International Conference on Cancer Research 2019

ICCR 2019 Proceeding

June 10-11, London, UK

Website: www.CancerConf.org

International e-Conference on Cancer Research

ICCR 2019

www.CancerConf.org

Contents

10-11 July 2019

■ Page 1-6

Performance of a Transfer Learning Module with Pretrained Neural Network and Logistic Regression in Detection of Breast Carcinoma from Microphotographs of Fine Needle Aspiration Cytology Smears

Parikshit Sanyal, Anirudh Sharma, Prosenjit Ganguli, Sanghita Barui

■ Page 7-7

Influence of MTHFR rs1801133 (C677T) Polymorphism upon Overall Methylation Levels of Glioblastoma Patients under Inhaled Perillyl Alcohol Treatment

Igor D.P. Soares, Giselle M. Faria, Marcia R. Amorim, Clovis O. da Fonseca, Thereza Quirico-Santos

■ Page 8-8

Investigation of Vascular Endothelial Growth Factor-A and Its Receptor in Canine Prostate Cancer

Antonio Fernando Leis-Filho, Patricia de Faria Lainetti, Priscila Emiko Kobayashi, Valeria Grieco, Chiara Palmieri, Renée Laufer-Amorim, Carlos Eduardo Fonseca-Alves

■ Page 9-13

Development of New Methods for the Detection, Isolation, Growth, and Re-collection of Cancer Cells In Blood Based on Size-discrimination of Cancer Cells and Normal Cells

Shin Aoki, Babita Shashni, Shinya Ariyasu, Hiroshi Takemura, Kazunori Akimoto, Naoyuki Aikawa, Ken-ichiro Iwasaki, Takayuki Nakanishi, Atsuo Yasumori, Tomohiro Osaki, Norihiko Itoh

■ Page 14-20

Flavonoids Effects on Breast Cancer Tumors

Sina Moradi Yeganmahale, Farahnaz Mohammadi Arab Abadi, Mohammad Hossin Abdoli, Mohammed Hosseini Goke

■ Page 21-32

Safety and Quality of Life in the Treatment of Non-metastasic Colorectal Cancer Patients: 5-fluorouracil Versus Capecitabine

Julia Sánchez-Gundín, Cristina Martín-Sabroso, Ana M. Fernández-Carballido, D. Barreda-Hernández, Ana I. Torres-Suárez

■ Page 33-37

Usefulness of Our Newly Designed Supplements for Reducing the High Risk of Pancreatic Cancer

Hidetoshi Ikeda, Takuma Ikeda, Hidetoshi Tahara

■ Page 38-38

BreastDefend Enhances Effect of Tamoxifen in Estrogen Receptor-positive Human Breast Cancer in Vitro and in Vivo

Isaac Eliaz, Dan Sliva

■ Page 39-54

Classic Herb Pair Sculellaria Barbata and Hedyotis Diffusa for Breast Cancer:Potential Mechanism with Method of Network Pharmacology

TingTing Ma, GanLin Zhang, BingXue Li, CunFang Dai, XiaoMin Wang

Contents

10-11 July 2019

■ Page 55-68

Breast Cancer Multi-therapy and Immune System Activation, Checkpoint Modulators, Signal Inhibitors and T Cells Reprogramming

Miguel A Galván Morales, Raúl Barrera Rodríguez, Julio R. Santiago Cruz, Luis M Terán Juárez

■ Page 69-85

The Hypercoagulability of a Murine Breast Cancer Model with Pulmonary Metastasis

Yang Wenjing,Yang Guowang, Zhang Ganlin

■ Page 86-105

Photodynamic Therapy and Lung Cancer Stem Cells – The effects of AlPcS4Cl on Isolated Lung Cancer Stem Cells

Anine Crous, Heidi Abrahamse

■ Page 106-117

Landscape of Clinically Actionable Mutations in Breast Cancer

Radheshyam Naik, Sheela ML, Sridhar PS, Shekar Patil, Satheesh C.T, Krithika Murugan, Srinivas B.J, Nalini Rao, Mahesh B, Shashidhara H.P, Krishna CR, Yogesh S, Nimmy Ramdas, Sunitha N, Ramya K, Ashwini R, Urvashi Bahadur, Pooja Agrawal, Veena R, Tejaswini BN, Sateesh Kunigal, Shanmukh Katragadda, Ashwini Manjunath, Amritanshu Ram, Raghavendra M Rao, Ajai Kumar, Mithua Ghosh

■ Page 118-127

Tumor Heterogeneity Uncovered by HLA-G Isoforms Expression

Diana Tronik-Le Roux, Jérôme Verine, Alix Jacquier, Raluca Stanciu, Julie Renard, Chantal Schenowitz, François Desgrandchamps, Nathalie Rouas-Freiss, Edgardo D. Carosella

■ Page 128-134

Soy Lecithin Liposome as Potential Platform for Intravenous Delivery of Quercetin in Cancer Treatment

Diem-Huong Nguyen Tran, Ngoc Thuy Trang Le, Hong Thao Truong, Van Du Cao, Cuu Khoa Nguyen, Dai Hai Nguyen, Minh Thanh Vu

■ Page 135-145

Novel BRCA1 and BRCA2 Deleterious Mutations and Unclassified Variants in Egyptian Female Breast Cancer Patients

Hala O. El-Mesallamy, Sherihan G. AbdelHamid, Hany AbdelAziz, Abdel-Rahman N. Zekri

■ Page 146-146

Proton Magnetic Spectroscopic Assess Metabolic Changes of Glioma Tumor of a Patient under Intranasal Perillyl Alcohol-based Therapy

Gisele M. Marques, Giselle M Faria, Alair S. dos Santo, Clovis O. da Fonseca, Thereza Quirico-Santos

■ Page 147-152

Effects of Vitamin C and Citicoline on Morphine-Inducing Tolerance in Mice

Mahrouz Salehpour, Bohloul Habibi Asl, Mohammad Charkhpur, Javad Mahmoudi

International e-Conference on Cancer Research

ICCR 2019

www.CancerConf.org

Contents

10-11 July 2019

■ Page 153-153

Influence of Microalgae Extracts on the Toxicity of a Carcinogenic Polycyclic Aromatic Hydrocarbon, Benzo(a) pyrene, in Endothelial Cells

Manon Le Goff, Antoine Delbrut, Rémi Pradelles, Odile Sergent, Dominique Lagadic-Gossmann, Eric Le Ferrec, Lionel Ulmann

■ Page 154-162

Antiproliferative Effects of Palmitoylethanolamide on Human Cervical Cancer Cells

Laura Bonfili, Valentina Cecarini, Anna Maria Eleuteri

■ Page 163-174

Evaluation of Cytotoxic and Antioxidant Activities of Purified Vegetal Extracts and Its Main Pure Compounds

J. Rocha-Pimienta, J. Espino, S. Martillanes, A.B. Rodríguez, J. Delgado-Adámez

■ Page 175-184

Hiroshima Black Rain Evidence Invalidates the A-bomb Survivor Life Span Study: the Basis of the Linear No-threshold Model

Shizuyo Sutou

■ Page 185-189

Study of the Prevalence of Chronic Diseases (Cancer, Diabetes, Heart Disease) and Its Relationship with the Elderly's Quality of Life

Samira Sangi, Majid Zargham Hajabi, Leila Zolghadr, Faegheh Miryousefiata, Sareh Sangi

■ Page 190-194

The Cytotoxic Properties and Anticancer Impacts of Zinc Oxide Nanoparticles on Human Breast, MCF7 Cell Lines

Ghasem Rahimi Kalateh Shah Mohammad, Vahid Pouresmaeil

■ Page 195-195

A Comprehensive Study of Possible Crosstalk between Angiogenic and Metabolic Signaling Pathways in Cancer

Hamid Latifi-Navid, Sepideh Taghizadeh, Zahra-Soheila Soheili, Shahram Samiei, Ehsan Ranaie Pirmardan

■ Page 196-205

A Survey of Anti-cancer Properties of Sea Buckthorn

Seyed MohammadReza Soltani Moghadas

International Conference on Cancer Research 2019

Website: www.CancerConf.org

June 10-11, London, UK



Performance of a Transfer Learning Module with Pretrained Neural Network and Logistic Regression in Detection of Breast Carcinoma from Microphotographs of Fine Needle Aspiration Cytology Smears

Parikshit Sanyal [1], Anirudh Sharma [2], Prosenjit Ganguli [3*], Sanghita Barui [1]

[1] *Dept of Pathology, Military Hospital Jalandhar, Jalandhar Cantt, PIN 144005, India*

[2] *Undergraduate student, Vellore Institute of Technology, Katpadi,Vellore, Tamil Nadu, PIN 632014, India*

[3] *Dept of Pathology, Command Hospital, Alipore, Kolkata 700027, India*

** Corresponding author: prosenjitganguli@hotmail.com*

Abstract

Fine needle aspiration cytology (FNAC) is an useful modality for initial assesment of a palpable breast lump. The aim of this study was to develop a computer model for classification of microphotographs from FNAC smears of breast lesions, into two classes 'benign' and malignant'. We have used the transfer learning method, i.e. using a neural network which has been trained on a different dataset, to extract features from the present datatset. Apart from being of valuable diagnostic utility, the model will also provide key insights on machine learning and how a learner, human or machine, distinguishes benign from malignant.

A pretrained neural network (VGG16) which has been trained on the ImageNet database, was used for the study. A total of 2037 processed microphotographs from Romanowky stained FNAC smears were taken, all at 40x magnification. Images from two different microphotography systems in two different tertiary care centers of India was used. The images were then split into two sets, 'training' (1544 images) and 'validation' (493 images). During training, features were extracted with VGG16 and fit with original labels using logistic regression. After completion of training, images from the validation set was processed with the VGG16 network and the trained logistic regression model was used to generate predictions.

The model achieved 90.38% sensitivity, 87.12% specificity, 88.67% positive predictive value and 89.03% negative predictive value. A diagnostic accuracy of 89% was achieved. Receiver operating characteristic shows area under curve of 0.89, indicating good perforamance. 12.8% false positives and 9.6% false negatives were also reported by the model. The principal difficulties encountered were the distinction between the dark staining nuclei of myoepithelial cells and the hyperchromasia of a malignant epithelial cell. Also, hypocellular foci with single malignant epithelial cells were often reported to be falsely negative by the model.

Overall, the sensitivity, specificity, positive and negative predictive value of the model is close to FNAC reported by pathologists. It shows potential to be used as a screening tool, after validation on a larger dataset.

Keywords:

Pretrained Neural Network,

Logistic Regression,

Breast Carcinoma,

Microphotographs.

1. Introduction

Breast cancer is the most common cancer in women worldwide, with 2 million new cases reported in 2018.[1 2] Fine needle aspiration cytology (FNAC) is part of the triple assessment of a suspected breast lump as it is minimally invasive and provides cytological material for identifying malignant lesions. In a study from Italy of 210 patients, sensitivity, specificity, diagnostic accuracy, positive predictive value (PPV) and negative predictive value (NPV) of 97%, 94%, 95%, 91% and 98% were found for FNAC breast.[3] A large systematic review found that the sensitivity of core needle biopsy (CNB) is better than that of FNAC [87% (95% CI, 84%-88%, I2 = 88.5%) versus 74% (95% CI, 72%-77%, I2 =

88.3%)] and the specificity of CNB is similar to that of FNAC [98% (95% CI, 96%-99%, I2 = 76.2%) versus 96% (95% CI, 94%-98%, I2 = 39.0%)].[4]

The aim of the present study was to develop a machine learning model which will be able to scan Romanowsky stained smears, mark areas with features suggestive of malignancy and present them to the pathologist; in effect the model will serve as a screening tool for FNAC smears of breast lesions. The performance characteristics of the model will have to be comparable to the established sensitivity, specificity, PPV and NPV of manual FNAC by the pathologist.

Machine learning methods have evolved sufficiently in complexity so that such a task can be undertaken. In particular, Artificial Neural Networks (ANNs) have been found to be suitable for image recognition tasks. [5]Artificial neural networks (ANN) are mathematical models based on systems of linear algebra. An ANN constitutes of several layers of 'neurones', individual nodes which take a number as input, perform a linear operation on it and return an output. For each neurone, presented with an input *x*, the output *y* is:

$$y = f(wx + b)$$

Where 'w' and 'b' are two parameters of the neuron, called 'weight' and 'bias' of the neuron respectively. *f(x)* is a function which transforms the input into output. The functions that are usually employed for this purpose are the sigmoid function or the rectified linear unit (ReLu) function. An ANN is made of up many such layers of neurones. The ANN calibrates it's coefficients 'w' and 'b' in each neuron, as to perform a certain task, e.g. pattern recognition.[6] Convolutional neural networks (CNNs) are a special class of ANNs which take a whole image as input and classifies the image in defined categories. A special operation called 'convolution' is performed in a CNN, which reduced the dimensions by averaging local pixels increase its depth. CNNs have been described in detail by Karpathy et al.[7] Multilayered deep neural networks have successfully been able to classify images in separate categories, from a large and diverse database.[8]

There has been use of neural networks in cytology. Savala et al have used neural networks based on morphometric features, to distinguish follicular adenoma from carcinoma in thyroid FNAC smears. [9] Conventional Pap smears have been successfully analysed with the PAPNET network by Mango et al.[10] However, these studies used morphometric data from the images as inputs to an ANN, and have not used a CNN.

Constructing a CNN requires thousands of training images and computer processing time. However, open source CNNs have been developed which have been trained over a very large dataset of diverse classes of images. Transfer learning is one of the emerging paradigms in machine learning which makes use of these pre-trained CNNs to perform a specific task. In the transfer learning approach, a neural network which has been pre-trained on a data set is used to analyse and predict on a different data set. The method of transfer learning has been described by Karpathy et al.[11] In the present study, we have used the VGG16 [12] neural network, which has been developed by the Visual Geometry Group at University of Oxford. [13] The VGG16 neural network has been pre-trained with the ImageNet dataset, consisting of 32326 different classes of images.[14]

2. Materials and Methods

Fine needle aspiration cytology smears from both benign and malignant lesions of breast were selected from the archives of two tertiary care hospitals of India. All smears were stained with Romanowsky stain (May-Grünwald Giemsa or Leishman Giemsa). The smears where diagnosed cytologically by a group of pathologists. A total of 288 micro photographs from malignant and 127 micro photographs from benign lesions were photographed. Images from one hospital was photographed using Olympus microphotography system on a Labomed LX300 microscope. Images from the other hospital were photographed in a DeWinter Digi510 Microphotography system. All microphotographs were taken at 40x maginification. Images of optimal quality were selected and a python script using openCV was then used to slice the photographs into 8 random slices of 341 x 256 pixels. The cropped images with trainable features specific to either the benign or the malignant categories were selected. A total of 2037 cropped images were thus produced. The images were then split into two data sets: one data set for training the CNN and another for validation. Distribution of the image data is shown in Table 1.

Table 1: Distribution of the processed microphotographs in different categories (N=2037)

	Training	**Validation**	**Total**
Benign	802	233	1035
Malignant	742	260	1002
Total	1544	493	2037

The images were read with the OpenCV library, and resized to a dimension 224 x 224, because the VGG16 neural network operates on this dimension. Weight of a VGG16 model trained on the ImageNet database were imported, using the Keras python library.[15] The model was imported after removing the Fully Connected Layers, i.e. the final step of prediction is skipped and the output of the penultimate layer of the neural network is extracted. We used this output as features vectors extracted from the image. Each of the 1544 training images generated a feature array, which is a 3-dimensional array of size 7 x 7 x 512. The feature array is then flattened into a feature vector of size 7 x 7 x 512 = 25088. This flattened feature vector of 25088 floating point numbers is then fitted with the original labels (0 for 'benign' and 1 for 'malignant) using a logistic regression model. After completion of training, the same algorithm was applied to the validation set of 493 images. Features were extracted by the VGG16 network, and the feature vectors were processed by the LR model to generate predictions, whether the image belongs to class '0' (benign) or '1' (malignant).

3. Results

Diagnostic accuracy achieved with the validation set was 0.89. Table 2 shows a contingency table of the predictions versus the original labels.

Table 2: Contingency table showing original labels and predicted labels of microphotographs of the validation set (N=493)

		Original label (diagnosed by pathologist)		Total
		Benign	**Malignant**	
Predicted by the model	**Benign**	203	25	228
	Malignant	30	235	265
		233	260	493
Sensitivity	90.38%	Specificity	87.12%	
Positive predictive value	88.67%	Negative predictive value	89.03%	

30 false positives (12.8% of benign microphotographs) and 25 false negative cases (9.6% of microphotographs with malignant foci) were reported by the predictor model. A receiver operating characteristic (ROC) curve (Figure 1) showed good performance with an area under curve (AUC) = 0.89.

Figure 2 shows few images from the validation set with their original and predicted labels.



Figure 1: Receiver operating characteristics of the predictor model

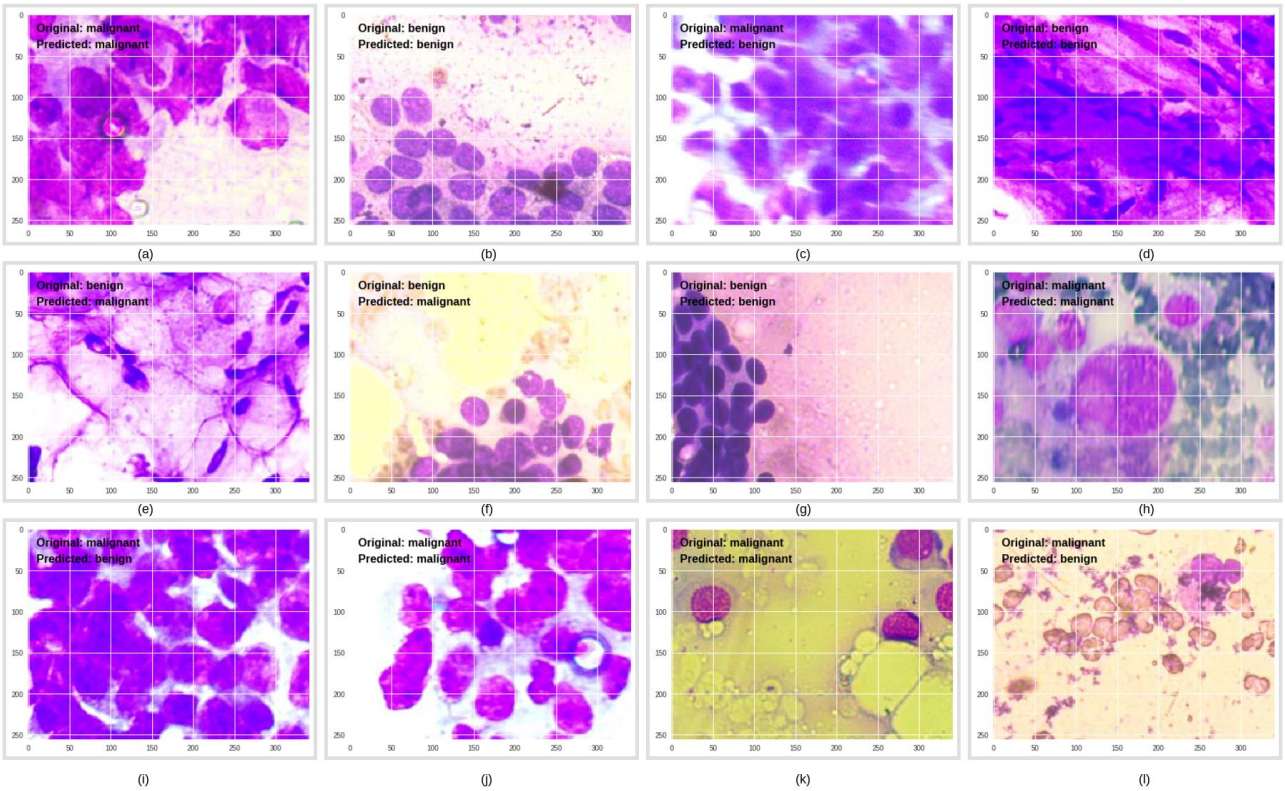


Figure 2: A subset of images in the validation set with original and predicted labels

4. Discussion

In a systematic review by Pouliakis et al in 2016, it was concluded that cytopathology is the ideal ground for application of artificial neural networks.[16] Machine learning tools are now available for screening Papanicolau stained cervical smears. [17] However, such models have not been extended to cytology of other organs. Several studies have used morphometric data from images as inputs to neural networks, which require the intervention of a pathologist or a morphometric device. Previous studies that have employed machine learning in cytological detection of breast cancer have also used morphometric data from images[18], such as radius, texture, perimeter, area, compaction (square perimeter divided by area), concavity, symmetry and fractals [19]. Using morphometric features requires an intermediary, either a human pathologist or a morphometric device. A few other studies have performed automated identification of breast cancer cells on immunohistochemically stained smears; a machine learning tool has been developed by Bolton for predicting immunohistochemical scores from tissue microarrays of breast cancer.[21] Algorithms have also been developed for automated screening of cytokeratin stained sections from sentinel lymph node biopsies.[22] In the present study, we have used whole images of Romanowsky stained cytological smears as input to the machine learning model.

The distinction between benign and malignant breast lesions from microphotographs of FNAC smears is a non-trivial machine learning problem. The criteria for identifying focus of carcinoma cells in FNAC smears from breast lesions include absence of myoepithelial cells, no single bare bipolar nuclei, and loss of cell cohesion moderate to severe nuclear atypia: enlargement, pleomorphism, irregular nuclear membrane and chromatin. In addition fibroblasts and fragments of collagen maybe present depending on presence of stromal desmoplasia. In contrast. FNAC from non-neoplastic breast tissue will include dark staining myoepithelial cells. Variable number of bare nuclei and bipolar cells are found in the background also the epithelial cells will have small round nuclei with bland chromatin.[20] such features are learnt by the trainee pathologist through exposure to several examples both benign and malignant. It is this reinforcement learning over repeated exposure to several training examples that impart learning to the brain. Neural networks operate on a similar principle. Recognition of individual cytological features by geometric methods is not computationally feasible because of the immense variability encountered in any field of biology, including cytology. Neural networks take a holistic approach to the problem and process the image as a whole.

The present study applies a neural network to whole image directly micro photographed from fine needle aspiration cytology smears of breast lesions. The sensitivity, specificity and diagnostic accuracy of the neural network was comparable to conventional fine needle aspiration cytology the network good successful identify features of carcinoma

in the micro photographs from the FNAC smears (Table 2).

Of the 233 images in the 'benign' category, 30 has been reported as false positive (12.8%). However, of the 260 images of the 'malignant' category, only 25 was reported false negative (9.6%). The low false negative rate has resulted in good negative predictive value (89.03%), suggesting potential utility in screening.

Figure 2(a), 2(h), 2(j) and 2(k) shows examples of foci where the model has successfully detected foci of malignancy. In Figure 2(a), 2(h) and 2(j), hyperchromatic, enlarged nuclei with uneven chromatin were recognised by the model. The model was also able to detect the isolated abnormal nuclei in an otherwise hypocellular focus (Figure 2(k)).

Figure 2(c) and 2(i) show a foci which has been reported false negative. In both these cases, the model has failed to distinguish epithelial cells with hyperchromatic nuclei from dark staining myoepithelial cells. In figure 2(j), in spite of obvious features of malignancy in the nuclei, the focus has been reported falsely negative, possibly due to hypocellularity in the focus.

Figure 2(e) and 2(f) represent clearly benign foci, which has been reported as false positives. The darker staining myoepithelial cells and nuclei of adipocytes have been falsely detected to be malignant. This might be attributable to overfitting on the training data, i.e. the model fitting both on the 'signal' (the actual epithelial and myoepithelial cells) as well as 'noise' (adipocytes, debris, background material) in the training data.

The present model depends on extracted features from the original image for its functioning. Each image produces a feature array of shape 7 x 7 x 512. Figure 3 shows systematic slices from this array, i.e. from 0 to 511, at each 60th slice. Each of these slices is a grayscale image, reproduced in figure 3 in artificial colors to highlight the features. All the 512 slices, each of shape 7 x 7, is flattened to produce a vector of 25088 dimensions, which is then fit with logistic regression to original label of the image.

5. Conclusion

We have demonstrated the performance of a predictor module based on transfer learning and logistic regression, to classify microphotographs from fine needle aspiration cytology smears of breast lesions, into two categories benign and malignant. The sensitivity of the model was 90.38%, suggestive of potential utility in screening. With further training with a diverse dataset, the model can evolve into an effective and accurate screening tool for FNAC smears of breast lesions.

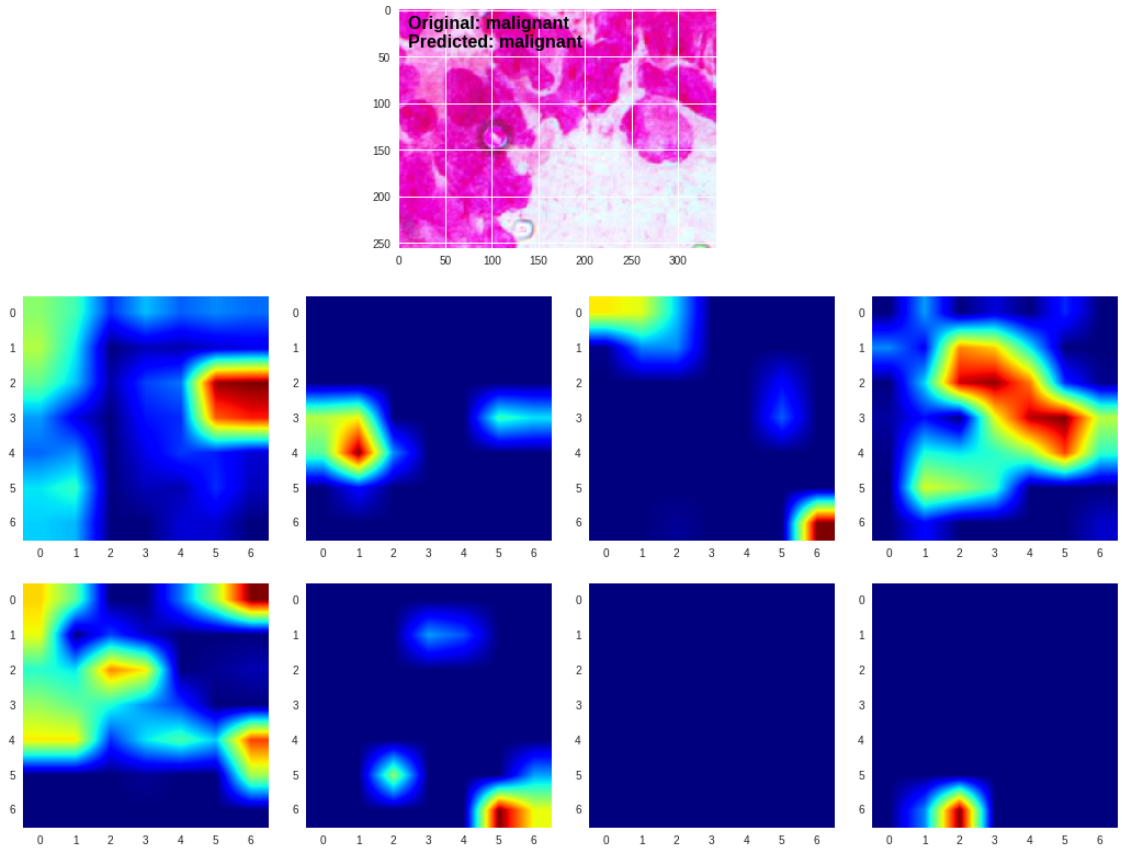


Figure 3: An image from the validation set and subset of its extracted features

5. References

1. Ghoncheh M. Incidence and Mortality and Epidemiology of Breast Cancer in the World. - PubMed - NCBI. Asian Pac J Cancer Prev. 2016; 17(S3):43–6.
2. Breast cancer statistics [Internet]. World Cancer Research Fund. 2018 [cited 2019 Jan 20]. Available from: https://www.wcrf.org/dietandcancer/cancer-trends/breast-cancer-statistics
3. Moschetta M M, Telegrafo, M. M, Carluccio DA, Jablonska JP, Rella L, Serio G, et al. Comparison between fine needle aspiration cytology (FNAC) and core needle biopsy (CNB) in the diagnosis of breast lesions. Il G Chir. 2014 Sep 1;35(7–8):171–6.
4. Wang M, He X, Chang Y, Sun G, Thabane L. A sensitivity and specificity comparison of fine needle aspiration cytology and core needle biopsy in evaluation of suspicious breast lesions: A systematic review and meta-analysis. Breast Edinb Scotl. 2017 Feb;31:157–66.
5. He K, Zhang X, Ren S, Sun J. Deep Residual Learning for Image Recognition. ArXiv151203385 Cs [Internet]. 2015 Dec 10 [cited 2018 Nov 12]; Available from: http://arxiv.org/abs/1512.03385
6. Haykin S. Neural Networks: A Comprehensive Foundation. 2nd ed. New York: Prentice Hall; 1999.
7. CS231n Convolutional Neural Networks for Visual Recognition [Internet]. [cited 2019 Jan 10]. Available from: http://cs231n.github.io/convolutional-networks/
9. Savala R, Dey P, Gupta N. Artificial neural network model to distinguish follicular adenoma from follicular carcinoma on fine needle aspiration of thyroid. Diagn Cytopathol. 2017 Dec 20;46.
10. Mango LJ. Computer-assisted cervical cancer screening using neural networks. Cancer Lett. 1994 Mar 15;77(2):155–62.
11. CS231n Convolutional Neural Networks for Visual Recognition [Internet]. [cited 2019 Feb 13]. Available from: http://cs231n.github.io/transfer-learning/
12. Simonyan K, Zisserman A. Very Deep Convolutional Networks for Large-Scale Image Recognition. ArXiv14091556 Cs [Internet]. 2014 Sep 4 [cited 2019 Feb 13]; Available from: http://arxiv.org/abs/1409.1556
13. Visual Geometry Group Home Page [Internet]. [cited 2019 Feb 13]. Available from: http://www.robots.ox.ac.uk/~vgg/
14. ImageNet [Internet]. [cited 2019 Feb 13]. Available from: http://www.image-net.org/
15. Home - Keras Documentation [Internet]. [cited 2019 Jan 20]. Available from: https://keras.io/
16. Pouliakis A, Karakitsou E, Margari N, Bountris P, Haritou M, Panayiotides J, et al. Artificial Neural Networks as Decision Support Tools in Cytopathology: Past, Present, and Future. Biomed Eng Comput Biol. 2016 Feb 18;7:1–18.
17. Cervical Cancer Screening - BD [Internet]. [cited 2019 Jan 10]. Available from: https://www.bd.com/en-us/offerings/capabilities/cervical-cancer-screening
18. Isa NAM, Subramaniam E, Mashor MY, Othman NH. Fine Needle Aspiration Cytology Evaluation for Classifying Breast Cancer Using Artificial Neural Network. Am J Appl Sci. 2007 Dec 31;4(12):999–1008.
19. Fiuzy M, Haddadnia J, Mollania N, Hashemian M, Hassanpour K. Introduction of a New Diagnostic Method for Breast Cancer Based on Fine Needle Aspiration (FNA) Test Data and Combining Intelligent Systems. Iran J Cancer Prev. 2012;5(4):169–77.
20. Cangiarella J. Breast. In: Orell & Steretts Fine Needle Aspiration Cytology. 5th ed. Edinburgh: Churchill Livingstone; 2012. p. 162.
21. Bolton KL, Garcia-Closas M, Pfeiffer RM, Duggan MA, Howat WJ, Hewitt SM, et al. Assessment of automated image analysis of breast cancer tissue microarrays for epidemiologic studies. Cancer Epidemiol Biomark Prev Publ Am Assoc Cancer Res Cosponsored Am Soc Prev Oncol. 2010 Apr;19(4):992–9.
22. Holten-Rossing H, Talman M-LM, Jylling AMB, Laenkholm A-V, Kristensson M, Vainer B. Application of automated image analysis reduces the workload of manual screening of sentinel lymph node biopsies in breast cancer. Histopathology. 2017 Dec;71(6):866–73.

International Conference on Cancer Research 2019

Website: www.CancerConf.org

June 10-11, London, UK



Influence of MTHFR rs1801133 (C677T) Polymorphism upon Overall Methylation Levels of Glioblastoma Patients under Inhaled Perillyl Alcohol Treatment

Igor D.P. Soares [1], Giselle M. Faria [2], Marcia R. Amorim [3], Clovis O. da Fonseca [4], Thereza Quirico-Santos [2]*

[1] *Instituto Nacional do Câncer, Centro de Medula Óssea, Divisão de Laboratórios, Laboratório de Células Tronco, RJ, Brasil*

[2] *Departmento de Biologia Celular e Molecular, Instituto de Biologia, Universidade Federal Fluminense, Niterói, RJ, Brasil*

[3] *Departmento de Biologia Geral, Universidade Federal Fluminense, Niterói, RJ, Brasil*

[4] *Departmento de Medicina Especializada , Escola de Medicina, Universidade Federal Fluminense , Niterói, RJ, Brasil*

** Corresponding author: tquirico@id.uff.br*

Abstract

Introduction: Glioblastoma (GBM) are primary brain tumor most common and aggressive in adults, highly proliferative with anabolic pattern and invasiveness. Deleterious genetic changes contribute to tumor agressivenes, low survival, treatment resistance and tumor recurrence. Intranasal administration of the naturally occurring monoterpene perillyl alcohol (POH) has been proven to halts glioma progression and prolongs GBM patients survival. Folate is crucial for biochemical processes with important role on carcinogenesis. MTHFR enzyme controls folic acid metabolic pathway and the balance between DNA synthesis and methylation, influencing global DNA methylation and carcinogenesis.

Aim: To evaluate the influence of *rs1801133* (C677T) functional polymorphism of *MTHFR* gene upon global genomic DNA (gDNA) methylation profile and survival of GBM patients under intranasal therapy with POH.

Material and methods: The study included 100 GBM patients (59 male; 41 female) at terminal stage according the clinical trial approved by Local Ethics Comitee. Genomic DNA from blood leukocytes was used for genotyping assay and global methylation status. Statistical analysis included non parametric tests, Spearman correlation, Chi-squared test, loglinear analysis, Kaplan-Meier analysis and Log-Rank test using SPSS program (version 20.0; 95% of confidence interval; $p<0.05$).

Results and discussion: the majority (73%) showed gDNA with hypomethylation pattern (median = 29.65%), with a significant difference ($p<0.0001$) compared to 27% from hypermethylated group (median = 133.25%). Survival plot of gDNA hypermethylated patients indicated high probability for longer survival, albeit no significat differences between the gDNA methylation beteween groups. Genotyping analysis showed frequencies of 38% for **CC** genotype; 49% for the heterozygous genotype **CT** and 13% for the **TT** genotype. **TT** genotype patients showed a significant ($p=0.037$) and marked reduction on gDNA hypomethylation levels (median = 13.35%) with approximatelly 2.5 fold decrease when compared to **CC** genotype (median = 33.02%). It was also observed a significant, moderate and negative correlation between the **TT** genotype and global gDNA hypomethylation (rho= -0,515; $p=0.006$).Genetic association studies did not found significant association between genotypes and global gDNA hypomethylation. However, it was found individual and significant contribution for the variables **gDNA hypomethylation below 25%** ($p=0,009$; Z score = -2.619), **additive model of contrast** (2TT+CT: $p<0.0001$; Z score = 5.083), **dominant model of contrast** (CT+TT: $p = 0.001$; Z score = 3.439) and **TT** genotype ($p<0.0001$; Z score = - 4.543). The survival plot of **TT** genotype showed high survival probability when compared to the heterozygous (**CT**) and wild type (**CC**) genotypes, but no significant differences were observed between median survival for each genotype of *rs1801133* (C677T), as well as no significant differences of survival times by Log Rank analysis by each genotype.

Conclusion: Even after tumor recurrence, it was possible to identify significant differences in hypomethylation degree among GBM patients, being the **TT** genotype of *rs180133* (C677T) a variable that contributed prominently for DNA hypomethylation pattern. Hypermethylated recurrent GBM patients tend to display a better survival profile, but curiously and controversially, the mutant variants of *rs1801133* (C677T) tends to be related to high survival probability when compared to wild variant which may be related to the efficacy of POH-base therapy.

Keywords:

Polymorphism,

Glioblastoma (GBM),

MTHFR Gene, DNA.

International Conference on Cancer Research 2019

Website: www.CancerConf.org

June 10-11, London, UK



Investigation of Vascular Endothelial Growth Factor-A and Its Receptor in Canine Prostate Cancer

Antonio Fernando Leis-Filho [1], Patricia de Faria Lainetti [1], Priscila Emiko Kobayashi [2], Valeria Grieco [3], Chiara Palmieri [4], Renée Laufer-Amorim [2], Carlos Eduardo Fonseca-Alves [1]*

[1] *São Paulo State University - UNESP, Department of Veterinary Surgery and Anesthesiology, School of Veterinary Medicine and Animal Science, Botucatu, Sao Paulo, Brazil.*

[2] *São Paulo State University - UNESP, Department of Veterinary Clinic, School of Veterinary Medicine and Animal Science, Botucatu, Sao Paulo, Brazil.*

[3] *Department of Veterinary Medicine, Università degli studi di Milano*

[4] *School of Veterinary Science, the University of Queensland, Gatton Campus, Gatton, Queensland, Australia.*

* *Corresponding author: carlos.e.alves@unesp.br*

Abstract

Vascular endothelial growth factor (VEGF) and its receptor (VEGFR) represent a complex family of angiogenic molecules, consisting of different ligands and different receptors. In both physiological and pathological processes, VEGFR2 receptor triggers angiogenesis after stimulation by VEGFA. In different human and canine tumors, cancer cells can express both VEGFR2 and VEGFA in a self-stimulation loop, resulting in angiogenesis and cell proliferation. Due to the importance of VEGF/VEGFR signaling in tumor proliferation and angiogenesis, this study aimed to evaluate VEGFA and VEGFR-2 protein and gene expression in canine prostate cancer (PC). We analyzed 12 normal prostates (NP), 12 proliferative inflammatory atrophy (PIA) lesions and 30 canine PC from the archives of the Sao Paulo State University and The University of Queensland. Protein expression and gene expression were evaluated by immunohistochemistry and RT-qPCR, respectively. The immunohistochemical staining for VEGFA and VEGFR-2 was quantified using a selected threshold from the Image J Software. The gene expression was evaluated comparing relative quantification (RQ). The survival curve was calculated for PCs using the Kaplan-Meier method, and the statistical significance was determined using a log-rank test. PC samples were classified according to the Gleason score (GS) in low GS tumors (scores 6 and 7) and high GS tumors (score 8, 9 and 10). A negative to weakly positive VEGF and VEGFR expression was observed in the epithelial cells of NP and PIA. On the other hand, canine PC expressed higher VEGF ($P<0.0001$) and VEGFR ($P<0.0001$) compared to normal samples. Regarding VEGF and VEGFR gene expression, we did not find significant statistical differences in all comparisons. A positive correlation between VEGF and VEGFR gene expression (Spearman $r= 0.68$ and $P=0.013$) and between VEGF and VEGFR protein expression (Spearman $r= 0.8$ and $P<0.0001$) was also observed in normal samples. This correlation was lacking in PC samples. Interestingly, we identified higher VEGF and VEGFR gene and protein expression in tumors with high Gleason score compared to the low GS group. Additionally, PC-affected patients with higher VEGFR expression experienced a lower survival time ($P=0.0372$) compared to patients with low VEGFR expression. In conclusion, VEGFR seems to be an independent prognostic factor in animals with prostate cancer.

Keywords:

VEGFA,

VEGFR-2,

Angiogenesis,

Prostate,

Dog Model.

International Conference on Cancer Research 2019

Website: www.CancerConf.org

June 10-11, London, UK



Development of Glass-Beads Filters for the Isolation, Culture, and Re-Collection of Cancer Cells from Blood

Shin Aoki [a,b*], Babita Shashni [a], Shinya Ariyasu [b], Hiroshi Takemura [b,c], Kazunori Akimoto [a,b], Naoyuki Aikawa [b,d], Ken-ichiro Iwasaki [d], Takayaski Nakanishi [d], Atsuo Yasumori [b,d], Tomohiro Osaki [e], Norihiko Itoh [e]

[a]*Faculty of Pharmaceutical Sciences, Tokyo University of Science, 2641 Yamazaki, Noda, Chiba 278-8510, Japan*

[b]*Research Institute for Science and Technology, Tokyo University of Science, 2641 Yamazaki, Noda, Chiba 278-8510, Japan*

[c]*Faculty of Science and Technology, Tokyo University of Science, 2641 Yamazaki, Noda, Chiba 278-8510, Japan*

[a]*Faculty of Industrial Scienc and Technology, Tokyo University of Science, 6-3-1 Nijuku, Katsushika-ku, Tokyo 125-8585, Japan*

[e]*Laboratory of Veterinary Surgery, Joint Department of Veterinary Medicine, Faculty of Agriculture; Tottori University, Tottori 680-8553, Japan*

** Corresponding author: shinaoki@rs.noda.tus.ac.jp*

Abstract

Circulating tumor cells (CTCs) are tumor cells that are considered to originate from primary cancer sites, go into the blood stream in the body, and metastasize to the other organs. Herein, we report on a simple and convenient method to trap, culture, and recollect cancer cells, the sizes of which are greater than that of normal hematologic cells by the use of glass-beads filters (GBF) having a diameter of 24 mm and a thickness of 0.4~1.2 mm, which were prepared by sintering round-shaped glass beads (diameter: 63–106 μm). A small integrated glass-beads filter (iGBF) with a diameter of ca. 9.6 mm for the use in filtering a small volume of blood was also designed and prepared. It was possible to efficiently capture mouse Lewis lung carcinoma cells expressing green fluorescent protein spiked in saline/blood by single and repeated (circulation) filtrations. In addition, we successfully captured B16 CTCs from the blood of a B16 melanoma metastasis mouse model by iGBF and grow them on/in iGBF. Filtration by GBF had negligible effect on the adherent and proliferative characteristics of cancer cells. We believe that the GBF protocols afford easy and efficient methods for early and convenient diagnosis and treatment of cancer and related diseases.

Keywords:

Glass-bead filter,

Filtration;

Circulating tumor cells;

Size based separation.

1. Introduction

Circulating tumor cells (CTCs) are tumor cells that are found in the peripheral blood of cancer patients.[1-4] It is reported that CTCs come out from the primary cancer tissues into the blood stream, travel around in the body, and then are arrested at other organ sites apart from the original cancer sites, resulting in the metastasis. It is assumed that such metastasis that causes 90% of cancer-associated human deaths could be detected, predicted, and/or managed if CTCs could be captured from the blood of cancer patients, analyzed, and used in drug testing.

Currently used methods for detection and capture of CTCs from whole blood mainly include biological and physical methods. Biological approaches include the capture of CTCs based on the expression of tumor specific antigens such as epithelial cell adhesion molecules (EpCAM), cytokeratins and so on. However, the limited number of such specific antibodies and cancer heterogeneity during epithelial-to-mesenchymal transition (EMT) hampers biological approaches as a less reliable approach.[4] On the other hand, physical methods for CTC capture are based on differences in biophysical properties such as hardness (deformity), size and shape between CTC and hematologic normal cells. It has been reported that the sizes of tumor cells are generally larger than those of hematologic cells, suggesting that the use of a size-based method for the capture of CTC using filtration systems might be a more convenient approach than biological-based methods. In this context, the use of microdevices such as microfilters, microfluidics, microsieve chips, and micropinching chips have been reported for use in the size-based enumeration and enrichment of CTCs.[5] To our knowledge, however, there is a few method that can treat a large volume (μL~L order) of non-diluted and/or diluted blood samples which isolates live cancer cells. Therefore, convenient and easy methods for isolation, growth, and re-collection of CTCs are highly required.

Herein, we report on new methods for detection of CTCs by using a particle size analyzer and PC software based on the size difference between normal blood cells and cancer cells (Figure 1).[6] For capture, growth, and re-collection of CTC, we have developed a new system using glass-bead filter (GBF) and small integrated GBF (iGBF), which possess suitable porous structures so that smaller normal hematologic cells such as red blood cells (RBC) to pass through the filters and larger cells such as cancer cells are trapped on/in the filters.[7] In this paper, these methods are reported.

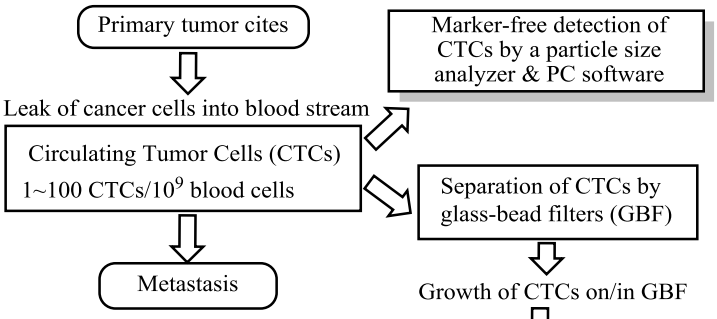
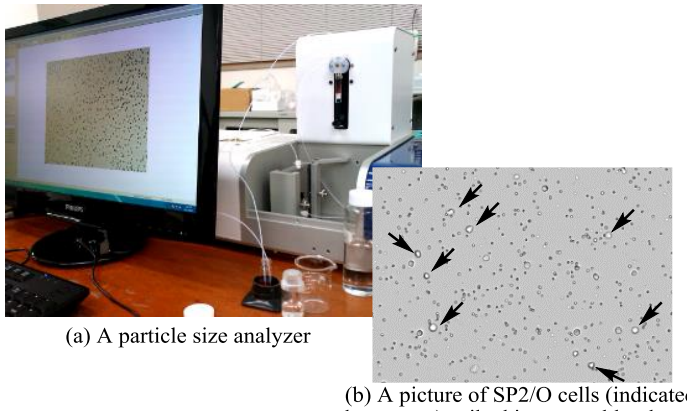


Figure 1. Convenient methods for detection, separation, growth, & re-collection of circulating tumor cells (CTC)

2. Marker-free detection of cancer cells in blood by a particle size analyzer and PC software "CCF". [6]

For the marker-free detection of cancer cells from hematologic/normal cells in blood, we have focused our effort on 1) the detection of cancer cells based on their size and shape and 2) the recognition of cancer cells based on cytomorphological deformity (surface contour). Namely, a Jasco-Occhio particle size analyzer IF nano-200 was employed for the comprehensive measurement of various size and shape parameters of cells (Figure 2). For the physical characterization of cells, a suspension of cells was introduced into a flow cell equipped with a high definition CCD camera that captures images by using stroboscopic illumination. The captured images are automatically analyzed for shape and size parameters by Particle Image Analysis Software that had been installed in particle size analyzer.[6]

In this work, SP2/O myeloma cells were chosen as the test example, because the results of our previous experiments suggested that the average inner diameter of SP2/O cells is 11.5 μm, which is greater than that of mouse red blood cells (4.4 μm on average).[4] Figure 3 displays a representative two-dimensional scatterplots of mouse blood containing SP2/O cells (the cell suspension in blood was diluted 51 X with PBS for the analysis to include 5.1 X 10^9/mL red blood cells (RBC) and ca. 2 x 10^4 SP2/O cells/mL) with respect to ISO inner diameter, which is a size parameter, on X-axis and ISO circularity, which is a shape parameter, onY-axis (each small dot in the scatterplot corresponds to a cell (particle)), suggesting that SP2/O cells and other cancer cells have greater inner diameters (≥10 μm) than those of normal cells.



(a) A particle size analyzer

(b) A picture of SP2/O cells (indicated by arrows) spiked in mouse blood taken on a particle size analyzer

Figure 2. (a) A particle size analyzer for discrimination of cancer cells from normal blood cells. (b) A picture of S/PO cells spiked in mouse blood.

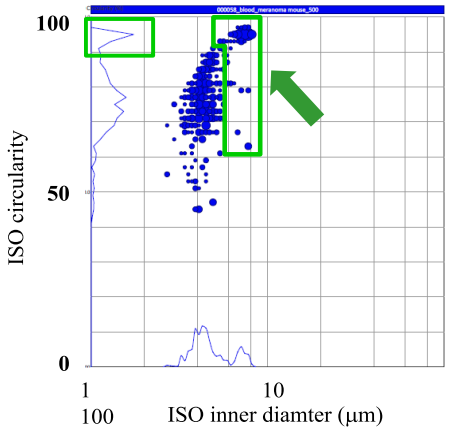


Figure 3. Two dimensional scatterplots of mouse blood containing cancer cells (SP2/O cells) with respect to ISO inner diameter (horizontal axis) & ISO circularity (vertical axis). Plots of SP2/O cells are indicated in a green box indicated by a green arrow.

It has been reported that the size of some white blood cells (WBC) is similar to that of cancer cells. In our study, we observed one WBC having an inner diameter of 10.3 μm among 777 particles (inner diameters of 4-50 μm). This information prompted us to develop a new computer software program "Cancer Cell Finder (CCF) ver. 1.0" to distinguish WBCs (inner diameter of >10.3 μm) and other normal cells from cancer cells using images obtained from the particle size analyzer. Deformity in cancer cells in contrast to normal cell is widely known and some reports have

linked the deformity in cancer cells with their metastatic propensity. In Figure 4, a WBC cell exhibits bright area in the center and darker area on the edge and smoother surface, while darkness curves of LLC are more complicated. Based on this observation, the numbers of stationary points (SP), at which the gradient of a darkness/brightness curve is zero, were counted for discriminating cancer cells from normal blood cells based on the following algorithm: 1) Prepared binarization (black and white) images of the microscopic images (or images from the particle size analyzer) of the cells with a given threshold. 2) Based on the obtained binarization images, cell areas were extracted and their center of gravity determined. 3) The defined two cross sections passing through the center of gravity of each cell (plain and dashed lines and respective luminance (darkness) functional curves of sections were obtained. 4) The total number of SP were counted on the aforementioned two luminance curves, based on which the cells were classified into two categories: i) a cell having SP number of less than or equal to 10 (≤ 10) is considered as a non-cancer cell, and ii) a cell having SP number greater than 10 (> 10) is considered as a cancer cell. The probabilities of "CCF ver. 1.0" for detecting normal cells such as WBC and lymph node cells was 83% and 100%, respectively, and for cancer cells, such as SP2/O cells and LLC cells, was 95% and 100%, respectively, as summarized in Table 1.

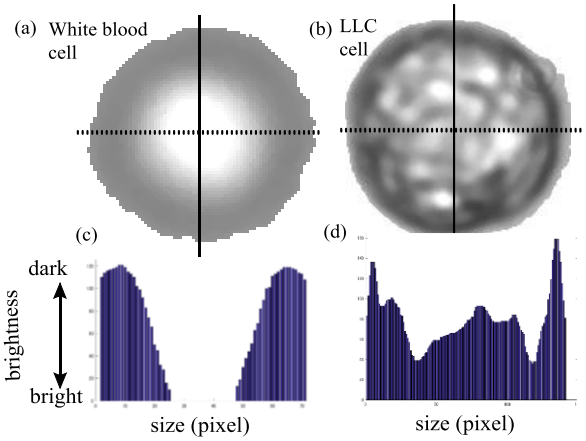


Figure 4. Particle size analyzer images of white blood cell (a) and LLC cell(b). The brightness functional curves of sections, which pass through the center of gravity of cells for white blood cell (c) and for LLC cell (d)

Table 1. Stationary poins observed for cancer and non-cancer cells as analyzed by the CLE value point method of "CCF ver. 1.0"

		Total cells	The number of cells that have >10 CLE value points	Probability of detection (%)
Normal cells	WBC	42	7	83 (as normal cells)
	Lymph node cells	42	0	100 (as normal cells)
Cancer cells	SP2/O	42	40	95
	LLC	42	42	100
	A549	41	41	100
	B16	42	41	98
	Colon-26	36	36	100
	HeLa	35	30	86
	Jurkat	42	21	50
	K562	42	41	98
	MC38	40	40	100
	MDA-MB-157	42	42	100
	MDA-MB-468	40	27	68
	Molt-4	42	10	24

3. Size-based separation of cancer cells from blood, and their growth and re-collection by means of glass-bead filters (GBF)[7]

The former GBFs were prepared by sintering (650–700°C for 1 h) commercially available round-shaped glass beads (diameter: 63–106 μm) to produce well-defined pores with an adequate porosity has a diameter of 24 mm and thickness of 1.2 and 0.4 mm, with a diameter of ca. 9 mm and thickness of ca. 2 mm (Figure 1). based on our assumption of the size threshold between cancer cells and hematologic cells. The entrapment of *in vitro* cancer cell lines and CTCs from an experimental model blood and from model mice using GBF and iGBF by a single filtration assembly and repeated (circulated) filtration system is also described. Furthermore, we also report that the cancer cells that were captured on/in GBF and iGBF could be further grown and re-collected by using the specific holder (designed especially for the culture and recollection of the trapped cancer cells). [7]

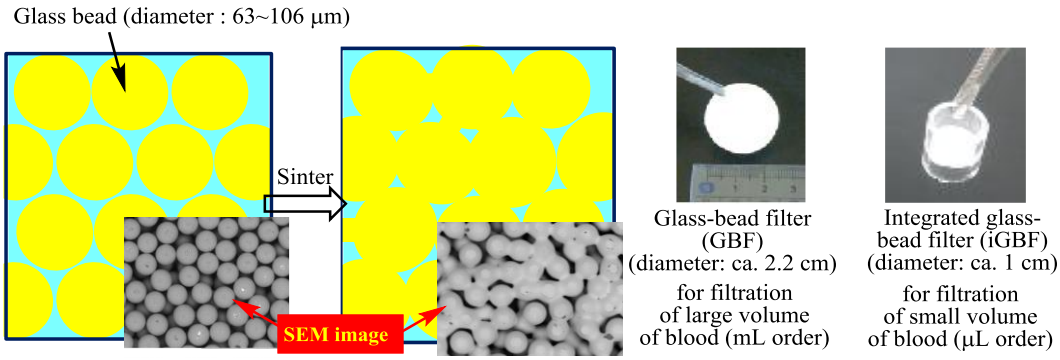


Figure 5. Preparation of glass-bead filter (GBF) by sintering glass beads

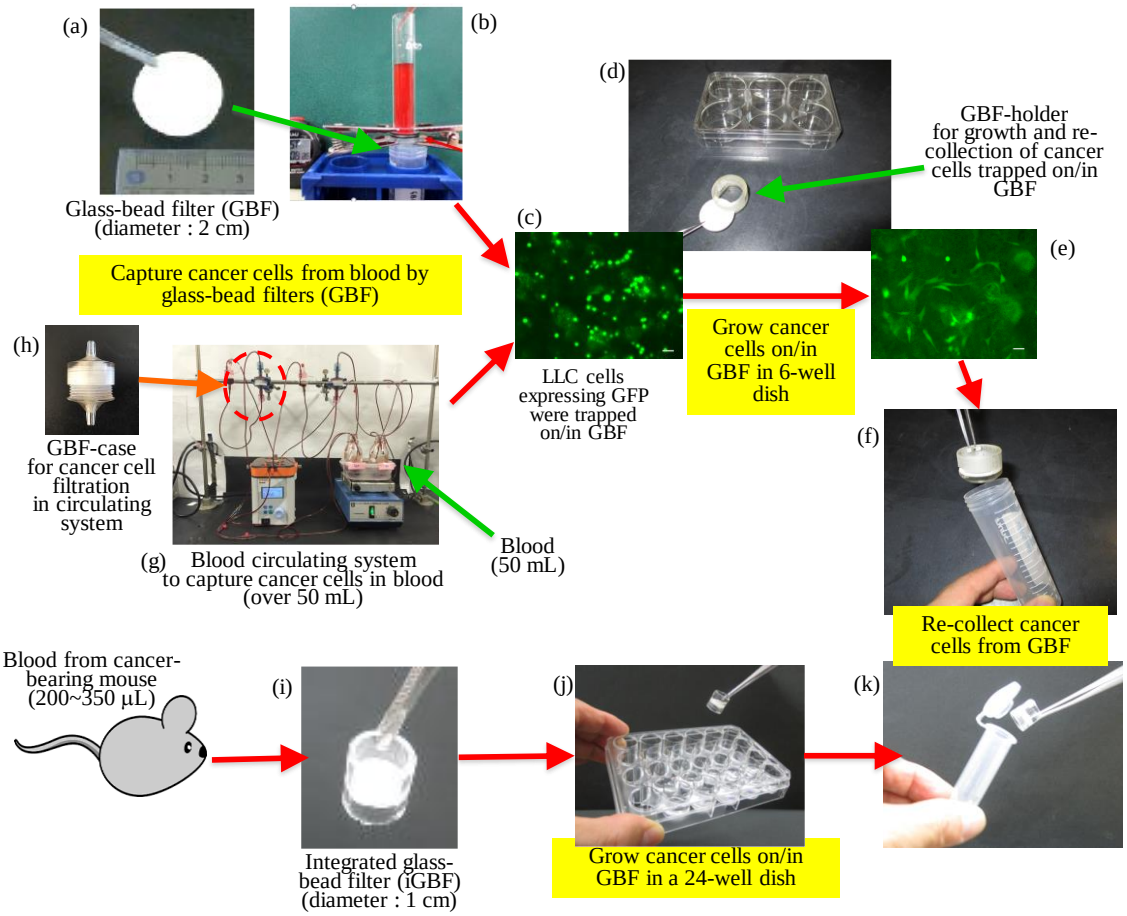


Figure 6. GBF-based methods for separatation, growth, and re-collection of CTC

4. Summary

In summary, we report on the convenient methods for detection, separation, growth, and re-collection of CTC in this paper. A convenient software program "CCF ver. 1.0" was developed to distinguish cancer cells from normal cells based on differences in the luminance (darkness) extent of curve of the cell surface. It is suitable for differentiating adherent cancer cells from WBCs and splenocytes, thus making it attractive for use in hospitals, medical facilities and laboratories, thereby overcoming the need for expensive CTC detecting devices. An analysis of blood samples (diagnosed with cancer) with a particle size analyzer or more simple and cheaper instruments assisted by a cell-recognition software such as "CCF" provides insights into possible clinical applications of our combination approach for detection CTCs and CTC clusters for evaluating the progression and theranostics of cancer and related diseases. The samples of these methods do not require any major preprocessing (e.g. cell fixation) and can be operated with any diluent, thereby permitting the

viability of the target cells to be maintained for *in vitro* establishment and for further characterization, contrary to immunological based detection which requires cells to be fixed.

5. Acknowledgements

This work was supported by grants-in-aid from the Ministry of Education, Culture, Sports, Science and Technology (MEXT) of Japan (No. 15H04129 for A.Y. and Nos. 15K00408, 16K10396, and 17K08225 for S.A.) and "Academic Frontiers" project for private universities: matching funds from MEXT, and the Tokyo University of Science fund for strategic research areas. We wish to acknowledge Prof. Ryo Abe, Prof. Masato Kubo, and Prof. Hiroyasu Esumi (Research Institute for Biomedical Science, Tokyo University of Science), Prof. Masanori Hayase (Faculty of Science and Technology, Tokyo University of Science), Dr. Masahiro Motosuke (Faculty of Engineering, Tokyo University of Science), Dr. Tomohiro Osaki and Dr. Norhiko Itoh (Faculty of Agriculture, Tottori University) for their helpful discussions.

6. References

[1] Cristofanilli, M., Budd, G. T., Ellis, M. J., Stopeck, A., Matera, J., Miller, M. C., Reuben, J. M., Doyle, G. V., Allard, W. J., Terstappen, L. W. M. M., Hayes, D. F. (2004) Circulating tumor cells, disease progression, and survival in metastatic breast cancer. *New Engl. J. Med.* 35, 781-791, doi: 10.1056/NEJMoa040766

[2] MoCellin, S., Hoon, D., Ambrosi, A., Nitti, D., Rossi, C. R. (2006) The prognostic value of circulating tumor cells in patients with melanoma. *Clin. Cancer Res.* 12, 4605-4613. doi: 10.1158/1078-0432.CCR-06-0823

[3] Parkinson, D. R.; Dracopoli, N.; Petty, B. G.; Compton, C.; Cristofanilli, M.; Deisserogh, A.; Hayes, D. F.; Kapke, G.; Kumar, P.; Lee, J. S. H.; McCormack, R.; Mikulski, S.; Nagahara, L.; Pantel, K.; Pearson-White, S.; Punnoose, E. A.; Roadcap, L. T.; Schade, A. E.; Scher, H. I.; Sigman, C. C.; Kelloff, G. J. (2012) Considerations in the development of circulating tumor cell technology for clinical use. J. Translat. Med. 10, 138.

[4] Okano, H., Suyama, K., Suzuki, T., Suzuki, T., Ariyasu, S., Aoki, S., Abe, R., Hayase, M. (2015) Enrichment of circulating tumor cells in tumor-bearing mouse blood by a deterministic lateral displacement microfluidic device. Biomed. Microdev., 17, 59 (11 pages). doi: 10.1007/s10544-015-9964-7.

[5] Lustberg, M.; Jatana, K. R.; Zborowski, M.; Chalmers, J. (2012) Emerging technologies for CTC detection based on depletion of normal cells. Recent results. Cancer Res. 195, 97-110.

[5] Ariyasu, S., Hanaya, K., Watanabe, E., Suzuki, T., Horie, K., Hayase, M., Abe, R., Aoki, S. (2012) The selective capture an collection of live target cells using a silicon wafer device modified with antibodies via a photocleavable linker. Langmuir, 28, 13118-13126. dOI: 10.1021/la302393p.

[6] Shashni, B.; Matsuura, H., Ariyasu, S., Takeda, R., Suzuki, T., Shiina, S., Akimoto K., Maeda, T., Aikawa, N., Abe, R., Osaki, T., Itoh, N., Aoki, S. (2018) Size-based differentiation of cancer and normal cells by a particle size analyzer assisted by a cell-recognition PC software. Biol. Pharm. Bull. 41, 487-503. doi: org/10.1248/bpb.b17-00776.

[7] Shashni, B., Matsuura, H., Saito, R., Hirata, T., Ariyasu, S., Nomura, K., Takemura, H., Akimoto, K., Aikawa, N., Yasumori A., Aoki, S. (2019) Simple and convenient method for the isolation, culture, and re-collection of cancer cells from blood by using glass-bead filters. ACS Biomaterials Sci. Eng, 5, 438-452. doi: 10.1021/acsbiomaterials.8b01335.

International Conference on Cancer Research 2019

Website: www.CancerConf.org

June 10-11, London, UK



Flavonoids Effects on Breast Cancer Tumors

Sina moradi yeganmahale[a *],farahnaz Mohammadi Arab abadi[b], Mohammadhossin Abdoli[c] Mohammed hosseini goke[ab]

[a]Department of Educational Sciences, Faculty of Imam Ali, Farhangian University, Rasht Iran

[b] Department of Radiology, Faculty of Paramedicine, Iran University of Medical Sciences, Tehran, Iran

[c] Department of Educational Sciences, Faculty of Imam Ali, Farhangian University, Rasht, Iran

[ab] Department of Educational Sciences, Faculty of Imam Ali, Farhangian University, Rasht, Iran

* *Corresponding author: sinamoradi98888@gmail.com*

Abstract:

Background: Breast cancer is one of the main causes of cancer deaths and the most common malignancy in women worldwide. Breast cancer accounts for 7% of total cancer deaths. There is a direct relationship between diet and cancer. One way to improve nutrition is good. Flavonoids Polyphenol compounds are found in some fruits, vegetables, seeds. This study examines the effects of flavonoids on breast cancer tumors.

Methods: This study was performed on 16 breeds of mice (Balb / c nu). First, the rats were divided into two groups: A and B; in the food group A, flavonoids were used, but in group B, these compounds were not used. Breast Cancer Tumor: 4t1 cancer cells were injected into 5 rabbits (balb / c) after culture. Following the appropriate size of the tumor, ethical standards were removed from the body of the mice. After 4 weeks, breast cancer tumors were cultured in groups A and B mice. Then, every 5 days, a mouse from each group was selected to examine tumor volume and lymphocyte proliferation.

Results: The results of 40-day studies showed that tumor volume in 8 mice in group A was less than group B ($P < 0.05$). Likewise lymphocyte proliferation in The spleens of the micea in group A were significantly more than group B($p<0.05$)

Conclusion: Nutrition is one of the most effective ways of preventing and preventing the spread of disease in the body, especially cancer. Flavonoids are found in some fruits, such as apples, pomegranates and red grapes, and are found in vegetables such as broccoli, celery and tomatoes in the brain such as walnuts and drinks such as green tea. Due to its antioxidant properties, flavonoids increase cellular immunity and increase the production of lymphocytes and strengthen the immune system. As seen in this study, the use of flavonoids in group A increases cellular immunity. By inducing breast cancer in the rat body, the expansion of the lymphocyte in group A was greater than that of group B, which the ability to cope with the tumor and reduced tumor volume. Based on the results, flavonoids play a major role in boosting the immune system so that they can be used for cancer drugs and cellular immunity. It is recommended that flavonoids are used daily to increase the immune system's strength against many diseases, including breast cancer.

Keywords: Flavonoids, Breast Cancer, Nutrition, Prevention.

Introduction:

Breast cancer is the most common cancer and also the primary cause of mortality due to cancer in female around the World. About 1.38 million new breast Cancer cases were diagnosed in 2008 with almost 50% of all breast cancer patients and approximately 60% of deaths occurring in developing countries. There is a huge diference in breast cancer survival rates worldwide, with an estimated 5-year survival of 80% in developed countries to below 40% for developing countries[1]. Only 5 to 10 % of all types of cancer are basically caused by inborn cancer predisposition such as the so-called familial breast cancer subtype know to be related to the BRCA1 and BRCA2 mutations. In contrast, the absolute majority of all cancer types carries a sporadic character based on modifiable risk factors[2]. modifiable risk factors play a central role in cancer prevention. Contextually, it has been estimated that almost one-third part of all cancers could be avoided through appropriate dietary habits and supplements[3,4]. Abundant evidence has been collected for beneficial effects of flavonoids compounds affecting a number of cancer-related pathways and can slow down the carcinogenic process by suppressing survival and proliferation of tumor cells as well as diminish invasiveness and angiogenesis of tumors. Some of them can stimulate detoxifying carcinogens and eliminating them from the body[5,6]more than 5000 flavonoids have been identified and are distributed in a wide range of plants. On the basis of their chemical structures, these flavonoids have been grouped into 10 categories, 6 of which including flavones, flavanones, anthocyanidins, flavonols, isoflavones, and catechins are commonly present in the human diet. Many

of these flavonoids possess documented anticancer activity both in animal and cellular model systems[7]. Flavonoids are natural substances that are widely used in many plant species. Especially in fruits and vegetables, such as celery, cherry, pepper, carrots, onion leaves, broccoli and parsley[8,9].Therefore, flavonoids are important antioxidants that have potent anticancer effpals[10]. The purpose of this paper is to increase the awareness of human societies about the impact of nutrition in preventing breast cancer and to help research institutes to produce drugs for the prevention and treatment of breast cancer using natural substances such as flavonoids .

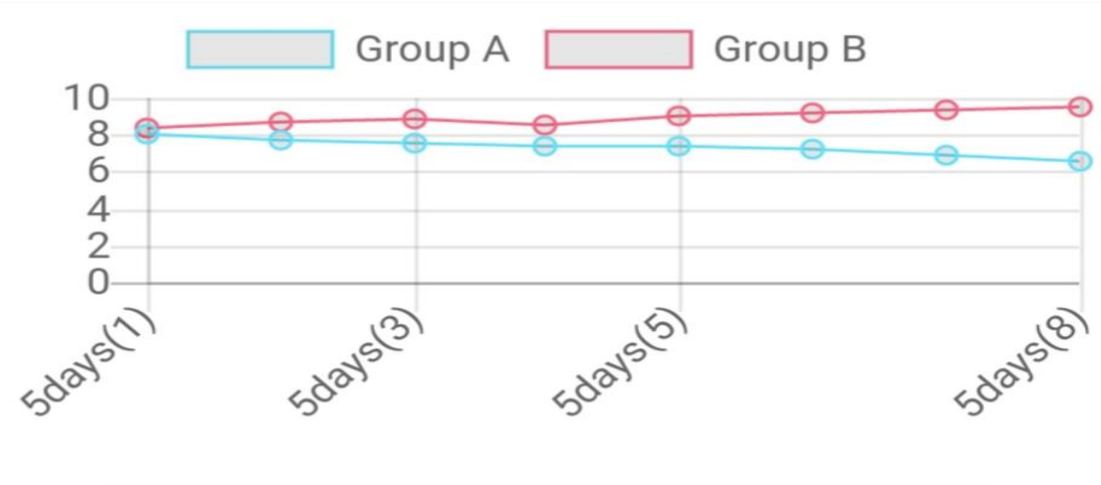
Methods :

This research studies the effects of flavonoid in fruits and vegetables on breast cancer . Healthy mice 16 (femal) (race balb/c) (Ten days passed from their birth) . were purchased from the Pasteur Institute of Iran. And divided into two groups A and B . In group A, foods made with apples, soybeans, beans, celery, carrots (made from flavonoids), but not in group B, were used.

Create a cancerous tumor : Breast cancer cells 4t1 race (balb / c) were purchased from the Pasteur Institute of Iran . The cells were cultured in (Dhg , dmem high cells were injected into the right chest of 7 mice (balb / glucose) medium. 6,000,000 c) . After suitable size of the tumor Following the appropriate size of the tumor, the body of mice was exited in accordance with ethical standards . Tumor graft:4 weeks after start feeding group A and B The 2 × 2 × 2 mm tumor was implanted to the right of the Under the skin mice. Two weeks after transplantation, every 5 days, a mice from each group was used to measure tumor volume and proliferating the spleen lymphocyte through the test (MTT (3-(4,5-Dimethylthiazol-2-yl)-2,5-Diphenyltetrazolium Bromide)) . Data analysis was performed using SPSS software version 19 with 95% confidence interval and p <0/05 as a meaningful level.

Results :

After a few weeks of using flavonoids, tumor growth was significantly lower in group A than in group B (p<0/05) (Fig. 1). Lymphocyte proliferation in the spleen: The rate of lymphocyte proliferation in group A mice was significantly higher than those in group B mice (p<0/05) (Fig,2) .



(Fig.1) Increased tumor volume in groups A and B, which has significant changes. During 40 days, 16 mice were examined (p<0/05) .



. (Fig.2): Stimulation of lymphocytes in the spleen was higher in group A than in group B.(p<0/05).

Conclusion:

Diet and nutrition have been considered as an effective preventive strategy for cancer. A bunch of dietary natural products have shown a potential role in prevention and treatment of cancers.[11,12,13]. . Fruits, vegetables, cereals, teas, essential oils, various beverages, or food products that are derived from them contain natural antioxidants and chemopreventive agents, such as popolyphens or flavonoids .[14]. Flavonoids reduce inflammation and cancer recurrence by (a) acting as an antioxidant or increasing antioxidant gene or protein expression;(b) decreasing cancer cell proliferation; (c) blocking pro-inflammatory cytokines or endotoxin-mediated kinases and transcription factors involved in cancer progression; (d) increasing histone deacetylase activity; or (e) activating transcription factors that antagonize chronic inflammation.[15,16].

One of the ways to prevent and treat breast cancer is proper nutrition. The use of natural ingredients like fruits and vegetables reduces weight, fat and, most importantly, reduces estrogen and progesterone. One of the natural ingredients that is effective in preventing and treating breast cancer is flavonoids .

Reference:

[1] Coleman, M . Quaresma,M. Berrino, F. Lutz ,JM. Angelis, R . Capocaccia ,R .(2008). Cancer survival in fve continents: a worldwide population-based study (CONCORD). Lancet Oncol, 9,730–56.doi : 10.1016/S1470-2045(08)70179-7.

[2] Golubnitschaja ,O.(2007). Cell cycle checkpoints: the role and evaluation for early diagnosis of senescence, cardiovascular, cancer, and neurodegenerative diseases. Amino Acids, 32,359–71. doi:10.1007/s00726-006.

[3] liu ,RH.(2013). Dietary bioactive compounds and their health implications. J FoodSci, 78,18–28.doi:10.1111/1750-3841.12101.

[4] magalova, T.(1999) Nutrition and female breast tumors. Bratisl Lek Listy. 100 : 14_503. (Pmid:10645042).

[5] Tanaka,T. Sugie, S.(2007). Inhibition of colon carcinogenesis by dietary non-nutritive compounds. J Toxicol Pathol, 20,215–35.

[6] Surh, YJ.(2003). Cancer chemoprevention with dietary phytochemicals. Nat Rev Cancer, 3,768_80 . Doi:10.1038/nrc1189.

[7] Kocic, B. Kitic, D. Brankovic, S.(2013) Dietary flavonoid intake and colorectal cancer risk : evidence from human population studies, J. Buon 1 , 34–43 .

[8] Chen, Z. Kong, S. Song, F. Li, L. Jiang, H. (2012). Pharmacokinetic study of luteolin, apigenin, chrysoeriol and diosmetin after oral administration of Flos Chrysanthemi extract in rats, Fitoterapia ,83, 1616–1622 .doi:10.1016/j.fitote.2012.09.011 .

[9] Lim, S.H. Jung, S.K. Byun, s. Lee, E.J. Hwang,J.A . Seo, S.G. (2013). Luteolin suppressesUVB- induced photoageing by targeting JNK1 and p90 RSK2, J. Cell. Mol. Med.17, 672_680 . DOI: 10.1111 / jcmm.12050 .

[10] Devi, K.P. Rajavel, T. Nabavi, S.F. Setzer, W.N. Ahmadi, A. Mansouri, K. Nabavi, S.M.(2015) . Hesperidin: a promising anticancer agent from nature, Ind. Crops Prod ,76, 582–589. doi:10.1016/j.indcrop.2015.07.051 .

[11] Zheng, J.; Zhou, Y.; Li, Y.; Xu, D.P.; Li, S.; Li, H.B.(2016) Spices for prevention and treatment of cancers. Nutrients,8,495. DOI: 10.3390/nu8080495.

[12] Zhou, Y.; Zheng, J.; Li, Y.; Xu, D.P.; Li, S.; Chen, Y.M.; Li, H.B. (2016).Natural polyphenols for prevention and treatment of cancer. Nutrients ,8,515. DOI: 10.3390/nu8080515 .

[13] Li, F. Li, S.Li, H.B. Deng, G.F. Ling, W.H. Xu, X.R.(2013). Antiproliferative activities of tea and herbal infusions. Food Funct,4 ,530–538. DOI: 10.1039/c2fo30252g .

[14] Kris-Etherton,PM . Lefevre,M . Beecher,GR .Gross,MD.Keen,CL . Etherton,TD .(2004).Bioactive compounds in nutrition and health-research methodologies for establishing biological function: the antioxidant and anti-inflammatory effects of flavonoids on atherosclerosis . Annu Rev Nutr ,24 ,511 – 38 . DOI: 10.1146 / annurev.nutr.23.011702.073237.

[15] Damianaki, A. Bakogeorgou, E. Kampa, M. Notas, G. Hatzoglou, A. Panagiotou, S. Gemetzi, C Kouroumalis, E. Martin, P.M. Castanas, E.(2000). Potent inhibitory action of red wine polyphenols on human breast cancer cells. J. Cell. Biochem,78 ,429–441. DOI:10.1002/1097-4644.

[16] Williamson, G.Manach, C.(2005). Bioavailability and bioefficacy of polyphenols in humans. II. Review of 93 intervention studies. Am. J. Clin. Nutr,81, 243–255. DOI: 10.1093 / ajcn / 81.1.243S / 81.1.243S.

International Conference on Cancer Research 2019

Website: www.CancerConf.org

June 10-11, London, UK



Safety and Quality of Life in the Treatment of Non-Metastasic Colorectal Cancer patients: 5-Fluorouracil versus Capecitabine

Sánchez-Gudín, J.[a]; Martín-Sabroso, C.[b]; Fernández-Carballido, A.M.[b]; Barreda-Hernández, D.[a]; Torres-Suárez, A.I.[b*]

[a]*Hospital Pharmacy Department. Virgen de la Luz Hospital, Hermandad de Donantes de Sangre, 16002, Cuenca (Spain)*

[b]*Department of Pharmaceutics and Food Technology, Complutense University, 28040 Madrid (Spain)*

**Corresponding author: galaaaa@farm.ucm.es*

Abstract

Colorectal cancer (CRC) is the most frequent neoplasm of the digestive system and the third most frequent tumour worldwide. In stages I and II the treatment is only surgical and, in high-risk stages II and stages III surgery is complemented with adjuvant chemotherapy. Traditional adjuvant therapy consists of 5-fluorouracil, in combination with leucovorin, and oxaliplatin (FOLFOX regimen, all for iv administration). Alternatively 5-fluorouracil can be substituted by capecitabine, precursor of 5-fluorouracil, which has the advantage that it is administered orally (XELOX regimen). Both regimes are considered interchangeable.

The aim of this study is to compare these regimens (FOLFOX and XELOX) in terms of safety and quality of life (QoL) in patients diagnosed with stage II and III non-metastatic CRC.

For this purpose, a descriptive prospective study with patients diagnosed with stage II and III non-metastatic CRC in adjuvant treatment with FOLFOX and XELOX schemes was carried out. The appearance of symptomatic, haematological and hepatic adverse events (AE) during the treatment was established by evaluating their clinical and pharmacotherapeutic history. The severity of the AE was established following the Common Terminology Criteria for Adverse Events (CTCAE v.4.03). To evaluate the QoL, the QoL EORTC QLQ-C30 version 3.0 questionnaire was given to patients at the beginning and the middle of the adjuvant treatment. The statistical analysis of the data was carried out with the SPSS®15.0 program.

33 patients were finally included in the study. All the patients treated with FOLFOX and with XELOX presented some of the AE studied. The most frequent AE for both groups were neurotoxicity, diarrhoea, constipation and thrombocytopenia, but only statistically significant difference was found in case of palmar-plantar erythrodysesthesia síndrome (PPE), and more frequent in patients treated with XELOX.

According to QoL, patients with FOLFOX presented a worsening in terms of daily activities, constipation and insomnia while in those treated with XELOX a worsening in daily activities, constipation, fatigue, nausea, vomiting, anorexia and diarrhoea was observed. Only statistically significant difference was found in the emotional role item at the middle of the treatment, at which point, patients treated with FOLFOX were better emotionally than those treated with XELOX.

As conclusion, both schemes seem to be safe, although differences in PPE (more frequent with XELOX) and emotional role (better with FOLFOX) were found. However, it should be taken into account that patients treated with FOLFOX presented higher frequency of haematological AE, which are difficult to perceive. In contrast, patients treated with XELOX had higher frequency of symptomatic AE, which probably leads to this slightly worse QoL.

Keywords:

Colorectal Cancer,

Safety,

Quality Of Life,

5-Fluorouracil,

Capecitabine.

1. Introduction

Colorectal cancer (CRC) is the most frequent neoplasm of the digestive system and the third most frequent tumor worldwide, with approximately one million people diagnosed annually [1]. It is also the fourth cause of death, after lung cancer, liver cancer and stomach cancer [2]. The incidence of CRC shows a marked geographical variation, being Central Africa the region with the lowest incidence rate (2.3 patients per 100,000 population) and Japan the region with the highest rate (49.3 patients per 100,000 population). This demographic variation is conditioned by the economic development of the country, with two-thirds of all CRCs diagnosed in developed countries [3].

More than 90-95% of these neoplasms seem to be sporadic [3] and only 5-10% seems to have a hereditary component. After CRC diagnosis, the best possible treatment is stablished acoording to the disease stage. The most used staging system is the TNM system of the American Joint Committee [4]. In stage 0 or carcinoma in situ, the tumor cells are located in the most superficial part of the mucosa, without grown beyond the mucosa. In stage I, the tumor affects the wall of the colon or rectum without passing through the muscle layer. In stage II, the tumor has infiltrated all the layers of the wall of the colon or rectum, being able to invade the surrounding organs. In stage III the tumor has invaded the nearest organs and affects the lymph nodes and in stage IV the tumor has spread to affect organs distant from the colon or rectum such as liver, lung, ovary or non-regional ganglion.

In stages I and II the treatment is only surgical and, in high-risk stages II and stages III surgery is complemented with adjuvant chemotherapy. Traditional adjuvant chemotherapy in these stages is based on the administration of 5-fluorouracil (5-FU) intravenously in monotherapy or in combination with another chemotherapeutic, also intravenously, such as oxaliplatin (FOLFOX regimen). The development of capecitabine, 5-FU precursor of oral administration [5], extended the therapeutic possibilities, since it is used orally as monotherapy or in combination with intravenous administration of oxaliplatin (XELOX regimen).

In the case of metastatic CRC (mCRC), the general therapeutic strategy depends on whether the metastatic disease is resectable or is only susceptible to palliative treatment. If the first case, the priority of the first-line treatment is the immediate control of the disease before the surgery, in order to reduce the related symptoms, to stabilize quickly the progression of the disease and to reduce the metastases. Currently, the regimens used as first-line treatment are FOLFOX, XELOX or FOLFIRI (combination of 5-FU with irinotecan) plus bevacizumab (recombinant humanized monoclonal antibody that binds and neutralizes vascular endothelial growth factor [VEGF]), without having found differences in long-term survival (LTS) or OS among the different combinations [6,7].

Several clinical trials have analized the safety and efficacy of these adjuvant therapies. In the case of capecitabine and 5-FU as monotherapy, numerous studies have shown that capecitabine is an alternative at least as effective and well tolerated as 5-FU in patients with stage III CRC [7,8], so that intravenous 5-FU can be replaced by capecitabine with the advantage of its oral administration.

When monotherapy was compared to combination therapy, an improvement in efficacy was observed, in general, when 5-FU or capecitabine were combined with oxaliplatin (FOLFOX and XELOX regimens respectively) [9]. For example, the MOSAIC study [10,11], which compares adjuvant treatment with 5-FU monotherapy and the treatment of 5-FU in combination with oxaliplatin, showed an increase in the 5-year LTS rate (from 67.4% to 73.3%) and the 6-year OS rate (from 76.0% to 78.5%) in the patients treated with FOLFOX regimen.

In the same way, the association of capecitabine and oxaliplatin (XELOX regimen) also improved survival when compared to the administration of 5-FU/leucovorin (5-FU/LV) monotherapy (leucovorin increases the effect of 5-fluorouracil by inhibiting thymidylate synthase) , data that are concluded from the XELOXA study [12,13], where the 3-year LTS rate was 70.9% for patients treated with the XELOX regimen and 66.5% for those treated with 5-FU/LV, and the 5-year OS rate was 77.6% for the XELOX group vs 74.2% for the 5-FU/LV group.

The duration of adjuvant chemotherapy should be 6 months, although the important cumulative neurotoxicity of oxaliplatin sometimes requires not to complete the treatment. In general, the benefits of the addition of oxaliplatin are less clear when the risk of recurrence is low or in case of high risk patients (associated comorbidities, elderly). In these patients the alternative treatment could be 5-FU or capecitabine in monotherapy [5].

FOLFOX and XELOX regimens are comparables in terms of efficacy. Regarding the toxicity profile of both regimens, it is worth mentioning the study carried out by Schmoll et al [14,15] in which the FOLFOX regimen is compared with XELOX regimen in patients with mCRC and CRC in state III. It was observed that, as in efficacy, both regimens haved a similar safety profile, although there were differences in terms of rates and severity of adverse reactions (AR). On the one hand, patients treated with the FOLFOX regimen showed, in general, more grade 3-4 AR (45% versus 36%) and more grade 3-4 AR associated with oxaliplatin, such as neurotoxicity (8% versus 6%), neutropenia (24% versus 5%) and febrile neutropenia (2% versus <1%). Similar results were already perceived in

previous studies where patients diagnosed with mCRC were analyzed [16]. On the other hand, patients treated with the XELOX regimen presented a higher frequency of grade 3-4 gastrointestinal disorders, such as diarrhea (15% versus 12%), vomiting or nausea (7% versus 5%) and palmar-plantar erythrodysesthesia (PPE) (12% versus <1%) [16].

Currently, in most of the countries FOLFOX and XELOX therapeutic schemes are considered, in general, interchangeable [17,18]. However, it is important when choosing a chemotherapeutic scheme over another, to take into account not only the efficacy and the adverse reactions associated with each scheme but also the quality of life (QoL) of the patients.

The measurement of the QoL is not easy, because it is conditioned, to a certain extent, by the subjectivity in the "perception of the disease" that each patient has. For this reason, questionnaires and scales are used trying to reflect as accurately as possible the impact of the disease and its treatment on this QoL and so standardize its evaluation. There are few clinical studies that include the evaluation of the QoL of patients with CRC. Commella P et al. [19] compared the QoL of patients diagnosed with mCRC in treatment with FOLFOX and XELOX regimens, by using of the European Organization for Research and Treatment of Cancer Quality of Life Questionnaire (EORTC QLQC30 version 3.0) at the beginning of the treatment and after 8 week, and differences in QoL between both groups were not found. Seymour MT et al. [20] also evaluated with the EORTC QLQ-C30 questionnaire the QoL of patients with mCRC in treatment with capecitabine or 5-FU with or without oxaliplatin. The questionnaire was completed at the beginning of treatment and at week 12, concluding that there were no differences in terms of QoL between both groups. Conroy T et al [21] obtained the same result.

Most of the comparative studies evaluating the safety and quality of life of chemotherapy schemes have focused on patients with mCRC, while there are almost no studies with patients diagnosed with stage II and stage III CRC.

The objective of this study is to evaluate whether the substitution of 5-FU, of intravenous administration, by capecitabine, of oral administration, in combination chemotherapy with oxaliplatin (FOLFOX and XELOX schemes) modifies the safety profile of the treatment and the quality of life (QoL) of patients diagnosed with stage II and III non-metastatic CRC.

2. Methods

2.1 Patients

A prospective descriptive study of patients diagnosed with stage II and III non-metastatic CRC, under adjuvant treatment with the FOLFOX-6 and XELOX regimens, was carried out. The study was conducted in the Hospital Virgen de la Luz (Cuenca, Spain) for 24 months (October 2015-October 2017) and included patients who during this period began and ended the adjuvant treatment, that is, they completed the 24 weeks of adjuvant treatment. The study was authorized by the Ethics Committee for Clinical Research of the region (Ref. 2015/PI1115).

All patients signed their consent to participate in the study after being informed of the objectives of the study.

2.2 Treatments

The patients were divided into two groups according to the chemotherapeutic regimen they followed [22,23]:

- FOLFOX: treated wih the FOLFOX-6 regimen, which consists of an initial intravenous administration of oxaliplatin (85 mg/m^2), leucovorin (400 mg/m^2) and 5-FU (400 mg/m^2) on the first day of the cycle, following of a continuous infusion for two days of 5-FU (1200 mg/m^2/day). All this repeated every two weeks until completing a total of 24 weeks (12 total cycles).

- XELOX: treated with the XELOX regimen, which consists of a dose of intravenous oxaliplatin (130 mg/m^2) on the first day of the cycle, and capecitabine orally administered twice a day (2,000 mg/m^2 daily) for 14 days since the first day of the cycle. All this repeated every three weeks for a total of 24 weeks (8 total cycles).

2.3 Control variables

Demographic data (age and gender), data related to the disease (location, stage and ECOG (scale developed by the Eastern Cooperative Oncology Group with the objective of measuring the functional repercussion of the oncology disease in the patient as a criterion for progression)) and data related to the treatment (existence or not of previous chemoradiation, number of cycles received, time from diagnosis to start of treatment, starting dose, reduction or not of

the dose during the treatment and reason for dose reduction or suspension, if any), were collected in all the patients finally included in the study.

2.4 Response variables

- Safety: The ARs were divided into:

  - Symptomatic ARs: diarrhea and/or constipation, nausea and/or vomiting, mucositis, PPE and neurotoxicity;
  - Haematological alterations: anemia, thrombocytopenia, lymphopenia, neutropenia;
  - Liver disorders: increase in total bilirubin and hypertransaminemia (increases in glutamic-oxalacetic transaminase (GOT) or aspartate aminotransferase, increases in glutamic-pyrubic transaminase (GPT) or alanine aminotransferase and increases in gamma glutamyl transpeptidase (GGT)).

  The severity of the ARs was established following the Common Terminology Criteria for Adverse Events (CTCAE v.4.03), except for liver disorders. These do not come stamped in this document and only the presence or absence of these alterations was analyzed, establishing the limit values according to those indicated by the Clinical Analysis Laboratory of the Hospital in which the study was conducted.

- Quality of life: it was evaluated from the EORTC QLQ-C30 questionnaire that consists of 30 questions divided into 3 scales:

  - Functional scale: physical function (questions 1 to 5), daily activities (questions 6 and 7), emotional role (questions 21 to 24), cognitive function (questions 20 and 25) and social function (questions 26 and 27).
  - Symptomatic scale: fatigue (questions 10, 12 and 18), pain (questions 9 and 19), nausea/vomiting (questions 14 and 15), dyspnea (question 8), insomnia (question 11), anorexia (question 13), constipation (question 16); diarrhea (question 17) and economic impact (question 28).
  - Global health status scale (questions 29 and 30).

2.5 Data collection

- Safety: The appearance of AR during the treatment was established through the review, for each patient, of the computerized clinical history (Mambrino XXI®), the pharmacotherapeutic history of the Farmatools-Dominion® External Patients module and the pharmacotherapeutic history of the Farhos Oncología®v.5.0 computer program. The data collection was carried out in an Excel database and another Access database. The management and maintenance of all the information guaranteed the rights of privacy and protection of personal data in accordance with current legislation on Protection of Personal Data [24].

- Quality of life: Patients completed the QoL questionnaire EORTC QLQ-C30 version 3.0 [25,26] at the beginning and half of the adjuvant treatment (in cycle 7 for patients treated with the FOLFOX regimen and in cycle 5 for those treated with XELOX).

2.6 Data Analysis

The statistical analysis of the data was carried out with the SPSS®15.0 program. (Windows® version). A descriptive analysis of the continuous or numerical variables was performed using measures of central tendency (mean and median) and dispersion (range), and absolute or relative frequencies were used for the categorical or qualitative variables. In the bivariate analysis, the relationship between the independent categorical variable (chemotherapeutic regimen administered) and the dependent variable was studied using the chi-square test (FISHER) in the case of the appearance or absence of any of the ARs studied. A level of significance of 0.05 was established.

For the analysis of the EORTC QLQ-C30 questionnaire, values of 1 and 2 (1: no, 2: yes) were assigned for questions 1 through 7; values between 1 and 4 for questions from 8 to 28 (1: nothing, 2: a little, 3: quite a bit, 4: a lot); and only in items 29 and 30 were evaluated with scores of 1 to 7 (1: extremely bad, 2: very bad, 3: bad, 4: fair, 5: good, 6: very good, 7: extremely good). The raw scores were obtained as the average of the items that contribute to the scale. The raw scores were standardized according equations 1, 2 and 3 obtaining a score between 0 and 100 (figure 1); so that higher values in the scale of global health status and functional scale indicated a better QoL and higher values in the symptomatic scale indicated a worse QoL [27].

Intra-group (at the beginning and half of the treatment) and inter-group (each therapeutic scheme) analysis of the scores were done. Changes on a scale from 5 to 10 points at the beginning and half of the adjuvant treatment were considered "small change", from 10 to 20 points were "moderate change" and greater than 20 points were "hight change". Only chages greater than 10 points were considered clinically relevant [28]. The comparison of means of a quantitative variable with a qualitative dichotomous one was carried out with the T test for independent samples. P <0.05 was considered statistically significant.

Equation 1	Functional scale	$S = \{1 - \frac{(RS-1)}{Range}\} * 100$
Equation 2	Symptomatic scale	$S = \{\frac{(RS-1)}{Range}\} * 100$
Equation 3	Global health status scale	$S = \{\frac{(RS-1)}{Range}\} * 100$

where RS is the raw score for each scale and Range is the difference between the maximum possible value of RS and the minimum possible.

Figure 1. Equations used for the standardization of the raw scores.

3. Results

3.1 Control variables

A total of 33 patients were finally included in the study, with an average age of 61 years (range: 21-76) and male predominance (24 patients, 73%). Regarding the data related to the disease, 17 (52%) patients presented colonic localization compared to 16 (48%) that presented rectal localization, and with respect to the stage of the disease, the majority of patients were classified as stage 3 (76%) and all patients (100%) had ECOG less than or equal to 2. The characteristics of the patients according to their demographic data and related to the disease are listed in Table 1. There were no statistically significant differences in the distribution of the patients between the two regimes when these variables were compared.

Table 1. Demographic data and disease data of the patients included in the study.

	FOLFOX regimen (n=12) N (%)	**XELOX regimen (n=21) N (%)**	**p value**
Age (years)			
Average (range)	61 (38-70)	62 (21-76)	p = 0.600
Gender			
Man	10 (83%)	14 (67%)	p = 0.289
Woman	2 (17%)	7 (33%)	
Desease location			
Rectal	7 (58%)	9 (43%)	p = 0.392
Colonic	5 (42%)	12 (27%)	
Desease stage			
II	3 (25%)	5 (24%)	p = 0.939
III	9 (75%)	16 (76%)	

Regarding the data related with the treatment, 21 patients (64%) received the XELOX regimen while 12 patients (36%) were treated with FOLFOX regimen. 12 patients, all of them diagnosed with rectal carcinoma, received previous chemoradiation (36%; 5 treated with FOLFOX and 7 treated with XELOX), and 6 of them received a lower number of cycles than the rest (1 patient received 10 cycles of FOLFOX and 5 patients received 6 cycles of XELOX). The average time period from diagnosis to the start of adjuvant treatment was 3 months (range: 1-7). The starting doses were all in agreement with that indicated in the data sheet with the exception of 4 patients (12%) who started the adjuvant treatment with reduced doses due to their bad general state. Regarding dose reduction or treatment suspension in the first half of adjuvant therapy (between cycles 1 and 7 for patients treated with FOLFOX and between cycles 1 and 5 for those treated with XELOX), 13 (39%) patients reduced the dose and 3 (9%) patients discontinued the oxaliplatin treatment, whereas that 11 (33%) patients reduced the dose of fluoropyrimidines, all due to AR. At the end of the adjuvant treatment (after 24 weeks of treatment), 15 (45%) patients had reduced the dose and 13 (39%) patients had discontinued the treatment with oxaliplatin, while 15 (45%) patients had reduced the dose and 7 patients (21%) had discontinued treatment of fluoropyrimidines. The data related to the treatment are shown in Table 2 and only statistically significant differences between chemotherapeutic regimes were found in the dose of oxaliplatin at the end of the treatment.

Table 2. Control variables related to treatment according to the received chemotherapeutic regimen. *statistically significant differences p<0.05.

	FOLFOX regimen (n=12) N (%)	XELOX regimen (n=21) N (%)	p value
Previous chemo-radiotherapy			
Yes	5 (42%)	7 (33%)	p = 0.633
Not	7 (58%)	14 (67%)	
Number of cycles received			
Average (range)	12 (10-12)	8 (6-8)	p = 0.105
Time from diagnosis to start of treatment (months)			
Average (range)	3 (1-7)	3 (1-6)	p = 0.431
Starting dose			
Complete	11 (92%)	18 (86%)	p = 0.605
Reduced	1 (8%)	3 (14%)	
Oxaliplatin dose in the middle of the treatment			
Complete	5 (42%)	12 (57%)	p=0.094
Reduced	7 (58%)	6 (29%)	
Suspended	-	3 (14%)	
Fluoropyrimidine dose in the middle of the treatment			
Complete	7 (58%)	15 (71%)	P = 0.446
Reduced	5 (42%)	6 (29%)	
Suspended	-	-	
Oxaliplatin dose at the end of treatment			
Complete	-	5 (24%)	p = 0.039*
Reduced	8 (67%)	7 (33%)	
Suspended	4 (33%)	9 (43%)	
Fluoropyrimidine dose at the end of treatment			
Complete	3 (25%)	8 (38%)	p = 0.734
Reduced	6 (50%)	9 (43%)	
Suspended	3 (25%)	4 (19%)	

3.2 Safety

When analyzing the appearance of AR according to the chemotherapeutic scheme administered, it was observed that 100% of the patients treated with FOLFOX regimen or with XELOX regimen presented some of the AR studied. The number of patients with grade 1-2 toxicity was 58% for the FOLFOX group and 81% for the XELOX group; and 42% and 19% patients with grade 3-4, respectively.

- Symptomatic ARs: The most frequent symptomatic ARs for both groups, FOLFOX or XELOX regimens, were neurotoxicity and diarrhea and/or constipation. In the group treated with the FOLFOX regimen, 100% of patients presented neurotoxicity, 83% of patients had diarrhea and/or constipation, 42% of patients had nausea and/or vomiting, 16% of patients mucositis and 8% of patient PPE. Regarding the group treated with the XELOX regimen, 90% of patients presented neurotoxicity, 67% of patients had diarrhea and/or constipation, 57% of patients nausea and/or vomiting, 38% of patients had PPE, and 28% of patients mucositis. The incidence of the symptomatic AR according to the chemotherapeutic regimen administered is shown in Figure 2a, finding statistically significant differences exclusively in the appearance of PPE, with a higher incidence in the group treated with the XELOX regimen. As can be seen in Figure 2g in the FOLFOX group all symptomatic ARs were grade 1-2 except for 8% of patient who presented mucositis grade 3 and other 8% that presented neurotoxicity also grade 3. For patients treated with the XELOX regimen, all these ARs were grade 1-2.

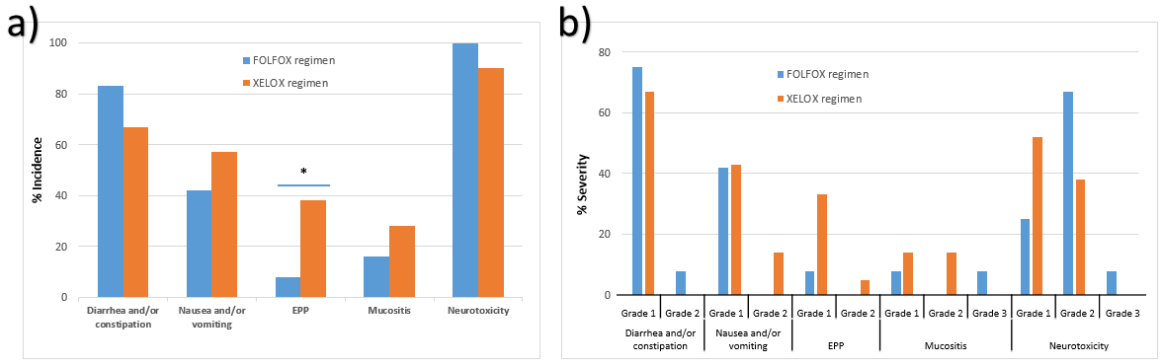


Figure 2. Frequency (2a) and severity (2b) of symptomatic AR according to the type of chemotherapeutic regimen administered. *statistically significant differences p<0.05.

- Haematological ARs: The most frequent hematologic AR for patients with both treatments was thrombocytopenia, and the less frequent was anemia for the group treated with FOLFOX and neutropenia for the group treated with XELOX. Specifically, in the group of patients treated with FOLFOX, 92% of patients had thrombocytopenia, 66% of patients had lymphopenia, 50% of patients had neutropenia and 33% of patients shown anemia. Regarding the group of patients treated with XELOX, 71% of patients had thrombocytopenia, 43% of patients anemia, 43% of patients lymphopenia and 38% of patients neutropenia. In addition, all anemia and thrombocytopenia were grade 1-2 for both treatments, and only lymphopenia and neutropenia (in the XELOX group) appeared in grade 3. The incidence and severity of the hematological AR depending on the drug administered are shown in Figure 3a and 3b. These differences between treatments were not statistically significant.

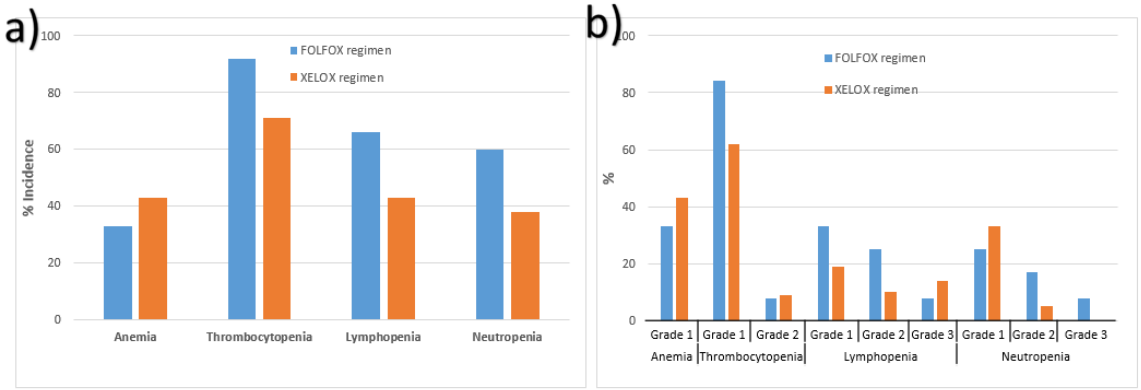


Figure 3. Frequency (3a) and severity (3b) of haematological AR according to the type of chemotherapeutic régimen administered.

- Hepatic ARs: The most frequent hepatic AR for the group treated with FOLFOX was the increase in GPT and for the group treated with XELOX the increase in GOT. Upon further analysis of hepatic ARs, within the group of patients treated with the FOLFOX regimen, in 75% of patients had increased GPT, in 50% of patients increased GOT and in 17% of patients increased GGT. Regarding the group of patients treated with the XELOX regimen, in 62% of patients had increased GOT, in 48% of patients increased GPT and in 14% of patients increased GGT. The incidence of hepatic ARs depending on the drug administered is shown in Figure 4, without finding statistically significant differences in any of the variables analyzed.

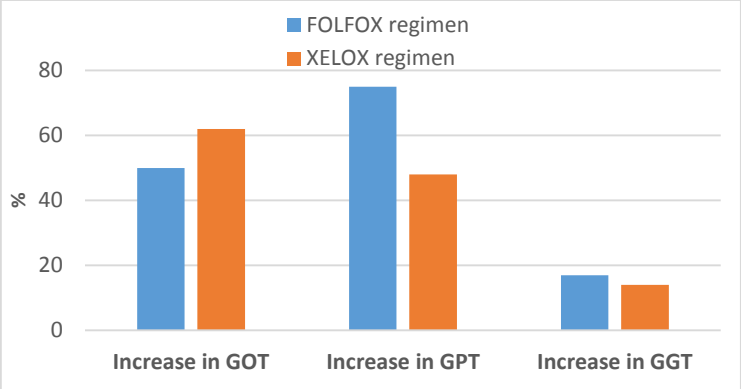


Figure 4. Frequency of hepatic ARs according to the chemotherapeutic regimen administered.

3.3 Quality of life

The results of the analysis of the different items of the questionnaire EORTC QLQ-C30 are shown in table 3. When comparing the scores obtained according to the treatment received, only statistically significant differences were found in the emotional role item (functional scale) at the middle of the treatment: patients treated with FOLFOX regimen exhibited better emotional state than those treated with XELOX.

When the scores obtained at the beginning and at the middle of the treatment are compared, moderate and hight clinically relevant changes are detected in several items. Regarding the daily activities, the patients of both groups presented a clinically relevant worsening, considered in both cases as "moderate".

The symptomatic scale worsened in both groups. Patients treated with FOLFOX presented a clinically relevant worsening in terms of constipation and insomnia throughout the treatment. The worsening of the first symotom was considered as moderate but in case of insomnia was a hight change. When analyzing patients treated with XELOX, a clinically relevant worsening was observed in constipation, fatigue, nausea, vomiting, anorexia and diarrhea throughout the treatment, considering this worsening for all items as "moderate".

Finally, when analyzing the global health scale, no variations were observed during the adjuvant treatment for any of the groups.

Table 3. Scores of the different items of the EORTC QLQ-C30 questionnaire at the beginning and half of the treatment. *statistically significant differences p<0.05.

	FOLFOX regimen		**XELOX regimen**		**p value**
	Mean	**Standard Deviation**	**Mean**	**Standard Deviation**	
Physical function					
Start	93	13.5	89	18.1	p = 0.609
Half of treatment	89	13.7	87	19.1	p = 0.777
Daily activities					
Start	95	15.1	92	18.7	p = 0.618
Half of treatment	82	33.7	79	30.3	p = 0.812
Emotional role					
Start	86	13.4	84	12.5	p = 0.705
Half of treatment	92	10.1	82	14.2	p = 0.036*
Cognitive function					
Start	94	11.2	96	11.9	p=0.569
Half of treatment	92	11.3	93	13.9	p=0.916
Social function					
Start	86	19.5	88	19.2	p=0.855
Half of treatment	85	21.7	85	18.3	p=0.976
Global functional scale					
Start	93	5.9	92	7.3	p=0.732
Half of treatment	93	7.3	90	7.9	p=0.283
Fatigue					
Start	15	17.4	18	20.3	p=0.686
Half of treatment	21	18.2	28	19.1	p=0.345
Pain					
Start	6	8.3	10	17.8	p=0.438
Half of treatment	9	17.2	10	14.8	p=0.819

Nausea/vomiting					
Start	0	0	3	8.8	p=0.104
Half of treatment	5	10.8	13	15.2	p=0.086
Dyspnoea					
Start	0	0	2	7.6	p=0.456
Half of treatment	9	15.4	5	16.7	p=0.550
Insomnia					
Start	2	39	24	34.9	p=0.839
Half of treatment	24	39.7	24	31.2	p=0.979
Anorexia					
Start	12	30.8	10	19.4	p=0.861
Half of treatment	15	31.1	30	24.7	p=0.165
Constipation					
Start	9	15.4	3	10.4	p=0.307
Half of treatment	21	22.4	14	23.1	p=0.420
Diarrhea					
Start	12	27.1	9	18.7	p=0.684
Half of treatment	21	34.2	24	21.8	p=0.753
Economic impact					
Start	18	34.6	14	32	p=0.740
Half of treatment	15	27.4	9	24.4	p=0.511
Global symptomatic scale					
Start	10	9.4	11	10.1	p=0.841
Half of treatment	15	13.6	18	17.1	p=0.468
Global health status					
Start	65	16.2	68	14	p=0.682
Half of treatment	69	15.3	66	16.7	p=0.663

4. Discussion

An study on safety and quality of life is presented, in which two therapeutc schemes, FOLFOX and XELOX, used as adjuvant chemotherapy in patients with CRC in stage II and III, are compared. All medication of FOLFOX scheme is administered intravenously: oxaliplatin and 5-FU+LV on the first day of the cicle, and 5-FU in continuous infusion the next two days, all repeated every two weeks until completing a total of 24 weeks (12 cycles). In XELOX scheme, 5-FU is substituted by capecitabine orally administered twice a day for 14 days, all repeated every three weeks until completing a total of 24 weeks (8 cycles). As previously commented, different clinical trials have evaluated the efficacy, safety and even the QoL of both schemes, but most of them in patients with mCRC. In these studies FOLFOX and XELOX showed an efficacy comparable, and although differences in terms of rates and severity of adverse reactions were detected, neither difference in QoL of the patients was demonstrated. However, there are very few studies performed on patients with stage III CRC and none with patients with stage II CRC. The lower overall deterioration of these patients could reveal differences between both schemes, especially in terms of QoL, due to the substitution of a continuous infusion administration for 2 days every two weeks (5-FU in FOLFOX scheme) by taking two tablets a day for 14 days every 3 weeks (capecitabine in XELOX scheme). The design of our study allows, in addition, to contrast the subjective results obtained with the QoL questionnaire with the objective results of adverse reactions reported in the same group of patients.

Several studies carried out in patients diagnosed with mCRC concluded that this type of patients preferred, in general, oral administration to intravenous administration [29,30], since oral treatment offers greater independence and control over therapy, it is easy to manage, avoid the problems associated with the insertion of venous access, such as infections and extravasations, and all with the same effectiveness. However, other studies showed that the safety profile of chemotherapeutic schemes plays an important role in the patient's preference for one route of administration or another, having little relevance the comfort that the route of administration may involve [31-34].

In our study of safety with stage II and III CRC patientes only statistical significant difference in the frecuency of appearance of PPE was detected, with a greater indicence in patients treated with XELOX. This coincides with other studies, which associate the highest incidence of PPE directly with the use of capecitabine [14,16].

Regarding QoL, it seems that it was better in patients treated with FOLFOX, although the scales of overall functionality and overall health status did not improve or worsen for both groups throughout the treatment and the overall symptomatic scale worsened only slightly for both groups. Lin JK et al. [8] studied the QoL in stage III CRC patients treated either with capecitabine or with 5-FU/LV, in monotherapy or associated with oxaliplatin, concluding that the

treatment with capecitabine did not offer a quality of life lower than the treatment with 5 –FU. In this study the EORTC QLQ-C30 questionnaire was completed at the beginning and end of the treatment.

In general, haematological ARs (thrombocytopenia, lymphopenia and neutropenia) were more frequent in patients who received FOLFOX, while patients treated with XELOX had a higher incidence of symptomatic ARs, such as PPE, nausea and vomiting and anemia. The study of Schmoll HJ. et al [14] also shows this higher incidence of nausea and vomiting in patients treated with XELOX. The fact that hematologic ARs, with the exception of anemia, are non-symptomatic ARs and that, therefore, the patient can not perceive them, may be the reason why patients treated with the FOLFOX scheme presented, in general, better results in the questionnaire QoL than patients treated with XELOX. Indeed, patients treated with XELOX showed a worsening during the treatment of fatigue (could be related to anemia), nausea/vomiting, anorexia and diarrhea, which did not manifest patients treated with FOLFOX. Patients treated with FOLFOX only showed a worsening of insomnia. This worsening in the symptomatology detected by patients treated with XELOX would be the cause of the statistically significant difference found when evaluating the emotional role in the middle of treatment in patients receiving FOLFOX and those receiving XELOX. The hematologic ARs such as neutropenia, lymphopenia and thrombocytopenia were not perceived by the patients because they did not limit their daily activities, but instead, the symptomatic ARs and anemia did condition and limit them in daily activities.

The clinically relevant worsening of insomnia detected in our study only in patients treated with FOLFOX, is not reported in other studies on QoL. On the contrary, the study by Cornmella et al [19] in patients diagnosed with mCRC showed that, with treatment, insomnia improved in patients who received FOLFOX and worsened in patients who received XELOX. The high standard deviation of the scores corresponding to this item in our study, could explain in part the different results.

The same occurs with the clinically relevant worsening in the perception of anorexia during XELOX treatment. In the study carried out by Conroy et al [21] no worsening of this item was detected with any of the treatments, probably because they performed the study with patients diagnosed with mCRC, who presented a significantly higher baseline incidence of anorexia than patients of our study. On the contrary, in the study carried out by Chen HH et al. in patients with stage III CRC, the questionnaire was completed at the beginning and after 12 and 28 weeks of treatment a lower loss of appetite in patients treated with capecitabine was detected [22].

In addition, in our study both groups of patients perceived constipation as a limiting symptom in their QoL, since this item presented a clinically relevant worsening throughout the adjuvant treatment for both the group treated with the FOLFOX scheme and the group treated with the XELOX scheme. In contrast, only patients treated with XELOX perceived diarrhea as a limiting and clinically relevant symptom. These data do not agree with the frequency of occurrence of these adverse reactions, greater in patients treated with FOLFOX (although the differences are not statistically significant). This disagreement is probably due to the difficulty in collecting this AR, as they were colostomized patients. In fact, the higher incidence of diarrhea/constipation associated with FOLFOX treatment is not reflected in other studies [14-16], and with respect to XELOX, in the study of Comella P. et al [19], with stage III CRC patients, there was even an improvement in the perception of constipation as the treatment progressed.

Although the differences were not statistically significant, grade 3-4 ARs were more frequent in patients treated with the FOLFOX scheme (42%), than in patients treated with XELOX (19%), especially due to the greater severity of the cases of mucositis, neurotoxicity and neutropenia. These results are consistent with those of other studies, such as that of Dureux M. et al, which reflects 45% of grade 3-4 ARs in patients treated with FOLFOX and 36% in patients treated with XELOX [16]. These differences are due, in part, to the higher incidence of neutropenia: it appeared in 24% of patients treated with FOLFOX compared to 5% in those treated with XELOX. This higher percentage of grade 3-4 ARs in patients treated with FOLFOX was probably the cause of greater number of dose reductions and discontinuations of treatment in these patients, specifically in the case of oxaliplatin due to the neurotoxicity associated with the use of this drug.

Probably the worsening in the performance of daily activities as treatment progressed, detected in all patients regardless of the therapeutic scheme, could be related to the neurotoxicity associated with oxaliplatin and also with the worsening of fatigue, dyspnoea, insomnia and nausea/vomiting.

5. Conclussions

The substitution of the continuous infusion of 5-FU for 3 days every two weeks (FOLFOX scheme) by the take of two tablets of capecitabine a day for 14 days every 3 weeks (XELOX scheme) slightly modifies the safety profile of the treatment and the quality of life of patients diagnosed with stage II and III CRC. Although statistically significant differences between both schemes were only found in the incidence of palmar-plantar erythrodysesthesia

(more frequent with XELOX), a higher incidence of non symptomatic hematologic adverse reactions was reported with FOLFOX while a higher incidence of symptomatic adverse reactions was related with XELOX, which led to a slightly worse assessment of the quality of life of these patients.

Patients relate their quality of life preferably to their perception of adverse reactions associated with the medication, and not to the route of administration used, so that the substitution of the intravenous route by the oral route is not perceived by the patient as a benefit.

Since the severity of an adverse reaction is independent of its perception by the patient, one scheme can not be generally selected over another, and an individual assessment of each patient is necessary in terms of general condition, comorbidity, lifestyle, age and even educational level.

6. References

[1]. Choong, M.K & Tsafnat, G. (2012). Genetic and Epigenetic Biomarkers of Colorectal Cancer. Clin Gastroenterol Hepatol., 10(1), 9-15.

[2]. Ferlay, J., Soerjomataram, I., Dikshit, R., Eser, S., Mathers, C. & Rebelo, M. (2015). Cancer incidence and mortality worldwide: sources, methods and major patterns in GLOBOCAN 2012. Int J Cancer, 136(5), 359-86.

[3] Watson, A.J.M. & Collins, P.D. (2011). Colon Cancer: A Civilization Disorder. Dig Dis. 29(2), 222-8.

[4] American Joint Committee on Cancer. Colon and rectum cancer staging (7th edition) [consulted October 2017]. Online: http://cancerstaging.org/referencestools/quickreferences/documents/colonmedium.pdf

[5] Yothers, G., O'Connell, M.J., Allegra, C.J., Kuebler, J.P., Colangelo, L.H. & Petrelli, N.J. (2011). Oxaliplatin as adjuvant therapy for colon cancer: updated results of NSABP C-07 trial, including survival and subset analyses. J Clin Oncol., 29(28), 3768-74.

[6] Ribecco, A.S., Pino, M.S., Cipriani, G., Marinozzi, C. & Fioretto, L. (2013). Molecularly targeted therapy: toxicity and quality of life considerations in advanced colorectal cancer. Expert Rev Anticancer Therapy, 13(10), 1181-91

[7] Summary of product charactheristics. Agencia Española de Medicamentos y Productos Sanitarios [Online]. [Accessed 25th May 2016]. Available at: http://www.aemps.gob.es/cima/fichasTecnicas.do?metodo=busca

[8] Lin, J.K., Tan, E.C. & Yang, M.C. (2015). Comparing the effectiveness of capecitabine versus 5-fluorouracil/leucovorin therapy for elderly Taiwanese stage III colorectal cancer patients based on quality-of-life measures (QLQ-C30 and QLQ-CR38) and a new cost assessment tool. Health Qual Life Outcomes, 13, 61.

[9] Cheng, Y., Yang, H., Chen, G. & Zhang, Z. (2013). Moleculary targeted drugs for metastatic colorectal cancer. Drug Des Devel Ther., 7, 1315–22.

[10] Inernational Multicentre Pooled Analysis of Colon Cancer Trials (IMPACT) investigators (1995). Efficacy of adjuvant fluorouracil and folinic acid in colon cancer. International Multicentre Pooled Analysis of Colon Cancer Trials (IMPACT) investigators. Lancet., 345(8955), 939-44.

[11] André, T., Boni, C., Mounedji-Boudiaf, L., Navarro, M., Tabernero, J. & Hickish, T. (2004). Oxaliplatin, fluorouracil, and leucovorin as adjuvant treatment for colon cancer. N Engl J Med., 350(23), 2343-51.

[12]. Twelves, .CJ. (2006). Xeloda in Adjuvant Colon Cancer Therapy (X-ACT) trial: overview of efficacy, safety, and cost-effectiveness. Clin Colorectal Cancer, 6(4), 278-87.

[13] Haller, D.G., Tabernero, J., Maroun, J., de Braud, F., Price, T. & Van Cutsem, E. (2011). Capecitabine plus oxaliplatin compared with fluorouracil and folinic acid as adjuvant therapy for stage III colon cancer. J Clin Oncol., 29(11), 1465-71.

[14] Schmoll, H.J., Twelves, C., Sun, W., O'Connell, M.J., Cartwright, T. & McKenna, E. (2014). Effect of adjuvant capecitabine or fluorouracil, with or without oxaliplatin, on survival outcomes in stage III colon cancer and the effect of oxaliplatin on post-relapse survival: a pooled analysis of individual patient data from four randomised controlled trials. Lancet Oncol., 15(13), 1481-92.

[15] Schmoll, H.J., Tabernero, J., Maroun, J., de Braud, F., Price, T. & Van Cutsem, E. (2015). Capecitabine Plus Oxaliplatin Compared With Fluorouracil/Folinic Acid As Adjuvant Therapy for Stage III Colon Cancer: Final Results of the NO16968 Randomized Controlled Phase III Trial. J Clin Oncol., 33(32), 3733-40.

[16] Ducreux, M., Bennouna, J., Hebbar, M., Ychou, M., Lledo, G. & Conroy, T. (2011). Capecitabine plus oxaliplatin (XELOX) versus 5-fluorouracil/leucovorin plus oxaliplatin (FOLFOX-6) as first-line treatment for metastatic colorectal cancer. Int J Cancer., 128(3), 682–90.

[17] Price, T.J., Segelov, E., Burge, M., Haller, D.G., Ackland, S.P. & Tebbutt, N.C. (2013). Current opinion on optimal treatment for colorectal cancer. Expert Rev Anticancer Ther., 13(5), 597-611.

[18] Guyatt, G.H., Ferrans, C.E., Halyard, M.Y., Revicki, D.A., Symonds, T.L. & Varricchio, C.G. (2007). Exploration of the value of health-related qualityof-life information from clinical research and into clinical practice. Mayo Clin Proc., 82(10), 1229-39.

[19]. Comella, P., Massidda, B., Filippelli, G., Farris, A., Natale, D. & Barberis, G. (2009). Randomised trial comparing biweekly oxaliplatin plus oral capecitabine versus oxaliplatin plus i.v. bolus flourouracil/leucovorin in metastasic colorectal cancer patients: results of the Southern Italy Cooperative Oncology study 0401. J Cancer Res Clin Oncol., 135(2), 217-26.

[20] Seymour, M.T., Thompson, L.C., Wasan, H.S., Middleton, G., Brewster, A.E. & Shepherd, S.F. (2011). Chemotherapy options in elderly and frail patients with metastatic colorectal cancer (MRC FOCUS2): an open label, randomised factorial trial. Lancet, 377(9779), 1749-59.F

[21] Conroy, T., Hebbar, M., Bennouna, J., Ducreux, M., Ychou, M. & Llédo, G. (2010). Quality-of-life findings from a randomised phase-III study of XELOX vs FOLFOX-6 in metastatic colorectal cancer. Br J Cancer, 102(1), 5967.

[22] Chen, H.H., Chen, W.T., Lee, H.C., Lin, J.K., Fang, C.Y. & Chou, Y.H. (2015). Health related quality of life and cost comparison of adjuvant capecitabine versus 5-fluorouracil/leucovorin in stage III colorectal cancer patients. Qual Life Res., 24(2), 473-84.

[23] NCCN guidelines. Colon cancer. [consulted 26 Julio 2017] https://www.nccn.org/professionals/physician_gls/default.aspx

[24] NCCN guidelines. Rectal cancer. [consulted 26 Julio 2017] https://www.nccn.org/professionals/physician_gls/default.aspx

[25] Ley Orgánica 15/1999, de 13 de diciembre, de Protección de Datos de Carácter Personal. [consulted 5 julio 2017]. Online: https://www.boe.es/boe/dias/1999/12/14/pdfs/A43088-43099.pdf

[26] Aaronson, N.K., Ahmedzai, S., Bergman, B., Bullinger, M., Cull, A. & Duez, N.J. (1993). The European Organization for Research and Treatment of Cancer QLQ-C30: a quality-of-life instrument for use in international clinical trials in oncology. J Natl Cancer Inst., 85(5), 365-76.

[27] Fayers, P.M., Aaronson, N.K., Bjordal, K., Groenvold, M., Curran, D. & Bottomley, A. (2001). The EORTC QLQ-C30 Scoring Manual (3rd Edition). Published by: European Organisation for Research and Treatment of Cancer, Brussels.

[28] Osoba, D., Rodrigues, G., Myles, J., Zee, B. & Pater, J. (1998). Interpreting the significance of changes in health-related quality-of-life scores. J Clin Oncol., 16, 139–44.

[29] Schmoll, H.J., Cartwright, T., Tabernero, J., Nowacki, M.P. & Figer, A. (2007). Phase III trial of capecitabina plus oxaliplatin as adjuvant therapy for stage III colon cancer: A planned safety analysis in 1,864 patients. Journal of Clinical Oncology, 25(1), 102–9.

[30] Liu, G., Franssen, E., Fitch, M.I. & Warner, E. (1997). Patient preferences for oral versus intravenous palliative chemotherapy. J Clin Oncol., 15(1), 110-5.

[31] Pelusi, J. (2006). Capecitabine versus 5-FU in metastatic colorectal cancer: considerations for treatment decision-making. Commun Oncol, 3(1), 19–27.

[32] Borner, M., Schoffski, P., de Wita, R., Caponigroa, F., Comellaa, G. & Sulkesa, A. (2002). Patient preferences and pharmacokinetics of oral modulated UFT versus intravenous fluorouracil and leucovorin: a randomised crossover trial in advanced colorectal cancer. Eur J Cancer, 38(3), 349–58.

[33] Twelves, C., Gollins, S., Grieve, R. & Samuel, L. (2006). A randomised cross-over trial comparing patient preference for oral capecitabine and 5 fluorouracil/leucovorin regimens in patients with advanced colorectal cancer. Ann Oncol., 17(2), 239-45.

[34] Pfeiffer, P., Mortensen, J.P., Bjerregaard, B., Eckhoff, L., Schønnemann, K. & Sandberg, E. (2006). Patient preference for oral or intravenous chemotherapy: a randomised cross-over trial comparing capecitabine and Nordic fluorouracil/leucovorin in patients with colorectal cancer. Eur J Cancer, 42(16), 2738-43.

International Conference on Cancer Research 2019

Website: www.CancerConf.org

June 10-11, London, UK



Usefulness of Our Newly Designed Supplements for Reducing the High Risk of Pancreatic Cancer

Hidetoshi Ikeda [1]*, Takuma Ikeda [2], Hidetoshi Tahara [3]

[1] *Research Institute for pituitary disease, Southern Tohoku General Hospital. 7-115 Yatsuyamada,Koriyama City, Fukushima963-8563, Japan.*

[2] *Department of Neurosurgery, Iwamisawa municipal central Hospital, 9-7-2 Iwamisawa 068-8555, Hokkaido, Japan.*

[3] *Department of Cellular and Molecular Biology, Hiroshima University, 1-2-3 Katsumi, Minami-ku, Hiroshima 734-8553, Japan.*

**Corresponding author: ikeda07@hotmail.co.jp*

Abstract

Early detection of pancreatic cancer became possible by analyzing micro RNA (miRNA) from peripheral blood. We report our new preventive intervention method to reduce the risk of pancreatic cancer by using our original supplements for patients with high risk of pancreas-bearing cancer.

Purpose; The risk determination of pancreatic cancer by using miRNA from blood was examined, and it was investigated whether it was effective to decrease the high risk of pancreatic cancer by using supplements that we newly devised.

Materials and Methods; For 14 adults who are not sick, the miRNA was extracted from the blood. They consisted of 7 men and 7 females, aged between 64 and 78 years old, averaging 67.6 years old. The encompassing analysis was performed using the next generation sequencer, and the risk of pancreatic cancer was calculated as expression score (ES). After confirming the absence of visible tumor, three months of our supplements (P-glucan and Methyl-resveratrol) were subjected to take.

Then the risk determination was carried out repeatedly by analyzing miRNA from blood samples. Changes in tumor-bearing risk treated by our tumor risk-reduction supplements were evaluated by ES calculated by next Generation sequencer before and after intervention and examined by Wilcoxon test.

Results; By the proactive intervention method of the tumor-bearing reduction supplements, the expression scores, in 11 cases (79%) in 14 cases, were reduced significantly (Wilcoxon test; $p<0.0052$) after taking supplements. Furthermore, 14 cases were divided into A group (N=8) who showed higher ES than the healthy mean average, and B group (B=4) who showed lower ES than the mean average of healthy persons. In A group 8 out of 8 (100%) showed significant ($p<0.009$) reduction of ES. While, in group B, no significant reduction of ES were obtained ($p = 0.465$) .

Conclusion; For those who have high risk of pancreatic cancer, we found it possible to reduce ES perfectly by means of our newly designed supplements. This shows an effective practice of preemptive medicine.

Keywords:

MicroRNA;

Pancreatic cancer;

Cancer risk;

Supplements;

Preemptive medicine.

1. Introduction

Diagnosis of pancreatic cancer in its early stage is difficult. Since pancreatic cancer usually found in Stage IV, there is no effective therapy for it [1]. The 5-year survival rate among patients with pancreatic cancer is 9%, which is the lowest among all cancers. Therefore, early detection of pancreatic cancer is desirable. Early detection of pancreatic cancer has become possible by analyzing microRNA (miRNA) from the peripheral blood [2]. Analysis of miRNA allows for detection of pancreatic cancer foci as small as 0.1 mm in diameter. The sensitivity of this test is more than 96% [3]. Because of this sensitivity and specificity of the test, the location of the tumor may not be indicated by conventional radiologic modalities such as CT, MRI, and PET-CT. Thus pancreatic cancer is often not found by imaging, it is a problem that the technical innovation of the diagnostic technology using miRNA analysis does not relate to treatment at once.

In order to make effective use of the early diagnosis method of high sensitivity, we found a method for reducing the risk of cancer bearing.

We examined the ability to determine the risk of pancreatic cancer using miRNA from blood. At the same time, we also investigated whether our newly developed supplements can efficiently decrease the risk of pancreatic cancer.

We will report here our new preventive intervention method to reduce the risk of pancreatic cancer using our original supplements for patients with a high risk of pancreatic cancer.

2. Materials and Methods

The approval to perform this study was obtained from ethical committee of Southern Tohoku General Hospital. Documented informed consent were obtained by each subject.

Blood samples were obtained from 14 healthy adults for miRNA extraction. The patients consisted of seven men and seven women ranging in age from 64 to 78 years (average, 67.6 years).

RNA extraction was performed using standard protocol of commercial miRNeasy 96 Kit (Qiagen, Netherland). Total RNA concentration was evaluated by Nanofrop2000 spectrometer (Thermo Scientific, USA). Quality assessment of total RNA samples was performed using Agilent 2100 Bioanalyzer (Agilent Technologies, USA). Small RNA libraries were prepared using TruSeq Small RNA Sample Preparation (Illumina) according to the manufacture's protocol with 1 ug RNA input per sample followed by RNA 3' adapter ligation, RNA 5' adapter ligation, cDNA synthesis, PCR amplification using unique barcode sequences for each sample and gel size-selection of small RNA library. The yield of sequencing libraries was assessed using the Agilent 2100 Bioanalyzer (Agilent Technologies). Multiplexed libraries were sequenced on Ion GeneStudio S5 next-generation sequencing platform (Thermo Fisher Scientific, Japan), and the risk of pancreatic cancer was calculated as the expression score (ES).

The presence of tumors was evaluated by radiographic images such as CT (160 channels, GE, USA), 3T -MRI (Signa, GE, Japan) and PET-CT (GE, USA). After confirming the absence of visible tumor, the patients took our newly designed supplements orally for 3months. The supplements consisted of beta-glucan (Meshima, 2 g/day) and methyl-resveratrol (pterostilbene; 2 caps/day).

Risk determination was then carried out repeatedly by analyzing miRNA from the patients' blood samples. Changes in the tumor-bearing risk after treatment with our tumor risk-reduction supplements were evaluated by the ES as calculated by next generation sequencing, just before and after the intervention and followed up 8 months after treatment, then the results were examined by the Wilcoxon test.

3. Results

The average ES before and after the intervention was -718 and -965, respectively.

After the proactive intervention of our tumor risk-reduction supplements, the ES significantly declared in 11 (Wilcoxon test, $p < 0.0052$) of 14 patients (79%) (Fig.1). Furthermore, the 14 patients were divided into Group A ($n = 8$), who shown a higher ES (mean; -564) than the average ES (-900) of healthy persons, and Group B ($n = 4$), who shown a lower ES (mean; -1007) than the average ES of healthy persons. In Group A, all eight patients (100%) showed a significant reduction of the ES ($p < 0.009$) (Fig. 2). In Group B, however, no significant reduction of the ES was obtained ($p = 0.465$) (Fig.3).

Supplement for 3 months in group A, without adding further intervention, and 8 months after completion of supplementation, ES were measured in three patients and found it remained unchanged.

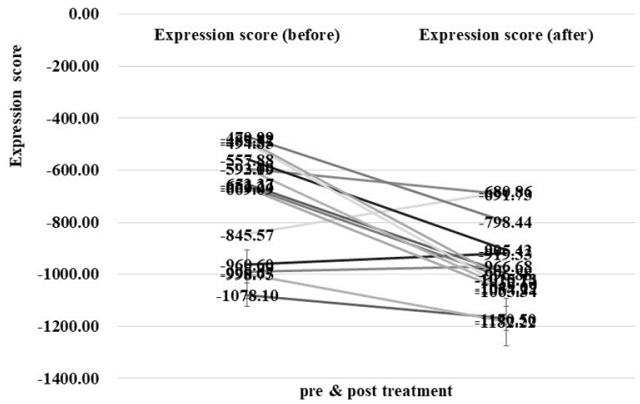


Fig.1 , Change in risk before and after intervention in all cases

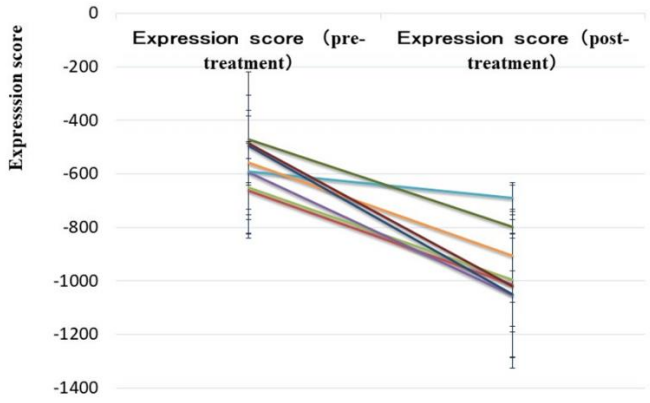


Fig.2, Changes in high risk before and after intervention

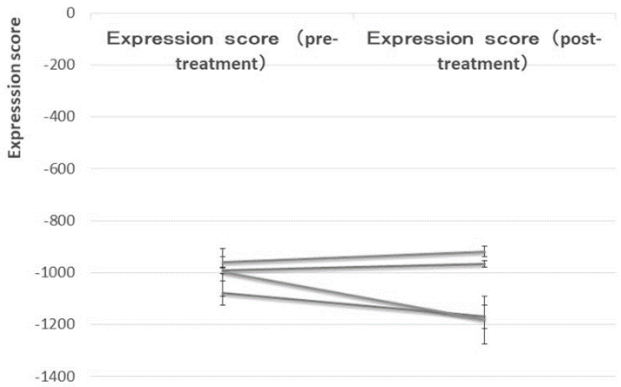


Fig.3, change in risk among low-risk individuals before and after intervention

4. Discussion

Pancreatic cancer remains one of the most lethal malignant neoplasms that caused 432,242 new deaths in 2018 (GLOBOCAN 2018 estimates). Globally, 458,918 new cases of pancreatic cancer have been reported in 2018, and 355,317 new cases are estimated to occur until 2040. Despite advancements in the detection and management of pancreatic cancer, the 5-year survival rate still stands at 9% only [1].

Worldwide incidence and mortality rate of pancreatic cancer in both males and females increases with age, and almost 90% of all deaths occur after the age of 55 years [4]. Pancreatic cancer is very difficult to detect and is often very advanced at the time of detection, making it a deadly and frightening cancer. That's why finding pancreatic cancer as soon as possible is the most important point.

Tumor markers used to diagnose pancreatic cancer include CA 19 -9, CEA, Dupan -2, and Span -1. Some tumor markers are more likely to appear in certain organ cancers, but many are made in more than one organ. It can also be elevated in diseases other than cancer (false positive), so high tumor markers do not make a cancer diagnosis [5]. Also, tumor markers are often not elevated in early stage cancers and cannot be used for early diagnosis of pancreatic cancer.

Abdominal ultrasonography (so-called abdominal echo)" is a standard and most sensitive imaging examination that may detect pancreatic cancer [6]. Pancreatic cancer must be detected early, when the tumor is 2 centimeters or smaller, but data show that abdominal ultrasound has only a 0.003% chance of detecting pancreatic cancer early. That means it's very difficult to detect pancreatic cancer early in a standard physical examination. Therefore, there are currently no definite guidelines for effective screening for pancreatic cancer.

The miRNA diagnosis used in this study is epoch-making because it has high specificity and sensitivity and can detect early lesions as small as 0.1 mm^3. However, diagnosis of pancreatic cancer with such sensitivity is difficult because the neuroradiological system and sensitivity do not catch up, and there is no other way than to closely follow patients. If the ES of the miRNA diagnosis is high, even if it is not visible in the image, the risk can be reduced by the supplement we devised, and if the lifestyle is not disturbed, the reduction in risk lasts more than 8 months.

Meshimas are mainly composed of P-glucan obtained from mushroom hyphae. P-glucan is known to activate natural killer T cells, T cells, B cells, and macrophages several times [7]. Pterostilbene also increases the activity of inhibitory miRNAs and exhibits anticancer effects [8]. Meshimakobu (1 pack/day) and pterostilbene (2 tablets/day) were taken after meals and continued for 3 months. After taking the drug for 3 months, a blood sample is taken, and risk is determined by miRNA.

Based on scientific evidence it is suggested that quitting smoking, drinking moderately, eating a balanced diet, physical activity, proper weight, and infection prevention are effective in preventing cancer. Those items are [1] related to daily life habits. By practicing the five health habits, we can lower the chance of getting cancer by our own efforts.

In conclusion, the paradigm of preventive medicine in the future is to use miRNA diagnostics to identify disease risk and, if there is no visible cancer, to take our cancer-reducing supplement for 3 months. After confirming that the cancer risk has decreased, it may be important to observe the five lifestyle behaviors such as quitting smoking, drinking moderately, eating a balanced diet, physical activity, and keep proper weight, and to protect your body so that the cancer risk does not rise again. This is what preemptive medicine should be and is a goal.

5. Conclusion

For patients at high risk of pancreatic cancer (e. g., those with a high ES), we found it possible to efficiently reduce the ES by means of our newly designed supplies. The risk reduction effect lasted at least eight months. This treatment represents effective practice of preemptive medicine.

6. References

[1] Rawla P, Sunkara T, Gaduputi V. (2019). Epidemiology of Pancreatic Cancer: Global Trends, Etiology and Risk Factors.

World J Oncol. Feb;10(1):10-27. doi: 10.14740/wjon1166. Epub 2019 Feb 26.

[2] Singh PK, Brand RE, Mehla K. (2012) MicroRNAs in pancreatic cancer metabolism. Nat Rev Gastroenterol Hepatol. 9:334-344.

[3] Tahara H. (2018) Risk assessment of age-associated disease using telomere and microRNA technologies. Rinsho Ketsueki. 59:1880-1885. doi:10.11406/rinketsu.59.1880.

[4] Bray F, Ferlay J, Soerjomataram I, Siegel RL, Torre LA, Jemal A. (2018) Global cancer statistics 2018: GLOBOCAN estimates of incidence and mortality worldwide for 36 cancers in 185 countries. CA Cancer J Clin.;68(6):394424.

[5] Ballehaninna UK, Chamberian RS.(2013) Biomarkers for pancreatic cancer: promising new markers and options beyond CA 19-9. Tumour Biol. 34:3279-92.

[6] Luz LP, Al-Haddad MA, Sey MSL, DeWitt JM. (2014) Application of endoscopic ultrasound in pancreatic cancer.

World J Gastroenterol. 28:7808-2840.

[7] Kim HM, Han SB, Oh GT, Kim YH, Hong DH, Hong ND, Yoo ID, (1996) Stimulation of humoral and cell mediated immunity by polysaccharide from mushroom Phellinus Inteus. Int J Immunopharmacology, 18:295-303,

[8] Chen RJ, Kuo HC, Cheng LH, Lee YH, Chang WT, Wang BJ, Wang YJ, Cheng HC. (2018) Apoptotic and nonapoptotic activities of pterostilbene against cancer. Int. Molecular Science 19,287、doi:ijimus19010287

International Conference on Cancer Research 2019

Website: www.CancerConf.org

June 10-11, London, UK



Breastdefend Enhances Effect of Tamoxifen in Estrogen Receptor-Positive Human Breast Cancer in Vitro and in Vivo

Isaac Eliaz [1]*, Dan Sliva [2,3]

[1] *Amitabha Medical Clinic and Healing Center, 398 Tesconi Ct., Santa Rosa, CA 95401*

[2] *Daniel Sliva, PhD, Cancer Research Laboratory, Methodist Research Institute, Indiana University Health, Indianapolis, IN 46202, USA*

[3] *DSTest-Laboratories, Purdue Research Park, 5225 Exploration Drive, Indianapolis, IN 46241, www.dstest-lab.com*

** Corresponding author: Isaac.eliaz@gmail.com*

Abstract

Background: Breast cancer is the leading cause of cancer death in females, and approximately 75% are estrogen receptor (ER)-positive breast tumors. Tamoxifen (TAM) has been a frontline treatment for both early and advanced ER-positive breast cancer in pre- and postmenopausal women. TAM is a selective ER modulator and its active metabolite, 4-hydroxytamoxifen (4-OHT), acts as an estrogen antagonist in breast cells that binds ER and blocks its activity to halt cell proliferation and induce apoptosis. Unfortunately, TAM resistance occurs in approximately 30% of patients. Additionally the development of side effects with long-term administration, including menopausal symptoms, fatigue, painful joints and mood changes, significantly affects quality of life and often leads to discontinuation of treatment. TAM in combination with other therapies is being actively investigated as a way to increase efficacy and decrease side effects. Numerous studies have demonstrated that natural compounds present in vegetables, fruits and mushrooms can affect multiple molecular targets and signaling pathways, leading to their possible use in combination therapy. BreastDefend® (BD) is a dietary supplement formula which contains a combination of medicinal mushrooms (Ganoderma lucidum, Coriolus versicolor, Phellinus linteus), herbal extracts (Curcuma longa, Scutellaria barbata, Astragalus membranaceus), and purified biologically active components (3, 3′ -diindolylmethane, quercetin). These natural agents have demonstrated anticancer activities against breast cancer in multiple studies. Prior studies on BD alone or combined with modified citrus pectin (MCP) showed significant inhibition of growth and invasive behavior of highly metastatic triple-negative human breast cancer cells in vitro and in vivo.

Study Purpose: We investigated the sensitivity of ER-positive MCF-7 cells and its tumor xenografts to BD, 4-OHT/TAM and their combination treatment.

Methods: In vitro: Cell proliferation and apoptosis determined in ER-positive human breast cancer cells (MCF-7) by MTT assay, quantitation of cytoplasmic histone-associated DNA fragments and expression of cleaved PARP, respectively. Molecular mechanism identified using RNA microarray analysis and western blotting.

In vivo: MCF-7 cells implanted (SQ) into inguinal mammary fat pads. E2 pellets (0.36 mg/pellet, 60-day release) also implanted. Mice with palpable tumors (~60 mm3) were randomly assigned to four groups (n = 13): control, TAM, BD, and TAM+BD (16–24 tumors/ group). TAM pellets (5 mg/pellet, 60-day release) were implanted (SQ). BD was suspended in water, administered by gavage 5 x/week (100 mg/kg) x 4 weeks. Tumor tissues analyzed by immunohistochemistry.

Results: Data clearly demonstrate that a combination of TAM with BD led to profound inhibition of cell proliferation and induction of apoptosis in MCF-7 cells, consistent with regulation of apoptotic and TAM resistant genes at the transcription and translation levels. In the xenograft model, TAM and BD co-treatment significantly enhanced apoptosis, suppressed tumor growth and reduced tumor weight.

Conclusions: We show, for the first time, that BD and TAM work synergistically against ER positive breast cancer by suppressing estradiol-induced proliferation of MCF-7

Cells in vitro and tumor growth in vivo, by inducing apoptosis and regulating expression of TAM resistant proteins (p21/CDKN1A and Bcl-2). The findings reveal a novel potential strategy against ER-positive human breast cancer using combination treatment of tamoxifen with BreastDefend.

Keywords:

Breast Cancer,

Vitro,

Vivo,

Tamoxifen.

International Conference on Cancer Research 2019

Website: www.CancerConf.org

June 10-11, London, UK



Classic Herb Pair Sculellaria Barbata and Hedyotis Diffusa for Breast Cancer: Potential Mechanism with Method of Network Pharmacology

TingTing Ma [ab], GanLin Zhang [a], BingXue Li [ab], CunFang Dai [a], XiaoMin Wang [a*]

[a] *Oncology Department, Beijing Hospital of Traditional Chinese Medicine,Capital Medical University.No.23. Back Road of Art Gallery, Dongcheng District, Beijing 100010, China.*

[b] *Beijing University of Chinese Medicine. No. 11 East North Third Ring Road, Chaoyang District, Beijing,100029, China.*

Abstract

Background: Although with diverse treatments and relative long survival times, the recurrences and metastasis are still prevalence after regular therapies, making breast cancer the most serious threatening disease for women all over the world. As empirical medicine, TCM are frequently and widely used for efficacy enhancing and toxicity reducing in the treatment of cancer. The combination using of scutellaria barbata and hedyotis diffusa is a classic herb pair SH prescribed by many famous Chinese oncologists. With the help of SH after western medicine therapeutics, recurrence reduction, metastasis reduction and even the decline of tumour markers can be observed in clinical cases. However, the underlying mechanism of SH for breast cancer is unclear. TCM network pharmacology approach provides a new research paradigm for translating TCM from an experience-based medicine to an evidence-based medicine system, potential mechanisms of TCM may be revealed with network pharmacology method. Based on clinical effectiveness observations, we did *in vitro* experiments and mined the network pharmacology of SH to analyse the role of SH and its potential mechanisms.

Methods: On the basis of TCM decoction process, lyophilized powder of SH is prepared. Both human-derived and mouse-derived breast cancer cells were used to evaluate the efficacy of SH. The active ingredients in SH lyophilized powder were identified by high performance liquid chromatography (HPLC). Cell proliferation test and cell scratch test were used to assess the effect of SH on breast cancer cells proliferation and migration. Then corresponding potential target genes were extracted from Swiss Target Prediction and SEA databases. For breast cancer, disease target genes were searched with "breast cancer" as keywords from databases Therapeutic Target Disease, Drug bank, Disease Gene NET and Genetic Association Database. In addition, with intersection genes of SH and breast cancer were mapped, the Protein-Protein Internetwork (PPI) network of shared genes was constructed with String Database. In the last, Gene Oncology (GO) and Kyoto Encyclopaedia of Genes and Genomes (KEGG) functional annotation clusters were acquired from String database and presented as top 30 pathways.

Results: SH lyophilized powder inhibited the proliferation and migration of both human-derived and mouse-derived breast cancer cells. Further, 75 active ingredients and 180 target genes were extracted for SH, simultaneously, 1305 related genes were extracted for breast cancer. Then 86 intersection genes of SH and breast cancer were mapped. With all the visualization process, combining the basis of physiology and pathology, MicroRNAs in cancer, steroid hormone biosynthesis, serotonergic synapse, VEGF signalling pathway, EFGR tyrosine kinase inhibitor resistance and NF-Kappa B signalling pathway et al were detected in the Top 30 KEGG clusters list from the intersection genes of SH and breast cancer, indicating possible effective mechanisms of SH for breast cancer.

Conclusion: SH can inhibit breast cancer with several potential mechanisms which provide more evidence for clinic. Further experiments and signal pathways analysis are needed to better understand SH.

Keywords:

Herb pair;

Sculellaria barbata;

Hedyotis diffus;

Breast cancer;

Network pharmacology.

* **CONTACT**: Xiao-Min Wang: wangxiaomin_bhtcm@126.com. Gan-Lin Zhang:kalinezhang@163.com.

Introduction

Breast cancer has always been the most serious threatening disease for women all over the world. Recurrence and metastasis are prevalence after those regular therapies such as operation, radiotherapy and chemotherapy, which usually lead to a decreased quality of life as well. As an empirical medicine, traditional Chinese Medicine (TCM) is frequently and widely used for efficacy enhancing and toxicity reducing in the treatment of cancer in China. With the ever-increasing acceptance of complementary and alternative medicine in the world, Chinese herbal medicine (CHM) appeared in many cancer centres in Asia, Africa and some western countries[1-3]

In the TCM theory, the pathological bases of breast cancer are Qi Deficiency, Blood Stasis and Toxin, and the corresponding treating principle are Tonifying Qi, Invigorating Blood Circulation and Detoxification. The combination using of scutellaria barbata and hedyotis diffusa (SH) is a classic herb pair in the detoxification method and frequently used by many Chinese oncologists. There was a study[4] claimed that Hedyotis diffusa plus Scutellaria barbata was the core treatment of CHM used to treat breast cancer in Taiwan. However, despite its curative effects, TCM has been trapped in the position of empirical drug use for its complex ingredients.

Network pharmacology approach, first proposed by Andrew L Hopkins in 2008[5], provides a new research paradigm for translating TCM from an experience-based medicine to an evidence-based medicine system. Active components, potential targets, biological processes and pathways of TCM may be revealed with network pharmacology method[6]. Chinese herbal formulae may influence many targets with many kinds of herbs, the use of TCM may become an advantage for aiming to multiple targets with multiple ingredients if we can explain the mechanisms more clear and logic. Wang et al have explored multiple targets of Ai Du Qing for breast cancer[7], as well as some other Chinese Medicine for different diseases[8-10].

In the present study, the efficacy of SH on breast cancer were analysed by experiments *in vitro* and the potential mechanisms were explored by network pharmacology.

Materials and Methods

The study mainly included three procedural modules: a. form evolution and ingredient identification of SH pair, b. clinical experiences and efficacy evaluation of cell experiments, c. network construction and pathways enrichment based on target genes fishing and mapping. (Figure1)

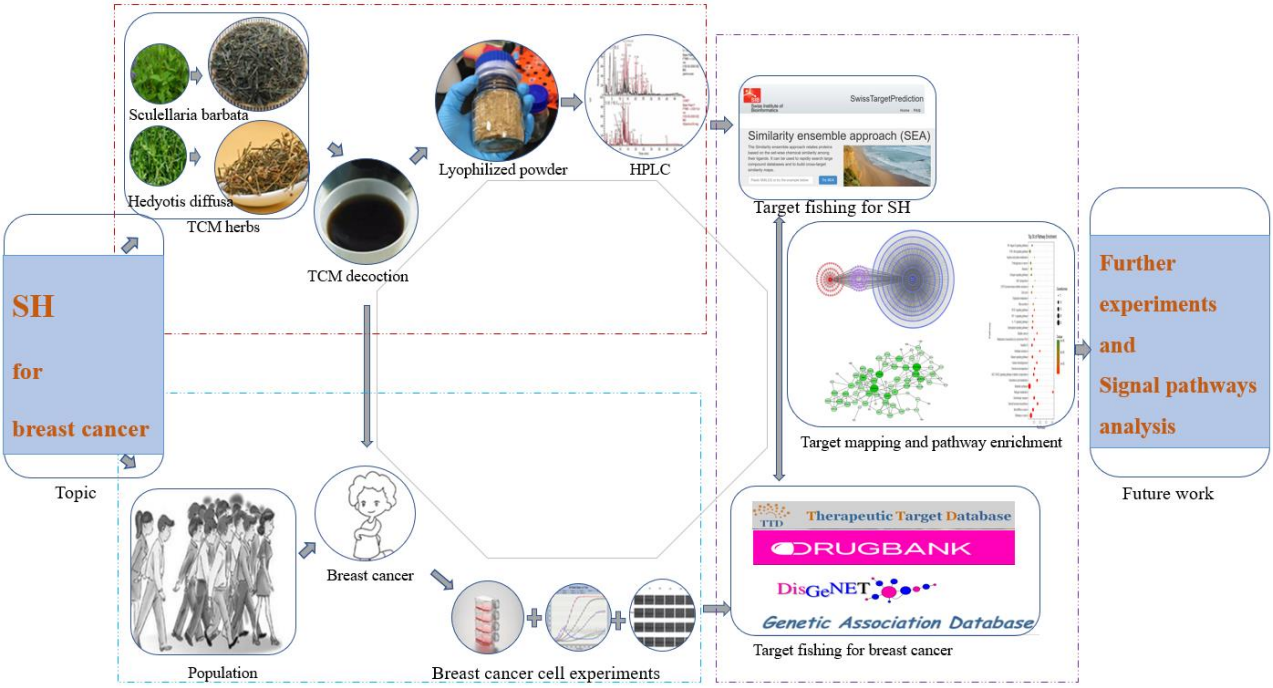


Figure 1 The framework for SH on breast cancer based on network pharmacology

SH is a herb pair with equal weight of Sculellaria barbata and Hedyotis diffusa, both of which were purchased from Beijing Hospital of Traditional Chinese Medicine, Capital Medical University. SH lyophilized powder was acquired by Vacuum cryogenic freeze dryer (Epsilon 2-4LSC, Chris, German). Mass spectrometry analysis was analysed by LTQ-Oribitrap XL linear ion trap tandem electrostatic field trap mass spectrometer: equipped with thermal spray ion source (HESI), Xcalibur 2.1 chemical workstation (Thermo Scientific company, USA); Dionex Utimate 3000 UHPLC Plus Focused ultra high liquid chromatography system (Thermo Scientific company, USA). Millipore Synergy UV Ultra

Pure Water Machine (Millipore Company, USA); Sartorious BT 25S 1/10000 Electronic Analysis Balance (Beijing Sedoris Instrument Co., Ltd.,China); Ultrasound Cleaner (Beijing Zhongsheng Technology Co., Ltd., China); 0.22 um Microporous Filtration Membrane (Tianjin Jinteng Experimental Equipment Co., Ltd.,China); Formic Acid and Methanol (Fisher Company, USA). Apigenin, scopolamine and caffeic acid were purchased from Chengdu Pfide Biotechnology Co., Ltd., China.

231-MDA-MB-Hpa cell and 4T1 cell are both breast cancer cell line, the former is human-derived and the latter is mouse-derived. 231-MDA-MB-Hpa cell was from Heparinase Sulphate Research Group, Department of Medical Biochemistry, University of Uppsala, Sweden. 4T1 cell was from Shanghai Institute of Cell Biology, Chinese Academy of Sciences, China. High glucose DMEM and foetal bovine serum (FBS) were purchased from Gibco Company ,USA. 0.25% trypsin was purchase from Hangzhou Gino Biomedical Technology Co., Ltd,China. Penicillin Streptomycin Solution was purchased from Shanghai Biyuntian Biotechnology Co., Ltd,China. PBS was purchased from Hyclone Company, USA. 25mm^2/75mm^2 Culture bottle, 96 well plate, 5ml/10ml/15ml centrifugal tube, 2ml cryogenic tube were purchased from Corning Company,USA. 0.22um filter membrane were purchased from Millipore Company ,USA. 10ul/100ul/1000ul pipette tips were purchased from Axygen Company, USA. The proliferation and migration of 4T1 was tested on IncuCyte ZOOM(Essen Bioscience, USA). 231-MDA-MB-Hpa cells were GFP labeled and the proliferation was tested on fluorescence channel on SYNERGY H1 microplate reader(BioTek,USA). While the migration was tested on IncuCyte ZOOM(Essen Bioscience, USA).

According to the ingredients of SH identified by HPLC, Canonical SMILES for each ingredient was matched with PubChem[11](https://pubchem.ncbi.nlm.nih.gov/),with which as ingredient ID, corresponding targets were predicted in Swiss Target Prediction [12](http://www.swisstargetprediction.ch/) database and SEA[13] (http://sea.bkslab.org/) databases respectively. The screening rules are possibility (> 0.6) for Swiss Target Prediction or Max TC (> 0.6) for SEA. Significant breast cancer target genes were obtained from Therapeutic Target Disease[14] (TTD, https://db.idrblab.org/ttd/), Drug Bank[15](https://www.drugbank.ca/), Disease Gene NET[16] (DisGeNET, http://www.disgenet.org/web/DisGeNET/menu/home) and Gene Association Database (GAD, https://geneticassociationdb.nih.gov/). The intersection genes of SH and breast cancer were mapped by Venn Diagram and visualized by Cytoscape3.2.1[17], after which, protein-protein internetwork (PPI) network of shared genes was constructed with String Database[18](https://string-db.org/cgi/input.pl?sessionId=PGNpo2jdjXVs).Kyoto encyclopaedia of genes and genomes (KEGG) functional annotation clusters were acquired from String database. To visualize PPI network with Cytoscape3.2.1 and top 30 pathways using bubble diagram with omic share(http://omicshare.com/) online annotation tool.

Results

Form evolution of SH

In this experiment, 2400ml SH decoction were made of 800g sculellaria barbata and hedyotis diffusa with a ratio of 1:1, then 480ml decoction were made into 13.25g lyophilized powder, the production rate was 8.28%. 100mg/ml mother liquor was formulated with deionized water and kept at -20℃ for later cell experiments. In the process of making lyophilized powder of SH, it took 72hours to mainly finish three steps: freezing, main drying and final drying. At least 10℃ lower than eutectic point was needed before the start of the process, the eutectic point of SH was detected between –30℃ and -40℃ in pre-experiment, so -50℃ was set as a start temperature. It is considered that lyophilized powder successfully produced when the resistivity is above 95%. Detection diagram of the whole process is as Figure 2.

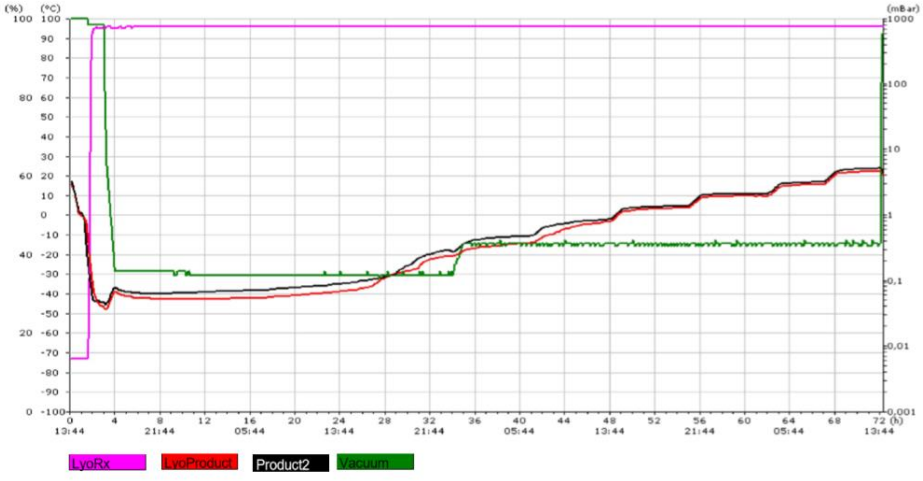
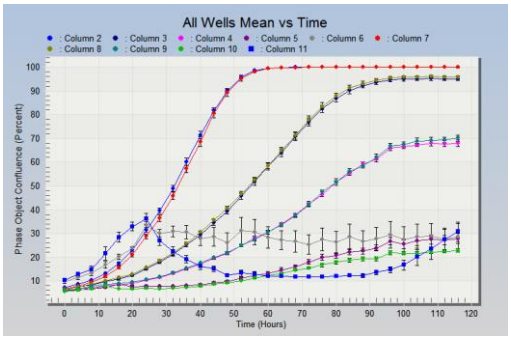


Figure 2 Formation process of lyophilized powder

SH lyophilized powder inhibits breast cancer cells proliferation and migration in vitro

All cells were cultured at 37 °C in a humidified atmosphere containing 5% CO2. Cells in the exponential phase of growth were used for all experiments.

For the proliferation of mouse-derived breast cancer cell 4T1with 96-well plate, PBS was filled the edge wells of the plate to keep the microenvironment moist, 2000 cells were seeded in every well of the 96-well plate, from line B to G, from row 2 to 11. The SH concentrations were 0mg/ml, 0.5mg/ml, 1mg/ml, 2mg/ml, 4mg/ml from row 2 to 6, and the same concentration from row 7 to 11. Each column was added with the same SH concentration. The proliferation was tested on Incu-Cyte ZOOM, it took pictures of fixed vision every 4 hours, the Y-axis showed the percentage of the confluence area of cells in the visual field, the X-axis showed the time point. By 60 hours, the confluence of cells in the visual field was up to 99%, meaning that the proliferation of 4T1 cell was limited. For row 6 and row 11, cells with concentration of 4mg/ml showed anomalous data, the results are presented as Figure 3-1. The values of detected percentage of the confluence area with time are presented as Table1-1, corresponding inhibition rate are presented as Table1-2. For cell scratch testing migration of mouse-derived breast cancer cell 4T1 with 96-well plate, PBS was filled the edge wells of the plate to keep the microenvironment moist, $6*10^4$ cells were seeded in every well of the 96-well plate, from line B to G, from row 2 to 11. The SH concentrations were 0mg/ml, 0.5mg/ml, 1mg/ml, 2mg/ml, 4mg/ml from row 2 to 6, each column was added with the same SH concentration. The migration was tested on Incu-Cyte ZOOM, the images of migration of 4T1 were taken every 2 hours, after picking out clear and typical images, the results are presented as Figure 3-2



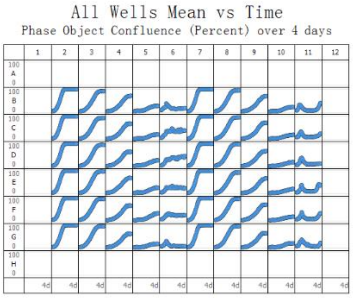


Figure 3-1a. All wells mean vs time grouped by column **Figure 3-1b. All wells mean vs time**

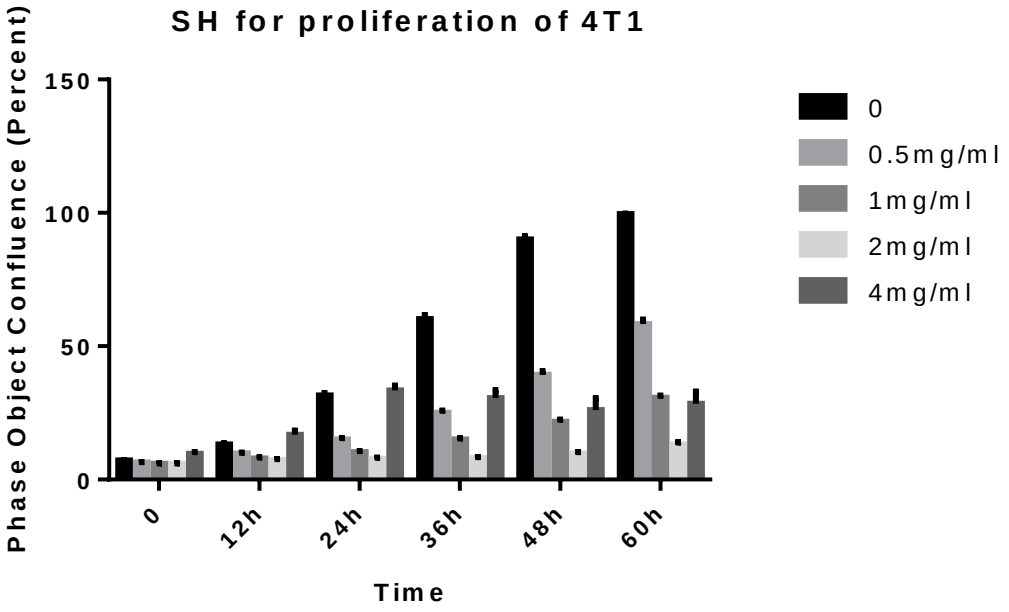


Figure 3-1c. All wells mean vs time grouped by column

Table 1-1. Mean phase object confluence (Percent) grouped by concentration

Confluence (Percent)	0mg/ml		0.5mg/ml		1mg/ml		2mg/ml	
	Mean	SD	Mean	SD	Mean	SD	Mean	SD
0	7.168746	0.174641	6.408026	0.160338	5.909254	0.214415	5.924113	0.175729
12h	13.198900	0.335550	9.789723	0.281281	7.985037	0.265762	7.357464	0.343418
24h	31.500640	0.938027	15.088650	0.496081	10.322470	0.318430	7.872883	0.366319
36h	60.192260	1.515052	25.123370	0.750464	15.021810	0.472186	8.078370	0.376362
48h	90.054750	1.093694	39.358920	1.166853	21.644630	0.755213	9.827250	0.531814
60h	99.557500	0.187575	58.310380	1.566535	30.626970	0.764860	13.236120	0.669873

Table 1-2. Inhibition rate for SH on 4T1

IR	0.5mg/ml	1mg/ml	2mg/ml
0	10.61%	17.57%	17.36%
12h	25.83%	39.50%	44.26%
24h	52.10%	67.23%	75.01%
36h	58.26%	75.04%	86.58%
48h	56.29%	75.97%	89.09%
60h	41.43%	69.24%	86.71%

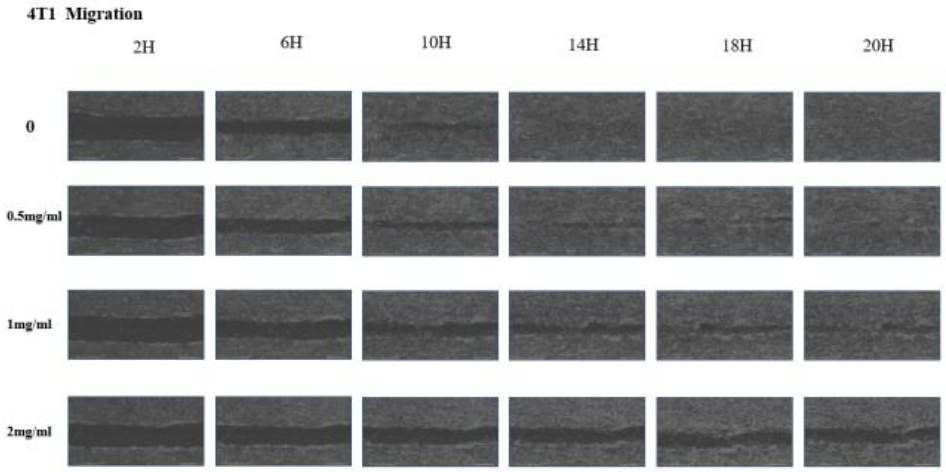


Figure 3-2. Pictures for the migration of SH on 4T1

For the proliferation of human-derived breast cancer cell 231-MDA-MB-Hpa with 96-well plate, PBS was filled the edge wells of the plate to keep the microenvironment moist, 2000 cells were seeded from line B to G, from row 2 to 11. The SH concentrations were 0mg/ml,0.25mg/ml, 0.5mg/ml, 1mg/ml, 2mg/ml, from row 2 to 6, and the same concentration from row 7 to 11. Each column was added with the same SH concentration. Hpa cells were GFP labelled and the proliferation was tested on fluorescence channel on SYNERGY H1 microplate reader. The Y-axis showed optical density (OD) of GFP, the X-axis showed the time point. For row 2 and row 7, cells with concentration of 0.25mg/ml showed almost the same growth trend with 0mg/ml. the results are presented as Figure 4-1. The values of detected OD of GFP with time are presented as Table2-1, corresponding inhibition rate are presented as Table2-2. For cell scratch testing migration of human-derived breast cancer cell 231-MDA-MB-Hpa with 96-well plate, PBS was filled the edge wells of the plate to keep the microenvironment moist, 6*104 cells were seeded in every well of the 96-well plate, from line B to G, from row 2 to 11. The concentrations were 0mg/ml, 0.5mg/ml, 1mg/ml, 2mg/ml from row 2 to

5, each column was added with the same SH concentration. The migration test was tested on Incu-Cyte ZOOM， the Y-axis showed the percentage of the confluence area of cells in the visual field, the X-axis showed the time point. The images of migration of 4T1 were taken every 2 hours, after picking out clear and typical images, the results are presented as Figure 4-2.

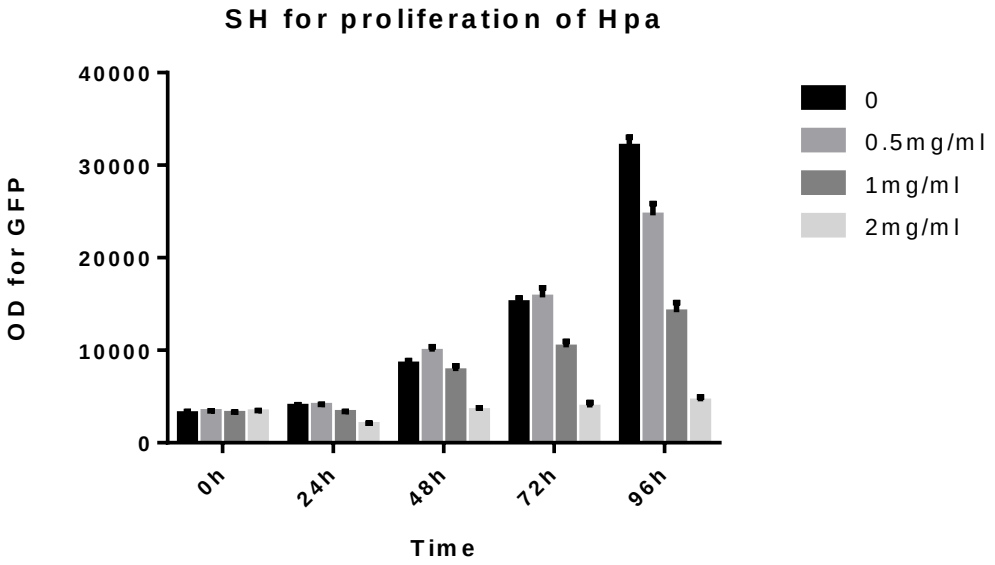


Figure 4-1. All wells mean vs time grouped by column

Table 2-1. Mean GFP OD grouped by concentration

GFP OD	0mg/ml		0.5mg/ml		1mg/ml		2mg/ml	
	Mean	SD	Mean	SD	Mean	SD	Mean	SD
0h	3126.667	246.8025	3341.167	114.6986	3159.667	166.3679	3306.333	167.8102
24h	3908.333	212.3268	4018.000	120.2664	3266.500	132.3174	1945.000	182.0824
48h	8477.000	411.8495	9858.167	510.9088	7761.667	568.9811	3435.333	343.6083
72h	15128.600	525.0093	15714.800	1032.168	10317.200	618.7982	3820.500	519.2012
96h	32018.600	998.5731	24588.800	1266.341	14128.000	1007.305	4485.167	476.5096

Table 2-2. Inhibition rate for SH on 4T1

IR	0.5mg/ml	1mg/ml	2mg/ml
24h	-6.86%	-1.06%	-5.75%
48h	-2.81%	16.42%	50.23%
72h	-16.29%	8.44%	59.47%
96h	-3.87%	31.80%	74.75%

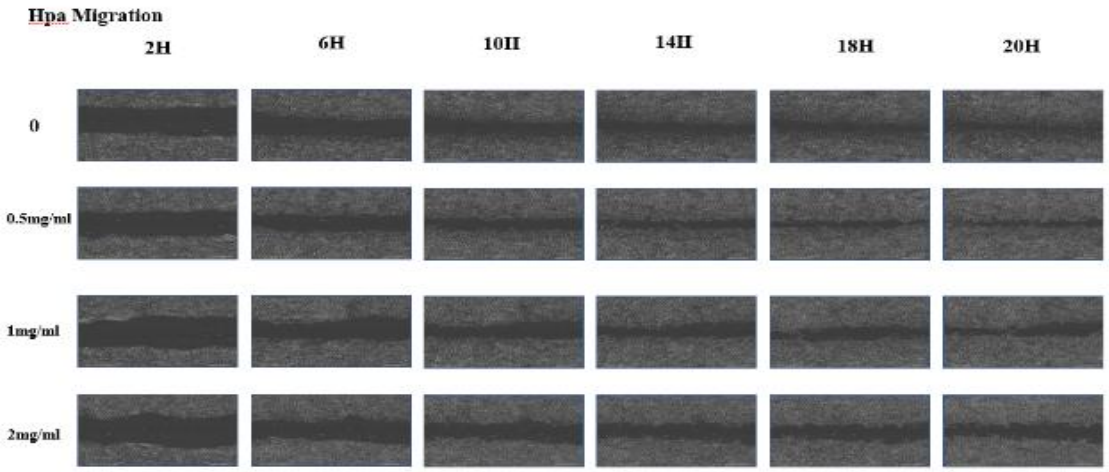


Figure 4-2. Pictures for the migration of SH on Hpa

High Performance Liquid Chromatography and Ingredient Identification.

High performance liquid chromatography (HPLC) was used to identify the main chemical constituents of HS.100mg Lyophilized powder of SH dissolved in 8 ml 50% methanol solution, ultrasonic vibration for 10 minutes, kept still for 5mins, then another ultrasonic vibration for 10 minutes, kept still for 5mins, 3000r/min centrifugation for 5 minutes, take the supernatant, filtered with 0.22um membrane dilution for testing. The extracts of Hedyotis diffusa and Scutellaria barbata were analysed and their total ion flow charts under positive and negative ion modes were obtained. According to the retention time, high resolution precise molecular weight and MSn multi-level fragment information obtained by LC-MS, and combined with the extraction of ion flow chart and standard product information, Scifinder database and related literature, 75 ingredients were identified, as shown in Figure 5-1. Among them, 53 ingredients were identified under positive ion mode, 34 ingredients were identified under negative ion mode, 12 shared ingredients were identified by both positive and negative ions, as shown in Figure 5-2. The 75 chemical constituents identified included 43 flavonoids, 9 terpenoids, 9 phenolic acids, 6 alkaloids, 3 coumarins or lignans, 2 anthraquinones and 3 other compounds, as shown in Figure 5-3. Details are listed in Table 3 and 4.

Table 3 Main chemical constituents in positive ion identification of extracts from SH

Peak No.	*t*R/ min	Molecular formula	Measured value *m/z*	Two level debris （MS/MS）	Possible Ingradient
1	12.39	$C_{15}H_{10}O_5$	271.06010	152.91;229.08;271.12;144.92	Baicalein
2	18.29	$C_{15}H_{10}O_5$	271.06010	152.81;229.08;271.03;144.92	Apigenin
3	11.13	$C_{15}H_{10}O_6$	287.05501	152.84;241.07;168.93; 118.90	Scutellarein
4	12.01	$C_{15}H_{10}O_6$	287.05501	269.00;240.97;168.79;118.88	Isoscutellarein
5	14.74	$C_{15}H_{10}O_6$	287.05501	269.05;241.07;168.88;118.91;287.1	5,7,2',5'-Tetrahydroxyflavone
6	16.36	$C_{15}H_{10}O_6$	287.05501	152.83;287.05;241.01;160.97;269.1	5,7,2',6'-Tetrahydroxyflavone
7	12.04	$C_{21}H_{18}O_{12}$	463.08710	287.08;301.13	Scutellarein 7-glucuronide
8	15.06	$C_{21}H_{18}O_{12}$	463.08710	287.08;288.18	5,6,7,2'-Tetrahydroxyflavone 7-glucuronide
9	10.31	$C_{15}H_{10}O_7$	303.04993	256.97;229.00;164.88;285.03;246.99	Viscidulin I
10	13.07	$C_{15}H_{10}O_7$	303.04993	257.01;229.02;164.92;285.07246.97	3,5,7,2',5'-Pentahydroxyflavone
11	13.68	$C_{21}H_{18}O_{11}$	447.09218	270.96;260.20	Baicalin
12	13.76	$C_{21}H_{20}O_{11}$	449.10783	271.00;285.08	Cinaroside
13	23.98	$C_{16}H_{12}O_4$	269.08083	254.07;223.03;237.00;255.05	Chrysin-5-methylether
14	18.32	$C_{16}H_{12}O_6$	301.07066	286.03;286.99	Hispidulin
15	13.92	$C_{22}H_{20}O_{12}$	477.10275	301.12;339.33	Hispidulin 7-O-beta-glucuronide
16	16.5	$C_{17}H_{14}O_6$	315.08631	302.02303.08	Skullcapflavone I
17	24.31	$C_{17}H_{14}O_6$	315.08631	299.23;281.13;239.20;257.13;271.10	5,7-Dihydroxy-8,2'-dimethoxyflavone
18	24.39	$C_{17}H_{14}O_6$	315.08631	295.18;267.09;108.84;285.13	5,8-Dihydroxy-6,7-dimethoxyflavone

19	26.94	$C_{18}H_{16}O_6$	329.10196	296.02;314.05;297.11;315.09	7-Hydroxy-5,8,2'-trimethoxyflavone
20	22.01	$C_{18}H_{16}O_7$	345.09687	330.08;312.13;331.22;313.08	Tenaxin I
21	24.80	$C_{19}H_{18}O_7$	359.11252	326.10;344.12;327.07;345.14	Altisin
22	21.83	$C_{19}H_{18}O_8$	375.10744	342.08;360.11;343.12;361.25;314.08	Skullcapflavone II
23	11.45	$C_{26}H_{28}O_{14}$	565.15518	547.23;433.31;403.10;521.30;548.40	Isoschaftoside
24	12.39	$C_{16}H_{14}O_4$	271.09648	152.91;229.08;271.12;144.92	(-)-Alpinetin
25	11.84	$C_{15}H_{12}O_6$	289.07066	168.85;146.87;188.86	Eriodictyol
26	12.62	$C_{15}H_{12}O_6$	289.07066	168.86;146.96;194.98;188.98	Carthamidin
27	14.96	$C_{15}H_{12}O_6$	289.07066	168.95;146.84;188.93	Isocarthamidin
28	14.32	$C_{16}H_{14}O_6$	303.08631	182.92;146.88;167.96	5,7,4'-Trihydroxy-6-methoxyflavanone
29	18.20	$C_{16}H_{14}O_6$	303.08631	182.95;146.86;167.85	Scutamoenin
30	13.79	$C_{15}H_{12}O_5$	273.07575	152.80;146.83;178.88	Dihydrobaicalein
31	10.31	$C_{15}H_{12}O_7$	305.06557	256.97;229.00;164.88;285.03;246.99	3,5,7,2',5'-Pentahydroxyflavanone
32	13.07	$C_{15}H_{12}O_7$	305.06557	257.01;229.02;164.92;285.07;246.97	3,5,7,2',6'-Pentahydroxyflavanone
33	18.07	$C_{22}H_{30}O_6$	391.21151	373.27;345.20;251.10	Jodrellin A
34	20.59	$C_{22}H_{30}O_6$	391.21151	373.25;313.30;331.15;295.32;345.27	Isomers of Jodrellin A
35	21.78	$C_{22}H_{30}O_6$	391.21151	331.24;313.20;275.13;295.09;247.20	Isomers of Jodrellin A
36	24.80	$C_{22}H_{30}O_6$	391.21151	331.13;313.08;295.20;257.20;271.26	Isomers of Jodrellin A
37	9.43	$C_{22}H_{32}O_7$	409.22207	229.12;202.95;247.05	11-Episcutecolumnin C
38	23.34	$C_{22}H_{32}O_8$	425.21699	407.15;274.08;408.32	Scutalbin C
39	11.04	$C_{10}H_{10}O_3$	179.07027	144.91;116.92	p-MCA
40	11.08	$C_{11}H_{14}O_2$	179.10665	144.88;148.96	Methyleugenol
41	12.92	$C_{10}H_{10}O_2$	163.07535	144.92;117.00;126.90	p-Hydroxybenzalacetone
42	12.95	$C_{10}H_{12}O_2$	165.09100	144.88;116.96;134.96;126.87	3'-Hydroxyanethole
43	25.97	$C_{30}H_{37}NO_9$	556.25411	514.32;313.17;235.03;295.11	Scutebarbatine F
44	26.70	$C_{32}H_{34}N_2O_7$	559.24387	436.23;295.26;313.19;249.22	Scutebarbatine A
45	20.10	$C_{26}H_{33}NO_7$	472.23297	455.21;454.25;313.16;249.06;389.30	Scutebarbatine G
46	28.20	$C_{28}H_{33}NO_7$	496.23297	295.21;313.13;271.03266.94;253.30	Scutebarbatine K
47	20.52	$C_{32}H_{34}N_2O_8$	575.23879	515.32;557.34;516.25;353.14	7-O-Nicotinoylscutebarbatine H
48	20.33	$C_{32}H_{34}N_2O_8$	575.23879	515.32;557.34;516.25;353.14	Isomers of 7-O-Nicotinoylscutebarbatine H
49	6.90	$C_{10}H_8O_4$	193.04954	146.89;174.95;165.02;148.90	Scopoletin
50	2.50	$C_{20}H_{18}O_6$	355.11761	192.95;324.08;325.12;184.98;323.32	Capitellataquinone A
51	24.07	$C_{15}H_{10}O_3$	239.07027	210.96;183.00;193.03;164.98	2-hydroxy-3-methylanthraquinone
52	13.98	$C_{32}H_{46}O_{11}$	607.31128	495.18;363.16;496.18	Scupontin B
53	15.91	$C_{32}H_{46}O_{11}$	607.31128	496.19;363.19	Isomers of Scupontin B

Table 4 Main chemical constituents in anion identification of extracts from SH

Peak No.	*t*R/ min	Molecular formula	Measured value *m/z*	Two level debris （MS/MS）	Possible Ingradient
1	12.44	$C_{15}H_{10}O_5$	269.04555	224.97；148.92；183.08；197.03	Baicalein
2	18.31	$C_{15}H_{10}O_5$	269.04555	225.09；148.94；200.98；182.96	Apigenin
3	13.74	$C_{15}H_{10}O_5$	269.04555	225.04；148.92；182.94；196.92	5,7,2'-Trihydroxyflavone
4	11.06	$C_{15}H_{10}O_6$	285.04046	266.93；238.93；185.02；164.88；213.04	Scutellarein
5	12.10	$C_{15}H_{10}O_6$	285.04046	241.08；212.98；257.06；266.95	Isoscutellarein
6	16.40	$C_{15}H_{10}O_6$	285.04046	240.98；198.91；174.96；216.89；150.84	5,7,2',6'-Tetrahydroxyflavone
7	12.21	$C_{21}H_{18}O_{12}$	461.07255	285.03；357.20；327.13	Scutellarein 7-glucuronide
8	15.10	$C_{21}H_{18}O_{12}$	461.07255	285.08；299.17	5,6,7,2'-Tetrahydroxyflavone 7-glucuronide
9	10.74	$C_{15}H_{10}O_7$	301.03540	286.04；181.02；255.06	Viscidulin I

10	13.35	$C_{15}H_{10}O_7$	301.03540	286.10；180.95；207.01	3,5,7,2',5'-Pentahydroxyflavone
11	13.73	$C_{21}H_{18}O_{11}$	445.07763	268.97；175.01	Baicalin
12	13.80	$C_{21}H_{20}O_{11}$	447.09328	271.05；174.92；285.05	Cinaroside
13	11.17	$C_{21}H_{20}O_{11}$	447.09328	271.06；175.06；327.09	Dihydrobaicalein 7-O-glucuronide
14	11.8	$C_{21}H_{20}O_{12}$	463.08820	286.97；269.09；174.98	3,5,7,2',6'-Pentahydroxyflavone 2'-glucoside
15	12.66	$C_{21}H_{20}O_{12}$	463.08820	287.18；445.24；401.39	Isomers of 3,5,7,2',6'-Pentahydroxyflavone 2'-glucoside
16	18.07	$C_{16}H_{12}O_4$	267.06628	252.02；239.11；223.11	Chrysin-5-methylether
17	24.39	$C_{16}H_{12}O_4$	267.06628	223.25；249.14；167.08；193.13	Isomers of Chrysin-5-methylether
18	12.43	$C_{21}H_{20}O_{10}$	431.09837	269.08；311.17	Isovitexin
19	13.8	$C_{22}H_{22}O_{10}$	445.11402	269.00；286.90	Baicalein 6-methyl ether 7-glucoside
20	9.56	$C_{23}H_{22}O_{11}$	473.10893	251.04；224.83；268.98；455.30；413.22	7-Hydroxy-5,8-dimethoxyflavone 7-glucuronide
21	17.73	$C_{22}H_{20}O_{11}$	459.09328	333.20；427.25；451.32	Baicalein 6-methyl ether 7-glucuronide
22	1.86	$C_{16}H_{20}O_{10}$	371.09793	353.19；208.91；191.08；164.93；134.92	Deacetyl asperuloside
23	10.10	$C_{16}H_{20}O_{10}$	371.09793	248.9；231.04	Isomers of Deacetyl asperuloside
24	16.00	$C_{31}H_{40}O_{15}$	651.22944	475.33；505.22；457.29；192.97	Isomartynoside
25	39.72	$C_{30}H_{48}O_3$	455.35307	407.55；386.86；318.75	Ursolic acid
26	4.26	$C_9H_8O_3$	163.04006	118.95；147.69	trans-p-Coumaric acid
27	7.60	$C_9H_8O_3$	163.04006	118.92；134.95	Isomers of trans-p-Coumaric acid
28	10.89	$C_9H_8O_3$	163.04006	118.91；134.96	Isomers of trans-p-Coumaric acid
29	8.25	$C_9H_8O_2$	147.04515	118.98；102.93；90.89	cinnamic acid
30	7.47	$C_7H_6O_2$	121.02950	92.81；120.81；105.58	HBA
31	9.88	C_8H_8O	119.05024	118.88；92.79	succinic acid
32	7.78	$C_9H_8O_4$	179.03498	134.87；150.93	Caffeic acid
33	3.95	$C_9H_8O_4$	179.03498	134.81；146.91	Isomers of Caffeic acid
34	14.02	$C_{31}H_{36}O_{11}$	583.21848	421.23；289.17；451.34	Hedyotol C

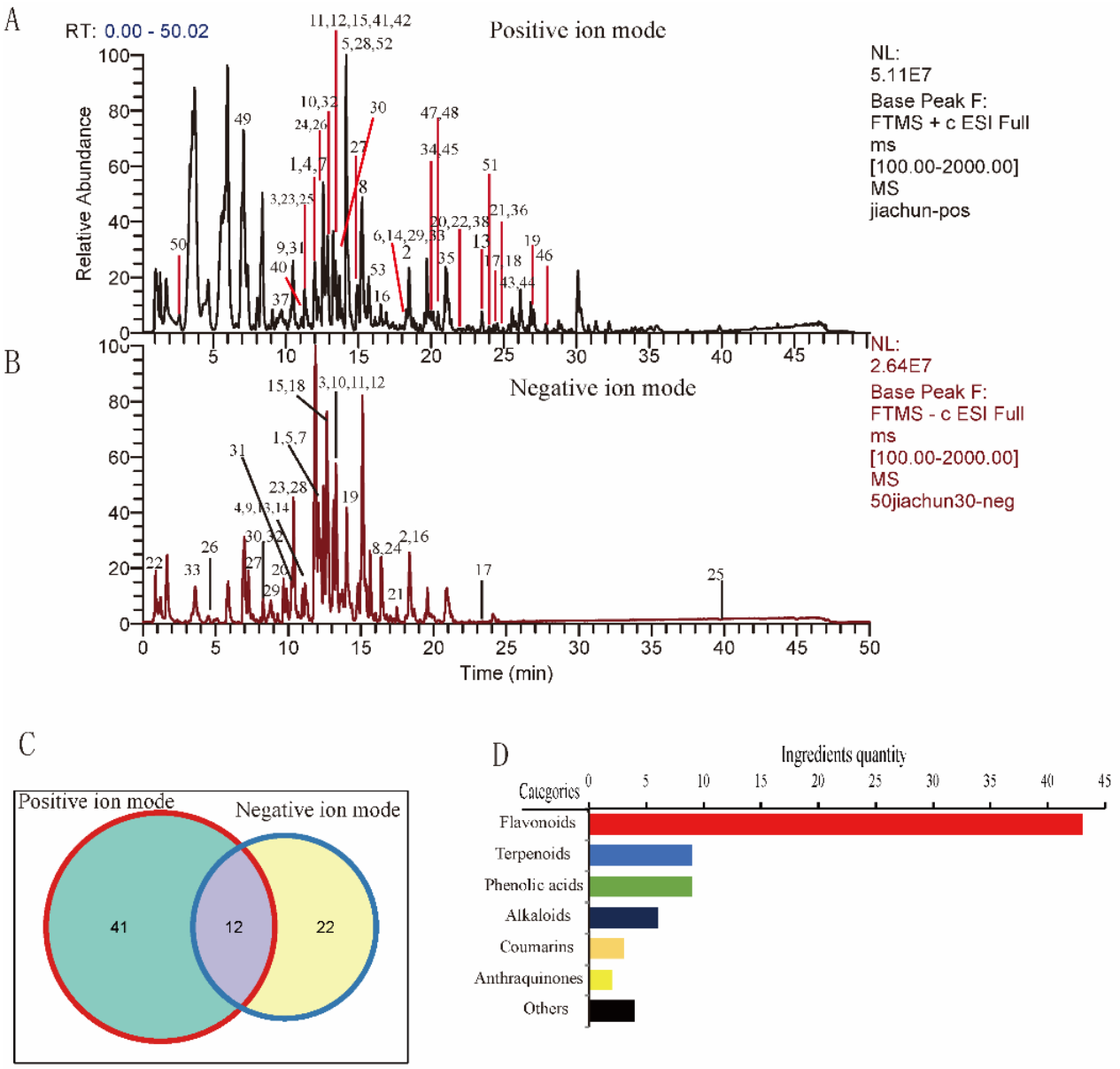


Figure 5 Main ingredients and categories

Target genes collection for SH and breast cancer

After searching and matching, 55 of 75 ingredients matched SMILES codes, while 8 ingredients that did not find matching SMILES codes, what worth noting is that SMILES represents two-dimensional ID and isomers share one SMILES code（Supplement table 1）. According to the screening rules mentioned before, 137 target genes in Swiss Target Prediction database and 106 target genes in SEA database were obtained, and 180 target genes were retained after cutting off duplicate values（Supplement table 2-4）.

A total of 1305 target genes were found for breast cancer candidate genes. 68 breast cancer targets from TTD, 198 from Drugbank, 329 from DisGeNET and 890 from GAD(Supplement 5). Targets of several databases intersect as shown in Figure 6.

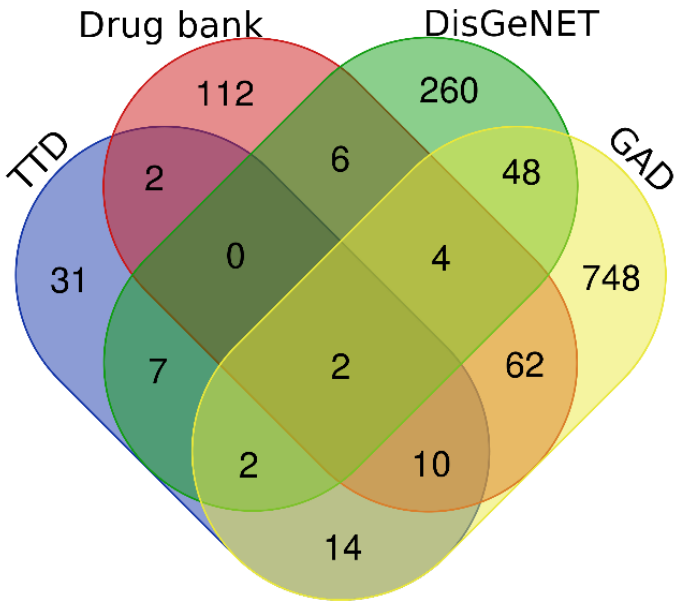


Figure 6 Venn for breast cancer target genes from different databases

Target genes mapping and network construction

Target genes were mapped for SH and breast cancer as shown in Figure 7. The PPI network of shared genes was constructed by Cytoscape3.2.1 on the basis on data from String database, as shown in Figure 8. Parameters were calculated by Network Analyzer shown in Table 5. Degree means the number of nodes directly interacting with some one node, the larger it is, the more biological functions the node participates in; Betweenness of one node means the proportion of all the shortest paths linked to this node in the network, the larger it is, the more important the node is; Closeness centrality means and average shortest path length also weigh a node in the network, the smaller they are, the more important for the node.

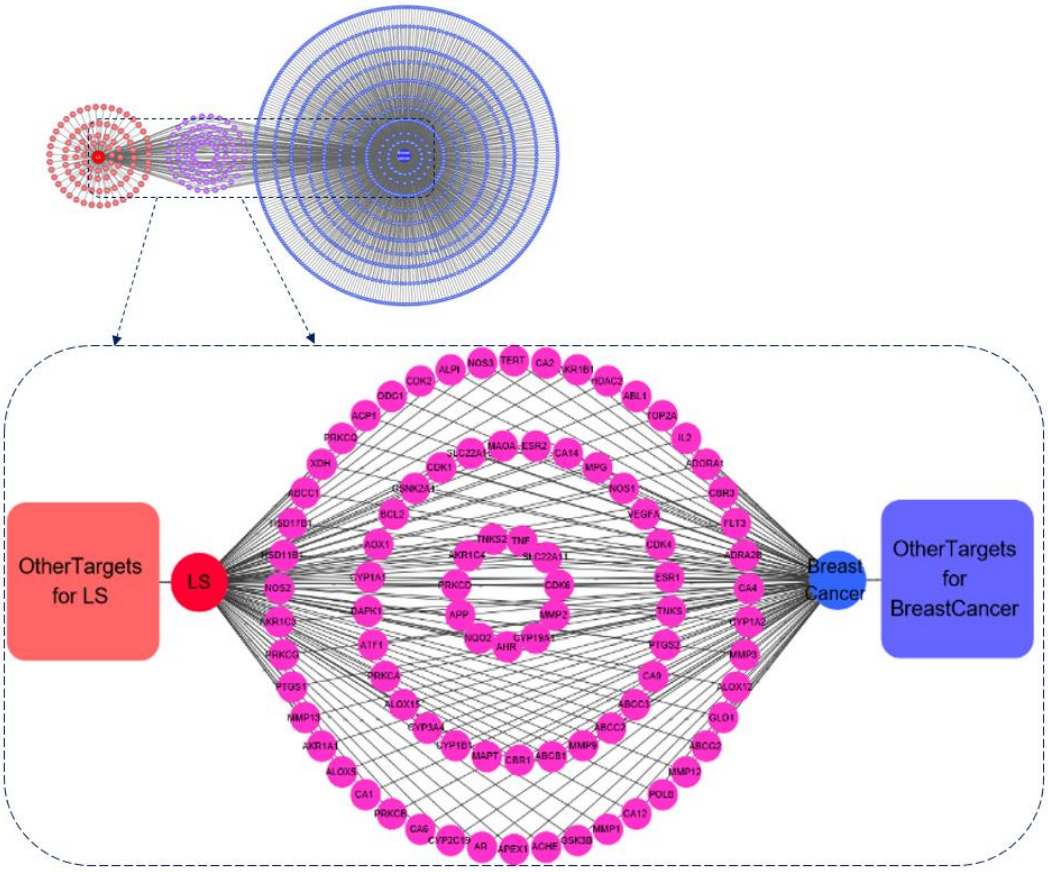


Figure 7 Target genes mapping for SH and breast cancer

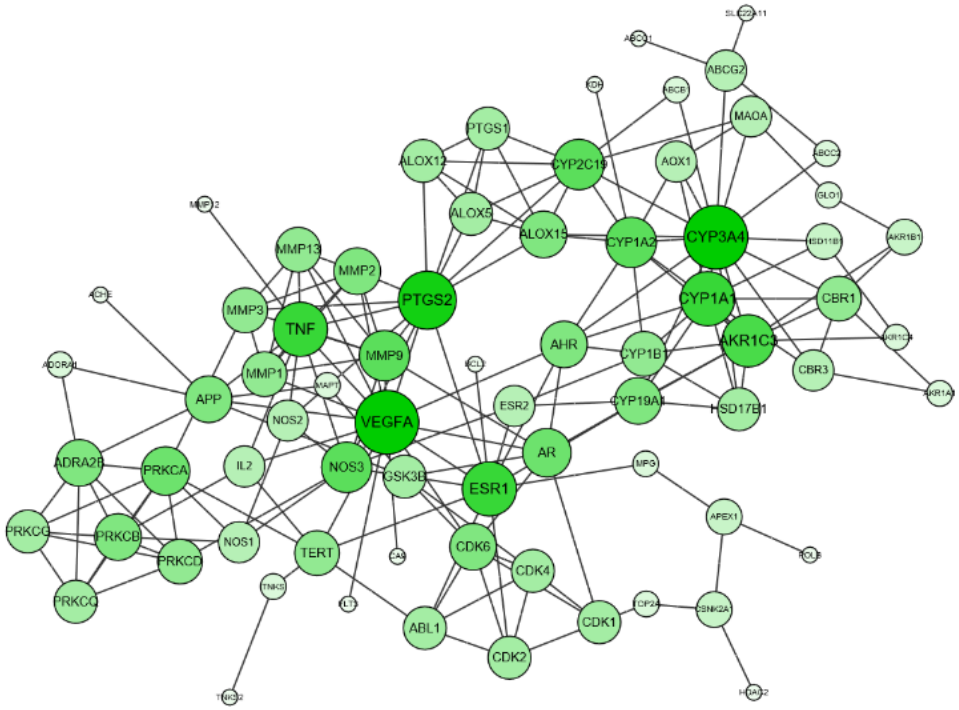


Figure 8. PPI network of shared target genes

Table 5 Parameters of genes in PPI network

Gene Name	Degree	Betweenness centrality	Closeness centrality	Average shortest path length
CYP3A4	16	0.21	0.37	2.69
VEGFA	16	0.25	0.45	2.23
PTGS2	13	0.16	0.41	2.45
CYP1A1	11	0.04	0.35	2.89
ESR1	11	0.22	0.43	2.32
TNF	11	0.05	0.36	2.76
AKR1C3	10	0.09	0.36	2.75
CYP1A2	9	0.04	0.35	2.85
CYP2C19	9	0.06	0.36	2.76
MMP9	9	0.02	0.37	2.69
NOS3	9	0.08	0.38	2.65
AR	8	0.13	0.40	2.52
PRKCA	8	0.04	0.31	3.27
ADRA2B	7	0.02	0.28	3.59
AHR	7	0.15	0.41	2.42
ALOX15	7	0.03	0.36	2.80
APP	7	0.09	0.34	2.92
CDK6	7	0.03	0.35	2.85
CYP19A1	7	0.08	0.39	2.59
MMP2	7	0.00	0.34	2.93
PRKCB	7	0.01	0.28	3.63
CBR1	6	0.02	0.29	3.39
CYP1B1	6	0.01	0.34	2.97
MMP1	6	0.00	0.33	3.06
MMP13	6	0.00	0.33	3.06
MMP3	6	0.02	0.33	3.03
PRKCD	6	0.02	0.30	3.34
TERT	6	0.09	0.36	2.79
ABL1	5	0.01	0.33	3.03
ALOX12	5	0.00	0.32	3.08
ALOX5	5	0.00	0.32	3.08

CDK1	5	0.06	0.31	3.24
CDK2	5	0.01	0.32	3.10
CDK4	5	0.01	0.29	3.49
GSK3B	5	0.03	0.32	3.15
HSD17B1	5	0.00	0.31	3.20
PRKCG	5	0.00	0.25	4.04
PRKCQ	5	0.00	0.25	4.04
PTGS1	5	0.00	0.32	3.08
ABCG2	4	0.06	0.28	3.61
AOX1	4	0.00	0.28	3.59
CBR3	4	0.01	0.28	3.59
ESR2	4	0.02	0.36	2.80
IL2	4	0.02	0.34	2.97
MAOA	4	0.02	0.30	3.38
NOS1	4	0.00	0.29	3.44
NOS2	4	0.00	0.32	3.13
AKR1B1	3	0.01	0.27	3.65
APEX1	3	0.05	0.25	4.04
CSNK2A1	3	0.03	0.21	4.70
HSD11B1	3	0.00	0.28	3.62
ABCB1	2	0.00	0.29	3.44
ABCC2	2	0.00	0.28	3.63
ADORA1	2	0.00	0.26	3.79
AKR1A1	2	0.00	0.23	4.37
AKR1C4	2	0.00	0.27	3.70
GLO1	2	0.00	0.24	4.14
MAPT	2	0.00	0.27	3.65
MPG	2	0.08	0.31	3.18
TNKS	2	0.03	0.27	3.75
TOP2A	2	0.03	0.24	4.10
ABCC1	1	0.00	0.22	4.59
ACHE	1	0.00	0.26	3.90
BCL2	1	0.00	0.30	3.31
CA9	1	0.00	0.31	3.21
FLT3	1	0.00	0.31	3.21
HDAC2	1	0.00	0.18	5.69
MMP12	1	0.00	0.27	3.75
POLB	1	0.00	0.20	5.03
SLC22A11	1	0.00	0.22	4.59
TNKS2	1	0.00	0.21	4.73

Pathway enrichment and analysis

Kyoto Encyclopedia of Genes and Genomes (KEGG) functional annotation clusters were acquired from String database (Supplement table 6). To visualize top 30 pathways with bubble diagram (Figure 9).

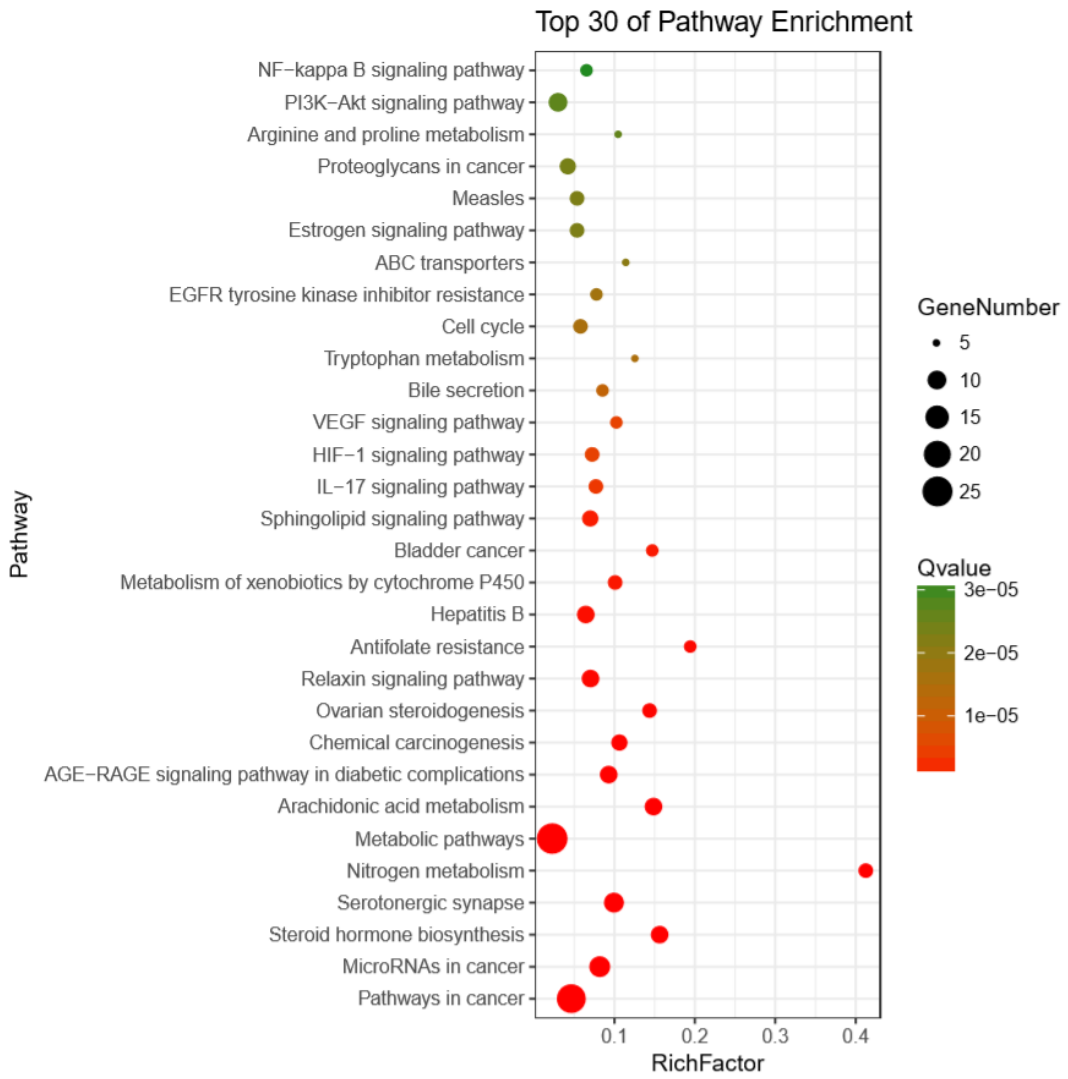


Figure 9 Top 30 KEGG pathways

Discussion:

This study evaluated the efficacy of SH lyophilized powder on human-derived and mouse-derived breast cancer cells *in vitro*. Besides, some key genes and many potential pathways were found through PPI network construction of intersection genes. Key genes like BCL-2 is one of the most important oncogenes in apoptotic research, similarly, 7 cell cycle related genes were mapped ABL1,CDK1,CDK2,CDK4,CDK6,GSK3B,HDAC2, as we all know that cell apoptosis and cell cycle are the most common drug effects, which can be considered as the preferred experiment validation. Some enriched pathways are widely discussed in cancer. Studies have shown that NF-KB can play an anti-apoptotic role in breast cancer, and it is related to the antibody of estrogen and progesterone and the expression of HER-2 gene in breast cancer[19].In addition, relevant studies have confirmed that [20-22] in some kinds of breast cancer cells, sustained activation of NF-KB was found. By inhibiting the activation of NF-KB, the sensitivity of breast cancer cells to anthracycline drugs could be reversed, further, migration and invasion of TNF-alpha-mediated breast cancer cells could be inhibited. Vascular endothelial growth factor (VEGF) is a highly sensitive marker of malignant tumours[23, 24]. It not only promotes the formation of blood vessels in breast tumours, but also promotes the metastasis of tumours through lymphatic channels [25]. Micro RNA in cancer is getting widely studied and discussed in recent years, it plays a major role in gene expression modulation and controlling major pathways. Dysregulation in micro RNA expression is associated with cancers [26, 27] and can act as promotor (oncomiR) or suppressors of tumorigenesis (antioncomiR) [28], miRNAs have been dysregulated in breast cancer as shown by profiling breast tissues from healthy individuals and those from breast cancer patients [29],they appear to be ideal biomarkers for diagnosis, follow-up, and prognosis prediction of cancer patients[30].

About SH form evolution, we all know that Chinese medicine come from herbs, process into slices and taken as decoction, however, due to too much large particles in the decoction, making it hard to be filtrated by 0.22um membrane. Derived from SH decoction and closest to the original state of TCM decoction, lyophilized powder is an indispensable form for cell experiments *in vitro*.

Target genes in TTD and Drug Bank were drug-validated, target genes in DisGeNET came from published literatures. GAD is a relatively primitive database with comprehensive content, which can complement the above verified targets. As figure 9 shows: several databases can not cover each other for the main direction each database is different, as network discussion, as comprehensive as possible target genes are necessary, so we took sum aggregate of these four databases for mapping and further discussion.

There are several limitations of the study: (i) It is unclear the efficiency proportion and possible side effects of each ingredient.(ii) There were only cell experiments for efficacy evaluation. (iii) Different target prediction and enrichment tools presented different results and even with visualized results of pathways, we have no idea of activation or inhibition effects, so further validations are essential. The efficacy validation of SH on nude mice model of triple-negative breast cancer and key proteins experimental validations such as cell cycle and apoptosis, EGFR pathway are two main parts of our present work. After that, precise efficacy of each ingredient is a long journey in the future.

In conclusion, SH plays an efficacy enhancing role in the treatment of breast cancer in accordance with detoxification principle in TCM. To our knowledge, Chinese medicine compatibilities sharing the same treating principle have the same or similar functions with different herbs, but the curative effects are imprecise from one herb to another for species diversity, better prescriptions with more definite efficacy will be optimized with the visualization process and validation of active ingredients, targets and pathways by network pharmacology.

References:

[1]Swarup AB, Barrett W, Jazieh AR. (2006) . The use of complementary and alternative medicine by cancer patients undergoing radiation therapy. Am J Clin Oncol 2006; 29(5): 468-473.

[2]Hyodo I, Amano N, Eguchi K, Narabayashi M, Imanishi J, Hirai M, Nakano T, Takashima S. (2005).Nationwide survey on complementary and alternative medicine in cancer patients in Japan. J Clin Oncol 2005; 23(12): 2645-2654.

[3]Evans MA, Shaw AR, Sharp DJ, Thompson EA, Falk S, Turton P, Thompson T. (2007).Men with cancer: is their use of complementary and alternative medicine a response to needs unmet by conventional care? Eur J Cancer Care (Engl) 2007; 16(6): 517-525.

[4]Yeh YC, Chen HY, Yang SH, Lin YH, Chiu JH, Lin YH, Chen JL. (2014).Hedyotis diffusa Combined with Scutellaria barbata Are the Core Treatment of Chinese Herbal Medicine Used for Breast Cancer Patients: A Population-Based Study. Evid Based Complement Alternat Med 2014; 2014: 202378.

[5]Hopkins AL. Network pharmacology: the next paradigm in drug discovery. (2008).Nat Chem Biol 2008; 4(11): 682-690.

[6]Li S, Zhang B. (2013).Traditional Chinese medicine network pharmacology: theory, methodology and application. Chin J Nat Med 2013; 11(2): 110-120.

[7]Wang N, Yang B, Zhang X, Wang S, Zheng Y, Li X, Liu S, Pan H, Li Y, Huang Z, Zhang F, Wang Z. (2018).Network Pharmacology-Based Validation of Caveolin-1 as a Key Mediator of Ai Du Qing Inhibition of Drug Resistance in Breast Cancer. Front Pharmacol 2018; 9: 1106.

[8]Gao L, Wang XD, Niu YY, Duan DD, Yang X, Hao J, Zhu CH, Chen D, Wang KX, Qin XM, Wu XZ. (2016).Molecular targets of Chinese herbs: a clinical study of hepatoma based on network pharmacology. Sci Rep 2016; 6: 24944.

[9]Yue SJ, Xin LT, Fan YC, Li SJ, Tang YP, Duan JA, Guan HS, Wang CY. (2017).Herb pair Danggui-Honghua: mechanisms underlying blood stasis syndrome by system pharmacology approach. Sci Rep 2017; 7: 40318.

[10]Gao L, Wang KX, Zhou YZ, Fang JS, Qin XM, Du GH. (2018).Uncovering the anticancer mechanism of Compound Kushen Injection against HCC by integrating quantitative analysis, network analysis and experimental validation. Sci Rep 2018; 8(1): 624.

[11]Kim S, Chen J, Cheng T, Gindulyte A, He J, He S, Li Q, Shoemaker BA, Thiessen PA, Yu B, Zaslavsky L, Zhang J, Bolton EE. (2019).PubChem 2019 update: improved access to chemical data. Nucleic Acids Res 2019; 47(D1): D1102-D1109.

[12]Gfeller D, Grosdidier A, Wirth M, Daina A, Michielin O, Zoete V. (2014).SwissTargetPrediction: a web server for target prediction of bioactive small molecules. Nucleic Acids Res 2014; 42(Web Server issue): W32-W38.

[13]Keiser MJ, Roth BL, Armbruster BN, Ernsberger P, Irwin JJ, Shoichet BK. (2007).Relating protein pharmacology by ligand chemistry. Nat Biotechnol 2007; 25(2): 197-206.

[14]Li YH, Yu CY, Li XX, Zhang P, Tang J, Yang Q, Fu T, Zhang X, Cui X, Tu G, Zhang Y, Li S, Yang F, Sun Q, Qin C, Zeng X, Chen Z, Chen YZ, Zhu F. (2018).Therapeutic target database update 2018: enriched resource for facilitating bench-to-clinic research of targeted therapeutics. Nucleic Acids Res 2018; 46(D1): D1121-D1127.

[15]Wishart DS, Feunang YD, Guo AC, Lo EJ, Marcu A, Grant JR, Sajed T, Johnson D, Li C, Sayeeda Z, Assempour N, Iynkkaran I, Liu Y, Maciejewski A, Gale N, Wilson A, Chin L, Cummings R, Le D, Pon A, Knox C, Wilson M. (2018).DrugBank 5.0: a major update to the DrugBank database for 2018. Nucleic Acids Res 2018; 46(D1): D1074-D1082.

[16]Pinero J, Bravo A, Queralt-Rosinach N, Gutierrez-Sacristan A, Deu-Pons J, Centeno E, Garcia-Garcia J, Sanz F, Furlong LI. (2017).DisGeNET: a comprehensive platform integrating information on human disease-associated genes and variants. Nucleic Acids Res 2017; 45(D1): D833-D839.

[17]Shannon P, Markiel A, Ozier O, Baliga NS, Wang JT, Ramage D, Amin N, Schwikowski B, Ideker T. (2003).Cytoscape: a software environment for integrated models of biomolecular interaction networks. Genome Res 2003; 13(11): 2498-2504.

[18]Szklarczyk D, Gable AL, Lyon D, Junge A, Wyder S, Huerta-Cepas J, Simonovic M, Doncheva NT, Morris JH, Bork P, Jensen LJ, Mering CV. (2019).STRING v11: protein-protein association networks with increased coverage, supporting functional discovery in genome-wide experimental datasets. Nucleic Acids Res 2019; 47(D1): D607-D613.

[19]Biswas DK, Shi Q, Baily S, Strickland I, Ghosh S, Pardee AB, Iglehart JD. (2004).NF-kappa B activation in human breast cancer specimens and its role in cell proliferation and apoptosis. Proc Natl Acad Sci U S A 2004; 101(27): 10137-10142.

[20]Choi YK, Cho SG, Woo SM, Yun YJ, Jo J, Kim W, Shin YC, Ko SG. (2013).Saussurea lappa Clarke-Derived Costunolide Prevents TNF alpha -Induced Breast Cancer Cell Migration and Invasion by Inhibiting NF- kappa B Activity. Evid Based Complement Alternat Med 2013; 2013: 936257.

[21]Zong H, Wang F, Fan QX, Wang LX. (2012).Curcumin inhibits metastatic progression of breast cancer cell through suppression of urokinase-type plasminogen activator by NF-kappa B signaling pathways. Mol Biol Rep 2012; 39(4): 4803-4808.

[22]Connelly L, Barham W, Onishko HM, Sherrill T, Chodosh LA, Blackwell TS, Yull FE. (2011).Inhibition of NF-kappa B activity in mammary epithelium increases tumor latency and decreases tumor burden. Oncogene 2011; 30(12): 1402-1412.

[23]Reiter MJ, Costello JE, Schwope RB, Lisanti CJ, Osswald MB. (2015).Review of Commonly Used Serum Tumor Markers and Their Relevance for Image Interpretation. J Comput Assist Tomogr 2015; 39(6): 825-834.

[24]Sharma G, Mirza S, Parshad R, Srivastava A, Gupta SD, Pandya P, Ralhan R. (2011).Clinical significance of Maspin promoter methylation and loss of its protein expression in invasive ductal breast carcinoma: correlation with VEGF-A and MTA1 expression. Tumour Biol 2011; 32(1): 23-32.

[25]Cohen-Kaplan V, Naroditsky I, Zetser A, Ilan N, Vlodavsky I, Doweck I. (2008).Heparanase induces VEGF C and facilitates tumor lymphangiogenesis. Int J Cancer 2008; 123(11): 2566-2573.

[26]Mendell JT, Olson EN. (2012).MicroRNAs in stress signaling and human disease. Cell 2012; 148(6): 1172-1187.

[27]Song S, Ajani JA. (2013).The role of microRNAs in cancers of the upper gastrointestinal tract. Nat Rev Gastroenterol Hepatol 2013; 10(2): 109-118.

[28]Svoronos AA, Engelman DM, Slack FJ. (2016).OncomiR or Tumor Suppressor? The Duplicity of MicroRNAs in Cancer. Cancer Res 2016; 76(13): 3666-3670.

[29]Hamam R, Hamam D, Alsaleh KA, Kassem M, Zaher W, Alfayez M, Aldahmash A, Alajez NM. (2017).Circulating microRNAs in breast cancer: novel diagnostic and prognostic biomarkers. Cell Death Dis 2017; 8(9): e3045.

[30]van Schooneveld E, Wouters MC, Van der Auwera I, Peeters DJ, Wildiers H, Van Dam PA, Vergote I, Vermeulen PB, Dirix LY, Van Laere SJ. (2012).Expression profiling of cancerous and normal breast tissues identifies microRNAs that are differentially expressed in serum from patients with (metastatic) breast cancer and healthy volunteers. Breast Cancer Res 2012; 14(1): R34.

International Conference on Cancer Research 2019

Website: www.CancerConf.org

June 10-11, London, UK



Breast Cancer Multi-Therapy and Immune System Activation, Checkpoint Modulators, Signal Inhibitors and T Cells Reprogramming

Miguel A Galván Morales [1], Raúl Barrera Rodríguez [2], Julio R. Santiago Cruz [3], Luis M Terán Juárez [4*]

[1] *Dept. of Immunogenetics and Allergy. National Institute of Respiratory Diseases. Calzada de Tlalpan 4502, Colonia Sección XVI, Delegación Tlalpan, 14080, Mexico City.*

[2] *Dept. Chronic Degenerative Diseases, Lab. Autoimmunity. National Institute of Respiratory Diseases. Mexico City.*

[3] *Laboratory of Autoimmunity, National Institute of Respiratory Diseases, Mexico. City, 14080. Department of Microbiology and Parasitology, Faculty of Medicine, National Autonomous University of México, México City.*

[4] *Dept. of Immunogenetics and Allergy. National Institute of Respiratory Diseases, 14080, Mexico City,.*

** Corresponding author: teranjlm@gmail.com, lmteran@iner.gob.mx*

Abstract

Cancer is one of the leading causes of death worldwide according to data from the U.S. National Cancer Institute, with approximately 14 million new cases and 8.2 million of cancer-related deaths in 2018. More than 60% of the new annual cases in the world occur in Africa, Asia, Central America, and South America, with 70% of cancer deaths in these regions. Recently they have been used for breast cancer, novel approaches among which several molecules that block signaling pathways and also reactivate the immune system by inhibiting the activities of two lymphocytes T receptor inhibitors; CTLA-4 and PD-1 in triple negative breast cancer. Although there is evidence, which supports the blocking of these inhibitory molecules, reactive the response of T cells does not always result, surely because in addition to need to reactivate the response Th1 is necessary co-activation of killer cells Natural (NK), the latter are the main actors of the anticancer response. Therefore, combining therapies with the coordinated activation of each cell of the immune response involved will probably produce better results. Through a better understanding of the interactions of the Th1 response and the action of the inhibitors of PD-1 and CTLA-4 and the intratumoral microenvironment, we believe that it would improve breast cancer therapy. In this article, recent advances in the treatment of cancer aimed at blocking signaling pathways and the use of monoclonal antibodies directed to receptors were reviewed. Likewise, it is proposed to combine therapies with antibodies that block PD-1 and CTLA-4 with the activation of the Th1 and NK response, in situ or with extracorporeal activation of autologous cells.

Keywords:

Breast cancer,

Immunotherapy,

EGFR,

PD-1,

CTLA-4,

Signal transduction inhibitors.

1. Introduction

In 2018, the National Cancer Institute declared 1,735,350 new cases of cancer in the United States, with 609,640 cancer deaths.[1] The most common types of cancer from 2016-2018 were breast cancer, lung cancer, prostate cancer, and colorectal cancer, followed by bladder cancer, melanoma, non-Hodgkin lymphoma, thyroid cancer, kidney cancer, and renal pelvis. The GLOBOCAN Annual Report shows that from 2002 to 2011 the mortality rate for most cancers decreased by approximately 1.8 percent per year among men, and 1.4 percent per year among women.[2] Therefore, although the mortality of most cancers in some countries has declined, the global incidence continues to grow and, according to current projections, cancer deaths will increase from 7.6 million in 2008 to 13 million in 2030. However, the development of new approaches for previous therapies and the success of new therapies, including immunotherapy, is expected to gradually reduce cancer mortality rates for the next decades. Breast cancer is the most common cancer in women, with 266,120 new cases in American women, and an estimated 40,920 deaths for 2018. Approximately one in six women diagnosed with breast cancer will die in the coming years. It is the main cause of cancer-related death in women in developing countries, and it is the second-leading cause in women in developed countries.[3] Mortality rates

are influenced by the occurrence of the disease, and the availability of screening programs and appropriate treatment. Despite lower breast cancer incidence, breast cancer mortality rates are higher in many developing countries because of advanced disease at presentation, suboptimal access to treatment, more aggressive biological subtypes, and younger age at diagnosis. In recent years a number of major medical advances have improved the treatment of primary breast cancer.[4] In the last decade, a great step forward has been taken with the discovery of molecular markers in breast cancer, originating "targeted therapies against cancer". Targeted therapies are drugs or other substances that block or inhibit specific molecules involved in cancer growth, progression and spread, specifically targeted to receptors and signaling pathways.

2. The immune system and cancer

The immune system has three main functions: to distinguish between the self and the exogenous, or in other words the immune system must be able to distinguish what is nonself (foreign) from what is self, to contain external invading agents (pathogens, molecules, etc.) and to destroy abnormal cells such as cancer cells. It is known that many tumors escape immune detection due to several factors such as a) lack of recognition of the HLA antigen, b) altered co-receptors that prevent their recognition and c) T cell anergy or natural killer (NK) cells that allow or promote the development of cancer through "immunoediting". Thus, many of the new anti-cancer strategies aim to redirect immune protection against these abnormal cells .[5] It should be noted that the adoptive immunotherapy treatment based on antibodies has not developed as dramatically as expected, due to the lack of specific markers in the tumors. However, inhibitors of several signaling pathways or antibodies that block receptors, such as blocking antigen 4 activity of cytotoxic T lymphocytes (CTLA-4) and programmed death protein 1 (PD-1) are being used to activate the antitumor response of T cells, with good results.[6] Therefore, for a more efficient antitumor response, it will probably be necessary to increase the degree of activation of the immune system, which could be achieved through the stimulation of cytotoxic T lymphocytes (CTL) and natural killer cells (NK), stimulated with cytokines such as: interleukin (IL)-2, interferon (IFN)-γ, tumor necrosis factor (TNF)-α and (IL)-12, plus the presentation of extracorporeal antigen.[7] This review highlights recent therapeutic approaches and their effectiveness for one of the most common cancers. Immunotherapy plus the use of specific inhibitors, the recent experience with new approaches to chemotherapy, and finally an evaluation of the effectiveness of therapies directed against cancer. Likewise, we make a treatment proposal, which contemplates reactivating the immune system: 1) Treating the explanted tumor cells of the patient *in vitro* with IFN-γ, IL-2 and TNF-α, confronting them with autologous T cells ($CD4^+$ and $CD8^+$) and NK cells ($CD56^{bright}$, $CD16^{dim}$), to subsequently reincorporate the reactivated T cells to the patient; and , 2) Treating the cells of the tumor explant with Th1 cytokines (IL-2 IFN-γ and TNF-α) IL-15, IL-22, and IL-23 and then encapsulate these in nanotubes or a material of the type used in hormone implants (pellets), to prevent the escape of tumor cells. Afterward, the encapsulated tumor will be implanted in the patient, to reactivate the immune response.

3. Anti-EGFR antibody therapy in breast cancer

The greatest impact in the treatment against breast cancer arose with the discovery of the over-expression of the HER-2 surface protein in some tumors. This transmembrane protein is a member of the human epidermal growth factor receptor family (HER/EGFR/ERBB). As an oncogene, it plays a crucial role in the development and progression of some aggressive breast cancers, such as invasive lobular carcinoma (ILC) or ductal carcinoma *in situ* (DCIS). In recent years, this protein has become an important biomarker of breast cancer, and about 30% of patients respond to therapy directed against this molecule.[8] The humanized monoclonal antibody (HuMab) trastuzumab (Herceptin®) recognizes the HER-2 receptor. The binding of trastuzumab to HER-2 promotes the increase of the p27kip1 protein that, in turn, stops cell proliferation.[9,10] Conceivably, treatment with trastuzumab is more effective if combined with surgery and chemotherapy.[11] Another HuMab used in breast cancer treatment is pertuzumab (Perjeta®) that inhibits dimerization of HER-2 and HER-3; it is used in combination with trastuzumab as neoadjuvant therapy for breast cancer at an early stage and, recently, also as adjuvant therapy to treat tumors in advanced stages (**Figure 1** and **Table 1**).[12] Unfortunately, a group of breast cancer tumors does not respond to treatment with HuMab anti-HER-2, and it comprises almost 70% of the cases. These tumors are classified into two categories according to their phenotype: 1) Tumors that do not express HER protein-2 ($HER\text{-}2^-$), but express hormone receptors (HR^+), such as estrogen receptor positive (ER^+), and progesterone receptor positive (PR^+); and 2) tumors that do not express HER-2, or hormone receptors, called triple negative (TNBC).[13,14] It should be noted that TNBCs are very aggressive and the number of treatment options limited, therefore, many new therapies are currently being investigated.[15] Additionally, in these tumors, heterogeneity makes specific biomarkers that may serve as target molecules for targeted therapies difficult to identify., Preclinical studies of these tumors have also identified several potential targets such as Src kinase, tyrosine-protein kinase Met (MET) and Poly [ADP-ribose] polymerase 1 and 2 (PARP-1/2).[16] Therapeutic agents such as bevacizumab (Avastin®), ranibizumab (Lucentis®) and aflibercept (Zaltrap®) (directed against vascular endothelial growth factor [VEGF]), have become elected treatments for retinal neovascular disorders, but their use in breast cancer treatment in combination with chemotherapy is increasing.[17] Some authorized combinations consist only on the use of standard chemotherapy and antibodies such as bevacizumab, even though they do not produce the expected results, mainly in metastatic breast cancer (MBC). Other neoadjuvant drugs such as gemcitabine, capecitabine, docetaxel, doxorubicin, and

cyclophosphamide have also been tested in several combinations with bevacizumab.[18] Unfortunately, these combinations have shown not too many benefits in TNBC patients.[19,20] Breast tumors that do not overexpress HER-2 could be treated by combining antibodies against EGFR, more inhibitors for other target molecules (such as PARP-1) and chemotherapy. Additionally, stimulation of antitumor immune activators such as cell-mediated cytotoxicity (ADCC) before or after surgery could prove to be a useful treatment. To obtain an effective anti-tumor immune response, the state of lymphocyte activation during treatment must be determined, since the success of the treatment depends on it.[20] The binding of several antibodies directed to specific molecules in tumor cells that act as target molecules of the immunotherapy, as well as their combinations according to the type of tumor are depicted in **Figure 1** and listed in **Table 1**.

Table 1. Molecular targeted therapy in Breast Cancer treatment.

	Approved agents	Molecular targets	Mechanism of action	Ref.
Monoclonal antibody	***Trastuzumab*** (Herceptin®)	HER2, HER3	RAS/Raf/MAPK Inhibition	9, 10, 21, 22, 70
	Pertuzumab (Perjeta®)	EGFR y HER4		12, 13, 21, 70
	Bevacizumab (Avastin®)	VEGF	VEGFR PI3K, PLCγ prevents neovascularization	17, 18
	Ranibizumab (Lucentis®)			17
	Aflibercept (Zaltrap®)			17, 19
	Cetuximab (Erbitux®)	EGFR	PI3K, RAS, STAT signaling inhibition	21, 24-26
	Panitumumab (Vectibix®)			27
Antibody-drug conjugate	***T-DM1***	HER2	Cytotoxic agent vinca alkaloid RAS/Raf/MAPK	70
	Vinorelbine- (Navelbine®)			
	Trastuzumab (Herceptin®)			22
Inhibitors conjugate	**Fulvestrant-Palbociclib** (Ibrance®)	HR+(HER2-)	CDK) 4/6 inhibitor	22, 71
	Palbociclib-Letrozole (Femara®)	(ER) Estrogen receptor positive	Cell cycle arrest	71
Signal transduction inhibitors				
Inhibitors	**Iniparib** (Sanofi® BSI 201)	BRCA1 or BRCA2 mutation.	Not repair their DNA	30, 40
	Talazoparib (BMN-673)			30
	Niraparib (Tesaro®)			34
	Olaparib (Lynparza® AZD-2281			31, 45

PARP-1/2	y TOPARP-A)	PARP-1 selective inhibitor		
	Rucaparib (AG014699, PF-01367338)			35
	Veliparib (ABT-888)			36
Preclinical studies phase 1 of Inhibitors PARP-1/2	CEP-9722	PARP-1/2 inhibitor	Not repair their DNA	37
	MK-4827			32
	MK-2206			38
	NMS-P118			39
Tyrosine Kinase Inhibitors	**Dasatinib** (Sprycel®)	Multiple tyrosine kinases (TK)	Bcr/Abl, Src, c-Kit and Eph receptor family	41
	Saracatinib (AZD0530)	Src protein	Src inhibitor Bcr/Abl	42
	Imatinib (Gleevec®)	Geminina y c-Abl nuclear	Inhibitor Geminina y c-Abl nuclear	43
	Nilotinib (Tasigna®)	Abl tyrosine kinases	Bcr/Abl	72
	Lapatinib (Tykerb®)	TK receptor		11, 44
	Palbociclib (Ibrance®) **Ribociclib** (Kisqali®)	Inhibitor kinases (CDK4,6)	Cell cycle	22, 71
	MK-2206	AKT inhibitors	Cell cycle arrest	38
	Vemurafenib (Zelboraf®)	inhibits the enzyme B-Raf. Serine/threonine-specific protein kinase	BRAF serine/threonine kinase inhibitor	60, 61
	Cobimetinib (Cotellic®)	MEK1 protein kinase	Inhibits the activity of ERK2 transcriptional	60, 61
Immunomodulators	**Nivolumab** (Opdivo®)	PD-1	Blocks ligands PD-L1 and PD-L2	49, 57, 59
	Pembrolizumab (Keytruda®)			55
	Durvalumab (Imfinzi®)	PD-L1	Block activation of PD1	56
	Atezolizumab (Tecentriq®)			57
	Avelumab			58

	(Bavencio®)			
	Ipilimumab (Yervoy®)	CTLA-4	B7-1/2	55
	Tremelimumab			56
TKIs	Afatinib Erlotinib Gefitinib Dacomitinib Neratinib Sorafenib Alectinib	EGFR, HER2 y ErbB-4, VEGFR	PI3K/Akt/	42 60, 61
	Crizotinib Ceritinib	competitive inhibitor Akt	ALK-fusión	

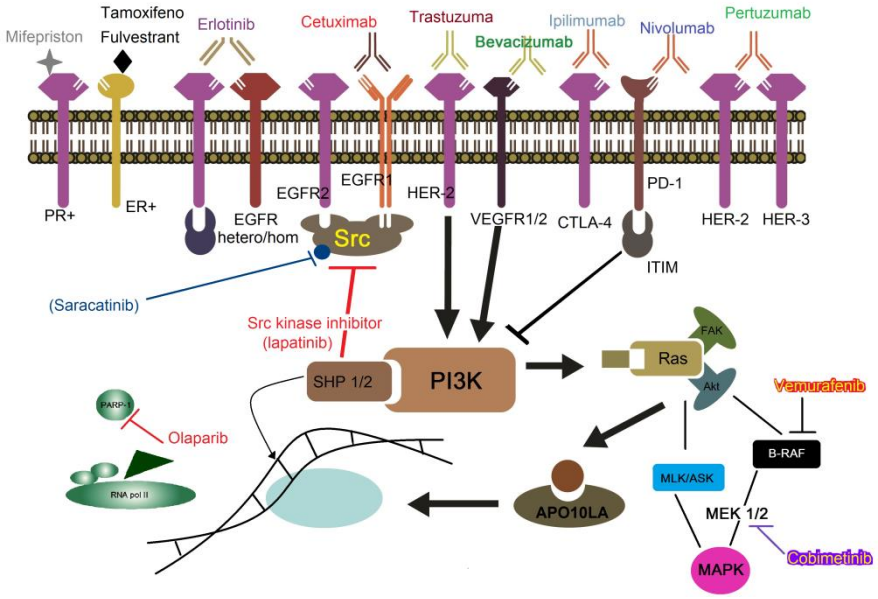


Figure 1. Tumoral receptors targeted for immune therapy. From right to left, HER-2 and HER-3 receptors which have a strong tendency to dimerize in cancer, *Pertuzumab* (green). Antibodies colored in blue are *Nivolumab* (anti-PD-1) and *Ipilimumab* (anti-CTLA-4),. *Bervacizumab* (dark green). HER-2 receptor is blocked by *Trastuzumab* (brown),. *Cetuximab* (red) is an antibody directed to EGFR that inhibits signal transduction for cell growth. Other mAbs similar are: *Rituximab*, *Bevacizumab* and *Ranibizumab*). Erlotinib (purple) is a drug that prevents dimerization of EGFR receptors from heterodimer to homodimer. Tamoxifen and Fulvestrant (black) can inactivate estrogen action by their competitive antagonism,. Mifepristone (gray) is an antagonist of the progesterone receptor, to be used in PR-dependent breast cancers. Lapatinib (red) is an inhibitor of tyrosine kinase from EGFR (ErbB1) and HER2 (ErbB2) receptors. Other inhibitors such as Saracatinib, Bosutinib or Dasatinib have also been used to avoid signaling on MAPK and PI3K pathway through Src or dimerization of Bcr-Abl tyrosine-kinase. Olaparib, is a molecule that inhibits PARP1. Cobimetinib is a reversible inhibitor of MEK that blocks MAPK's (yellow with purple) and Vemurafenib (red-yellow) inhibitors used for breast cancer metastatic.

For instance, the treatment of breast cancer HER-2^{+} with antibodies such as trastuzumab and pertuzumab has shown good results, while cetuximab, discussed later, is used successfully in TNCB.[21] On the other hand, the combination of vinorelbine-trastuzumab, palbociclib and fulvestrant or palbociclib and letrozole seems to be a successful therapy in MBC. Fulvestrant degrades the receptors while palbociclib for the cell cycle.[22] Regarding hormone-dependent breast tumors (HR^{+}), their treatment is tamoxifen and hormonal suppression, while the use of antibodies against the estrogen receptor α (ER-α) or another natural molecule. Like to Genistein, Isoliquiritigenin, Kurarinone, Sceptrin, Silibinin or Soranjidiol is not recommended despite the possibility of blocking ER-α by means of a humanized monoclonal antibody (similar to that of clone SP1 used for immunohistochemistry). However, it is not possible to deny the good results

obtained in the treatment with selective estrogen receptors pharmacological blockers or with aromatase inhibitors that prevent the conversion of androgens to estrogens such as tamoxifen, anastrozole, Letrozole or Exemestane.[23]

4. Other monoclonal antibodies in breast cancer treatment

Recent findings indicate that the treatment of patients with basal inflammatory type breast cancer or TNCB with anti-EGFR antibodies improves their prognosis.[24] Although predictive biomarkers in breast cancer have not yet been established, it is highly possible that EGFR expression in the three types of breast is not related to the main oncogenic factor responsible of inducing the proliferative alteration, but none the less, playing an important role in the disease and its control. Cetuximab (Erbitux®) is a chimeric monoclonal antibody (mAb) approved for the treatment of human metastatic colorectal cancer (mCRC), squamous cell carcinoma of the head and neck (HNSCC) and advanced non-small cell lung cancer (NSCLC). This mAb inhibits EGFR activation by blocking its ligand binding or hindering its interaction with other proteins (**Figure 1**).[25] Although the first clinical trials with cetuximab were costly, a new anti-EGFR mAb has been developed at a lower cost. Noticeably, their blockade with cetuximab contributes to the suppression of several signaling pathways such as JAK/STAT, Raf/MEK/ERK, and PI3K/Akt, which seems to be sufficient to inhibit the aggressive behavior in the TNCB.[26] Panitumumab (Vectibix®) is a huMab used primarily in the treatment of metastatic colorectal cancer and acts in the same way as cetruximab. Vectibix is in phase III clinical studies and is being used in combination with gemcitabine and carboplatin for treatment in women with triple negative metastatic breast cancer.[27]

5. Signal transduction inhibitors

Along with therapies targeting surface markers overexpressed as EGFR, inhibitors of PARPs have been used, along with chemotherapy based on liposomal doxorubicin (Caelyx®, Myocet®), or nanoliposomal irinotecan (Onivyde®). These treatments are recommended against TNBC (**Figure 2**).[28] Paradoxically, the effectiveness of PARPs activators relies on cancer cells undergoing oxidative stress, increasing DNA damage and depletion of cellular ATP that leads to lysis and cell death (necrosis). However, cancer therapy seeks to inhibit PARPs, because knock-out mice for PARP-1 and -2, showed profound deficiencies in the mechanisms of DNA repair, as well as greater sensitivity to ionizing radiation or alkylating agents.[29] These and others evidence allow us to propose the convenience of inhibiting PARPs as a treatment method for breast cancer. Some examples of PARP inhibitors are iniparib (Sanofi® BSI 201), talazoparib (BMN-673), olaparib (Lynparza® AZD-2281 and TOPARP-A), and niraparib (Tesaro®) (**Figure 1**).[30-34] Rucaparib (AG014699, PF-01367338) and veliparib (ABT-888) have also been used in phase III clinical trials for the treatment of breast cancer and metastatic melanoma.[35,36] Other PARP inhibitors such as CEP- 9722, MK -4827, MK-2206 and NMS-P118 are in phase I trials, some combined with chemotherapy in patients with different types of cancer *in situ* or in metastatic tumors.[37,39] In 2014, Sanofi gave up the use of iniparib after phase III trial results were reported on the "first Word pharma" portal. However, based on previous studies as well as the recent good results obtained from phase II clinical trials in metastatic breast cancer and TNBC, the use of PARP inhibitors including iniparib is being recommended as first-line treatment of these cancer types. On the other hand, inhibitors targeting Src proto-oncogene family could also be adopted for breast cancer therapy.[40] These drugs inhibit the signal transduction pathway that promotes critical processes for the development and progression of cancer such as proliferation, adhesion, invasion, migration, and tumorigenesis of cancer cells. For example, dasatinib (Sprycel® or BMS-354825), a multi-target inhibitor approved for first-line use in patients with chronic myeloid leukemia, was developed since 2006 and was authorized for use by the FDA in 2013. This drug inhibits several tyrosine kinases, including Bcr-Abl, Src, c-Kit, and the Eph receptor, but has no effect on EGFR.[41] Saracatinib (AZD-0530) is an experimental inhibitor of Src, that acts as a dual inhibitor of kinases: Src and Bcr-Abl. However, and despite several studies demonstrating its ineffectiveness against cancer, recently (2018) published articles still promote its use in cancer.[42] We previously mentioned several components participate in the development of TNCB and one of them is the over-expression of c-Abl, a tyrosine kinase that phosphorylates and activates geminin. While in the cytoplasm, c-Abl protein plays an important role in differentiation, proliferation and cell migration. Contrastingly, its translocation to the nucleus promotes apoptosis, damaged DNA repair and chromatin dynamics regulation by histones phosphorylation. In a study where 800 samples of TNBC were analyzed, overexpression of germinin was found in 90% of the cases and most of them were negative to c-Abl in the nucleus. When the activity of c-Abl was inhibited by imatinib (Gleevec®) or nilotinib (Tasigna®), the phosphorylation of geminin in the Y150 residue was prevented, inactivating it and converting the overexpressed geminin into an inducer of apoptosis.[43] Lapatinib (Tykerb®) is a tyrosine kinase inhibitor in HER-1/EGFR/ERBB1 and HER-2/ERBB2, and was authorized to be used in combination with capecitabine (Xeloda®); very good results in the treatment of metastatic breast cancer, and particularly in the treatment for ER/EGFR/HER-2 positive breast tumors that did not respond to trastuzumab, anthracyclines or taxanes.[45] Currently, immunotherapy based on antibodies is being incorporated into almost all cancer treatments. However, a combination therapy of an inhibitory mAb of any of several overexpressed markers, a PARP inhibitor such as olaparib (Lynparza®) and liposomal chemotherapy, appears to be one of the most promising combinations in the treatment against cancer (**Figure 2**).[45] For that, we propose that after surgery, therapy for mammary tumors *in situ* or metastatic should include: i) at least one PARP inhibitor (avoiding repair of DNA damage) or an Src inhibitor, ii) the use of the chemotherapy encapsulated in liposomes (i. e CAELYX®),. The application of CAELYX®, plus spores of *Clostridium* (spores of *C. novyi-NT*) in the site of the tumor or metastasis, will aid *in situ* release.[46,47] iii) Additionally,

the use of antibodies directed to target molecules that promote cell cytotoxicity and blockade in the proliferation of cancer cells together with a specific inhibitor of overexpressed receptors. Also, it is recommendable to verify the production/expression of TNF-α, IFN-γ, and IL-2. This triple approach in the treatment of breast tumors (**Figure 2**) would be a better option compared to first-line treatments with EGFR inhibitors alone or with standard chemotherapy, that have ineffective response rates. Recently, in the treatment of breast cancer and other types of tumors, treatment with nivolumab-ipilimumab (anti-PD-1 and anti-CTLA-4) has been started as an immunotherapy basis.[48,49]

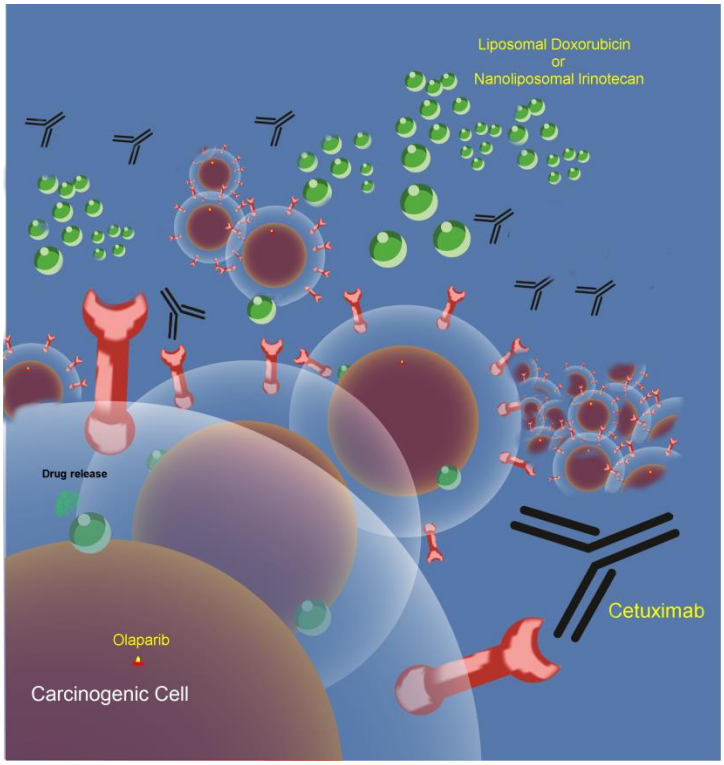


Figure 2. First-line treatment for TNBC. In personalized medicine, this treatment could be very effective since the administration of doxorubicin or irinotecan both encapsulated in liposomes (green balls) to help their delivery into the site of action and diminish their secondary effects on other tissues, which helps to avoid the patient worsening. In the larger cell, the delivery of doxorubicin (or irinotecan) can be observed. In addition to antibodies against EGFR, such as Cetuximab, a PARP-1 inhibitor, such as Olaparib, could be added to avoid cells repairing the DNA damage. The activity of the PARP-1 inhibitor potentiates the chemotherapy.

6. Reactivation of the immune response in combination with antibodies

Despite the therapeutic resources already mentioned, there are still several difficulties in the use of targeted therapies. One of the main problems is adverse effects, secondary reactions and interactions with other therapies, occasionally with altered responses. Still, breast cancer therapy with a combination of liposome-encapsulated chemotherapy, inhibitors and blocking antibodies has given a variety of responses.[50] The promising possibilities of immunotherapy in lung cancer have promoted treatment development for other cancer types. The main objective of immunotherapy is to recognize and eradicate tumors by restoring the immune capacity of the host. One interesting approach is the activation of macrophages (MΦs) with the application of retinoic acid and stimulation of NK cells with IL-15, IL-22 and IL-23 and cytotoxic T cells (CTLs) stimulated with IL-2, TNF-α, IFN-γ, plus the presentation of the antigen. One further step in cancer therapy could be depletion or maintenance of the Treg/Th17 cells balance.[51,52] So, an approach that we propose to boost the anticancer response of the immune system is to "tag" cancer cells with specific antibodies, activate both the antigen presentation and lymphocytes with cytokines or IFN-α, TNF-α, IL-2, IFN-γ and IL-12 (Th1). To minimize the promoted attack, if not physiologically stopped, the IL-10, TGF-β and autologous regulatory T cells (Treg) would be applied to restore equilibrium (**Figure 3B**).[53] In an experimental proposal, autologous $CD4^+$ T cells could be robustly polarized *in vitro* towards Th1 and Th17 subtypes, through cytokines and chemokines, to subsequently identify their activation with molecular adhesion profiles and surface markers, which will open the possibility of detecting effector function *in vitro* and then *in vivo* to treat cancer. Th1 response is generally considered as the main source of tumor rejection, but there is also evidence that Th17-polarized cells mediate the destruction of advanced B16 melanoma.[54] The Th1 therapeutic effect critically depends on the production of IFN-γ, while apparently; depletion of IL-17A and IL-23 has little impact. Visibly,

the appropriate *in vitro* polarization of the effector $CD4^+$ T cells could be decisive for the elimination of the tumor; design of preclinical and clinical trials should consider this therapy based on *in vitro* stimulation of the response and posterior transferring of these immune cells, capable of recognizing the tumor *in vivo*, back to the original tumor (**Figure 3 A**).

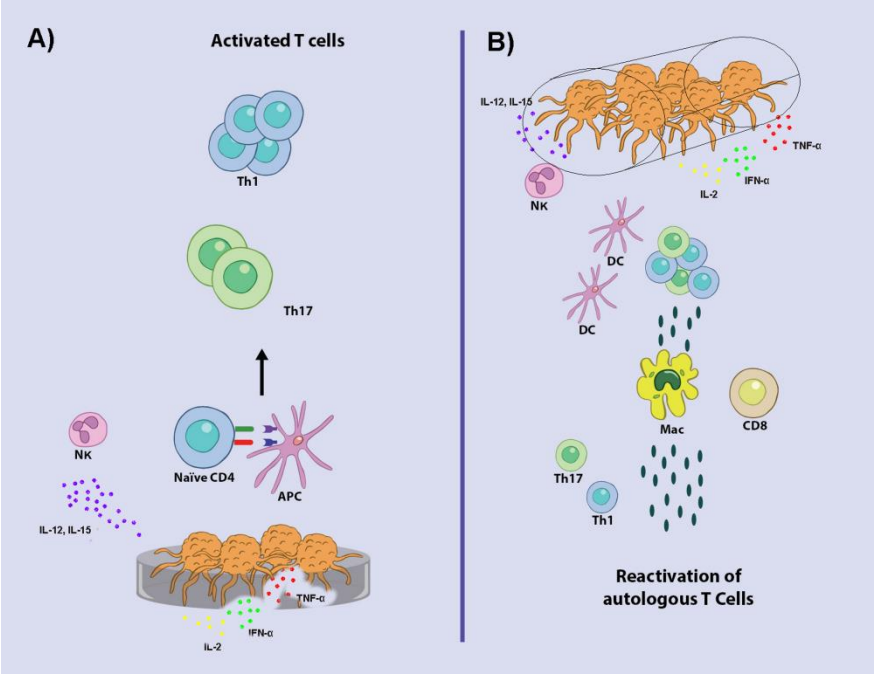


Figure 3

Figure 3. Extracorporal activation of autologous cells to stimulate Th1 and NK responses. A) Several lineages of bystander immune cells are obtained from the cancer patient to be activated. T cells are challenged with chimeric antigens. Further, the experimental in vitro boost of tumoral cells with NK cells and T cells costimulated with interleukin accordingly to the lineage for the maturation and differentiation of immune cells. Later, theoretically stimulated cells are reincorporated to attack the tumor. B) The same tumoral piece can be embedded into a no-degradable synthetic polymeric tube with hexagonal holes. This encapsulated tumoral piece is going to be embedded with Th1 cytokines and chemokines: IL-2, IFN-alpha or -gamma, and TNF-alpha to activate the cell-mediated cytotoxicity, and the NK cells with IL-12, IL-15, and IL-18; for at the last reincorporate the encapsulated piece. Monitoring of maturation of response and the new immune awakening should be screened with the attack to other sites with free tumor.

7. Immunotherapy control point blocking in cancer with PD-1 and CTLA-4 blocking antibodies.

In cancer, T cells are repressed and cannot respond against the tumor through the interaction between T cell receptors: PD-1 and its corresponding ligands (PD-L1/PD-L2 or B7.H1/B7.DC) and CTLA-4 (CD152) and its ligands CD80 (B7-1) and CD86 (B7-2) present in the cancer cell. Recent treatments with nivolumab (PD-1 target), ipilimumab (CTLA-4 target), durvalumab (PD-L1 target) and tremelimumab (CTLA-4 target) used in breast tumors HER-2 negative and TNBC reported that they respond to blocking therapy at the immune control point, due to their high immunogenicity. Atezolizumab (Tecentriq®), a humanized monoclonal antibody of the isotype IgG1 against PD-1, and pembrolizumab (Keytruda®), and which act by blocking PD-1, are also available but they should not be used in immunosuppressed or treated patients with corticosteroid (see **Figure 4A and B**).[55] Recently, Polk et al. conducted a meta-research of the studies for breast cancer treatments until 2017; it highlights the results obtained with chemotherapy, radiotherapy and targeted immunotherapy with HuMab against the PD-1 and CTLA-4 receptors in T cells (durvalumab-tremelimumab and nivolumab-ipilimumab) and other combinations. Other studies have begun the evaluation of the combination of durvalumab and tremelimumab antibodies in breast cancer in early stages, as the treatment in MBC and TNBC has demonstrated good results.[56, 57] Other anti-PD-L1 antibodies for the treatment of breast cancer such as avelumab (Bavencio®) are also being studied, and it must be combined with surgery, chemotherapy, and radiotherapy.[58] Until now, targeted therapy anti-PD-1 and anti-PD-L1 has made great strides in the treatment of breast cancer. Simultaneously, it is also possible to inhibit CTLA-4 with ipilimumab (Yervoy®), a mAb that inhibits its activation, which makes cytotoxic T lymphocytes capable of recognizing and destroying cancer cells. Both nivolumab and ipilimumab are being

tested and their clinical results have been promising in the treatment of several cancers (**Figures 1** and **4**).[59] Clearly, the use of these checkpoint inhibitors has shown great therapeutic potential in several clinical trials, which is why they have been proposed for the first-line treatment of breast cancer. The use of this type of inhibitors is generating great interest in the field of immunotherapy. Nivolumab and ipilimumab are the most used and promising antibodies; Applied in a cocktail for cancer without mutation in the proto-oncogene B-RAF (V600 BRAF) and for metastatic breast cancer. In addition to the combination that has been tested with vemurafenib and cobimetinib (Cotelli®), which is a reversible inhibitor, selective allosteric blocking, the MAPK pathway specifically directed to an extracellular signal regulating protein kinase (MEK) 1 and MEK 2, which causes an inhibition of ERK1/2 phosphorylation.[60] Currently, available agents include the ALK inhibitors certinib and crizotinib and the EGFR inhibitors afatinib, erlotinib, and gefitinib. Four oral targeted therapies are used in the treatment of solid tumor associated with the B-Raf proto-oncogene (BRAF): cobimetinib, dabrafenib, trametinib, and vemurafenib, oral agents for treatment.[61]

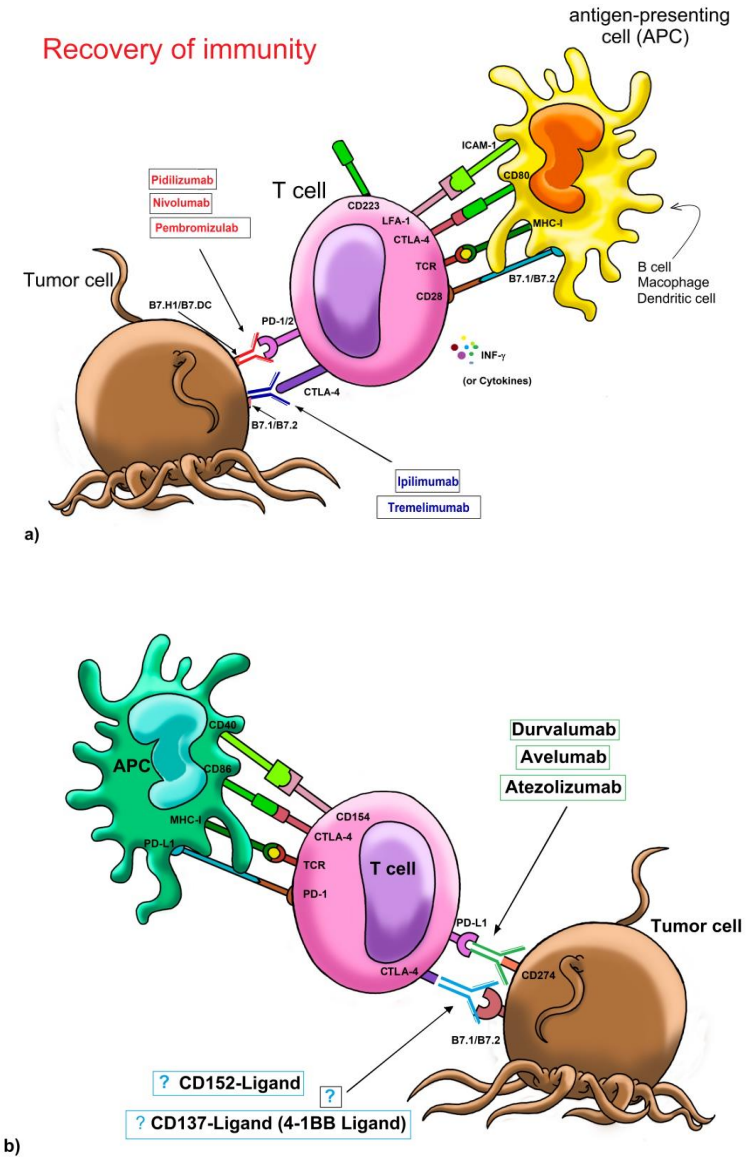


Figure 4. a) Restoring the immune capacity. Binding of PD-1 with its ligand B7.H1 and B7.DC delivers inhibitory signals to T lymphocytes, this lead to anergy and dysfunction of cells. Both activation mechanisms of T cells by antigen presenting cells (APC), and blocking by mAb targeted to PD-1/2 (red) and mAb directed to CTLA-4 (blue) will restore the ability of T lymphocytes for destroying cancerous cells, especially if accompanied by the action of IFN-gamma and other cytokines. b) The PD-L1 interaction of cancerous cells favors the conversion of bystander T cells and the decrease of cytokine secretion. The mAb anti-PD-L1 (green) binding to tumor cells avoid the inactivation of T cells; and further, can function as a marker for the attack to the membrane by the MAC, CTL-mediated death by perforin and granzyme, or NK CD16 cells with its Fc receptor that recognizes the antibodies bound to the cell. On the other side, there are not antibodies targeted to ligands of CTLA-4 (CD152 or CD137).

8. Cytokines and immunoregulation

In the early days of immunotherapy against cancer, some cytokines that regulate the Th1 response, (IFN-γ, IL-2) were used together with the inhibitors nivolumab and ipilimumab. These cytokines can promote a better antitumor response after activating the T cells since the activated cells are able to recognize tumor antigens, while these antibodies would release the brake imposed on the reactive T cells.[62] In experimental studies *in vivo* and *in vitro*, the use of these therapies has been favorable with the administration of IFN-α or IFN-γ and exogenous IL-2 (to activate the antitumor T cells) and the presence of regulatory T cells (Treg) or helper T cells 17 (Th17). Results of retrospective studies with patients who were treated with high doses of cytokines were not as encouraging; still, it is possible that the combined use of cytokines and inhibitors will aid reduce the damages of advanced breast cancer (stages III and IV) and decrease recurrences. Furthermore, these substances can be administered in combination with stage IV breast cancer chemotherapy. Although side effects with the use of cytokines may be a limiting factor, careful management by an immunotherapy medical specialist can significantly reduce the risks.[63,64]

9. NK activation

NK cells are the main cellular effectors of the innate immune system, which mediate the lack of self-recognition, lysis of a marked target and are also a potent and early source of cytokines and chemokines, which does not require prior exposure to antigens. In healthy individuals 90% of NK cells are in peripheral blood (PB) and are mature and cytotoxic, characterized by expressing $CD16^{bright}$ and $CD56^{dim}$, while the remaining 10% of NK cells is a subset of immature cells, which produce cytokines and express $CD56^{bright}$ $CD16^{dim}$ or $CD16^{-}$ and $CD25^{+}$.[65] The activity of NK is regulated by inhibition or stimulation of signals upon contact with tumor cells, where the prevalence of stimulating signals or the absence of inhibitors leads to triggering the lytic effect. That is, if healthy cells do not express high levels of HLA class I, but do not express activating ligands, tolerance will be induced in NK cells.[66] On the other hand, tumor cells, in general, may show a reduction in the expression of HLA class I and at the same time an increase in the activation of ligands such as NKp30 or NKG2D, which facilitate the attack of NK cells to the tumor.[67] During the last decade, it was established that NK cells are activated by IL-12, IL-15, and IL-18, but the NK lineage is sufficiently exclusive since it is not easy to obtain functional NK cells. Colucci et al. proposed three stages in the development of NK cells in vitro.[68] Under these conditions, NK cells show cytotoxicity and are producers of proinflammatory cytokines such as IFN-γ, TNF-α, IL-13, IL-10, and GM-CSF, when there is contact with tumor cells susceptible to be recognized (**Figure 3 A**). However, in most cancer patients, NK cell populations are depleted or almost eliminated or non-existent, resulting in low control of tumor growth. It should be mentioned that the recognition of the tumor by NK cells can be carried out through an activation signal or through the inhibition of the receptors on the surface of the cell, either measured by the MHC, by their KIR receptors; or they can be activated through an event independently of this recognition, and known as CIK (killer cells induced by cytokines). Therefore, we believe that the use of cytokines, to activate autologous NK cells *in vitro*, and then to be perfused back into the patient, so that they can respond against cancer cells, could be excellent immunotherapy (**Figure 3A and B**).[69]

10. Conclusion

The current standard treatment for different types of breast cancer is still chemotherapy since they are highly sensitive. However, patients have high relapse rates. Today the therapeutic target with mAbs that block both PD-1 and PD-L1 and CTLA-4 is being supported by several novel studies. In addition, several studies have reported that the TNBC and the BC hormone receptor have a very high level of genomic instability and high rates of genetic mutations, which may involve the probable generation of more neoantigens and increased immunogenicity. In addition, several inhibitors of signaling pathways (MAPKs) are being studied, as well as the application in the treatment of drugs that inhibit PARP-1/2 cause multiple breaks in double strands and in tumors with BRCA1, BRCA2 present in some tumors of BC. Preliminary data from the clinical trials showed promising results for patients with advanced stage / metastatic TNBC and with possibilities of application in other early stages. Some tests in patients responded to the treatment having a favorable prognosis and frequently showed a significant increase in overall survival. Even so, the objective response rate was relatively low. The design of several mAbs directed to tumor antigens have proven successful in the treatment of various malignancies and are now widely used in the clinic, such as: Trastuzumab, Pertuzumab, Bevacizumab, Ranibizumab, Aflibercept, Cetuximab, Panitumumab, and others. However, the current mAbs directed to the immunological control point are playing a preponderant role in the immunological awakening. In addition, tyrosine kinase inhibitor (TKI) tests have shown that, despite the preservation of tyrosine kinase domains, tyrphostins can be designed and synthesized that discriminate even between closely related tyrosine kinase proteins, such as EGFR, and its close relationship HER2 and thus can be used in breast cancer that expresses it. As well as the use of inhibitors of AKT, Scr and other downstream signal molecules for the activation of genes for growth, differentiation, and proliferation. Therefore, it is necessary to find strategies to improve the response to this therapy in BC and to transform those that do not respond.

We know that through the immunotherapy with mAb the expected response is not always present, either due to the

activation of the response only in some places or without presenting a good response through the antibodies. But we also need to keep in mind that there are zones of immune response development and other areas without immune activity in tumors. In addition, immunotherapy with antibodies apparently does not always activate the immune system efficiently. Consequently, in some cases, the evolution of the therapy does not improve the prognosis and only a partial resolution of the problem is achieved. In the worst scenarios, even with several types of treatment, only a few more years of life are provided to the patient and in some cases, they produce severe adverse reactions. An autoimmune response is a frequent complication that, besides, prevents the adequate identification of the tumor. This event raises several questions: Why do tumors escape immune surveillance? Is tolerance due to the early presence of cancer cells, evading, therefore, immune recognition of the self and nonself? Lack of response is due to molecules that fulfill their role in an abnormal way? Does the immunoediting happen in all cancers? The processes carried out by the immune system to recognize and eliminate a tumor are explained by immunoediting that comprises three stages: elimination, equilibrium, and escape. If in the elimination phase the tumor is not controlled, it enters a stage of equilibrium, escapes and will be allowed. There is a possibility that the recognition of antigens does not occur, there are T anergic cells or the activation of cytokines is not carried out. Taking all this into account, our proposed immunotherapy against tumors includes the reactivation of the immune response through a new screening and activation, using activated T cells and external cytokines, which may be re-implanted in the patient to establish an effective and lasting recognition towards the tumor.

This proposal might be validated as a common treatment against cancer, since, theoretically, the type of cancer in question does not matter because it is based on reactivation of the immune system for the recognition of new variants and the activation of the immune antitumor response. Briefly, our first proposal would be extracting activated or virgin T lymphocytes and tumor cells from the patient, and co-cultivate them in the presence of cytokines that activate the cytotoxic response: i.e. IL-2, INF-α and γ, and TNF-α. Additionally, macrophages or dendritic cells should be obtained; they are to be activated in a classical way (M1) to be lately exposed to cancer cells for them to carry out the antigen processing. An additional possibility is that the excised tumors of patients are confronted with NK cells and exogenous cytokines IL-15, IL-18, IL-22, IL-23, to reactivate the immune response and establish specific tumor recognition. As a result of all these interactions, T cells and antigen presenting cells already activated could be re-implanted into the patient, to raise an efficient and sustained antitumor immune response (**Figure 3A**).

A second immunotherapy proposal consists of tumor extirpation, to infiltrate it later with Th1 and IL-15 cytokines, IL-18 and exogenous IFN-α, and, finally, re-implant the tumor into the patient, in a subcutaneous region closer to some lymph nodes. It must be noted that this implant should be covered in a nanoparticulate network to prevent the escape of tumor cells (**Figure 3B**). As a result, a reactivation of the local immune response mediated by T cells, APC (antigen presenting cells) and NK cells is expected. Through the active migration of immune response cells to the implanted tumor, the stimulated area might be monitored. The immunotherapy success will only be achieved through a deep understanding of the T cells and NKs activation mechanisms, and delicate handling of cytokines, reaching adequate cytotoxic T cells reprogramming. All this additionally depends on the uptake and presentation of tumor antigens by macrophages and dendritic cells, coupled with the expression of various co-stimulatory molecules and cytokines of the antitumor response. Once the antitumor immune response is established, it can be kept under control by regulatory mechanisms, such as immune control points mediated by PD-1 and CTLA-4, as well as other types of immunosuppressive cells such as Treg and TH17. With the recent advances in antitumor immunology and the development of new inhibitors of target molecules, the implementation of multi-therapy against cancer seems to be the most promising option in years to come. This goal will only be reached with further research, increasing the number of clinical studies and obtaining the experience that will allow the future achievement of an effective therapy against one of the diseases that cause many deaths in the world.

11. Funding Information

This study was supported by Instituto Nacional de Enfermedades Respiratorias “Ismael Cosio Villegas” Mexico City.

12. Conflict Of Interest

None declared.

13. Authors’ Contributions

Each and every one contributed equally. Galván-Barrera; Conceptualization original draft and writing. Santiago; Orthography and images, Terán; Review and editing.

14. Acknowledgments

The authors thank Ph.D. Betinna Sommers Cervantes.

15. References

1. Siegel RL, Miller KD, Jemal A. Cancer statistics, 2018. CA Cancer J Clin. 2018;68(1):7-30.

2. Torre LA, Bray F, Siegel RL, Ferlay J, Lortet-Tieulent J, Jemal A. 2015. Global cancer statistics, 2012. CA Cancer J Clin. 65(2):87–108.

3. Siegel RL, Miller KD, Jemal A. Cancer statistics, 2015. CA Cancer J Clin. 2015;65(1):5-29.

4. Modena MG, Sismondi P, Mueck AO, et al. New evidence regarding hormone replacement therapies is urgently required transdermal postmenopausal hormone therapy differs from oral hormone therapy in risks and benefit. Maturitas. 2005;52(1):1-10.5.

5. Vesely MD, Schreiber RD. Cancer immunoediting: antigens, mechanisms, and implications to cancer immunotherapy. 2013. Ann N Y Acad Sci. 1284:1-5.

6. Mahoney KM, Rennert PD, Freeman GJ. Combination cancer immunotherapy and new immunomodulatory targets. Nat Rev Drug Discov. 2015;14(8):561-84.

7. Pardoll DM. The blockade of immune checkpoints in cancer immunotherapy. Nat Rev Cancer. 2012; 12(4):252-64.

8. Mates M, Fletcher GG, Freedman OC, et al. Systemic targeted therapy for HER-2-positive early female breast cancer: a systematic review of the evidence for the 2014 Cancer Care Ontario systemic therapy guideline. Curr Oncol. 2015;22(Suppl 1):S114-22.

9. Li H, Shao B, Yan Y, et al. Efficacy and safety of trastuzumab combined with chemotherapy for first-line treatment and beyond progression of HER2-overexpressing advanced breast cancer. Chin J Cancer Res. 2016;28(3):330-8.

10. Le XF, Pruefer F, Bast RC Jr. HER-2-targeting antibodies modulate the cyclin dependent kinase inhibitor p27Kip1 via multiple signaling pathways. Cell Cycle. 2005;4(1):87–95.

11. Press MF, Finn RS, Cameron D, et al. HER-2 gene amplification, HER-2 and epidermal growth factor receptor mRNA and protein expression, and lapatinib efficacy in women with metastatic breast cancer. Clin Cancer Res. 2008;14(23):7861-70.

12. Harbeck N, Beckmann MW, Rody A, et al. HER-2 Dimerization Inhibitor Pertuzumab Mode of Action and Clinical Data in Breast Cancer. Breast Care (Basel). 2013;8(1):49-55.

13. Kawajiri H, Takashima T, Kashiwagi S, Noda S, Onoda N, Hirakawa K. Pertuzumab in combination with trastuzumab and docetaxel for HER2-positive metastatic breast cancer. Expert Rev Anticancer Ther. 2015;15(1):17-26.

14. Meng L, Ma P. Apparent diffusion coefficient value measurements with diffusion magnetic resonance imaging correlated with the expression levels of estrogen and progesterone receptor in breast cancer: A meta-analysis. J Cancer Res Ther. 2016;12(1):36-42.

15. Gierach GL, Burke A, Anderson WF. Epidemiology of triple negative breast cancers. Breast Dis. 2010;32(1-2):5-24.

16. Fong PC, Boss DS, Yap TA, et al. Inhibition of poly(ADP-ribose) polymerase in tumors from BRCA mutation carriers. N Engl J Med. 2009;361(2):123-34.

17. Schauwvlieghe AM, Dijkman G, Hooymans JM, et al. Comparing the Effectiveness of Bevacizumab to Ranibizumab in Patients with Exudative Age-Related Macular Degeneration. The BRAMD Study. PLoS One. 2016;11(5):e0153052.

18. Bertucci F, Fekih M, Autret A, et al. Bevacizumab plus neoadjuvant chemotherapy in patients with HER-2-negative inflammatory breast cancer (BEVERLY-1): a multicentre, single-arm, phase 2 study. Lancet Oncol. 2016;17(5):600-11.

19. Wu FT, Paez-Ribes M, Xu P, et al. Aflibercept and Ang1 supplementation improve neoadjuvant or adjuvant chemotherapy in a preclinical model of resectable breast cancer. Sci Rep. 2016;6:36694

20. Lee A, Djamgoz MBA. Triple negative breast cancer: Emerging therapeutic modalities and novel combination therapies. Cancer Treat Rev. 2018; 62:110-122.

21. Brockhoff G, Heckel B, Schmidt-Bruecken E, et al. Differential impact of Cetuximab, Pertuzumab and Trastuzumab on BT474 and SK-BR-3 breast cancer cell proliferation. Cell Prolif. 2017;40(4):488-507.

22. Walker AJ, Wedam S, Amiri-Kordestani L, et al. FDA Approval of Palbociclib in Combination with Fulvestrant for the Treatment of Hormone Receptor-Positive, HER2-Negative Metastatic Breast Cancer. Clin Cancer Res. 2016;22(20):4968-4972.

23. De Placido S, Gallo C, De Laurentiis M, et al. Adjuvant anastrozole versus exemestane versus letrozole, upfront or after 2 years of tamoxifen, in endocrine-sensitive breast cancer (FATA-GIM3): a randomised, phase 3 trial. Lancet Oncol. 2018;S1470-2045(18):30116-5.

24. Tanei T, Choi DS, Rodriguez AA, et al. Antitumor activity of Cetuximab in combination with Ixabepilone on triple negative breast cancer stem cells. Breast Cancer Res. 2016;18(1):6.

25. Matsuda N, Lim B, Wang X, Ueno NT. Early clinical development of epidermal growth factor receptor targeted therapy in breast

cancer. Expert Opin Investig Drugs. 2017;26(4):463-479.

26. Costa R, Shah AN, Santa-Maria CA, et al. Targeting Epidermal Growth Factor Receptor in triple negative breast cancer: New discoveries and practical insights for drug development. Cancer Treat Rev. 2017;53:111-119.

27. Yardley DA, Ward PJ, Daniel BR, et al. Panitumumab, Gemcitabine, and Carboplatin as Treatment for Women With Metastatic Triple-Negative Breast Cancer: A Sarah Cannon Research Institute Phase II Trial. Clin Breast Cancer. 2016;16(5):349-355.

28. Drummond DC, Noble CO, Guo Z, Hong K, Park JW, Kirpotin DB. Development of a highly active nanoliposomal irinotecan using a novel intraliposomal stabilization strategy. Cancer Res. 2006;66(6):3271-7.

29. Klapacz J, Pottenger LH, Engelward BP, Heinen CD, Johnson GE, Clewell RA. Contributions of DNA repair and damage response pathways to the non-linear genotoxic responses of alkylating agents. Mutat Res Rev. 2016;767:77-91.

30. Wang B, Chu D, Feng Y, Shen Y, Aoyagi-Scharber M, Post LE. Discovery and Characterization of (8S,9R)-5-Fluoro-8-(4-fluorophenyl)-9-(1-methyl-1H-1,2,4-triazol-5-yl)-2,7,8,9-tetrahydro-3H-pyrido[4,3,2-de]phthalazin-3-one (BMN 673, Talazoparib), a Novel, Highly Potent, and Orally Efficacious Poly(ADP-ribose) Polymerase-1/2 Inhibitor, as an Anticancer Agent. J Med Chem. 2016;59(1):335-57.

31. Robson M, Im SA, Senkus E, et al. Olaparib for Metastatic Breast Cancer in Patients with a Germline BRCA Mutation. N Engl J Med. 2017;377(6):523-533.

32. Carey JPW, Karakas C, Bui T, et al. Synthetic Lethality of PARP Inhibitors in Combination with MYC Blockade Is Independent of BRCA Status in Triple-Negative Breast Cancer. Cancer Res. 2018;78(3):742-757.

33. McCann KE, Hurvitz SA. Advances in the use of PARP inhibitor therapy for breast cancer. Drugs Context. 2018;7:212540.

34. Sisay M, Edessa D. PARP inhibitors as potential therapeutic agents for various cancers: focus on niraparib and its first global approval for maintenance therapy of gynecologic cancers. Gynecol Oncol Res Pract. 2017;4:18.

35. Drew Y, Ledermann J, Hall G, et al. Phase 2 multicentre trial investigating intermittent and continuous dosing schedules of the poly(ADP-ribose) polymerase inhibitor rucaparib in germline BRCA mutation carriers with advanced ovarian and breast cancer. Br J Cancer. 2016;114(7):723-30.

36. Werner TL, Sachdev J, Swisher EM, et al. Safety and pharmacokinetics of veliparib extended-release in patients with advanced solid tumors: a phase I study. Cancer Med. 2018;7(6):2360-2369.

37. Awada A, Campone M, Varga A, et al. An open-label, dose escalation study to evaluate the safety and pharmacokinetics of CEP-9722 (a PARP-1 and PARP-2 inhibitor) in combination with gemcitabine and cisplatin in patients with advanced solid tumors. Anticancer Drugs. 2016; 27(4):342-8.

38. Jiao P, Zhou YS, Yang JX, et al. MK-2206 induces cell cycle arrest and apoptosis in HepG2 cells and sensitizes TRAIL-mediated cell death. Mol Cell Biochem. 2013;382(1-2):217-24.

39. Papeo G, Posteri H, Borghi D, et al. Discovery of 2-[1-(4,4-Difluorocyclohexyl)piperidin-4-yl]-6-fluoro-3-oxo-2,3-dihydro-1H-isoindole-4-carboxamide (NMS-P118): A Potent, Orally Available, and Highly Selective PARP-1 Inhibitor for Cancer Therapy. J Med Chem. 2015;58(17):6875-98.

40. O'Shaughnessy J, Schwartzberg L, Danso MA, et al. Phase III study of iniparib plus gemcitabine and carboplatin versus gemcitabine and carboplatin in patients with metastatic triple-negative breast cáncer. J Clin Oncol. 2014;32(34):3840-7.

41. Schott AF, Barlow WE, Van Poznak CH, et al. Phase II studies of two different schedules of dasatinib in bone metastasis predominant metastatic breast cancer: SWOG S0622. Breast Cancer Res Treat. 2016; 159(1):87-95.

42. Jin J, Sun Z, Yang F, Tang L, Chen W, Guan X. miR-19b-3p inhibits breast cancer cell proliferation and reverses saracatinib-resistance by regulating PI3K/Akt pathway. Arch Biochem Biophys. 2018;645: 54-60.

43. Blanchard Z, Mullins N, Ellipeddi P, et al. Geminin overexpression promotes imatinib sensitive breast cancer: a novel treatment approach for aggressive breast cancers, including a subset of triple negative. PLoS One. 2014;9(4):e95663.

44. Sonnenblick A, de Azambuja E, Agbor-Tarh D, et al. Lapatinib-Related Rash and Breast Cancer Outcome in the ALTTO Phase III Randomized Trial. J Natl Cancer Inst. 2016;108(8). pii: djw037

45. Schouten PC, Dackus GM, Marchetti S, et al. A phase I followed by a randomized phase II trial of two cycles carboplatin olaparib followed by olaparib monotherapy versus capecitabine in BRCA1- or BRCA2-mutated HER-2-negative advanced breast cancer as first line treatment (REVIVAL): study protocol for a randomized controlled trial. Trials. 2016;17(1):293

46. Roberts NJ, Zhang L, Janku F, et al. Intratumoral injection of Clostridium novyi-NT spores induces antitumor responses. Sci Transl Med. 2014;6(249):249ra111.

47. Tejada-Berges T, Granai CO, Gordinier M, Gajewski W. Caelyx/Doxil for the treatment of metastatic ovarian and breast cancer.

Expert Rev Anticancer Ther. 2002;2(2):143-50.

48. Polk A, Svane IM, Andersson M, Nielsen D. Checkpoint inhibitors in breast cáncer-Current status. Cancer Treat Rev. 2018;63:122-134.

49. Sanchez K, Page D, McArthur HL. Immunotherapy in breast cancer: An overview of modern checkpoint blockade strategies and vaccines. Curr Probl Cancer. 2016;40(2-4):151-162.

50. Cox K, Alford B, Soliman H. Emerging Therapeutic Strategies in Breast Cancer. South Med J. 2017;110(10):632-637.

51. Schlom J, Gulley JL. Vaccines as an Integral Component of Cancer Immunotherapy. JAMA. 2018;320(21):2195-2196.

52. Abdolahi M, Yavari P, Honarvar NM, et al. Molecular Mechanisms of the Action of Vitamin A in Th17/Treg Axis in Multiple Sclerosis. J Mol Neurosci. 2015;57(4):605-13.

53. Pichler R, Gruenbacher G, Culig Z, et al. Intratumoral Th2 predisposition combines with an increased Th1 functional phenotype in clinical response to intravesical BCG in bladder cancer. Cancer Immunol Immunother. 2017;66(4):427-440.

54. Guéry L, Hugues S. 2015. Th17 Cell Plasticity and Functions in Cancer Immunity. Biomed Res Int. 2015:314620.

55. Wang J, Yuan R, Song W, Sun J, Liu D, Li Z. PD-1, PD-L1 (B7-H1) and Tumor-Site Immune Modulation Therapy: The Historical Perspective. J Hematol Oncol. 2017;10(1):34.

56. Santa-Maria CA, Kato T, Park JH, Kiyotani K, et al. A pilot study of durvalumab and tremelimumab and immunogenomic dynamics in metastatic breast cancer. Oncotarget. 2018;9(27):18985-18996.

57. Katz H, Alsharedi M. Immunotherapy in triple-negative breast cancer. Med Oncol. 2017;35(1):13.

58. Juliá EP, Amante A, Pampena MB, Mordoh J, Levy EM. Avelumab, an IgG1 anti-PD-L1 Immune Checkpoint Inhibitor, Triggers NK Cell-Mediated Cytotoxicity and Cytokine Production Against Triple Negative Breast Cancer Cells. Front Immunol. 2018;9:2140.

59. Monneur A, Gonçalves A, Bertucci F. PD-L1 expression and PD-1/PD-L1 inhibitors in breast cancer. Bull Cancer. 2018;105(3):263-274.

60. Wagle MC, Kirouac D, Klijn C, et al. A transcriptional MAPK Pathway Activity Score (MPAS) is a clinically relevant biomarker in multiple cancer types. NPJ Precis Oncol. 2018:7;2(1):7.

61. Roskoski R Jr. Small molecule inhibitors targeting the EGFR/ErbB family of protein-tyrosine kinases in human cancers. Pharmacol Res. 2018;139:395-411.

62. Kleef R, Moss R, Szasz AM, Bohdjalian, Bojar H, Bakacs T. Complete Clinical Remission of Stage IV Triple-Negative Breast Cancer Lung Metastasis Administering Low-Dose Immune Checkpoint Blockade in Combination With Hyperthermia and Interleukin-2. Integr Cancer Ther. 2018;17(4):1297-1303.

63. Faghih Z, Erfani N, Haghshenas MR, Safaei A, Talei AR, Ghaderi A. Immune profiles of CD4+ lymphocyte subsets in breast cancer tumor draining lymph nodes. Immunol Lett. 2014;158(1-2):57-65.

64. Faghih Z, Rezaeifard S, Safaei A, Ghaderi A, Erfani N. IL-17 and IL-4 producing CD8+ T cells in tumor draining lymph nodes of breast cancer patients: positive association with tumor progression. Iran J Immunol. 2013;10(4):193-204.

65. Romagnani C, Juelke K, Falco M, et al. CD56brightCD16- killer Ig-like receptor- NK cells display longer telomeres and acquire features of CD56dim NK cells upon activation. J Immunol. 2007;178(8):4947-55.

66. Farag SS, Caligiuri MA. 2006. Human natural killer cell development and biology. Blood Rev. 20(3):123-37.

67. Colucci F, Di Santo JP, Leibson PJ. Natural killer cell activation in mice and men: different triggers for similar weapons? Nat Immunol. 2002;3(9):807-13.

68. Mata-Molanes JJ, Sureda González M, Valenzuela Jiménez B, Martínez Navarro EM, Brugarolas Masllorens A. Cancer Immunotherapy with Cytokine-Induced Killer Cells. Target Oncol. 2017;12(3):289-299.

69. Ferreira-Teixeira M, Paiva-Oliveira D, Parada B, et al. Natural killer cell-based adoptive immunotherapy eradicates and drives differentiation of chemoresistant bladder cancer stem-like cells. BMC Med. 2016;14(1):163.

70. Martin M, Fumoleau P, Dewar JA, Albanell J, Limentani SA, Campone M. Trastuzumab emtansine (T-DM1) plus docetaxel with or without pertuzumab in patients with HER2-positive locally advanced or metastatic breast cancer: results from a phase Ib/IIa study. Ann Oncol. 2016;27(7):1249-56.

71. Finn RS, Martin M, Rugo HS, et al. Palbociclib and Letrozole in Advanced Breast Cancer. N Engl J Med. 2016;375(20):1925-1936.

72. Meirson T, Genna A, Lukic N, et al. Targeting invadopodia-mediated breast cancer metastasis by using ABL kinase inhibitors. Oncotarget. 2018;9(31):22158-22183.

International Conference on Cancer Research 2019

Website: www.CancerConf.org

June 10-11, London, UK



The High-Efficiency and Stable Hypercoagulation-Breast-Cancer Models for Study the Mechanism of Hematogenous Metastasis

Yang Wenjing [1], Yang Guowang [1]*, Zhang Ganlin [1]*

[1] *Oncology Department, Beijing Hospital of Traditional Chinese Medicine, China.*

** Corresponding author: yangguowang_bhtcm@126.com，kalinezhang@163.com*

Abstract

Breast cancer is the commonest malignancy cancer in women. Accumulated research showed that more than 60% of patients with malignant tumor were accompanied by hypercoagulable state, which in turn cause cancer progression, followed by long distant metastasis, alert the worse tumor prognosis and even affect treatment strategy. In the clinical study, we showed that the MA (mm) were significantly higher in the patients with stage IV breast cancer than in stage I/II/ III patients(P=0.01), which indicated that platelet hyperfunction was positively associated with tumor metastasis in breast cancer patients. In order to explore the relational mechanisms, we were committed to construction of efficient models in vivo and in vitro. In vivo study, as tumor-bearing period (TBP) and postoperative incubation period (PIP) are two key factors for coagulation and metastasis, we established 4T1-luc breast-tumor-bearing mice model of 4 groups (1a= TBP25+PIP17, 1b= TBP25+PIP1, 1c= TBP20+PIP17, 1d= TBP20+PIP1) with different TBP and PIP. Through evaluation of the breast tumors, lung metastases, animal welfare, operational feasibility and TEG Assay, indicated that: Lung metastasis and hypercoagulability were successfully established in all tumor groups; The TBP and PIP were both played a decisive role in the occurrence of lung metastasis; The model hypercoagulation state was characterized not by coagulation factors, but by the hyperactivity of fibrin and platelet. Given animal welfare and operational feasibility, recommended 4Tl-luc cells be injected into the fourth intramammary gland fat pad with 1 x 106, and with TBP of 3 weeks and PIP of 2 weeks, then an ideal in vivo model can be established. In vitro study, we established an in vitro model (platelet-breast cancer co-action) by platelets (female BALB/c mice) and 4T1 cells co-incubation for 30 minutes (represent the early phase of platelet-breast cancer co-action in vivo) or 24 hours (represent the late phase of platelet-breast cancer co-action in vivo), then the co-incubation supernatants were obtained by differential centrifugation. Through evaluation of the physical characteristics and procoagulant activity of the supernatants, indicated that co-incubation of platelets and 4T1 cells could activate each other and promote the release of substance and procoagulant activity with prolonging the co-incubation time, and the reaction supernatants can be used for interest factors detection and bioactivity verification. In conclusion, we provided powerful hypercoagulation-breast-cancer model for research in this field in vivo and in vitro, which will also provide important insights into the intervention of hematological metastasis in breast cancer.

Keywords:

Breast Cancer;

Hypercoagulable State;

In Vivo Model;

In Vitro Model.

Introduction

Activation of the hemostatic system contributes significantly to the hypercoagulable state, thrombotic diathesis, metastasis and even death in these patients [1-6]. And the elevated of platelets function or counts were reported widely in numerous clinical cancer researches [7-8]. Furthermore, aberrant platelet activation and aggregation include disseminated intravascular coagulation, migratory thrombophlebitis and pulmonary embolism frequently discovered in cancer patients too [9]. However, reducing platelet count or inhibiting platelet function can effectively inhibit the number of experimental metastases [10-12]. In addition, clinical randomized controlled trials (RCTs) studies have revealed the anticancer effects of low-dose aspirin, and recommending it for primary prevention of cancer [13-17]. All of the above evidences suggest that platelets play a vital role of the hypercoagulable state formation and tumor metastasis.

Breast cancer is the commonest malignancy cancer in women and is considered to be associated with high risk of hypercoagulable state to make tumor progression [18]. The clinical data of our hospital showed that the degree of hypercoagulability worsens with cancer progression, and the hyperfunction of platelet is only appears in metastasis

breast cancer patients. Which prompted us to doubt whether the hyperfunction of platelet has a more directly relationship with metastasis than coagulation factors in breast cancer. Currently, the relevant mechanism researches indicated that the procoagulant microparticles (MPS), especially those expressing tissue factor (TF) or phospholipid (PS), which mainly come from tumor cells, platelets or both [19-22]. Contribute most to the hypercoagulability and metastasis of breast cancer.

Extracellular vesicles (EVs) which are classified into three groups, (a) exosomes, (b) microvesicles (MVs), and (c) apoptotic bodies (ABs), based on their sizes, origins, makers, shapes and derivation mechanism [23-25]. They act as carriers of nucleic acids, lipids and proteins and have been recognized as critical mediators of extracellular communications, which promote transformation, growth invasion, hypercoagulability and drug-resistance of cancer cells. PS exposure on MPS (belonging to MV) promote hypercoagulable state and metastasis have been reported largely in breast cancer. However, PS exposure on other EVs especially the small ones like exosomes, which whether contributes to hypercoagulability and progression in patients with breast cancer or not has not been investigated, so the interesting function of small EVs maybe a promising research direction.

For research in this field, construction of an in vivo model of tumor metastasis with hypercoagulability is the key. However, a high-efficiency and stable condition to establish the in vivo model suitable for study in this field has not been clearly elucidated. We took tumor-bearing period (TBP) and postoperative incubation period (PIP) as the two main intervention factors to build 4 groups, through the evaluation of the breast and lung metastases tumor, the characteristics of hypercoagulation state, animal welfare and operational feasibility, we got an excellent in vivo model which characterized not by coagulation factors, but by the hyperactivity of fibrin and platelet.

A lot of research indicated the dynamic crosstalk between tumors and platelet is charming which increasingly recognized as a key regulator of hypercoagulable state and malignant progression. For our research, we established an in vitro model (platelet-breast cancer co-action) by platelets and 4T1 cells co-incubation for 30 minutes (represent the early phase of platelet-breast cancer co-action in vivo) or 24 hours (represent the late phase of platelet-breast cancer co-action in vivo), then the co-incubation supernatants were obtained by differential centrifugation. Through the evaluation of the co-incubation supernatants in physical characteristics (concentration and size) and procoagulant activity (PS exposure), we confirmed co-incubation of platelets and 4T1 cells could activate each other and promote the release of substance and procoagulant activity with prolonging the co-incubation time. In addition, the reaction supernatant is rich in nucleic acids, lipids, proteins and numerous bioactive substances. You can use this model to detect anything you are interested in and set up intervention conditions.

This study provides a powerful research tool for the study of the correlation between hypercoagulable state and breast cancer progression through establishment of in vivo and in vitro research models, and novel antithrombotic treatments may arise from a better understanding of breast cancer associated hypercoagulable state.

Materials and methods

1. Clinical information of patients.

A retrospective analysis was performed on breast cancer patients who tested Thrombelastograph (TEG) assay in the Beijing Traditional Chinese Medicine Hospital Capital Medical University from July 2016 to January 2019. Clinical and test information were extracted via the institutional electronic data warehouse. We obtained pathological, clinical stage, combined disease, medical history, sex, age and the results of TEG assay included R (min), K (min), Angle (deg), MA (mm). Inclusion criteria: Breast cancer diagnosed by pathology; Patients have been tested for TEG assay. Exclusion criteria: Patients with unavailable clinical stage; Patients received anticoagulant therapy; Patients combined with coagulation-related diseases.

2. Cell culture

4T1/ 4T1-luc are a murine breast carcinoma cell line, which from Caliper (USA) were cultured in RPMI-1640 medium supplemented with 10% fetal calf serum (FBS; Sigma-Aldrich, Oakville, ON) and 1% penicillin-streptomycin (Gibco; 10000 units/ml Penicillin, 10000 μg/ml Streptomycin) at 37˚C in a humidified atmosphere containing 5% CO2. The cells were passaged every two to three days to maintain exponential growth.

3. Animal

6-8-week-old female BALB/c mice used in this study were obtained from Beijing Vital River Laboratory Animal Technology Co. Ltd, and were approved by China Laboratory Animal Welfare and Animal Experimental Ethical Committee. All mice were maintained in specific pathogen-free barrier facilities at the Beijing Institute of Traditional Chinese Medicine, and fed with a regular diet. They were carefully bred and would be humanely sacrificed by cervical dislocation at study endpoint.

4. Established of the 4T1-luc breast-tumor-bearing mice model / lung metastasis model

4T1-luc cells seeded at log phase were treated with 0.25% Trypsin-EDTA (Gibco) for two minutes and washed once with PBS prior to being passaged. Then the viability and number of 4T1-luc cells were measured by Trypan blue staining, and the cell concentration was adjusted to 2×10^7/mL with PBS. Finally, 50 ul cell suspension (1×10^6) were stead injected into the fourth intramammary gland fat pad of female BALB/c mice on each side at a uniform speed.

When the TBP of each group was reached to the design requirement, we removed the breast tumors as follows: Animals were fixed on the paraffin table in supine position after gas (oxygen: isoflurane = 98:2) anesthesia. After 70% alcohol disinfection, the skin was incised beside the tumors on the side of the body. Surgical scissors were used to carefully remove the tumor from the breast pad. During the operation, attention should be paid to the detachment of the blood vessel and the complete elimination of the tumor capsule according to the radical principle. The iatrogenic dissemination of the tumor cells was avoided according to the tumor-free principle. Attention also should be paid to sterilization of instruments and protection of surgical incision according to aseptic principle. Avoid animal death due to excessive bleeding or excessive anesthesia time and avoid secondary recurrence due to incomplete resection. Complete separation of main nutrient vessels and proximal ligation are important steps to reduce blood loss (fig 1). 5-0 non-absorbable surgical sutures to suture the skin, ligation of instruments, cutting of excess sutures, skin closure of incisions, daily observation.

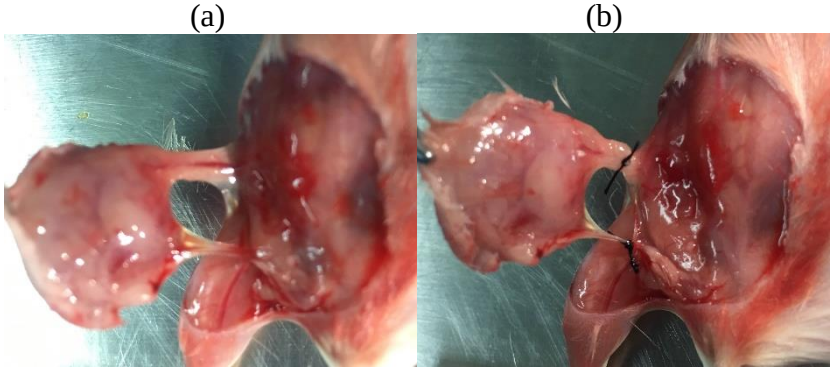


Fig. 1 Complete separation of the main nutrient vessels and proximal ligation: (a). Complete separation of the main nutrient vessels: Peeled off the main nutrient vessels along the blood vessel as carefully and rapidly as possible at the 5-6 o'clock position and the 10-11 o'clock position of the breast tumor. (b) Proximal ligation of the main nutrient vessels: After complete separation of the main nutrient vessels, they were ligated by instrument knotting at the proximal end of them, then severed sharply.

5. In vivo experimental design

In order to study the effect of TBP and PIP on lung metastasis in mice, different experimental groups were set up in this study. According to the TBP, the mice were divided into group 1 (27 days ± 2 days, n=17), and group 2 (20 days ± 2 days, n=14). According to the PIP (15 days ± 2 days/ 1 day), the group 1 and the group 2 were further divided into 4 subgroups: group 1a (with TBP 25 days and PIP 17 days, n=8), group 1b (with TBP 29 days and PIP 1 days, n=9), group 2a (with TBP 22 days and PIP 13 days, n=9), group 2b (with TBP 18 days and PIP 1 days, n=5), and set up a blank control group (n=11). After modeling, the mice were observed for general activity, nutritional status, and tumor formation rate.

6. Evaluation of the in vivo model

6.1 Evaluation of the breast tumors

To investigate and verify the ability of tumorigenesis at breast. The breast tumors were measured using a caliper once every 3 days from the 10th day after model established. The tumor volume was calculated using the formula: tumor volume (mm3) = $0.5\times a\times b^2$, where a represents the shortest diameter and b represents the longest diameter of the tumor. For pathological confirmation, mice were euthanized to collection of breast tumors according to the study design. All tissues were weighed and took photos for recording, then embedded in paraffin using standard procedures, sectioned, and stained with hematoxylin and eosin (H & E).

6.2 Evaluation of the lung metastases

Lung and extrapulmonary metastasis was assessed by optical in vivo imaging (IVIS-Lumina Ⅲ) before the experiment was terminated according to the study design. The specific operation was as follows: Each mouse was injected with 200 ul fluorescein substrates in the subcutaneous space, isoflurane was inhaled and anesthetized for 3 minutes, then placed into a living fluorescence imaging system to record lung metastases and extrapulmonary

metastases. Finally, using Living Image 4.5 software for analysis.

After recorded photon number of lung and extrapulmonary metastases. The mice were humanely sacrificed by cervical dislocation to collection their lung and extrapulmonary metastases. All tissues were weighed and took photos for recording, then embedded in paraffin using standard procedures, sectioned, and stained with hematoxylin and eosin (H & E).

6.3 Evaluation of the animal welfare/ operational feasibility

Based on the principle of animal welfare, we compare the following indicators between experiment groups: 1. Total time (anesthesia duration) spent on complete removal of breast tumors, the shorter the time, the less harmful the animal is; 2. The length and the stitches of the breast surgical incision, the shorter the incision, the less harmful the animal is; 3. The trend of animal weight change, the milder the trend, the less harmful the animal is.

6.4 Routine blood tests

For hypercoagulation state analysis, 20μL mice whole blood was collected into the prepared tubes with special diluent, then routine blood tests were immediately performed using a Sysmex XT-2000i automated hematology analyzer (Sysmex Corp., Hyogo, Japan) for the platelets (PLT) counts.

6.5 TEG Assay

For hypercoagulation state analysis, 500μL mice whole blood was collected into the prepared anti - coagulation tubes (sodium citrate 3.8%). Then the TEG test which measures clot formation, clot strength, and clot degradation in whole blood by adding kaolin and calcium chloride (final concentration, 10.5mMol/L) were carry out for enable a quantitative analysis of blood coagulation factor and platelet function. The specific operation is as follows: After the instrument is calibrated, 20 ul of calcium chloride is pushed to the bottom of the test cup, 500 ul of anticoagulant is thoroughly mixed with 20 ul of kaolin, 360 ul of the stimulated blood is pushed to the TEG test cup, and the TEG analyzer is started to measure the blood. The entire process of clot formation and degradation.

The parameters of the TEG are explained as follows: R(min) reflects the prothrombin start-up time, which reflects the function of coagulation factor, and the prolongation of R (min) indicates that the activity of coagulation factor is decreased or absent, and conversely, the activity of coagulation factor is hyperactive; K (min) and Angle (deg) reflect the rate of blood clot formation, which reflects fibrin function. K-time prolongation or Angle (deg) reduction suggests that fibrin function is reduced, and vice versa. MA (mm) reflects the absolute intensity of fibrin clot which reflecting platelet function, a decrease in the MA (mm) indicates a decrease in platelet function, and conversely indicates an increase in platelet function.

7. Preparation of mice platelets

Blood samples were obtained from female BALB/c mice. Washed platelet suspensions were prepared from blood in Tyrode's solution as previously described ($1*10^8$ /ml) [26].

8. Established of the in vitro model

We established the in vitro model to study the crosstalk between platelets and breast tumor cells in cancer progression. As we all known, the life-span of platelets in vivo is 7-10 days, and in vitro, the survival time is greatly shortened. So, we cultured platelets and 4T1 cells in vitro for 24 hours to represent the late phase of platelet-breast cancer co-action in vivo, and 30 minutes to represent the early phase of platelet-breast cancer co-action in vivo. The specific operation is as follows: 4T1 cells seeded at log phase were treated with 0.25% Trypsin-EDTA for two minutes and washed once with PBS prior to being passaged. Then the viability and number of 4T1 cells were measured by Trypan blue staining, and the cell concentration was adjusted to 1×10^6/mL with RPMI-1640 (10% FBS and 1% penicillin-streptomycin), Washed platelet suspensions(1ml) and 4T1 cells suspensions(1ml) co-incubation for 30 minutes or 24 hours at 37˚C in a humidified atmosphere containing 5% CO2. Then the co-incubation supernatants were centrifuged twice (first at 1400×g for 20 minutes and then at 13000×g for 2 min) at 4˚C to complete removal all of the 4T1 cells and platelets [27]. Platelets/4T1 cells incubation lonely for 24 hours/30 minutes all as control, and the supernatants stored at −80°C until assayed.

9. Identification of the co-incubation supernatants

To evaluation of the co-incubation supernatants in physical characteristics, we used a nano-flow cytometer (N30 Nanoflow Analyzer, NanoFCM Inc., Xiamen, China) to quantify the co-incubation supernatants and control supernatants by their concentration, size. As phosphatidylserine (PS) is an anionic phospholipid generally distributed in the cell membrane. But when the cells are activated or upon apoptosis, PS will externalize to the outer membrane to enhance the procoagulant activity, A large number of research reports circulating MPs and exposed PS from different cells contribute to the procoagulant activity in patients with cancer [27-28]. To evaluation of the co-incubation supernatants in procoagulant activity, we used a nano-flow cytometer to quantify the co-incubation supernatants and control supernatants by their PS exposure.

10. Statistical analysis

Data was analyzed using SPSS 16.0 (IBM, Armonk, NY, USA) or GraphPad Prism 5 (GraphPad, CA, USA). Groups were compared by using Mann-Whitney test or Kruskal-Wallis test. p-value<0.05 was considered statistically significant.

Results

1. Clinical results

Between July 2016 and January 2019, 81 subjects who had undergone TEG testing in our hospital were identified. Based on the criteria for inclusion and exclusion, 76 women subjects were eligible for analysis (Fig 2).

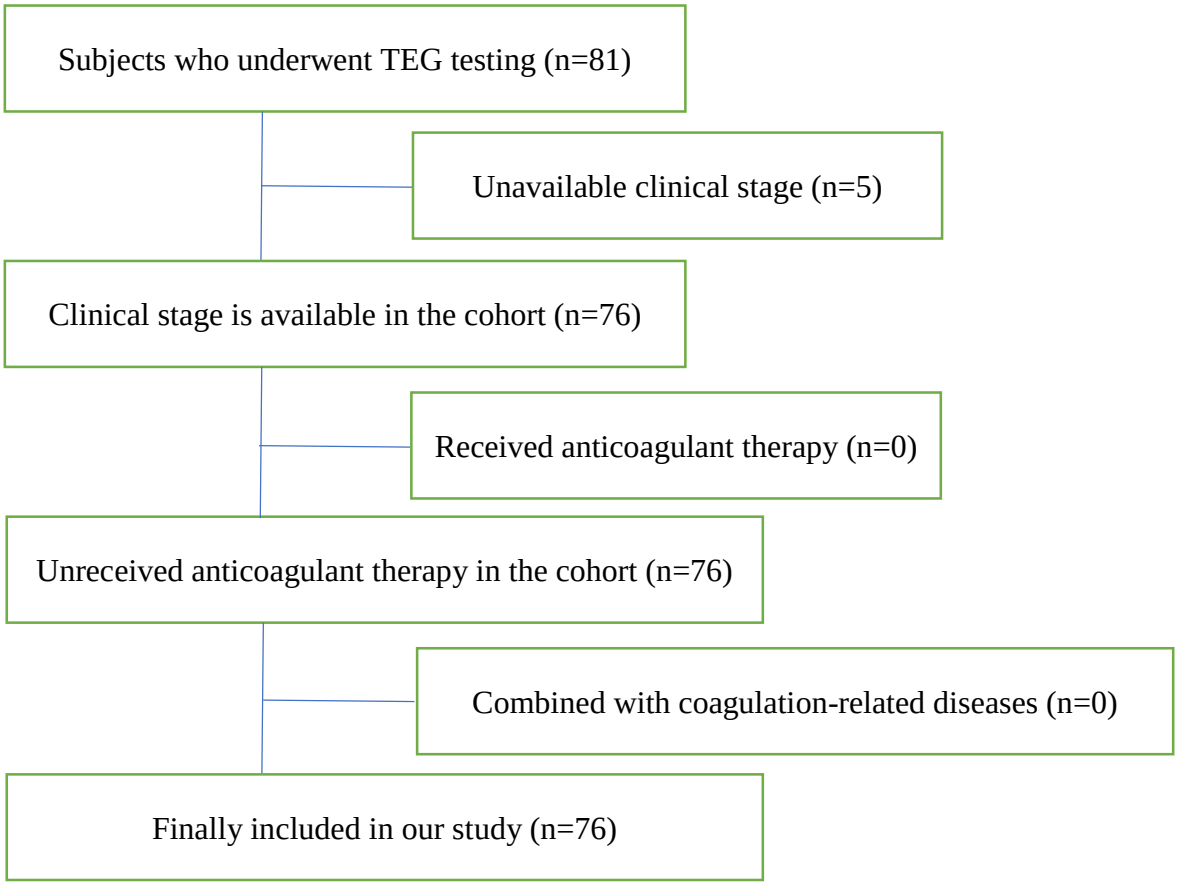


Fig. 2 Study flow chart showing step-wise exclusion algorithm based on eligibility

Among the eligible subjects (age from 34 to 88), the characteristic of clinical stage is: stage Ⅰ is 12, stage Ⅱ is 16, stage Ⅲ is 12, stage Ⅳ is 36; M0 is 40, M1 is 36. The results of TEG assay showed that the R (min) among stage Ⅰ, stage Ⅱ, stage Ⅲ with stage Ⅳ is no difference, and the MA (mm) among stage Ⅰ, stage Ⅱ, stage Ⅲ with stage Ⅳ is no difference. In order to explore the difference of coagulation state between metastasis and no metastasis subjects, we take M0 compare to M1 with the results of TEG assay. Which showed that the R (min) between M0 and M1 is no difference (P＞0.05), but the MA (mm) between M0 and M1 is difference (P=0.01). In other words, the hyperfunction of coagulation factor is appears in all clinical stages, but the hyperfunction of platelet is only appears in metastasis subjects. We doubt that maybe the hyperfunction of platelet has a more directly relationship with metastasis than coagulation factor in breast cancer (Fig 3).

Table 1. Comparison of the coagulation status between the two groups by TEG assay: The R (min) between M0 and M1 is no difference (P＞0.05), but the MA (mm) between M0 and M1 is difference (P=0.01).

	M0	M1	x^2	p value
R (min)			1.11	>0.05
<5	10	13		
≥5	30	23		
MA (mm)				=0.01

<70	40	30
≥70	0	6

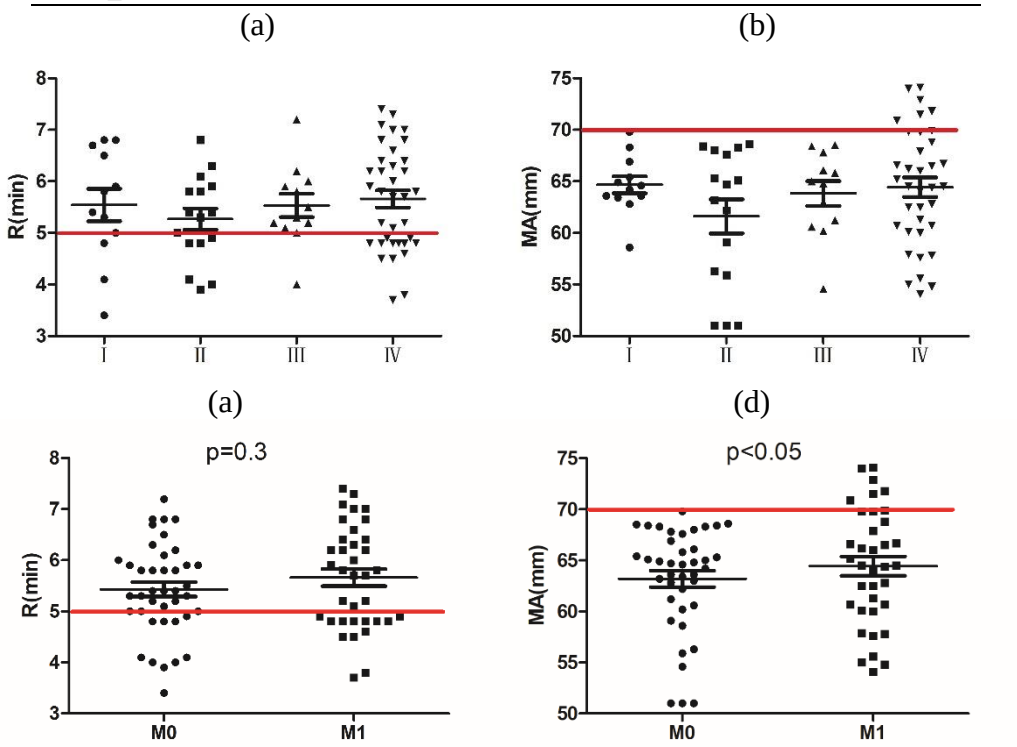


Fig. 3 Comparison of TEG assay among different clinical stages. (a) R(min): There is no difference of the R(min) among stage Ⅰ, stage Ⅱ, stage Ⅲand stage Ⅳ; (b) MA (mm): There is no difference of the MA (mm) among stage Ⅰ, stage Ⅱ, stage Ⅲand stage Ⅳ; (c) R(min): There is no difference of the R(min) between M0 and M1, P=0.3 ; (d) MA (mm): There is a statistical difference between M0 and M1, P＜0.05.
*The red line represents the normal value, the normal value of R is no less than 5.0(min), the normal value of MA is less than 70(mm).

2. The characteristics of breast tumor among four groups

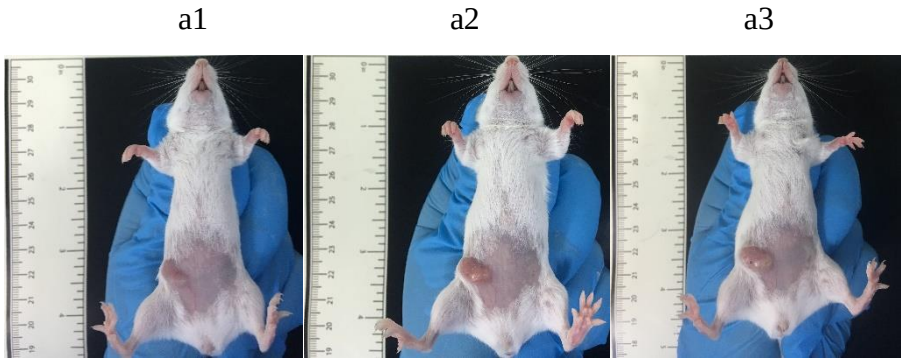
2.1 Comparison the volume of breast tumor

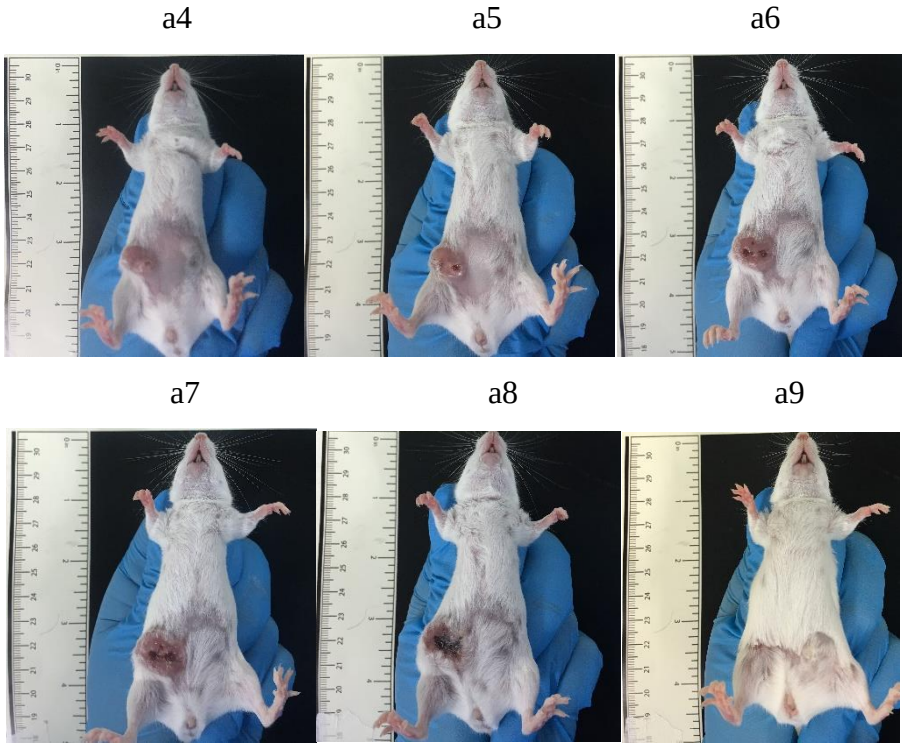
The volume of breast tumors was measured every 3 days from the 8th day after in vivo model established, the growth trend was consistent among the four groups, and the growing pictures were also collected (Fig 4 a).

2.2 Comparison the weight of breast tumor

Compliance with the termination time of the in vivo experimental design, tumor weight recorded immediately after resection (Fig 4 b). Comparison the weight of breast tumor among the groups: The breast weights of experimental group 1a, 2a increased significantly compared with group 2b, the differences were statistically significant, and the P value was 0.0006, 0.0041, respectively; The breast weights of experimental group 1b, increased significantly compared with group 1a, 2a and 2b, the differences were statistically significant, and the P value was 0.0006, 0.0021 and 0.0021, respectively.

(a)





(b)

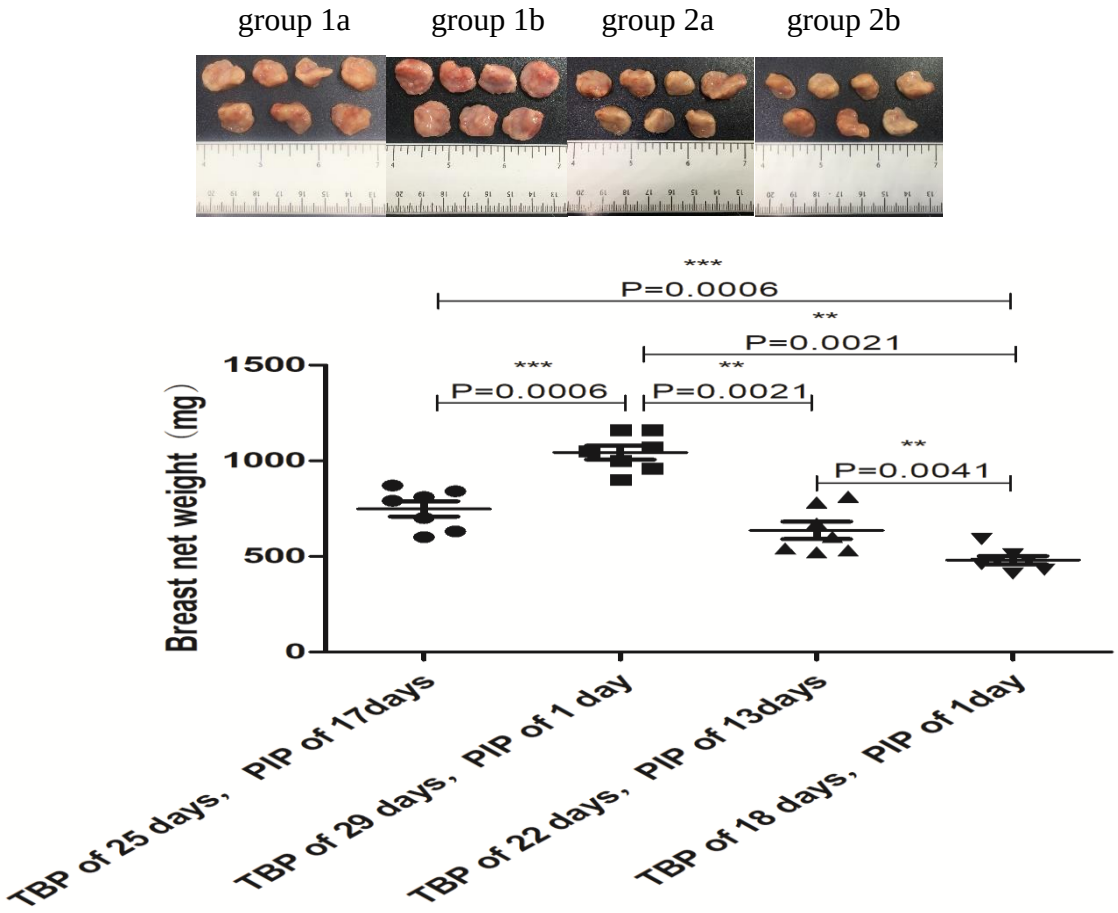


Fig. 4 The growth trend of breast tumors: (a). The picture collection of breast tumors from the 8th day after in vivo model established. a1=8th day, a2=11th day, a3=14th day, a4=17th day, a5=20th day, a6=23th day, a7=26th day, a8=33th day, a9=7th day after the breast tumor resection. (b). Comparison the weight of breast tumor among the groups:

The breast weights of experimental group 1a, 2a increased significantly compared with group 2b, the differences were statistically significant, and the P value was 0.0006, 0.0041, respectively; The breast weights of experimental group 1b, increased significantly compared with group 1a, 2a and 2b, the differences were statistically significant, and the P value was 0.0006, 0.0021 and 0.0021, respectively.

3. The characteristics of lung and extrapulmonary metastases among four groups

3.1 Comparison of the lung weight

The results of lung weight showed that: 1. Comparison between the experimental groups and the blank group: The lung weights of experimental group 1a, 1b, 2a and 2b increased significantly compared with the blank group, the differences were statistically significant, and the P value was 0.0024, 0.0002, 0.0003 and 0.0025, respectively (Fig. 5 a). 2. Comparison between the experimental groups: Compared with experimental group 1b, 2a and 2b, the lung weight of experimental group 1a increased significantly, and the P value was 0.0181, 0.0123 and 0.0295, respectively. Which means the lung metastasis of the experimental group 1a was more obvious than that of the other experimental groups (Fig. 5 a).

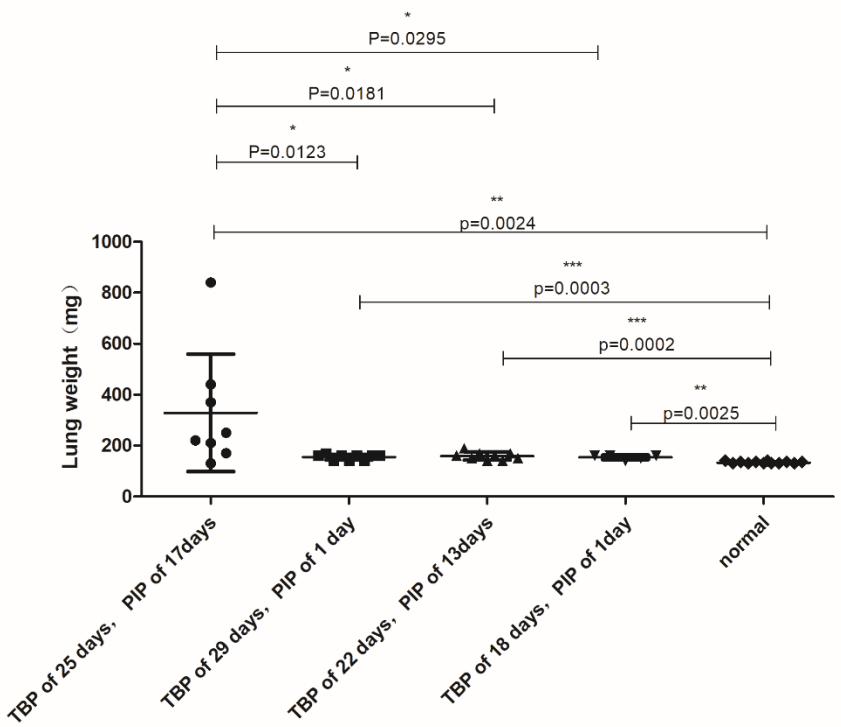
3.2 Comparison photon number of lung metastasis

The result of optical in vivo imaging analysis showed that the photon number of experiment 1a group > experiment 2a group > experiment 1b group > experiment 2b group. The general view of lung specimens showed that the lung metastases in group 1a were mostly fused, and the single lung metastases were larger, but there was no obvious lung metastases in group 2b (Fig 5 b).

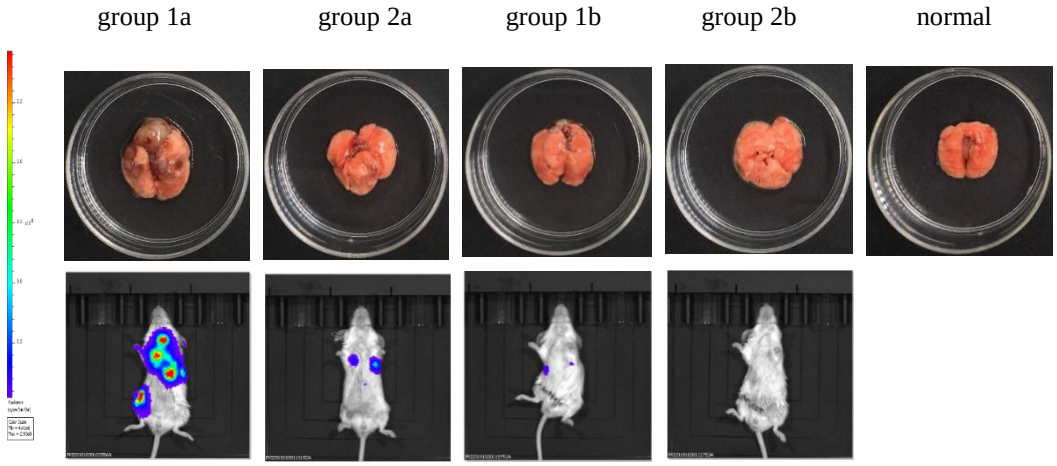
4. The characteristics of extrapulmonary metastases

To our surprise, the group 1a, besides lung metastasis, extrapulmonary metastases such as chest wall, back subcutaneous, axillary lymph nodes, inguinal lymph nodes and pericardium were also found (Fig 5 c).

(a)



(b)



(c)

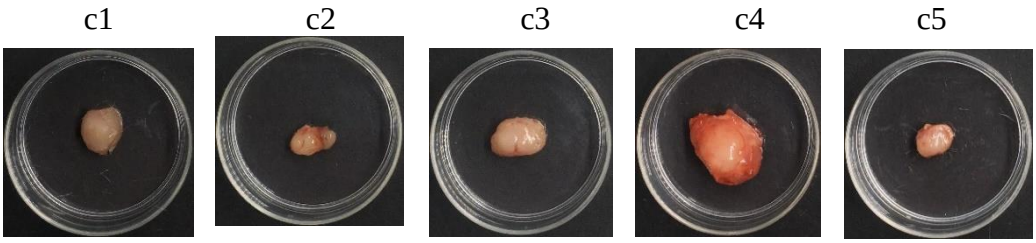


Fig. 5 The characteristics of lung and extrapulmonary metastases among four groups: (a). Comparison of the lung weight: The lung weights of experimental group 1a, 1b, 2a and 2b increased significantly compared with the blank group, the differences were statistically significant, and the P value was 0.0024, 0.0002, 0.0003 and 0.0025, respectively; The lung weights of experimental group 1a increased significantly compared with group 1b, 2a, 2b, the differences were statistically significant, and the P value was 0.0181, 0.0123, 0.0295. (b). Comparison photon number of lung metastasis: The photon number of group1a > group 2a> group 1b> group 2b, and the photos of lung specimens are displayed simultaneously. (c). The extrapulmonary metastases of group 1a: c1= chest wall metastases, c2=back subcutaneous metastases, c3=axillary lymph nodes metastases, c4=inguinal lymph nodes metastases, c5=pericardium metastases.

5. The characteristics of hypercoagulation state

TEG results showed that: 1. Comparison between the experimental groups and the blank group: The K(min) of experimental group 1a, 1b, 2a and 2b had significantly shorter than the blank group, and the P values were 0.0087, 0.0009, 0.0060 and 0.0012, respectively (Fig.6 a). Suggesting the fibrin function is hyperactive in all the experimental groups; The Angle (deg) of experimental group 1a, 1b, 2a and 2b had significantly increased than the blank group, and the P values were 0.0104, 0.0083, 0.0018 and 0.0022, respectively (Fig.6 b). Suggesting the fibrin function is hyperactive in all the experimental groups; The MA (mm) of experimental group 1a, 1b, 2a and 2b had significantly increased than the blank group, and the P values were 0.0022, 0.0001, 0.0018 and 0.0046 respectively (Fig.6 c). Suggesting the platelet function is hyperactive in all the experimental groups. However, the R(min) had no significant difference between the experimental groups and the blank group (Fig.6 d). Suggesting there was no significant abnormality in coagulation factor function in all of the experimental groups. 2. Comparison between the experimental groups: The only statistically significant was the MA (mm) of the experimental group 2a increased than group 1b, and P value was 0.0274 (Fig.6 c). Suggesting prolonged tumor-bearing time and post-operative stress may cause hyper platelet function in group 1b.

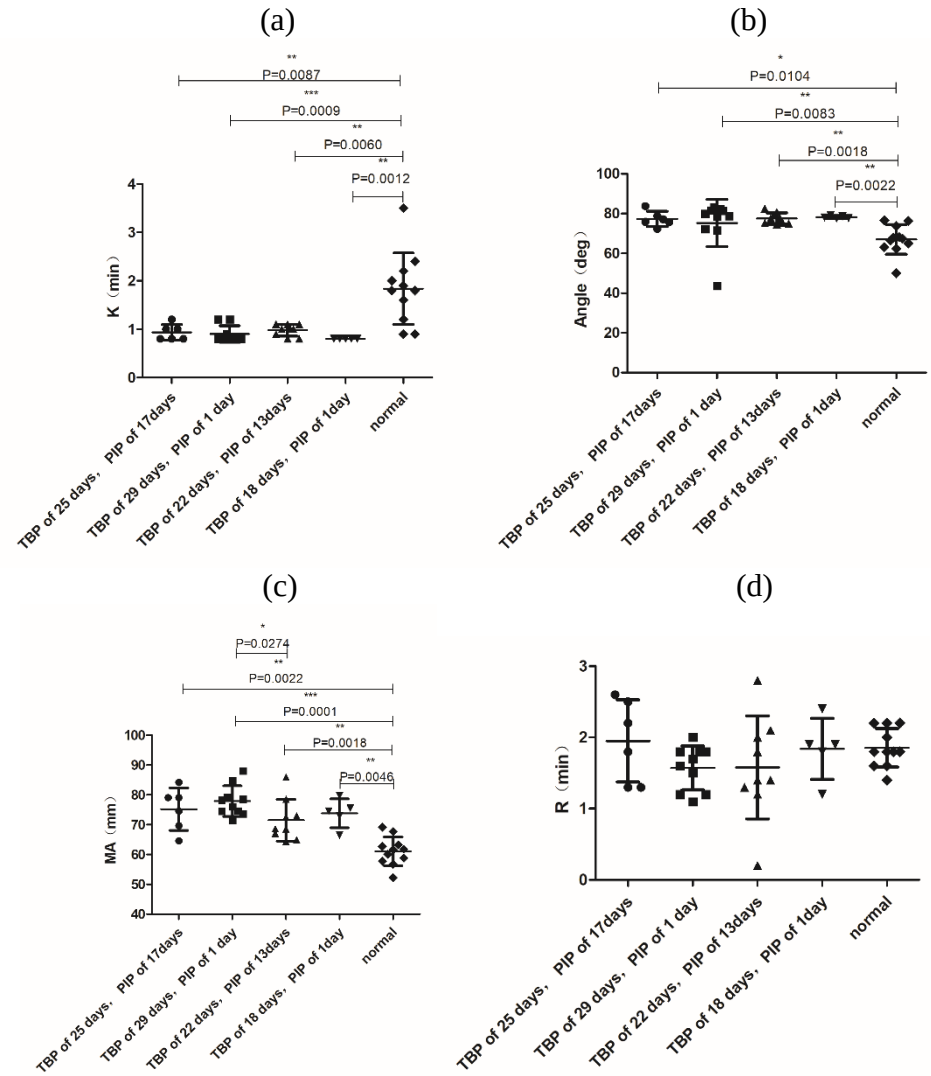


Fig. 6 The characteristics of hypercoagulation state: a. Comparison between the experimental groups and the blank group: The K(min) of experimental group 1a, 1b, 2a and 2b had significantly shorter than the blank group, and the P values were 0.0087, 0.0009, 0.0060 and 0.0012, respectively; b. The Angle (deg) of experimental group 1a, 1b, 2a and 2b had significantly increased than the blank group, and the P values were 0.0104, 0.0083, 0.0018 and 0.0022, respectively; c. The MA (mm) of experimental group 1a, 1b, 2a and 2b had significantly increased than the blank group, and the P values were 0.0022, 0.0001, 0.0018 and 0.0046 respectively, The MA (mm) of the group 2a increased than group 1b, the differences were statistically significant, and P value was 0.0274.d. the R(min) had no significant difference between the experimental groups and the blank group.

5. Animal welfare/ Feasibility analysis of operation

Increased size of breast tumors caused by prolonged TBP significantly prolonged the operation time, the length and stitches of the incision, which all brought animal trauma undoubtedly.

5.1 The weight records of mice

Mice weight records (Once a week) showed that the weight of the mice increased smoothly, there were no statistically differences among all the groups, and the tumors did not cause them obvious pain.

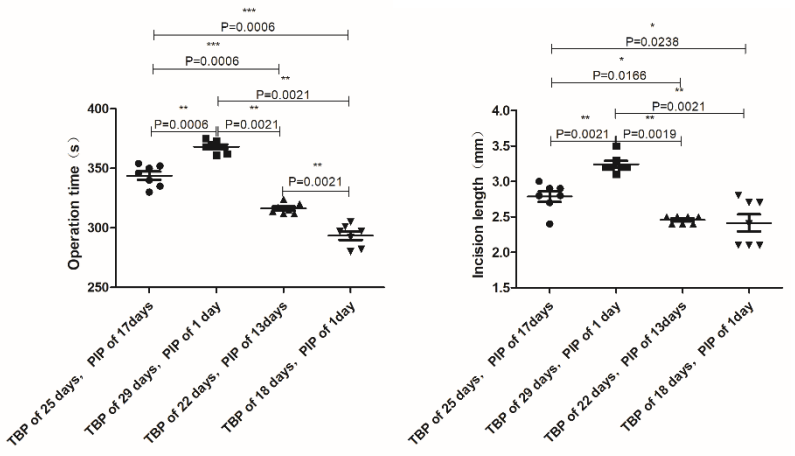
5.2 Comparison of the operation time

The operation time of experimental group 1b had significantly longer than group 1a, 2a and 2b, and the P values were 0.0103, 0.0014 and 0.0021, respectively. The operation time of experimental group 1a had significantly longer than group 2a and 2b, and the P values were 0.0006, 0.0006, respectively. The operation time of experimental group 2a had significantly longer than group 2b, and the P values was 0.0021. (Fig.7 a).

5.3 Comparison of the incision length and stitches

Because the size of breast tumors varies with the time of tumor-bearing, so the lengths and stitches of incisions were different. The incision length of experimental group 1b had significantly longer than group 1a, 2a and 2b, and the P values were 0.0021, 0.0019, and 0.0021, respectively. The incision length of experimental group 1a had significantly longer than group 2a and 2b, and the P values were 0.0166, 0.0238, respectively. But there was no obvious statistical difference between group 2a and 2b. (Fig.7 b). The incision stitches of experimental group 1a had significantly longer than group 2a and 2b, and the P values were 0.0093, 0.0020, respectively. The incision stitches of experimental group 1b had significantly longer than group 1a, 2a and 2b, and the P values were 0.0103, 0.0014 and 0.0014, respectively. And the incision stitches of experimental group 2a had significantly longer than group 2b, and the P values was 0.0075. c= group 1a, d= group 2a, e= group 2b. (d). The pictures of the incisions were collected after operation. (Fig.7 c).

(a) (b)



（c）

group 1a group 1b group 2a group 2b



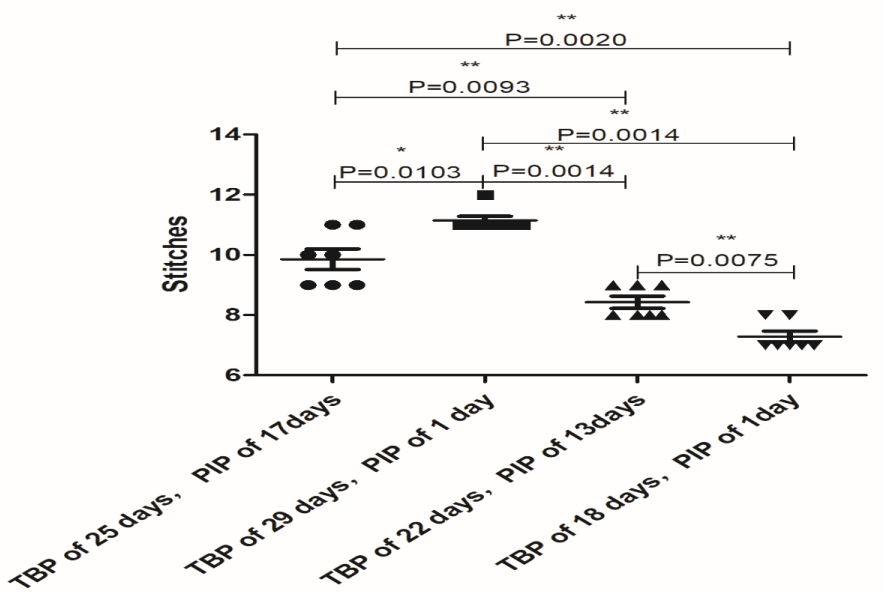


Fig. 7 Animal welfare/ Feasibility analysis of operation: (a). Comparison of the operation time: The operation time of experimental group 1b had significantly longer than group 1a, 2a and 2b, and the P values were 0.0103, 0.0014 and 0.0021, respectively. The operation time of experimental group 1a had significantly longer than group 2a and 2b, and the P values were 0.0006, 0.0006, respectively. The operation time of experimental group 2a had significantly longer than group 2b, and the P values was 0.0021. (b). Comparison of the incision length: The incision length of experimental group 1b had significantly longer than group 1a, 2a and 2b, and the P values were 0.0021, 0.0019, and 0.0021, respectively. The incision length of experimental group 1a had significantly longer than group 2a and 2b, and the P values were 0.0166, 0.0238, respectively. But there was no obvious statistical difference between group 2a and 2b. (c). Comparison of the incision stitches: The incision stitches of experimental group 1a had significantly longer than group 2a and 2b, and the P values were 0.0093, 0.0020, respectively. The incision stitches of experimental group 1b had significantly longer than group 1a, 2a and 2b, and the P values were 0.0103, 0.0014 and 0.0014, respectively. And the incision stitches of experimental group 2a had significantly longer than group 2b, and the P values was 0.0075. c= group 1a, d= group 2a, e= group 2b. (d). The pictures of the incisions were collected after operation.
*Increased size of breast tumors caused by prolonged TBP significantly prolonged the operation time, the length and stitches of the incision, which all brought animal trauma undoubtedly.

6. The characteristics of supernatants

Co-incubation of platelets and 4T1 cells could activate each other and promote the release of substance and procoagulant activity with prolonging the co-incubation time.

6.1 The physical characteristics of supernatants

The concentration and size characteristics of supernatants were listed as follows (Table 2), (Fig.8 a), (Fig.8 b): 1. The concentration of supernatants increased with the incubation time, 4T1 (24h) > 4T1 (30min), PLT (24h) > PLT (30min), 4T1+PLT(24h) >4T1+PLT (30min); 2. Co-incubation promoted release, and the efficiency increased with prolonging the co-incubation time, 4T1+PLT (30min) > 4T1 (30min) + PLT (30min), 4T1+PLT (24h) > 4T1 (24h) + PLT (24h); 3. There were no obvious size difference among the supernatants.

Table 2. The physical characteristics of supernatants: The concentration of supernatants increased with the incubation time, 4T1 (24h) > 4T1 (30min), PLT (24h) > PLT (30min), 4T1+PLT (24h) >4T1+PLT (30min); Co-incubation promoted release, and the efficiency increased with prolonging the co-incubation time, 4T1+PLT (30min) > 4T1 (30min) + PLT (30min), 4T1+PLT (24h) > 4T1 (24h) + PLT (24h);

	Sample	Size(nm)	Concentration
1	4T1 (30min)	61.14 ± 16.45	5.45×10^9
2	4T1 (24h)	57.63 ± 16.91	9.47×10^9
3	PLT (30min)	64.26 ± 27.31	2.39×10^{10}
4	PLT (24h)	57.35 ± 19.73	3.28×10^{10}
5	4T1+PLT (30min)	61.79 ± 24.34	2.97×10^{10}
6	4T1+PLT (24h)	57.37 ± 19.55	5.73×10^{10}

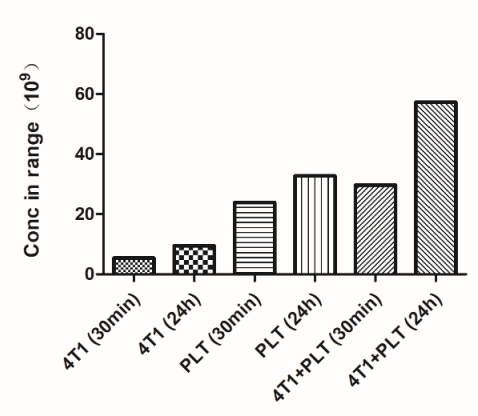
6.2. The procoagulant activity of supernatants

The small EVs with PS-exposed in the 24-hour co-incubation supernatant were significantly more than 24-hour platelet supernatant (Table 3) (Fig.8 c).

Table 3. The procoagulant activity of supernatants: PS-exposed microparticles in the 24-hour co-incubation supernatant were significantly more than 24-hour platelet supernatant, co-incubation significantly increased the procoagulant activity.

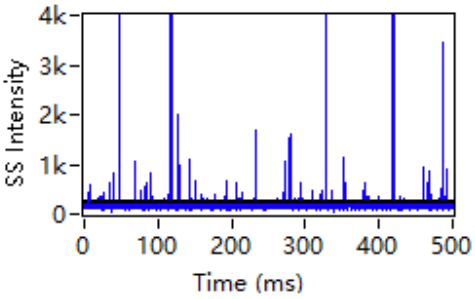
	Sample	Size(nm)	Concentration
1	PLT (24h)	82.36±28.29	5.84×10^9
2	4T1+PLT (24h)	76.91±29.26	9.86×10^9

（a）

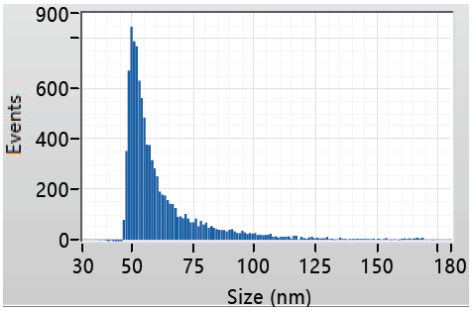


(b)

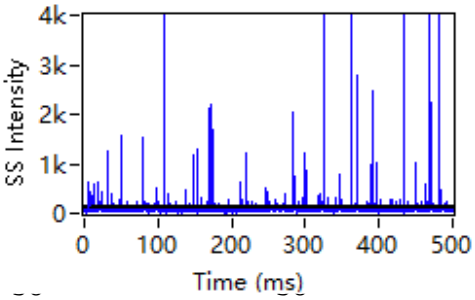
b1



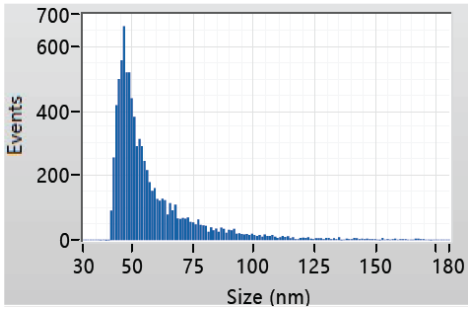
b2



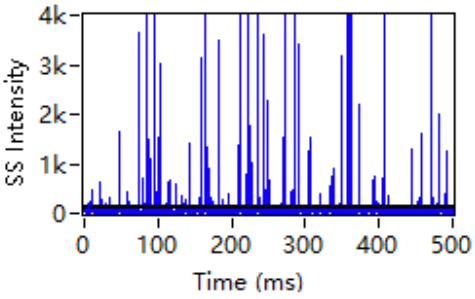
b3



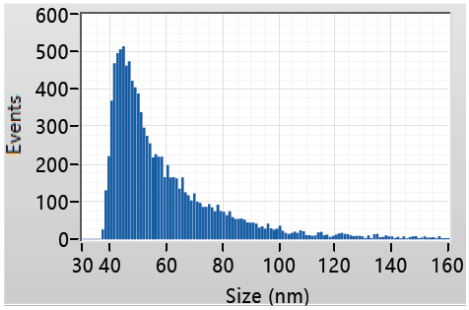
b4

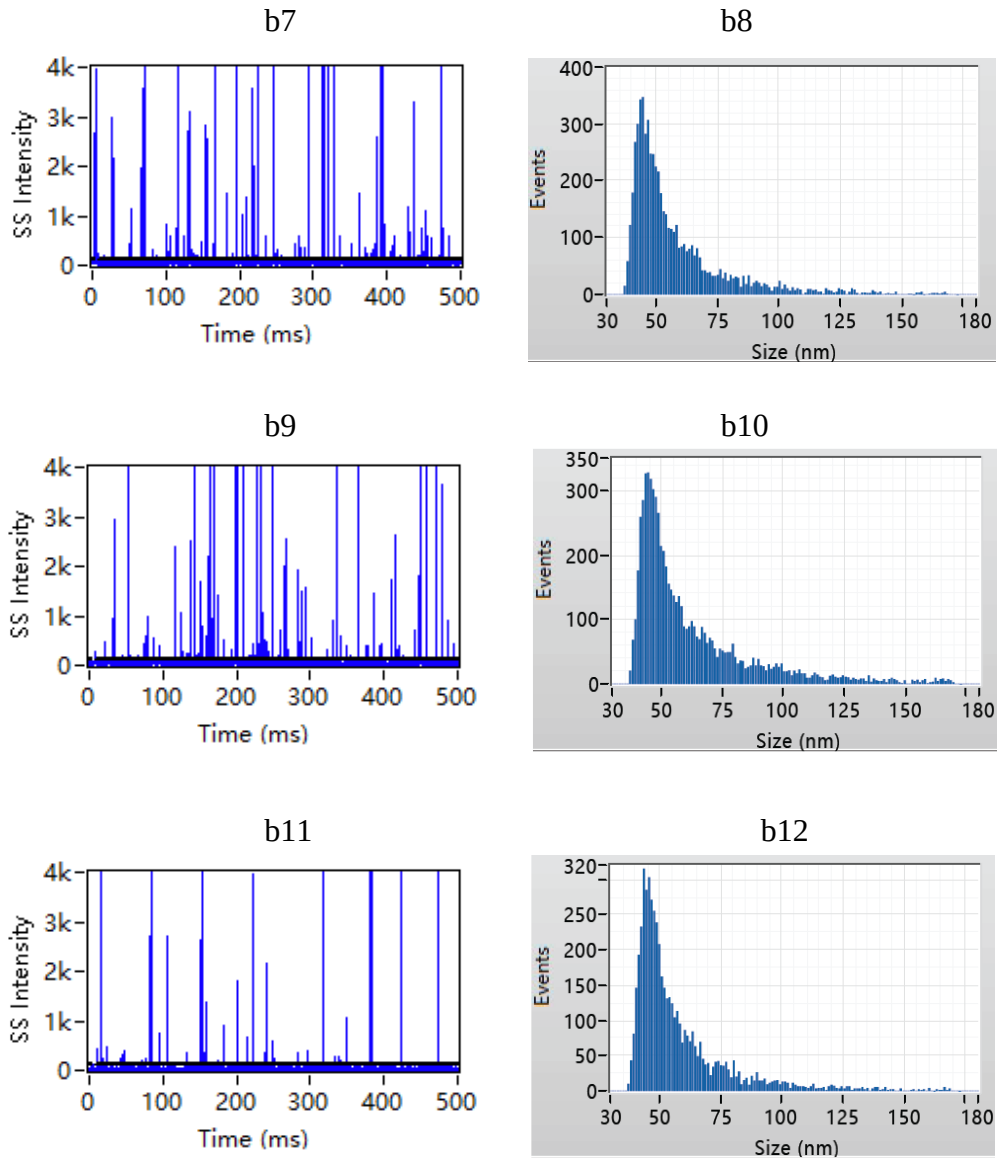


b5

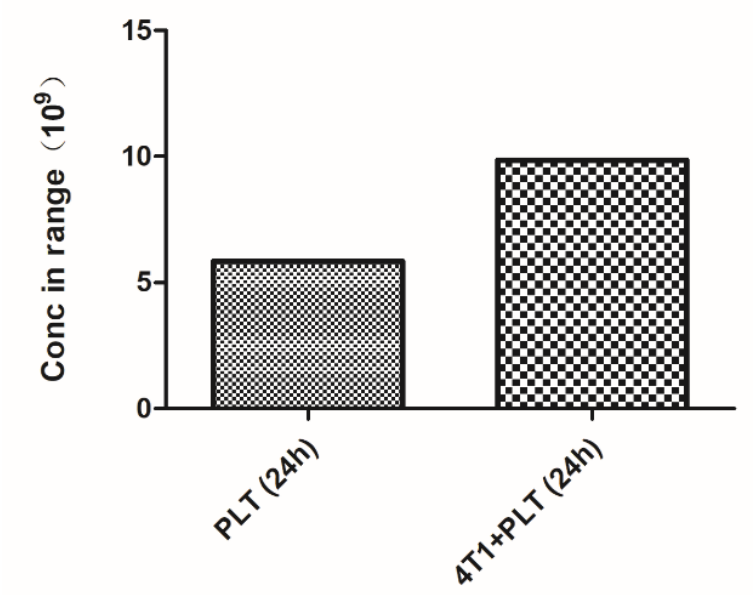


b6




b7
b8
b9
b10
b11
b12
SS Intensity
Time (ms)
Events
Size (nm)

(c)


Conc in range（10⁹）
PLT (24h)
4T1+PLT (24h)

(d)

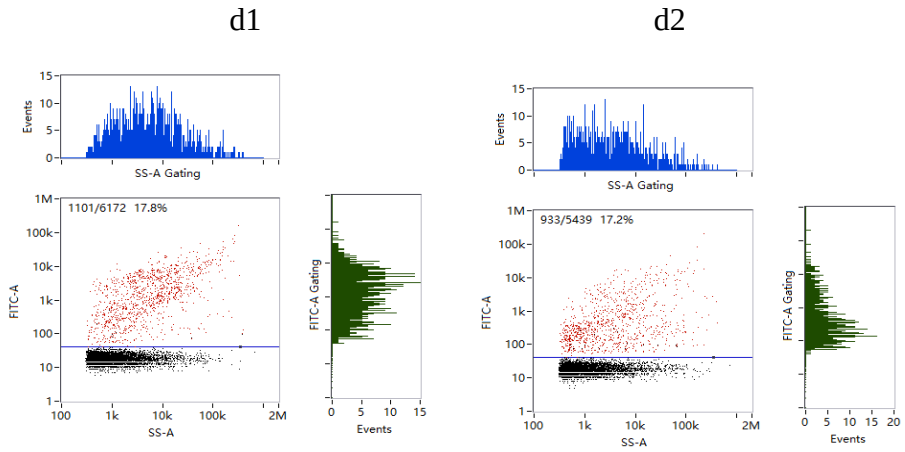


Fig.8 (1). The physical characteristics of supernatants: (a). The concentration of supernatants increased with the incubation time, 4T1 (24h) > 4T1 (30min), PLT (24h) > PLT (30min), 4T1+PLT (24h) >4T1+PLT (30min); Co-incubation promoted release, and the efficiency increased with prolonging the co-incubation time, 4T1+PLT (30min) > 4T1 (30min) + PLT (30min), 4T1+PLT (24h) > 4T1 (24h) + PLT (24h); (b). b1=the concentration of 4T1 (30min) supernatant, b2= the microparticle size of 4T1 (30min) supernatant, b3=the concentration of 4T1 (24h) supernatant, b4= the microparticle size of 4T1 (24h) supernatant, b5=the concentration of PLT (30min) supernatant, b6= the microparticle size of PLT (30min) supernatant, b7=the concentration of PLT (24h) supernatant, b8= the microparticle size of PLT (24h) supernatant, b9=the concentration of 4T1+PLT (30min) supernatant, b10= the microparticle size of 4T1+PLT (30min) supernatant, b11=the concentration of 4T1+PLT (24h) supernatant, b12= the microparticle size of 4T1+PLT (24h) supernatant. (2). The procoagulant activity of supernatants: (c). PS-exposed microparticles in the 24-hour co-incubation supernatant were significantly more than 24-hour platelet supernatant; (d). d1. PS-exposed microparticles of 24-hour platelet supernatant; d2. PS-exposed microparticles of 24-hour co-incubation supernatant. * Co-incubation of platelets and 4T1 cells could activate each other and promote the release of substance and procoagulant activity with prolonging the co-incubation time.

Discussion

Breast cancer is the commonest malignancy cancer in women, and about 3%-8% of patients are with distant metastasis at the time of initial diagnosis [29]. Even 30% of the early patients who underwent radical resection and standardized treatment would still have recurrence and metastasis [30], even lead to death. Accumulated studys showed that more than 60% of patients with malignant tumor were accompanied by hypercoagulable state, which in turn cause cancer progression, followed by long distant metastasis, alert the worse tumor prognosis and even affect treatment strategy. In the clinical study, we showed that the MA (mm) were significantly higher in the patients with stage IV breast cancer than in stage I/II/ III patients(P=0.01), which indicated that platelet hyperfunction was positively associated with tumor metastasis in breast cancer patients. The interesting clinical phenomenon has inspired us to explore the mechanisms related to platelet hyperactivity and breast cancer metastasis.

Given construction of models in vivo and in vitro are the key and the basis of study in this field [31], which both play a decisive role in mimic blood hypercoagulability and the biological characteristics of hematogenous metastasis with clinical efficiently. We were committed to the construction of efficient models in vivo and in vitro.

For selected an excellent in vivo model, we established four experimental groups by limiting the TBP and PIP. Through evaluation of the lung metastasis, we found: 1. The TBP and PIP were both played a decisive role in the occurrence of lung metastasis. For the decisive role of TBP, all of the group 1a, 1b and 2a achieved lung metastasis successfully, but there was no obvious lung metastasis in the group 2b. Given the influence of TBP on metastasis is mainly decided by the follows: When the TBP is too short, the tumor has not yet occurred invasion and metastasis, which directly affects the success of metastasis; When the TBP is too long, the tumor neovascularization increases and the rent increases, the tumor adheres to the surrounding tissue, and is prone to local necrosis, which brings difficulties to radical resection of the tumor, and also easy to cause death by excessive bleeding and prolonged anaesthesia during resection, even leads to incomplete tumor resection to cause recurrence. Combined with the characteristics of our in vivo models, it is indicated that 3 weeks is the baseline of TBP to achieve lung metastasis. 2. For the decisive role of PIP, we found the lung metastasis of the group 1a was more obvious than that of the group 1b, and the group 1a even achieved extrapulmonary metastases. But the fact was TBP of group 1a was longer than that of group 1b, which indicated if the TBP was over 3 weeks, continued extension of it does not increase the incidence of lung metastasis. On the contrary,

the PIP of group 1a was longer than that of group 1b, which indicated when TBP was over 3 weeks prolonged PIP (about 2 weeks) can increase the incidence of lung metastasis. In conclusion, with TBP of 3 weeks and PIP of 2 weeks is the optimum modeling conditions for achieve lung metastasis.

Through evaluation of the hypercoagulation state, we found: 1. Compared with the blank group, all of the experimental groups showed hypercoagulable state, and the remarkable characteristic is the hyperfunction of fibrin and platelet, but the function of coagulation factors were normal. It is further suggested that our in vivo model is particularly suitable for the study of the hematological mechanism of hypercoagulation with hyperactivity of fibrin and platelet; 2. The difference between the group 1b and the blank group was more obvious than that of the other experimental groups. Because the prolonged TBP is the most significant feature of the group 1b, which indicated that the TBP had a great influence on the hyperfunction of platelet; 3. The group 2b showed hypercoagulability before the obvious lung metastasis, indicating that the hypercoagulable state of our model is an early event of metastasis, which can effectively mimic the biology process of hypercoagulable state promoting metastasis.

By compared the operation time, the incision length and stitches among the experimental groups, animal welfare and feasibility analysis of operation were evaluated. We found: Increased size of breast tumors caused by prolonged TBP significantly prolonged the operation time, the length and stitches of the incision, which all brought animal trauma undoubtedly. Therefore, we should shorten the TBP as much as possible on the premise that the model can be successfully established. However, for surgical techniques, we emphasize that complete separation of main nutrient vessels and proximal ligation are important steps to reduce blood loss, which decreased animal trauma obviously.

In conclusion, our study recommended that 4Tl-luc cells be injected into the fourth intramammary gland fat pad with 1 x 10^6, and with TBP of 3 weeks and PIP of 2 weeks, then an ideal in vivo model can be established.

For further promote the study of in vitro mechanism, we established an in vitro model (platelet-breast cancer co-action) by platelets (female BALB/c mice) and 4T1 cells co-incubation for 30 minutes (represent the early phase of platelet-breast cancer co-action in vivo) or 24 hours (represent the late phase of platelet-breast cancer co-action in vivo), then the co-incubation supernatants were obtained by differential centrifugation. Through compared the physical characteristics of supernatants, we found: 1. The concentration of supernatants increased with the incubation time, 4T1 (24h) > 4T1 (30min), PLT (24h) > PLT (30min), 4T1+PLT(24h) >4T1+PLT (30min); 2. Co-incubation promoted release, and the efficiency increased with prolonging the co-incubation time, 4T1+PLT (30min) > 4T1 (30min) + PLT (30min), 4T1+PLT (24h) > 4T1 (24h) + PLT (24h); 3. There were no obvious size difference among the supernatants. The results of physical characterization showed that co-incubation of platelets and 4T1 cells could activate each other and promote substance release with prolonging the co-incubation time, and the reaction supernatants can be used for interest factors detection and bioactivity verification.

From the study of our in vivo model, we known the TBP had a great influence on the hyperfunction of platelet, which means in vitro model, the reaction supernatants by 4T1 and platelet co-incubation for 24 hours (represent the late phase of platelet-breast cancer co-action in vivo) should have a more obvious procoagulant activity, and through compared the PS-exposed, we found the small EVs in the 24-hour co-incubation supernatant were significantly more than 24-hour platelet supernatant, which means co-incubation significantly increased the procoagulant activity with prolonging the co-incubation time.

In conclusion, through the clinical study, we found platelet hyperfunction was positively associated with tumor metastasis in breast cancer patients. And through established models in vivo and in vitro, we have helped to provide powerful research tools for understanding the underlying mechanism related to platelet hyperactivity and breast cancer metastasis. Maybe these models will also provide important insights into the intervention of hematological metastasis in breast cancer.

References

1. Trousseau A. Clinique médicale de l'Hôtel-Dieu de Paris [M]. Baillière, 1865.

Blom J W, Doggen C J M, Osanto S, et al. Malignancies, prothrombotic mutations, and the

2. risk of venous thrombosis[J]. Jama, 2005, 293(6): 715-722.

3. Lee K W, Bang S M, Kim S, et al. The incidence, risk factors and prognostic implications of venous thromboembolism in patients with gastric cancer[J]. Journal of Thrombosis and Haemostasis, 2010, 8(3): 540-547.

4. Lyman G H, Khorana A A. Cancer, clots and consensus: new understanding of an old problem [J]. Journal of Clinical Oncology, 2009, 27(29): 4821.

5. Erdemir F, Kilciler M, Bedir S, et al. Clinical significance of platelet count in patients with renal cell carcinoma[J]. Urologia internationalis, 2007, 79(2): 111-116.

6. Taucher S, Salat A, Gnant M, et al. Impact of pretreatment thrombocytosis on survival in primary breast cancer[J]. Thrombosis and haemostasis, 2003, 89(06): 1098-1106.

7. Bensalah K, Leray E, Fergelot P, et al. Prognostic value of thrombocytosis in renal cell carcinoma[J]. The Journal of urology, 2006, 175(3): 859-863.

8. Brockmann M A, Giese A, Mueller K, et al. Preoperative thrombocytosis predicts poor survival in patients with glioblastoma[J]. Neuro-oncology, 2007, 9(3): 335-342.

9. Thrombosis and cancer[M]. Taylor & Francis, 2004.

10. Patrignani P, Patrono C. Aspirin and cancer[J]. Journal of the American College of Cardiology, 2016, 68(9): 967-976.

11. Patrignani P, Patrono C. Aspirin, platelet inhibition and cancer prevention[J]. Platelets, 2018, 29(8): 779-785.

12. Gasic G J, Gasic T B, Stewart C C. Antimetastatic effects associated with platelet reduction[J]. Proceedings of the National Academy of Sciences of the United States of America, 1968, 61(1): 46.

13. Cole B F, Logan R F, Halabi S, et al. Aspirin for the chemoprevention of colorectal adenomas: meta-analysis of the randomized trials[J]. JNCI: Journal of the National Cancer Institute, 2009, 101(4): 256-266.

14. Baron J A, Cole B F, Sandler R S, et al. A randomized trial of aspirin to prevent colorectal adenomas[J]. New England Journal of Medicine, 2003, 348(10): 891-899.

15. Algra A M, Rothwell P M. Effects of regular aspirin on long-term cancer incidence and metastasis: a systematic comparison of evidence from observational studies versus randomised trials[J]. The lancet oncology, 2012, 13(5): 518-527.

16. Rothwell P M, Wilson M, Price J F, et al. Effect of daily aspirin on risk of cancer metastasis: a study of incident cancers during randomised controlled trials[J]. The Lancet, 2012, 379(9826): 1591-1601.

17. Bibbins-Domingo K, Grossman D C, Curry S J. The US Preventive Services Task Force 2017 draft recommendation statement on screening for prostate cancer: an invitation to review and comment[J]. Jama, 2017, 317(19): 1949-1950.

18. DeSantis C E, Lin C C, Mariotto A B, et al. Cancer treatment and survivorship statistics, 2014[J]. CA: a cancer journal for clinicians, 2014, 64(4): 252-271.

19. Chaari M, Ayadi I, Rousseau A, et al. Impact of breast cancer stage, time from diagnosis and chemotherapy on plasma and cellular biomarkers of hypercoagulability[J]. BMC cancer, 2014, 14(1): 991.

20. Jaiswal R, Johnson M S, Pokharel D, et al. Microparticles shed from multidrug resistant breast cancer cells provide a parallel survival pathway through immune evasion[J]. BMC cancer, 2017, 17(1): 104.

21. Toth B, Liebhardt S, Steinig K, et al. Platelet-derived microparticles and coagulation activation in breast cancer patients[J]. Thrombosis and haemostasis, 2008, 100(10): 663-669.

22. van der Spuy W J, Augustine T N. Ultrastructural investigation of the time-dependent relationship between breast cancer cells and thrombosis induction[J]. Micron, 2016, 90: 59-63.

23. Van der Pol E, Böing A N, Harrison P, et al. Classification, functions, and clinical relevance of extracellular vesicles[J]. Pharmacological reviews, 2012, 64(3): 676-705.

24. Théry C, Ostrowski M, Segura E. Membrane vesicles as conveyors of immune responses[J]. Nature reviews immunology, 2009, 9(8): 581.

25. Maas S L N, Breakefield X O, Weaver A M. Extracellular vesicles: unique intercellular delivery vehicles[J]. Trends in cell biology, 2017, 27(3): 172-188.

26. Radomski M, Moncada S. An improved method for washing of human platelets with prostacyclin[J]. Thrombosis research, 1983, 30(4): 383-389.

27. Su Y, Deng X, Ma R, et al. The Exposure of Phosphatidylserine Influences Procoagulant Activity in Retinal Vein Occlusion by Microparticles, Blood Cells, and Endothelium[J]. Oxidative medicine and cellular longevity, 2018.

28. Schwertz H, Rondina M T. Platelets and their Microparticles go hand in hand[J]. Thrombosis research, 2018, 168: 164-165.

29. Siegel R L, Miller K D, Jemal A. Cancer statistics, 2016[J]. CA: a cancer journal for clinicians, 2016, 66(1): 7-30.

30. Gonzalez-Angulo A M, Morales-Vasquez F, Hortobagyi G N. Overview of resistance to systemic therapy in patients with breast cancer[M]//Breast Cancer Chemosensitivity. Springer, New York, NY, 2007: 1-22.

31. Zhang L, Bi L, Shi J, et al. A quantitative diagnostic method for oral mucous precancerosis by Rose Bengal fluorescence spectroscopy[J]. Lasers in medical science, 2013, 28(1): 241-246.

International Conference on Cancer Research 2019

Website: www.CancerConf.org

June 10-11, London, UK



Photodynamic Therapy and Lung Cancer Stem Cells – The effects of $AlPcS_4Cl$ on Isolated Lung Cancer Stem Cells

Anine Crous[a], Heidi Abrahamse[b1]

[a,b] *Laser Research Centre, Faculty of Health Sciences, University of Johannesburg, PO Box 17011, Johannesburg 2028, South Africa*

Abstract

Cancer is a worldwide burden. Claiming the lives of millions annually. Lung cancer is the leading contributor to mortality rates caused by cancer. Lowering risk factors such as tobacco consumption and industrial pollution can reduce lung cancer incidence. Yet it is noted to be counter-intuitive in emerging nations. An important disease entity is people who develop lung cancer regardless of avoiding factors leading to cancer. A subset of cells known to contribute to the high mortality rates seen in lung cancer is cancer stem cells (CSCs). Studies on CSCs have shown that they can evade conventional cancer treatment. Attributing to their stem-like characteristics is self-renewal, differentiation leading to phenotypical heterogeneity of tumor cells, metastasis and cancer recurrence. Expression of genetic markers involved in drug efflux, regeneration and motility contribute to the stem-like nature of CSCs. Photodynamic therapy (PDT) is an effective yet underutilized treatment modality for a variety of cancers. This form of alternative chemotherapy uses a non-toxic drug that has an affinity for cancerous cells. The drug localizes in intracellular organelles exerting an effect upon laser activation of the drug at a specific wavelength. Extensive research has been focused on the development of operative photosensitizers (PS), enhancing its selectivity and uptake into cancerous cells. Aluminium (III) Phthalocyanine Chloride Tetrasulphonate (AlPcS4Cl) is an improved second generation PS with ideal PDT characteristics including high photochemical reactivity, it is amphiphilic, has low dark toxicity, good localization and little light sensitivity. The effects and efficacy of PSs in the eradication of CSCs are not well studied. PDT can be a useful therapeutic tool in the eradication of CSCs, where factors such as fluence, dose, and localization play a crucial role. In this study, we evaluated the effects of (AlPcS4Cl) on isolated lung CSCs expressing stem-like markers involved in metastasis and drug resistance. Our findings suggest that treating CSCs using PDT is advantageous over standard cancer treatments. The results can be attributed to PDT not inducing drug resistance upon initial application of treatment to CSCs. This is due to passive absorption of the PDT drug which doesn't activate drug efflux pumps in the CSCs. This enables the PS to localize in the cell, ensuring biochemical responses upon laser activation leading to cellular toxicity and cellular death.

Keywords:

Photodynamic Therapy,

Photosensitizer,

Lung Cancer Stem Cells,

Surface Markers,

Cell Death,

Cytotoxicity,

Proliferation,

Viability.

1. Introduction

Malignancy is a disease that had formed part of a global problem over many decades. It has driven broad research and modern medicine to seek prevention and treatment to combat cancer and its mortality rates. Along with preventative treatment research, the causes of cancer and its dynamics are also investigated [1]. Cancer development starts on a cellular level where genetic mutations lead to defective instructions in the DNA sequence. These mutations can affect normal cell cycle function where the cells evade apoptosis along with genetic instability contributing to further cancer-promoting mutations [2]. Along with cancer cells evading cell cycle arrest cancer can have the ability to metastasize and return even after conventional therapy.

Lung cancer is a noteworthy supporter of disease fatalities. Carcinoma of the lung emerges because of hazardous factors, for example, smoking, inhalation of destructive synthetics and air contamination; prompting mutagenic transformations of typical lung tissue. Along with risk factors promoting lung cancer development there are still patients who avoid these risks, yet are still the victim of mutagens leading to cancer development. These genetic transformations

[1] **CONTACT**: habrahamse@uj.ac.za

cause hereditary adjustments that can change cell cycle regulations, prompting cellular expansion, tissue invasion, tumor development and metastasis [3]. Patients undergoing lung cancer treatment can still only expect a 5-year survival rate. This is due to treatment resistance before and during chemo and radiation therapy. Treatment resistance contributes to disease progression, recurrence and mortality [4]. This poses a significant clinical challenge for lung cancer treatment. Novel agents have been used alone and in combination with conventional therapy to overcome this problem. However, the basic systems presenting this resistant phenotype in malignant lung growth stay obscure [5]. The complete treatment of cancer depends on revealing its origin.

Research findings suggest that a small heterogeneous subpopulation of cells are the origin for cancer development. This small population of cells display stem-like characteristics. These cells are called cancer stem cells (CSCs). CSCs can self-renew, have multi-differentiation potential and are known to evade drug-induced cell death and can metastasize [6]. CSCs differ from the bulk of a tumor by its characteristic ability to repopulate a malignant growth. Giving rise to both CSCs and non-stem cancerous cells. Asymmetric division enables the CSCs to self-perpetuate and generate a differentiated progeny. Giving rise to a heterogeneous tumor whilst maintaining the CSC subpopulation. CSCs undergo symmetric division during periods of stress. Whereas non-stem-like lung cancer cells undergo only symmetric division. Resulting in a pure non-CSC cell population. This may explain the ineffectiveness of many conventional therapies and patient relapse [5]. These important clinical observations have stimulated intense interest in experimental approaches for further investigation of CSCs and their role in the treatment of drug resistant lung cancer. CSCs show strong treatment opposition and endurance because of expanded telomere length, initiation against apoptotic pathways, expanded membrane transporter action and their capacity to relocate and metastasize [7]. Lung CSCs identified, showed resistance to various lung cancer treatment options. These include: conventional therapy, biological molecules and targeted therapy. Eliminating lung CSCs during therapeutic intervention is of utmost importance. As this can prevent CSC expansion, cancer recurrence, relapse and metastasis. While little is at present known about lung CSC biology, various CSC markers have been distinguished and considered. These markers incorporate ALDH1, CD133, side population (Hoechst-negative), CD44, CD87 and CD117. These markers have been connected to chemo resistance in various first line disease treatments [5]. It is therefore widely accepted that CSCs are closely related to pathological features resulting in poor clinical prognosis [8].

Photodynamic therapy (PDT) or Alternate/ Photo chemotherapy is an innovative form of cancer treatment. PDT is not intrusive and can be used as a stand-alone treatment or in combination with conventional cancer treatments showing excellent therapeutic outcomes [9]. Non-oncological diseases can also benefit from PDT. It has been successfully used in dermatology, oncology, gynecology and urology. The photosensitive compound or photosensitizer (PS) is used either locally or applied systemically. Where it concentrates in malignant tissues. This leads to selective destruction of cancerous cells via the absorption of light from a particular wavelength. Due to its selectivity, this form of treatment is well tolerated by patients. Despite PDT achieving high success rates in treating various cancers. Researchers are investigating the improvement of PDT by enhancing its selectivity and effectiveness by developing new PS compounds and improving PS delivery methods [10].

The mechanism of action for PDT comprises of the photosensitive compound being activated through photon absorption from a specific light wave. The activated PS generates reactive oxygen species (ROS) leading to cell membrane damage and cell death. The PS moves from its ground state to its excited singlet state. The PS in its excited triplet state can follow two pathways. Type I the PS reacts with biomolecules, transferring hydrogen atoms via the radical mechanism generating free radicals and radical ions. These radicals then react with oxygen resulting in ROS generation. Type II the PS reacts with oxygen in its triplet ground state. Yielding singlet oxygen which is highly reactive and cytotoxic [11].

Characteristics of an ideal PS include no dark toxicity, little aggregation, photo stability, absorbs light at long wavelengths, high singlet oxygen yield, fluorescent, minimum daylight absorption, is not retained by non-cancerous cells and is highly concentrated in cancerous tissue [12]. Clinical anticancer therapy uses the first generation PSs from the porphyrin class. However, these PS tend to have important drawbacks such as short wavelength light absorption that can interfere with tissue absorption. They have low extinction coefficients and induces photosensitivity of the skin [13]. Phthalocyanines (Pc) are synthetic dyes that have a high molar absorption coefficient in the red part of the spectrum. Pcs belong to the group of 2nd generation PSs which exhibit a high extinction coefficient around 670 and 750 nm and even up to 1,000 nm. Thus allowing increased tissue penetration of the activating light [14]. Most phthalocyanine derivatives exhibit high hydrophobicity, which limits their clinical efficacy [13]. Modifying the axial and peripheral substituents changes the tendency for aggregation, pharmacokinetics, bio distribution, solubility, as well as fine-tuning of near infra-red (NIR) absorbance. Extinction coefficients higher than 10^5 M^{-1} cm^{-1} have been reported [15]. These mixes are porphyrin-like PSs, showing tetrapyrrolic, aromatic macrocycles with each cycle connected to the next by nitrogen particles. Each pyrrolic ring is reached out by a benzene ring bringing about the red-shift of their last retention band. Attaching substituents to the peripheral and non-peripheral ring sites can alter the Q band location and complexity of a Pc. Furthermore, the Pc can be adjusted depending on the substituents nature, size and number. Electron donating groups, for example, – NH2, OR and SR at the non-peripheral and periphery result in a red shift to the NIR area. Substitution at

the non-peripheral position indicates more red-shift than at the peripheral position [16]. Other than their solid assimilation in the NIR, Pcs show low retention at wavelengths somewhere in the range of 400 and 600 nm driving possibly to a lower skin photosensitization when presented to daylight. In addition, the nearness of a diamagnetic focal metal, for example, Al3+ in the Pc core appears to improve the triplet state life time (τt), just as its yield (Φt) and singlet oxygen yields (ΦΔ) contrasted with paramagnetic metals [15]. Low lethality of phthalocyanines makes them promising for PDT application. Both lipophilic and water-dissolvable phthalocyanines have been considered as a possibility for PDT. Sulfonation essentially expands Pc dissolvability in polar solvents including water, evading the requirement for elective conveyance vehicles [14]. When comparing sulfonated AlPc ($AlPcS_4$) to other PSs, such as porphyrin and a hydrophobic hydroxyphenylchlorin, most frequently used in clinical settings. $AlPcS_4$ showed increased cellular uptake [17], due to sulfonation enhancing its hydrophilic nature it is more acceptable to antibody conjugation. Even when compared to a hydrophilic form of porphyrin, $AlPcS_4$ has much better photochemical characteristics for use in PDT ($\epsilon_{675} = 1.7 \times 10^5$ vs. $\epsilon_{595} = 7 \times 10^3\ M^{-1}cm^{-1}$) [18]. Proving that Pc have a vast array of photo physical and spectral characteristics [15]. Aluminium (III) Phthalocyanine Chloride Tetrasulphonate ($AlPcS_4Cl$) is an improved second generation PS with ideal PDT characteristics. Along with the afore mentioned characteristics $AlPcS_4Cl$ shows little to no dark toxicity and is amphiphilic in nature due to it being both water soluble and can bind to cytochrome c located in the mitochondrial membrane [14].

The CSC theory has attracted the development of targeted therapies. These therapies are aimed at destroying CSCs specifically, not only reducing the tumor bulk but cancer as a whole. PDT should not be viewed as a replacement therapy but rather as an adjunct to conventional cancer treatment. The concentration of PSs in cancerous cells alone could provide a solution for CSC resistance. PDT can, therefore, be used as an alternative treatment for lung cancer. Or combination treatment alongside standard cancer therapies in advanced cases. Current research is focused on finding a therapeutic modality that eradicates both the cancer tissue and the more resistant CSCs. The novel application of the eradication of CSCs using PDT will provide insight into the therapeutic potential of PDT in the treatment of lung cancers. Successful killing of CSCs in due course will reduce cases of treatment failures, recurrences and progression to other sites, subsequently driving down the disease burden of lung cancer in the world.

2. Materials and methods

To date, because so little is known regarding the response of CSCs to PDT, the aim of this research was to observe the cellular responses of lung CSCs after exposure to PDT using laser light and Aluminium (III) Phthalocyanine Chloride Tetrasulphonate ($AlPcS_4Cl$) (Frontier Scientific, AlPcS-834) as a PS. A side population of cells, isolated from the lung cancer cell line A549 (ATCC®, CCL185™), positive for the CSC antigenic markers CD 133, CD 56 and CD 44 were isolated using antibody conjugated magnetic microbeads and were verified by fluorescent protein detection using flow cytometry and immunofluorescent (IFL) microscopy. Localization of the PS was established in order to determine the effectiveness that PDT may have on CSCs using fluorescence (FL) and differential interference contrast (DIC) microscopy. The isolated lung CSCs received treatment using $AlPcS_4Cl$ for PDT. Post irradiation biochemical responses where measured in order to establish the anticancer effect of $AlPcS_4Cl$ on lung CSCs after 24h. These assays included morphology of cells, LDH cytotoxicity, ATP proliferation, Trypan Blue viability and Annexin VPI cell death. Reagent grade solvents and reagents were used as received.

2.1. Cell culture

Commercially accessible epithelial lung carcinoma cells from the ATCC were utilized in this investigation A549 (ATCC®, CCL185™). The media utilized for maintaining of the lung cancer cells and separated CSCs comprised of the accompanying: Rosewell Park Memorial Institute 1640 medium (RPMI-1640) (SIGMA, R8758) enhanced with 10% fetal bovine serum (FBS) (Biochrom, S0615) and 0.5% penicillin/streptomycin (SIGMA, P4333) and 0.5% amphotericin B (SIGMA, A2942).

Cell lines used for control purposes in the characterization of the isolated lung CSCs included: Colorectal adenocarcinoma cells Caco2 (Cellonex, Caco-2) were cultured in Dulbecco's Modified Eagle's Medium - high glucose, with 4500 mg/L glucose, L-glutamine, and sodium bi carbonate (DMEM) (SIGMA, D5796) supplemented with 10% FBS, 4 mM Sodium pyruvate solution (SIGMA, S8636), 0.5% penicillin/ streptomycin and 0.5% amphotericin B.

Uterine epithelial cells consistent with leiomyosarcoma SK-UT-1 (ATCC® HTB-114™) was cultured in Minimum Essential Medium Eagle, with Earle′s salts and sodium bicarbonate (MEM) supplemented with 1% MEM Non-essential Amino Acid Solution (NEAA) (SIGMA, M7145), 2 mM L-glutamine (SIGMA, G7513), 1 mM sodium pyruvate,10% FBS and 0.5% penicillin/ streptomycin and 0.5% amphotericin B.

Skin fibroblast cells WS1 (ATCC® CRL-1502™) were cultivated in MEM, supplemented with 1% NEAA, 2 mM L-glutamine,1 mM sodium pyruvate,10% FBS and 0.5% penicillin/ streptomycin and 0.5% amphotericin B.

Mesenchymal stem cells immortalized with hTERT ASC52telo (ATCC® SCRC-4000™) were cultured in Mesenchymal Stem Cell Basal Medium (ATCC® PCS-500-030™) supplemented with Mesenchymal Stem Cell Growth Kit (ATCC® PCS-500-040™).

All cultured cells were maintained and incubated at 37°C in 5% CO_2 and 85% humidity.

2.2. Isolation of CSCs

A magnetic bead isolation pack and division unit (Miltenyi Biotec, QuadroMACS™ partition unit 130-091-051) was utilized to separate lung CSCs from lung cancer cells. The cells were magnetically labelled with microbead conjugated antibodies coordinated at the antigenic surface marker CD 133, CD 56 and CD44. The cell populace was enhanced for CD 133+, CD 56+ and CD 44+ lung CSCs by utilizing the CD 133/CD 56/CD 44 MicroBead Kit (Miltenyi Biotec, MicroBead Kit, human 130-050-801) intended for the positive selection of cells expressing the human CD 133/CD 56 and CD 44 antigen. Cells were suspended and counted. The cell suspension was re-suspended in 80 µl buffer and 20 µl Micro-beads per 10^7 total cells, followed by incubation for 15 minutes at 4°C. Cells were washed 3 times using buffer and centrifugation at 3000rpm for 10 min., and re-suspended in 500 µl buffer per 10^7 cells. Cells homogenously suspended in buffer were then added to prepared separation columns (Miltenyi Biotec, 130-042-201). Unlabeled cells are collected and discarded passing through the column, whereas positively selected cells that are conjugated to the magnetic beads would remain in the magnetic column, and flushed out into a suitable collection tube using buffer and a plunger.

2.3. Characterization of isolated lung CSCs

2.3.1. Flow Cytometry

To confirm whether cells isolated using the magnetic bead kit, were of CSC origin, cells were fluorescently labelled using the secondary antibody conjugation technique. Primary mouse anti human antibody CD133, CD 56 and CD44 was used. Isolated cells were placed in a suspension where they were washed twice using centrifugation and resuspension with ice-cold washing buffer: PBS/BSA/azide buffer (PBS/ 0.1% w/v bovine serum albumin (BSA) (Sigma, A2153)/ 0.01% w/v azide (Sigma, S8032)), and then incubated with blocking buffer (10 % (w/v) BSA (bovine serum albumin) 30 min on ice as a blocking step and washed twice as previously described. Cells were then incubated with primary mouse anti human antibody in working buffer (2% serum in PBS BSA/azide buffer) for 30 min, keeping the cells suspended in tubes on ice. Cells were then rinsed three times with washing buffer and incubated with secondary fluorescent (FL) antibodies FITC Goat anti-Mouse (NovusBio, NB720-F-1mg), Cy5 Goat anti-Mouse (NovusBio, NB7602) and PE Goat anti-Mouse (NovusBio, NB7594) in working buffer for 30 min on ice, protected from light where after they were washed again with washing buffer. The antigenic detection was done using the BD Accuri™ C6 flow cytometer (BD Biosciences, BD ACCURI C6) which detects the fluorescence on the conjugated antibody, indicating if the cells are CD 133, CD 56 and CD 44 positive/negative.

2.3.2. Immuno Fluorescence

The isolated CSCs were characterized using indirect immunofluorescence (IFL) a method that uses FL imaging detection. Whereby cultured cells are labelled with a primary antibody directed at a target antigen and made visible using fluorochromes attached to secondary antibodies directed at the primary antibodies.

Cells were cultured on heat-sterilized coverslips placed in petri dishes (3.5 cm culture dish, Corning, 430588), at a concentration of 5 x 10^5 cells in complete media. Cells were incubated and allowed to attach to the coverslip. After cells were cultured on the coverslips, they were washed twice with ice-cold washing buffer: PBS/BSA/azide buffer (PBS/ 0.1% w/v bovine serum albumin (BSA) (Sigma, A2153)/ 0.01% w/v azide (Sigma, S8032)), and then incubated with blocking buffer (10 % (w/v) BSA (bovine serum albumin) for 30 min on ice as a blocking step and washed twice again using ice cold buffer.

Cells were then incubated with 100 µl primary mouse anti human antibody (CD133 Antibody; CD 56 Monoclonal Anti-N Cam; CD44 Antibody), in working buffer (2% serum in PBS BSA/azide buffer) for 30 min on ice. Cells were then rinsed three times with washing buffer. The cells were then labelled and incubated with 100 µl of the secondary FL FITC Goat anti-Mouse (NovusBio, NB720-F-1mg), Cy5 Goat anti-Mouse (NovusBio, NB7602) and PE Goat anti-Mouse (NovusBio, NB7594) antibody, in working buffer for 30 min on ice, protected from light. Cells were rinsed three times as before and fixed in 4 % Paraformaldehyde (Sigma, P6148) for 10 minutes. After fixation, cells were rinsed once briefly with PBS, before being stained with 4'- 6- diamidino-2-phenylindole (DAPI) (Invitrogen™, D1306) 358Ex/461Em and mounted on glass slides using Fluoromount™ Aqueous Mounting Medium (Sigma, F4680). Slides were viewed using a FL microscope, live cell station from Zeiss (Zeiss, Axio Observer Z1). The images were compiled using a Java image processing program ImageJ developed at the National Institutes of Health and the Laboratory for Optical and Computational Instrumentation, License: Public Domain, BSD-2.

2.4. Localization of AlPcS$_4$Cl in intracellular organelles of lung CSCs

Localization of AlPcS$_4$Cl into lung CSC cellular organelles was confirmed by FL and DIC microscopy, in order to establish the suitability of AlPcS$_4$Cl as a PS for PDT. Intracellular organelles such as mitochondria and lysosomes were fluorescently labelled. Cells were grown on glass coverslips in 35 mm culture dishes in complete media, at a seeding density of 5 x 10^5 cells until the cells have attached. Once the cells were attached, they received AlPcS$_4$Cl at a concentration of 20 µM which was used as the treatment concentration. The cells were incubated for at least 4 hours allowing the PS to penetrate the cells. Cells were then washed with HBSS and stained with MitoTracker™ Green FM 490Ex/516EM (Invitrogen™, M7514) for mitochondria at a working concentration of 100 nM or LysoTracker™ Green DND-26 504Ex/511EM (Invitrogen™, L7526) for lysosomes using a working concentration of 50 nM for 30 min. Cells were then washed with HBSS and counterstained using DAPI. Cells were then rinsed with PBS, and excess buffer from the coverslip drained. Coverslips were then mounted onto glass microscope slides. Where after the slides were examined using the live cell station from Zeiss (Zeiss, Axio Observer Z1) to determine localization of the AlPcS$_4$Cl. Images were compiled using ImageJ.

2.5. Photodynamic Therapy

2.5.1. Photosensitizer

The PS Al (III) Phthalocyanine Chloride Tetrasulfonic Acid (AlPcS4Cl) (Frontier Scientific, AlPcS-834) was used in this study. Its formula is C32H16AlClN8O12S4, formula weight 895.21, TLC > 95 % with an absorbance wavelength of 674 nm. Figure 1 shows the structural components of AlPcS$_4$Cl. A predetermined concentration of the PS was used as established in a previous study conducted using AlPcS$_4$Cl on A549 lung cancer cells where a concentration of 20 µM delivered an inhibitory concentration of 50 % [IC 50] along with a predetermined laser energy output of 10 J/cm^2 [19].

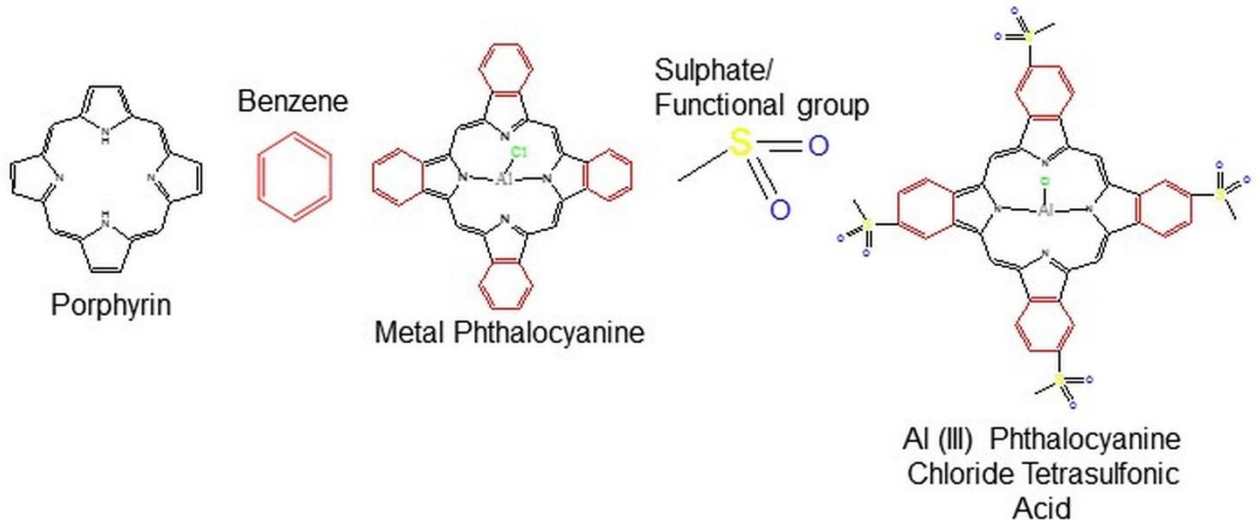


Figure 1. Structural components of AlPcS$_4$Cl, comprising of a porphyrin ring, pyrrolic/benzene rings and sulphate functional groups attached to a metalized phthalocyanine.

2.5.2. Laser irradiation

A 673.2 nm diode laser (Arroyo, High Power Laser, 1000 mA Laser source 4210 (S/N 070900108)) provided by the National Laser Center of South Africa, was used to irradiate the cells. Prior to exposing the cells to irradiation, the power output of the laser was measured using a FieldMate Laser Power Meter (FieldMate, Coherent, Power Sens detector (0496005)). The value from the meter reader was used to calculate the exposure time. Laser parameters are seen in Table 1.

Table 1. PDT drug and laser parameters using the 673.2 nm diode laser.

PARAMETERS	
Laser type	Semiconductor (Diode)
Wavelength (nm)	673.2
Wave emission	Continuous
Fluence (J/cm^2)	10
Photosensitiser (PS)	$AlPcS_4Cl$
PS Concentration (µM)	20

The laser is setup with a fiber optic to deliver red light onto the monolayer of cells. The fiber optic is placed 8 cm above the cell culture dish, giving an irradiation spot size of 9.1 cm^2 covering the entire area of the culture dish. Cells were irradiated without the culture dish lid on at room temperature. In order to eliminate light interference, all irradiation protocols were performed in the dark. Irradiation time was calculated as follows:

$$mW/cm^2 = \frac{mW \times 4}{\pi \times 3.4^2}$$

$$W/cm^2 = \frac{mW/cm^2}{1000}$$

$$Time\ (s) = \frac{J/cm^2}{W/cm^2}$$

Cells were cultured at a total of 5 x 10^5 cells per petri dish in complete media. Cultures were divided into 4 study groups. Group 1 was the control and received no irradiation or PS, group 2 contained PS but no irradiation, group 3 was irradiated but no PS was added. Group 4 was treated with $AlPcS_4Cl$ and was irradiated. All samples were incubated for 24 h after PDT treatment followed by biochemical analysis.

2.5.3. Morphology

Any morphological changes of the isolated lung CSCs post PDT treatment were observed and studied using an Olympus CKX41 inverted light microscope (Wirsam, Olympus CKX41) 24 hours post irradiation, whereby changes were captured using the SC30 Olympus camera.

2.5.4. Cytotoxicity

To determine the toxicity induced by PDT. The amount of LDH released from the cells into the culture medium was measured. This determines the amount of cell membrane damage and cell death. This oxidoreductase inter-converts lactate into pyruvate. Its discharge from the cytosol leads to an unusual increase of the enzyme in culture media *in vitro*. Formazan a product of tetrazolium salt conversion through NADH reduction, was measured using a nonradioactive colorimetric assay. The amount of formazan is proportional to the number of cells that have membrane damage and lysed due to undergoing cell death induced by PDT treatment. The CytoTox96® nonradioactive cytotoxicity assay (Promega, G400) was used according to manufacturer specifications. We evaluated cytotoxicity by measuring formazan with a multilabel Counter (Perkin Elmer, VICTOR3™, 1420) at 490 nm.

2.5.5. Proliferation

The effect of PDT on CSC metabolism was determined by measuring the amount of ATP present in the cells after treatment. Intracellular ATP was measured using the CellTiter-Glo® luminescent cell proliferation assay (Promega, G7570) and used according to manufacturer specifications. Luciferase present in the reagent catalyzes the oxidation of luciferin to oxyluciferin and illuminates in the presence of cellular ATP. Luminescence was read and quantified using a Multilabel Counter (Perkin Elmer, VICTOR3™, 1420) expressed in RLU. The amount of luminescence is directly proportional to ATP levels indicative of metabolically active cells. A reduction in luminescence is representative of cell inhibition and cell death induced by the anticancer treatment causing a reduction in intracellular ATP.

2.5.6. Viability

The adjustment in cell numbers because of development restraint instigated by PDT on the CSCs was resolved utilizing the trypan blue viability assay. This color prohibition test permits live (feasible) cells with flawless membranes to bar the color and stay unstained, though dead (non-suitable) cells will hold the color and stain blue. An equivalent volume of cells and 0.4% Trypan blue (Sigma Aldrich, T8154) was homogenously blended and exchanged to a chamber slide which was then embedded into a computerized cell counter (Countess® Automated Cell Counter) which visually delineates the cells and after that electronically calculates the level of viable cells.

2.5.7. Cell Death

Annexin V propidium iodide (PI) was used to measure cell death post irradiation. The assay gives an indication of cell death either as necrotic or apoptotic. The test makes use of fluorescently labelled dyes which are then read using a flow cytometer quantifying the amount of fluorescently labelled cells.

24 Hours after PDT treatment, cells were detached and washed with HBSS. Cells were re-suspended in 1X binding buffer at a concentration of 1 x 10^6 cells/ml and 100 µl of the cell suspension was transferred into flow cytometry tubes. Five microliters of each Annexin V-FITC and PI reagents (BD Pharmingen™, 559763) were added and the tubes were thoroughly mixed and incubated for 10 min at room temperature in the dark. Within 1 h, flow cytometric analysis was performed on the BD Flow cytometer (BD Accuri™ C6 Cytometer) and Annexin V-FITC and PI was detected as a green and red fluorescence, respectively.

2.6. Statistics

All experiments were repeated four times. Data processing was done using Sigma plot version 12/13. Error bars are representative of the mean (SEM) (n = 3). Data accumulated was statistically evaluated by Student's paired t-test, and the significance was defined as $p<0.05$(*), $p<0.01$(**) or $p<0.001$(***). All colorimetric, luminescent and absorbance assays was performed using a background control that was subtracted from the raw data obtained.

3. Results/ discussion

3.1. Characterization of isolated lung CSCs

CSCs have been isolated from solid tumors and cell lines and their intense ability to initiate tumor formation as well as differentiate upon *in vivo* application has been demonstrated [20]. Studies on how to identify and isolate CSCs have elaborated on the various markers, gene expression molecules and cell signaling pathways involved in CSC research. The most common method applied in identifying and isolating sub populations of cells is through protein marker detection or cluster of differentiation molecules. Over expression of common stem cell genes or markers representative of the tissue of origin has been seen in various stem cells including CSCs. Allowing for identification of stem ness inside a tumor population [21]. One way of differentiating CSCs from non-tumorous stem cells and cancerous cells is that CSCs undergo altered glycosylation during malignant transformation. Giving CSCs cancer specific glycans and their tumorous characteristics of tumor aggressiveness, progression, and metastasis along with increased levels of stem marker expression [22].

After isolation of the subpopulation of stem like cells from the lung cancer cell line A549 using magnetic beads attached to protein markers we had to identify whether the population of cells were of stem cell origin. This was done using CD markers specific to lung CSCs including CD 133, CD 56 and CD 44. The methods used to identify these markers included antibody identification through flow cytometry and IFL staining.

3.1.1. Flow Cytometry

In order to determine whether the cells isolated were of stem cell origin, antigenic detection was assessed using the BD Accuri™ C6 Flow Cytometer. Indirect antibody labelling allowed to fluorescently express whether or not the primary antibody is present on the cells. FL detection using flow cytometry showed that the isolated cells expressed the markers CD 133, CD 44 and CD 56 (Figure 2).

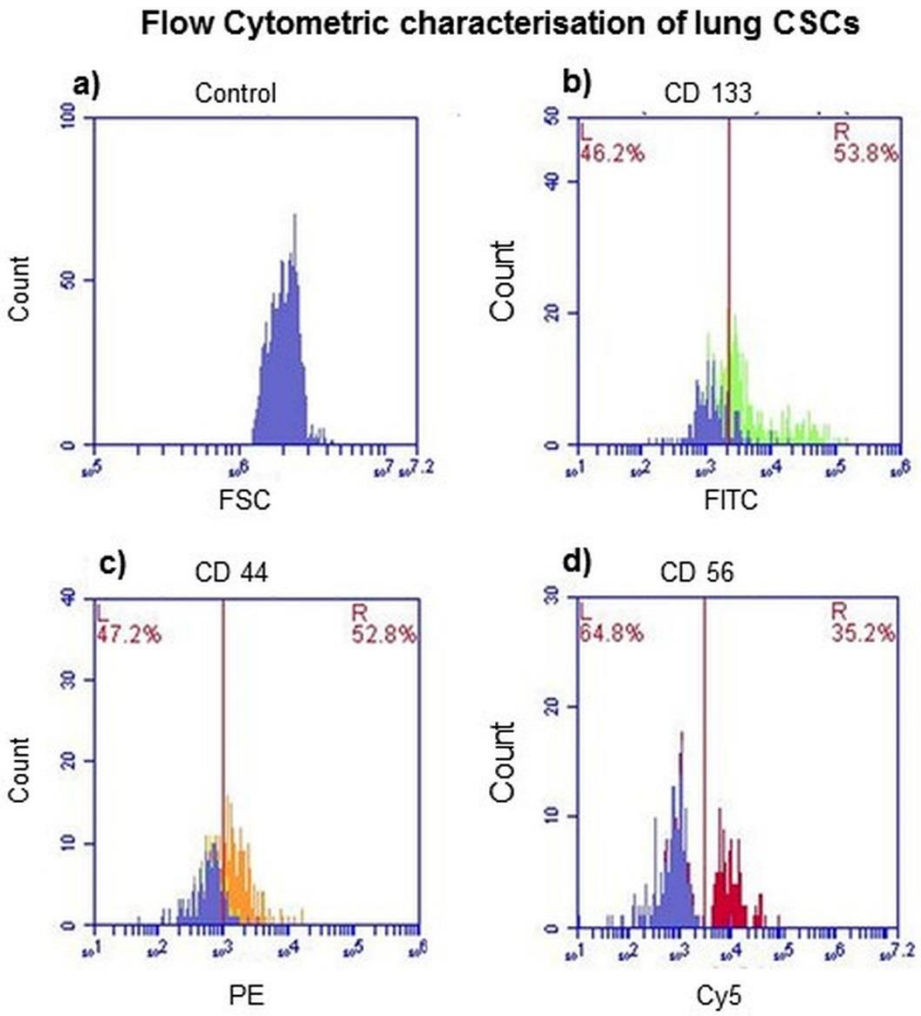


Figure 2. Fluorescence protein detection using flow cytometry. a) Unstained lung CSCs (control). b) Lung CSCs positive for CD 133 (FITC), c) Lung CSCs positive for CD 44 (PE), and Lung CSCs positive for CD 56 (Cy5). All positive samples are overlaid with the control to distinguish between the color shifts.

Analysis of the flow cytometric results was performed by running a control sample in order to establish the population group by gating the cell population on the density plot and expressing it as a blue peak on the histogram (Figure 2 a)). Experimental samples labelled with the primary antigenic markers and fluorophore tags were run and gated and further analyzed for the expression of the respective markers. Cells labelled with, CD 133 was tagged with FITC (green) and fluorescence was detected using FL-1 with a 533/30 filter and 488 nm laser (Figure 2 b)); CD 44 was tagged with PE (orange) and fluorescence detected using FL-2 with a 585/40 filter and 488 nm laser (Figure 2 c)); and CD 56 was tagged with Cy5 (red) and fluorescence detected using FL-3 with a 670 LP filter and 488 nm laser (Figure 2 d)). Results expressing two peaks are indicative of the unstained control population that is overlaid onto the positively stained populations in order to differentiate between the two. Results indicate that the cells isolated are lung CSCs.

3.1.2. Immuno Fluorescence

Expression of the antigenic CSC markers after isolation of the side population was determined by IFL microscopy. Isolated lung CSCs expressed the surface marker CD 133, CD 44 and CD 56. Control cell lines positive for the antigenic markers confirmed the antigenic expression as seen by the fluorescence detected. No fluorescence was observed from the negative control cell lines, indicating that these cells do not express the surface markers. DAPI was used to counterstain the nuclei. Positive expression of the antigenic surface markers confirmed positive isolation of lung CSCs (Figure 3 - 5).

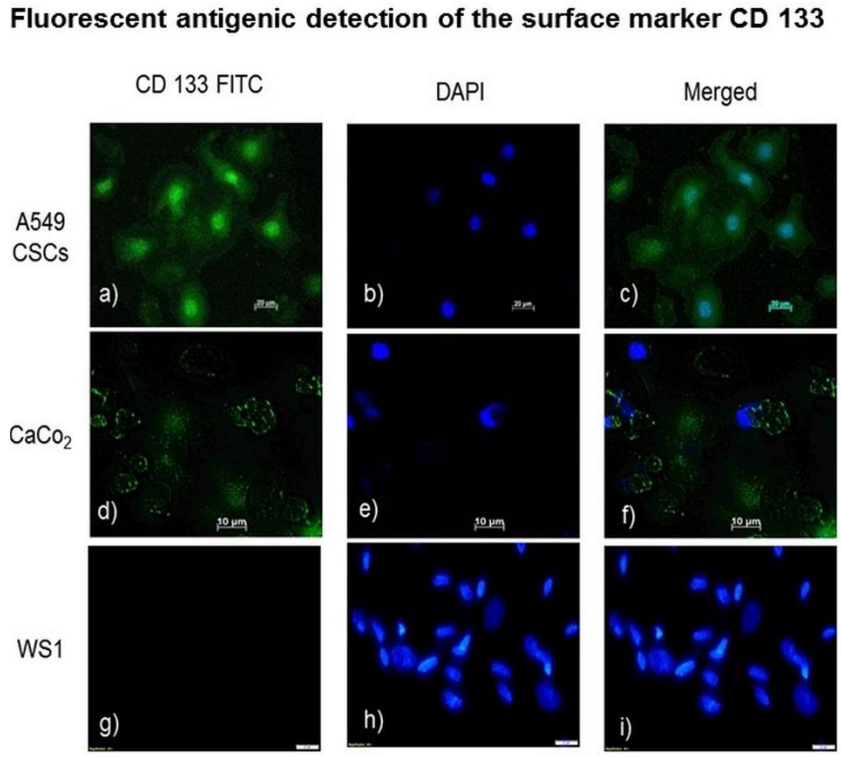


Figure 3. Fluorescent antigenic detection of the surface marker CD 133. Immunofluorescent staining of the isolated side population of Lung CSCs (a) and control cell CaCo2 (d) positive for the antigenic marker CD 133 indicated positive fluorescence with FITC (green). Negative control cell line WS1 (g) indicated no fluorescence. All cell lines were counter stained with DAPI indicated by blue fluorescence seen in the nuclei (b, e, and h). Merged fluorescent images of the labelled cell lines are indicated by image c, f and i.

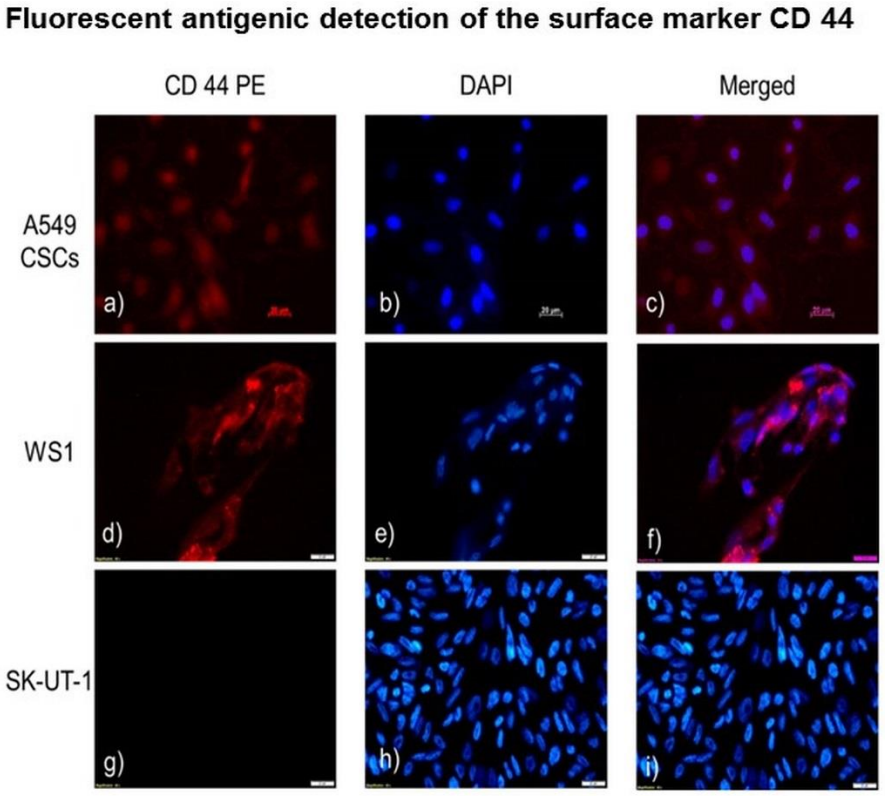


Figure 4. Fluorescent antigenic detection of the surface marker CD 44. Immunofluorescent staining of the isolated side population of Lung CSCs (a) and control cell WS1 (d) positive for the antigenic marker CD 44 indicated positive fluorescence with PE (red). Negative control cell line SK-UT-1 (g) indicated no fluorescence. All cell lines were counter stained with DAPI indicated by blue fluorescence seen in the nuclei (b, e, and h). Merged fluorescent images of the labelled cell lines are indicated by image c, f and i.

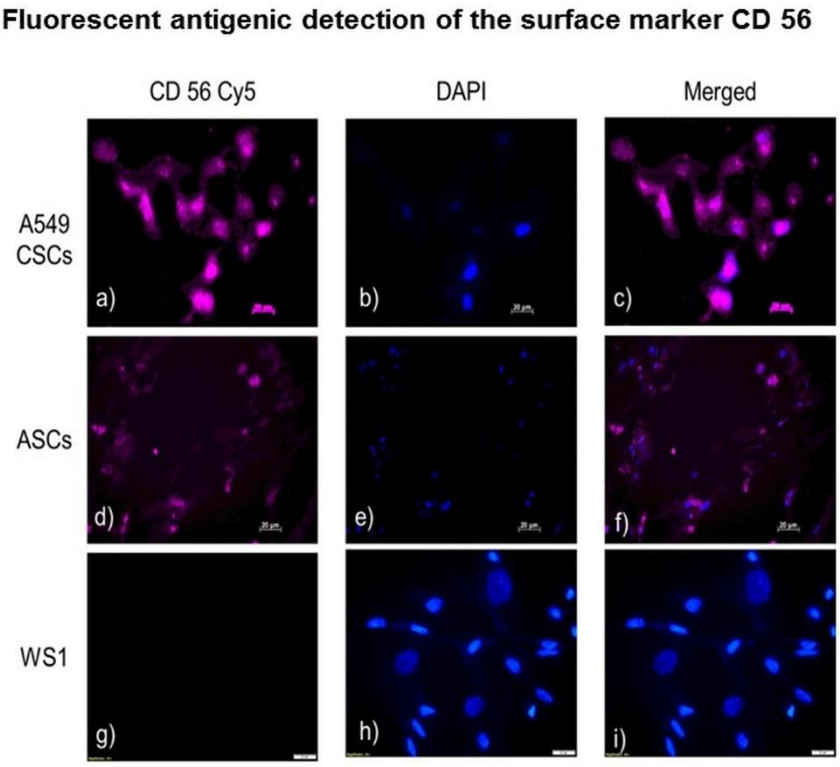


Figure 5. Fluorescent antigenic detection of the surface marker CD 56. Immunofluorescent staining of the isolated side population of Lung CSCs (a) and control cell ASC (d) positive for the antigenic marker CD 56 indicated positive fluorescence with Cy5 (magenta). Negative control cell line WS1 (g) indicated no fluorescence. All cell lines were counter stained with DAPI indicated by blue fluorescence seen in the nuclei (b, e, and h). Merged fluorescent images of the labelled cell lines are indicated by image c, f and i.

3.2. Localization of PS in lung CSCs

The intracellular confinement of a PS is critical to characterize the system and effectiveness of photo actuated cell death. This is expected by PDT following two sorts of components including a type I system where through a redox procedure an energized triplet state PS interface with intracellular targets including film lipids, proteins, DNA and sub-atomic oxygen, framing radicals. Radicals can be oxidized to shape superoxide or associate with oxygen, hydrogen peroxide, redox-dynamic progress metals, nitrogen oxide or redox-dynamic locales of biomolecules framing ROS. Type II system the energized triplet state PS exchanges energy to atomic oxygen framing $^1O_2$ an exceedingly cytotoxic species. The two ROS and $^1O_2$ actuate annihilation of biological targets [11]. Mitochondria are associated with cell homeostasis by directing ATP levels just as framing synthetic substances for breakdown of poisons, they contain different atoms including DNA, ribosomes and compounds for protein and phospholipid combination. Focusing on the mitochondria as a PDT target will prompt cell destruction. Lysosomes contain proteins for hydrolysis or processing of biomolecules just as outside particles to help in the expulsion of atoms from the cell. Focusing on lysosomes can prompt downregulation of cell homeostasis and obviously cell death. In order to establish the suitability of $AlPcS_4Cl$ as a PS we determined whether $AlPcS_4Cl$ localizes in intracellular organelles such as mitochondria and lysosomes. This was confirmed using IFL and DIC, where mitochondria and lysosomes were fluorescently labelled using FITC and the PSs' auto fluorescence exploited and detected using FL microscopy (Figure 6 and 7).

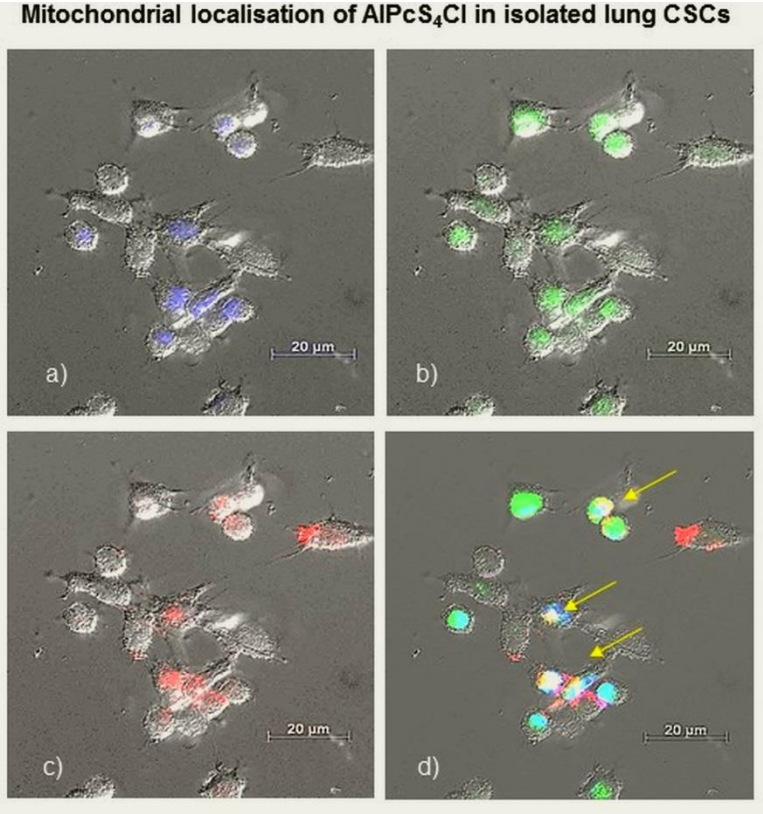


Figure 6. Mitochondrial localization of $AlPcS_4Cl$ in isolated lung CSCs. a) Nuclei are stained blue using DAPI, b) Mitochondria fluoresces green (FITC), c) $AlPcS_4Cl$ auto fluoresces red (Cy5), d) Intermediate yellow is seen in the superimposed images where the green and red channels are merged and fluorescence from the mitochondrion and PS are overlapping.

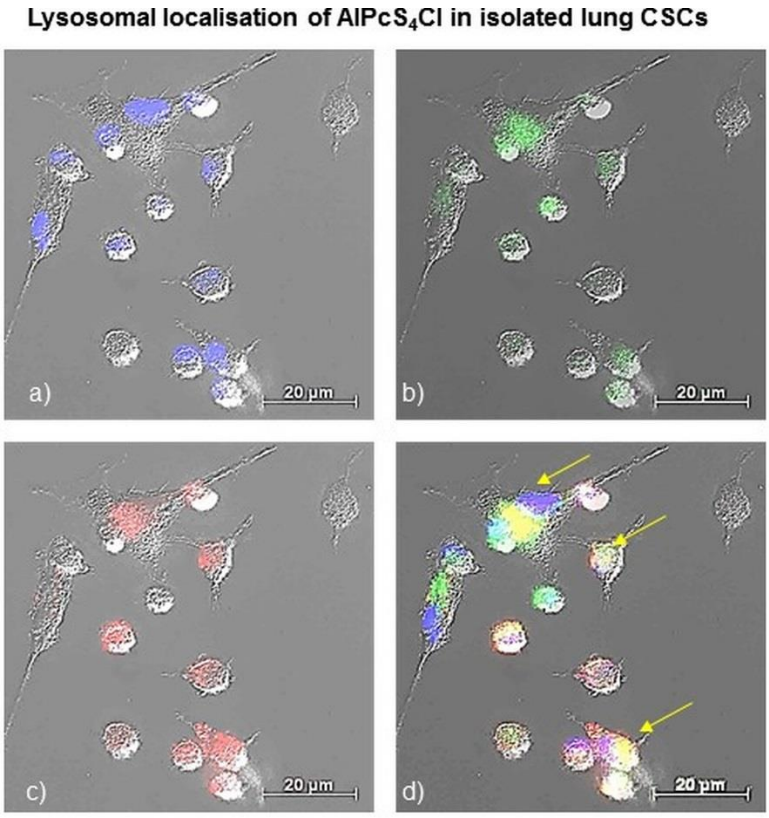


Figure 7. Lysosomal localization of $AlPcS_4Cl$ in isolated lung CSCs. a) Nuclei are stained blue using DAPI, b) Mitochondria fluoresces green (FITC), c) $AlPcS_4Cl$ auto fluoresces red (Cy5), d) Intermediate yellow is seen in the superimposed images where the green and red channels are merged and fluorescence from the lysosomes and PS are overlapping.

Figure 6 and 7 shows the intracellular localization of the PS, where $AlPcS_4Cl$ localizes in the perinuclear area in the mitochondrion as well as the lysosomes of the isolated lung CSCs. The images show superimposed DIC microscopy and FL imaging of a) the nucleus (DAPI - blue), b) mitochondria / lysosomes (FITC - green), c) $AlPcS_4Cl$- auto fluorescence (Cy 5 - red) and d) a superimposed image of all the fluorescent markers combined. Figure 6 d) and 7 d) shows intracellular localization of $AlPcS_4Cl$ in both the mitochondria and lysosomes depicted by a resultant yellow fluorescence seen when merging the two color channels (FITC and Cy 5), white fluorescence is noted due to all the color channels overlapping, where the primary colors (red, blue and green) result in white, giving an indication that the PS surrounds the perinuclear area. This in turn signifies that organelles involved in cell function and viability will be targeted upon photo activation of $AlPcS_4Cl$, whereby ROS or $^1O_2$ formation and accumulation will destroy these organelles that can lead to CSC death.

3.3. Photodynamic Therapy

In order to determine whether the PS $AlPcS_4Cl$ exerts any responses in isolated lung CSCs an array of biochemical assays were tested along with morphological features. This gives an indication of the extent of PDT damage by assessing post-irradiation cellular phenotypic components.

3.3.1. Morphology

Following PDT on the isolated lung CSCs, the cells were characterized morphologically. All the treatment groups were compared to the respective control sample which did not receive any treatment. The results indicated that the isolated lung CSCs receiving irradiation alone had an increase in cell proliferation indicated by an increase in the monolayer density. This is in accordance with previous studies conducted using photobiomodulation (PBM) of 10 J/cm^2 and wavelengths ranging from 630 – 830 nm on lung CSCs and various cancer cell lines, having an increase in cell proliferation and viability [23; 24]. Isolated lung CSCs receiving PS at a concentration of 20 µM alone did not indicate changes in morphology when compared to its respective control. The cells presented with a dense monolayer of cells that are viable with no membrane damage or signs of cytotoxicity. Thus indicating the safety of using $AlPcS_4Cl$ as a PS [25; 26]. CSCs that received PDT treatment showed alterations in morphology. Cell death due to intrinsic apoptosis was noted, where changes included cell shrinkage, chromatin condensation, cell blebbing and cytoplasmic vacuolization; and programmed necrosis, indicated by cell swelling and lysis (Figure 8).

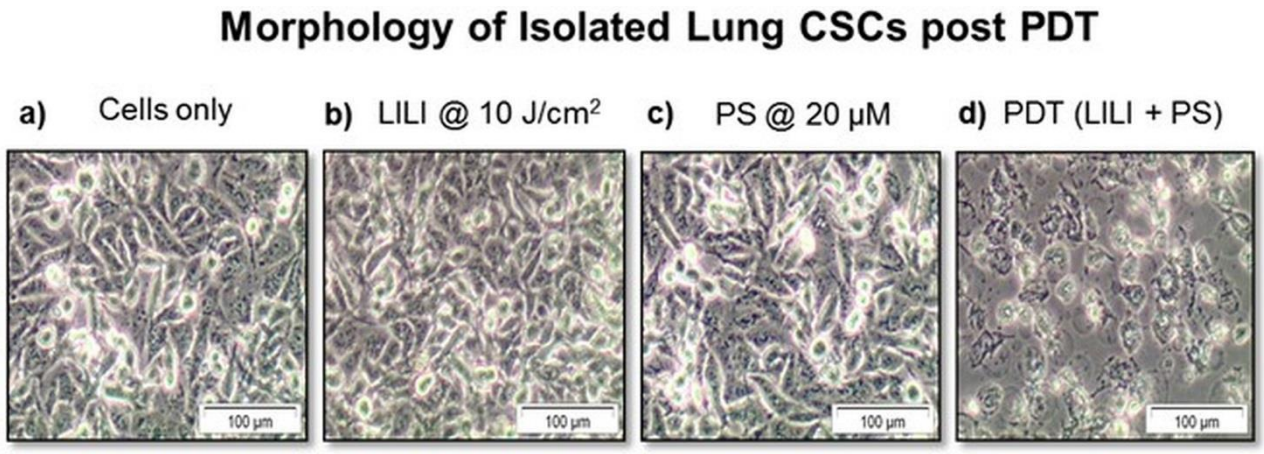


Figure 8. Morphology of Isolated Lung CSCs post PDT. Cells only represent healthy viable lung CSCs. CSCs receiving LILI with an energy of 10 J/cm^2 indicated an increase in cell proliferation, seen by an increase in the cell monolayer density when compared to the density of the control sample. No cytotoxic morphological changes are seen in lung CSCs after receiving $AlPcS_4Cl$ of 20 µM without photo activation. Cellular morphology resemble that of the control sample receiving no PS. Lung CSCs that received PDT with a 20 µM $AlPcS_4Cl$ concentration activated using 10J/cm^2 irradiation, show indications of cell death, following an apoptotic and necrotic pathway.

3.3.2. Cytotoxicity

To explore the PDT activity of $AlPcS_4Cl$ on isolated lung CSCs, a series of LDH cytotoxicity assays were performed. Results seen in Figure 9 indicated that there was no significant cytotoxicity associated with exposure to light irradiation alone in the absence of the PS. This result is due to red photobiomodulation which is used at a low power and low fluence output having a bio stimulatory effect on cells [27; 28], thus having no indication of cytotoxicity. The results seen from

the group treated with PS alone in the absence of excitation light had shown no significant cytotoxicity. One of the characteristics of an ideal PS is to have negligent dark toxicity [29], which was seen when using $AlPcS_4Cl$ [26]. A significant increase in cytotoxicity was observed in CSCs receiving both PS and LILI/ PDT treatment. In order to establish the percentage of cytotoxicity induced a positive control sample was used, whereby the cells were completely lysed prior to running LDH cytotoxicity assays using the cell lysates in the culture media. The positive control sample represents 100 percent (%) cytotoxicity. The percentage cytotoxicity achieved using PDT with $AlPcS_4Cl$ on isolated lung CSCs were seen to be 36.13 % when using 20 µM $AlPcS_4Cl$ and 10 J/cm^2 LILI.

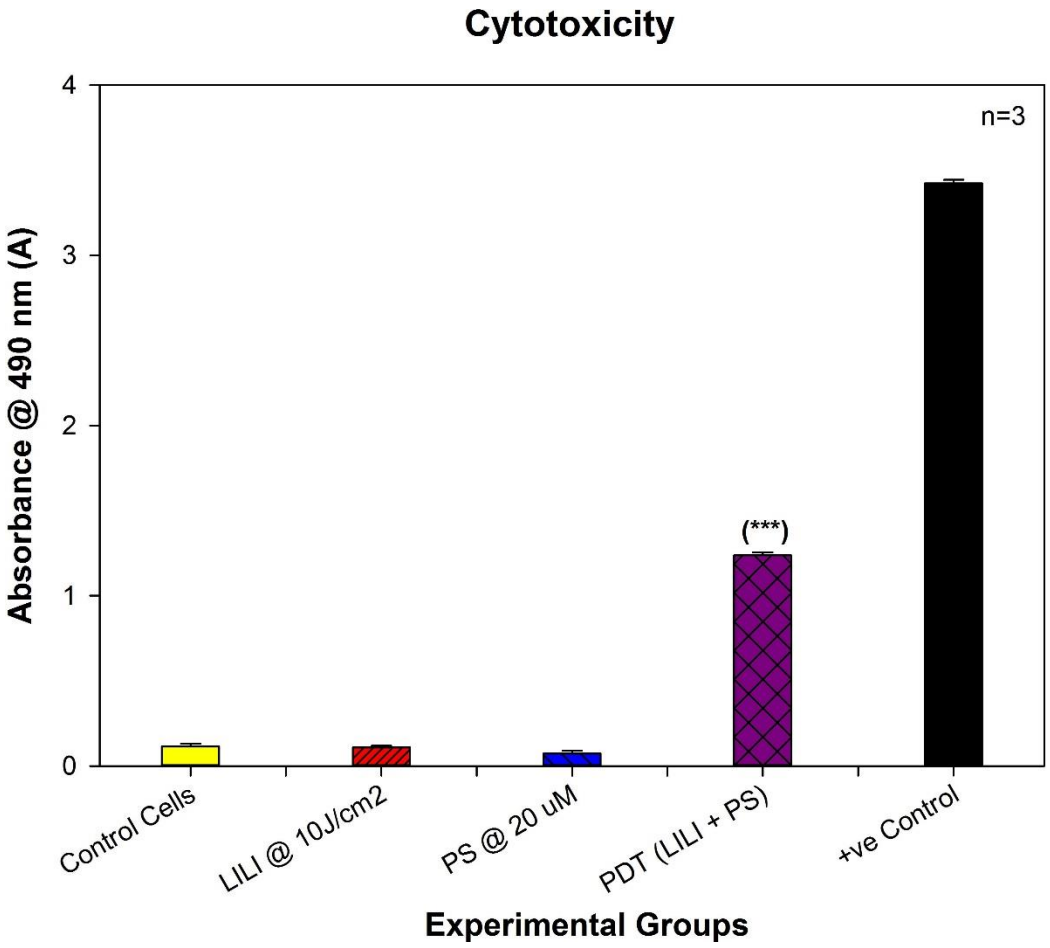


Figure 9. LDH Cytotoxicity of Isolated Lung CSCs post PDT. Cytotoxicity was measured as an absorbance value @ 490 nm. All test samples were compared to their respective control cells. No statistical significance was seen when exposing the cells to PS or LILI alone. A statistical significance of p<0.001 in LDH cytotoxicity was observed when treating the cells with PDT using 20 µM $AlPcS_4Cl$ and 10 J/cm^2 LILI, which was calculated as a percentage value in comparison to the positive control sample representing 100 %. The percentage cytotoxicity achieved in isolated lung CSCs was 36.13 %.

3.3.3. Proliferation

All metabolically active cells require energy in order to perform cellular processes such as proliferation. Most cancerous cells produce ATP energy through aerobic glycolysis [30]. To determine whether PDT had an effect on isolated lung CSCs, we measured the amount of ATP present in the test samples in order to determine what amount of ATP is present in metabolically functional lung CSCs and whether PDT reduces cellular processes, which can be seen by a decrease in intracellular ATP measured. Proliferation results (Figure 10) indicate that cells treated with LILI and PS only, had no significant impact when compared to their control cells receiving no treatment. Although previous studies established that LILI at wavelengths between 630 nm and 800 nm using low energy densities of 10 J/cm^2 had a proliferatory effect on various cell lines [31-33], it was noted that LILI had no significant effect on lung CSCs. This is in accordance with research stating that CSCs or stem cells have a decreased or quiescent metabolism [34], which ultimately impacts the metabolic rate and the effect LILI has on lung CSCs, also considering the fluence and wavelength used to irradiate the cells. Due to $AlPcS_4Cl$'s negligent dark toxicity, it is noted that the CSCs receiving only PS had a similar metabolic rate as its control cells, due to the PS having no effect in its un-activated state. Lung CSCs that was treated with PDT showed a significant decrease in cell metabolism, seen by a decrease in ATP luminescence. Indicating

when using 20 µM $AlPcS_4Cl$ and 10 J/cm^2 LILI, it can significantly decrease the proliferation rate of lung CSCs and lead to CSC death *in vitro.*

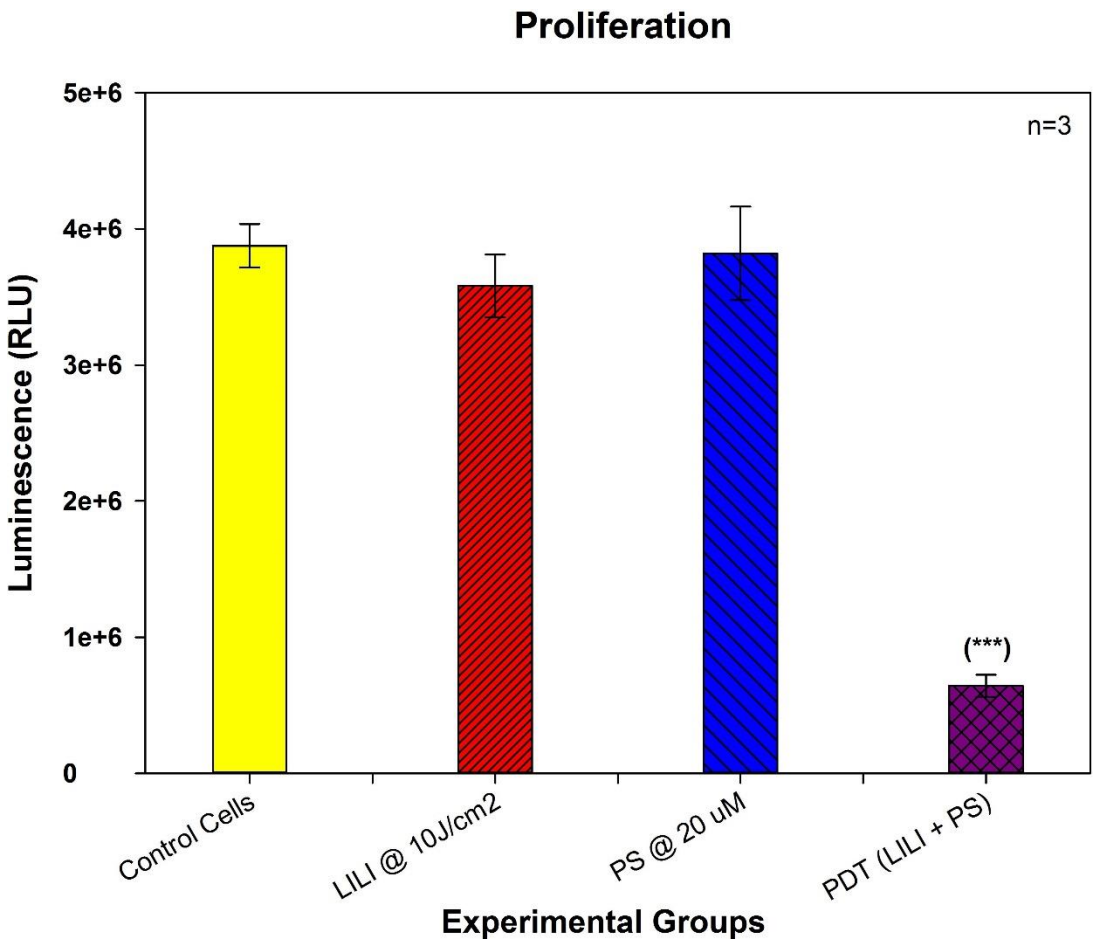


Figure 10. ATP Proliferation of Isolated Lung CSCs post PDT. ATP was measured as a luminescent value in relative light units (RLU). All test samples were compared to their respective control cells. No statistical significance was seen when exposing the cells to PS or LILI alone. A statistical significant decrease in ATP proliferation of p<0.001 was observed when treating the cells with PDT using 20 µM $AlPcS_4Cl$ and 10 J/cm^2 LILI.

3.3.4. Viability

Trypan Blue exclusion assay is a well-established method for identifying viable and dead cells, as it reflects the viability based on cell membrane integrity [35]. Viable cells that have not undergone any stress induction will exclude the dye. Whereas cells exposed to treatments or environmental factors inducing stress, whereas in the case of PDT ROS mediated cytodamage, will have diminished cell membrane integrity, permeable to the dye, indicative of cell death. This method permits us to establish the effect PDT has on isolated lung CSC viability. Results were recorded as a percentage value of the proportion of viable cells after experimental treatment as seen in Figure 11. The results show that there is no significant difference in viability in CSCs treated with LILI and PS alone, as compared to the control sample. Confirming that LILI at 10 J/cm^2 does not have a significant stimulatory action on lung CSCs, as well as $AlPcS_4Cl$ having no dark toxicity when exposing the cells to the PS without light activation. There is however a significant decrease seen in viability after PDT treatment of the lung CSCs. This is indicated by a 46 % decrease in viability as compared to the respective control cells.

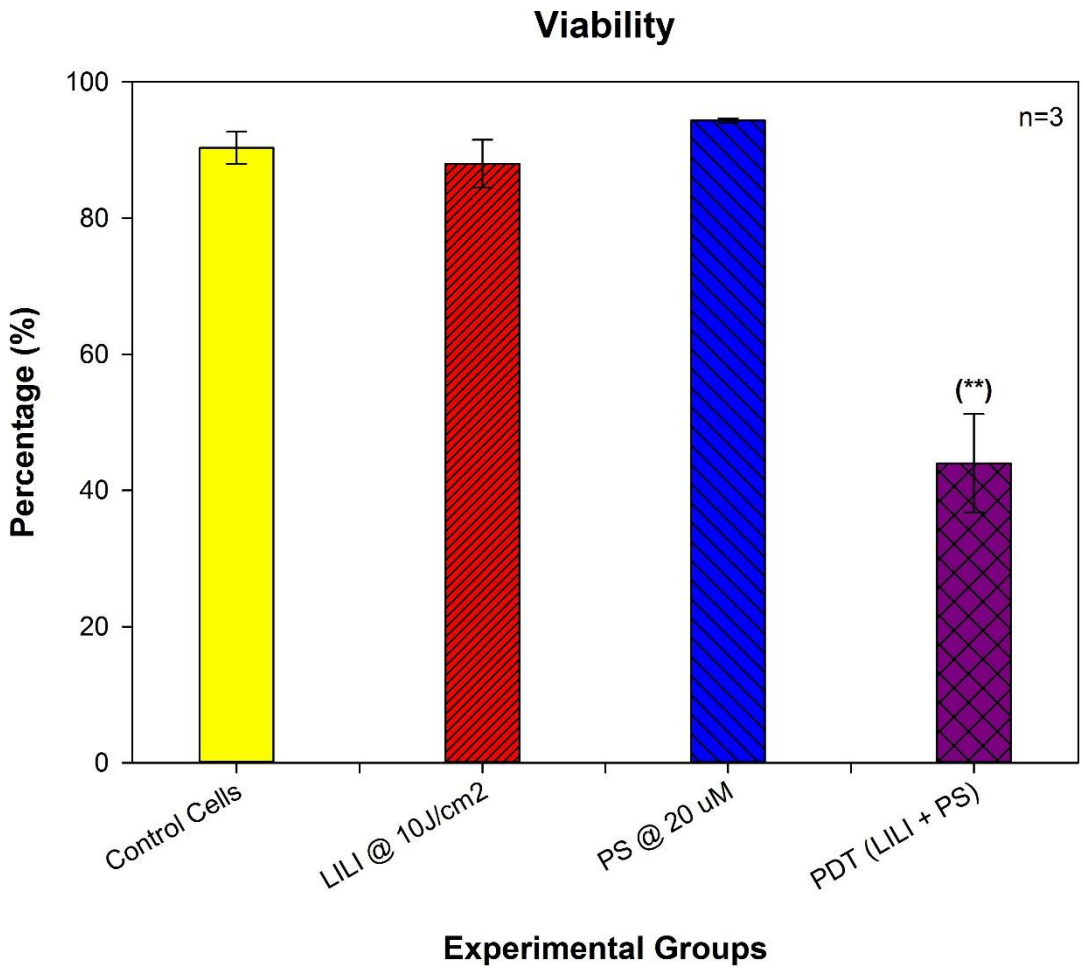


Figure 11. Trypan Blue Viability of Isolated Lung CSCs post PDT. Trypan Blue was used as a dye exclusion assay, where viable cells excluding the dye was recorded as a percentage value. All test samples were compared to their respective control cells. No statistical significance was seen when exposing the cells to PS or LILI alone. A statistical significant decrease ($p<0.01$) in viability of 46 % was seen when treating the cells with PDT using 20 µM $AlPcS_4Cl$ and 10 J/cm^2 LILI, when compared to the respective control samples.

3.3.5. Cell death

It has been established that PDT directly destroys cancer cells by inducing either apoptotic or necrotic cell death where these mechanisms can occur concurrently [36]. Photodynamic induced cell death is seen due to the formation of ROS associated with oxidative stress and subsequent cell damage by oxidizing and degrading cell components [37]. In order to establish whether PDT induced apoptotic or necrotic cell death in isolated lung CSCs, an Annexin V PI cell death assay was done. In apoptotic cells, phosphatidylserine is translocated from the internal to the external part of the plasma membrane, exposing phosphatidylserine, making it available for Annexin V a phospholipid binding protein to attach to it [38]. Phosphatidylserines' translocation is an initial occurrence preceding the loss of membrane integrity associated with later cell death pathways. For this reason propidium iodide (PI) is used in conjunction with Annexin V, as a nucleic acid intercalator that penetrates porous cell membranes, enabling it to attach to DNA. Making it possible to distinguish between cells that are viable, cells that are in early apoptosis, late apoptosis and necrotic [39]. Flow cytometric results (Figure 12) show that PDT does induce apoptosis and necrosis in lung CSCs. This was established by running an unstained sample of cells to determine the cell population. A sample of lung CSCs where apoptosis was induced using hydrogen peroxide as a positive control to establish apoptotic events and the control cell sample with no PS or LILI along with cells receiving PS alone or LILI alone which showed no significant cell death. Whereas lung CSCs treated with PDT indicated statistical significant ($p<0.001$) increases in early apoptotic, late apoptotic and necrotic cell death.

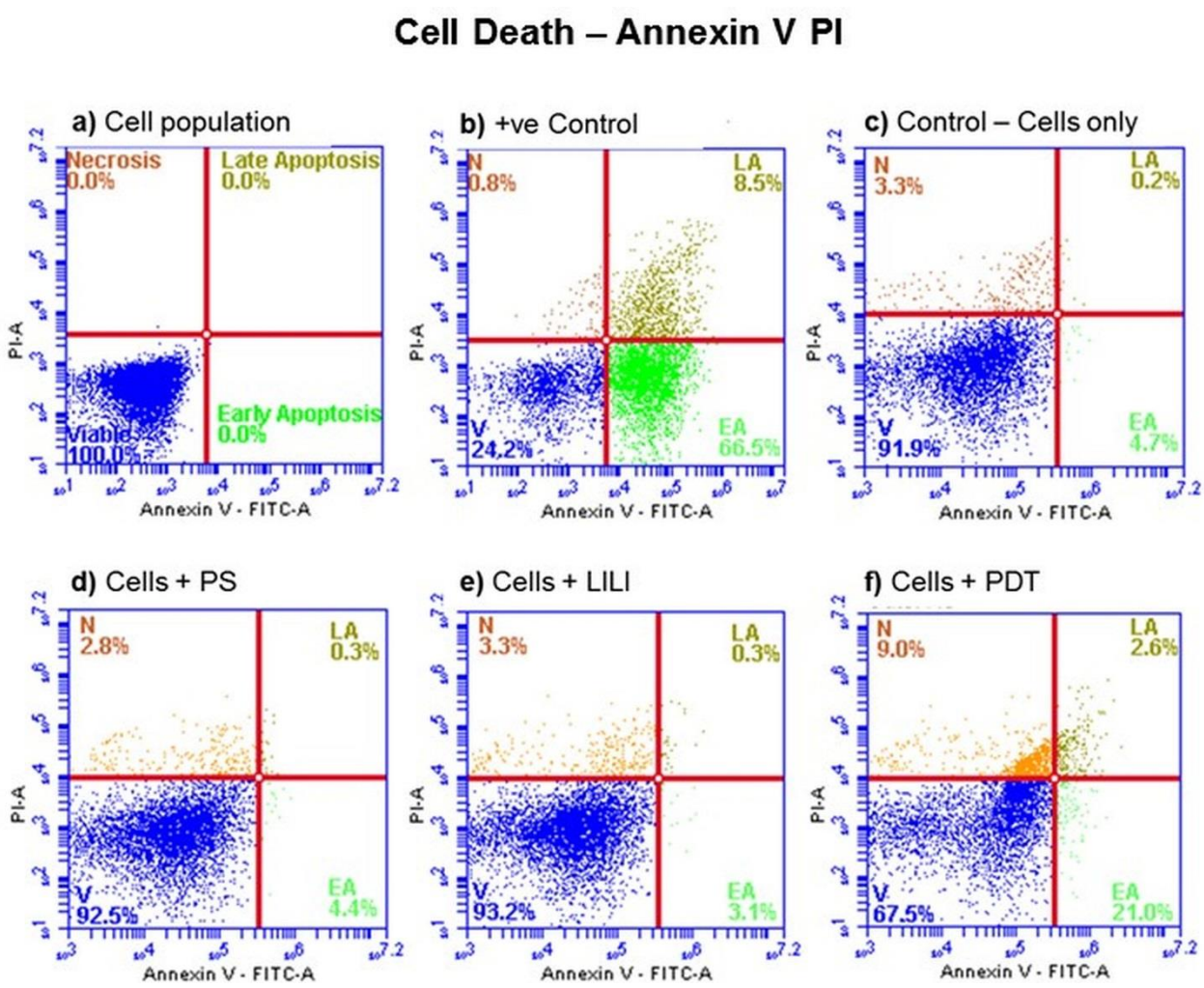


Figure 12. Cell Death – Annexin VPI of Isolated Lung CSCs post PDT. Unstained cells were used to establish the cell population (a). A positive control sample was used where apoptosis was induced using hydrogen peroxide (b). Cells receiving no treatment was used as the control (c). Cells receiving PS or LILI alone had no significant cell death with viabilities of 92.5 % and 93.2 % respectively (d – e). Cells receiving PDT showed a statistical significant increase ($p<0.001$) in early apoptosis (21 %), late apoptosis (2.6 %) and necrosis (9 %).

At present, PDT using different types of PSs, has proven effective in treating most solid tumors both *in vitro* and *in vivo*. Although the outcomes of PDT on isolated lung CSCs have yet to be elucidated until now. In this study we elaborated on the effects that PDT using $AlPcS_4Cl$ has on isolated lung CSCs in order to establish its treatment potential for lung cancer. Morphologic and biochemical assessments were performed on several groups of isolated lung CSCs displaying stem like markers including CD 133, CD 44 and CD 56 all of which has been identified to promote cancer recurrence and metastasis. Where CD 133 is the most frequently found CSC marker. This cell surface glycoprotein aids in self-renewal, tumor initiation and drug resistance where it has been shown to maintain cancer stem-like and chemo, radio resistant properties in lung cancer derived CD 133+ cells [40]. CD 44 has been reported to be associated with poor prognosis of lung cancer, where it has been established that lung cancer cell lines that are CD 44+ had increased proliferative and colony forming potential [41]. Neural cell adhesion molecule CD 56 has been reported to be highly expressed in cases of lung cancer recurrence, where this marker has been established as a diagnostic tool for lung cancer as well a potential target for drug immuno-therapy [42]. Due to the severity of tumorigenic potential seen when lung CSCs express these markers we used them as a treatment population in our experiment. The lung CSCs were effectively isolated using magnetic cell sorting and characterized by IFL and flow cytometric protein detection.

The PS chosen for this study, $AlPcS_4Cl$, was used due to its preferential features for a successful PS, demonstrated by its photo stability and amphipathic nature, negligent toxicity in the dark, localizes in intracellular organelles that upon membrane damage and ROS formation cause apoptotic cell death and its activation wavelength which is optimal for tissue penetration [26]. Results confirmed that the intracellular confinement of this PS in lung CSCs are optimal for cell death induction via apoptosis. This was seen where the PS localizes in intracellular organelles that upon photo activation will result in the production of ROS and free radicals which will ultimately destroy these cellular structures inhibiting their functions leading to cell death.

PDT treatment of the lung CSCs was arranged in several treatment groups where the control group consisted of cells not exposed to either variables including irradiation or PS, ruling out possible effects not indicated by PDT. Similarly a group of cells received PS alone and LILI alone, whereby the influence of the PS in its inactive state could be measured and the effect of LILI in the absence of a PS was evaluated. Results indicated that neither individual components induced any significant changes to the lung CSCs, However, PDT had significant changes when analyzing the morphological and biochemical assessments. Changes in morphology were in accordance with those seen induced by apoptosis caused by the activated PS forming cytotoxic species that interact with cellular components causing the observed cell damages. Morphological results were confirmed by LDH cytotoxicity, which quantifies enzymes released into the culture medium upon cell destruction. Results indicated a significant increase in LDH cytotoxicity. Results were further corroborated by ATP proliferation and Trypan Blue viability analysis showing a significant decrease in CSC proliferation and viability as compared to the control samples. When comparing results to those established in a previous study using a similar PS and laser parameters on lung cancer cells it was noted that the amount of cytotoxicity achieved was higher in lung CSCs than lung cancer alone. Similarly the findings showed a greater decrease in proliferation for CSCs than lung cancer, viability comparisons indicated a similar result in viability of ± 43 % [26]. Further validating the above mentioned findings was cell death analysis using Annexin V PI, confirming cell death via apoptosis and necrosis. This would suggest that $AlPcS_4Cl$ show a desired effect when used on lung CSCs as a photodynamic drug.

4. Conclusion

Lately, CSCs have been identified in numerous tumors and have been proposed to explain metastatic capacity, recurrence, and resistance to radiotherapy and chemotherapy that some tumors poses. Research suggest that tumors contain a small subpopulation of cells that can self-renew, proliferate infrequently, express several pluripotency genes and are responsible for tumor initiation and metastasis [43]. Anticancer agents that destroy highly proliferative tumor cells do not affect CSCs, therefore treatments need to destroy CSCs in particular to eradicate the tumor. CSCs that evade cancer therapy will be responsible for tumor drug resistance and relapse. Stem cell markers have been associated with CSCs that can be used to isolate and enrich a population of cells displaying these stem cell markers [44]. CSCs can be identified and isolated using different approaches including flow cytometry and magnetic-associated cell sorting. This study proves that PDT using $AlPcS_4Cl$ has the desired effects of killing lung CSCs. This is seen in morphological features of apoptosis and necrosis that included cell shrinkage, chromatin condensation, cell blebbing, cytoplasmic vacuolization and cell swelling and lysis. Furthermore, results on cell toxicity, proliferation, viability and cell death corroborated these morphological findings, where $AlPcS_4Cl$-PDT caused a significant increase in cytotoxicity, and significant decreases in cell proliferation and viability, as well as cell death analysis presenting significant increases in early-, late-apoptosis and necrosis. It should be mentioned that PDT can be considered as a palliative treatment along with established lung cancer therapies, which can enhance the prognostic outcome of the treatments by killing of CSCs. Photodynamic anticancer therapy is aimed at destroying cancerous cells alone, preserving normal cells [45]. Therefore the effects of the particular PS need to be explored on normal lung cells.

5. Conflict of interest

The authors declare no conflict of interest

6. Acknowledgements / Funding

This work is based on the research supported by the South African Research Chairs Initiative of the Department of Science and Technology and National Research Foundation of South Africa (Grant No 98337). The authors sincerely thank the University of Johannesburg and the National Laser Centre – Council for Scientific and Industrial Research South Africa (CSIR) for their facilities and laser equipment and the National Research Foundation of South Africa (SARChI-DST) for their financial grant support.

7. References

[1] Colditz, G. A., & Wei, E. K. (2012). Preventability of cancer: The relative contributions of biologic and social and physical environmental determinants of cancer mortality. Annual Review of Public Health, 33(1), 137-156. doi: 10.1146/annurev-publhealth-031811-124627.

[2] Salem, M. S. Z. (2015). Cancer: Some genetic considerations. Egyptian Journal of Medical Human Genetics, 16(1), 1-10. doi: https://doi.org/10.1016/j.ejmhg.2014.09.003.

[3] Crous, A., & Abrahamse, H. (2018). Targeted photodynamic therapy for improved lung cancer treatment. In Torres, A. F. C. (Ed.), Lung cancer: IntechOpen.

[4] Lemjabbar-Alaoui, H., Hassan, O. U., Yang, Y.-W., & Buchanan, P. (2015). Lung cancer: Biology and treatment options. Biochimica et biophysica acta, 1856(2), 189-210. doi: 10.1016/j.bbcan.2015.08.002.

[5] MacDonagh, L., Gray, S. G., Breen, E., Cuffe, S., Finn, S. P., O'Byrne, K. J., & Barr, M. P. (2016). Lung cancer stem cells: The root of resistance. Cancer Lett, 372(2), 147-156. doi: https://doi.org/10.1016/j.canlet.2016.01.012.

[6] Kreso, A., & Dick, J. E. (2014). Evolution of the cancer stem cell model. Cell Stem Cell, 14(3), 275-291. doi: 10.1016/j.stem.2014.02.006.

[7] Sleeman, J., & Steeg, P. S. (2010). Cancer metastasis as a therapeutic target. European Journal of Cancer, 46(7), 1177-1180. doi: https://doi.org/10.1016/j.ejca.2010.02.039.

[8] Eun, K., Ham, S. W., & Kim, H. (2017). Cancer stem cell heterogeneity: Origin and new perspectives on csc targeting. BMB reports, 50(3), 117-125. doi: 10.5483/BMBRep.2017.50.3.222.

[9] Arruebo, M., Vilaboa, N., Sáez-Gutierrez, B., Lambea, J., Tres, A., Valladares, M., & González-Fernández, A. (2011). Assessment of the evolution of cancer treatment therapies. Cancers, 3(3), 3279-3330. doi: 10.3390/cancers3033279.

[10] Kwiatkowski, S., Knap, B., Przystupski, D., Saczko, J., Kedzierska, E., Knap-Czop, K., Kotlinska, J., Michel, O., Kotowski, K., & Kulbacka, J. (2018). Photodynamic therapy - mechanisms, photosensitizers and combinations. Biomed Pharmacother, 106, 1098-1107. doi: 10.1016/j.biopha.2018.07.049.

[11] Usacheva, M., Swaminathan, S. K., Kirtane, A. R., & Panyam, J. (2014). Enhanced photodynamic therapy and effective elimination of cancer stem cells using surfactant-polymer nanoparticles. Mol Pharm, 11(9), 3186-3195. doi: 10.1021/mp5003619.

[12] Plaetzer, K., Krammer, B., Berlanda, J., Berr, F., & Kiesslich, T. (2009). Photophysics and photochemistry of photodynamic therapy: Fundamental aspects. Lasers Med Sci, 24(2), 259-268. doi: 10.1007/s10103-008-0539-1.

[13] Muehlmann, L. A., Ma, B. C., Longo, J. P., Almeida Santos Mde, F., & Azevedo, R. B. (2014). Aluminum-phthalocyanine chloride associated to poly(methyl vinyl ether-co-maleic anhydride) nanoparticles as a new third-generation photosensitizer for anticancer photodynamic therapy. Int J Nanomedicine, 9, 1199-1213. doi: 10.2147/ijn.s57420.

[14] Amin, R. M., Hauser, C., Kinzler, I., Rueck, A., & Scalfi-Happ, C. (2012). Evaluation of photodynamic treatment using aluminum phthalocyanine tetrasulfonate chloride as a photosensitizer: New approach. Photochem Photobiol Sci, 11(7), 1156-1163. doi: 10.1039/c2pp05411f.

[15] Sekkat, N., Bergh, H. v. d., Nyokong, T., & Lange, N. (2012). Like a bolt from the blue: Phthalocyanines in biomedical optics. Molecules, 17(1), 98.

[16] Thomas. (1990). Phthalocyanine research and applications.

[17] Berg, K., Bommer, J. C., & Moan, J. (1989). Evaluation of sulfonated aluminum phthalocyanines for use in photochemotherapy. Cellular uptake studies. Cancer Lett, 44(1), 7-15.

[18] Vrouenraets, M. B., Visser, G. W., Stigter, M., Oppelaar, H., Snow, G. B., & van Dongen, G. A. (2002). Comparison of aluminium (iii) phthalocyanine tetrasulfonate- and meta-tetrahydroxyphenylchlorin-monoclonal antibody conjugates for their efficacy in photodynamic therapy in vitro. Int J Cancer, 98(5), 793-798.

[19] Crous, A., Kumar, S. S. D., & Abrahamse, H. (2019). Effect of dose responses of hydrophilic aluminium (iii) phthalocyanine chloride tetrasulphonate based photosensitizer on lung cancer cells. Journal of Photochemistry and Photobiology B: Biology. doi: https://doi.org/10.1016/j.jphotobiol.2019.03.018.

[20] Chen, K., Huang, Y.-h., & Chen, J.-l. (2013). Understanding and targeting cancer stem cells: Therapeutic implications and challenges. Acta Pharmacologica Sinica, 34, 732. doi: 10.1038/aps.2013.27.

[21] Khan, M. I., Czarnecka, A. M., Helbrecht, I., Bartnik, E., Lian, F., & Szczylik, C. (2015). Current approaches in identification and isolation of human renal cell carcinoma cancer stem cells. Stem cell research & therapy, 6(1), 178-178. doi: 10.1186/s13287-015-0177-z.

[22] Barkeer, S., Chugh, S., Batra, S. K., & Ponnusamy, M. P. (2018). Glycosylation of cancer stem cells: Function in stemness, tumorigenesis, and metastasis. Neoplasia (New York, N.Y.), 20(8), 813-825. doi: 10.1016/j.neo.2018.06.001.

[23] Crous, A., & Abrahamse, H. (2016). Low-intensity laser irradiation at 636 nm induces increased viability and proliferation in isolated lung cancer stem cells. Photomed Laser Surg, 34(11), 525-532. doi: 10.1089/pho.2015.3979.

[24] Kiro, N. E., Hamblin, M. R., & Abrahamse, H. (2017). Photobiomodulation of breast and cervical cancer stem cells using low-intensity laser irradiation. Tumour Biol, 39(6), 1010428317706913. doi: 10.1177/1010428317706913.

[25] Rocha, M. S., Lucci, C. M., Longo, J. P., Galera, P. D., Simioni, A. R., Lacava, Z. G., Tedesco, A. C., & Azevedo, R. B. (2012). Aluminum-chloride-phthalocyanine encapsulated in liposomes: Activity against naturally occurring dog breast cancer cells. J Biomed Nanotechnol, 8(2), 251-257.

[26] Crous, A., Dhilip Kumar, S. S., & Abrahamse, H. (2019). Effect of dose responses of hydrophilic aluminium (iii) phthalocyanine chloride tetrasulphonate based photosensitizer on lung cancer cells. J Photochem Photobiol B, 194, 96-106. doi: 10.1016/j.jphotobiol.2019.03.018.

[27] Wang, Y., Huang, Y.-Y., Wang, Y., Lyu, P., & Hamblin, M. R. (2017). Red (660 nm) or near-infrared (810 nm) photobiomodulation stimulates, while blue (415 nm), green (540 nm) light inhibits proliferation in human adipose-derived stem cells. Scientific Reports, 7(1), 7781. doi: 10.1038/s41598-017-07525-w.

[28] Crous, A. M. (2016). Photobiomodulatory effects of low intensity laser irradiation on isolated lung cancer stem cells.

[29] Kiesslich, T., Gollmer, A., Maisch, T., Berneburg, M., & Plaetzer, K. (2013). A comprehensive tutorial on in vitro characterization of new photosensitizers for photodynamic antitumor therapy and photodynamic inactivation of microorganisms. BioMed research international, 2013, 840417-840417. doi: 10.1155/2013/840417.

[30] Vander Heiden, M. G., Cantley, L. C., & Thompson, C. B. (2009). Understanding the warburg effect: The metabolic requirements of cell proliferation. Science (New York, N.Y.), 324(5930), 1029-1033. doi: 10.1126/science.1160809.

[31] Ziago, E. K., Fazan, V. P., Iyomasa, M. M., Sousa, L. G., Yamauchi, P. Y., da Silva, E. A., Borie, E., Fuentes, R., & Dias, F. J. (2017). Analysis of the variation in low-level laser energy density on the crushed sciatic nerves of rats: A morphological, quantitative, and morphometric study. Lasers Med Sci, 32(2), 369-378. doi: 10.1007/s10103-016-2126-1.

[32] Ayuk, S. M., & Abrahamse, H. (2018). Photobiomodulation alters matrix protein activity in stressed fibroblast cells in vitro. 11(3). doi: 10.1002/jbio.201700127.

[33] Fekrazad, R., Asefi, S., Allahdadi, M., & Kalhori, K. A. (2016). Effect of photobiomodulation on mesenchymal stem cells. Photomed Laser Surg, 34(11), 533-542. doi: 10.1089/pho.2015.4029.

[34] Peiris-Pagès, M., Martinez-Outschoorn, U. E., Pestell, R. G., Sotgia, F., & Lisanti, M. P. (2016). Cancer stem cell metabolism. Breast cancer research : BCR, 18(1), 55-55. doi: 10.1186/s13058-016-0712-6.

[35] Strober, W. (2001). Trypan blue exclusion test of cell viability. Curr Protoc Immunol, Appendix 3, Appendix 3B. doi: 10.1002/0471142735.ima03bs21.

[36] Yoo, J. O., & Ha, K. S. (2012). New insights into the mechanisms for photodynamic therapy-induced cancer cell death. Int Rev Cell Mol Biol, 295, 139-174. doi: 10.1016/b978-0-12-394306-4.00010-1.

[37] Mfouo-Tynga, I., & Abrahamse, H. (2015). Cell death pathways and phthalocyanine as an efficient agent for photodynamic cancer therapy. Int J Mol Sci, 16(5), 10228-10241. doi: 10.3390/ijms160510228.

[38] Demchenko, A. P. (2013). Beyond annexin v: Fluorescence response of cellular membranes to apoptosis. Cytotechnology, 65(2), 157-172. doi: 10.1007/s10616-012-9481-y.

[39] Rieger, A. M., Nelson, K. L., Konowalchuk, J. D., & Barreda, D. R. (2011). Modified annexin v/propidium iodide apoptosis assay for accurate assessment of cell death. Journal of visualized experiments : JoVE(50), 2597. doi: 10.3791/2597.

[40] Chen, Y. C., Hsu, H. S., Chen, Y. W., Tsai, T. H., How, C. K., Wang, C. Y., Hung, S. C., Chang, Y. L., Tsai, M. L., Lee, Y. Y., Ku, H. H., & Chiou, S. H. (2008). Oct-4 expression maintained cancer stem-like properties in lung cancer-derived cd133-positive cells. PLoS One, 3(7), e2637. doi: 10.1371/journal.pone.0002637.

[41] Hu, B., Ma, Y., Yang, Y., Zhang, L., Han, H., & Chen, J. (2018). Cd44 promotes cell proliferation in non-small cell lung cancer. Oncology letters, 15(4), 5627-5633. doi: 10.3892/ol.2018.8051.

[42] Teicher, B. A. (2014). Targets in small cell lung cancer. Biochemical Pharmacology, 87(2), 211-219. doi: https://doi.org/10.1016/j.bcp.2013.09.014.

[43] Chang, J. C. (2016). Cancer stem cells: Role in tumor growth, recurrence, metastasis, and treatment resistance. Medicine (Baltimore), 95(1 Suppl 1), S20-25. doi: 10.1097/md.0000000000004766.

[44] Phi, L. T. H., Sari, I. N., Yang, Y.-G., Lee, S.-H., Jun, N., Kim, K. S., Lee, Y. K., & Kwon, H. Y. (2018). Cancer stem cells (cscs) in drug resistance and their therapeutic implications in cancer treatment. Stem cells international, 2018, 5416923-5416923. doi: 10.1155/2018/5416923.

[45] Agostinis, P., Berg, K., Cengel, K. A., Foster, T. H., Girotti, A. W., Gollnick, S. O., Hahn, S. M., Hamblin, M. R., Juzeniene, A., Kessel, D., Korbelik, M., Moan, J., Mroz, P., Nowis, D., Piette, J., Wilson, B. C., & Golab, J. (2011). Photodynamic therapy of cancer: An update. CA Cancer J Clin, 61(4), 250-281. doi: 10.3322/caac.20114.

International Conference on Cancer Research 2019

Website: www.CancerConf.org

June 10-11, London, UK



Landscape of Clinically Actionable Mutations in Breast Cancer

Radheshyam Naik[1*], Sheela ML[2], Sridhar PS[1], Shekar Patil[1], Satheesh C.T[1], Krithika Murugan[1], Srinivas B.J[1], Nalini Rao[1], Mahesh B[1], Shashidhara H.P[1], Krishna CR[2], Yogesh S[2], Nimmy Ramdas[2], Sunitha N[2], Ramya K[2], Ashwini R[2], Urvashi Bahadur[2], Pooja Agrawal[2], Veena R[2], Tejaswini BN[2] Sateesh Kunigal[2], Shanmukh Katragadda[2], Ashwini Manjunath[2], Amritanshu Ram[1], Raghavendra M Rao[1], Ajai Kumar[1], Mithua Ghosh[2]

[1] *Health Care Global Enterprises Ltd., Bangalore, India*

[2] *Strand Life Sciences Private Limited, Bangalore, India*

** Corresponding author: radheshyam_n@yahoo.com*

Abstract

Breast cancer (BC) is a heterogeneous disease. Numerous chemotherapeutic agents are available for early diagnosed or advanced/ metastatic breast cancer to provide maximum benefit with minimum side effects. However, the clinical outcome of patients with the same clinical and pathological characteristics and treated with similar treatments may show major differences and a vast majority of patients still develop treatment resistance and eventually succumb to disease. It remains an unmet need to identify specific molecular defects, new biomarkers to enable clinicians to adopt individualized treatment for every patient in terms of endocrine, chemotherapy or targeted therapy which will improve clinical outcomes in BC. Our study aims to identify frequent hotspot mutation profile in Indian BC by targeted deep sequencing in cancer-related genes using Swift Accel-Amplicon panel and MiSeq technology in an IRB-approved prospective study in a CLIA compliant laboratory. All the cases had pathology review for stage, histological type, hormonal status and Ki67. Data was processed using Strand NGS™. Mutations identified in the tumor were assessed for 'actionability' i.e. response to therapy and impact on prognosis.

Keywords:

Breast Cancer,

Next Generation Sequencing,

NGS,

Genetic Profiling,

Somatic Mutations,

PIK3CA,

Signaling Pathway.

Introduction

Breast Cancer (BC) is the most frequently diagnosed malignancy worldwide and is the second leading cause of cancer death among females accounting to approximately 40,000 deaths every year [1]. Breast cancer mainly affects post-menopausal women, however, it is estimated that 4.8-5.0% of cases occur in young adults, less than 40 years [2]. The most important risk factors include: genetic predisposition, exposure to oestrogens (endogenous and exogenous), ionising radiation, low parity and a history of atypical hyperplasia. The western-style diet, obesity, ethnicity, lifestyle and the consumption of alcohol also contribute to the rising incidence of BC [3]. There is a significant increase in the incidence and cancer-associated morbidity and mortality in Indian subcontinent as described in global and Indian studies [4]. The factors for BC in western populations have been extensively investigated and has been suggested that reproductive and life-style related factors are strongly associated with increased risk for BC [5]. Not much data is available about the role of various risk factors for BC in Indian women [6]. BC in males is rare, contributing to approx. 1% of cases. The major risk factors include clinical disorders carrying hormonal imbalances (especially gynaecomastia and cirrhosis), radiation exposure and, in particular, a positive family history and genetic predisposition [7].

The disease is very heterogeneous (both intra and inter tumour) clinically and at molecular level. Current clinical management of the disease comprises morphological assessment (size, grade, lymph node status), and testing for hormone receptor(HR) as Estrogen (ER), progesterone (PR), human epidermal growth factor receptor 2 (HER2) and Ki67 for proliferation index [8]. Classification of breast cancer at the molecular level based on gene expression studies started in the year 2000 and explained that breast cancer is not one single entity but can be subdivided into distinct subtypes Luminal A (HR+/HER2−, tumor grade 1 or 2), luminal B/HER2+ (HR+/HER2+), luminal B/HER2− (HR+/HER2−, tumor grade 3 or 4), triple negative (HR−/HER2−) or HER2 overexpressing (HR−/HER2+) [9]. Of all the breast cancer cases, luminal A and B subtypes account for 65% to 70%, triple negative breast cancer (TNBC) about 10% to 15% and Her-2 overexpressing about 10% to 20% [10]. The ER positive groups are about three quarters of all breast cases treated using ER modulators or aromatase inhibitors [11]. Several genomic tests are available to predict the outcome of ER+ patients receiving endocrine therapy and only about 20% to 40% respond to the treatment [12]. Among the subtypes, the luminal A has good outcome with 95% 5-year survival whereas luminal B tend to have worst outcome as they are less sensitive to endocrine therapy and are more sensitive to chemotherapy [12]. TNBC also known as basal like breast cancers are known to be aggressive with only chemotherapy option and are associated with germline BRCA mutations [13]. TNBC subgroup cannot be regarded as a single disorder but rather as a trunk of heterogeneous diseases which have different characteristics, behaviours, and prognoses and also respond differently to

Drug treatments. Further, these findings are supported by gene expression studies which have thrown light on prognostic and predictive subgroups in TNBC [14]. HER-2 subtypes may be eligible for targeted therapy but still the rate of metastasis is high and prognosis is poor as they are resistant to current chemotherapies [15].

The development of distant metastases is the strongest negative prognostic factor associated with BC mortality [16]. Although breast cancer metastases are detected in approximately 5%–10% newly diagnosed cases, 25%–50% of patients affected by early-stage lesions or by locally advanced tumors may develop metachronous metastatic disease [1, 17].

Despite recent advances in the treatment of BC with the advent of better surgical expertise, radiotherapy techniques and chemotherapeutic advances over the past 20 years the outcome of metastatic BC has increased marginally and remains the second leading cause of female-specific cancer-related mortality, accounting for approximately 40,000 deaths every year [18]. Many major drugs have initial response but the non-responder rates vary between 30% and 70%. The variation in the clinical outcomes of patients can be accounted to inherent variability because of the genomic instability, which generates somatic mutations/alterations leading to clonal expansion. For eg. although trastuzumab has revolutionized the treatment of Her2 positive BC , a significant number of patients with HER2-overexpressing breast cancer do not benefit from it due to acquired or *de novo* resistance Understanding the mechanisms of action and resistance to trastuzumab is therefore crucial for the development of new therapeutic strategies [19] . The phosphatidylinositol 3′-kinase/protein kinase B/mammalian target of rapamycin (PI3KCA, AKT, mTOR) pathway , cross-talk with ER receptors, immune response, cell cycle control mechanisms, and other tyrosine kinase receptors such as insulin-like growth factor I receptor are potential pathways involved in trastuzumab resistance [19]. Moreover, drug resistance is common in all breast cancer types despite the different treatment modalities applied. The development of resistance to different therapeutics is not mutually exclusive. It seems that tumor could be resistant to multiple treatment strategies, such as being both chemoresistant and monoclonal antibody resistant. However, the underlying mechanisms are complicated and need further investigation. It is well known that cancer progression is due to the genetic alteration in the cancer genome and hence understanding the genomic drivers is essential to develop new therapies [20]. Evidences suggest that the risk assessments, treatments and patient outcome are not just by the biology of the tumor but are also influenced by somatic and germline mutations [21]. Somatic mutations in AKT1, PICK3CA, PTEN and TP53 genes have been found at high frequency in breast cancer with PICK3CA as 26.4%, TP53 as 24.7%, PTEN as 3.8% and AKT1 as 2.8% as per Catalogue of Somatic Mutations in Cancer (COSMIC) database [22]. Large genomic landscape studies have shown that the mutations in these four genes showed subgroup specificity with clinical implications which helped extensively in cancer classification and treatment [23-24].

PI3KCA/AKT/mTOR signalling pathway is critical to both normal and malignant cellular processes, like proliferation, apoptosis, and metabolism [25]. Spontaneous mutations in PIK3CA are very common with almost 25% of breast cancer patients harbouring a mutation in this gene [26]. Reports show that there are recurrent somatic mutations in different types of cancer and particularly in breast cancer. Particularly, the p110α catalytic component of phosphoinositide-3-kinase (PI3K) termed as *PIK3CA*, the gene that encodes, is commonly mutated in approximately 36% of breast cancers, and 80% to 90% of mutations which aggregates in exon 9 (E545K and E542K) and exon 20 of *PIK3CA* into 3 hotspot regions [27]. PI3K phosphorylates membrane phosphatidylinositols leading to recruitment of AKT and its activator (phosphoinositide dependent kinase -PDK1) to the cell membrane via pleckstrin homology domain and 3’ phosphorylated lipids. This enforced co localization of AKT and PDK1 phosphorylates the latter in turn activates the former. PDK1 and PDK2, likely components of TORC2 complex, phosphorylate the AKT initiating a downstream signalling cascade [28]. The same site is dephosphorylated by the tumor suppressor or PTEN on membrane phosphatidylinositols that is phosphorylated by PI3K, which reverses the effect of PI3K signalling

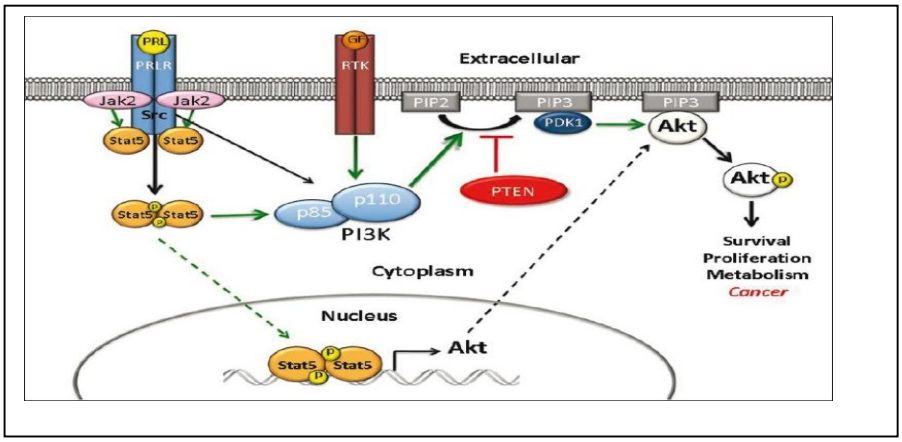


Figure 1: PI3K- AKT Signalling Pathway

Preclinical and clinical studies support *PIK3CA* mutations may predict sensitivity to treatment with PI3K/AKT/mTOR inhibitors in breast tumors in particular and also a multiple tumor types [29]. Multiple molecular alterations like PI3K mutation, PTEN loss and AKT1 mutation follow this abnormal activation of PI3K-AKT-mTOR pathway. Additionally, as a result of crosstalk between the PI3K-AKT-mTOR pathway and MAPK pathway, KRAS and BRAF activate the members of PI3K-AKT-mTOR pathway [30-31]. Activation of PI3K lipase get aggravated by PIK3CA mutation and in turn upregulates the downstream AKT signalling. There are reports of negative feedback regulation of the PI3K pathway, in which PTEN plays an important role. PTEN is absent in 25% of breast cancer patients and mutated in 5% of the patients and this inactivation leads to phosphorylation of AKT, mTOR and S6K1[32].

PIK3CA is the second most commonly mutated gene in hormone receptor positive breast cancer [33] for which the inhibitor everolimus is recommended as a therapeutic option for metastatic breast cancer [34].Though PIK3CA

mutations have been associated with good prognosis for few subtypes, they have also been shown to impart resistance to trastuzumab which is a common treatment option for Her-2 overexpressing breast cancers [35]. The therapeutic efficacy of a number of inhibitors of AKT, PIK3CA and mTOR inhibitors are under clinical investigations for breast as well as other cancers [36]. Moreover, in case of TNBC's, there are no targeted treatments and so identifying gene mutations becomes important. Hence, it is very important to establish the genetic profile of BC and to identify the gene mutations for treatment options and to avoid unnecessary drug toxicities [21]. Also the mutation spectrum of these genes and other driver mutations is not well studied in Indian population Therefore It remains an unmet need to identify specific molecular defects, new biomarkers for Indian BC patients to enable the clinician to adopt individualized treatment for every patient in terms of endocrine, chemotherapy or targeted therapy which will improve clinical outcomes in BC

The advance of next-generation sequencing (NGS) technology enables massively parallel deep sequencing of patients at with breast cancer 'one go' to analyse the mutation profile of tumors, identify genomic markers as response predictors to therapy to thus making personalized treatment a reality for patients. This breaks the cycle of 'trial and error' medicine, and link the test to patient tailored action and evidence based therapy/ treatment plan in breast cancer

In the present study, we have analysed the frequent hotspot mutation profile in BCs by targeted deep sequencing in cancer-related genes using Swift Accel-Amplicon panel and MiSeq technology in an IRB-approved prospective study in a CLIA compliant laboratory. Further, the clinical and pathological features of breast cancer associated with the mutations detected have been analysed.

Materials and Methods:

Ethics Statement

The study has been approved by the Human Research Ethics Committee of the institute (Health Care Global Enterprises, India) .The institutional ethics committee recommended the need for consent for formalin-fixed, paraffin-embedded (FFPE) tumor samples obtained from the tumor tissue bank at the hospital's department of Pathology. All samples and medical data used in this study have been irreversibly anonymized.

Patient / Study subjects and sample preparation

570 women with BC(early diagnosed or advanced/ metastatic) aged 26-75 yrs (median age 50.5yrs) diagnosed at the hospital from April 2014-17 were counselled/ consulted to be profiled by targeted deep sequencing for somatic hotspot mutations in 56 cancer-related genes. For the study, Swift Accel-Amplicon panel was used on MiSeq technology in an IRB-approved prospective study in a CLIA compliant laboratory. Out of 570 BC cases 275 (48%) patients consented for undergoing the genetic testing. Formalin-fixed, paraffin-embedded (FFPE) tumor samples were obtained from the tumor tissue bank at the hospital's Department of Pathology. All the cases had pathology review for stage, histological type, hormonal status and Ki67.

DNA preparation

FFPE tissue samples were first deparaffinized in xylene, 3–5-µm-thick sections were extracted, and DNA was isolated using the QIAamp DNA Mini Kit (QIAGEN) as per the manufacturer's instructions. DNA was quantified using Qubit, as well as a qPCR assay.

Histopathology and Immunohistochemistry (IHC)

IHC for ER, PR and Her-2/neu was done on tissue sections that were fixed in 10% neutral buffered formalin. FFPE blocks from these sections were cut into 3micron thickness and taken on positively charged slides coated with PLL. The primary and secondary antibodies from Biocare, USA were used (ERSP1 clone for ER, PRSP2clone for PR and EP3clone for Her-2/neu).The slides were incubated at 35 0 degree overnight, followed by treatment with Antigen retrieval in citrate buffer at pH 6.0 for 30min at 93 0C. The slides were then stained as per protocol with DAB. All the stainings were done along with known positive controls tissue. Internal control where available was also used for validation of the staining. The stained slides were interpreted as per Alred Score for ER, PR and as per American Society of Clinical Oncology (ASCO) / College of American Pathologists (CAP) guidelines using a cutoff of > 1% stained tumor nuclei and evaluated by Allred score guidelines for Her-2/neu [37] . Her-2/neu score of 0 and 1+ were reported as negative where there was either absence or barely perceptible incomplete membrane staining in <10% of tumor cells, while a score of 3+ was interpreted as positive when >10% cells showed complete strong membrane staining. Fluorescent in situ hybridization (FISH) testing was recommended for a score of 2+(equivocal) where there was incomplete membrane staining in >10% tumor cells. All hematoxylin and eosin (H&E)-stained slides and immunohistochemistry slides were reviewed by two pathologists.

Her2/neu by FISH

Detection of Her2/neu amplification in human breast carcinoma via fluorescence in situ hybridization (FISH) on FFPE tissue specimen, is the alternative technique used to overcome the limitations of immunohistochemistry. Her2/neu by FISH was tested usingst an FDA-approved PathVysion HER-2 DNA Probe Kit (Abbott PathVysion Kit Catalogue number 06N46-03). IHC evaluation of breast tissue that was considered inconclusive/ equivocal with a 2+ score was reflexed for FISH testing. Four µm thick paraffin sections fixed on positively charged slides were pretreated chemically and enzymatically to remove wax and proteins, thereby making the nucleus permeable to the fluorescent probes. The pretreatment was followed by denaturation and hybridization of the fluorescently labeled DNA probes complementary to the her2/neu genomic DNA sequence . The slide was further subjected to post- hybridization washes to remove un-annealed probes. The sample was counterstained with a nucleus staining dye to visualize the signals under an epifluorescence microscope (Nikon Eclipse 80i) fitted with appropriate filter set. Enumeration of the signals is done in accordance with the manufacturers guidelines and interpretation based on recent ASCO and CAP guidelines [38]. The signals for Her2/ neu gene to the centromere enumeration probe (CEP) on chromosome 17 was counted to provide a comprehensive report to the clinicians. Her2/neu gene was reported to be amplified if , Her2/CEP17 ratio greater than or equal to two, and the average copy number of her2/neu gene was less than, equal to or greater than four OR Her2/CEP17 ratio is less than two and the average copy number of her2/neu gene was greater than or equal to six. Her2/neu gene is not amplified when the Her2/CEP17 ratio was reported to be less than two and the average copy number of her2/neu was less than four. Her2/ neu gene ratio equal to or greater than two indicates amplification or over expression, whereas a ratio less than two does not indicate amplification of the gene.

Next Generation sequencing (NGS) - Multigene panel selection

NGS was performed using Accel Amplicon 56G for comprehensive and hotspot coverage of 56 clinically-relevant oncology-related genes .This panel utilizes a 263-amplicon design, covering over 16,000 COSMIC mutations (Forbes et al. Oxford Journals. 2014), to generate targeted libraries compatible with Illumina MiSeq sequencing .The genes in the panel are ABL1, AKT1, ALK, APC, ATM, BRAF, CDH1, CDKN2A, CSF1R, CTNNB1, DDR2, DNMT3A, EGFR, ERBB2, ERBB4, EZH2,FBXW7, FGFR1, FGFR2, FGFR3, FLT3, FOXL2, GNA11, GNAQ, GNAS, HNF1A, HRAS, IDH1, IDH2, JAK2, JAK3, KDR,KIT, KRAS, MAP2K1, MET, MLH1, MPL, MSH6, NOTCH1, NPM1, NRAS, PDGFRA, PIK3CA, PTEN, PTPN11, RB1, RET,SMAD4, SMARCB1, SMO, SRC, STK11, TP53, TSC1, VHL

Library Preparation and Sequencing

10-100 ng of DNA depending on the quality of DNA was used for Accel Amplicon 56G amplicon library generation. Individually amplified libraries were tagged with adaptors/barcodes and quantified using NEBNext Library Quant Kit (NEB, USA). Up to 20 libraries were pooled and loaded on Illumina MiSeq platform using a V2 kit to yield multitude of reads for each region of interest.

Analysis

The trimmed FASTQ files were generated using MiSeq Reporter from Illumina. The amplicon primers were trimmed from the reads using cutadapt v1.13. The reads were processed using STRAND® NGS v2.6 (http://www.strand-ngs.com) via the analysis pipeline 'Swift_56G_ST_v4'. In this pipeline, reads were aligned against the whole genome build hg19 (UCSC). Before aligning, one base pair from the 3' end of the reads was trimmed, as were 3' end bases with quality below 20. Reads which have length less than 25 bp after trimming were not considered for alignment. A maximum of 5 matches of alignment score of at least 90% were computed. Reads that failed vendor QC, reads with average quality less than 20, reads with ambiguous characters, and reads with alignment score less than 95% were all filtered out. The Strand®NGS binomial variant caller was used to detect variants. Variants are called at locations in the target regions covered by a minimum of 10 reads having at least 2 variant reads. Variants with a decibel score of at least 50 were reported. Substitution variants with a StrandBias > 50%, and InDel variants in homopolymer stretches longer than 4bp with supporting reads<10% were filtered out. Also, all variants with supporting reads <2% were filtered out. All the variants were then imported into StrandOmics for further interpretation and reporting. Annotation and prioritization of variants was done by automated pipelines in StrandOmics. The StrandOmics user interface was then used for identifying variants of interest and for reporting these variants. All variants reported were verified to have good read quality using the Strand® NGS v2.6 genome browser before final reporting. The Limit of Detection (LOD) for this test is 3% variant allele frequency (VAF) at coverage of 200X. It has a sensitivity of ~96% and a specificity of ~100%.

Statistical analysis

One objective of the statistical analyses was to evaluate if there was an impact of gene mutation on the proportions of hormonal subtype and pathological response to Neo-adjuvant treatment. This was ascertained by Fisher's Exact Test and χ2-Sqaure test with Bonferroni Corrections on post-hoc analyses for subgroups. All inferential tests were two-tailed and α was considered to be 0.05. All statistical tests were done using SPSS version 18.

Results:

275 patients of Indian ethnicity with a known diagnosis of early/ advanced-metastatic BC diagnosed at a tertiary hospital from April 2014-16 were consented to be profiled by targeted deep sequencing for hotspot mutations in 56

cancer-related genes. The cohort comprised of 2 male and 273 female breast cancer patients The clinicopathological features of the patients were summarized in Table 1A and 1B. The maximum number of patients were in the age group of 40-65 years (67%), whereas 24% of patients were below the age of 40 years. There were only 25 (9%) patients above 65 years of age. The median age of patients was found to be 52 years. The cohort was predominantly of common histological type of infiltrating ductal carcinoma (IDC) (73%) and presented at stage III (18%) or IV (55%) of breast cancer. About 60% of patients were hormonal positive (HR+ive) out of which 12% were triple positive (TPBC- HR+ve Her2+ive-) and 48% were HR+ve and Her2-ive (HR+ve Her2-ive). Among the 40% hormonal negative (HR-ve) cohort, 10% of patients were Her2+ive (HR-ive, HER2+ive) and 30 % were triple negative breast cancer TNBC-HR-ive, HER2-ive-). Notably, the number of TNBC cases reported in the tertiary cancer centre in India is higher than the global data [10]. Based on hormonal status and Ki67, the cohort was classified into Luminal A (7%), Luminal B (34%), basal like

/ TNBC (30%) and HER 2 enriched (11%) (Table 1B). The stage and hormonal status were not available in the medical records for 33 patients.

Table 1 A. Statistics of total number of cases

	Total cases	**Percentage**
Ca breast cases from 2014-2017	**570**	
Ca breast cases who have undergone Somatic testing	**275**	**48%**
Female patients	**273**	**99%**
Male patients	**2**	**1%**
Cases with mutations detected	**195**	**71%**
Cases with actionable mutations detected	**126**	**46%**
Cases with no mutation	**80**	**29%**

Table 1B. Clinicopathological Characteristics of 275 breast cancer patients

Sl No	**Characteristics**		**Number of patients**	**n(%)**
a	**Age at diagnosis**	<40	65	24
		40-65	185	67
		>65	25	9
b	**Tumor Grade**	1	4	1
		2	79	29
		3 or 4	67	24
		Unknown	125	45
c	**Tumor Stage**	1	15	5.5
		2	25	9.1
		3	50	18.2
		4	151	54.9
		Unknown	34	12.4
d	**Tumor type**	IDC	201	73.1
		ILC	2	0.7
		Mucinous	1	0.4
		Mixed	6	2.2
		DCIS	4	1.5
		Unknown	61	22.2
e	**Hormonal Status**			
	HR	Positive (+)	147	60.7
	HR Her2	Positive (+) Positive (+)	29	12.0
	HR Her2	Positive (+) Negative (-)	118	48.8
	HR Her2	Negative (-) Positive (+)	22	9.1
	HR Her2	Negative (-) Negative (-)	73	30.2
	HR Her2	Unknown	33	13.6
f	**Molecular subtype**	Luminal A	19	7
		Luminal B	93	34
		Basal like/TNBC	75	30
		HER 2 enriched	29	11
		Unknown	61	22

Detection of Mutations by NGS

The somatic mutation landscape was analysed in these patients (Table 2). Somatic variants were detected in 195 BC patients (71%) comprising of mutation in single gene or co mutation in multiple genes. "Actionable" mutations were found in 46% BC cases with direct impact on therapy or prognosis.

Table 2. Frequencies of most prevalent somatic mutations compared with TCGA data

Mutation Pattern	In this study of 275 patients(195 harbouring somatic mutation		In TCGA data (n=507)	
	# patients	Percentage	# patients	Percentage
Mutation in gene				
AKT1	6	3	23	4.5
PIK3CA	82	42	179	35.3
PTEN	25	12.8	16	3.2
TP53	121	62	179	35.3
others	16	8.2	NA	NA
Mutation in single gene				
AKT1	2	1	9	1.8
PIK3CA	35	18	130	25.6
PTEN	4	2	6	1.2
TP53	61	31	127	25.0
Co-mutation in two genes				
AKT1+PIK3CA	0	0.0	1	0.2
AKT1+PTEN	1	0.5	0	0.0
AKT1+TP53	3	1.5	2	0.4
PIK3CA+PTEN	3	1.5	4	0.8
PIK3CA+TP53	37	19	44	8.7
PTEN+TP53	7	3.6	6	1.2
PI3K + others	43	22	NA	NA
Co-mutation in three genes				
AKT1+PIK3CA+TP53	0	0.0	0	0.0
PIK3CA+PTEN+TP53	1	0.5	0	0.0

Genetic aberrations were identified in PI3KCA/AKT/PTEN signalling pathway in substantial fraction (57.8 %) in Indian BC patients PI3KCA was found to be altered in 42 % cases where as deletion in pTEN was found in 12.8 % and mutation in AKT in 3 % of BC patients. The somatic mutation frequency of these genes reported by TCGA [39] was 35.5%, 3.2% and 2.4% respectively. Overall ,the mutation frequency of these genes is higher in Indian patients thus offering important biomarkers for targeted therapy in metastatic setting.

Multiple – gene and recurrent mutations

Among the 195 somatic mutation carriers, 102 (102/195, 52%) harboured mutation in single gene mutation, 94 (94/195 48%) harboured co-mutation in two genes , and 1 patient (0.005%) harboured co-mutation in three genes .

The mutation landscape was correlated with the clinicopathological characteristics of the patients (Table 3)

Table 3. Clinicopathological characteristics and associations with PIK3CA and TP53 in 275 breast cancer patients

	Total (275)	PIK3CA co- mutation (82)		TP53 co mutation (121)		PIK3CA + TP53 (39)	
Characteristic	**Number**	**Mutant (%)**	**WT**	**Mutant (%)**	**WT**	**Mutant (%)**	**WT**
Age at diagnosis							
<40	65 (23.6)	11 (13.4%)	54 (28.0%)	29 (23.9%)	36 (23.4%)	4 (10.8%)	61 (25.8%)
40-65	185 (67.3)	63 (76.8%)	122 (63.2)	84 (69.4%)	101 (65.6%)	31(83.7%)	154 (65.3%)
>65	25 (9%)	8 (9.8%)	17 (8.8)	8 (6.6%)	17 (11.0%)	2 (5.4%)	23 (9.7%)
Hormonal Status							
HR (+)	147(60.7%)	56 (38%)	91 (62%)	41 (33.9%)	95 (61.7%)	28 (71.8%)	108 (45.8%)
HR (+) Her2 (+)	29 (19%)	11 (38%)	18(62%)	9 (7.4%)	12 (7.8%)	4 (10.3%)	17 (7.2)
HR (+) Her2(-)	118 (83%)	45 (38%)	73 (62%)	32 (26.4%)	83 (53.9%)	20 (51.3%)	95 (40.3)
HR (-)Her2 (+)	22 (11%)	4 (18%)	18 (82%)	16 (13.2%)	13 (8.4%)	2 (5.1%)	27 (11.4%)
HR (-)Her2 (-)	73 (30%)	13 (18%)	60 (82%)	51 (42.1%)	25 (16.2%)	8 (20.5%)	68 (28.8%)
HR Her2 (unknown)	33 (13.6)	25 (13.0%)	9 (11%)	13 (10.7%)	21 (13.6%)	5 (12.8%)	29 (12.3%)
Ki 67 Expression							
< 15	25 (9.1%)	6 (24%)	19 (9.8)	4 (16%)	21 (13.6%)	3 (12%)	22 (9.3%)
> 15	162 (58.9%)	54 (33%)	108 (56.0%)	75 (46.3%)	87 (56.5%)	23 (14.2%)	139 (58.9%)
Unknown	88 (32.0%)	22 (25%)	66 (34.2%)	42 (47.8%)	46 (29.9%)	13 (14.8%)	75 (31.8%)

Comparing mutation carriers with activating mutations in PI3KCA/AKT/PTEN signalling pathway and non-carriers, mutations were found to be the common genetic event in hormone receptor-positive HR+ve BC (38%). Using Fischer Exact (P=0.001) test, mutations in PI3KCA/AKT/PTEN signalling pathway was found to be significantly higher in HR+ve BC compared to HR –ve cohort of IDC histology.

It is also important to note that PI3KCA/AKT/PTEN signalling pathway was also found to be altered 1n 18% of TNBC. Also, using Pearson Chi Square test ($\chi 2 = 11.180$; p=0.011), the mutations in PI3KCA/AKT/PTEN signalling pathway was found to be significantly higher in HR+ve , HER2-ive BC. These findings are consistent with a study by Kalinsky et al. which showed PIK3CA mutations were more in HER2− tumors than HER2+ tumors (61.5% vs. 38.5%, respectively) and patients with HR+ tumors had a higher likelihood of having a PIK3CA mutation than those with

HR− tumors. However, no statistical significance was shown in this study [40]. The findings have a potential clinical implication as targeted mTOR inhibitors like everolimus, a rapamycin derivative that inhibits PI3K/ATK/mTOR signaling, have been approved to treat advanced HR+/HER2− breast cancer patients after other treatments have failed and have been shown to increase progression-free survival [41-43] Also activation of the PI3K/ATK/mTOR pathway has been shown to confer resistance to trastuzumab treatment in HER2+ breast tumors [44-45], specific mutation may offer a potential prognostic value identifying these mutations in all breast cancer patients regardless of subtype may serve as a potential tool to stratify patients as responders and non- responders of anti Her2 therapy

Several different PIK3CA mutations were identified: p.N345K in the C2 domain encoded by exon 4, p.E542K and p.E545K in the helical domain encoded by exon 9, and p.H1047R and p.H1047L in the kinase domain encoded by exon 20 (Table 4). Mutations in p.H1047R was found to be most prevalent (40/82cases) followed by p.E542K, p.E545K. Three patients had other variants of PIK3CA (p.Glu 542 Gln , p.Glu 542 Gln and p. Pro 539 Arg) along with p.H1047R. These three mutations have been found in previous studies to be the most prevalent in human breast cancers and are associated with an increase in kinase activity in the PI3K pathway [44-45], and accounted for 88.5% of all PIK3CA mutations in our study.

Table 4. Pathogenic mutations of PIK3CA gene (single mutation+ co-mutation) detected in 82 Ca breast cases of 275 cases

Gene	# of Patients	Frequency of mutation	Status	Nucleotide change	Variant	Mutation type	Previously reported
PIK3CA	1	1.2	Somatic	c.3140A>T	p.His 1047 Leu	Missence	dbSNP[COSMIC]ClinVar
	1	1.2	Somatic	c.3132T>A	p.Asn 1044 Lys	Missence	dbSNP[COSMIC]ClinVar
	10	12.2	Somatic	c.1035T>A	p.Asn 345 Lys	Missence	dbSNP[COSMIC]ClinVar
	3	3.7	Somatic	c.1258T>C	p. Cys 420 Arg	Missence	dbSNP[COSMIC]ClinVar
	1	1.2	Somatic	c.1637A>G	p.Gln 546 Arg	Missence	dbSNP[COSMIC]ClinVar
	1	1.2	Somatic	c.1636C>G	p. Gln 546 Glu	Missence	dbSNP[COSMIC]ClinVar
	1	1.2	Somatic	c.1636C>A	p. Gln 546 Lys	Missence	dbSNP[COSMIC]ClinVar
	1	1.2	Somatic	c.1625A>G	p. Glu 542 Gly	Missence	dbSNP[COSMIC]ClinVar
	7	8.5	Somatic	c.1624G>A	p. Glu 542 Lys	Missence	dbSNP[COSMIC]ClinVar
	2	2.4	Somatic	c.1634A>C	p. Glu 545 Ala	Missence	dbSNP[COSMIC]ClinVar
	1	1.2	Somatic	c.1634A>G	p. Glu 545 Gly	Missence	dbSNP[COSMIC]ClinVar
	7	8.5	Somatic	c.1633G>A	p. Glu 545 Lys	Missence	dbSNP[COSMIC]ClinVar]ExAC
	37	45.1	Somatic	c.3140A>G	p. His 1047 Arg	Missence	dbSNP[COSMIC]ClinVar]ExAC
	1	1.2	Somatic	c.3140A>G c.1624G>C	p.His 1047 Arg p.Glu 542 Gln	Missence Missence	dbSNP[COSMIC]ClinVar]ExAC dbSNP[COSMIC]ClinVar
	1	1.2	Somatic	c.3140A>G c.1633G>A	p. His 1047 Arg p.Glu 545 Lys	Missence Missence	dbSNP[COSMIC]ClinVar]ExAC dbSNP[COSMIC]ClinVar
	1	1.2	Somatic	c.3140A>G c.1616C>G	p. His 1047 Arg p. Pro 539 Arg	Missence Missence	dbSNP[COSMIC]ClinVar]ExAC dbSNP[COSMIC]ClinVar
	4	4.9	Somatic	c.3140A>T	p. His 1047 Leu	Missence	dbSNP[COSMIC]ClinVar]ExAC
	1	1.2	Somatic	c.3129G>C	p. Met 1043 Ile	Missence	dbSNP[COSMIC]ClinVar
	1	1.2	Somatic	c.1633G>A	p. Pro 278 Ser	Missence	dbSNP[COSMIC]ClinVar

While the study of Kalinsky *et al* found overall patient survival to be significantly improved in patients with PIK3CA mutations [40], in a short follow up study , we found that patients with PIK3CA mutations collectively had a roughly equal DFS time to patients with WT PIK3CA. Since the cohort of patients for whom we had clinical follow up was small, more patients have been enrolled in the investigator imitated trials and are being followed up.

PIK3CA mutations are an early event in breast cancer development. In our study, we found mutations in this gene at all stages and all breast cancer subtypes. While previous research has found PIK3CA mutations to be associated with older patient age [45], we did not find significant differences between age and PIK3CA mutations among all patients. No correlation was found with stage and Ki67 index of the tumor also. Notably 67% of BC cases presented with liver metastases at the time of diagnosis were detected with PIK3CA mutation indicating its role as a surrogate marker of organ specific metastasis. Similar findings have been reported in a recent study where PI3KCA mutations have been frequently observed in BC with liver metastasis (LM) and persist along with the recurrence [32]. This finding can be very useful in serial monitoring of the clinical response by identifying the PI3KCA mutations in circulating tumor cells through "liquid biopsy" of the patient and can serve as a useful biomarker in the routine practice of breast cancer management to prevent tumor recurrence and overcome the problems of intra- and inter-tumoral heterogeneity.

Disruptive and non-disruptive mutations in TP53 alone and co-mutated with other genes were found in 31% and 62 % of BC. TP53 was also found to be commutated with PI3KCA in 19 % BC patients. P53 mutation had been found to be significantly higher in Indian patients compared to what has been reported in TCGA data [39]. Previous in vivo study has confirmed that TP53 and PIK3CA mutation show cooperation in mammary tumor formation in mice [46]. It have been reported that TP53-PIK3CA co-mutation carriers had worst disease-free survival comparing with non-mutation carriers, PIK3CA-mutation-only or TP53-mutation-only carriers [47]. Since a high frequency of TP53-PIK3CA co-mutations was detected in our cohort, this mutation pattern needs to be evaluated closely in clinical settings for Indian breast cancer patients in the future . Also in our cohort, TP53 mutation carriers had a significant higher proportion of patients to be triple negative BC. A follow up of few cases showed shorter disease free survival(DFS) and poor outcome in resected BC treated with NACT, indicating its robust prognostic value in NACT setting.

Furthermore, somatic mutations were also detected in cKIT indicating sensitivity to imatinib and therefore enrolled on a clinical trial. The other variants were found in RB1, Her2 genes , FGFR amplification, KRAS, NRAS, CDH1, FBXW 7 and EGFR. All these variants identified indicated resistance to conventional therapy and suggested sensitivity

to alternative targeted therapy, either approved or in clinical trials.

Pathological complete response rates (pCR) with PI3KCA mutation status

We retrospectively selected patients with invasive breast cancer who underwent surgery at the surgery unit of HCG hospital after neoadjuvant chemotherapy (NACT) and had undergone somatic mutation testing in our laboratory. Information on the treatment protocol was obtained from the medical records. Out of total 46 selected patients, follow up data were available for 35 cases. All patients underwent at least three cycles of NACT before surgery. The NACT regimens without trastuzumab included anthracycline based (doxorubicin with cyclophosphamide) or anthracycline and taxane-based (doxorubicin and docetaxel with or without cyclophosphamide) regimens. The NACT regimens including trastuzumab were anthracycline-based, taxane-based (docetaxel), or anthracycline and taxane-based (doxorubicin with docetaxel and cyclophosphamide) regimen. The histopathology reports of sequential FFPE blocks including pre-NACT and post-NACT, and recurrent specimens of each patient were collected. Patients were excluded if they did not have either pre-NAC or post-NAC specimen blocks. Tumor recurrence/ progressive disease (PD) was defined as involving both local recurrence and distant metastasis, while pCR was defined as no invasive tumor in the breast or lymph nodes, and no lymphovascular invasion. The patients were categorized into pathological partial response (PR) if the invasive tumor in the breast or lymph nodes is more than 25% and stable disease (SD) if invasive tumor in the breast or lymph nodes is less than 25%.

In total 5 patients (14%) achieved pCR after NACT, 15 patients had PR (43%) , 7 patients(20%) were found to achieve SD while 8 patients (23%) had PD. Overall 27 patients (77%) responded to NACT either with a pCR or a stable disease whereas 8 patients(23%) had progressive disease. *PIK3CA* mutation in post-NACT specimens correlated with a lower pCR rate than that observed in the post-NACT wild-type specimens. Majority of these patients were HER2+ve and had undergone NACT regimen that included trastuzumab. Although the cohort is small to perform a statistical analysis but the overall data clearly indicates that activation of the PI3K/ATK/mTOR pathway could be a potential factor conferring resistance to trastuzumab treatment in HER2+ breast tumors thus suggestive of using combination therapy/ alternate therapy

Conclusions

Understanding the genetic profile of cancer and identifying hotspot mutations serve as valuable tool for correct diagnosis, prognosis and treatment. This study provides a comprehensive mutation profile of Indian breast cancer cases and has a potential implication in clinical management of BC. The findings also confirm the utility of multigene profiling in Indian cohort of breast cancer patients, both early diagnosed and advanced cases to identify markers/signature which will help to stratify them based on their molecular profile who could potentially benefit from targeted therapy. Prospective studies and randomized clinical trials are ongoing to confirm the independent prognostic and therapeutic value of the mutations in a larger cohort of Indian population. and design more optimal genome specific next generation clinical trials in the future.

References

1. Siegel RL, Miller KD, Jemal A. Cancer statistics, CA Cancer J Clin. 2016; 66:7-30.
2. Encinas G, Sabelnykova VY *et al*. Somatic mutations in early onset luminal breast cancer, Oncotarget. 2018; 9: 22460-22479.
3. McTiernan. Behavioral risk factors in breast cancer: can risk be modified? Oncologist. 2003; 8: 326-334.
4. Babu GR, Lakshmi SB, Thiyagarajan JA. Epidemiological correlates of breast cancer in South India. Asian Pac J Cancer Prev. 2013; 14(9):5077-83.
5. Rockhill B, Weinberg CR, Newman B. Population attributable fraction estimation for establish, Am J Epidemiol. 1998; 147:826-33.
6. Navneet Kaur, Amit Attam, Sudipta Saha, S. K. Bhargava. Breast Cancer Risk Factor Profile in Indian Women. JIMSA. October - December 2011; 24:4.
7. Ottini L PalliDRizzoS*et al*. Male breast cancer, Crit Rev Oncol Hematol. 2010; 73:141-155.
8. Senkus S. Kyriakides S. Ohno F. Penault-Llorca P. PoortmansE. Rutgers S. Zackrisson F. Cardoso. Primary breast cancer: ESMO Clinical Practice Guidelines for diagnosis, treatment and follow-up, Annals of Oncology. 2015; 26:5:v8-v30.
9. Parise CA, Caggiano V. Breast cancer survival defined by the ER/PR/HER2 subtypes and a surrogate classification according to tumor grade and immunohistochemical biomarkers, J Cancer Epidemiol. 2014; 2014:469251.
10. Perou CM, Sorlie T, Eisen MB, van de Rijn M, Jeffrey SS, Rees CA, *et al*. Molecular portraits of human breast tumours, Nature. 2000; 406:747-52.

11. Ciruelos Gil EM. Targeting the PI3K/AKT/mTOR pathway in estrogen receptor-positive breast cancer, Cancer Treat Rev. 2014; 40:862-71.
12. Johnston SR. New strategies in estrogen receptor-positive breast cancer, Clin Cancer Res. 2010; 16:1979-87.
13. Abramson VG, Lehmann BD, Ballinger TJ, Pietenpol JA. Subtyping of triple-negative breast cancer: implications for therapy, Cancer. 2015; 121:8-16.
14. Brian D. Lehmann and Jennifer A. Pietenpol. Clinical implications of molecular heterogeneity in triple negative breast cancer, Breast. Nov 2015; 24:02:S36-S40.
15. Slamon DJ, Clark GM, Wong SG, Levin WJ, Ullrich A, McGuire WL. Human breast cancer: correlation of relapse and survival with amplification of the HER-2/neu oncogene, Science. 1987; 235:177-82.
16. MeiHua Jin, Ah-Rong Nam, Ji Eun Park, Ju-Hee Bang, Yung-Jue Bang and Do Youn Oh. Resistance Mechanism against Trastuzumab in HER2-Positive Cancer Cells and Its Negation by Src Inhibition, Molecular Cancer Therapeutics. 2016; 16:6:1145-1154.
17. Dawood S, Broglio K, Ensor J, Hortobagyi GN, Giordano SH. Survival differences among women with de novo stage IV and relapsed breast cancer, Ann Oncol. 2010; 21:2169-74.
18. Cheng YC, Ueno NT. Improvement of survival and prospect of cure in patients with metastatic breast cancer, Breast Cancer. 2012; 19:191-9.
19. Mariaelena Pierobon1, Corinne Ramos *et al*. Enrichment of PI3K-AKT–mTOR Pathway Activation in Hepatic Metastases from Breast Cancer, Clin Cancer Res. 2017; 23:16: 4919-4928.
20. Stratton MR, Campbell PJ, Futreal PA. The cancer genome, Nature. 2009; 458:7239: 719-24.
21. Liu S, Wang H, Zhang L, Tang C, Jones L, *et al*. Rapid detection of genetic mutations in individual breast cancer patients by next-generation DNA sequencing, Human Genomics. 2015; 9:1:2.
22. Forbes SA, Beare D, Boutselakis H, Bamford S, Bindal N, Tate J, *et al*. COSMIC: somatic cancer genetics at high-resolution, Nucleic acids research. 2017; 45(D1):D777-D83.
23. Nik-Zainal S, Davies H, Staaf J, Ramakrishna M, Glodzik D, Zou X, *et al*. Landscape of somatic mutations in 560 breast cancer whole-genome sequences, Nature. 2016; 534: 7605:47-54.
24. Pereira B, Chin SF, Rueda OM, Vollan HK, Provenzano E, Bardwell HA, *et al*. The somatic mutation profiles of 2,433 breast cancers refines their genomic and transcriptomic landscapes, Nature communications. 2016; 7:11479.
25. Liu P, Cheng H, Roberts TM, Zhao JJ. Targeting the phosphoinositide 3-kinase pathway in cancer, Nat Rev Drug Discov. 2009; 8:627-644.
26. Lee JW, Soung YH, Kim SY, Lee HW, Park WS, Nam SW, *et al*. PIK3CA gene is frequently mutated in breast carcinomas and hepatocellular carcinomas. Oncogene. 2004; 24:1477-80.
27. Stephens PJ, Tarpey PS, Davies H, Van Loo P, Greenman C, Wedge DC, *et al*. The landscape of cancer genes and mutational processes in breast cancer, Nature. May 2012; 486:7403:400-4.
28. Ronit Weisman, Adiel Cohen, Susan M Gasser. TORC2 - a new player in genome stability, EMBO Mol Med. Aug 2014; 6:8:995-1002.
29. Elisavet Paplomata, Ruth O'Regan. The PI3K/AKT/mTOR pathway in breast cancer: targets, trials and biomarkers, Ther Adv Med Oncol. Jul 2014; 6:4:154-166.
30. Markman B, Atzori F, Perez-Garcia J, Tabernero J, Baselga J. Status of PI3K inhibition and biomarker development in cancer therapeutics, Ann Oncol. 2010; 21:683-691.
31. Populo H, Soares P, Faustino A, Rocha AS, Silva P, Azevedo F, *et al*. mTOR pathway activation in cutaneous melanoma is associated with poorer prognosis characteristics, Pigment Cell Melanoma Res. 2011; 24: 254-257.
32. Hennessy BT, Smith DL, Ram PT, Lu Y, Mills GB. Exploiting the PI3K/AKT pathway for cancer drug discovery, Nat Rev Drug Discov. 2005; 4:988-1004.
33. Kandoth C, McLellan MD, Vandin F, Ye K, Niu B, Lu C, *et al*. Mutational landscape and significance across 12 major cancer types, Nature. 2013; 502:333-9.
34. Generali D, Venturini S, Rognoni C, Ciani O, Pusztai L, Loi S, *et al*. A network meta-analysis of everolimus plus exemestane versus chemotherapy in the first- and second-line treatment of estrogen receptor-positive metastatic breast cancer, Breast Cancer Res Treat. 2015; 152:95-0117.

35. Mukohara T. Mechanisms of resistance to anti-human epidermal growth factor receptor 2 agents in breast cancer, Cancer Sci. 2011; 102:1-8.

36. Mariaelena Pierobon1, Corinne Ramos , Shukmei Wong *et al*. Enrichment of PI3K-AKT–mTOR Pathway Activation in Hepatic Metastases from Breast Cancer, Clin Cancer Res. Aug 2017; 23:16: 4919-4928.

37. Hammond ME, Hayes DF, Dowsett M, Allred DC, Hagerty KL, Badve S, et al. American Society of Clinical Oncology/College of American Pathologists guideline recommendations for immunohistochemical testing of estrogen and progesterone receptors in breast cancer. J Clin Oncol 2010;28:2784-95.].

38. Wolff AC, Hammond ME, Hicks `DG, Dowsett M, McShane LM, Allison KH, et al. Recommendations for human epidermal growth factor receptor 2 testing in breast cancer: American Society of Clinical Oncology/College of American Pathologists clinical practice guideline update. J Clin Oncol 2013;31:3997-4013].

39. Cancer Genome Atlas N. Comprehensive molecular portraits of human breast tumours. Nature. 2012;490(7418):61±70. https://doi.org/10.1038/nature11412 PMID: 23000897

40. Kalinsky K, Jacks LM, Heguy A, Patil S, Drobnjak M, Bhanot UK, *et al*. PIK3C mutation associates with improved outcome in breast cancer, Clin Cancer Res. 2009; 15:5049-59.

41. Di Nicolantonio F, Arena S, Tabernero J, Grosso S, Molinari F, Macarulla T *et al*. Deregulation of the PI3K and KRAS signaling pathways in human cancer cells determines their response to everolimus, J Clin Invest. 2010; 120:2858-66.

42. Atkins MB, Yasothan U, Kirkpatrick P. Everolimus. Nat Rev Drug Discov. 2009; 8:535-6.

43. Baselga J, Campone M, Piccart M, Burris HA, Rugo HS, Sahmoud T, *et al*. Everolimus in postmenopausal hormone-receptor-positive advanced breast cancer. N Engl J Med. 2012; 366:520-9.

44. Lai Y-L, Mau B-L, Cheng W-H, Chen H-M, Chiu H-H, Tzen C-Y. PIK3CA exon 20 mutation is independently associated with a poor prognosis in breast cancer patients, Ann Surg Oncol. 2008; 15:1064-9.

45. Nahta R, Yu D, Hung M-C, Hortobagyi GN, Esteva FJ. Mechanisms of disease: understanding resistance to HER2-targeted therapy in human breast cancer, Nat Clin Prac Oncol. 2006; 3:269-80.

46. Adams JR, Xu K, Liu JC, Agamez NM, Loch AJ, Wong RG, et al. Cooperation between Pik3ca and p53 mutations in mouse mammary tumor formation, Cancer research. 2011; 71(7):2706-17

47. Croessmann S, Wong HY, Zabransky DJ, Chu D, Rosen DM, Cidado J, et al. PIK3CA mutations and TP53 alterations cooperate to increase cancerous phenotypes and tumor heterogeneity, Breast CancerResearch and Treatment. 2017;162(3):451-64.

International Conference on Cancer Research 2019

Website: www.CancerConf.org

June 10-11, London, UK



Tumor Heterogeneity Uncovered by HLA-G Isoforms Expression

Diana Tronik-Le Roux [ab]*, Jérôme Verine [c], Alix Jacquier [ab], Raluca Stanciu [ab], Julie Renard [ab], Chantal Schenowitz [ab], François Desgrandchamps [d], Nathalie Rouas-Freiss [ab] and Edgardo D. Carosella [ab]

[a]*CEA, DRF-Francois Jacob Institute, Research Division in Hematology and Immunology (SRHI), Saint-Louis Hospital, Paris, France*

[b]*University of Paris, IRSL, UMRS 976, Paris, France*

[c]*Service d'Anatomo-Pathologie, AP-HP, Hôpital Saint-Louis, Paris, France.*

[d]*Service d'Urologie, AP-HP, Hôpital Saint-Louis, Paris, France.*

Abstract

The heterogeneity of cancer cells introduces significant challenges in designing effective therapeutic approaches. This tremendous flexibility is maintained via the expression of multiple isoforms mainly produced by alternative splicing, in a non-uniform distribution, constituting probably one cause of treatment failure. Characterizing isoforms heterogeneity might therefore allow for a better understanding of tumorigenesis and facilitate the development of more suitable therapeutic strategies. In this study we have explored the level of tumor heterogeneity by studying HLA-G as paradigm in clear cell renal cell carcinoma (ccRCC).

HLA-G is a non-classical HLA-class I molecule whose best known role is to inhibit the cytotoxic activity of natural killer and T-cells. This molecule was first described to play a crucial role in feto-maternal tolerance. HLA-G expression is not ubiquitous, in contrast to other HLA-class I molecules. Its physiological expression is mainly restricted to extravillous cytotrophoblasts. However, under pathological conditions, HLA-G expression can be induced in almost all tissues. Particularly, HLA-G has been found in most of the tumors analyzed, such as ccRCC, the most common human renal malignancy, in which a high incidence of HLA-G was described. More recently, we have reported novel HLA-G isoforms in addition to the seven already reported that include spliced forms having an extended 5'-region and lacking the transmembrane and/or alpha1 domains. In the present study we have extended our analysis by simultaneous assessment of immunohistochemistry (IHC) labeling and RT-PCR. Combining both methods was necessary since the specificity of the different antibodies have been questioned. The study of tumors retrieved from ccRCC patients reveal that the expression of HLA-G is highly variable among tumors and distinct areas of the same tumor. In particular, we have repeatedly noticed that ccRCC samples contain eosinophilic hyaline globules exhibiting glassy appearance with a clear surrounding halo. These hyaline globules represent a well-characterized morphologic and functional entity associated with a more aggressive behavior and seem to be directly linked to autophagy defects. Interestingly, we observed that hyaline globules are associated with enhanced expression of HLA-G. Moreover, the novel isoforms were also detected in placental trophoblast cells demonstrating that they did not arise from spontaneous mutations in the process of tumor formation. The absence of alpha1 domain from one of the membrane-bound isoforms prevents its detection by immunostaining since all antibodies recognize an epitope located into the alpha1 domain common to all HLA-G isoforms. Therefore, we also report here the development of a lentivirus-vector cellular model to specifically analyze the characteristics of this particular novel isoform. Collectively, our approach extends the portrait of HLA-G isoforms expression and provides data that might facilitate the development of more-effective personalized therapies.

Keywords:

HLA-G;

Immune-checkpoints;

Isoforms;

ccRCC;

Tumor heterogeneity.

* **CONTACT**: diana.le-roux@cea.fr

Introduction

The heterogeneity of cancer cells introduces significant challenges in designing effective therapeutic approaches. Given this heterogeneity, a relevant number of patients has unsatisfactory responses or tumor recurrence following an initial clinical benefit. The expression of multiple isoforms in tumors, mainly produced by alternative splicing in a non-uniform distribution, might be in part, responsible for treatment failure. An accurate assessment of tumor heterogeneity based on the characterization of isoform diversity might therefore allow for a better understanding of tumorigenesis and facilitate the development of more effective therapeutic strategies.

Cancer immunotherapy has positively revolutionized outcomes and basic concepts of oncological treatments. Most of such breakthroughs are due to the discovery and therapeutic modulation of key immune-regulatory molecules (checkpoints) at the interface between tumor cells and immune effectors [1]. These immune-checkpoints (IC) have been broadly defined as cell-surface molecules that can transduce signals into effector cells to positively (stimulatory receptors) or negatively (inhibitory receptors) modulate signaling upon ligand binding. Tumor cells take advantage of these associations to escape destruction by the immune system. At present, antibody-based therapeutics targeting IC proved to improve prognosis and help establishing a more effective antitumor response.

Among IC, the interaction between HLA-G and its receptors, ILT2 and ILT4 (LILRB1/CD85j and LILRB2/CD85d) has lately arouses great interest [2]. HLA-G was originally described on trophoblast cells at the maternal-fetal interface where it plays a critical role in protecting fetal allograft from maternal immune rejection [3]. Its primary transcript is alternatively spliced, producing at least seven mRNAs encoding four membrane-bound (HLA-G1 to HLA-G4) and three soluble (HLA-G5 to HLA-G7). These isoforms display one, two or three extracellular domains. The soluble proteins have retained intron sequences that include stop signals that prevent the translation of the transmembrane and intracytoplasmic domains.

HLA-G has a broad immunoregulatory function that affects both innate and adaptive immunity. Via its interaction with the inhibitory receptors ILT2 and ILT4 which are differentially expressed by immune cells, HLA-G inhibits the cytolytic function of NK cells, the Ag-specific cytolytic function of cytotoxic T cells, the alloproliferative response of CD4+ T cells, and the maturation and function of dendritic cells. Unlike other IC, HLA-G is characterized by a restricted expression in normal tissues which would make HLA-G particularly pertinent as therapeutic target. Besides its limited distribution in healthy tissues, HLA-G expression can be ectopically induced under malignant transformation in tumor cells and/or in tumor-infiltrating immune cells [2].

The first demonstration of the *in vivo* role of HLA-G as a tumor escape mechanism was shown in immunocompetent mice by direct injection of cells expressing or not the full length HLA-G1 or HLA-G5 protein. We demonstrate that xenograft tumors expressing these isoforms promoted tumor progression while control tumor cells not expressing HLA-G were rejected. Of note, there was no tumor development when HLA-G was blocked by a specific antibody providing the proof of concept for new antitumor therapeutic strategy based on anti-HLA-G antibodies [4, 5].

Over the past few years, we showed heterogeneous expression of HLA-G/ILT in tumor cells and in infiltrating CD8+ and CD4+ T cells of patients with clear cell renal cell carcinoma (ccRCC) [6]. In addition to the seven known HLA-G isoforms, we also revealed the presence of yet undescribed spliced HLA-G isoforms in tumors derived from these patients. These included transcripts that have an extended 5'-region, or may lack the transmembrane and/or α1 domains (HLA-GΔα1) [7]. It is likely that HLA-G expression in tumors might have been underestimated since currently available antibodies cannot detect the HLA-GΔα1 isoform.

Therefore, to consider HLA-G as a potential target for cancer therapy, a critical issue is to characterize and quantify the degree of functional specificity or overlap exhibited by the different isoforms. To this end, we have extended our analysis of HLA-G isoforms in ccRCC lesions and carried out a systematic analysis of placenta trophoblasts to assess whether the new isoforms arise as a consequence of spontaneous mutations in the process of tumor formation. In addition, the different isoforms were expressed in two different cell lines: the RCC7 cell line which derives from a tumor of a patient with ccRCC [8] and the erythroleukemic K562 cell line, which is commonly used as target cell for NK function studies [9] in order to derived human cellular ccRCC models and conduct structure-function studies.

Marked subcellular heterogeneity of HLA-G isoforms distribution in ccRCC

To consider HLA-G as a potential target for cancer therapy, we ought to assess whether different HLA-G isoforms are expressed in tumor cells. We use as paradigm tumors derived from patients with ccRCC. All patients of this study underwent a radical nephrectomy for ccRCC as first therapeutic intervention in the urology department of Saint-Louis Hospital (Paris, France). We have analyzed different sections for each tumor with two different antibodies directed against HLA-G: 4H84, which recognizes an epitope located into the α1 domain common to all seven reported

HLA-G isoforms and the antibody 5A6G7 that only recognizes soluble HLA-G5 and HLA-G6 isoforms. This latter antibody targets the amino acids encoded by the retained intron 5 (previously known as intron 4 according to the IMGT/HLA nomenclature).

The immunostaining patterns revealed that even though all tumors expressed HLA-G in at least one area, this expression was distinct between and inside tumors. Four representative ccRCC tumors are illustrated in Figure 1. Tumors of patients 1 and 2 showed a strong immunostaining with 4H84 antibody in all regions. The staining was membranous and cytoplasmic. Noteworthy, an additional very strong staining of hyaline globules located in the cytoplasm of the tumor cells was also detected. In H&E staining, these eosinophilic hyaline globules exhibited a glassy appearance with a clear surrounding halo located in the cytoplasm of the tumor cells. The immunostaining pattern obtained with the 4H84 antibody was similar for tumors 1 and 2 whereas the profiles obtained with 5A6G7 were distinct. A moderate and fine granular intracytoplasmic stain was observed in patient 1's tumor whereas this staining was discrete in patient 2's tumor. Nevertheless, in these two cases, the hyaline globules weren't stained by this antibody. In tumor of patient 3, the expression of HLA-G evaluated by 4H84 antibody was noted in a small microscopic area of only one tumor region. Of note, this HLA-G positive area corresponded precisely to the tumor area containing intracytoplasmic hyaline globules. In addition, no stain was observed for 5A6G7 in the different regions of this tumor.

These results contrasted with the pattern observed for patient 4, which revealed a complete negative staining with antibody 4H84. The lack of labeling of tumor sections with this antibody normally accounts for the absence of HLA-G expression. However, a strong granular intracytoplasmic 5A6G7 immunostaining, particularly in hyaline globules, was observed in this patient's tumor. This was unexpected within the boundaries of our prevailing knowledge on the structure of the seven reported HLA-G isoforms since they all contain the α1 domain recognized by the 4H84 antibody.

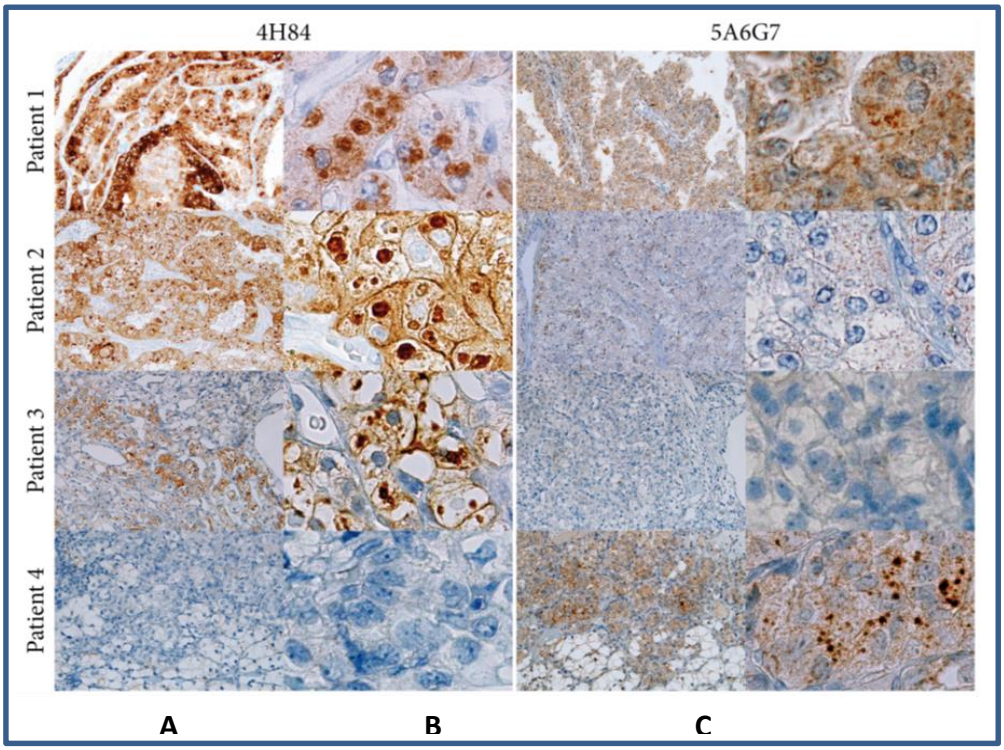


Figure 1: Representative immunohistochemistry analysis of HLA-G expression probed with mAbs 4H84 and 5A6G7. A and C are overall primary ccRCC sections. B and D, specifically show hyaline globules.

Together, the results of the immunohistochemical study clearly demonstrate intra- and inter-heterogeneity of HLA-G expression in ccRCC tumors and are consistent with the presence of several isoforms expressed in different subcellular regions of ccRCC patients' tumors.

Novel HLA-G isoforms present in trophoblasts

To assess whether the new isoforms arise from spontaneous mutations in the process of tumor formation, we have performed a systematic analysis of HLA-G isoform diversity in placenta trophoblasts by RT-PCR. We have used specific combinations of primers (Figure 2) that allow distinguish the different isoforms. All primer sequences were described previously [7].

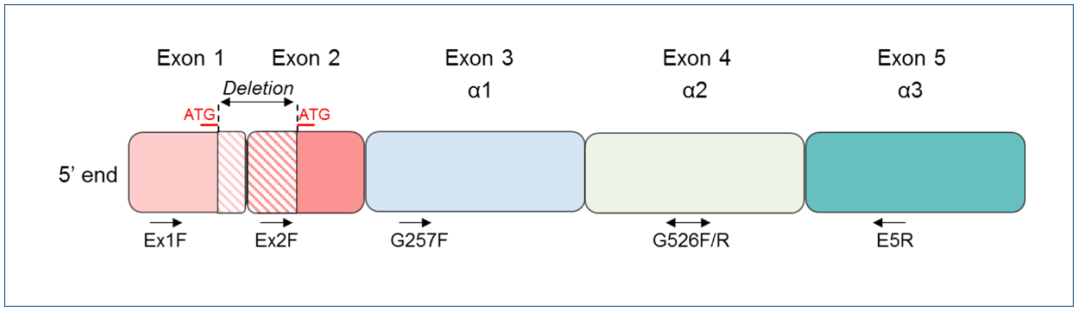


Figure 2: Localization of primers used for the different RT-PCR strategies to amplify HLA-G isoforms.

First, cDNA derived from RNA prepared from 14 throphoblasts were amplified by RT-PCR using primer Ex2F and G526R. Primer Ex2F is complementary to the region immediately upstream of the ATG located in exon 2, which was found in all reported HLA-G isoforms (Figure 2). The 3'-amplification primer G526R is located in exon 4 (the Ensembl nomenclature will be used throughout the whole text). The results of the RT-PCR reveal the presence of an amplified fragment of 560 bp in almost all trophoblasts analyzed. Trophoblasts 6 and 13, however, produce a band smaller than expected (Figure 3).

We next ought to determine whether transcripts containing the supplementary 5' exon 1 absent from the IMGT/HLA database can be detected in physiological conditions since no transcript initiated at exon 1 was previously reported. To this end, we use the primer named Ex1F, which binds a region complementary to the exon1 (schematically represented in Fig 2). If the extended 5'-region that is absent from the IMGT/HLA-G database is indeed transcribed, the amplification with Ex1F in combination with G526R will produce a band of 690bp. The results of the RT-PCR analysis have effectively revealed amplification products of 690 bp in 4 out of the 14 trophoblast samples (7, 11, 13, 14). Notably, for six other trophoblasts, we found at least three supplementary transcripts. This shows that trophoblasts might express one or different isoforms. The heterogeneity of transcripts starting in exon 1 was not reported before in trophoblasts.

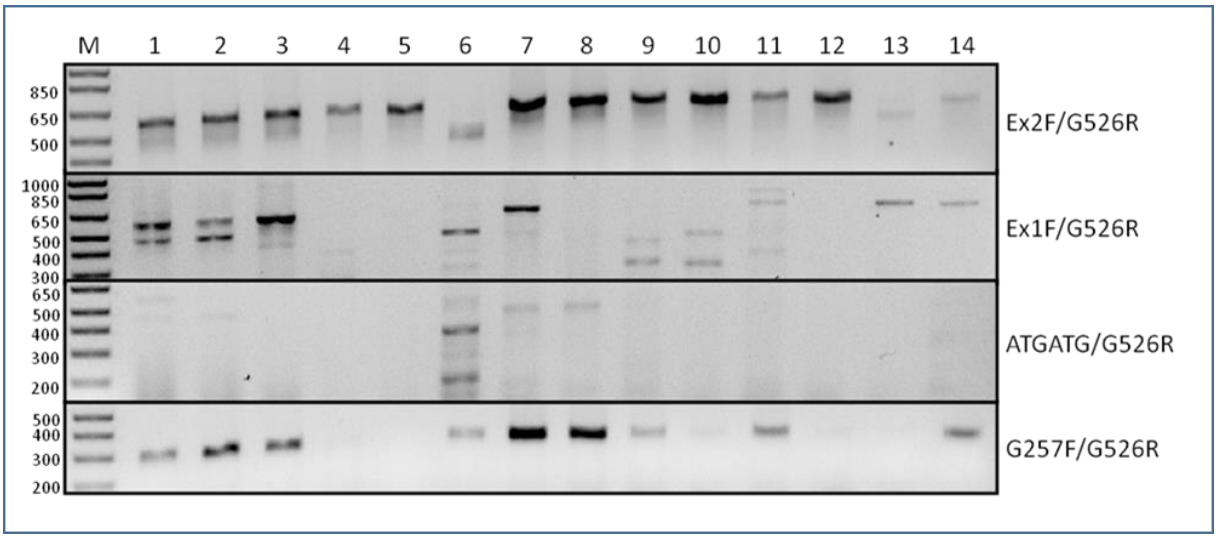


Figure 3: Expression of HLA-G isoforms in 14 placenta trophoblasts. RNA were subjected to RT-PCR using specific primers whose locations were shown in Figure 2. M: 100-bp size marker.

To assess for the presence of the novel isoform HLA-G1L that results from the deletion of a 106 bp fragment 5' of the ATG situated in exon 2, we designed a specific primer, named ATGATG, complementary to the region, surrounding the area between the two ATG, that has been deleted (Fig 2). This deletion reduces the distance between the ATG located at the end of exon1 and exon 2's ATG from 118 bp to 12 bp. Resulting from this deletion, the ATG present at the end of exon 1 becomes in frame with the ATG located in exon 2, which was previously considered as the only suitable translation initiation site. This primer located therefore at the junction of exon 1 and exon 2, when used in combination with G526R, only allows to amplify HLA-G1-L transcripts, which have deleted the 106 bp-sequence. In contrast, the Ex1F primer cannot amplify HLA-G1L since the complementary region is deleted in this isoform (Fig 2). The results of this analysis showed a 560 bp-amplification fragment (Fig 3), consistent with the presence of HLA-G1L in 4 out of 14 trophoblasts (1, 2, 7 and 8). The RT-PCR profile of trophoblast 6 suggests that other undescribed isoforms might also exist that have spliced out supplementary exons.

Finally, we amplified the cDNA from the fourteen trophoblasts with the well-known G257F and G526R primers currently used for the amplification of HLA-G1 transcripts. These primers amplify a region of 290 bp that contains the epitope recognized by the 4H84 antibody. The results of the RT-PCR amplification (Figure 3) reveal that 4 out of 14 trophoblasts (4, 5, 12 and 13) are not amplified with this couple of primers. This is consistent with the presence of an isoform that lacks the exon encoding the α1 domain.

Table 1: Summary of HLA-G isoforms expressed in placenta trophoblasts.

Trophoblastes	*1*	*2*	*3*	*4*	*5*	*6*	*7*	*8*	*9*	*10*	*11*	*12*	*13*	*14*
Ex2F/G526R	+	+	+	+	+	+	+	+	+	+	+	+	+	+
Ex1F/G526R	+	+	+	-	-	+	+	-	+	+	+	-	+	+
ATGATG/G526R	+	+	-	-	-	+	+	+	-	-	-	-	-	-
G257F/G526R	+	+	+	-	-	+	+	+	+	-	+	-	-	+

Altogether, the RT-PCR analysis, summarized in Table 1, shows that the novel HLA-G isoforms that we have previously found in tumors of patients with ccRCC are also expressed in trophoblasts. These isoforms are not mutually exclusive and may co-exist in physiological and pathological conditions. In addition, the survey of the 14 trophoblasts further indicates that several HLA-G isoforms are yet to be discovered.

Cellular models expressing different HLA-G isoforms.

To analyze the expression and function of the different isoforms we have engineered lentivirus encoding HLA-G1, HLA-G1L and HLA-GΔα1. The cDNA corresponding to the three isoforms were introduced into plasmid pWPXL (Addgene plasmid # 12257). Since HLA-GΔα1 cannot be detected with available antibodies directed against HLA-G nor other technique, we inserted in frame with the HLA-GΔα1 cDNA, the sequence encoding the peptide DYKDDDDK at the 3'end of the molecule. This peptide constitutes a tag that can be detected by a highly specific anti-tag antibody and allows tracking the protein in any cell. These plasmids were used to further obtain lentivirus specifically expressing each isoform.

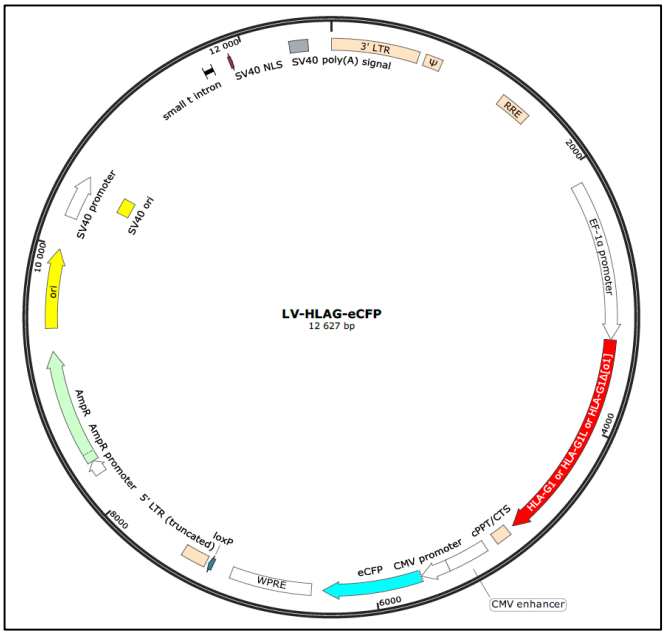


Figure 4: Schematic representation of lentivirus carrying the HLA-G isoforms

In these constructs, the expression of all HLA-G isoforms is directed by the EF-1α promoter. The constructs also include a variant of the green fluorescent protein (GFP), named "enhanced Cyan Fluorescent Protein (eCFP), which expression is under the control of the CMV promoter (Figure 4). These plasmids were used to produce lentivirus WPXL ΔU3 SIN, VSV-G envelope, at the Plateforme Vecteurs Viraux et Transfert de Gènes (VVTG), SFR Necker, US 24, UMS 3633, Paris. The lentivirus were successfully introduced in K562 and ccRCC7cell lines to generate valuable models to specifically analyze the function of individual HLA-G isoforms and obtain ccRCC cellular models expressing different HLA-G isoformes.

To verify the HLA-G expression in these cells, RNA transcripts were analyzed by RT-PCR (Figure 5). First, actin primers were used as control for RNA integrity. Then HLA-G isoforms were assessed using primers EX1-526R; G257-G526R ATGATG-526R and G526F-E5R, which specifically detect the isoforms described in the previous section.

A specific amplification was obtained with primers G257F and G526R for HLA-G1 and HLA-G1L. As expected, no amplification was detected for HLA-GΔα1 since primer G257F is located in the exon encoding the alpha 1 domain which is absent from HLA-GΔα1. As expected, the amplification with primers ATGATG/G526R reveals only the expression of HLA-G1L. Finally, amplification with primers G526F-E5R allows identifying the three isoforms. No HLA-G expression was found in wild type cells under these conditions. The same expression profiles were obtained for K562 or RCC7 cell lines.

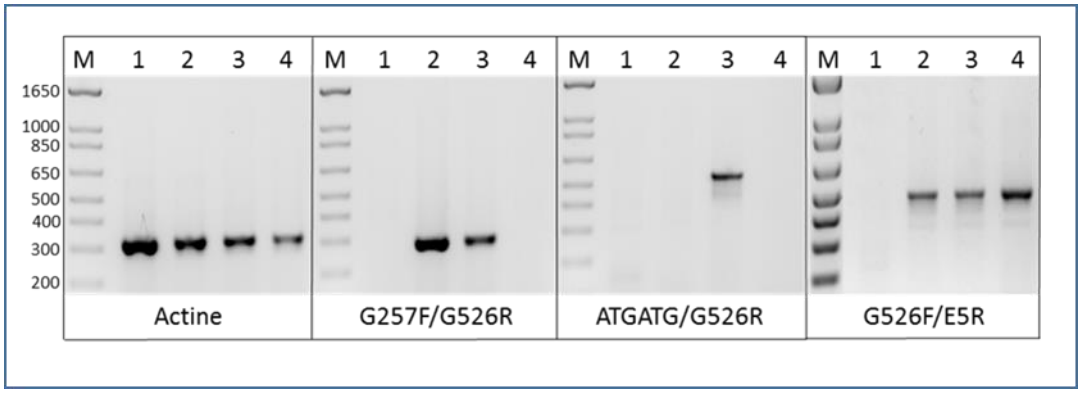


Figure 5: RT-PCR analysis of HLA-G transduced cells. Line 1:WT, line 2: HLA-G1, line 3: HLA-G1L and line 4: HLA-G Δα1. M: 100-bp size marker.

HLA-G1, HLA-G1L and HLA-GΔα1 are addressed at the cell-surface.

To determine whether the transcripts encoding the three HLA-G isoforms: HLA-G1, HLA-G1L and HLA-GΔα1 are translated into proteins, we carried out both Western blot and flow cytometry analysis of HLA-G-transduced cell lines. The corresponding wild type (WT) cell lines were used as controls. Western blot experiments were first conducted using the 4H84 mAb, which specifically detects denatured HLA-G via the α1 domain epitope. As expected we found that HLA-G1 and HLA-G1L transcripts were translated into a 39- to 40-kDa protein, in both K562 and RCC7 cell lines (Fig. 6). As predictable, the HLA-GΔα1 protein missing the α1 domain could not be detected in any cell line with 4H84 mAb (Fig. 6).

To determine whether the proteins were found at the cell surface, flow cytometry experiments were further carried out using the K562 cell line model because it does not express any HLA class I molecule in the WT form and allows to specifically analyzing individual HLA-G isoforms. The results showed that both HLA-G1 and HLA-G1L were detected at the cell surface of K562 transduced cells (Figure 7). Indeed, both HLA-G1 and HLA-G1L were stained by the MEM-G/9 antibody which recognizes a conformational epitope located in the α1 domain, dependent upon the association with the β2m.

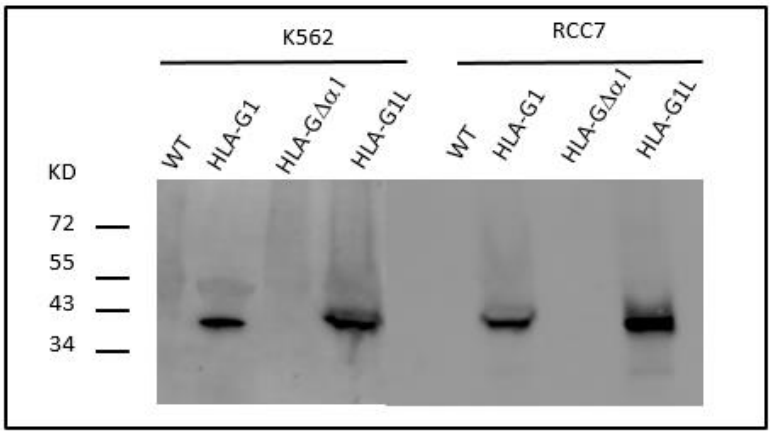


Figure 6: Western blot analysis of K562 and RCC7 cell lines

Western blot analysis of lysates from K562 and RCC7 cell lines was conducted using the 4H84 mAb under reducing conditions. Briefly, total protein aliquots from the corresponding cell line lysate were separated on SDS-PAGE gels (mini-protean TGX stain-free precast Gels, Bio-Rad). The gels were blotted onto nitrocellulose membranes (Transblot turbo transfer pack, Bio-Rad). The membranes were then probed with the 4H84 mAb (Exbio) at a 1:1000 dilution, and then with peroxidase-conjugated sheep anti-mouse IgG Ab (Sigma) at 1:10,000. Finally, the membranes were stained with enhanced chemiluminescence reagent (Amersham). Numbers at the *left* of each figure refer to *M*r in kilodaltons. One of three representative experiments is shown.

Since this, or any other commercially available anti-HLA-G antibodies (i.e., 87G, MEM-G/9, G233, 01G, 4H84) directed against the HLA-G-α1 domain, the HLA-GΔα1 protein could not be detected. Therefore, we tested a panel of anti-HLA class I antibodies kindly provided by Soldano Ferrone (Harvard Medical School, Boston, USA) to determine whether one of this could detect another domain of the HLA-G protein. We found that one antibody, TP123, was able to detect the novel HLA-GΔα1 protein transduced into the K562 cell line as well as HLA-G1 and HLA-G1L (Fig. 7A). All three proteins were detected at the cell surface. This observation constitutes the first demonstration that such truncated HLA-G isoform missing the α1 domain can be translated into protein and can reach the cell surface.

To determine whether the β2m-associated protein could also be directed to the membrane in the absence of the α1 domain, we have used the B1G6 mAb that recognizes specifically the β2microglobuline (Fig. 7A). The results show that the β2microglobuline was found at the surface of cells expressing HLA-G1 and HLA-G1L whereas this protein could not be detected at the surface of K562 cells expressing HLA-GΔα1 protein (Fig. 7A).

To further study the function of the HLA-GΔα1 protein in cells expressing other HLA class I molecules and purify those that specifically express HLAGda1, we have analyzed the eCFP fluorescence and used the antibody directed against the Tag to detect the expression of this isoform. The α-tubulin was used as positive intracellular marker. The results of the cytometric analysis reported in Figure 6B clearly show the fluorescence emitted by the eCFP and the positive stain with the tag antibody, which further demonstrates the expression of the HLA-GΔα1 /Tag protein. The results are therefore consistent with the use of this model in future strategies.

Discussion

Despite recent breakthroughs in immuno-oncology and the use of therapeutic antibodies targeting checkpoint molecules, only a portion of patients respond to these therapeutic antibodies. This was attributed in part to the heterogeneity of cancer cells, which results at least from the expression of several tumor relevant protein isoforms, mainly produced by alternative splicing in a non-uniform distribution.

Alternative splicing imparts distinct functions by allowing single genes to produce several distinct protein isoforms. These isoforms have prominent role in many biological processes [10], and may alter the function, cellular localization, and stability of the corresponding RNA or protein [11, 12] A large majority of human genes uses alternative isoforms. In some cases, the functions of two isoforms of the same protein can have opposing effects on a cellular process (cell survival versus death, anti- or pro-angiogenic, etc.). Despite the enormous body of experimental knowledge accumulated on different aspects of gene expression, there still remain many fundamental unanswered questions regarding the biology and functional significance of the different isoforms of a particular gene.

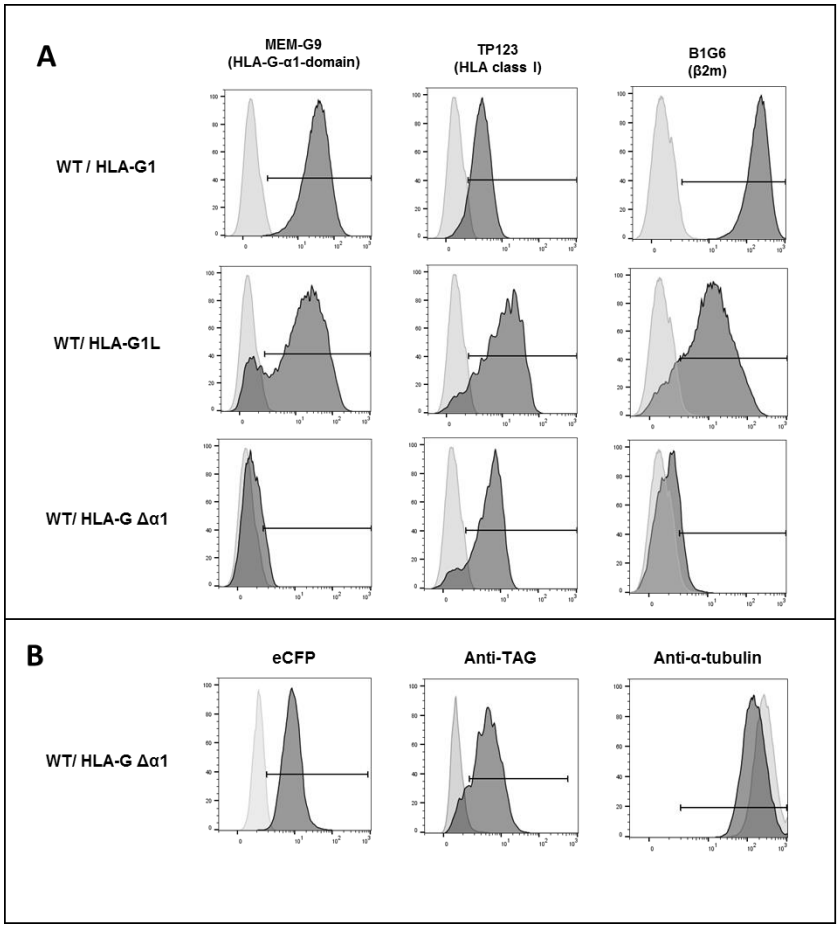


Figure 7 : Flow cytometry analysis of transduced K562 cell lines.

Panel (A) Membrane staining shows HLA-G cell surface expression level on K562 transduced cell lines (dark histogram) compared to K562 WT cell line (light histogram). The following antibodies were used: the anti-HLA-G MEM-G9-PE conjugated (Exbio) (left column), the anti-HLA class I TP123, kindly provided by S. Ferrone (USA) (middle column), the anti-β2-microglobulin B1G6 (Exbio) (right column). (B) Intracellular staining of K562 WT (lighter histogram) compared to K562 transduced by the HLA-GΔα1 lentiviral construct (dark histogram) shows the expression level of (left) the lentiviral construct through eCFP fluorescence, (middle) the HLA-GΔα1 protein using anti-TAG-APC conjugated antibody (Miltenyi Biotec) and, (right) the-α-tubulin protein (Sigma) as positive control for cell permeabilization. When the first antibody used was not conjugated to fluochrome, cells were secondly labelled with PE-conjugated $F(ab')_2$ goat anti-mouse IgG (Beckman Coulter). Only viable cells were analyzed in these experiments. Acquisition was made on a MACSQuant 10 flow cytometer (Miltenyi biotec); analysis was performed using the MACSQuantify software (Miltenyi biotec) and Flowjo software. One of three representative experiments is shown.

In this study, by combining immunohistochemistry with transcripts and proteins analysis we have provided an overview of structurally different HLA-G isoforms expressed in tumors from patients with ccRCC. Our molecular survey has not only revealed a high intra- and inter-tumor heterogeneity regarding HLA-G expression, but also highlighted distinct subcellular locations and, for the first time, we observed that hyaline globules are associated with expression of particular HLA-G isoforms. The hyaline globules represent a well-characterized morphologic and functional entity. They constitute a very uncommon aspect of tumor cells associated with aggressive behavior and seem to be directly linked to autophagy defects [13].

Autophagy, although beneficial to normal cells, helps malignant cells to adapt to an unfavorable environment, and hence, promotes tumor cell survival. This decreases the effectiveness of chemotherapy by enhancing cancer cell metabolism inhibiting thus its cell death pathway. Recent studies have shown that autophagy significantly controls immune responses by modulating the functions of immune cells and the production of cytokines. In fact, the induction of autophagy may also benefit tumor cell escape from immune surveillance and result in intrinsic resistance to immunotherapy [14]. Conversely, some cytokines and immune cells have a prominent effect on the function of autophagy. Thus, opposite properties have been reported where autophagy may attenuate or enhance the effects of immunotherapies [15].

Immunomodulatory molecules, such as indoleamine 2,3 dioxygenase(IDO), CTLA-4 and PD-1 have been involved in tumor immune tolerance through autophagy pathways. Blocking the PD-L1/PD1 axis via antibodies such as anti-PD1 or anti-PD-L1 triggers autophagy in tumor cells [16]. Therefore, understanding the synergistic interaction between autophagy and IC, in particular with each isoform of HLA-G, is important for developing tumor immunotherapy strategies.

To further understand the role of HLA-G isoforms in cancer, we asked whether the subset of alternative splicing events observed in tumors may represent independent oncogenic mutations that could be relevant to explain the functional transformations in cancer. Here, we clearly demonstrate that the different splicing events are also found in trophoblasts since similar expression patterns were obtained in both cell types. Trophoblasts, as tumor cells, can also express one or several isoforms simultaneously. The analysis of expression profiles also reveal that other isoforms are yet to be identified.

The novel HLA-G isoforms encoded mainly by transcripts initiated in exon 1, may have or not a deletion of 106 bp 5'of the ATG located in exon 2. The identification of these transcripts may result in a modification of the promoter localization, the length of the 5'-untranslated region and the transcription/translation initiation sites and therefore the regulation of the expression of HLA-G and its cellular fate. In particular, the HLA-G1L isoform might exhibit an extended N-terminal end if the translation initiation occurs at the ATG located in the first exon. The presence of five supplementary amino acids (MKTPR) may have extremely important physiological consequences. In fact it might modify the transport and targeting of the molecule to different cellular compartments of the cell, and hence, its function.

Although the HLA-G1L transcript displays an extended peptide signal, the mature processed HLA-G1L protein is expected to be similar to the HLA-G1 isoform, constituted by three extracellular domains α1, α2, α3, a transmembrane part and a short cytoplasmic tail. Here we demonstrate that HLA-G1L and HLA-G1 are translated into a 39/40 KDa cell surface proteins that can be associated with the β2m. Accordingly, we may expect that this isoform, like HLA-G1, interacts with both ILT2 and ILT4 receptors and may thus affect the immune function of NK, T, B, dendritic cells, monocytes, and neutrophils, which all express one or both receptors [17]. Even though the extracellular domains of ILTs bind to the α3 domain of the HLA class I molecules, the highest affinity is for that of HLA-G [18]. Structural analysis showed that ILT4 could recognize both HLA-G/β2m associated forms and free HLA-G heavy chains, whereas ILT2 only recognized HLA-G associated with β2m. Of note, HLA-G isoforms can be presented as homo- and hetero-multimers resulting from intermolecular disulphide bonds between Cys42 or Cys147 located in the α1 or α2 domain, respectively. These multimeric forms are of particular importance since they exhibit higher affinity for the ILT receptors and thus constitute the biologically active forms [19, 20].

The HLA-GΔα1 isoform, whose transcript lacks the exon coding for the α1 domain, is a totally novel HLA-G isoform since all reported HLA-G isoforms have in common the α1 domain. Our present results demonstrate for the first time the cell-surface expression of such HLA-G lacking the α1 domain isoform. This isoform has several features which are distinct from the other HLA-G molecules. First, this isoform, although presenting the α3 domain, does not associate with the β2m. The association between β2m and the heavy chain of HLA class I molecules is dependent on the conformational structure adopted by all 3 extracellular domains. Another specific feature of this novel HLA-G isoform is related to the absence of the peptide binding groove classically exhibited by HLA class I molecules due to the assembly of both α1 and α2 domains. Accordingly, the HLA-GΔα1 isoform may not be able to present peptides to T cells. Regarding interaction with ILT receptor, the HLA-GΔα1 isoform may not be able to interact with ILT2 because of the absence of β2m-associated forms, while binding to ILT4 may be effective. Homodimers of the HLA-GΔα1 isoform may be formed through disulfide bonds engaging the Cys 147 present in the α2 domain. Thus, the Cys147- Cys147 homodimers that might be formed in the α1-deleted α2α3 molecules may affect the specificity or modulate the affinity of such HLA-G isoforms for their receptors. Recently, the group of Maenaka reported that HLA-G2, which lack the α2-domain, naturally forms a β2-microglobulin-free and non-disulfide-linked homodimer having an overall structure that resembles that of the HLA class II heterodimer [21].

Based on these particularities, whether the HLA-GΔα1 isoform exhibits specific functions and interacts with receptors distinct from those well-known for the other HLA-G isoforms, remains to be explored.

The HLA-GΔα1 isoform cannot be recognized by the currently available HLA-G antibodies which all target the α1 domain and/or are dependent to the association with β2m. In particular, this isoform would not be recognized by the 4H84 mAb, largely used in immunohistochemical studies of cancer lesions. Consequently, HLA-G expression in cancer patients may be underestimated and novel antibodies aimed at recognizing all HLA-G isoforms are now required. In this regard, a recent study in colorectal cancer patients showed that different structural HLA-G molecules, in particular an α1 deleted isoform, may have different clinical significance [22]. The unexpected level of complexity emerging with the discovery of these unannotated transcripts and the molecules that might encode, strengthen the idea that the use of current commercial antibodies may bias diagnostic, signifying that a large campaign to develop new antibodies is ineluctable.

In conclusion, our molecular survey revealed a layer of complexity whereby a single gene can produce distinct proteins, which in turn may have functional consequences in cancer cells. The still unrecognized transcripts that might encode novel HLA-G proteins may have far-reaching implications. Accordingly, the cellular models expressing independently each isoform, that we have produced, might help defining whether the different proteins might play specific or overlapping functional roles in physiological and pathological conditions. Uncovering isoforms that are expressed in tumor cells might assuredly open new perspectives in the cancer research field, in particular, for use in diagnosis and therapeutic strategy design.

References

[1] Marin-Acevedo JA, Dholaria B, Soyano AE, Knutson KL, Chumsri S, Lou Y. (2018). Next generation of immune checkpoint therapy in cancer: new developments and challenges. J Hematol Oncol, 11(1):39.

[2] Carosella ED, Ploussard G, LeMaoult J, Desgrandchamps F. (2015). A Systematic Review of Immunotherapy in Urologic Cancer: Evolving Roles for Targeting of CTLA-4, PD-1/PD-L1, and HLA-G. European urology 2015, 68(2):267-279.

[3] Rouas-Freiss N, Goncalves RM, Menier C, Dausset J, Carosella ED. (1997). Direct evidence to support the role of HLA-G in protecting the fetus from maternal uterine natural killer cytolysis. Proceedings of the National Academy of Sciences of the United States of America 1997, 94(21):11520-11525.

[4] Agaugue S, Carosella ED, Rouas-Freiss N. (2011). Role of HLA-G in tumor escape through expansion of myeloid-derived suppressor cells and cytokinic balance in favor of Th2 versus Th1/Th17. Blood, 117(26):7021-7031.

[5] Loumagne L, Baudhuin J, Favier B, Montespan F, Carosella ED, Rouas-Freiss N. (2014). In vivo evidence that secretion of HLA-G by immunogenic tumor cells allows their evasion from immunosurveillance. International journal of cancer Journal international du cancer 2014, 135(9):2107-2117.

[6] Rouas-Freiss N, LeMaoult J, Verine J, Tronik-Le Roux D, Culine S, Hennequin C, Desgrandchamps F, Carosella ED. (2017). Intratumor heterogeneity of immune checkpoints in primary renal cell cancer: Focus on HLA-G/ILT2/ILT4. Oncoimmunology, 6(9):e1342023.

[7] Tronik-Le Roux D, Renard J, Verine J, Renault V, Tubacher E, LeMaoult J, Rouas-Freiss N, Deleuze JF, Desgrandschamps F, Carosella ED. (2017). Novel landscape of HLA-G isoforms expressed in clear cell renal cell carcinoma patients. Molecular oncology, 11(11):1561-1578.

[8] Wittnebel S, Jalil A, Thiery J, DaRocha S, Viey E, Escudier B, Chouaib S, Caignard A. (2005). The sensitivity of renal cell carcinoma cells to interferon alpha correlates with p53-induction and involves Bax. European cytokine network, 16(2):123-127.

[9] Rouas-Freiss N, Marchal RE, Kirszenbaum M, Dausset J, Carosella ED. (1997). The alpha1 domain of HLA-G1 and HLA-G2 inhibits cytotoxicity induced by natural killer cells: is HLA-G the public ligand for natural killer cell inhibitory receptors? Proceedings of the National Academy of Sciences of the United States of America, 94(10):5249-5254.

[10] Vitting-Seerup K, Sandelin A. (2017). The Landscape of Isoform Switches in Human Cancers. Molecular cancer research : MCR, 15(9):1206-1220.

[11] Wang ET, Sandberg R, Luo S, Khrebtukova I, Zhang L, Mayr C, Kingsmore SF, Schroth GP, Burge CB. (2008). Alternative isoform regulation in human tissue transcriptomes. Nature, 456(7221):470-476.

[12] Davuluri RV, Suzuki Y, Sugano S, Plass C, Huang TH: The functional consequences of alternative promoter use in mammalian genomes. Trends in genetics : TIG 2008, 24(4):167-177.

[13] Krishnan B, Truong LD: Renal epithelial neoplasms: the diagnostic implications of electron microscopic study in 55 cases. Human pathology 2002, 33(1):68-79.

[14] Degenhardt K, Mathew R, Beaudoin B, Bray K, Anderson D, Chen G, Mukherjee C, Shi Y, Gelinas C, Fan Y et al: Autophagy promotes tumor cell survival and restricts necrosis, inflammation, and tumorigenesis. Cancer cell 2006, 10(1):51-64.

[15] Marinkovic M, Sprung M, Buljubasic M, Novak I. (2018). Autophagy Modulation in Cancer: Current Knowledge on Action and Therapy. Oxidative medicine and cellular longevity, 2018:8023821.

[16] Robainas M, Otano R, Bueno S, Ait-Oudhia S. (2017). Understanding the role of PD-L1/PD1 pathway blockade and autophagy in cancer therapy. OncoTargets and therapy, 10:1803-1807.

[17] Carosella ED, Rouas-Freiss N, Tronik-Le Roux D, Moreau P, LeMaoult J. (2015). HLA-G: An Immune Checkpoint Molecule. Advances in immunology, 127:33-144.

[18] Shiroishi M, Kuroki K, Rasubala L, Tsumoto K, Kumagai I, Kurimoto E, Kato K, Kohda D, Maenaka K. (2006). Structural basis for recognition of the nonclassical MHC molecule HLA-G by the leukocyte Ig-like receptor B2 (LILRB2/LIR2/ILT4/CD85d). Proceedings of the National Academy of Sciences of the United States of America, 103(44):16412-16417.

[19] Gonen-Gross T, Achdout H, Gazit R, Hanna J, Mizrahi S, Markel G, Goldman-Wohl D, Yagel S, Horejsi V, Levy O. (2003).Complexes of HLA-G protein on the cell surface are important for leukocyte Ig-like receptor-1 function. Journal of immunology, 171(3):1343-1351.

[20] Gonen-Gross T, Achdout H, Arnon TI, Gazit R, Stern N, Horejsi V, Goldman-Wohl D, Yagel S, Mandelboim O. (2005). The CD85J/leukocyte inhibitory receptor-1 distinguishes between conformed and beta 2-microglobulin-free HLA-G molecules. Journal of immunology, 175(8):4866-4874.

[21] Kuroki K, Mio K, Takahashi A, Matsubara H, Kasai Y, Manaka S, Kikkawa M, Hamada D, Sato C, Maenaka K. (2017). Cutting Edge: Class II-like Structural Features and Strong Receptor Binding of the Nonclassical HLA-G2 Isoform Homodimer. Journal of immunology, 198(9):3399-3403.

[22] Lin A, Zhang X, Zhang RL, Zhang JG, Zhou WJ, Yan WH. (2018). Clinical Significance of Potential Unidentified HLA-G Isoforms Without alpha1 Domain but Containing Intron 4 in Colorectal Cancer Patients. Frontiers in oncology, 8:361.

International Conference on Cancer Research 2019

Website: www.CancerConf.org

June 10-11, London, UK



Soy Lecithin Liposome as Potential Platform for Intravenous Delivery of Quercetin in Cancer Treatment

Diem-Huong Nguyen Tran[a], Ngoc Thuy Trang Le[a,b], Hong Thao Truong[c], Van Du Cao[c], Cuu Khoa Nguyen[a,b], Dai Hai Nguyen[a,b], Minh Thanh Vu[d*]

[a] *Institute of Applied Materials Science, Vietnam Academy of Science and Technology, Ho Chi Minh City 700000, Vietnam*

[b] *Graduate University of Science and Technology, Vietnam Academy of Science and Technology, Ha Noi 100000, Vietnam*

[c] *Faculty of Pharmacy, Lac Hong University, Buu Long Ward, Bien Hoa City, Dong Nai Province 810000, Vietnam*

[d] *Institute of Chemistry and Materials, 17 Hoang Sam, Cau Giay, Ha Noi 100000, Vietnam*

Abstract

Naturally occurring compounds having anticancer properties are considered as attractive candidates for the treatment of cancer. Quercetin (QR; 3,3′,4′,5,7- pentahydroxylflavone), one of the most important and abundant flavonoid in the human diet, recently gained much attention for its direct proapoptotic effect on various types of tumors and little to no toxicity to normal cells, which were well-documented in numerous *in vitro* and *in vivo* studies. In spite of the common presence in many edible fruits and vegetables, QR has poor oral absorption, resulting in very low bioavailability. Besides, the poor aqueous solubility, rapid body clearance, and instability in physiological environment also hinder the intravenous administration of QR. In this study, liposome formulated from eco-friendly soy lecithin (SLP) was developed and exploited for QR encapsulation, creating an aqueous intravenous delivery platform to overcome QR's limitations. QR-SLP was prepared by thin film hydration method, followed by the investigation into the influence of hydration media (deionized water, PBS pH 5.7, and PBS pH 7.4) on QR-SLP's size, polydispersity index (PDI), zeta potential, and drug encapsulation capacity. Transmission electron microscopy (TEM), dynamic light scattering (DLS), zeta potential measurement, differential scanning calorimetry (DSC), and UV-Vis spectrophotometer method were used for the characterizations. Results showed that hydration media had a strong influence on the size, PDI, and encapsulation capacity of the formulations, in which QR-SLPs hydrated with PBS pH 7.4 possess the smallest size (93.7 ± 4.9 nm) with low polydispersity and the highest drug loading efficacy (~95.18% for loading efficiency (LE) and ~8.65% for loading capacity (LC)) whereas those hydrated with PBS pH 5.7 have the largest size (303.7 ± 3.5 nm) with high PDI value and the lowest loading efficacy (~87.33% for LE and ~7.99% for LC). Moreover, all synthesized formulations were spherical in shape and had negative surface charges from -40 to -50 mV. QR was slowly released from QR-SLPs up to 24 h, showing a controlled and long-lasting release. Taken together, all of the obtained results demonstrated that QR-SLP hydrated with PBS pH 7.4 could serve as a potential platform for intravenous QR delivery, thus improving the applicability of QR in cancer treatment.

Keywords:

Quercetin, Soy Lecithin,

Liposome,

Drug Delivery System,

Cancer Treatment.

1. Introduction

Anticancer agents derived from naturally occurring plant-based compounds has gained increasing attention for cancer treatment and prevention [1]. Among various phytochemicals found in plants, Quercetin (QR) is an important and ubiquitous flavonoid in the human diet that owns antiproliferative and direct proapoptotic effect on multiple malignant tumors such as breast, ovarian, cervical, prostate, pancreas, colon, liver, and lung. It exerts anticancer properties also in the cells of osteosarcoma, melanoma, several leukemia and lymphoma [2-5]. In *in vivo* studies, the inhibitory effect of QR on carcinogen-induced tumors has been demonstrated in several animal models and considered as Phase I clinical

* **CONTACT**: vmthanh222@yahoo.com.

trial anticancer drug [2, 5]. Moreover, its little to no toxicity to normal cells with lack of adverse side effects have been proved in human [6, 7]. Hence, there is no doubt that QR could become a highly potential anticancer drug. Unfortunately, dietary consumption of QR cannot provide sufficient amount to compatible with the anticancer effectiveness since oral bioavailability of QR is only ~2% [6, 8] in spite of its common presence in many edible fruits and vegetables (i.e. apples, onions, capers, berries, lovage leaves, etc.) [6, 7]. Besides, the poor aqueous solubility, rapid body clearance, and instability in physiological environment also hinder the intravenous administration of QR [2, 6, 9]. In this case, higher dose together with increased administration frequency of QR are needed, leading to increased tendency of side effects and cost of treatment. Various strategies have been taken into consideration to overcome those limitations, including chemical modification of QR to improve its solubility. However, the drug potency could be lost [6, 10]. Therefore, utilization of drug delivery systems for QR delivery has been focused.

Liposomes – spherical vesicles comprising of at least one lipid bilayer enclosed aqueous core have been widely known as versatile carrier for drug delivery application by virtue of their biodegradability, high compatibility, ability to entrap both hydrophilic and hydrophobic agents, preferential accumulation at tumor site through enhanced permeation and retention (EPR) effect, and release the cargo in controlled manner. In addition, drug entrapped inside liposomes can be better protected from the degradation in physiological condition [11, 12]. Properties of liposomes are considerably altered with reference to lipid composition, synthetic method, and particle size and surface charge. Regarding the choice of bilayer components, the rigidity/fluidity of liposomes' lipid bilayer were strongly influenced as well. Among the choices, the use of soy lecithin (SL), which is a natural and unsaturated phospholipid obtained from soybean, for liposomes preparation not only yields much more permeable liposomes but also facilitates large-scale industrial production thanks to the reduced production costs compared to saturated phospholipids [11]. Several studies have been carried out on the benefit of using SL to prepare soy lecithin liposomes (SLPs) [11, 13, 14].

Previous study reported that in the presence of lipids, the absorption of QR is improved and the elimination of QR is also delayed. QR displayed a high affinity towards liposomes as well which was attributed to QR's planar configuration, thus facilitating the embedding of QR into organized structure of phospholipid bilayer of liposomal vesicles [15, 16]. As revealed in other studies, better entrapment of QR in lipid layers during film formation would be refer to the apparent lipophilicity of QR [17]. Furthermore, liposomes are considered as one of the most successful nano-platform as compared to other nanocarriers with many liposomal formulations that are underwent clinical trials and approved. Thus, encapsulation of QR into liposomes, specifically SLPs, would be of great interest.

Herein, liposome formulated from eco-friendly SL (SLP) was developed and exploited for QR encapsulation, creating an aqueous intravenous delivery platform to overcome QR's limitations, improving the applicability of QR in cancer treatment. QR-SLP was prepared by thin film hydration method. Notably, the influences of different hydration media at different pH (deionized water, PBS pH 5.7, and PBS pH 7.4) on QR-SLP's size, polydispersity index (PDI), zeta potential, and drug encapsulation capacity were investigated. Differential scanning calorimetry (DSC), transmission electron microscopy (TEM) image and release behavior of entrapped QR from optimized QR-SLP were characterized.

2. Materials and methods

2.1. Materials

Quercetin and cholesterol were purchased from Sigma-Aldrich (St Louis, MO, USA). Lecithin from soybean (SL) and Tween 80 (polyoxyethylene sorbitan monooleate) were obtained from Tokyo Chemistry Industry Co., Ltd. (Kita-ku, Tokyo, Japan). Cetyltrimethylammonium bromide (CTAB) was purchased from Merck (Darmstadt, Germany). Methanol and chloroform were supplied by Fisher Scientific (Houston, TX, USA). All chemicals and solvents were of highest analytical grade and used without further purification.

2.2. Preparation of QR-SLPs using different hydration media

QR-SLPs were prepared by thin film hydration method. Briefly, SL and cholesterol (molar ratio 9:1) together with 1% CTAB dissolved in chloroform was mixed with QR dissolved in methanol at room temperature (chloroform: methanol = 2:1 v/v), in which the weight ratio between lipid phase and QR is 10:1. The mixture was dried to thin film using a rotary evaporator (Buchi Rotavapor R-144, Essen, Germany) for 4 h at 45^{o}C and maintained under vacuum condition overnight to remove all traces of solvents. Next, the thin film was hydrated with different hydration media (deH_2O, PBS pH 5.7, or PBS pH 7.4) containing Tween 80 (0.5%, v/v) by stirring at 60^{o}C for 2 h, followed by the intermittent probe sonication of 30 min. Finally, the suspension was homogenized using ULTRA-TURRAX® Tube Drive (IKA, Germany) to give QR-SLPs.

2.3. Characterizations

Differential scanning calorimetry (DSC) of SLPs, QR, QR-SLP prepared with deH_2O as hydration medium (QR-SLP-1), QR-SLP prepared with PBS pH 5.7 as hydration medium (QR-SLP-2), and QR-SLP prepared with PBS pH 7.4

as hydration medium (QR-SLP-3) were measured using TGA/DSC 3^+ (Mettler Toledo, USA). Samples were heated in range of 30-400°C at a scanning rate of 5°C/min.

Hydrodynamic size, polydispersity index (PDI), and zeta potential of synthesized QR-SLPs were determined by dynamic light scattering (DLS) Zetasizer (SZ-100, Horiba, Japan). All samples were sonicated for 15 min and measured at the detection angle of 90° and the temperature of 25°C using helium-neon (He-Ne) at 633 nm as incident beam. Zeta potential of QR-SLPs was also analyzed using SZ-100. Experiment was performed in triplicate.

Transmission electron microscopy (TEM) (JEM-1400; 300 kV, JEOL, Tokyo, Japan) was utilized to illustrate the morphology of optimized batch. Sample was prepared by placing a drop of sample solution (1 mg/mL in deH_2O) onto a carbon-copper grid (300-mesh, Ted Pella, Inc., USA) and air-drying for 10 min.

2.4. Determination of QR loading capacity

The loading capacities of QR-SLP-1, QR-SLP-2, and QR-SLP-3 were determined by indirect method regarding the initial fed QR and loaded QR, which was calculated indirectly from unloaded QR. QR-SLPs suspension was transferred to centrifuge tubes and centrifuged at 1000 rpm for 10 min in refrigerated ultracentrifuge (HERMLE Z 32 HK, Germany). The drug loading capacity including loading efficiency (LE) and loading content (LC) of QR-SLPs were quantified from supernatant after centrifugation by UV-Vis spectrophotometer (Shimadzu UV-1800, USA) at a wavelength of 372 nm and calculated according to equations as follows:

$$\text{LE (\%)} = \frac{\text{weight of fed QR - weight of unloaded QR}}{\text{weight of fed QR}} \times 100 \quad (1)$$

$$\text{LC (\%)} = \frac{\text{weight of fed QR - weight of unloaded QR}}{\text{weight of SLPs and QR}} \times 100 \quad (2)$$

2.5. In vitro QR release study

Dialysis method was used to analyze the release behavior of QR from optimized batch of QR-SLPs. A dialysis bag (MWCO 6-8 kDa) filled with 1 mL of QR-SLPs was immersed into vial containing 20 mL of PBS buffer (0.01 M, pH 7.4) containing 2% Tween 80. Then, the vial was placed in an orbital shaker bath for the horizontal shaking at 50 rpm and maintained temperature of 37°C. At specific time intervals, release medium (1 mL) was collected and equally substituted with fresh media. The collected samples were filtered (pore size = 0.22 µm) before being measured in triplicate by UV- Vis spectrophotometer.

3. Results and discussion

Regarding two aromatic rings linked by oxygen-containing heterocyclic ring, QR has lipophilic nature and a tendency to be entrapped within liposomal bilayer [3]. After being encapsulated into QR-SLPs, determination of the efficiency and the content of QR that are successfully entrapped inside SLPs is needed; and these parameters are important characteristic that directly affect the therapeutic effect of delivery nano-platform. Three formulations QR-SLP-1, QR-SLP-2, and QR-SLP-3 prepared using three different hydration media at different pH including deionized water, PBS pH 5.7, and PBS pH 7.4, respectively, were investigated firstly for the QR loading capacity. As shown in Figure 1, the overall loading capacity of SLPs for QR are high, which is mainly attributed to the lipophilicity of QR that ease the entrapment of it into SLPs' lipid phase and minimize the loss of QR to external aqueous medium. QR-SLP-3 hydrated with PBS pH 7.4 possess the highest LE (95.18 ± 2.91%) and highest LC (8.65 ± 0.91%) whereas those hydrated with PBS pH 5.7 have lowest loading efficacy (87.33 ± 1.27% for LE and 7.99 ± 0.27% for LC). This difference might be explained by the effect of pH of hydration media on the phospholipid membrane of QR-SLPs. At acidic pH (PBS pH 5.7), polar head groups of phospholipid chains are protonated and gained positive charge, causing destabilization of liposomal lipid layer and thus the leakage of entrapped QR within lipid bilayer. This phenomenon was also observed in cation lipids at low pH [18]. In physiological pH of 7.4, QR remains largely ionized since QR is a weak acid with a pK_a (negative log of dissociation constant) of 6.74. Proton from ionized QR now can partly compensate for the negative charge-gained phospholipid chains, thus stabilizing liposomal membrane. As expect, QR-SLP-3 has the most effective QR entrapment, impressively high as compared to previously reported QR-loaded liposomal systems [17, 19].

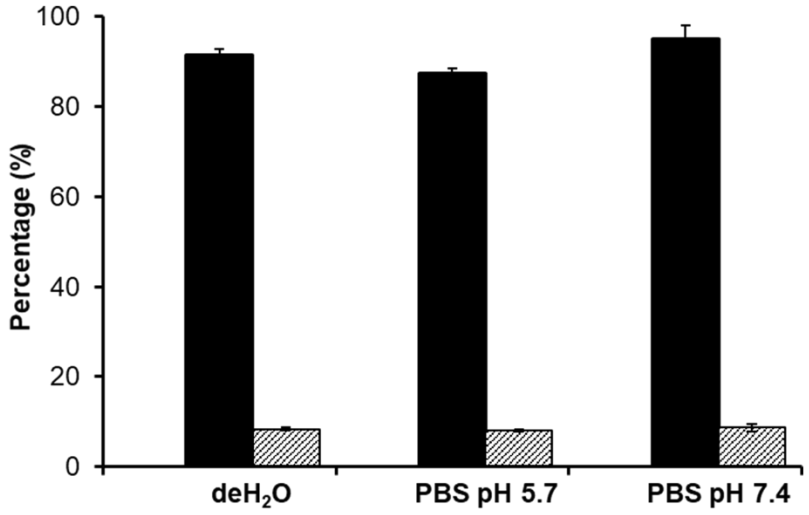


Figure 1. LE (black) and LC (diagonal) of QR-SLPs hydrated with deH_2O (QR-SLP-1), PBS pH 5.7 (QR-SLP-2), and PBS pH 7.4 (QR-SLP-3), respectively.

Others important properties that affect *in vivo* integrity and biological fate of a nano-platform are particle size and surface charge. As reported, nano-platforms with the size in range of 10-200 nm can be entrapped easily by endosome during endocytosis, thus facilitating the passive targeting and intracellular accumulation of nano-platforms within tumor cells through the EPR effect [20]. Consequently, both QR-SLP-1 (99.93 ± 3.45 nm), and QR-SLP-3 (93.70 ± 4.97 nm) have the potential to deliver QR more effectively to tumors, excepted for QR-SLP-3 with the size larger than 200 nm (Figure 2a). PDI values of them were very close to 0.4, indicating relatively homogenous nano-platforms.

The result showed that hydration media had a slight influence on the zeta potential of synthesized QR-SLPs. QR-SLP-1 hydrated with deH_2O depicted no significant change in zeta potential (~ -42 mV) in comparison with blank SLPs (-41.7 mV). Those hydrated with PBS media, especially at pH 7.4, showed drastic increased in zeta potential, which was around -50.8 mV. Negative surface charge not only averts the aggregation of nanoparticles but also prevent them from being phagocytized, improving the stability of QR-SLPs. Taken together, QR-SLP-3 with highest loading capacity as well as desirable particle size and stability might serve as optimized platform among three synthesized formulations.

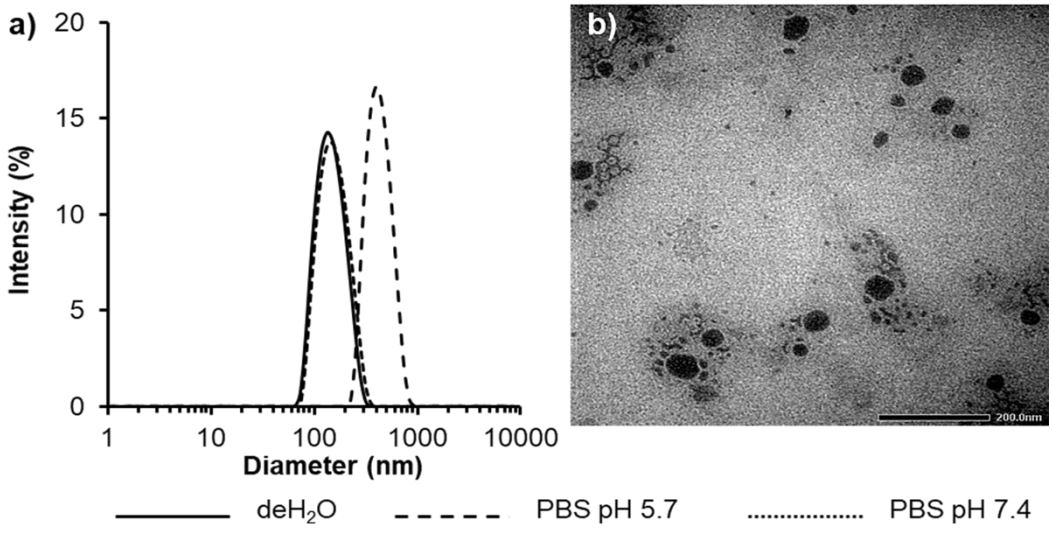


Figure 2. Particle size distribution of QR-SLP-1, QR-SLP-2, and QR-SLP-3 (a) and TEM image of QR-SLP-3 (scale bar = 200 nm) (b).

In the corresponding TEM image of QR-SLP-3 (Figure 2b), it is apparent that all particles are nearly spherical in shape and well separated. Further, DSC analysis confirmed the encapsulation of QR into SLPs (Figure 3). The complete absence of melting peak of QR at 308^{o}C implied the interaction of entrapped QR with liposomal lipid components, which is in accordance with previous results [17, 21, 22]. Moreover, an endotherm at 109^{o}C indicated the dehydration of QR as well as the evaporation of water from liposomal platform as aqueous dispersion [22].

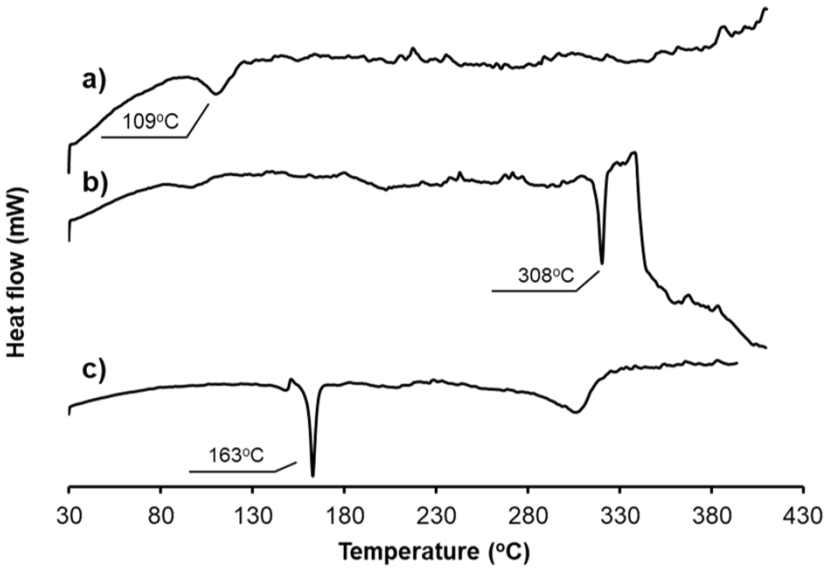


Figure 3. DSC thermograms of QR-SLP-3 (a), QR (b), and SLP (c).

Besides the ability to efficiently load the drug, efficient platform for intravenous delivery of QR should be capable of releasing them at controlled and sustained rate at the target site. As demonstrated in Figure 4, about 26.05% of QR was released in the first hour. This could be explained by the release of QR molecules that are absorbed into the outer phospholipid layer or loosely bound at lipid-water interface at the surface of SLPs. The cumulative amount of released QR increased up to 41% for the next 5 h, followed by a slower sustained release with merely 3.5% of cumulative QR detected more in the media for the last 18 h. It is clear that the entrapment of QR into SLPs platform led to sustained release manner thanks to the well-known reservoir effect of liposomes, as expected [17, 21]. This result suggest that it would be promising for utilizing SLPs to control and sustain the release rate of QR in intracellular delivery.

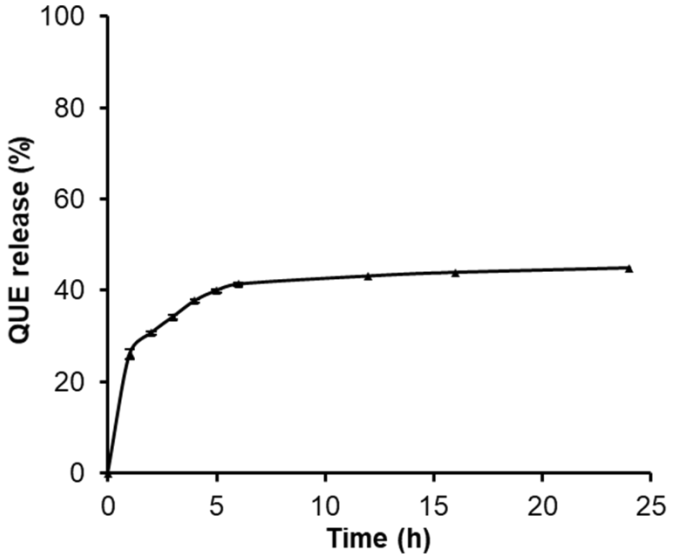


Figure 4. *In vitro* release profile of QR from QR-SLP-3.

4. Conclusion

To overcome QR's limitations, poorly soluble QR was successfully encapsulated into liposomes formulated from eco-friendly SL prepared by thin film hydration method using different hydration media at different pH values. Overall, QR-SLP-3 prepared with PBS pH 7.4 is the most promising one with the desirable size, low PdI, and good stability. More importantly, highest amount of QR (~95%) was detected in QR-SLP-3, which was impressively high as compared to previously reported QR-loaded liposomal systems. QR was released from QR-SLP-3 in a sustained manner as well. These obtained results demonstrated that QR-SLPs hydrated in PBS pH 7.4 could be a potential platform for QR delivery.

5. Conflict of Interest

The authors declare no conflict of interest.

6. Acknowledgements

This research is funded by the Vietnam National Foundation for Science and Technology Development (NAFOSTED) under grant number 104.06-2018.320.

7. References

[1] Srivastava, S., Somasagara, R.R., Hegde, M., Nishana, M., Tadi, S.K., Srivastava, M., Choudhary, B., Raghavan, S.C. (2016). Quercetin, a natural flavonoid interacts with DNA, arrests cell cycle and causes tumor regression by activating mitochondrial pathway of apoptosis. Scientific reports, 6, 24049. doi:10.1038/srep24049.

[2] Men, K., Duan, X., Wei Wei, X., Ling Gou, M., Juan Huang, M., Juan Chen, L., Yong Quian, Z., Quan Wei, Y. (2014). Nanoparticle-delivered quercetin for cancer therapy. Anti-Cancer Agents in Medicinal Chemistry (Formerly Current Medicinal Chemistry-Anti-Cancer Agents), 14(6), 826-832.

[3] Pawlikowska-Pawlęga, B., Dziubińska, H., Król, E., Trębacz, K., Jarosz-Wilkołazka, A., Paduch, R., Gawron, A., Gruszecki, W. I. (2014). Characteristics of quercetin interactions with liposomal and vacuolar membranes. Biochimica et Biophysica Acta (BBA)-Biomembranes, 1838(1), 254-265. doi:10.1016/j.bbamem.2013.08.014.

[4] Zhou, J., Fang, L., Liao, J., Li, L., Yao, W., Xiong, Z., Zhou, X. (2017). Investigation of the anti-cancer effect of quercetin on HepG2 cells in vivo. PloS one, 12(3), e0172838. doi:10.1371/journal.pone.0172838.

[5] Baby, B., Antony, P., Al Halabi, W., Al Homedi, Z., Vijayan, R. (2016). Structural insights into the polypharmacological activity of quercetin on serine/threonine kinases. Drug design, development and therapy, 10, 3109. doi:10.2147/dddt.s118423.

[6] Sak, K. (2014). Site-specific anticancer effects of dietary flavonoid quercetin. Nutrition and cancer, 66(2), 177-193. doi:10.1080/01635581.2014.864418.

[7] Hashemzaei, M., Delarami Far, A., Yari, A., Heravi, R. E., Tabrizian, K., Taghdisi, S. M., Sadegh, S. E., Trasouhas, K., Kouretas, D., Tzanakakis, G., Nikitovic, D., Anisimov, N. Y., Spandidos, D. A., Tsatsakis, A., Nikitovic, D. (2017). Anticancer and apoptosis‐inducing effects of quercetin in vitro and in vivo. Oncology reports, 38(2), 819-828. doi:10.3892/or.2017.5766.

[8] Jain, A.K., Thanki, K., Jain, S. (2013). Co-encapsulation of tamoxifen and quercetin in polymeric nanoparticles: implications on oral bioavailability, antitumor efficacy, and drug-induced toxicity. Molecular pharmaceutics, 10(9), 3459-3474. doi:10.1021/mp400311j.

[9] Tefas, L.R., Muntean, D. M., Vlase, L., Porfire, A. S., Achim, M., & Tomuță, I. (2015). Quercetin-loaded liposomes: formulation optimization through a D-optimal experimental design. Farmacia, 63(1), 26-33. doi:10.3109/21691401.2014.975238.

[10] Yuan, Z.P., Chen, L. J., Fan, L. Y., Tang, M. H., Yang, G. L., Yang, H. S., Du, X., Wang, G. Q., Yao, W. X., Zhao, Q. M., Ye, B., Wang, R., Diao, P., Zhang, W., Wu, H. B., Zhao, X., Ye, B. (2006). Liposomal quercetin efficiently suppresses growth of solid tumors in murine models. Clinical Cancer Research, 12(10), 3193-3199. doi:10.1158/1078-0432.CCR-05-2365.

[11] Nguyen, T.L., Nguyen, T. H., Nguyen, D. H. (2017). Development and in vitro evaluation of liposomes using soy lecithin to encapsulate paclitaxel. International journal of biomaterials, 2017, 1-7. doi:10.1155/2017/8234712.

[12] Nguyen, D.H., Lee, J. S., Choi, J. H., Lee, Y., Son, J. Y., Bae, J. W., Lee, K., Park, K. D. (2015). Heparin nanogel-containing liposomes for intracellular RNase delivery. Macromolecular Research, 23(8), 765-769. doi:10.1007/s13233-015-3093-2.

[13] Imran, M., Revol-Junelles, A. M., Paris, C., Guedon, E., Linder, M., Desobry, S. (2015). Liposomal nanodelivery systems using soy and marine lecithin to encapsulate food biopreservative nisin. LWT-Food Science and Technology, 62(1), 341-349. doi:10.1016/j.lwt.2014.12.046.

[14] Zawada, Z.H. (2012). Liposomes from hydrogenated soya lecithin formed in sintered glass pores. Acta Pol. Pharm, 69(1), 107-111.

[15] Lesser, S., Cermak, R., Wolffram, S. (2004). Bioavailability of quercetin in pigs is influenced by the dietary fat content. The Journal of nutrition, 6, 1508-1511. doi:doi.org/10.1093/jn/134.6.1508.

[16] van Dijk, C., Driessen, A. J., Recourt, K. (2000). The uncoupling efficiency and affinity of flavonoids for vesicles. Biochemical pharmacology, 60(11), 1593-1600. doi:10.1016/S0006-2952(00)00488-3.

[17] Shaji, J., Iyer, S. (2014). Double-loaded liposomes encapsulating Quercetin and Quercetin beta-cyclodextrin complexes:

Preparation, characterization and evaluation. Asian Journal of Pharmaceutics (AJP): Free full text articles from Asian J Pharm, 6(3), 218. doi:10.4103/0973-8398.104840.

[18] Balazs, D.A., Godbey, W. T. (2011). Liposomes for use in gene delivery. Journal of drug delivery, 2011. doi:10.1155/2011/326497.

[19] Gang, W., Jie, W. J., Ping, Z. L., Ming, D. S., Ying, L. J., Lei, W., Fang, Y. (2012). Liposomal quercetin: evaluating drug delivery in vitro and biodistribution in vivo. Expert opinion on drug delivery, 9(6), 599-613. doi:10.1517/17425247.2012.679926.

[20] Tran, D.H.N., Nguyen, T. H., Vo, T. N. N., Pham, L. P. T., Vo, D. M. H., Nguyen, C. K., Bach, L. G., Nguyen, D. H. (2019). Self‐assembled poly (ethylene glycol) methyl ether‐grafted gelatin nanogels for efficient delivery of curcumin in cancer treatment. Journal of Applied Polymer Science, 136(20), 47544. doi:10.1002/app.47544.

[21] Shaji, J.E.S.S.Y., Iyer, S. (2012). Preparation, optimization and in-vivo hepatoprotective evaluation of quercetin liposomes. Int J Curr Pharm Res, 4(2), 24-32. doi:10.3109/21691401.2014.975238.

[22] Jain, A.S., Shah, S. M., Nagarsenker, M. S., Nikam, Y., Gude, R. P., Steiniger, F., Thamm, J., Fahr, A. (2013). Lipid colloidal carriers for improvement of anticancer activity of orally delivered quercetin: formulation, characterization and establishing in vitro–in vivo advantage. Journal of biomedical nanotechnology, 9(7), 1230-1240. doi:10.1166/jbn.2013.1636.

International Conference on Cancer Research 2019

Website: www.CancerConf.org

June 10-11, London, UK



Novel BRCA1 and BRCA2 Deleterious Mutations and Unclassified Variants in Egyptian Female Breast Cancer Patients

Hala O. El-Mesallamy [a], Sherihan G. AbdelHamid [a*], Hany AbdelAziz [b], Abdel-Rahman N. Zekri [c]

[a] *Biochemistry Department, Faculty of Pharmacy, Ain Shams University, Cairo 11566, Egypt*

[b] *Clinical Oncology Department, Faculty of Medicine, Ain Shams University, Cairo 11591, Egypt*

[c] *Virology and Immunology Unit, Cancer Biology Department, National Cancer Institute, Cairo University, Giza 11796, Egypt*

Abstract

Introduction: Breast cancer is the most common malignancy among females worldwide and the leading cause of cancer death in economically developing countries. The world's oldest documented cancer case hails from Ancient Egypt 3500 years BC and the Egyptian population shows high-degree of genetic diversity due to its complex ethnic origins. The contribution of *BRCA1*/*BRCA2* mutations to the burden of breast cancer in Egypt has not been extensively evaluated. **Methods:** A series of 103 Egyptian female breast cancer patients, unselected for age of onset or family history, were included in the study. Mutational screening of exons 2 and 20 of *BRCA1* and exons 9 and 11 of *BRCA2* genes was performed using HRM analysis followed by direct sequencing of detected variants. The potential clinical effect of the novel missense mutations on protein structure and function was evaluated using *In Silico* prediction tools. **Results:** Deleterious mutations were observed in 29 (28.15%) cases. Of those, 13 (44.8%) carried *BRCA1* mutations, 13 (44.8%) carried *BRCA2* mutations and 3 (10.34%) carried both *BRCA1* and *BRCA2* mutations. Thirteen carriers (44.8%) reported positive family history of breast cancer, 14 (48.27%) had early onset and 5 cases had bilateral disease. Twenty different sequence variants were identified: 5 novel frame shift mutations; 1 in *BRCA1* (c.5205delA) and 4 in *BRCA2* (c.3641delT, c.3291dupT, c.3292delA, and c.787dupA), 1 novel nonsense mutation (*BRCA2* c.3280A>T), 2 previously described missense mutations (*BRCA1* c.117T>G and c.110C>A), 1 silent mutation (*BRCA2* c.3396A>G) and 11 unclassified variants, 8 of which were novel. Novel mutations were submitted to NCBI Clinvar database. All the observed deleterious mutations were recurrent, except *BRCA1* c.110C>A mutation which was detected once. The *BRCA1* frame shift mutation c.5205delA was observed in high frequency (16/103, 15.5%) in our cohort. Unclassified variants were identified in 32 (31%) cases, 15 of them had a co-occurring deleterious mutation. Patients with BRCA mutations tended to have early onset breast cancer compared to non-carriers (P=0.002), more often premenopausal (P=0.006), with a familial history of breast cancer as well as other cancers (P=0.005).**Conclusion:** This study provides the results of our attempt to delineate the genetic aspect of breast cancer among the Egyptian population and emphasizes the necessity of implementing screening and preventive strategies as part of the national public health policy to facilitate early diagnosis and proper counseling for breast cancer patients in Egypt.

Keywords:

BRCA1;

BRCA2;

Breast Cancer;

Egypt;

HRM;

Germline Mutations;

Unclassified Variants.

Introduction

Breast cancer is the most commonly diagnosed cancer and the leading cause of death among females worldwide [1]. The world's oldest documented cancer case hails from Ancient Egypt 3500 years BC [2], and the Egyptian population shows high-degree of genetic diversity compared to other populations due to its complex and diverse ethnic origins

* **CONTACT**: dr.sherehan@pharma.asu.edu.eg.

[3,4]. Currently, breast cancer accounts for more than 34.4% of cancer cases among Egyptian females [5] and is responsible for 29.1% of cancer deaths [6]. Although incidence rates in Egypt are lower than other populations, rates are steadily increasing and mortality rates in Egypt are worse [7]. Furthermore, the current demographic trends favor the likelihood that breast cancer will become an even greater public health concern in Egypt in the future [8]. The age at diagnosis in Egypt is one decade younger than the corresponding age in Europe and North America with exceptionally high incidence in the age group 25 to 34 years [7]. In addition, 60-80% of breast cancers in Egypt present with advanced disease at time of diagnosis [9], and family history of breast cancer, possibly related to high rate of consanguineous marriage [10]. Taken together, this evidence may imply that a high proportion of breast cancer cases in Egypt may be attributable to genetic factors.

The most well characterized genetic risk factors for breast and/or ovarian cancer to date are germline mutations of the breast-cancer susceptibility gene 1, *BRCA1* (MIM#113705) [11] and breast-cancer susceptibility gene 2, *BRCA2* (MIM#600185) [12]. Molecular analysis of *BRCA1/2* in different populations has demonstrated a very large mutational spectrum and variable mutation prevalence [13]. Identification of mutation carriers is important for early diagnosis and prevention of breast cancer as it provides the opportunity for healthy carriers to consider various risk-reducing options and intensive screening; and can also imply novel treatment strategies for affected patients such as poly (ADP-ribose) polymerase (PARP) inhibitors [14]. Unfortunately, cancer genetic services in developing countries such as Egypt are still lagging behind, due to lack of financial and practical resources, and so knowledge of the prevalence and spectrum of *BRCA1*and *BRCA2* mutations in the Egyptian population is sparse.

Mutation scanning analysis of *BRCA1/2* genes using high-resolution melting (HRM) analysis followed by direct sequence analysis is a sensitive, specific, cost- effective and reliable screening method for the identification of genetic variants while avoiding the unnecessary sequencing of wildtype genotypes, and is also capable of detecting new variants [15,16].

Few studies have addressed *BRCA1/2* mutations in the Egyptian population [17,18,19,20]. To the best of our knowledge, this is the first study on the frequency and profile of *BRCA1* and *BRCA2* mutations in a cohort of unselected Egyptian female breast cancer patients using HRM and direct sequencing on some exons of *BRCA1* and *BRCA2* genes. Our goal was to evaluate the burden of breast cancer in Egypt attributable to germline mutations in *BRCA1/2* genes using a rapid and cost-effective approach, as well as determine the profile of *BRCA1/2* mutations in this population; which can in turn guide breast cancer screening and thus help in reducing mortality and morbidity in this poor resource country. In the current study we describe novel deleterious mutations and unclassified variants (UVs) that were detected for the first time in the Egyptian population.

Methods

Recruitment of Subjects

All recruited patients provided a signed informed consent. The study protocol was approved by the Ethical Committee of Ain Shams University, Cairo, Egypt. The study was conducted in accordance with the regulations and recommendations of the Declaration of Helsinki.

A series of 103 unrelated Egyptian female breast cancer patients diagnosed with primary invasive breast cancer were recruited from the Breast Cancer Unit, Clinical Oncology Department, Ain Shams University, Cairo, Egypt. The enrolled patients were not selected on the basis of age of onset of breast cancer, family history or any other criterion that would enrich for *BRCA1/2* mutation carriers.

Eligibility criteria were female patients aged 18 years and above with histologically proven breast cancer, and the first line of treatment was surgery with curative intent followed by adjuvant therapy. Exclusion criteria were any previous history of malignancy other than breast cancer, and the evidence of distant metastases at the time of diagnosis.

All recruited patients agreed to genetic testing with the understanding that they would receive the results and would be counseled regarding the implications. The clinicopathological characteristics were extracted from hospital records.

Sample Collection and Storage

About 5 mL peripheral blood was collected from each case in blood vacutainer tubes having EDTA as anticoagulant. For storage, transportation and preservation, recommended guidelines were followed [21]. Genomic DNA was isolated from peripheral blood using QIAamp DNA Mini kit (Qiagen, Hilden, Germany), according to the manufacturer's instructions. The DNA concentration and quality for each extraction was determined by spectrophotometric measurement using Nanodrop ND2000 Spectrophotometer (Nanodrop Technologies, USA).

Mutational analysis of BRCA1 and BRCA2

The PCR and HRM were performed in a single run on Applied Biosystems 7500 Fast Real-Time PCR according to the manufacturer's instructions (Applied Biosystems, USA). The reaction mix contained 1 µl (20 ng) of genomic DNA, 5 µM of each primer and 10 µl MeltDoctor™ HRM Master Mix with PCR grade water adjusted to a total volume of 20 µl. The reaction conditions included an activation step at 95°C for 10 minutes followed by 40 cycles of 95°C for 15 seconds, a touch down of 60°C for 1 minute. Before the HRM step, the products were heated to 95°C for 10 seconds. The HRM was carried out over the range from 60°C to 95°C rising at 1°C per second with 30 acquisitions per degree. All reactions were performed in a 96-well microtiter plate. Upon completion of the run, HRM curve analysis was performed using the Applied Biosystems 7500 Software version 2.0.2 supplied with the Applied Biosystems 7500 fast.

To check and confirm the mutations detected by HRM analysis, aliquots of patients' DNA with suspected variants were subjected to PCR/direct sequencing analysis (Macrogen Lab, South Korea). Sequencing was performed using Big Dye® termination technology in both forward and reverse directions. Detected mutations and other sequence alterations are described at the cDNA level according to the *BRCA1* reference sequence (GenBank U14680) and *BRCA2* reference sequence (NM_000059.3), using the nomenclature recommendation guidelines used by Human Genome Variation Society (HGVS) (http://www.hgvs.org) using the A of the ATG translation initiation codon as nucleotide +1 [22]. Mutations are also provided using the BIC nomenclature, where the A of the ATG translation initiation codon is at position 120 of the *BRCA1* mRNA and at position 229 of the *BRCA2* mRNA, respectively. In the tables, all sequence variants are listed according to both BIC and HGVS. Potential clinical effect of UVs on protein structure and function was evaluated by analyses of the severity of the amino acid changes and their conservation across species. These analyses were performed using *In Silico* prediction analysis web tools: Alignment-Grantham variation Grantham deviation (Align GVGD; http://agvgd.iarc.fr/agvgd_input.php) [23], Polymorphism Phenotyping-2 (PolyPhen2); http://genetics.bwh.harvard.edu/pph2/) [24], and Sorting Intolerant From Tolerant (SIFT; http://blocks.fhcrc.org/sift/SIFT.html) [25] scores, and PMUT (http://mmb.irbbarcelona.org/PMut/).

Results

A total of 103 cases with invasive breast cancer were ultimately included in the study. The median age at diagnosis of breast cancer in the study cohort was 43 years (ranged from 24 to 66). Forty-three cases (41.75%) had early onset breast cancer (≤40 years). Forty-one cases (39.8%) reported a positive family history of breast cancer in first, second or third degree relative. The clinical characteristics of the study cohort are given in Table 1.

Table 1. The clinical characteristics of the study cohort.

Character	No. (%)	Median (Range)
Age at diagnosis		43 (24-66)
≤40	43 (41.75%)	
>40	60 (58.25%)	
Family history of cancer		
Breast cancer	41 (39.8%)	
Other cancers	23 (22.33%)	
No	39 (37.86%)	
Age at menarche, years		12 (10-16)
Age at first live birth, years		23 (15-33)
Parity		3 (0-8)
Hormonal contraception		
Yes	67 (65.05%)	
No	36 (34.95%)	
Onset of breast cancer		
Premenopausal	69 (67%)	
Postmenopausal	4 (33%)	

In total, 20 sequence variants were detected: 9 (45%) in *BRCA1* and 11 (55%) in *BRCA2*. The detected variants comprised 8 deleterious mutations, 11 UVs and one silent mutation. Deleterious mutations were observed in 29 (28.15%) cases. The clinicopathological characteristics of breast cancer patients carrying *BRCA1* or *BRCA2* deleterious mutations are shown in Table 2. Positive family history of breast cancer was observed in 13 mutation carriers (44.8%) and 9 patients reported family history of other cancers. Fourteen carriers had early onset breast cancer ≤40 years (48.27%) and 8 carriers were diagnosed between 41 and 50 years (27.5%). Seven patients (24.13%) had both early onset and family history of breast cancer. Bilateral breast cancer was diagnosed in 5 mutation carriers, 3 of them had early onset and

family history of cancer. Patients with *BRCA* mutations tended to have early onset breast cancer compared to non-carriers (P=0.002), more often premenopausal (P=0.006), with a familial history of breast cancer as well as other cancers (P=0.005).

Table 2. Clinicopathological characteristics of breast cancer patients carrying *BRCA1* or *BRCA2* deleterious mutations

Patient ID	Mutation	Age (years)	Laterality	Family history of cancer	Affected family members	
					Breast Cancer	Other cancers
1025	*BRCA1* c.110C>A, c.117T>G, c.5205delA	44	Unilateral	+	Sister	-
1006	*BRCA1* c.117T>G, c.5205delA	39	Unilateral	-	-	-
1002	*BRCA1* c.5205delA	53	Unilateral	+	Daughter	Son (brain)
1003	*BRCA1* c.5205delA	36	Bilateral	+	Aunt	-
1008	*BRCA1* c.5205delA	39	Unilateral	-	-	-
1011	*BRCA1* c.5205delA *BRCA2* c.3280A>T	34	Unilateral	+	Sister, 2 Aunts	-
1018	*BRCA1* c.5205delA	40	Unilateral	+	Sister	-
1024	*BRCA1* c.5205delA	43	Bilateral	-	-	-
1029	*BRCA1* c.5205delA	24	Unilateral	+	Aunt, Grandmother	Grandfather (colon)
1032	*BRCA1* c.5205delA	61	Unilateral	+	-	Mother (colon)
1033	*BRCA1* c.5205delA	41	Unilateral	+	Aunt	-
1035	*BRCA1* c.5205delA *BRCA2* c.787dupA	40	Unilateral	+	Cousin	-
1036	*BRCA1* c.5205delA	56	Unilateral	+	Sister	-
1040	*BRCA1* c.5205delA	39	Unilateral	-	-	-
1052	*BRCA1* c.5205delA *BRCA2* c.3641delT	40	Unilateral	+	Aunt, 2 cousins	-
1099	*BRCA1* c.5205delA	42	Bilateral	+	Mother, Sister, Aunt	
1023	*BRCA2* c.787dupA	40	Unilateral	-	-	-
1056	*BRCA2* c.787dupA	38	Bilateral	+	-	Mother (abdomen)
1082	*BRCA2* c.787dupA	63	Unilateral	+	-	Mother (liver)
1083	*BRCA2* c.787dupA	60	Unilateral	-	-	-
1087	*BRCA2* c.787dupA, c.3280A>T	40	Unilateral	+	-	Brother (leukemia)
1084	*BRCA2* c.3280A>T	61	Unilateral	+	-	Niece, Son (leukemia)
1085	*BRCA2* c.3280A>T	36	Bilateral	+	Mother	-
1061	*BRCA2* 3291dupA	50	Unilateral	-	-	-
1089	*BRCA2* c.3291dupA	40	Unilateral	+	Aunt, Grandmother	-
1093	*BRCA2*c.3291dupA	50	Unilateral	+	-	Uncle (colon)
1031	*BRCA2* c.3292delA	47	Unilateral	-	-	-
1034	*BRCA2* c.3292delA	35	Unilateral	-	-	-
1009	*BRCA2* c.3641delT	49	Unilateral	+	-	Son (colon)

Age, age of breast cancer diagnosis

The spectra of the deleterious mutations identified are illustrated in Table 3. They included 2 previously described missense mutations, 1 novel nonsense mutation and 5 novel frameshift mutations. The novel mutations were submitted to NCBI Clinvar database and accession numbers obtained:

NM_007294.3(*BRCA1*):c.5205delA (SCV000172260)
NM_000059.3(*BRCA2*):c.3280A>T (SCV000191885)
NM_000059.3(*BRCA2*):c.3291dupT (SCV000191886)
NM_000059.3(*BRCA2*):c.3292delA (SCV000191887)
NM_000059.3(*BRCA2*):c.3641delT (SCV000191888)
NM_000059.3(*BRCA2*):c.787dupA (SCV000191884)

Table 3. Spectrum of *BRCA1* and *BRCA2* deleterious mutations identified in the study cohort.

Gene	BIC Nomenclature	HGVS Nomenclature	Amino acid change	Type of Mutation	No. Observations	Reference
BRCA1	229C>A	c.110C>A	p.T37K	Missense	1	BIC, HGMD, LOVD
BRCA1	236T>G	c.117T>G	p.C39W	Missense	2	UMD-*BRCA1*, HGMD
BRCA1	5324delA	c.5205delA	p.(Val1736Serfs*29)	Frameshift	16	Novel
BRCA2	1014insA	c.787dupA	p.(Ser263Lysfs*13)	Frameshift	6	Novel
BRCA2	3509A>T	c.3280A>T	p.K1094*	Nonsense	4	Novel
BRCA2	3519insT	c.3291dupT	p.(Asn1098*)	Frameshift	3	Novel
BRCA2	3520delA	c.3292delA	p.(Asn1098Ilefs*6)	Frameshift	2	Novel
BRCA2	3869delT	c.3641delT	p.(Val1214Glyfs*14)	Frameshift	2	Novel

***BRCA1*/*BRCA2*, breast cancer-susceptibility genes 1 and 2, respectively; BIC, Breast Cancer Information Core Database; HGVS, Human Genome Variation Society; HGMD, Human Gene Mutation Database; LOVD, Leiden Open Variation Database; UMD, Universal Mutation Database; T, threonine; K, lysine; C, cysteine; W, tryptophan; del, deletion; ins, insertion; dup, duplication.**

These mutations were predicted to be deleterious because each generated a stop codon in the open reading frame leading to premature termination of translation at the same positions as other mutations reported to be of clinical significance in BRCA mutational databases including ClinVar [26], BRCA exchange [27], Human Gene Mutation Database (HGMD-Professional) [28], Universal Mutation Database (UMD) [29] or Leiden Open Variation Database (LOVD) [30]. The *BRCA1* frameshift mutation c.5205delA (p.Val1736Serfs*29) was observed in high frequency (15.5%) in the study group. Most of the carriers of this mutation (9 out of 16) had early onset breast cancer, and 4 patients were diagnosed between 40 and 45 years. This novel mutation occurs within the *BRCA1* C-terminal (BRCT) repeats. The clinicopathological characteristics of the patients harboring this mutation are given in Table 4.

Table 4. Clinical characteristics of Egyptian female breast cancer patients carrying the *BRCA1* mutation c.5205delA p.(Val1736Serfs*29).

Sample	Age (years)	Tumor size	Histo- pathology	Grade	Lymph node involvement	Family history of breast cancer	Family members with breast cancer	
							Number	Degree
1025	44	T2	IDC	2	-	+	1	1st
1006	39	T3	ILC	2	+	-	-	-
1002	53	T2	IDC+ILC	3	+	+	1	1st
1003	36	T2	IDC	2	+	+	1	2nd
1008	39	T3	IDC	2	-	-	-	-
1011	34	T2	IDC	2	+	+	3	1st, 2nd
1018	40	T2	IDC	2	+	+	1	1st
1024	43	T2	IDC	2	+	-	-	-
1029	24	T2	IDC	2	-	+	1	1st, 2nd
1032	61	T2	IDC	2	+	-	-	-
1033	41	T2	IDC	2	-	+	1	2nd
1035	40	T2	IDC	2	-	+	1	3rd
1036	56	T2	ILC	2	-	+	1	1st
1040	39	T3	IDC	2	+	-	-	-
1052	40	T2	IDC	2	+	+	3	2nd, 3rd
1099	42	T2	IDC	2	-	+	3	1st, 2nd

Age, age of breast cancer diagnosis; IDC, invasive ductal carcinoma; ILC, invasive lobular carcinoma.

The *BRCA1* missense mutation c.110C>A (p.T37K) was observed only once in this study and c.117T>G (p.C39W) mutation was observed in 2 patients. They both lie within 100% conserved cysteine residues of the *BRCA1* RING domain.

Five novel deleterious mutations were detected in *BRCA2* gene, 4 of them occur in the ovarian cancer cluster region spanning nucleotides 3035 to 6629. However, the precise family history of ovarian cancer was not available for the patients harboring these mutations. They comprised the nonsense mutation c.3280A>T (4 patients), the frameshift mutations c.3291dupT (3 patients), c.3292delA (2 patients), c.3641delT (2 patients), and c.787dupA (6 patients).

Of note, 3 of the 29 mutation carriers (10.34%) had deleterious mutations in both *BRCA1* and *BRCA2* genes. The first case was found to carry both *BRCA1* c.5205delA and *BRCA2* c.3280A>T mutations; the second case had both *BRCA1* c.5205delA and *BRCA2* c.3641delT mutations and the third case carried both *BRCA1* c.5205delA and *BRCA2* c.787dupA mutations. Interestingly, the 3 cases had early onset and positive family history breast cancer.

Furthermore, 11 UVs (6 in *BRCA1* 5 in *BRCA2*) were detected in 32 cases, 15 of them had a co-occurring deleterious mutation. Twelve cases (37.5%) had a family history of breast cancer. The spectrum of the UVs identified is given in Table 5. Among these UVs, 8 were novel. The functional effects of the novel UVs were predicted using the prediction analysis tools SIFT, PolyPhen-2 and PMUT (Table 6). Align-GVGD categorized 1/8 (12.5 %) as C65, 0/8 as C55, C45, C35 or C25, and 7/8 (87.5 %) as C0.

Table 5. Spectrum of *BRCA1* and *BRCA2* unclassified variants (UVs) identified in Egyptian female breast cancer patients.

Gene	BIC Nomenclature	HGVS Nomenclature	Amino acid change	Type of Mutation	No. observations	Reference
BRCA1	150G>T	c.31G>T	p.V11L	Missense	5	Novel
BRCA1	161C>A	c.42C>A	p.V14V	Silent	1	BIC
BRCA1	162A>T	c.43A>T	p.I15F	Missense	2	Novel
BRCA1	235G>T	c.116G>T	p.C39F	Missense	8	Novel
BRCA1	5387G>T	c.5268G>T	p.Q1756H	Missense	1	Novel
BRCA1	5394A>G	c.5275A>G	p.K1759E	Missense	1	Novel
BRCA2	968T>C	c.740T>C	p.I247T	Missense	1	BIC
BRCA2	967A>T	c.739A>T	p.I247F	Missense	9	Novel
BRCA2	3520 A>T	c.3292A>T	p.N1098Y	Missense	5	Novel
BRCA2	3744 G>A	c.3516G>A	p.S1172S	Silent	1	BIC
BRCA2	3868 G>T	c.3640G>T	p.V1214L	Missense	2	Novel

***BRCA1/BRCA2*, breast cancer-susceptibility genes 1 and 2, respectively; BIC, Breast Cancer Information Core Database; V, valine; L, leucine; I, isoleucine; F,phenylyalanine; C, cysteine; Q, glutamine; H, histidine; K, lysine; E, glutamic acid; T, threonine; N, asparagine; Y, tyrosine; S, serine, W, tryptophan.**

Table 6. Predicted effect of novel unclassified missense variants of *BRCA1* and *BRCA2*.

Gene	BIC	HGVS	Amino acid	GV	GD	Align-	SIFT	Polyphen2	PMUT

	nomenclature	nomenclature	Change	GVGD					
BRCA1	150G>T	c.31G>T	p.V11L	28.68	4.86	C0	0.00 (not tolerated)	0.993 (probably damaging)	Neutral
BRCA1	162A>T	c.43A>T	p.I15F	4.86	21.28	C0	0.00 (not tolerated)	0.068 (benign)	Neutral
BRCA1	235G>T	c.116G>T	p.C39F	0	204.39	C65	0.00 (not tolerated)	0.996 (probably damaging)	Pathological
BRCA1	5387G>T	c.5268G>T	p.Q1756H	152.42	0	C0	0.03 (not tolerated)	0.129 (benign)	Pathological
BRCA1	5394A>G	c.5275A>G	p.K1759E	164.69	20.36	C0	0.00 (not tolerated)	0.01 (benign)	Neutral
BRCA2	967A>T	c.739A>T	p.I247F	242.23	0	C0	0.05 (Tolerated)	0.838 (possibly damaging)	Neutral
BRCA2	3520 A>T	c.3292A>T	p.N1098Y	231.68	79.14	C0	0.1 (Tolerated)	0.868 (possibly damaging)	Pathological
BRCA2	3868 G>T	c.3640G>T	p.V1214L	172.62	12.95	C0	0.33 (Tolerated)	0.006 (benign)	Neutral

***BRCA1/BRCA2*, breast cancer-susceptibility genes 1 and 2, respectively; BIC, Breast Cancer Information Core Database; HGVS, Human Genome Variation Society; GV, Grantham Variation score; GD, Grantham Deviation score; Align-GVGD, Align Grantham Variation Grantham Deviation; SIFT, Sorting Intolerant from Tolerant; PolyPhen; Polymorphism Phenotyping; V, valine; L, leucine; I, isoleucine; F, phenylyalanine; C, cysteine; Q, glutamine; H, histidine; K, lysine; E, glutamic acid; N, asparagine; Y, tyrosine.**

The *BRCA1* c.116G>T (p.C39F) mutation which was shown to be deleterious according to SIFT, Polyphen and PMUT and is placed in class C65 in Align-GVGD, was observed in 8 cases in our study cohort. It lies within the RING domain of *BRCA1* protein. Additionally, *BRCA1* c.5268G>T (p.Q1756H) and c.5275A>G (p.K1759E) mutations occurring within *BRCA1* BRCT repeats were predicted to be deleterious according to SIFT. Both mutations were identified only once in the same patient with early onset breast cancer. Noteworthy, this case was found to harbor the deleterious mutation *BRCA2* c.787dupA.

Discussion

The Egyptian population has many unique genetic features developed during its evolution history [3]. Breast cancer patients in Egypt have not been extensively studied for *BRCA1/2* mutations; knowledge of which can lead to better understanding of genetic risk factors of this disease. In the present study, we have determined the spectrum and frequency of *BRCA1/2* mutations in a cohort derived from hospital-based Egyptian female breast cancer population not selected on the basis of age of onset or family history, aiming to elucidate the contribution of mutations in these genes to the burden of breast cancer in Egypt. We have performed HRM analysis and direct sequencing of exons 2 and 20 of *BRCA1* gene and exons 9 and 11 of *BRCA2* gene. These exons contain frequently recurring mutations described worldwide, but the type of mutations identified can differ considerably in different populations.

In this study, *BRCA1* and *BRCA2* deleterious mutations were identified in 29 patients representing a prevalence of 28.15%. The frequency of *BRCA1/2* mutations display considerable variation among populations that coincides with ethnic and geographical diversity [13]. A high prevalence of 28% has been reported in the Levant region [31]. The Moroccan, Tunisian and Algerian populations have reported frequencies of 25.64%, 19.4% and 20%, respectively [32,33,34].

Our data are in line with prior studies in the Egyptian population that reported high mutation rate, supporting enrichment for genetic risk factors among Egyptian breast cancer patients. Ibrahim *et al* [17] have detected *BRCA1/2* mutations in 86% among 60 breast cancer patients and 120 cases of their asymptomatic female first degree relatives. The study reported five mutations, previously described in other populations, 2 in *BRCA1* (5454delC, 185delAG) and 3 in *BRCA2* (999del5, 4446C--T and 738C--A) using the combination of SSCP and heteroduplex analysis. A similar rate was detected by Fattoh *et al* [18]. El-Debaky *et al* [19] identified *BRCA1* mutations in 73.35% of breast cancer patients with family history (15 patients), 68.35% of breast cancer patients without family history (15 patients) and 55% of healthy controls (20 cases). They used primers for detection of 185delAG, 5382insC and C61G mutations using multiplex mutagenically separated PCR and RFLP. On the other hand, Saied *et al* [20] found a carrier frequency of 2.5% for heterozygous mutation of *BRCA1* AG185del using pyrosequencing technique.

In the current study, the spectrum of mutations identified differs from that previously reported in the Egyptian population. The aforementioned studies used primers designed for detection of specific mutations. In contrast, HRM analysis in our study allowed the detection of any sequence variations which were then confirmed and checked for by sequencing, allowing the detection of novel mutations as well as UVs. Taken together, these findings underline the importance of the development of Egyptian breast cancer mutational database.

Our findings show that all mutation carriers had either early onset, family history of breast cancer or bilateral disease; which are all suggestive of genetic predisposition. Thirteen mutation carriers reported positive family history of breast cancer, representing 31.7% of all familial cases. This is in agreement to that reported in Moroccan, Algerian and Tunisian hereditary breast cancer patients [33,35,36]. Fourteen mutation carriers had early onset breast cancer, providing a frequency of 32.5% of all early onset cases, which is similar to that detected in Ashkenazi Jews (30- 35%) [37,38]. Five mutation carriers had bilateral breast cancer, representing 31.2% of all cases with bilateral disease, which is consistent to that reported elsewhere [39]. This data highlights the need to use these clinical criteria for routine testing for *BRCA* genes mutations in Egyptian breast cancer patients.

Some of the mutations identified in our study were previously described in other populations. The *BRCA1* missense mutation c.110C>A (p.T37K) was detected before in the American population. The *BRCA1* missense mutation c.117T>G (p.C39W) was reported in the UMD-*BRCA1*and HGMD databases in the French population. The *BRCA2* silent mutation c.3396A>G (p.K1132K), observed in 2.9% of the studied cases, was cited in BIC database (232 reports), LOVD database and UMD database (6 reports) where it is described as polymorphism.

An important finding in our study is the detection of 6 novel deleterious mutations, and all of them were recurrent. The *BRCA1* frameshift mutation c.5205delA was observed in 15.5% of the study cohort, mainly in cases with early onset and positive family history of breast cancer. Interestingly, 3 patients had double mutations in both *BRCA1* and *BRCA2* genes, which is a rare condition in most populations. The 3 patients of them had early onset and positive family history of breast cancer. Frank *et al* [40] found 10 patients with both mutations in *BRCA1* and *BRCA2* out of 10,000 patients. On the other hand a higher frequency was observed by Choi *et al* [41], who detected 2 patients out of 9 carriers in a sample size of 60 young Korean breast cancer females.

To our knowledge, this report is the first to include information on the prevalence of missense mutations of unknown significance in the Egyptian population. About one-third of the genetic variants in *BRCA1* and 50% of those found in *BRCA2* reported by the BIC are considered genetic variants of unknown clinical significance, because of the uncertainty about their cancer risks [42]. We identified 11 different *BRCA1* and *BRCA2* UVs, 8 of them are novel. They may have a functional role in breast cancer development, which deserves further elucidation.

A major strength of the current study was the detection of novel deleterious mutations and UVs, which may imply that the Egyptian population has genetic peculiarity. Screening for these mutations in extended breast cancer families could help in the identification of specific effect. Further studies on larger sample size are warranted to better elucidate the role of *BRCA1/2* in breast cancer in Egypt. Studying the association of *BRCA1/2* mutational status and clinicopathological characteristics as well as its impact on clinical outcome is ongoing in another study.

Conclusions

This study provides the results of our attempt to delineate the genetic aspect of breast cancer among the Egyptian population. For the first time, we used HRM and direct sequencing to identify *BRCA1/2* mutations in Egyptian patients, providing a rapid, reliable and cost-effective approach for *BRCA* mutation detection in this resource constraint country. The accumulating evidence from this study and previous studies about the profile and frequency of *BRCA1/2* mutations in the Egyptian population emphasize the necessity of implementing screening and preventive strategies as part of the national public health policy in Egypt to facilitate early diagnosis and proper counseling for breast cancer patients.

List of Abbreviations

BRCA1: breast cancer susceptibility gene 1; *BRCA2*: breast cancer susceptibility gene 2; HRM: High-resolution melting; UVs: Unclassified variants; BIC: Breast Cancer Information Core Database; HGMD-Professional: Human Gene Mutation Database; UMD: Universal Mutation Database; LOVD: Leiden Open Variation Database; HGVS: Human Genome Variation Society; Align GVGD: Alignment-Grantham variation Grantham deviation; PolyPhen2: Polymorphism Phenotyping-2; SIFT: Sorting Intolerant From Tolerant; IARC: International Agency for Research on Cancer; BRCT: *BRCA1* C-terminal.

Competing interests

The authors declare that they have no competing interests.

Authors' contributions

HOE: Participated in study design, participated in analysis of clinical data and helped in the revision of the manuscript. SGA: Participated in study design, performed mutational analyses, analyzed clinical data and drafted the manuscript. HAA: Participated in the study design, revised clinical and pathological data and helped in the revision of the manuscript. ANZ: Participated in the study design, participated in sequence alignment and the analysis of the mutational data and revised the manuscript. All authors read and approved the final manuscript.

Acknowledgements

We would like to thank Dr. Ahmed Mahmoud and Dr. Mostafa El-berry at the National Cancer Institute, Egypt, for technical assistance with HRM.

References:

1. Bray F, Ferlay J, Soerjomataram I, Siegel RL, Torre LA, Jemal A (2018). Global cancer statistics 2018: GLOBOCAN estimates of incidence and mortality worldwide for 36 cancers in 185 countries. CA: A Cancer Journal for Clinicians, 68: 394- 424. doi: 10.3322/caac.21492.
2. Donegan W (2002). History of breast cancer. In: Donegan W, Spratt J, eds. Cancer of the Breast. Philadelphia, PA: WB Saunders; c2002.
3. Pagani L, Schiffels S, Gurdasani D, Danecek P, Scally A, Chen Y, Xue Y, Haber M, Ekong R, Oljira T, Mekonnen E, Luiselli D, Bradman N, Bekele E, Zalloua P, Durbin R, Kivisild T, Tyler-Smith C (2015). Tracing the route of modern humans out of Africa by using 225 human genome sequences from Ethiopians and Egyptians. Am J Hum Genet., 96:986-991. doi: 10.1016/j.ajhg.2015.04.019.
4. Kim YC, Soliman AS, Cui J, Ramadan M, Hablas A, Abouelhoda M, Hussien N, Ahmed O, Zekri, AN, Seifeldin IA, Wang SM (2017). Unique Features of Germline Variation in Five Egyptian Familial Breast Cancer Families Revealed by Exome Sequencing. PLoS ONE, 12: e0167581. https://doi.org/10.1371/journal.pone.0167581
5. Ibrahim AS, Khaled HM, Mikhail NN, Baraka H, Kamel H (2014). Cancer Incidence in Egypt: Results of the National Population-Based Cancer Registry Program. Journal of Cancer Epidemiology, 18. http://dx.doi.org/10.1155/2014/437971
6. Ismail GM, Abd El Hamid A, Abd ElNaby AG (2013). Assessment of Factors that Hinder Early Detection of Breast Cancer among Females at Cairo University Hospital. World Applied Sciences Journal, 23: 99-108. DOI: 10.5829/idosi.wasj.2013.23.01.73124
7. Rennert G (2006). Breast cancer. In: Cancer Incidence in Four Member Countries (Cyprus, Egypt, Israel, and Jordan) of the Middle East Cancer Consortium (MECC) Compared with US SEER. NIH Publication: 06- 5873, chapter 8, National Cancer Institute, Bethesda, Md, USA. http://seer.cancer.gov
8. Hirko KA, Soliman AS, Hablas A, Seifeldin IA, Ramadan M, Banerjee M, Harford J, Robert M. Chamberlain RM, and Merajver SD (2013). Trends in Breast Cancer Incidence Rates by Age and Stage at Diagnosis in Gharbiah, Egypt, over 10 Years (1999–2008). Journal of Cancer Epidemiology, 7. https://doi.org/10.1155/2013/916394.
9. Dey S, Soliman AS, Hablas A, Seifeldein IA, Ismail K, Ramadan M, El-Hamzawy H, Wilson ML, Banerjee M, Boffetta P, Harford J, Merajver SD (2010). Urban-rural differences in breast cancer incidence in Egypt (1999-2006). Breast, 19(5):417-23. doi: 10.1016/j.breast.2010.04.005.
10. Bedwani R, Abdel-Fattah M, El-Shazly M, Bassili A, Zaki A, Seif HA, Weber W (2001). Profile of familial breast cancer in Alexandria, Egypt. Anticancer Res, 21(4B): 3011–3014.
11. Miki Y, Swensen J, Shattuck-Eidens D, Futreal PA, Harshman K, Tavtigian S, et al (1994). A strong candidate for the breast and ovarian cancer susceptibility gene BRCA1. Science, 266(5182):66–71. doi:10.1126/science.7545954.
12. Wooster R, Bignell G, Lancaster J, Swift S, Seal S, Mangion J, Collins N, Gregory S, Gumbs C, Micklem G (1996). Identification of the breast cancer susceptibility gene BRCA2. Nature, 378(6559):789-92. doi: 10.1038/378789a0
13. Fackenthal J, Olopade O (2007). Breast cancer risk associated with BRCA1 and BRCA2 in diverse populations. Nature Reviews Cancer, 7: 937-948. doi:10.1038/nrc2054
14. Salhab M, Bismohun S, Mokbel K. (2010). Risk-reducing strategies for women carrying BRCA1/2 mutations with a focus on prophylactic surgery. BMC Womens Health, 20;10:28. doi: 10.1186/1472-6874-10-28.

15. Hondow HL, Fox SB, Mitchell G, Scott RJ, Beshay V, Wong SQ; kConFab Investigators, Dobrovic A (2011). A high-throughput protocol for mutation scanning of the BRCA1 and BRCA2 genes. BMC Cancer, 24;11:265. doi: 10.1186/1471-2407-11-265.

16. van der Stoep N, van Paridon CD, Janssens T, Krenkova, P, Stambergova A, Macek M, Matthijs G, and Bakker E. (2009). Diagnostic guidelines for high-resolution melting curve (HRM) analysis: An interlaboratory validation of BRCA1 mutation scanning using the 96-well LightScanner™. Hum. Mutat., 30: 899-909. doi:10.1002/humu.21004.

17. Ibrahim SS, Hafez EE, Hashishe MM (2010). Pre-symptomatic breast cancer in Egypt: role of BRCA1 and BRCA2 tumor suppressor genes mutations detection. J Exp Clin Cancer Res, 29(1):82. doi: 10.1186/1756-9966-29-82.

18. Fattouh M, Ahmed H, Hafez Eel S (2011). Detection of BRCA1 and BRCA2 gene mutation in Egyptian females with breast cancer and their relatives by PCR- SSCP method. Egypt J Immunol, 18: 9-16. PMID:23082475

19. El-Debaky F, Azab N, Alhusseini N, Eliwa S, Musalam R (2011). Breast cancer gene 1 (Brca 1) mutation in female patients with or without family history in Qalubia Governorate. Journal of American Science, 7(2):82–93. ISSN: 1545-1003.

20. Saied MH, El Boraie S, Elfayoumy T, El Guizery D (2017). Detection of BRCA1 Founder Mutation 185DELAG in Breast Cancer Patients using Pyrosequencing Technique. Breast Can Curr Res, 2:117. doi:10.4172/2572-4118.1000117

21. Anderson D, Yu T-W, Dobrzyńska MM, Ribas G, Marcos R (1997). Effects in the comet assay of storage conditions on human blood. Teratog Carcinogens Mutagen., 17(3):115-25. doi:10.1002.

22. Dunnen JT, Antonarakis SE (2000). Mutation nomenclature extensions and suggestions to describe complex mutations: a discussion. Human Mutat., 15(1):7-12. doi: 10.1002/(SICI)1098-1004(200001)15:1<7:AID-HUMU4>3.0.CO;2-N

23. Tavtigian SV, Deffenbaugh AM, Yin L, Judkins T, Scholl T, Samollow PB, de Silva D, Zharkikh A, Thomas A (2006). Comprehensive statistical study of 452 BRCA1 missense substitutions with classification of eight recurrent substitutions as neutral. J Med Genet., 43(4):295-305. doi:10.1136/jmg.2005.033878

24. Ramensky V, Bork P, Sunyaev S (2002). Human non-synonymous SNPs: server and survey. Nucleic Acids Res., 30(17):3894-900. doi: 10.1093/nar/gkf493

25. Ng PC, Henikoff S (2003). SIFT: Predicting amino acid changes that affect protein function. Nucleic Acids Res., 31(13):3812-4. doi: 10.1093/nar/gkg509.

26. NCBI Clinvar. Available from URL: https://www.ncbi.nlm.nih.gov/clinvar/ [accessed 15.1. 2019].

27. The BRCA Exchange. Available from URL: https://brcaexchange.org [accessed 15.1 2019].

28. Human Gene Mutation Database (HGMD). Available from URL: www.hgmd.org [accessed 15.1.2019].

29. Universal Mutation Database (UMD). Available from URL: www.umd.be [accessed 15.1.2019].

30. Leiden Open Variation Database (LOVD). Available from URL: www.lovd.nl [accessed 11.12.2019

31. Abdulrashid K, AlHussaini N, Ahmed W, Thalib L (2019). Prevalence of BRCA mutations among hereditary breast and/or ovarian cancer patients in Arab countries: systematic review and meta-analysis. BMC Cancer, 21;19(1):256. doi: 10.1186/s12885-019-5463-1.

32. Tazzite A, Jouhadi H, Nadifi S, Aretini P, Falaschi E, Collavoli A, Benider A, Caligo MA (2012). BRCA1and BRCA2 germline mutations in Moroccan breast/ovarian cancer families: Novel mutations and unclassified variants. Gynecol Oncol., 125(3):687-92. doi: 10.1016/j.ygyno.2012.03.007.

33. Troudi W, Uhrhammer N, Sibille C, Dahan C, Mahfoudh W, Bouchlaka Souissi C, Jalabert T, Chouchane L, Bignon YJ, Ben Ayed F, Ben Ammar Elgaaied A (2007). Contribution of the BRCA1 and BRCA2 mutations to breast cancer in Tunisia. J Hum Genet., 52(11):915-20. DOI:10.1007/s10038-007-0195-5

34. Henouda S, Bensalem A, Reggad R, Serrar N, Rouabah L, Pujol P (2016). Contribution of BRCA1 and BRCA2 Germline Mutations to Early Algerian Breast Cancer. Dis Markers, 7869095.doi: 10.1155/2016/7869095.

35. Laraqui A, Uhrhammer N, Lahlou-Amine I, El Rhaffouli H, El Baghdadi J, Dehayni M, Moussaoui RD, Ichou M, Sbitti Y, Al Bouzidi A, Amzazi S, Bignon YJ (2013). Mutation screening of the BRCA1 gene in early onset and familial breast/ovarian cancer in Moroccan population. Int J Med Sci., 10 (1):60-7. doi: 10.7150/ijms.5014.

36. Uhrhammer N, Abdelouahab A, Lafarge L, Feillel V, Ben Dib A, Bignon YJ (2008). BRCA1 mutations in Algerian breast cancer patients: high frequency in young, sporadic cases. Int J Med Sci., 8;5(4):197-202. PMID: 18645608

37. Gershoni-Baruch R, Dagan E, Fried G, Bruchim Bar-Sade R, Sverdlov-Shiri R, Zelicksson G, Friedman E (2000). Significantly lower rates of BRCA1/BRCA2 founder mutations in Ashkenazi women with sporadic compared with familial early onset breast cancer. Eur J Cancer., 36(8):983-6. doi: https://doi.org/10.1016/S0959-8049(00)00045-9

38. Hodgson SV, Heap E, Cameron J, Ellis D, Mathew CG, Eeles RA, Solomon E, Lewis CM (1999). Risk factors for detecting germline BRCA1 and BRCA2 founder mutations in Ashkenazi Jewish women with breast or ovarian cancer. J Med Genet., 36(5):369-73. http://dx.doi.org/10.1136/jmg.36.5.369

39. Rogozińska-Szczepka J, Utracka-Hutka B, Grzybowska E, Mąka B, Nowicka E, Smok-Ragankiewicz A, Zientek H, Steffen J, Wojciechowska-Łącka A (2004). BRCA1 and BRCA2 mutations as prognostic factors in bilateral breast cancer patients. Ann Oncol., 15: 1373-1376. doi:10.1093/annonc/mdh352

40. Frank TS, Deffenbaugh AM, Reid JE, Hulick M, Ward BE, Lingenfelter B, Gumpper KL, Scholl T, Tavtigian SV, Pruss DR, Critchfield GC (2002). Clinical characteristics of individuals with germline mutations in BRCA1 and BRCA2: analysis of 10,000 individuals. J Clin Oncol., 15;20(6):1480-90. doi: 10.1200/JCO.2002.20.6.1480

41. Choi DH, Lee MH, Bale AE, Carter D, Haffty BG (2004). Incidence of BRCA1 and BRCA2 Mutations in Young Korean Breast Cancer Patients. J Clin Oncol., 1;22(9):1638-45. doi: 10.1200/JCO.2004.04.179

42. Gómez García EB, Oosterwijk JC, Timmermans M, van Asperen CJ, Hogervorst FB, Hoogerbrugge N, Oldenburg R, Verhoef S, Dommering CJ, Ausems MG, van Os TA, van der Hout AH, Ligtenberg M, van den Ouweland A, van der Luijt RB, Wijnen JT, Gille JJ, Lindsey PJ, Devilee P, Blok MJ, Vreeswijk MP (2009). A method to assess the clinical significance of unclassified variants in the BRCA1 and BRCA2 genes based on cancer family history. Breast Cancer Res., 11(1):R8. doi: 10.1186/bcr2223

International Conference on Cancer Research 2019

Website: www.CancerConf.org

June 10-11, London, UK



Proton Magnetic Spectroscopic Assess Metabolic Changes of Glioma Tumor of a Patient under Intranasal Perillyl Alcohol-Based Therapy

Gisele M. Marques[1,2], Giselle M Faria [1], Alair S. dos Santo [3], Clovis O. da Fonseca[3], Thereza Quirico-Santos [1]*

[1] *Instituto de Biologia, Universidade Federal Fluminense, Brasil.*

[2] *Instituto Nacional de Cancer, RJ, Brasil;*

[3] *Faculdade de Medicina, Universidade Federal Fluminense, Niteroi, Rio de Janeiro, Brasil 24020-141*

* *Corresponding author: tquirico@id.uff.br*

Abstract

Glioblastoma (GBM) is the primary brain tumor most common and aggressive in adults, characterized by intense cellular proliferation and accumulation of deleterious genetic changes which contribute to the aggressive behavior, low survival, resistance to chemotherapy and tumor recurrence. Tumor cells shows specific metabolic alteration, such as increased choline (Cho) which is characteristic of highly proliferative tumor cells, reduced N-acetyl-aspartate (NAA) a marker for neuronal density and viability and phosphocreatine (Cr) peak serves as a marker for energy-dependent systems. Metabolic information within the tumor microenvironment can be detected by proton magnetic spectroscopy (^{1}HMRS) considered a noninvasive procedure that also provides anatomical and functional image data for diagnosis and patient follow-up. Perillyl alcohol (POH), a naturally occurring monoterpene has recognized antitumor effect inhibits tumor proliferation and increase survival of GBM patients under intranasal POH-based therapy.

To assess by HMRS metabolic changes within the tumor microenvironment and survival rate up to 8 months of a patient with GBM after intranasal administration of the monoterpene perillyl alcohol.

The present study was approved by CONEP (number 2.218.551); UFF Ethics Committee (UFFCAAE: 14613313.8.0000.5243) and was carried out at the Hospital Universitário Antonio Pedro, UFF. This case report covers a 60 years-old male GBM patient who had failed current standard treatment (surgery, radio and chemotherapy) for malignant glioma and was at terminal stage under palliative care. The patient signed a written informed consent prior to enroll in this clinical trial to assess the therapeutic efficacy (BR Patent Number PI 0107262-5) of POH (55 mg; 0.3% v/v) daily inhalation 4 times per day totaling 266.8 mg/day. MRS image and brain metabolism data (NAA/Cr; NAA/Cho, Cho/Cr ratios) were collected at the time of protocol inclusion and after 1, 5 and 8 months of POH-based treatment.

One month after POH based-therapy it was observed a marked increase of NAA/Cr and NAA/Cho ratios 23.7 and 33.5 fold respectively. Such metabolic ratios maintained a sustained increase with ongoing POH treatment (5 and 8 months). Conversely it was observed a gradual and consistent reduction of Cho/Cr ratio. During the period of this study the patient showed no image of recrudescence and was considered with partial response with reduction of the lesion size.

The present findings corroborate the already described therapeutic efficacy of POH inhalation for recurrent GBM patients due to its anti-inflammatory, antiangiogenic and antiproliferative properties. It is also highlighted the importance of including HMRS metabolic data evaluation as a monitoring tool for these patients follow up, considering the expected increment of NAA/Cr and NAA/Cho as well as the decrease of Cho/Cr.

Keywords:

Glioblastoma,

Perillyl Alcohol,

Proton Magnetic Spectroscopy,

Tumor Metabolic Indicators..

International Conference on Cancer Research 2019

Website: www.CancerConf.org

June 10-11, London, UK



Effects of Vitamin C and Citicoline on Morphine-Inducing Tolerance In Mice

Mahrouz Salehpour [a,b*], Bohloul Habibi Asl [a], Mohammad Charkhpur [a], Javad Mahmoudi [c]

[a] *Graduate pharmacologist, Tabriz, 5167738564, Iran*

[b] *Department of Pharmacology, Faculty of Pharmacy, Tabriz University of Medical Sciences, Tabriz, Iran*

[c] *Department of Physiology, Faculty of Medicine, Tabriz University of Medical Sciences, Tabriz, Iran*

Abstract

Introduction: The issue of evolving tolerance to opioid analgesia is a major problem in relation to pain management within the field of medicine, as in cancer patients. This paper seeks to remedy this problem by evaluating *vitamin C* and *citicoline* on tolerance postponement, depending on proven founded inhibiting effects on "glutamatergic system" of which hyper activation will result in tolerance.

Aim: This study set out to assess effects of vitamin C and citicoline on morphine-induced tolerance postponement in male mice.

Methods: Nine male albino mice groups (n=8, 0.02-0.03 g) received certain drug regimens for four days concurrently with daily morphine in order to tolerance development. On the fifth day, through *the Hot-plate test*, pain response to thermal stimulation at 15, 30, 45 and 60 minutes after the test dose of morphine was recorded. MDA and TAC were also assayed through blood serum. Statistical analyses were carried out using one-way analysis of variance (ANOVA) and Tukey post-test, where differences with *p* values less than 0.05 were intended significant.

Results: Vitamin C could significantly attenuate the tolerance, with maximum analgesic effect against thermally induced pain at 15 and 60 min (p-values<.05). However, no significant variation of MDA and TAC levels was remarked.

Conclusion: Vitamin C could postpone morphine-induced tolerance due to possible mechanisms, N-Methyl-D-Aspartate (NMDA) receptor antagonism and glutamate release inhibition, respectively.

Keywords:

Pain;

Morphine;

Tolerance;

Vitamin C;

Citicoline;

Mice.

1. Introduction

Opioids are one of the most widely used groups of antinociceptive agents. Morphine, an important component, plays a key role in severe and chronic pain management especially within cancer patients. Despite its safety and efficacy, prolonged application suffers from several major drawbacks. A major problem with this kind of application is tolerance evolution which has been a controversial and much disputed subject and received considerable critical attention within the field of medicine. By the evolution of tolerance within chronic consumption, opioid administered dose must be increased to achieve the prior analgesic effect[1,2].

The causes of this event have been the subject of intense debate within the scientific community. A number of factors found to be influencing tolerance development have been explored in several studies which show an unambiguous relationship between N-methyl-D-aspartate receptor (NMDAR, which found at most excitatory synapses and belongs to the family of glutamate receptors) and tolerance. Previous studies have indicated that NMDA antagonisms have a positive impact on tolerance postponement[3-6]. Related findings have identified that redox

* **CONTACT**: tabrizu.salehpoor@gmail.com

phenomena regulate the function of NMDA receptor in brain. Vitamin C (L-ascorbic acid), a well-known example of an antioxidant, has been found to oppose NMDA actions by inhibiting glutamate-NMDAR binding and subsequent events rooted from NMDA-gated currents in neurons[7-9].

As Hurtado et al. (2005) have indicated, citicoline (cytidine-5′-diphosphocholine or CDP-choline), contributing factor in neuronal membrane proteins generation from choline, plays the neuroprotective role in cerebral ischemic injury by decreasing brain glutamate release via glutamate uptake enhancement through astrocyte stimulation and increasing expression of EAAT2 glutamate transporter[10].

The main purpose of this study was to contest the claim whether vitamin C and citicoline can postpone tolerance development or not.

2. Materials and methods

2.1. Materials

The compounds which were utilized, are: Morphine sulfate and Vitamin C (Ascorbic acid) (Darupakhsh pharmaceutical company - Iran), Citicoline (Caspiantamin pharmaceutical company - Iran), Normal saline 0.9% (Shahid Qazi factory - Iran), Ketamine 10% (Alfasan veterinary medicines manufacturer- Holland), Xylazine 2% (Alfasan veterinary medicines manufacturer- Holland).

2.2. Animals

Nine groups of male albino mice (0.02-0.03 kg, n=8) were treated under conditions in which constant temperature (25 ± 0.5°C), air ventilation and available food and water were provided.

Prior to commencing the study, ethical clearance was sought from the Ethic Committee for Animal Experiments of Tabriz University of Medical Sciences (code: IR.TBZMED.REC.1396.670) and the procedures were carried out according to the National Institutes of Health guide for the care and use of Laboratory animals (NIH Publications No. 8023, revised 1978).

2.3. Treatment

Drugs were administered by intraperitoneal (i.p.) injection over the course of a 4-day period, according to the following protocols designed for examined groups:

1) Normal saline (10 ml/kg) + Normal saline (10 ml/kg)

2) Normal saline (10 ml/kg) + Morphine (50 mg/kg); control group

3,4,5) Citicoline (5, 10, 15 mg/kg) + Morphine (50 mg/kg)

6,7,8) Vitamin C (25, 50, 75 mg/kg) + Morphine (50 mg/kg)

9) Citicoline (10 mg/kg) + Vitamin C (50 mg/kg) + Morphine (50 mg/kg)

The morphine treated group was considered as the "control group".

2.4. Tolerance evaluation method

For the purpose of tolerance evaluating, on the fifth day, pain response (hand licking) to thermal stimulation was examined at intervals of 15 minutes (till one hour) after the 9 mg/kg test dose of morphine, test latency time; while the procedure is called Hot-plate test, although base latency time was recorded before test dose administration. The temperature of the Hot-plate instrument was stabilized at 54 °C (varied from 53.7 to 54.8°C). With the provision of outlasting threshold of stimulation more than 40 seconds, the test was discontinued. Maximum Possible Effect (MPE %) was calculated in accordance with the equation below:

MPE% = [(TL-BL) / (cut off time- BL)] x 100; where TL indicates time latency and BL, base latency time.

2.5. Evaluation of preventing effects on oxidative stress

On completion of analyzing vitamin C and citicoline effects on tolerance, the process of evaluating oxidative stress was carried out. Traditionally, tissue damage caused by oxidative stress have been assessed by measuring Malondialdehyde (MDA) and Total antioxidant capacity (TAC)[11,12], although there are certain drawbacks associated with the current MDA measuring method resulting in unreliability, which have been amended by recent studies[13-15]. Thus, it can be considered as a source for error affecting the result. However, for our purpose, the animal was deeply anesthetized by ketamine and xylazine (80 and 8 mg/kg, i.p., respectively). Blood sample was then obtained through cutting off the head[16] and poured in non-anticoagulant tube. Subsequently, the plasma serum was isolated by centrifuge

device (rpm= 3500, temperature=4°C, centrifuging time: 20 minutes). Finally, the samples were frozen with liquid nitrogen, recovered and stored at -70 °C until TAC and MDA assays.

2.6. Statistical analysis

The data were managed and analyzed using SPSS 16.0 (2010). To compare the average scores of treated groups with the control group, one-way ANOVA (analysis of variance) Tukey post hoc test were used; where significant levels were set at less than 5%.

3. Results

3.1. Development of tolerance to analgesia

As can be seen from the Figure 1, feeling of pain in daily *morphine-treated* mice occurred significantly more quickly (p<.05) at 15 minutes after the morphine test dose administration than *normal saline-treated* ones; accordingly, incidence of tolerance turns out to be definite.

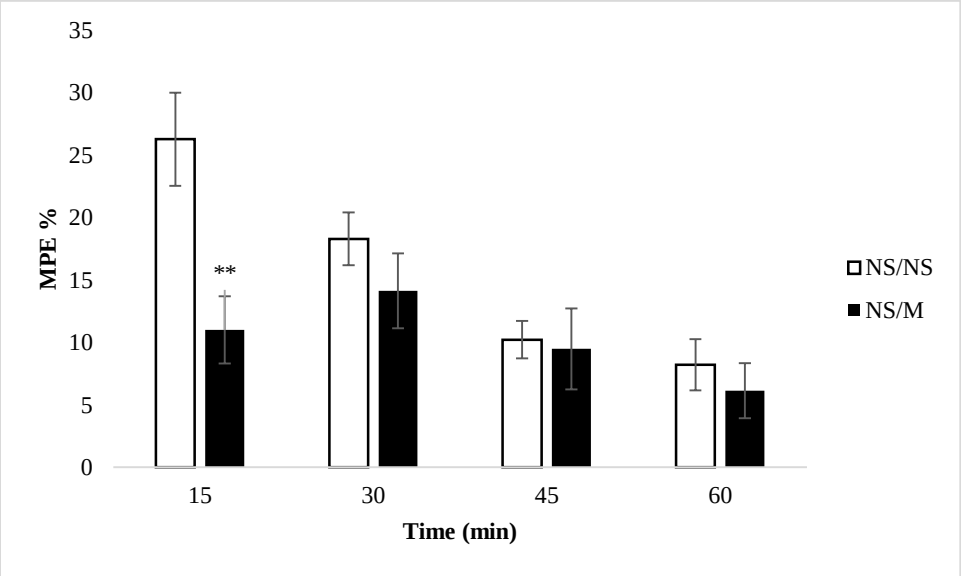


Figure 1. Mean MPE (%) (± SEM), pertaining to tolerant and non-tolerant mice (respectively treated with daily morphine 50 mg/kg, i.p. and normal saline 10 mL/kg, i.p.); $^{**}p < .01$

3.2. Effects of Vitamin C on morphine-inducing tolerance

Figure 2 presents the experimental data on vitamin C. Results showed that vitamin C (50, 75 mg/kg) attenuated the degree of tolerance to morphine.

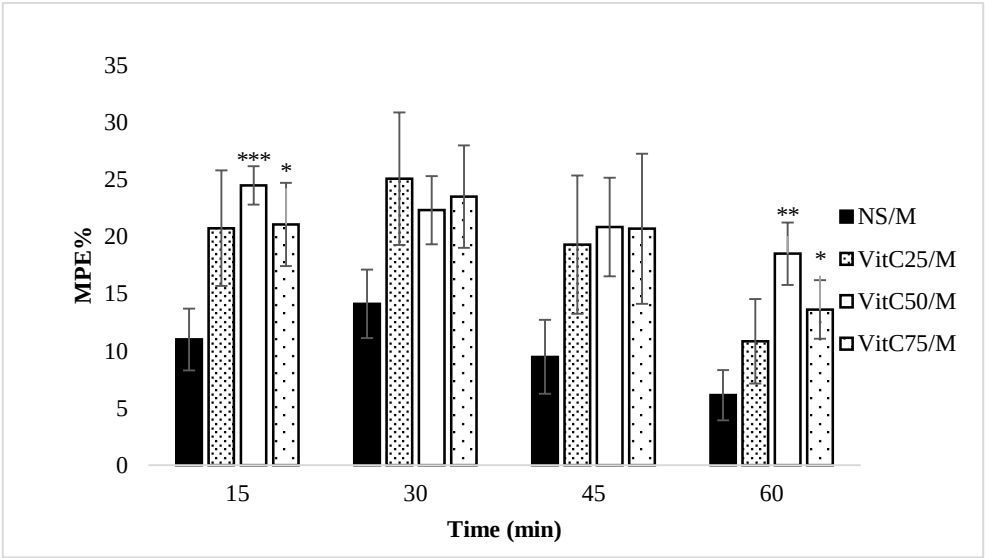


Figure 2. Mean MPE (%) (± SEM), pertaining to vitamin C treated groups (25, 50, 75 mg/kg, i.p.) and the control group through the Hot-plate test; *$p < .05$, **$p < .01$, ***$p < .001$

3.3. Effects of Citicoline on morphine-inducing tolerance

It can be seen from the Figure 3 that citicoline failed to significantly reduce tolerance to morphine analgesia.

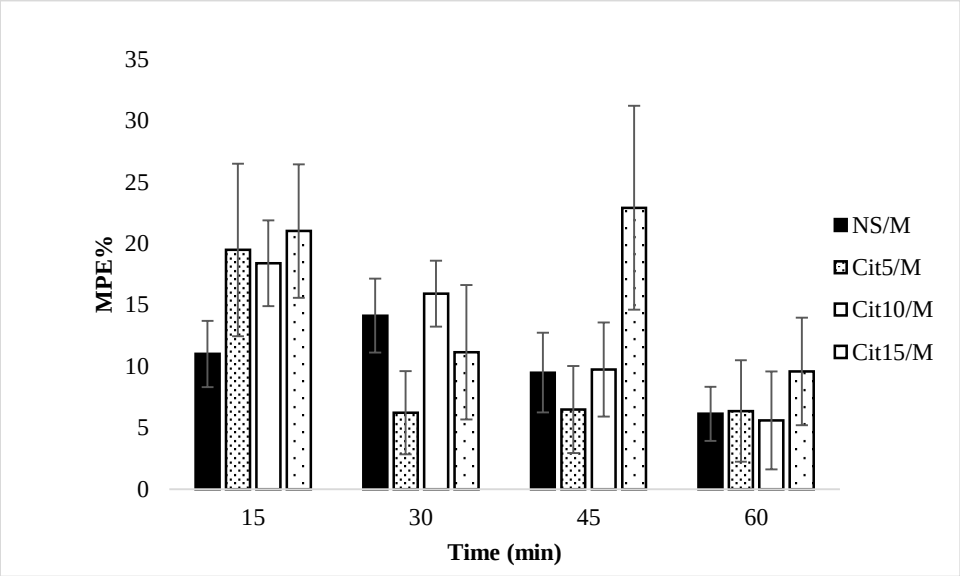


Figure 3. Mean MPE (%) (± SEM), pertaining to citicoline treated groups (5, 10, 15 mg/kg, i.p.) and the control group through the Hot-plate test.

3.4. Effects of parallel Vitamin C, Citicoline treatment on morphine-inducing tolerance

As Figure 4 shows, the concurrent treatment of vitamin C and citicoline did not significantly eventuate in tolerance postponement.

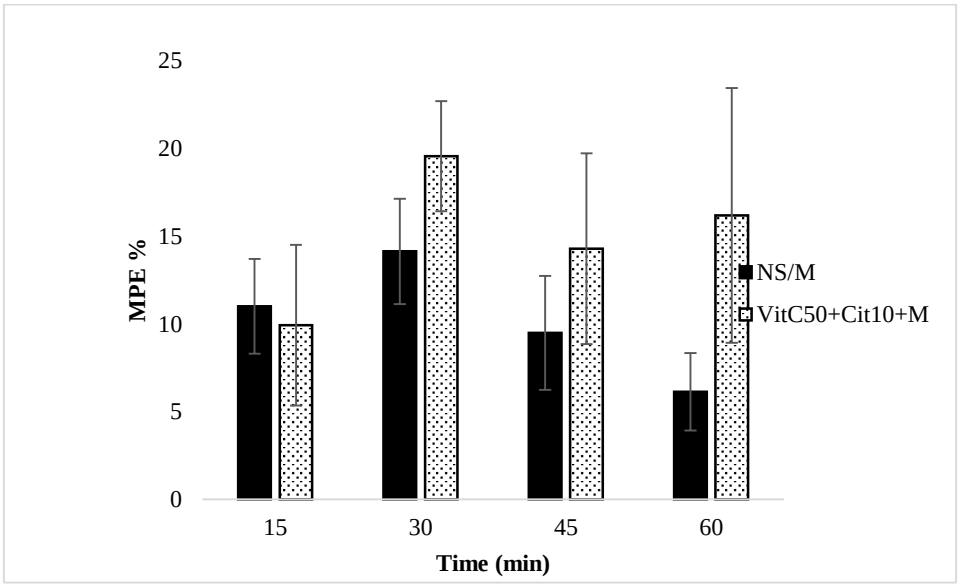


Figure 4. Mean MPE (%) (± SEM), pertaining to citicoline concurrently with vitamin C treated group (10 and 50 mg/kg, i.p.) and the control group through the Hot-plate test.

3.5. Effects of parallel Vitamin C, Citicoline treatment on MDA and TAC serum levels

Table 5 presents the results of malondialdehyde (MDA) and total antioxidant capacity (TAC) assay. No significant differences were found compared with the control group.

Table 5: Malondialdehyde (MDA) and total antioxidant capacity (TAC) assay

Groups of mice	MDA (μM)	TAC (Mm)
Ns/Ns	2.04 ± 0.22	1.05 ± 0.31
Ns/M*	2.34 ± 0.2	1.05 ± 0.23
Cit5+M	2.7 ± 0.6	1.23 ± 0.16
Cit10+M	1.62 ± 0.99	1.13 ± 0.06
Cit15+M	1.56 ± 0.1	1.19 ± 0.78
VitC25+M	1.74 ± 0.22	1.14 ± 0.11
VitC50+M	1.7 ± 0.24	1.09 ± 0.08
VitC75+M	1.68 ± 0.14	1.00 ± 0.07
VitC50+ Cit10+M	1.89 ± 0.24	0.99 ± 0.09

4. Discussion

The present study was designed with the aim of assessing vitamin C, citioline and the co-administration effects on tolerance postponement during morphine consumption based on prior studies noting their importance for modifying the glutamatergic system in neurons, of which hyper activation results in *tolerance*[17-19]. Contrary to expectations, only vitamin could significantly put off tolerance.

In correlation with this study, a number of important limitations need to be considered. First, the numbers of subjects were relatively small which could have prominently affected the evaluations of which especially oxidation biomarkers. However, approaches of behavior studies carry with them noticeable limitations including influencing environmental conditions such as unavoidable noise, researcher's mood, etc.

Thirdly, another weakness of the investigation is the use of current measuring method for MDA as well as small sample size.

In addition, there are, however, other possible explanations for the unanticipated results. For instance, inappropriate doses, inefficaciousness of intraperitoneal injection and drug kinetics or dynamics being affected by the other drug or in the body. It is recommended that further studies which take these variables into account be undertaken.

5. Conclusion

Although the study has successfully demonstrated postponing ability of tolerance to morphine analgesia for vitamin C, the precise mechanisms interfering in different findings of citicoline and concurrent utilization of vitamin c and citicoline remain to be elucidated.

6. Acknowledgments

We thank the research deputy of Tabriz University of Medical Sciences for providing technical support for this study.

7. References

[1] Sobczak M, Sałaga M, Storr MA, Fichna J. (2014). Physiology, signaling, and pharmacology of opioid receptors and their ligands in the gastrointestinal tract: current concepts and future perspectives. Journal of gastroenterology, 49(1), 24-45. doi: 10.1007/s00535-013-0753-x.

[2] Feng Y, He X, Yang Y, Chao D, H Lazarus L, Xia Y. (2012). Current research on opioid receptor function. Current drug targets, 13(2), 230-46. doi: 10.2174/138945012799201612.

[3] Vanderah TW, Ossipov MH, Lai J, Malan Jr PT, Porreca F. (2001). Mechanisms of opioid-induced pain and antinociceptive tolerance: descending facilitation and spinal dynorphin. Pain, 92(1), 5-9. doi: 10.1016/S0304-3959(01)00311-6.

[4] DuPen A, Shen D, Ersek M. (2007). Mechanisms of opioid-induced tolerance and hyperalgesia. Pain Management Nursing, 8(3), 113-21. doi: 10.1016/j.pmn.2007.02.004.

[5] Song L, Wu C, Zuo Y. (2015). Melatonin prevents morphine-induced hyperalgesia and tolerance in rats: role of protein kinase C and N-Methyl-D-Aspartate receptors. BMC anesthesiology, 15(1), 12. doi: 10.1186/1471-2253-15-12.

[6] Fischer BD, Ward SJ, Henry FE, Dykstra LA. (2010). Attenuation of morphine antinociceptive tolerance by a CB1 receptor agonist and an NMDA receptor antagonist: interactive effects. Neuropharmacology, 58(2), 544-50. doi: 10.1016/j.neuropharm.2009.08.005.

[7] Majewska MD, Bell JA. (1990). Ascorbic acid protects neurons from injury induced by glutamate and NMDA. Neuroreport, 1(3-4), 194-6.

[8] Domith I, Socodato R, Portugal CC, Munis AF, Duarte-Silva AT, Paes-de-Carvalho R. (2018). Vitamin C modulates glutamate transport and NMDA receptor function in the retina. Journal of neurochemistry, 144(4), 408-20. doi: 10.1111/jnc.14260.

[9] Portugal CC, Miya VS, Calaza KD, Santos RA, Paes-de-Carvalho R. (2009). Glutamate receptors modulate sodium-dependent and calcium-independent vitamin C bidirectional transport in cultured avian retinal cells. Journal of neurochemistry, 108(2), 507-20. doi: 10.1111/j.1471-4159.2008.05786.x.

[10] Hurtado O, Moro MA, Cárdenas A, Sánchez V, Fernández-Tomé P, Leza JC, Lorenzo P, Secades JJ, Lozano R, Dávalos A, Castillo J. (2005). Neuroprotection afforded by prior citicoline administration in experimental brain ischemia: effects on glutamate transport. Neurobiology of disease, 18(2), 336-45. doi: 10.1016/j.nbd.2004.10.006.

[11] Grotto D, Maria LS, Valentini J, Paniz C, Schmitt G, Garcia SC, Pomblum VJ, Rocha JB, Farina M. (2009). Importance of the lipid peroxidation biomarkers and methodological aspects for malondialdehyde quantification. Quimica Nova, 32(1), 169-74. doi: 10.1590/S0100-40422009000100032.

[12] Kusano C, Ferrari B. (2008). Total antioxidant capacity: a biomarker in biomedical and nutritional studies. J Cell Mol Biol, 7(1), 1-5.

[13] Khoubnasabjafari M, Ansarin K, Jouyban A. (2016). Critical review of malondialdehyde analysis in biological samples. Current Pharmaceutical Analysis, 12(1), 4-17.

[14] Azizi S, Shahrisa A, Khoubnasabjafari M, Ansarin K, Khoubnasabjafari M, Soleymani J, Jouyban A. A possible reason for the low reproducibility of malondialdehyde determinations in biological samples. doi: 10.4155/bio-2016-0228.

[15] Azizi S, Khoubnasabjafari M, Shahrisa A, Khoubnasabjafari M, Soleymani J, Jouyban A. (2017). Effects of analytical procedures on the repeatability of malondialdehyde determinations in biological samples. Pharmaceutical Sciences, 23(3), 193-7. doi: 10.15171/PS.2017.29.

[16] Mahjal Naebi A, Mahmoudi J. (2010). Laboratory Animals Practice. volume 1. Tabriz: University of Tabriz Medical Sciences.

[17] Fischer MJ, Mak SW, McNaughton PA. (2010). Sensitisation of nociceptors—what are ion channels doing. Open Pain J, 3, 82-96.

[18] Freye E, Latasch L. (2003). Development of opioid tolerance--molecular mechanisms and clinical consequences. Anasthesiologie, Intensivmedizin, Notfallmedizin, Schmerztherapie: AINS, 38(1), 14-26. doi: 10.1055/s-2003-36558.

[19] Mao J, Price DD, Mayer DJ. (1995). Mechanisms of hyperalgesian and morphine tolerance: a current view of their possible interactions. Pain, 62(3), 259-74. doi: 10.1016/0304-3959(95)00073-2.

International Conference on Cancer Research 2019

Website: www.CancerConf.org

June 10-11, London, UK



Influence of Microalgae Extracts on the Toxicity of a Carcinogenic Polycyclic Aromatic Hydrocarbon, Benzo(a)pyrene, in Endothelial Cells

Manon Le Goff [1,2], Antoine Delbrut [3], Rémi Pradelles [3], Odile Sergent [2], Dominique Lagadic-Gossmann [2], Eric Le Ferrec [2*], Lionel Ulmann [1*]

[1] *Metabolism, Engineering of Microalgal Biomolecules and Applications (MIMMA)- UBL, IUML - FR CNRS 3473, EA 2160 MMS, Mer Molécules Santé, Le Mans University, CERIUM2, 53020 Laval, France*

[2] *Univ Rennes, Inserm, EHESP, Irset (Institut de recherche en santé, environnement et travail) - UMR_S 1085, F-35000 Rennes, France*

[3] *Microphyt, 34670 Baillargues, France*

**Co-supervisors*

manon.le_goff@univ-lemans.fr; antoine.delbrut@microphyt.eu; remi.pradelles@microphyt.eu; odile.sergent@univrennes1.fr; dominique.lagadic@univ-rennes1.fr; eric.leferrec@univ-rennes1.fr lionel.ulmann@univ-lemans.fr

Abstract

Exposure to environmental contaminants is known to cause cancer in humans. Polycyclic aromatic hydrocarbons (PAHs) generated during the incomplete combustion of organic matter, constitute an ubiquitous family of environmental contaminants whose main source of exposure is from human activities (industrial activities, cigarette smoke, food processing...). Among them, benzo(a)pyrene(B(a)P), found in all mixtures humans are exposed to, is classified in group 1, i.e. carcinogenic to humans, by the International Agency for Research on Cancer. Most of B(a)P deleterious effects (i.e. apoptosis, induction of pro-inflammatory cytokines and CYP450 enzymes) are mediated by the activation of a ligand-activated transcription factor : aryl hydrocarbon receptor (AhR).

Marine microalgae are photosynthetic microorganisms, known to be a source of bioactive molecules of interest to human health, such as n-3 polyunsatured fatty acids (n-3 PUFAs) and pigments (carotenoids: fucoxanthin, violaxanthin…). The fact that some of the natural compounds are known to exhibit antiinflammatory, antioxidant, anti-proliferative, apoptosis-inducing effects demonstrates their potential interest in preventing cancers.

In this context, we have used two microalgae extracts in order to evaluate and compare their potential effects towards B(a)P-induced toxicity in endothelial HMEC-1 cells (human microvascular endothelial cells-1). Endothelial cells were chosen because they express AhR eceptor and CYP450s and they are well known targets of PAHs.

The cytotoxicity, apoptosis, expression of CYP1B1 (P450 isoenzyme involved in B(a)P bio-activation) and of pro-inflammatory cytokines have been studied during exposure of B(a)P or microalgae extracts alone and upon co-exposure using MTT assay, Hoechst fluorescent staining and mRNA expression analysis, respectively

The microalgae extracts are derived from *Ostreoccoccus tauri* (OT), a green microalgae rich in docosahexaenoic acid (DHA, 22 :6 n-3) and *Phaeodactylum tricornutum* (PT), a diatom rich in eicosapentanenoic acid (EPA, 20 :5 n-3). The lipid and pigment composition of the extracts were determined.

Our results show that OT and PT extracts can significantly decrease B(a)P-induced CYP1B1 mRNA levels. MTT assay, as expected under our experimental conditions, revealed B(a)P toxicity, but does not show any toxicity for the extracts alone, nor increased toxicity upon co-exposure. Interestingly, using Hoechst staining, we have observed that OT extract, unlike PT extract, significantly decreased B(a)P-induced apoptosis. Concerning the effects of OT and PT extracts on mRNA expression of two pro-inflammatory cytokines, IL-8 and IL-β, we have observed that both OT and PT extracts inhibited B(a)P-induced IL-8 and IL-1β mRNA expression.

Taken together, our data indicate that microalgae extracts can influence the toxicity of B(a)P at least by decreasing the induction of CYP1B1 mRNA and of pro-inflammatory cytokines (IL-8 and Il1-β), and only for OT extract, the B(a)P-induced-apoptosis. The differential effects obtained between the two extracts on the toxicity of B(a)P is probably related to their different composition, such as EPA and DHA among others. Indeed, it has been recently reported that EPA and DHA may differently affect B(a)P metabolism.

In conclusion, these results are promising concerning the possible use of microalgae extracts to counteract the B(a)P-induced toxicity but remain to be confirmed by further study *in vivo.*

Keywords:

Microalgae,

Benzo(a)pyrene,

Endothelial Cells,

PAHs.

International Conference on Cancer Research 2019

Website: www.CancerConf.org

June 10-11, London, UK



Antiproliferative Effects of Palmitoylethanolamide on Human Cervical Cancer Cells

Laura Bonfili *, Valentina Cecarini, Anna Maria Eleuteri

School of Biosciences and Veterinary Medicine, University of Camerino, via Gentile III da Varano, 62032 Camerino (MC), Italy.

Abstract

Palmitoylethanolamide (PEA) is a bioactive fatty acid amide that accumulates during certain types of inflammation. PEA has been identified as a potent analgesic and anti-inflammatory agent, thus representing a promising molecule in the treatment of chronic pain and inflammation. Several studies evidenced the coexistence of multiple mechanisms of action of PEA. For example, PEA may act as an enhancer of the anti-inflammatory and antinociceptive activity exerted by other endogenous compounds (i.e. anandamide), either by increasing their affinity for receptors or inhibiting their metabolic degradation. The ubiquitin-proteasome system is the main extra-lysosomal proteolytic pathways and it is involved in the removal of inflammatory proteins, cell cycle regulators, oxidized and misfolded proteins. The modulation of the proteasome functionality represents an established target in a number of pathologic conditions such as cancer, neurodegenerations and inflammation.

In the present study, we investigated the ability of PEA to modulate the enzymatic activity of the proteasome. At first, we studied the effect of different concentrations of PEA on isolated constitutive and immuno-proteasomes. Successively, human cervical carcinoma cells were used as a model to measure PEA effect on tumour cell viability. The effect of PEA on the proteolytic activities of cellular proteasomes has been evaluated and the expression level of several proteasome substrates were determined. Our data propose an additional mechanism of action of PEA, precisely the modulation of proteasome-mediated proteolysis and demonstrate that PEA can affect tumour cells survival through the activation of apoptosis. These findings could represent an important preliminary step in considering PEA as a possible anti-cancer tool.

Keywords:

Palmitoylethanolamide;

Proteasome,

Anticancer.

1. Introduction

N-palmitoylethanolamine (PEA) is a naturally occurring fatty acid amide belonging to the class of endocannabinoids and it is present in most mammalian tissues. PEA is known for its anti-inflammatory properties which has been observed in vitro and in clinically relevant animal models of inflammatory pain [1, 2]. PEA is a signalling molecule, which can inhibit mast cell activation and microglial cell activities [3-5] thus reducing central pain hypersensitization [6]. The exact mechanisms of action of PEA are still under discussion, although it seems that the antinociceptive effects are mediated by multimodal mechanisms [7]. Membrane receptors (i.e., cannabinoid receptors) [4], nuclear receptors (i.e. PPAR, perossisome proliferator receptor) [8, 9], neurosteroid synthesis [10], mast cell down-modulation [3, 11, 12] and control of microglial activation [13] are all supposed mechanisms of action of PEA. These may coexist, depending upon the physiological and pathophysiological circumstances [14]. Additionally, a distinct entourage-effect has been hypothesized to explain PEA biological activities [15] with PEA acting as enhancer of the anti-inflammatory and antinociceptive activity exerted by other endogenous compounds and increasing their affinity for receptors or inhibiting their metabolic degradation. One of these endogenous compounds is anandamide, whose activity may be potentiated by PEA [7]. PEA antinociceptive effects are prevented by the cannabinoid receptor antagonists [16] although its affinity for cannabinoid receptors (CB1 and CB2) is very low [17]. Although PEA has affinity for other PPAR isoforms, G

* **CONTACT**: laura.bonfili@unicam.it

coupled receptors and novel cannabinoid receptors, PPAR-α can be considered the main biological target of PEA [18]. PEA up-regulation of PPAR-α results in decreased output of inflammatory mediators like tumor necrosis factor-α and interleukins, thus supporting PEA's role as a modulator of inflammation and pain [12]. Additionally, PEA reduced neurological deficits in a spinal trauma model, via reduction of mast cell infiltration and activation [12].
Considering PEA affinity for PPAR-α and the widespread presence of this receptor in CNS microglia and astrocytes, it is reasonable to think to PEA possible applications in the treatment of neuropathic pain [18].
The increase of the local synthesis of a compound with documented anti-inflammatory properties, during certain types of inflammation, raises the possibility that compounds affecting the metabolism of PEA may be therapeutically useful. In this work, the hypothesis that PEA can induce apoptosis in cancer cells through proteasome modulation has been investigated.

2. Material and methods

2.1. Reagents and chemicals

Substrates for assaying the ChT-L, T-L, PGPH activities (Suc-Leu-Leu-Val-Tyr-AMC, Z-Leu-Ser-Thr-Arg-AMC, Z-Leu-Leu-Glu-AMC, respectively) were all purchased from Sigma-Aldrich (Italy) while PEA was from EPITECH (Italy). The substrate Z-Gly-Pro-Ala-Phe-Gly-pAB and the inhibitor Z-Gly-Pro-Phe-Leu-CHO to test the BrAAP activity were the kind gift of Prof. Cardozo (Department of Medicine, Mount Sinai School of Medicine, New York). Media and reagents for cell cultures were purchased from Euroclone (Italy). Antibodies used in western blotting were purchased from Santa Cruz Biotechnology (CA. USA). The western blot stripping buffer was from Pierce (USA). All chemicals and solvents were of the highest analytical grade available. Human cervical carcinoma cells (HeLa) and the non-tumorigenic epithelial cell line MCF10A were from ATCC (Manassas, VA, USA).

2.2 20S proteasome in vitro assays

The effects of increasing concentrations of PEA on constitutive and immuno- 20S proteasomes functionality were evaluated through fluorimetric assays. The following synthetic substrates were used: Suc-Leu-Leu-Val-Tyr-AMC for ChT-L, Z-Leu-Ser-Thr-Arg-AMC for T-L, Z-Leu-Leu-Glu-AMC for PGPH, and Z-Gly-Pro-Ala-Phe-Gly-pAB for BrAAP. The tests for the BrAAP activity were performed in the presence of aminopeptidase-N. 20S proteasome and immunoproteasome were isolated from bovine brain and thymus respectively. The incubation mixture contained increasing concentrations of PEA (from 0 to 20 μM), 1 μg of isolated 20S proteasome or immunoproteasome, the appropriate substrate and 50 mM Tris-HCl pH 8.0 up to a final volume of 100 μL. Incubation was carried out at 37°C and, after 60 min, the measurements of the hydrolyzed 7-amino-4- methyl-coumarin (AMC) and 4-aminobenzoic acid (PABA) were detected (AMC: λexc=365 nm, λem=449 nm; PABA λexc=304 nm, λem=664 nm) on a SpectraMax® Gemini™ XPS Microplate spectrofluorometer (Molecular Device®). Control assays were performed to evaluate a possible effect of the molecules on the proteolytic activity of aminopeptidase-N.

2.3 Cell viability assay

Cell viability upon PEA treatment was evaluated by MTT assay, an index of mitochondrial activity and cell viability. It is based on viable cells' ability to convert a soluble yellow tetrazolium salt, 3-(4,5-dimethylthiazol-2-yl)-2,5-diphenyltetrazolium bromide, to a purple–blue formazan crystal by mitochondrial succinate dehydrogenase. In detail, cells were treated with increasing concentrations (0-50μM) of PEA for 24-72 hours. After experimental treatment, media were replaced with serum-free media containing 0.5 mg/mL MTT. Plates were incubated at 37 °C for 2 h. After discarding the supernatant, the formazan product was solubilized in 100 μL of dimethyl sulfoxide and absorbance was measured at 550 nm. The MTT assay was also carried out in the
presence and in the absence of the caspase inhibitor zVADfmk (10 μM concentration in the assay; Sigma-Aldrich, St Louis, MO, USA). Each time point was performed in sixtuplicate.

2.4 Cells treatment

HeLa cells were grown in DMEM medium supplemented with 10% FBS, antibiotic, antimycotic and L-glutamine at 37°C. MCF10A cells (an in vitro model for studying normal epithelial cell function) were cultured in a DMEM/F12 Ham's mixture supplemented with 5% equine serum, 20 $ng \cdot mL^{-1}$ epidermal growth factor, 10 $\mu g \cdot mL^{-1}$ insulin, 0.5 $mg \cdot mL^{-1}$ hydrocortisone, antibiotics and antimycotic. Cells were incubated with growth medium at 37°C equilibrated with 95% air and 5% CO_2 in flasks or 96- or 6-well plates depending on the assay. Cells were treated with 10 μM palmitoylethanolamide (PEA) for 6 and 24 h. Control cells were treated with DMSO. Upon treatment, cells were harvested in PBS, centrifuged and the pellet was resuspended in lysis buffer (20 mM Tris, pH 7.4, 250 mM sucrose, 1 mM EDTA and 5 mM β-mercaptoethanol). Lysates were centrifuged at 12000xg for 15 min and the supernatants were stocked at -80 °C. Protein concentration in cell lysates was determined by the method of Bradford using bovine serum albumin as a standard.

2.5 Proteasomal activities on cell lysates

20S proteasome activity assays in cell lysates (1 μg of total proteins in the mixture) were performed using the substrates listed above; control experiments were done in the presence of specific proteasome inhibitors: Z-Gly-Pro-Phe-Leu-CHO and lactacystin (5 μM in the reaction mixture). Incubation was carried out at 37°C for 60 min, then the measurements of the release AMC and PABA groups were detected on a SpectraMax® Gemini™ XPS Microplate spectrofluorometer (AMC: λexc = 365 nm, λem= 449 nm; PABA: λexc= 304 nm, λem= 664 nm). 26S proteasome ChT-L activity was measured including 10 mM $MgCl_2$, 1 mM DTT and 2 mM ATP in the reaction mixture. Incubation was carried out at 37°C and, after 60 min, the AMC release was detected.

2.6 Caspase 3 activity

Caspase 3 activity was measured in cell lysates (20 μg of total proteins in the mixture) using the Ac-Asp-Glu-Val-Asp-AMC substrate in 50 mM Tris–HCl, 50 mM NaCl, 5 mM $CaCl_2$, 1 mM EDTA, 0.1% CHAPS, 5 mM β-mercaptoethanol, pH 7.5. Incubation was carried out at 37 °C for 60 min, then the fluorophore hydrolysis product was detected (AMC: λexc= 365 nm, λem= 449 nm) on a spectrofluorimetric microplate reader Gemini XPS.

2.7 Western blotting analyses

Intracellular levels of ubiquitinated proteins, IkBα and p27 after PEA treatment were analyzed through western blotting assays. Cell lysates (15 μg) were loaded on sodium dodecyl sulfate polyacrilamide gel electrophoresis (SDS-PAGE) and electroblotted onto PVDF membranes. After incubation with specific primary and secondary antibodies the immunoblot detections were carried out with Enhanced ChemiLuminescence western blotting analysis system (Amersham-Pharmacia-Biotech). Every gel was loaded with molecular weight markers including proteins with MW from 6.5 to 205 kDa (SigmaMarker Wide Molecular Weight Range, Sigma-Aldrich S.r.l., Milano, Italy). As a control for equal protein loading glyceraldehyde-3-phosphate dehydrogenase (GAPDH) was utilized: membranes were stripped and reprobed for GAPDH using a monoclonal antibody diluted 1:500. A densitometric algorithm has been developed to quantitate the Western Blot results. Each Western Blot film has been scanned (16 bits greyscale) and the obtained digital data were processed to calculate the background mean value and its standard deviation. The background-free image was then obtained subtracting the background intensity mean value from the original digital data. The integrated densitometric value associated to each band was then calculated as the sum of the density values over all the pixels belonging to the considered band having a density value higher than the background standard deviation. The band densitometric value was then normalized to the relative GAPDH signal intensity. The ratios of band intensities were calculated within the same Western Blot. All the calculations were carried out using the Matlab environment (The MathWorks Inc., MA, USA) [19].

2.8 Statistical analysis

Values are expressed as mean values and standard deviation of results obtained from separate experiments. Student's t-test was used to compare differences between the means of control and treated groups. Statistical tests were performed with Sigma-stat 3.1 software (SPSS, Chicago, IL, USA). P-values < 0.05 and < 0.01 were considered to be significant.

3. Results

3.1 Effect of PEA on isolated 20S proteasomes

The ability of PEA to inhibit 20S proteasomes was assayed by incubating both constitutive proteasome and immunoproteasome with increasing concentrations of PEA. All proteasomal activities were significantly inhibited. In particular, a strong inhibition of the BrAAP activity of the constitutive 20S proteasome was observed (60% at 10 μM). ChT-L, T-L and PGPH activities of constitutive proteasome showed a 30-40% inhibition upon incubation with the highest PEA concentration (20 μM). When the immunoproteasome was incubated with 20 μM PEA, the BrAAP component resulted inhibited of a 60%, while the ChT-L, T-L and PGPH showed a 30-40% inhibition (Figure 1). Interestingly, relatively low concentrations of PEA (1-2.5 μM) were already able to significantly affect only the BrAAP component of both enzymes (Fig. 1)

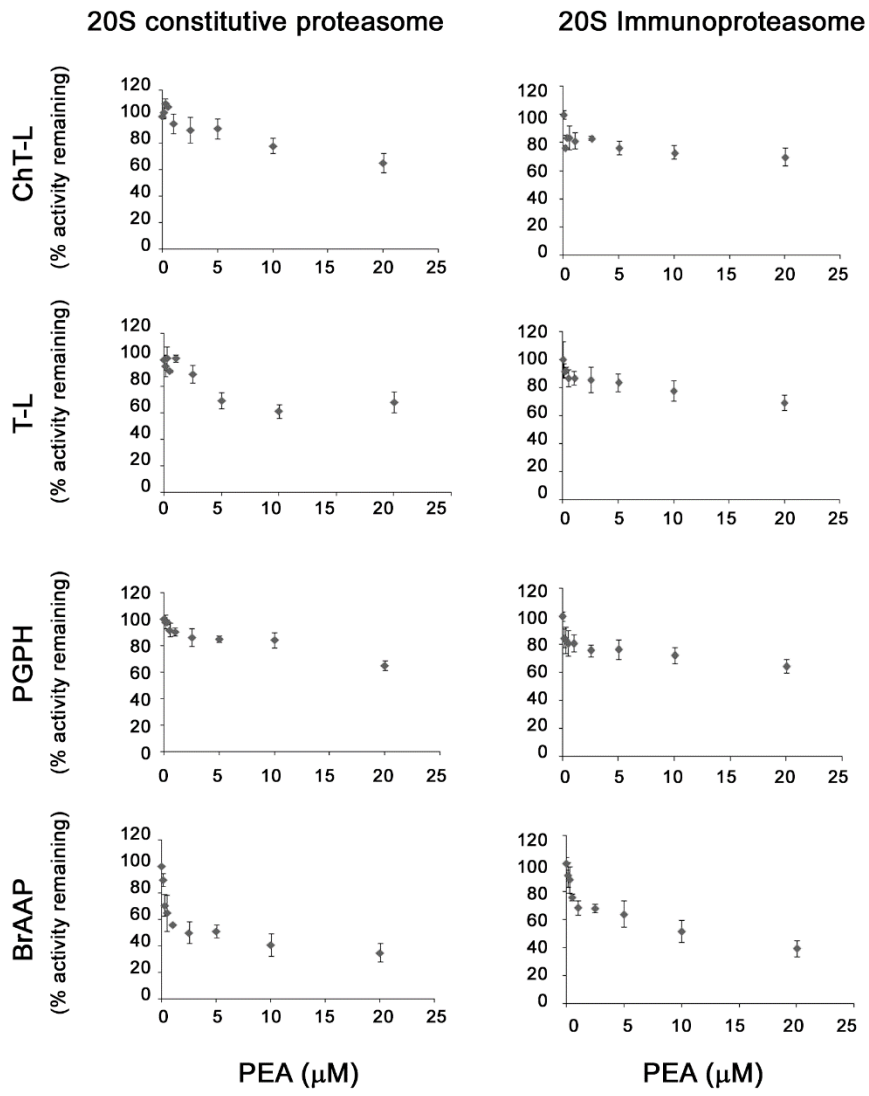


Fig. 1 Effects of PEA on isolated 20S proteasomes. Effect of increasing concentration of PEA on the ChT-L, T-L, PGPH and BrAAP proteolytic components of constitutive (Left) and immuno- (Right) 20S proteasomes, isolated from bovine brain and thymus respectively. Data shown are expressed as mean values ± SE obtained from six distinct determinations.

Interestingly, relatively low concentrations of PEA (1-2.5 μM) were already able to significantly affect only the BrAAP component of both enzymes (Fig. 1).

3.2. HeLa cells viability upon PEA exposure

Upon cell treatment with increasing concentrations (0-50μM) of PEA for 24-72 hours a concentration-dependent effect on HeLa cells viability has been observed. Upon 24h treatment with 15 μM PEA a significant decrease of HeLa cell viability occurred, whereas 5 μM PEA significantly decreased HeLa cell survival at 48 and 72 h. Conversely, MCF10A viability was not influenced by the treatment, suggesting a selective effect on cancer cells (Fig 2).

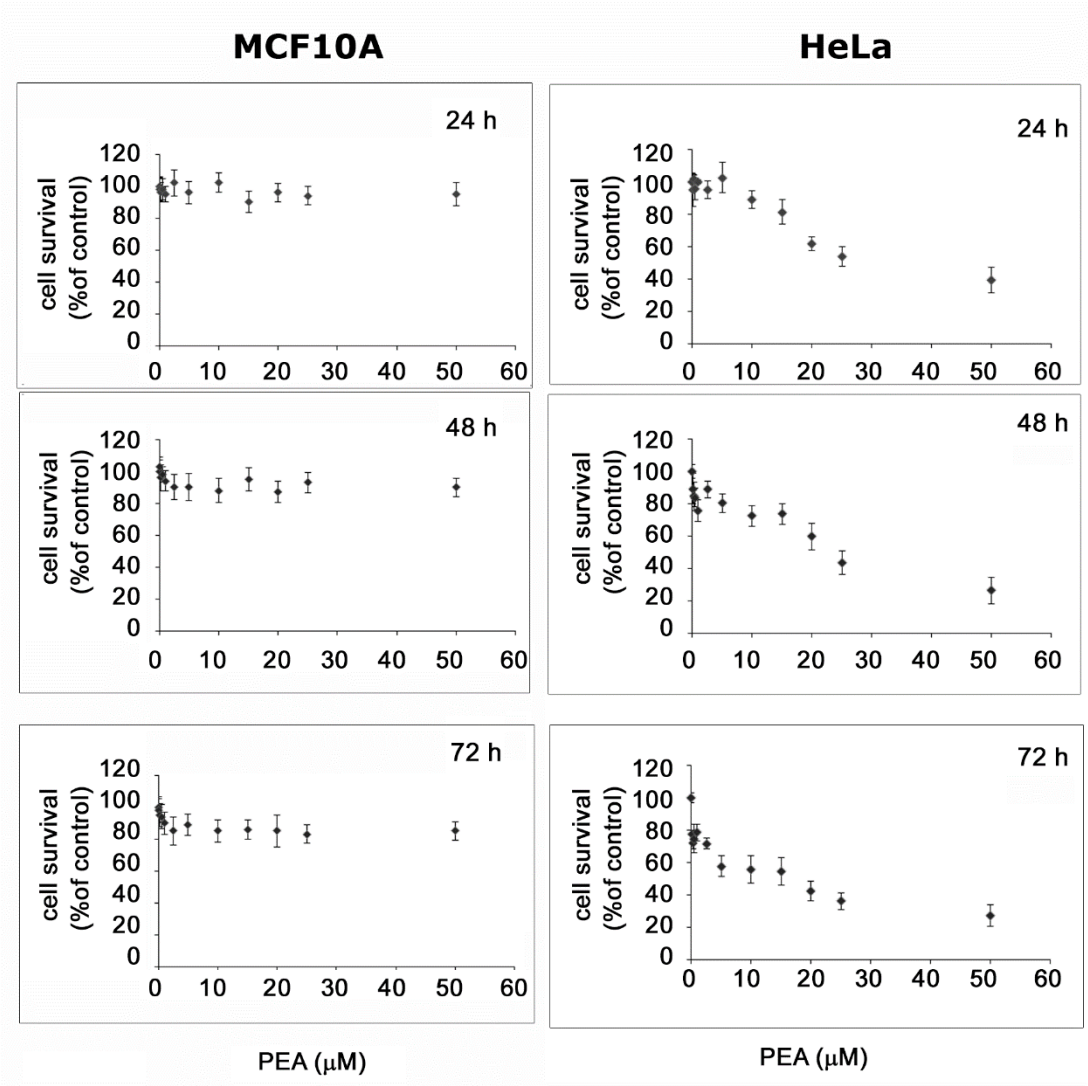


Fig 2. Cell survival analyzed with the MTT assay. Cell viability plots of MCF10A (left) and HeLa (right) cells treated with increasing concentrations (0-50μM) of PEA for 24, 48 and 72 h as described in Materials and methods section. Data are reported as % of cell viability. Data shown are expressed as mean values ± SE obtained from six distinct determinations.

3.3 Effects of PEA on cellular proteasomes

20S proteasomal activities were measured in cells treated with 10 μM PEA for 6 and 24 h. PEA significantly inhibited 20S proteolytic components, mainly the ChT-L (25% inhibition at each time point) and T-L activities (50% and 35% at 6 and 24 h respectively) in HeLa cells. BrAAP activity decreased of 15% and 35% at 6 and 24 h, respectively, and PGPH activity was inhibited of 10% at 24h (Figure 3).

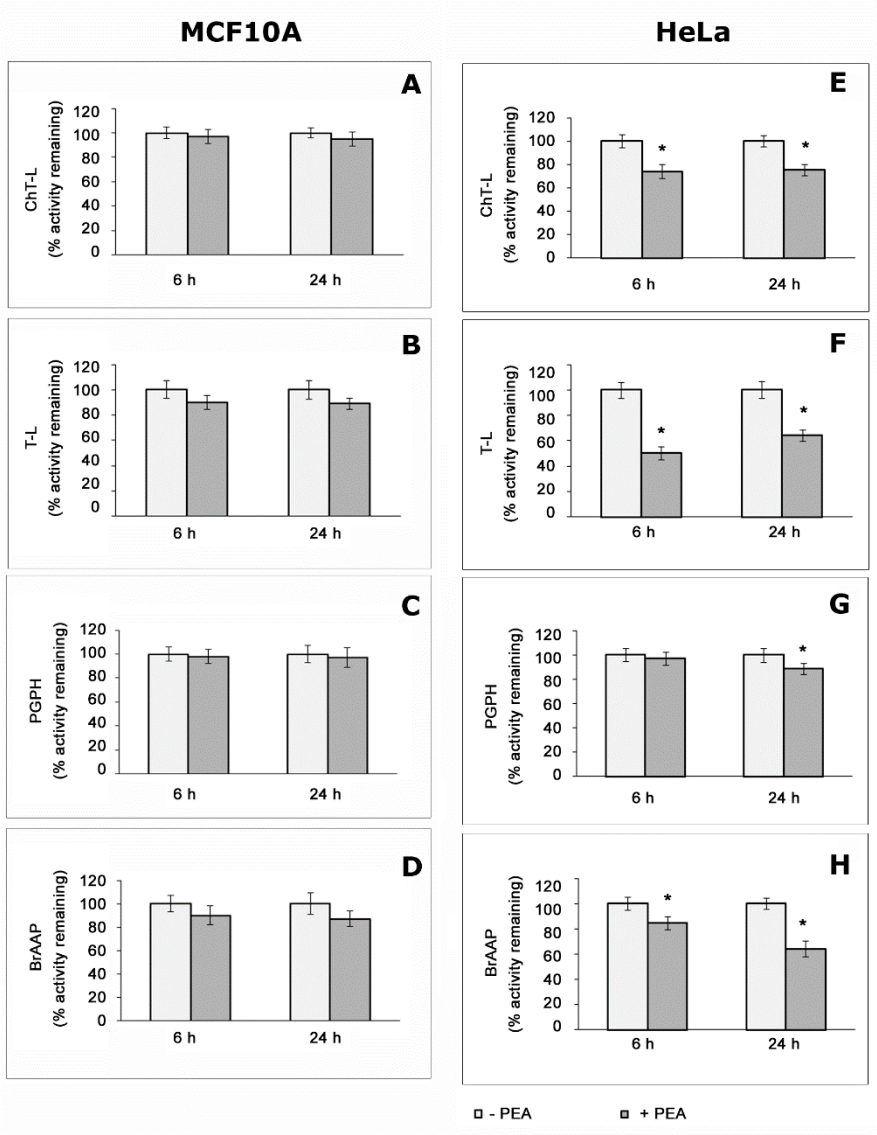


Fig 3 Proteasomal activities measured in cell lysates. Upon treatment with PEA, MCF10A (left) and HeLa (right) cells lysates were tested for the ChT-L (panel A), T-L (panel B), PGPH (panel C) and BrAAP (panel D) activities of 20S proteasomes, using fluorescent substrates. Data are reported as % of cell viability. Data shown are expressed as mean values ± SE obtained from six distinct determinations.

The 26S ChT-L activity was measured to explore the functionality of the ubiquitin-proteasome system. The activity resulted inhibited of 35% upon 6 and 24 h treatment exclusively in Hela cells (Figure 4)

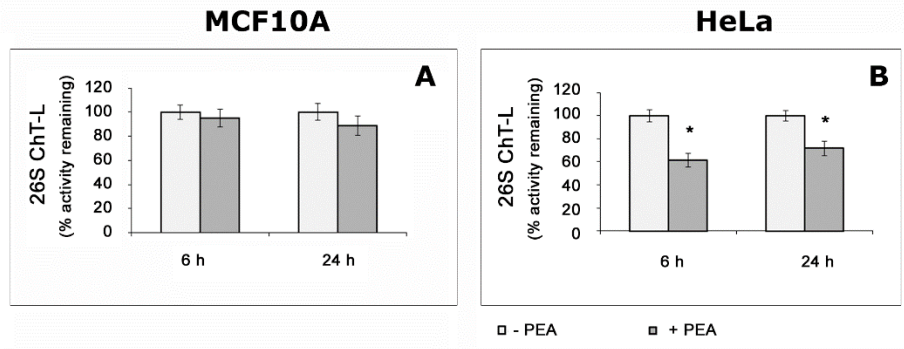


Fig 4 26S proteasome ChT-L activity. MCF10A and HeLa cells were treated with PEA for 6 and 24 h, as described in the Materials and methods section. 26S ChT-L activity was measured in cell lysates including in the

reaction mixture 10 mM MgCl2, 1 mM DTT and 2 mM ATP. Data are expressed as % activity remaining compared to their respective control in each time set (*p <0.05).

PEA-dependent proteasome inhibition was also confirmed by the accumulation of ubiquitinated proteins and increase in the levels of other proteasomal substrates, such as IkBα and p27 in HeLa cells (Fig 5).

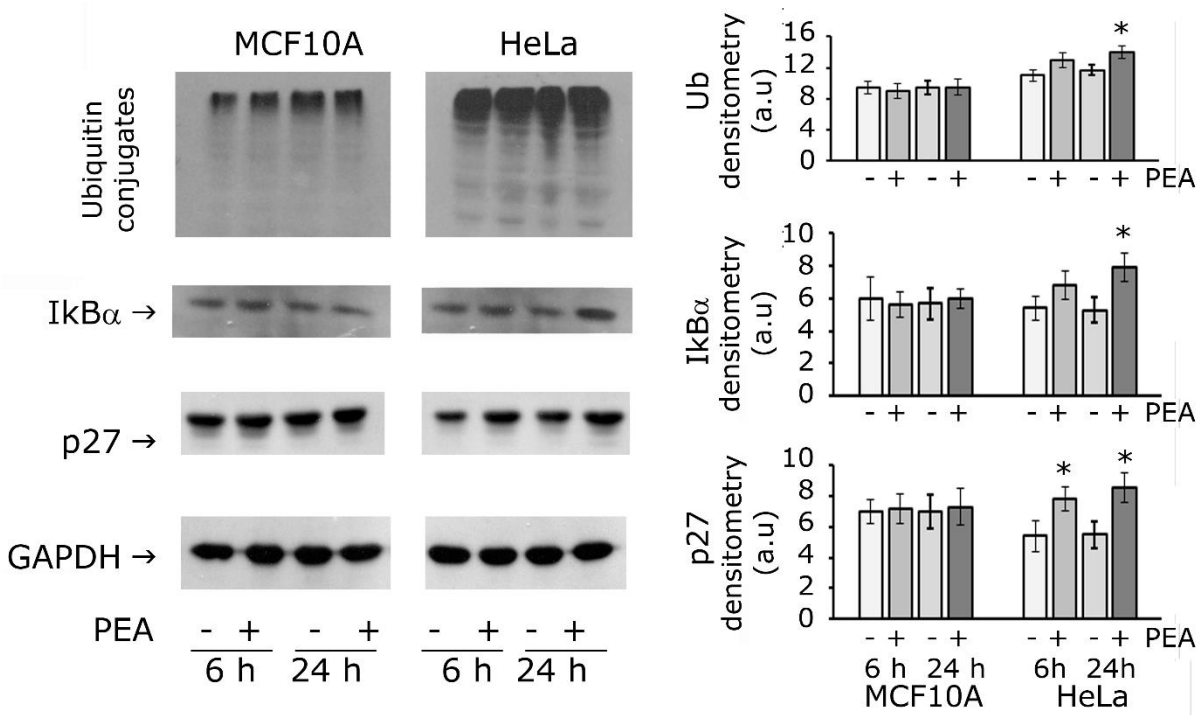


Fig. 5. Proteasome substrates accumulation in HeLa cells treated with PEA. Representative western blotting of proteasome substrates levels in MCF10 and HeLa cells treated with 10 μM PEA for 6 and 24 h. The densitometric analyses from six separate blots provided for quantitative analysis are presented. Equal protein loading was verified by using an antibody directed against GAPDH. Data points marked with an asterisk are statistically significant compared to their respective not treated control cells in each time set (*p<0.05).

3.4 Caspase-3 activity

Caspase 3 is a crucial enzyme in apoptosis, since it catalyzes the proteolysis of many cellular regulatory proteins, finally resulting in DNA fragmentation. Caspase 3 activity was measured to elucidate the basis for the observed cellular death. Its activity was significantly enhanced selectively in HeLa cells at 6 and 24 h in the presence of 10 μM PEA (Fig. 6).

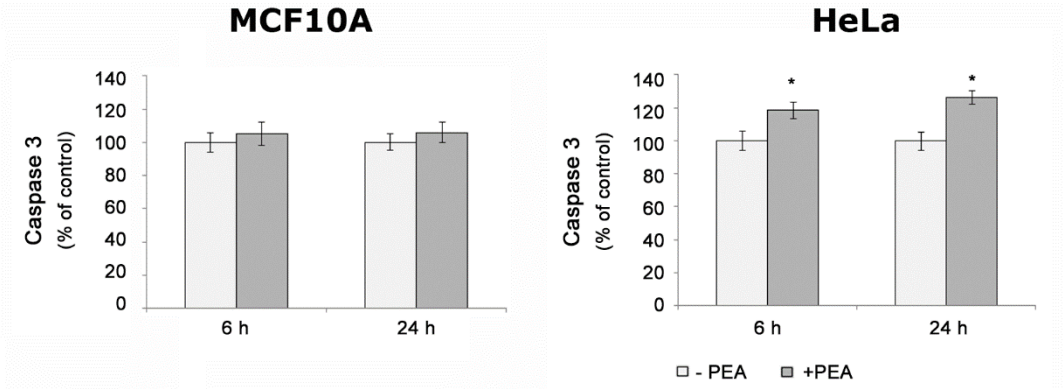


Fig. 6. Caspase 3 activity. Caspase-3 activity measured using the fluorogenic substrate Ac-Asp-Glu-Val-Asp-AMC. Data are expressed as percentage of the respective untreated control cells (100%) in both MCF10A (left) and HeLa (right) cell lines.

4. Discussion

The endogenous fatty acid amide palmitoylethanolamide (PEA) was initially considered acting mainly as an anti-inflammatory agent. In fact, recent data have demonstrated that PEA may play an important key role in the regulation of complex systems involved in the inflammatory response, pruritus, neurogenic and neuropathic pain [7]. PEA was suggested to exert its actions via several molecular mechanisms, including direct activation of peroxisome proliferator-activated receptor-α (PPAR-α), or indirect activation of cannabinoid receptors and transient receptor potential vanilloid type-1 (TRPV1) channels following potentiation of AEA activity at these targets [20]. However, its precise mechanism of action remains debated. The aim of the present study was to evaluate if PEA effects could also be mediated by the modulation of the proteasome activity, the major complex in charge of the removal of misfolded and oxidized proteins with a pivotal role in cell proliferation, apoptosis, inflammation and diseases onset and progression.

In a first phase, the investigation was conducted on isolated constitutive and immuno-proteasomes and successively on human cervical carcinoma cells (HeLa) and a normal counterpart (MCF10A). In detail, PEA was able to significantly modulate isolated proteasome activities in both a subunit- and concentration-dependent manner, exerting an inhibitory effect mainly on the BrAAP component of both complexes. HeLa cells viability upon PEA treatment was evaluated exposing cells to increasing concentration of PEA for 24, 72 and 48h. The amide was able to decrease cell survival in a concentration dependent way, 15 μM of PEA being the lowest concentration able to affect cell survival at 24h exposure. Tests on cell cultures were then performed using a concentration of PEA of 10 μM, as this treatment did not caused significant changes in cell survival.

Cellular proteasomes functionality, both 20 and 26S, resulted significantly inhibited upon PEA treatment. Comparing these results with those obtained treating isolated enzymes, we once more detected a subunit-dependent inhibition of the complex, but in this test the most affected activities resulted the T-L of the 20Sproteasome and 26S-ChT-L activity. The inhibition of the complex was further confirmed by the finding of accumulated proteasomal substrates including Ub-protein conjugates, IκBα and p27. Together, such results demonstrate for the first time that PEA mechanisms of action also include the modulation of the proteasome functionality.

In addition, the anti-inflammatory properties of PEA may also be mediated by its direct effects on the proteasome as it results from IκB-α accumulation.

As abovementioned, the proteasome plays a role in numerous cellular pathways, including apoptosis. In this study, we show that proteasome inhibition is accompanied by increased levels of p27 and IκBα, which are recognized apoptosis markers [21]. To better explore this pathway, we tested PEA effects on caspase-3 activity, an enzyme involved in the last step of the apoptotic cascade. As expected, a significant enhancement of the enzyme activity in HeLa cells at 6 and 24 h in the presence of 10 μM of the amide was observed. This result confirms that PEA, at the concentration used in the present study, is able to promote the activation of the apoptotic pathway selectively in tumor cells.

Concluding, in the present study we identify an additional mechanism of PEA action, precisely the induction of proteasome inhibition. Moreover, we demonstrate that PEA can affect tumor cells survival through the activation of apoptosis. This finding could represent an important preliminary step in considering PEA as a possible anti-cancer drug, however further studies are needed to better explore the involved pathways.

5. Acknowledgements

The authors thank the University of Camerino for financial support.

6. References

[1] D.G. Couch, H. Cook, C. Ortori, D. Barrett, J.N. Lund, S.E. O'Sullivan, Palmitoylethanolamide and Cannabidiol Prevent Inflammation-induced Hyperpermeability of the Human Gut In Vitro and In Vivo-A Randomized, Placebo-controlled, Double-blind Controlled Trial. *Inflammatory bowel diseases*, **2019**,25, 1006-1018.

[2] S. Boccella, C. Cristiano, R. Romano, M. Iannotta, C. Belardo, A. Farina, F. Guida, F. Piscitelli, E. Palazzo, M. Mazzitelli, R. Imperatore, L. Tunisi, V. de Novellis, L. Cristino, V. Di Marzo, A. Calignano, S. Maione, L. Luongo, Ultra-micronized palmitoylethanolamide rescues the cognitive decline-associated loss of neural plasticity in the neuropathic mouse entorhinal cortex-dentate gyrus pathway. *Neurobiology of disease*, **2019**,121, 106-119.

[3] S. Cerrato, P. Brazis, M.F. della Valle, A. Miolo, A. Puigdemont, Effects of palmitoylethanolamide on immunologically induced histamine, PGD2 and TNFalpha release from canine skin mast cells. *Veterinary immunology and immunopathology*, **2010**,133, 9-15.

[4] L. Facci, R. Dal Toso, S. Romanello, A. Buriani, S.D. Skaper, A. Leon, Mast cells express a peripheral cannabinoid receptor with differential sensitivity to anandamide and palmitoylethanolamide. *Proceedings of the National Academy of Sciences of the United States of America*, **1995**,92, 3376-3380.

[5] L. Luongo, F. Guida, S. Boccella, G. Bellini, L. Gatta, F. Rossi, V. de Novellis, S. Maione, Palmitoylethanolamide reduces formalin-induced neuropathic-like behaviour through spinal glial/microglial phenotypical changes in mice. *CNS & neurological disorders drug targets*, **2013**,12, 45-54.

[6] S.D. Skaper, L. Facci, M. Fusco, M.F. Della Valle, M. Zusso, B. Costa, P. Giusti, Palmitoylethanolamide, a naturally occurring disease-modifying agent in neuropathic pain. *Inflammopharmacology*, **2014**,22, 79-94.

[7] G. Re, R. Barbero, A. Miolo, V. Di Marzo, Palmitoylethanolamide, endocannabinoids and related cannabimimetic compounds in protection against tissue inflammation and pain: potential use in companion animals. *Vet J*, **2007**,173, 21-30.

[8] J. Lo Verme, J. Fu, G. Astarita, G. La Rana, R. Russo, A. Calignano, D. Piomelli, The nuclear receptor peroxisome proliferator-activated receptor-alpha mediates the anti-inflammatory actions of palmitoylethanolamide. *Mol Pharmacol*, **2005**,67, 15-19.

[9] G. D'Agostino, G. La Rana, R. Russo, O. Sasso, A. Iacono, E. Esposito, G.M. Raso, S. Cuzzocrea, J. Lo Verme, D. Piomelli, R. Meli, A. Calignano, Acute intracerebroventricular administration of palmitoylethanolamide, an endogenous peroxisome proliferator-activated receptor-alpha agonist, modulates carrageenan-induced paw edema in mice. *J Pharmacol Exp Ther*, **2007**,322, 1137-1143.

[10] O. Sasso, R. Russo, S. Vitiello, G.M. Raso, G. D'Agostino, A. Iacono, G.L. Rana, M. Vallee, S. Cuzzocrea, P.V. Piazza, R. Meli, A. Calignano, Implication of allopregnanolone in the antinociceptive effect of N-palmitoylethanolamide in acute or persistent pain. *Pain*, **2012**,153, 33-41.

[11] D. De Filippis, L. Luongo, M. Cipriano, E. Palazzo, M.P. Cinelli, V. de Novellis, S. Maione, T. Iuvone, Palmitoylethanolamide reduces granuloma-induced hyperalgesia by modulation of mast cell activation in rats. *Mol Pain*, **2011**,7, 3.

[12] E. Esposito, I. Paterniti, E. Mazzon, T. Genovese, R. Di Paola, M. Galuppo, S. Cuzzocrea, Effects of palmitoylethanolamide on release of mast cell peptidases and neurotrophic factors after spinal cord injury. *Brain Behav Immun*, **2011**,25, 1099-1112.

[13] Luongo L, Guida F, Gatta L, e. al., Palmitoylethanolamide systemic treatment reduces spinal and supraspinal formalin-induced neuroinflammation and allodynia, in: XIV Congress of the European Shock Society, Taormina, Italy, **2011**.

[14] M. Pistis, M. Melis, From surface to nuclear receptors: the endocannabinoid family extends its assets. *Curr Med Chem*, **2010**,17, 1450-1467.

[15] W.S. Ho, D.A. Barrett, M.D. Randall, 'Entourage' effects of N-palmitoylethanolamide and N-oleoylethanolamide on vasorelaxation to anandamide occur through TRPV1 receptors. *Br J Pharmacol*, **2008**,155, 837-846.

[16] A. Calignano, G. La Rana, D. Piomelli, Antinociceptive activity of the endogenous fatty acid amide, palmitylethanolamide. *Eur J Pharmacol*, **2001**,419, 191-198.

[17] D.M. Lambert, F.G. DiPaolo, P. Sonveaux, M. Kanyonyo, S.J. Govaerts, E. Hermans, J. Bueb, N.M. Delzenne, E.J. Tschirhart, Analogues and homologues of N-palmitoylethanolamide, a putative endogenous CB(2) cannabinoid, as potential ligands for the cannabinoid receptors. *Biochim Biophys Acta*, **1999**,1440, 266-274.

[18] J.M.K. Hesselink, New Targets in Pain, Non-Neuronal Cells, and the Role of Palmitoylethanolamide. *The Open Pain Journal*, **2012**.

[19] C. Marchini, M. Angeletti, A.M. Eleuteri, A. Fedeli, E. Fioretti, Aspirin modulates LPS-induced nitric oxide release in rat glial cells. *Neuroscience letters*, **2005**,381, 86-91.

[20] D. De Filippis, A. D'Amico, M. Cipriano, S. Petrosino, P. Orlando, V. Di Marzo, T. Iuvone, Levels of endocannabinoids and palmitoylethanolamide and their pharmacological manipulation in chronic granulomatous inflammation in rats. *Pharmacol Res*, **2010**,61, 321-328.

[21] J. Adams, The proteasome: structure, function, and role in the cell. *Cancer Treat Rev*, **2003**,29 Suppl 1, 3-9.

International Conference on Cancer Research 2019

Website: www.CancerConf.org

June 10-11, London, UK



Evaluation of Cytotoxic and Antioxidant Activities of Purified Vegetal Extracts and Its Main Pure Compounds

J. Rocha-Pimienta [a*], J. Espino [b], S. Martillanes [a], A.B. Rodríguez [b], J. Delgado-Adámez [a]

[a] *Technological Agri-Food Institute (CICYTEX-INTAEX). Junta of Extremadura. Avda. Adolfo Suárez s/n 06007 Badajoz, Spain.*

[b] *Department of Physiology, Neuroimmunophysiology and Chrononutrition Research Group, Faculty of Science, University of Extremadura, Avda. Elvas s/n, 06006 Badajoz.*

Abstract

Vegetal aqueous extracts are an important source of phytochemicals with biological activities. Concretely, olive leaf extract (OLE) and green tea extract (GTE) contain a high amount of phenolic compounds that present antioxidant, antibacterial and cytotoxic properties, among others. As described in literature, plant extracts containing photosynthetic pigments, such as chlorophylls, may cause an undesirable pro-oxidant effect when applied in food matrices. Such pro-oxidant effect, however, must be analysed according to the final applicability of the extract.

The aim of this work was to purify natural extracts' phenolic content by elimination of chlorophyll compounds and evaluate the cytotoxic and antioxidant activity of the extracts, the importance of the individual major phenolic compounds and the influence of chlorophylls. The extracts were characterized by HPLC which showed that they contained different phenolic compounds in high concentration, particularly, OLE contained mainly hydroxytyrosol, oleuropein and tyrosol, while GTE contained caffeine, gallocatechin, epigallocatechin, epigallocatechin gallate, gallocatechin gallate as main phenolics. Afterwards, extracts were subjected to purification process by column chromatography and the amount of phenolic compounds decreased because the column yield was 33-58%.

The antioxidant capacity of the extracts was evaluated by ABTS method. Pro-oxidant or anti-oxidant activity of individual phenolic compounds were concentration-dependent because when the extracts were doped with individual compounds, this fact generated a decrease in antioxidant activity compared to fresh extracts. The individual phenolic compounds did not show synergic effect when combined, and the elimination of chlorophyll compounds did not generate a change in the antioxidant activity of extracts, suggesting that these vegetal pigments are not relevant to such capacity. On the other hand, the cytotoxic activity of the extracts was tested against HL-60 leukemic cells using the MTS tetrazolium salt reduction assay. The results showed that both OLE and GTE had a high antiproliferative activity, 66.3% and 70.1%, respectively and, in contrast to their antioxidant activity, the elimination of chlorophyll compounds generated an important decrease of cytotoxic effect in both cases. Only hydroxityrosol and caffeine phenolic compounds individually showed important antiproliferative activity, 44.5% and 25.2%, respectively. But when the fresh extracts were doped with some individual compounds, the cytotoxic capacity was increased. This can be explained by the extract's matrix effect on the individual compounds.

In conclusion, these results highlight the great antioxidant and antiproliferative potential of the natural extracts tested. In addition, these findings showed that photosynthetic pigments acquired a considerable relevance in the cytotoxic capacity of OLE and GTE.

Keywords:

Green Tea;

Olive Leaf;

Pro-oxidant;

Chlorophyll;

Bioactivity.

1. Introduction

Over the years, plants have been an important source of bioactive and phytochemical compounds which have been used for application in many fields, including medicine and food industry. A large number of functional and nutraceutical ingredients are currently being developed from plant derivatives and their phytochemicals. Medicinal plants used as food for the prevention and/or control of diseases are natural sources of antioxidant substances such as phenolic compounds [1]. Epidemiological studies have shown that people who eat diets rich in fruits and vegetables have a lower risk of degenerative diseases, such as cancer, cardiovascular disease and diseases derived from these [2], among many others. These potential benefits for humans are attributed to their phytochemical components such as vitamins, lycopenes, carotenoids and phenolic compounds.

Phenolic compounds are secondary metabolites with a considerable physiological and morphological importance in plants. Our body cannot naturally synthesize phenolic compounds, so they must be incorporated into the diet along with

* **CONTACT**: javier.rocha@juntaex.es

other essential nutrients in order to enjoy their benefits. This group of compounds mainly possesses antioxidant activity to prevent the oxidation damage by reactive species [1], avoid the initiation stages of cancer [3], and exert positive effects against cardiovascular problems [4]. Besides, some authors have described pro-oxidant effects of this molecules [5], a capacity that needs to be studied in depth to determine its mechanisms and the possible future applicability due to its relationship with anti-cancer properties.

These bioactive molecules have been found in important concentrations in many parts of plants such as olive leaves [6] and green tea leaves [7]. The major individual phenolic compounds identified in olive leaves aqueous extract (OLE) are caffeic acid, hydroxytyrosol, quercetin, luteolin, ligstroside, oleuropein, demethyloleuropein, vanillic acid, verbascoside and tyrosol [6]. The main responsible for its antioxidant properties is oleuropein [8], a secoiridoid recognized by European Food Safety Authority (EFSA) as suitable substance for use in food supplements due to its health benefits, such as increase in glucose tolerance. Moreover, it has been described that oleuropein and hydroxytyrosol (phenolic alcohol) decrease the number of MCF-7 cells by inhibiting the rate of cell proliferation and inducing cell apoptosis [9]. Other biological properties of OLE include its antiviral [10] and antimicrobial activity against human pathogens [11].

On the other hand, Rusak et al. [7] confirmed that green tea is a richer source of phenolics than other tea species, in which eight catechins (epigallocatechin gallate (EGCG), epigallocatechin (EGC), epicatechin gallate (ECG), epicatechin, gallocatechin gallate, gallocatechin, catechin gallate and catechin), caffeine and eight other minor phenolic compounds are identified [12]. These major phenolic compounds in green tea mainly present antioxidant and anti-cancer properties. Catechins, when combined with anti-cancer compounds, have anti-cancer capacity against numerous cancer cell lines as human head, neck, lung, breast, prostate, liver, ovarian, leukemia, malignant neuroblastoma and various organs cancer cells [13]. Its mechanisms of action are very varied including the induction of apoptosis by enhancing the expression of genes that regulate it, synergistic inhibition of cell proliferation and colony formation, and inhibition of kinases as well as activation of caspases, among many others. Three of the main green tea catechins, namely EGCG, EGC and ECG, have cancer-preventive activity, and the combination of them has synergistic effects on the induction of apoptosis and inhibition of cell growth in PC-9 cells, and inhibits the release of TNF-α, an endogenous tumor promoter [14]. Concretely, it has been described the synergistic enhancement of apoptosis, gene expression, and anti-cancer effects using various combinations of EGCG and anti-cancer drugs such as COX‐2 inhibitors [15]. Also, catechins possess other properties such as antimicrobial and anti-inflammatory actions, among many others [16].

Furthermore, plant extracts contain photosynthetic pigments such as chlorophylls, which are necessary for the absorption of sunlight in photosynthesis. Chlorophyll and its various derivatives present biological activities such as cancer prevention, induction of apoptotic events, antioxidant activity and antimutagenic activity. These encouraging results have led to the investigation of their chemopreventive effects in humans [17]. Due to their light-absorbing properties, the energy absorbed by these molecules can be transferred to oxygen, resulting in the production of reactive oxygen species (ROS) and thus presenting pro-oxidant activity. In addition, Wanasundara and Shahidi [18] reported that the presence of chlorophyll in green tea extracts (GTE) was responsible for their pro-oxidant effect on the oxidation of marine oils. Nonetheless, not only the chlorophylls are responsible for such pro-oxidant activity, the concentration of individual phenolic compounds can also generate this effect [5].

The pro-oxidant properties of chlorophylls and catechins [19] are relevant for the anticancer capacity of these extracts. This is a field worth to be investigated to clarify its mechanisms of action for a putative application in cancer therapy. Many studies have evaluated the properties of bioactive compounds individually, but these compounds are not isolated in nature but interact with each other, thereby enhancing their activity in some cases. This is the so-called synergic effect. On the other hand, these compounds can act in one way or another depending on the medium in which they are located and the composition thereof. The modification of its properties depending on the set of molecules that surround them is known as matrix effect.

Therefore, the aim of the present study was to investigate the cytotoxic and antioxidant capabilities of an OLE and a GTE before and after a purification process to eliminate their chlorophylls. Additionally, it was intended to determine the possible synergic or matrix effects of the main phenolic compounds of the extracts and the influence of the chlorophylls on these bioactivities.

2. Materials and methods

2.1. Preparation of raw material

Olive leaves were picked up from a local company (Badajoz, Spain). The samples were immediately transported to the laboratory in ventilated storage trays, vacuum-packaged (Gustav Müller VS 100, Germany) in plastic bags (500 gr) and frozen until their use (-80ºC). These processes were carried out with care to avoid changes in the composition of the material. Dried green tea leaves were obtained from a local market.

2.2. Extraction of bioactive compounds from extracts

Before extraction treatment, fresh olive leaves were washed with distilled water and partially dried (model 210, Selecta® P, Spain) during 12 min at 120ºC. Dried samples (green tea and olive leaves) were ground in a domestic knife mill to obtain particles (0.5-3.0 mm). Then, bioactive compounds were extracted with water (1:10 w/v) at 118ºC for 15 min, the samples were filtered and centrifuged to remove solid particles. Finally, the extracts were frozen at -80°C until

further analysis. The extracts purification was carried out using a column (1.25 cm internal diameter and 20cm height) packed with Toyopearl HW-40F (Tosoh Bioscience LLC) was used. Crude extracts were dissolved in 80% (v/v) aqueous ethanol and introduced onto the column. The column was eluted with hexane until all the residual green colour had disappeared. The column was then washed with 80% (v/v) aqueous ethanol to recover the dechlorophyllized green tea extracts. Ethanol was removed by evaporation under vacuum at 40°C using a rotary evaporator and the residual water was removed by lyophilization.

2.3. Experimental design

The extracts were analysed in crude and after the purification process. The composition of phenolic compounds, the antioxidant and cytotoxic activities were evaluated to detect changes in the bioactive compounds present in the extracts. In order to evaluate the possible synergic or matrix effect on the antioxidant and cytotoxic activities of individual phenolic compounds present in GTE and OLE, the extracts were diluted (1:10 v/v) and mixed with standards of oleuropein, hydroxytirosol (Extrasynthése, Genay, France) and tyrosol (Sigma-Aldrich Chemie, Steinheim, Germany) in the case of OLE, and with caffeine (Enzo Biochem, Farmingdale, USA), gallocatechin (Extrasynthése, Genay, France), epigallocatechin, gallocatechin gallate (Chengdu Biopurify Phytochemicals, Sichuan, China) and epigallocatechin gallate (Adipogen, Liestal, Switzerland) in the case of GTE. The combinations analysed are summarized in table 1 and table 2.

Table 1. Experimental design followed to evaluate the matrix effect between phenolic compounds of GTE. Individual standards of phenolic compounds, a mixture of them (multi-standard) as well as diluted GTE mixed with standards were evaluated.

	Caffeine (mg/kg)	Gallocatechin (mg/kg)	Epigallocatechin (mg/kg)	Epigallocatechin gallate (mg/kg)	Gallocatechin gallate (mg/kg)	Abbreviations
Multi-standard	2000	2000	2000	2000	2000	TMIX
Individual Standards	2000	-	-	-	-	CA
	-	2000	-	-	-	GC
	-	-	2000	-	-	EGC
	-	-	-	2000	-	EGCG
	-	-	-	-	2000	GCG
Fresh extract	-	-	-	-	-	GTEC
	2000	-	-	-	-	GTEC+CA
	-	2000	-	-	-	GTEC+GC
	-	-	2000	-	-	GTEC+EGC
	-	-	-	2000	-	GTEC+EGCG
	-	-	-	-	2000	GTEC+GCG
Purified extract	-	-	-	-	-	GTENC
	2000	-	-	-	-	GTENC+CA
	-	2000	-	-	-	GTENC+GC
	-	-	2000	-	-	GTENC+EGC
	-	-	-	2000	-	GTENC+EGCG
	-	-	-	-	2000	GTENC+GCG

Table 2. Experimental design followed to evaluate the matrix effect between phenolic compounds of OLE. Individual standards of phenolic compounds, a mixture of them (multi-standard) as well as diluted OLE mixed with standards were evaluated.

	Oleuropein (mg/kg)	Tyrosol (mg/kg)	Hydroxytyrosol (mg/kg)	Abbreviations
Multi-standard	2000	2000	2000	OMIX
Individual Standards	2000	-	-	O
	-	2000	-	TY
	-	-	2000	HY
Fresh extract	-	-	-	OLEC
	2000	-	-	OLEC+O
	-	2000	-	OLEC+TY
	-	-	2000	OLEC+HY
Purified extract	-	-	-	OLENC
	2000	-	-	OLENC+O
	-	2000	-	OLENC+TY
	-	-	2000	OLENC+HY

2.4. HPLC analysis of phenolic compounds of the OLE and GTE before and after purification

Standards of polyphenolic compounds were prepared in methanol and stored in darkness at -20ºC. HPLC mobile phases were prepared with HPLC grade methanol and acetonitrile (Fisher Chemical, Loughborough, UK) and P.A. grade formic acid (PANREAC, Barcelona, Spain). The HPLC analysis was carried out following the method and conditions described by Cabrera-Bañegil et al. [20]. Main phenolic compounds analysis was carried out with an Agilent 1100 HPLC system (Hewlett-Packard, Waldbronn, Germany), which was equipped with a diode array detector (DAD) and fluorescence detector (FLD). Also, for this determination, a Gemini-NX C18 column was used (150x4.6 mm i.d., 3 µm thickness, Phenomenex).

2.5. Antioxidant activity assays of the extracts

The antioxidant capacity of the extract samples was determined by the ABTS•+ method [21]. In this assay, 100 µl of ABTS solution (2.2'-azinobis (3-ethylbenzoithiazolone 6-sulphonate)) were mixed with different combinations of extracts samples (Tables 1 and 2) and these mixtures were added to 96-well microtiter plates. Absorbance was measured at 730 nm and results were expressed as mmol Trolox 10 mL^{-1} using a calibration curve of Trolox.

2.6. Cell culture

Human promyelocytic leukemia HL-60 cell line (ECACC No. 88120805; Dorset, UK) was grown in RPMI 1640 medium (Lonza) supplemented with 2 mM L-glutamine, 10% heat-inactivated fetal bovine serum, 100 U/mL penicillin and 100 µ/mL streptomycin. Cells were cultured in a humidified atmosphere containing 5% CO_2 at 37ºC.

2.7. In vitro cytotoxicity assay

The cytotoxic effects of the different extracts were assayed on HL-60 cell line by means of the CellTiter 96® AQueous One Solution Cell Proliferation Assay (Promega, Madrid, Spain), which is based on the reduction of an MTS tetrazolium compound. Cells were seeded in 96-well plates at a density of 2×10^4 cells/well. After treating cultures for 24h, assays were performed by adding 10 µl of the CellTiter 96® AQueous One Solution Reagent directly to culture wells, incubating for 2h at 37 ºC, and then recording absorbance on a microplate reader (Infinite M200; Tecan Austria GmbH, Groedig, Austria) at a test wavelength of 490 nm and a reference wavelength of 650 nm to subtract background. All analyses were run in triplicate. The cell viability was calculated as percentage of control values (untreated samples).

2.8. Statistical analysis

Three replicates were carried out for each treatment and analysis. The results were represented as means and standard deviations and were analysed by SPSS 18.0 statistical software (SPSS Inc., Chicago, IL). One-way analysis of variance

(ANOVA) was used to compare the data, and all the tests were considered statistically significant at $p<0.05$. When analysis detected significant differences, means were compared using Tukey's test and Student's t-test.

3. Results and discussion

3.1. Phenolic compounds content of extracts and changes after purification

The quantification of the main phenolic compounds content in OLE and GTE before and after purification are shown in Table 3.

Table 3. Concentration of main phenolic compounds of OLE and GTE (mg/L) in fresh extracts and after purification. Results are expressed as means ± SD of three sample replicates. *Significant statistical differences between purified and its fresh extract (Student's t-test, p<0.05).

Compounds (mg/L)	Fresh OLE	Purified OLE
Phenolic Alcohols		
Hydroxytyrosol	445.73±3.10	187.30±7.68*
Tyrosol	12.09±2.58	5.83±0.16*
Secoiridoids derivatives		
Oleuropein	2173.52±110.80	679.53±12.73*
Compounds (mg/L)	**Fresh GTE**	**Purified GTE**
Alkaloid		
Caffeine	2232.52±208.16	1483.30±23.61*
Catechins		
Gallocatechin	2536.82±16.55	2215.18±59.39*
Epigallocatechin	948.80±36.29	802.00±93.18
Epigallocatechin gallate	1829.27±172.21	109.32±3.27*
Gallocatechin gallate	658.52±18.44	70.73±6.52*

The purification of the phenolic compounds from the extracts and the elimination of the chlorophylls produced the loss of polyphenols. The total phenolic content was 8205,94 mg/L and 4680.52 mg/L for fresh GTE and purified GTE, respectively, while it was 2631.34 mg/L and 872.67 mg/L for fresh OLE and purified OLE, respectively. Therefore, the efficiency of the purification column was 57.03% and 33.16% for GTE and OLE, respectively. After these results, the main phenolic compounds and caffeine in fresh GTE were quantified individually by HPLC (table 3): gallocatechin (2536.82 mg/L), caffeine (2232.52 mg/L), epigallocatechin gallate (1829.27 mg/L), epigallocatechin (948.80 mg/L) and gallocatechin gallate (658.52 mg/L).

These results are in agreement with previous findings described by other researchers, such as Kang et al. [22], who identified them as majority compounds in the Korean GTE, with epigallocatechin gallate being the most concentrated. Perva-Uzunalić et al. [23] also identified these compounds as the most abundant in GTE, wherein EGCG represented 67.5% of the main catechins of green tea leaves.

The purification process generated a significant decrease in all these compounds found in the GTE (table 3). The most relevant decrease was observed in EGCG and gallocatechin gallate which was significantly different.

On the other hand, major phenolic compounds in OLE were oleuropein (2173.52 mg/L) and hydroxytyrosol (445.73 mg/L). Despite the fact that it was found at much lower concentration, tyrosol (12.09 mg/L) was also analysed, because it is an important biomolecule. In fact, the phenolic compounds identified represented more than 80% of the total compounds of the OLE [24]. In the same way, the purification of the extract caused a considerable decrease in the phenolic compounds analysed, with a significant reduction in oleuropein and hydroxytyrosol (table 3).

The elaboration process of the extracts was optimized for the preservation of phenolics compounds [25]. These compounds were water-soluble since we used aqueous phase to obtain the extracts. Methanol or hexane were rejected owing to its toxicity [26] with a view to future applications of the extracts in fields like medicine or agroindustry.

The loss in phenolic content during purification of the extracts is due to the fact that these compounds may be retained in the purification column and not fully recovered or that some of them may undergo transformations. This has been reported when extracts are subjected to a column purification process, whose phenolic compounds can react and suffer transformations into simpler compounds or interact with each other [27]. Specifically, this is what usually happens to gallates, which are transformed during similar processes into other compounds such as gallic acid. Another factor influencing the final efficiency of the purification process by a chromatographic column is the retention of compounds into the column. The final passage of the eluent through it to entrain the compounds of interest does not separate them all and, therefore, its final efficiency decreases.

This evident decrease in the phenolic content due to the process of purification and elimination of the chlorophylls may also generate a decrease in their bioactive properties, an undesirable side-effect in some cases, since the elimination of photosynthetic pigments is intended to enhance them.

The chemical data discussed in this research can be considered useful in providing information about the presence of major and minor compounds in olive leaves and green tea leaves. The amount of phenolic compounds is an important factor when the quality of extracts is assessed and because of the beneficial effects of these components on human health.

3.2. Antioxidant activity of extracts and effects of chlorophylls

The antioxidant activity of the phenolic compounds of green tea and olive leaves has been identified as one of their most important benefits, with catechins and oleuropein being the most powerful antioxidants in these groups [28, 8]. In order to verify that the possible loss of antioxidant activity is due to the loss of phenolic compounds during the purification process, the raw extract data were normalised to compare them with the purified extract. In case of GTE, the efficiency of the purification column was 57.03%, a figure proportional to the remaining antioxidant activity in the purified extract (no statistical differences). Then, it can be ruled out that chlorophylls play an important role in the antioxidant capabilities of GTE, which therefore indicates that the antioxidant activity appearing in the purified extract corresponds only to the effect exerted by phenolic compounds.

Results of antioxidant activity of fresh GTE, purified GTE and their different combinations (table 1) is showed in figure 1.

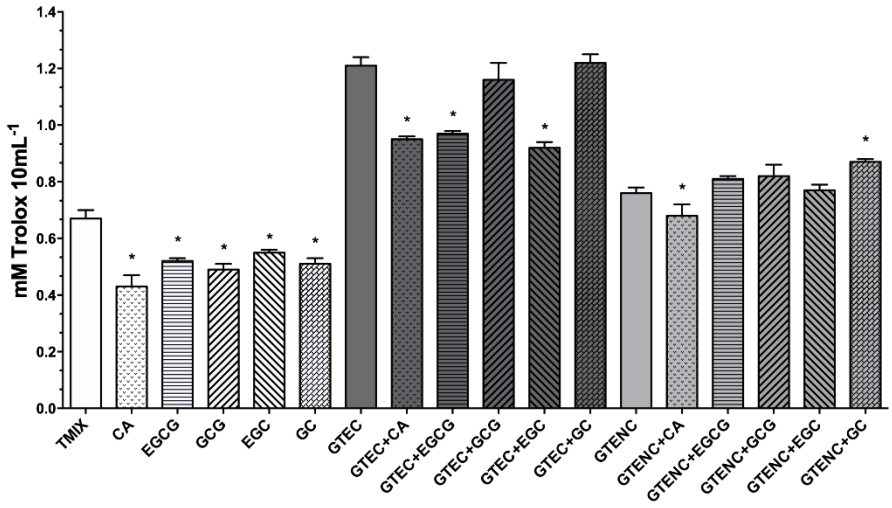


Figure 1. Antioxidant activity of GTE showed as mM Trolox 10 mL^{-1}. Mixed pure majority phenolic compounds of GTE (TMIX), caffeine (CA), epigallocatechin gallate (EGCG), gallocatechin gallate (GCG), epigallocatechin (EGC), gallocatechin (GC), GTE crude (GTEC), GTE crude with caffeine (GTEC + CA), GTE crude with epigallocatechin gallate (GTEC + EGCG), GTE crude with gallocatechin gallate (GTEC + GCG), GTE crude with epigallocatechin (GTEC + EGC), GTE crude with gallocatechin (GTEC + GC), purified GTE (GTENC), purified GTE with caffeine (GTENC + CA), purified GTE with epigallocatechin gallate (GTENC + EGCG), purified GTE with gallocatechin gallate (GTENC + GCG), purified GTE with epigallocatechin (GTENC + EGC) and purified GTE with gallocatechin (GTENC + GC) are analyzed. Results are showed as means ± SD. *Means show significant differences ($p<0.05$) by Tukey's multiple test between the doped extracts with their corresponding non-doped and between the individual compounds with the mix.

As previously described in literature and corroborated by our own results, GTE has a high antioxidant capacity of 1.2 mM Trolox 10 mL^{-1}. All pure GTE compounds individually showed antioxidant activity, with EGC showing the highest antioxidant activity (significant differences; $p<0.05$). The mix of GTE compounds (TMIX) showed more antioxidant capacity than the individual compounds by themselves but it was not enough to confirm an accumulative or synergic effect between them. Numerous studies have shown the great antioxidant capacity of catechins, which are more effective in protecting the oxidative damage caused to DNA by free radicals than vitamin C [29], vitamin E, tocopherol and

carotenes [30]. Other researchers such as Lee et al. [31] stated that the total antioxidant capacity of tea is not related to a particular type of polyphenols, but to the combined activity of various antioxidants, including phenolic acids and polyphenols.

As for fresh extracts doped with pure compounds, the tendency is to maintain their antioxidant activity or a decreased onet with respect to undoped extract. This phenomenon is due to the pro-oxidant activity shown by phenolic compounds, which depends on the applied dose [5]. In fact, the increase of their concentration in the extract generates the appearance of pro-oxidant activity instead of increasing the antioxidant effect. The purified extract doped with the standards showed the same pattern of action as the non-purified extracts, with the exception of the gallocatechin-doped extract (GTENC+GC), which significantly increased its antioxidant activity. Similarly, saturation in the concentration of compounds added to the extract generated the appearance of pro-oxidant activity or no increase in antioxidant effect.

This experimental design is based on the results obtained by Wanasundara and Shahidi [18], which showed that GTE exhibited a pro-oxidant effect when applied to edible marine oils due to the catalytic effect of their chlorophyll, presenting an important antioxidant activity after pigment removal. These results indicate that the extract may present a negative dose-dependent matrix effect because, in some cases, the increase in the concentration of phenolic compounds causes a negative effect, thus decreasing the antioxidant capacity and in some cases even a pro-oxidant effect.

This pro-oxidant activity may be a positive feature for potential therapeutic applications against cancer. Therefore, consumption of green tea may induce oxidative stress, which may lead to ROS-mediated death of cancer cells or may eliminate ROS under conditions of high oxidative stress, thus preventing cell damage [32]. In addition, Azam et al. [19], stated that these pro-oxidant effects appear to be responsible for the induction of apoptosis in tumor cells, and may also induce activation of endogenous antioxidant systems in normal tissues that offer protection against tumor threat.

On the other hand, results of antioxidant activity of fresh OLE, purified OLE and its different combinations (table 2) is showed in figure 2.

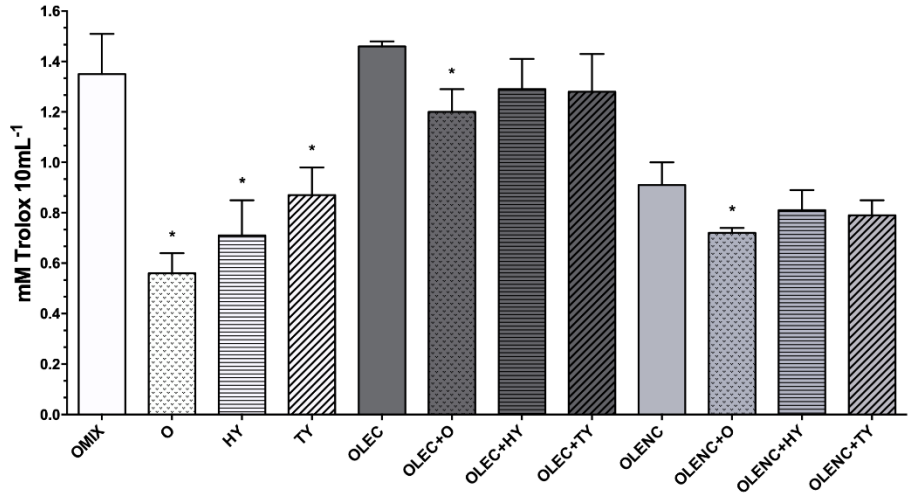


Figure 2. Antioxidant activity of OLE showed as mM Trolox 10 mL^{-1}. Mixed pure majority phenolic compounds of OLE (OMIX), oleuropein (O), hidroxytyrosol (HY), tyrosol (TY), OLE crude (OLEC), OLE crude with oleuropein (OLEC + O), OLE crude with hydroxytyrosol (OLEC + HY), OLE crude with tyrosol (OLEC + TY), purified OLE (OLENC), purified OLE with oleuropein (OLENC + O), purified OLE with hydroxytyrosol (OLENC + HY), purified OLE with tyrosol (OLENC + TY) are analyzed. Results are showed as means ± SD. *Means show significant differences ($p<0.05$) by Tukey's multiple test between the doped extracts with their corresponding non-doped and between the individual compounds with the mix.

Normalized data from fresh OLE reflected that the decrease in the antioxidant activity of the purified extract was not proportional (lower) to the reduction in phenolic content due to the purification process (statistical differences), thereby indicating that chlorophylls are not important for the antioxidant activity of OLE. This piece of data corroborated that a superior concentration of phenolic compounds generates a pro-oxidant activity [5]. Fresh OLE presented high antioxidant activity with value of 1.46 mmol Trolox 10 mL^{-1}. In fact, the OLE used herein had much higher antioxidant activity, 15-fold higher, than other foods such as virgin olive oil [25]. The OLE showed a similar behaviour to the GTE. Pure standard compounds had an important antioxidant activity when used individually: tyrosol had the greatest capacity and oleuropein the lowest. This activity increased when the compounds were put together, but the mixture (OMIX) did not show a synergic effect because this activity was lower than the sum of their individual activities. In addition, both the fresh and the purified OLE displayed the same behaviour. All the doped extracts exhibited decrease antioxidant activity but only the oleuropein-doped extracts (OLEC+O and OLENC+O) presented statistically significant differences. These reductions support the previous results observed on the dose-dependent pro-oxidant activity of phenolic compounds.

The preservation of phenolic compounds in OLE is desirable for its use for preventive and/or therapeutic purposes due to their protective effect against oxidative damage in human red blood cells [33]. Likewise, some authors reported the anticancer potential shown by olive phenolic compounds like oleuropein [34]. Not only the oleuropein displayed cytotoxic activity, but also hydroxytyrosol induce the death of MCF-7 cells by inhibiting the rate of cell proliferation and inducing cell apoptosis [9]. Finally, other studies corroborated that polyphenolic antioxidants exhibited a dose-dependent toxicity against human promyelocytic leukemia cells (HL- 60), which was accompanied by malondialdehyde formation [35]. For these reasons, the goal of this study was to explore in depth the relationship between different molecules that compose the extracts and their antioxidant and anti-cancer activity.

3.3. Cytotoxic activity of extracts and chlorophylls effects

There is a lot of literature describing the anti-cancer or cytotoxic activity of plant extracts and phytochemicals contained in them. However, it is necessary to deepen and investigate the mechanisms of action of these molecules, the influence of others present in the extracts, and the interaction between them.

Figure 3 shows the results of cytotoxic activities of the different GTE assayed (table 1) against human promyelocytic leukemia HL-60 cell line.

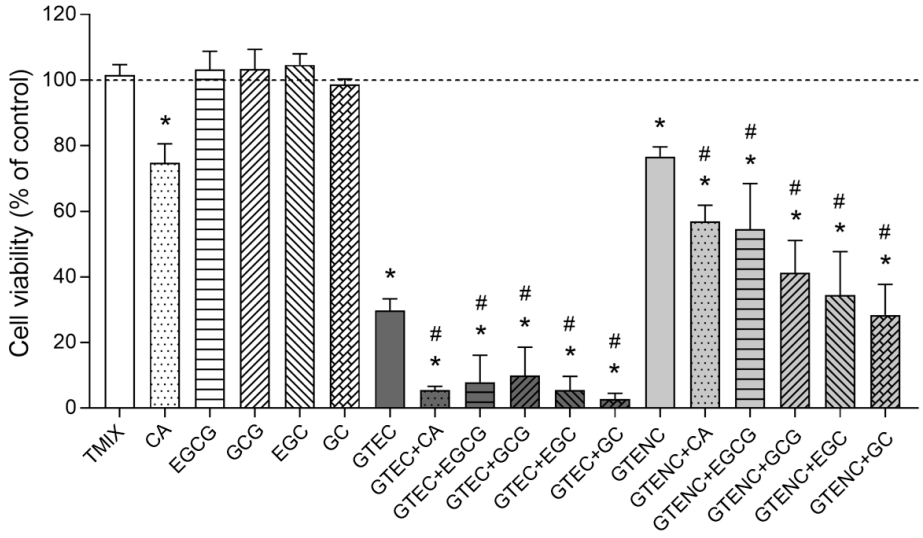


Figure 3. Antiproliferative activity of mixed pure majority phenolic compounds of GTE (TMIX), caffeine (CA), epigallocatechin gallate (EGCG), gallocatechin gallate (GCG), epigallocatechin (EGC), gallocatechin (GC), GTE crude (GTEC), GTE crude with caffeine (GTEC + CA), GTE crude with epigallocatechin gallate (GTEC + EGCG), GTE crude with gallocatechin gallate (GTEC + GCG), GTE crude with epigallocatechin (GTEC + EGC), GTE crude with gallocatechin (GTEC + GC), purified GTE (GTENC), purified GTE with caffeine (GTENC + CA), purified GTE with epigallocatechin gallate (GTENC + EGCG), purified GTE with gallocatechin gallate (GTENC + GCG), purified GTE with epigallocatechin (GTENC + EGC), and purified GTE with gallocatechin (GTENC + GC). Results are showed as means ± SD. *Means show significant differences against the control (100 % of viability) by Tukey's multiple test ($p<0.05$). #Means show significant differences between the doped extract and its corresponding non-doped extract by Tukey's multiple test ($p<0.05$).

Normalized data of fresh GTE showed that the elimination of chlorophylls produced a negative effect on the cytotoxic potential of the fresh GTE as cytotoxic activity was decreased by 50% after the purification process (statistically significant). These results, in contraposition of antioxidant capacity of GTE, indicate that the photosynthetic pigments have an important role in the extract's cytotoxic capacity.

As for the individual compounds of GTE, the only compound with cytotoxic activity was caffeine (74.85% of cell viability). The other compounds and the mix (TMIX) did not show activity, the latter probably due to a negative matrix effects of the other compounds on caffeine. The cytotoxicity of caffeine had been described by other authors, who affirmed that caffeine inhibited ATM and ATR kinases which leads to the disruption of multiple DNA damage-responsive cell cycle checkpoints and greatly sensitized tumor cells to antitumor agents [36]. Caffeine may also block repair of DNA lesions through a direct interference with DNA-PK activity and other DNA repair enzymes [37].

In addition, the doped extracts showed an important positive matrix effect. Both purified and non-purified doped extracts further increased their cytotoxicity as the concentration of pure compounds present in them also increased (statistically significant differences). The compound with the highest increase in cytotoxic activity was galocatechin (GC). This fact, together with the results showing that the individual compounds did not have cytotoxic capacity, reinforces the idea that catechins act by potentiating the cytotoxic activity presented by other molecules. As mentioned above, green tea catechins such as EGCG combined with anticancer drugs generate synergistic enhancement of

apoptosis, gene expression changes and anti-cancer effects [15]. Besides, Fujiki and Suganuma [38] confirmed that the combination of anti-cancer drugs with green tea catechins synergistically induces apoptosis of human cancer cells, inhibits tumor formation in mice, and enhances inhibition of tumor growth in xenograft mouse models.

On the other hand, figure 4 shows the results of cytotoxic activities of the different OLE assayed (table 2).

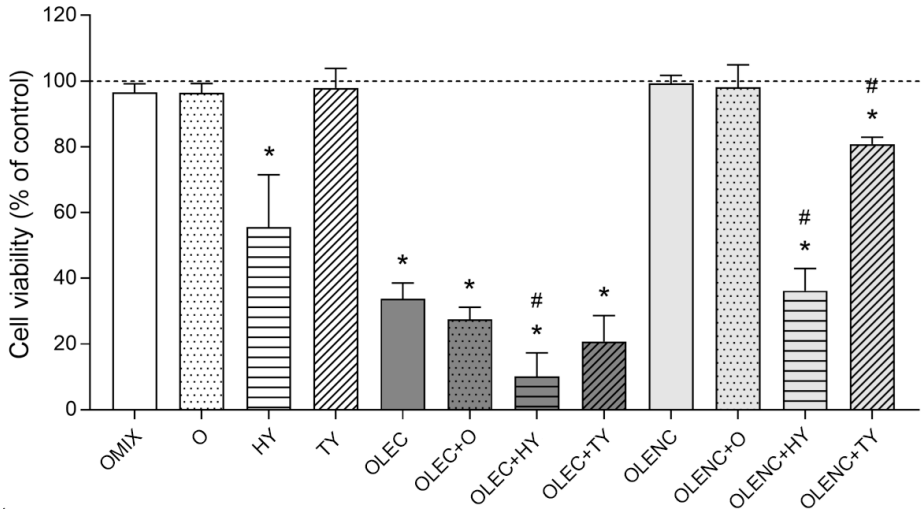


Figure 4. Antiproliferative activity of mixed pure majority phenolic compounds of OLE (OMIX), oleuropein (O), hidroxytyrosol (HY), tyrosol (TY), OLE crude (OLEC), OLE crude with oleuropein (OLEC + O), OLE crude with hydroxytyrosol (OLEC + HY), OLE crude with tyrosol (OLEC + TY), purified OLE (OLENC), purified OLE with oleuropein (OLENC + O), purified OLE with hydroxytyrosol (OLENC + HY), and purified OLE with tyrosol (OLENC + TY). Results are showed as means ± SD. *Means show significant differences against the control (100 % of viability) by Tukey's multiple test ($p<0.05$). #Means show significant differences between the doped extract and its corresponding non-doped extract by Tukey's multiple test ($p<0.05$).

Like in fresh GTE, normalized data of fresh OLE demonstrated that the elimination of chlorophylls generated a marked decrease in its cytotoxic activity due to the purification process. The purification process allowed to recover 33% of the phenolic compounds found in the extract with the consequent elimination of chlorophylls. This fact, together with the results already described, indicates that chlorophylls play a major role in the anti-cancer activity of OLE. The importance of the chlorophylls in chemoprevention has been previously described. Thus, chlorophyll and chlorophyllin can form complexes with certain chemicals that cause cancer such as aflatoxin-B1. These complexes may interfere with gastrointestinal absorption of potential carcinogens, and the amounts of carcinogenic substances in susceptible tissues may be reduced [17]. Also, this molecule is credited with the ability to prevent cancer by means of different mechanisms including its antioxidant and antimutagenic activity, mutagen trapping, modulation of xenobiotic metabolism, and induction of apoptosis [39]. Although, the direct action of chlorophylls against cancer cells have not been described yet, it is clear the importance of these compounds for future anti-cancer therapies.

In addition, with regard to the OLE pure compounds, only the hydroxytyrosol showed a cytotoxic activity (55.56% of cell viability). The OMIX did not show cytotoxic activity probably for the same reason as TMIX, i.e., the other compounds produced a negative matrix effect on hydroxytyrosol.

Finally, the doped extracts showed the same behaviour (both fresh and purified) in so that oleuropein and tyrosol generated a slight increase in cytotoxic capacity while hydroxytyrosol caused a large increase on such activity (statistically significant). The anti-cancer capacity of hydroxytyrosol is well known, although the mechanisms of action are not completely clear. Several studies demonstrated that this phenolic compound is a potent antioxidant phenol and also possesses antiproliferative, pro-apoptotic, as well as anti-inflammatory activities. These activities have the potential to counteract specific cancer hallmarks, thus representing the expectant biological activities underlying the anti-tumor properties of hydroxytyrosol [40]. It has been also reported that hydroxytyrosol has a significantly protective effect against UVB-induced oxidative DNA damage due to its antioxidant activity [41]. Moreover, it has been shown that hydroxytyrosol protects against other different cancer cell types, such as those derived from gut [42], blood [43], prostate [44], and breast [45].

Given the results obtained in this study and those from previous experiments which remark the importance of chlorophylls, one can speculate that there are substantial possibilities for using both extracts (GTE and OLE) as potential tools in future human anti-cancer research and therapy. Nevertheless, it is necessary to further investigate on the mechanism of action of these molecules and the interaction effect between them to potentiate their activity.

4. Acknowledgements

The authors thanks to INIA (RTA2 015-00001-00-0), the Regional Government of Extremadura and FEDER funds for the economic aid received (IB16208 and GR18192 (AGA002)). S. Martillanes thanks the Valhondo Calaff Foundation for the predoctoral formation contract granted. J. Espino holds a post-doctoral fellowship financed by Ministerio de Ciencia, Innovación y Universidades (IJCI-2016-28030).

5. References

[1]. Balasundram, N., Sundram, K., & Samman, S. (2006). Phenolic compounds in plants and agri-industrial by-products: Antioxidant activity, occurrence, and potential uses. Food Chemistry, 99(1), 191–203. https://doi.org/10.1016/j.foodchem.2005.07.042

[2]. Van't Veer, P., Jansen, M. C., Klerk, M., & Kok, F. J. (2008). Fruits and vegetables in the prevention of cancer and cardiovascular disease. Public Health Nutrition, 3(01), 103–107. https://doi.org/10.1017/s1368980000000136

[3]. Moon, Y. J., Wang, X., & Morris, M. E. (2006). Dietary flavonoids: effects on xenobiotic and carcinogen metabolism. Toxicology in vitro, 20(2), 187-210. https://doi.org/10.1016/j.tiv.2005.06.048

[4]. Kris-Etherton, P. M., Hecker, K. D., Bonanome, A., Coval, S. M., Binkoski, A. E., Hilpert, K. F., ... & Etherton, T. D. (2002). Bioactive compounds in foods: their role in the prevention of cardiovascular disease and cancer. The American journal of medicine, 113(9), 71-88. https://doi.org/10.1016/S0002-9343(01)00995-0

[5]. Dintcheva, N. T., Arrigo, R., Baiamonte, M., Rizzarelli, P., & Curcuruto, G. (2017). Concentration-dependent anti-/pro-oxidant activity of natural phenolic compounds in bio-polyesters. Polymer Degradation and Stability, 142, 21–28. https://doi.org/10.1016/j.polymdegradstab.2017.05.022

[6]. Talhaoui, N., Taamalli, A., Gómez-Caravaca, A. M., Fernández-Gutiérrez, A., & Segura-Carretero, A. (2015). Phenolic compounds in olive leaves: Analytical determination, biotic and abiotic influence, and health benefits. Food Research International, 77, 92–108. https://doi.org/10.1016/j.foodres.2015.09.011

[7]. Rusak, G., Komes, D., Likić, S., Horžić, D., & Kovač, M. (2008). Phenolic content and antioxidative capacity of green and white tea extracts depending on extraction conditions and the solvent used. Food Chemistry, 110(4), 852–858. https://doi.org/10.1016/j.foodchem.2008.02.072

[8]. Škerget, M., Kotnik, P., Hadolin, M., Hraš, A. R., Simonič, M., & Knez, Ž. (2005). Phenols, proanthocyanidins, flavones and flavonols in some plant materials and their antioxidant activities. Food Chemistry, 89(2), 191–198. https://doi.org/10.1016/j.foodchem.2004.02.025

[9]. Han, J., Talorete, T. P. N., Yamada, P., & Isoda, H. (2009). Anti-proliferative and apoptotic effects of oleuropein and hydroxytyrosol on human breast cancer MCF-7 cells. Cytotechnology, 59(1), 45–53. https://doi.org/10.1007/s10616-009-9191-2

[10]. Micol, V., Caturla, N., Pérez-Fons, L., Más, V., Pérez, L., & Estepa, A. (2005). The olive leaf extract exhibits antiviral activity against viral haemorrhagic septicaemia rhabdovirus (VHSV). Antiviral Research, 66(2–3), 129–136. https://doi.org/10.1016/j.antiviral.2005.02.005

[11]. Sudjana, A. N., D'Orazio, C., Ryan, V., Rasool, N., Ng, J., Islam, N., … Hammer, K. A. (2009). Antimicrobial activity of commercial Olea europaea (olive) leaf extract. International Journal of Antimicrobial Agents, 33(5), 461–463. https://doi.org/10.1016/j.ijantimicag.2008.10.026

[12]. Nishitani, E., & Sagesaka, Y. M. (2004). Simultaneous determination of catechins, caffeine and other phenolic compounds in tea using new HPLC method. Journal of Food Composition and Analysis, 17(5), 675–685. https://doi.org/10.1016/j.jfca.2003.09.009

[13]. Fujiki, H., Sueoka, E., Watanabe, T., & Suganuma, M. (2015, September 28). Synergistic enhancement of anticancer effects on numerous human cancer cell lines treated with the combination of EGCG, other green tea catechins, and anticancer compounds. Journal of Cancer Research and Clinical Oncology. Springer Berlin Heidelberg. https://doi.org/10.1007/s00432-014-1899-5

[14]. Suganuma, M., Okabe, S., Kai, Y., Sueoka, N., Sueoka, E., & Fujiki, H. (1999). Synergistic effects of (-)-epigallocatechin gallate with (-)- epicatechin, sulindac, or tamoxifen on cancer-preventive activity in the human lung cancer cell line PC-9. Cancer Research, 59(1), 44–47.

[15]. Suganuma, M., Saha, A., & Fujiki, H. (2011, February 1). New cancer treatment strategy using combination of green tea catechins and anticancer drugs. Cancer Science. John Wiley & Sons, Ltd (10.1111). https://doi.org/10.1111/j.1349-7006.2010.01805.x

[16]. Sinija, V. R., & Mishra, H. N. (2008, January 13). Green tea: Health benefits. Journal of Nutritional and Environmental Medicine. https://doi.org/10.1080/13590840802518785

[17]. Egner, P. A., Muñoz, A., & Kensler, T. W. (2003). Chemoprevention with chlorophyllin in individuals exposed to dietary aflatoxin. In Mutation Research - Fundamental and Molecular Mechanisms of Mutagenesis (Vol. 523–524, pp. 209–216). https://doi.org/10.1016/S0027-5107(02)00337-8

[18]. Wanasundara, U. N., & Shahidi, F. (1998). Antioxidant and pro-oxidant activity of green tea extracts in marine oils. Food Chemistry, 63(3), 335–342. https://doi.org/10.1016/S0308-8146(98)00025-9

[19]. Azam, S., Hadi, N., Khan, N. U., & Hadi, S. M. (2004). Prooxidant property of green tea polyphenols epicatechin and epigallocatechin-3-gallate: Implications for anticancer properties. Toxicology in Vitro, 18(5), 555–561. https://doi.org/10.1016/j.tiv.2003.12.012

[20]. Cabrera-Bañegil, M., Pérez-Nevado, F., Montaño, A., Pleite, R., & Martín-Vertedor, D. (2018). The effect of olive fruit maturation in Spanish style fermentation with a controlled temperature. LWT - Food Science and Technology, 91, 40–47. https://doi.org/10.1016/j.lwt.2018.01.018

[21]. Turoli, D., Testolin, G., Zanini, R., & Bellù, R. (2004). Determination of oxidative status in breast and formula milk. Acta Paediatrica, International Journal of Paediatrics, 93(12), 1569–1574. https://doi.org/10.1080/08035250410022495

[22]. Kang, J. H., Chung, S. T., Go, J. H., & Row, K. H. (2000). Separation of epigallocatechin gallate from Korean green tea by RP-HPLC. Journal of Liquid Chromatography and Related Technologies, 23(17), 2739–2749. https://doi.org/10.1081/JLC-100101831

[23]. Perva-Uzunalić, A., Škerget, M., Knez, Ž., Weinreich, B., Otto, F., & Grüner, S. (2006). Extraction of active ingredients from green tea (Camellia sinensis): Extraction efficiency of major catechins and caffeine. Food Chemistry, 96(4), 597–605. https://doi.org/10.1016/j.foodchem.2005.03.015

[24]. Martín-Vertedor, D., Garrido, M., Pariente, J. A., Espino, J., & Delgado-Adámez, J. (2016). Bioavailability of Bioactive Molecules from Olive Leaf Extracts and its Functional Value. Phytotherapy Research, 30(7), 1172–1179. https://doi.org/10.1002/ptr.5625

[25]. Delgado-Adámez, J., Baltasar, M. N. F., Yuste, M. C. A., & Martín-Vertedor, D. (2014). Oxidative stability, phenolic compounds and antioxidant potential of a virgin olive oil enriched with natural bioactive compounds. Journal of Oleo Science, 63(1), 55–65. https://doi.org/10.5650/jos.ess13114

[26]. Japón-Luján, R., & Luque De Castro, M. D. (2008). Liquid-liquid extraction for the enrichment of edible oils with phenols from olive leaf extracts. Journal of Agricultural and Food Chemistry, 56(7), 2505–2511. https://doi.org/10.1021/jf0728810

[27]. Balentine, D. A., Wiseman, S. A., & Bouwens, L. C. M. (1997). The chemistry of tea flavonoids. Critical Reviews in Food Science and Nutrition, 37(8), 693–704. https://doi.org/10.1080/10408399709527797

[28]. Vinson, J. A., Dabbagh, Y. A., Serry, M. M., & Jang, J. (1995). Plant Flavonoids, Especially Tea Flavonols, Are Powerful Antioxidants Using an in Vitro Oxidation Model for Heart Disease. Journal of Agricultural and Food Chemistry, 43(11), 2800–2802. https://doi.org/10.1021/jf00059a005

[29]. Kim, D.-O., Lee, K. W., Lee, H. J., & Lee, C. Y. (2002). Vitamin C equivalent antioxidant capacity (VCEAC) of phenolic phytochemicals. Journal of Agricultural and Food Chemistry, 50(13), 3713–3717. https://doi.org/10.1021/JF020071C

[30]. Sharangi, A. B. (2009, June 1). Medicinal and therapeutic potentialities of tea (Camellia sinensis L.) - A review. Food Research International. Elsevier. https://doi.org/10.1016/j.foodres.2009.01.007

[31]. Lee, K. W., Lee, H. J., & Lee, C. Y. (2018). Antioxidant Activity of Black Tea vs. Green Tea. The Journal of Nutrition, 132(4), 785–785. https://doi.org/10.1093/jn/132.4.785

[32]. Forester, S. C., & Lambert, J. D. (2011, June 1). The role of antioxidant versus pro-oxidant effects of green tea polyphenols in cancer prevention. Molecular Nutrition and Food Research. John Wiley & Sons, Ltd. https://doi.org/10.1002/mnfr.201000641

[33]. Paiva-Martins, F., & Gordon, M. H. (2001). Isolation and characterization of the antioxidant component 3,4-dihydroxyphenylethyl 4-formyl-3-formylmethyl-4-hexenoate from olive (Olea europaea) leaves. Journal of Agricultural and Food Chemistry, 49(9), 4214–4219. https://doi.org/10.1021/jf010373z

[34]. Shamshoum, H., Vlavcheski, F., & Tsiani, E. (2017, July 8). Anticancer effects of oleuropein. BioFactors. John Wiley & Sons, Ltd. https://doi.org/10.1002/biof.1366

[35]. Sergediene, E., Jönsson, K., Szymusiak, H., Tyrakowska, B., Rietjens, I. M. C. M., & Čenas, N. (1999). Prooxidant toxicity of polyphenolic antioxidants to HL-60 cells: Description of quantitative structure-activity relationships. FEBS Letters, 462(3), 392–396. https://doi.org/10.1016/S0014-5793(99)01561-6

[36]. DeFrank, J. S., Tang, W., Powell, S. N., Roos, P., Taya, Y., Karnitz, L. M., & Abraham, R. T. (1996). p53-null cells are more sensitive to ultraviolet light only in the presence of caffeine. Cancer Research, 56(23), 5365–5368.

[37]. Block, W. D., Merkle, D., Meek, K., & Lees-Miller, S. P. (2004). Selective inhibition of the DNA-dependent protein kinase (DNA-PK) by the radiosensitizing agent caffeine. Nucleic Acids Research, 32(6), 1967–1972. https://doi.org/10.1093/nar/gkh508

[38]. Fujiki, H., & Suganuma, M. (2012, November 28). Green tea: An effective synergist with anticancer drugs for tertiary cancer prevention. Cancer Letters. Elsevier. https://doi.org/10.1016/j.canlet.2012.05.012

[39]. Ferruzzi, M. G., & Blakeslee, J. (2007, January 1). Digestion, absorption, and cancer preventative activity of dietary chlorophyll derivatives. Nutrition Research. Elsevier. https://doi.org/10.1016/j.nutres.2006.12.003

[40]. Bernini, R., Merendino, N., Romani, A., & Velotti, F. (2013). Naturally Occurring Hydroxytyrosol: Synthesis and Anticancer Potential. Current Medicinal Chemistry, 20(5), 655–670. https://doi.org/10.2174/092986713804999367

[41]. Guo, W., An, Y., Jiang, L., Geng, C., & Zhong, L. (2010). The protective effects of hydroxytyrosol against UVB-induced DNA damage in HaCaT cells. Phytotherapy Research, 24(3), 352–359. https://doi.org/10.1002/ptr.2943

[42]. Manna, C., Galletti, P., Cucciolla, V., Moltedo, O., Leone, A., & Zappia, V. (2018). The Protective Effect of the Olive Oil Polyphenol (3,4-Dihydroxyphenyl)- ethanol Counteracts Reactive Oxygen Metabolite–Induced Cytotoxicity in Caco-2 Cells. The Journal of Nutrition, 127(2), 286–292. https://doi.org/10.1093/jn/127.2.286

[43]. Nousis, L., Doulias, P. T., Aligiannis, N., Bazios, D., Agalias, A., Galaris, D., & Mitakou, S. (2005). DNA protecting and genotoxic effects of olive oil related components in cells exposed to hydrogen peroxide. Free Radical Research, 39(7), 787–795. https://doi.org/10.1080/10715760500045806

[44]. Quiles, J. L., Farquharson, A. J., Simpson, D. K., Grant, I., & Wahle, K. W. J. (2002). Olive oil phenolics: effects on DNA oxidation and redox enzyme mRNA in prostate cells. British Journal of Nutrition, 88(3), 225–234. https://doi.org/10.1079/BJN2002620

[45]. Warleta, F., Quesada, C. S., Campos, M., Allouche, Y., Beltrán, G., & Gaforio, J. J. (2011). Hydroxytyrosol protects against oxidative DNA damage in human breast cells. Nutrients, 3(10), 839–857. https://doi.org/10.3390/nu3100839

International Conference on Cancer Research 2019

Website: www.CancerConf.org

June 10-11, London, UK



Hiroshima Black Rain Evidence Invalidates the A-Bomb Survivor Life Span Study: The Basis of the Linear No-Threshold Model

Shizuyo Sutou [a*]

[a] *School of Pharmacy, Shujitsu University, 1-6-1 Nishigawara, Naka-Ku, Okayama-Shi 703-8516, Japan*

** Corresponding author: sutou@shujitsu.jp*

Abstract

The National Academy of Sciences of the United States of America (NAS) presented the linear no-threshold model (LNT) in 1956, which asserts that the lowest doses of ionizing radiation are hazardous in proportion to the dose. In 2006, NAS put forward the BEIR VII report as evidence supporting LNT. This report is based on the data of the Life Span Study of A-bomb survivors in Hiroshima and Nagasaki (LSS). Radiation doses of the survivors were estimated using initial radiation (5% of blast energy); residual radiation (10%) was neglected. The major component of residual radiation was fallout. Black rain poured down soon after the detonation. Most fallout must have come down to the ground with rain. Three major black rain maps show that black rain covered wide areas of Hiroshima city. Considering that black-rain-affected areas were wide and that these areas were contaminated with residual radiation, an important conclusion is reached that not only A-bomb survivors but also not-in-the-city control subjects (NIC) were irradiated by residual radiation to a greater or lesser degree. Therefore, exposure doses in LSS were underestimated. The use of NIC as a negative control is invalid. Moreover, LSS ignores radiation hormesis: ionizing radiation is not always hazardous; it can be beneficial depending on the dose and dose rate. Consequently, LNT based on LSS is unsound. Indeed, examination of LSS data of longevity reveals a clear J-shaped dose-response, a hallmark of radiation hormesis. Additionally, the average lifespan of A-bomb survivors is longer than that of the nation as a whole.

Keywords:

BEIR VII;

Hormesis;

LNT;

LSS.

1. Introduction

The tolerated dose of radiation exposure for workers had remained at 500 mGy/year from 1934 until 1956 with no difficulties, but the linear no-threshold model (LNT) was then recommended without solid supporting data by the National Academy of Sciences of the United States of America (NAS) [1]. Actually, LNT relies upon the assumption that even the lowest doses of ionizing radiation are hazardous in proportion to the dose. In 2006, NAS reported its support of LNT [2] based on the Life Span Study of Hiroshima and Nagasaki A-bomb survivors (LSS). That report is invalid: 1) dose estimation was based only on the initially sustained doses (5% of total A-bomb energy), neglecting residual radiation (10%) and underestimating radiation doses; 2) control subjects (not-in-the-city control subjects, NIC, who entered Hiroshima and Nagasaki after A-bomb detonation) were assumed for the study to have zero exposure and zero risk of cancer, but they had been irradiated to a greater or lesser degree by residual radiation, compromising their status as negative controls; and 3) analyses were premised on the invalid LNT to emphasize hazardous effects of ionizing radiation, neglecting radiation hormesis (high doses are hazardous, but low doses are beneficial).

The three issues presented above are closely associated with black rain because black rain was the carrier of fallout, which was the major component of residual radiation. Black-rain-affected areas were so wide that most A-bombed people and NIC must have been irradiated with residual radiation. Some NIC died of acute radiation symptoms (ARS).

Therefore, elucidation of black rain is indispensable to elucidate the effects on health from ionizing radiation from A-bombs. In 1957, Obo indicated clearly that the area around the epicenter in Hiroshima was heavily contaminated with residual radiation [3]. The reports appeared in a rather minor Japanese journal that the author had translated and summarized into English [4]. The Oak Ridge National Laboratory (ORNL) holds a document clearly illustrating that black rain readily induced ARS such as fever, vomiting, diarrhea, sore throat, and epilation [5]. However, the Radiation Effects Research Foundation (RERF), a Japan–US scientific organization and the center of LSS, is apparently reluctant to admit the effects of black rain [6]. Although the black rain issue involves many complicated factors such as time of onset, duration of rain, affected areas, intensity of rain, and intensity of radioactivity, intensive efforts have been made to clarify the nature of black rain. Its exact reproduction is difficult, however, mainly because data of scientific measurements were scant. Eyewitness accounts by A-bomb survivors constitute the major information sources.

Three major questionnaire studies are often cited in the context of black rain [7, 8, and 9]. These three are mainly reviewed. Results of other studies are also introduced here.

2. Three Major Black Rain Maps

2.1. Uda map

The Uda map is important for Hiroshima residents to obtain an A-Bomb Survivor Certificate from the Ministry of Health, Labour and Welfare (MHLW). Uda and his colleagues had worked for the Hiroshima Regional Headquarters of the Japan Meteorological Agency. They collected materials related to general conditions at the detonation, states of clouds and winds, whirlwinds induced by the ensuing inferno, rain showers caused by the detonation and inferno, thunder, falling objects, destruction of houses and buildings, and conditions of fires and burning [7]. The research was conducted during August–December, 1952, but Uda himself started data collection immediately after the bombing in 1945. Of a survey of at least 170 inhabitants, 116 testimonies are attached to the end of their article, from which four maps associated with black rain and destruction have come to be cited here (Fig. 1).

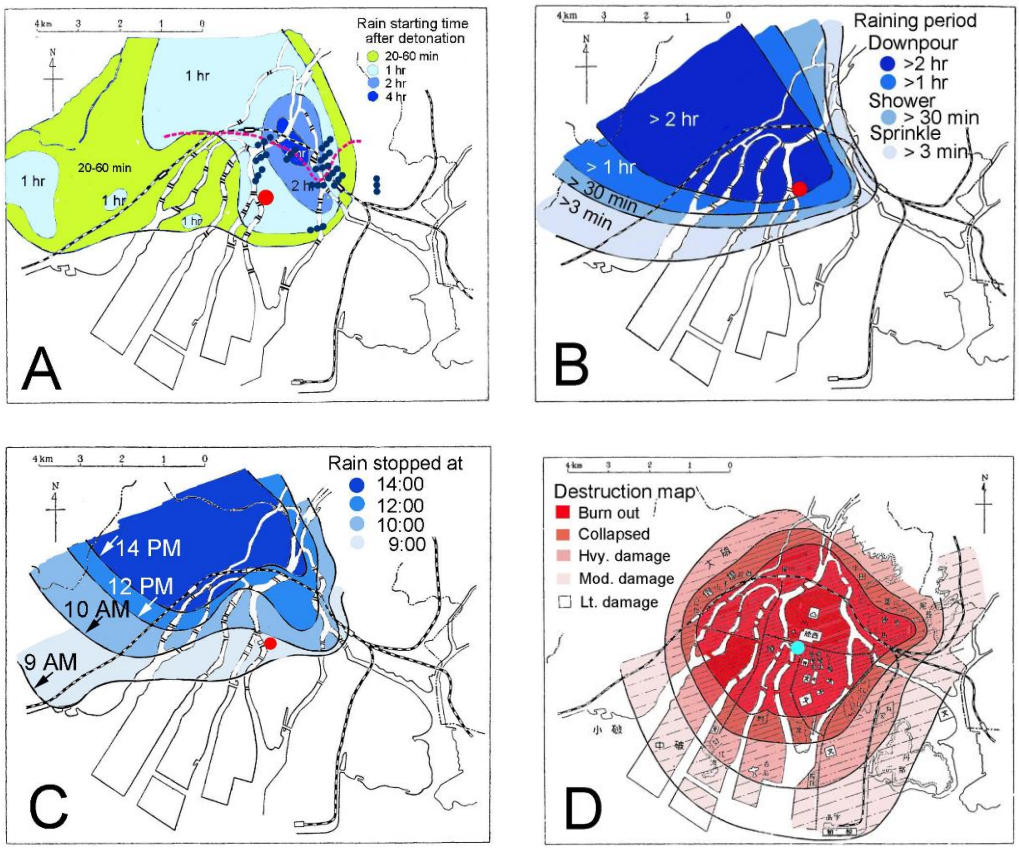


Figure 1. Uda map: A, rain starting time after detonation, wind front (pink dashed line), and whirlwinds (triple dots); B, rain period; C, rain stopping time; and D, destruction map. The epicenter is shown as a red circle in A–C and as a light blue circle in D. The original maps are colorless, but are colored above for ease of understanding.

The Hiroshima A-bomb was detonated at 8:15 AM 600 m above the ground in the clear sky. Regarding the epicenter, black rain started at around 9 AM (Fig. 1A) and poured down torrentially for more than two hours (Fig. 1B). Figure 1C shows, however, that the rain stopped before 10 AM, meaning that the black rain lasted for about 1 hr around the epicenter. The reason for this discrepancy is not known. Because Fig. 1B shows the blast center as located at the border of 1 hr and 2 hr areas, the actual raining period might be close to 1 hr.

The rain started to pour around the epicenter and moved northwest. Ascending air currents produced by the A-bomb blast itself and resultant fire seemed to reinforce the rain synergistically. The heavy rain poured down in an oval area with the major axis of 19 km and minor axis of 11 km. The whole rain area including slight rain constituted an oval with the major axis of 29 km and minor axis of 15 km (Fig. 2A).

Initially, the rain contained black and sticky components. A rumor circulated that the black fluid must be oil spilt to burn Hiroshima city, but it had neither the characteristics of oil nor an oily smell. Rushing black streams in the rivers produced foams. The naked skin hurt when huge rain drops as large as hail hit it. During the heavy rain, the temperature dropped drastically; people shivered with cold. Later analyses showed that the rain was radioactive. Fish such as carps in ponds and eels in rivers floated to the surface. Cattle had diarrhea. People in some areas had diarrhea for more than three months, probably because water pipes were destroyed. They drank well water or underground water. Harmful insects disappeared from rice fields. Rice plants showed abnormal growth, as if they had been treated with special fertilizers. Farmers looked forward to rich harvests. These latter observations hint at hormetic effects on plants. Typhoons struck this area twice on September 17 and 18 and on October 9 and 10, dooming their expectations of good harvests.

In heavy rain areas, black rain lasted for 1–2 hr; then ordinary colorless rain came down. Components of the black rain seemed to contain the A-bomb fallout, with soil and debris produced by a Mach wave, and soot from fires. Black rain-affected areas were expected to be highly radioactive.

Actual rainfall was not measured, but heavy rain areas were flooded to an almost equal degree as that experienced from the typhoon on September 17 and 18, which suggests that the rain was 60–110 mm in 1–3 hr. The total rainfall was estimated as 10–20 million m^3. The rain was so heavy that some bushfires were extinguished by the rain alone.

During or after the rain, thunder rumbled several times around 10–11 AM. The thunder was peculiar, sounding like explosions or the roar of cannons. Thunder occurred in remote areas more than 20 km distance from the epicenter.

Black dust fell several kilometers outside of the rain areas, blackening the leaves of vegetables. Falling objects were galvanized iron sheets, wooden plates from roofs, pieces of mosquito netting, cotton rags, remnants of clothes, paper scraps, name cards, paper money, debentures, and so on. Of those, paper scraps including slips from governmental offices, banks, and post offices and strips of papers of account books were the most abundant. The areas of falling objects were distinct from the rain areas. The areas were southwest of the major axis from the epicenter and extended 30 km. Falling objects were carried at a speed of 1–3 m/s.

Hiroshima city was destroyed concentrically from the epicenter to the outskirts (Fig. 1D). Fires started about 5 min after detonation in shattered houses and buildings that had been using open flames at the time of the blast. Others caught fire from the heat of the A-bomb blast. People were unable to the extinguish fires. The cumulative fires began to rage around 9 AM, becoming most furious from 10 AM to 2 PM, but abated in the evening. Most areas of Hiroshima city were wrapped in smoke on the afternoon of August 6, 1945. The fire lasted for three days. Smoldering lasted for a weak. The heat of the A-bomb and inferno evaporated water from the rich waterways. Burning of organic materials produced water and CO_2. Rain poured down from 9 AM to 4 PM.

Spontaneous fires were visible on straw roofs, straw in the fields, shrines thatched with *hinoki* bark, *shouji* screens, crude rubber, cement bags, the tops of electric poles, railroad ties, stakes beside railways, hemp, palms, and so on. Black objects collected heat more than white ones. A man dressed in white was burned slightly, but his wife in black beside him died from severe burns. People close to the epicenter were charred or evaporated. The skin of people between 0.5–2 km sometimes peeled off (drawings can be viewed at the Hiroshima Peace Memorial Museum (HPMM)). Most people outdoors at 2–4 km from the center were burned slightly, as though they had been suntanned.

Most people outdoors at 1–2 km felt violent heat. Those at 4–5 km felt hot. Some people 20 km away from the epicenter felt warm. Leaves of plants such as rice plants, corns, eggplants, pumpkins, lotuses, and sweet potatoes and trees such as pine, oak, cherry, and holly were charred or burned depending on their distance from the epicenter. Many trees died of heat at 2.5 km from the epicenter. Trees were partially burned at 4 km from the epicenter. It was midsummer, but colored leaves of wooded hills impressed people as if it were fall. After one month or so, new shoots emerged. Then the normal landscape was recovered.

The time of detonation was close to a morning calm: weakening land winds were blowing from the north in the northern parts of Hiroshima city, with growing sea winds in the southern parts from the central area of the city, forming a front close to the railway (Fig. 1A). The epicenter was located south of the front. Strong sea winds blew into fierce ascending air currents after the detonation and big fire. Great whirlwinds (Fig. 1A) appeared along the front between 11 AM and 15 PM. Some whirlwinds developed into tornados. Drums, thick wood boards, galvanized iron sheets, suitcases, beer bottles, water, some people, and other objects were whirled upward.

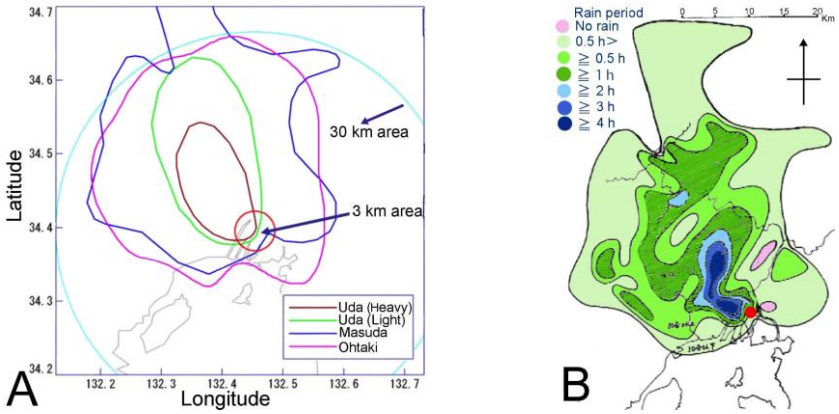
Uda's house was located in Takasu Area, a heavily contaminated area. Wooden sliding shutters were blown out into the garden and were pelted by black rain. When radioactivity of a muddy sample was measured at RIKEN, it was 50 times higher than the natural background level even 2 months after the blast. When his second son came back home from the evacuated place 3 months after the blast and slept beside the contaminated sliding shutters, his hair began to

fall out. Astonished, Uda soon removed the shutters.

2.2. Masuda map

A new law, "Act for Atomic Bomb Sufferers' Medical Care," was passed in 1957 to support the A-bomb survivors medically. The survivors were issued an A-Bomb Survivor Certificate by the Ministry of Health, Labour and Welfare (MHLW). This law had been revised several times. In 1965, parts of "Heavily Contaminated Areas with Residual Radiation" were designated as "Specially Irradiated Areas." This change opened a path to supporting people living in black rain-affected areas. The Specially Irradiated Areas, however, were so limited. In 1968, another new law, "Act on Special Measures of the Atomic Bomb Survivors," was enacted to assist survivors' livelihood in addition to medical measures. People asked Hiroshima city and Hiroshima prefecture to expand the Specially Irradiated Areas. In 1976, the heavy rain area of the Uda map (Fig. 2A) was designated as "Special Areas for Physical Examination." When specified illnesses were detected, the relevant person was regarded as an A-bomb survivor and was given an A-Bomb Survivor Certificate. In 1978, "the Association of Liaison Committees of Hiroshima prefecture of 'Black Rain and Home Nursing' A-bomb Victims" (Black Rain Association) was established. This group pushed for expansion of the Special Areas for Physical Examination.

Masuda used to work for the Meteorological Research Institute, the Japan Meteorological Agency. He learned through the Black Rain Association that the Uda map was not always correct, e.g., black rain dropped outside the rain areas that Uda and his colleagues had determined. He decided to reconstruct the black rain areas using various materials. He collected data for three years from 1985. 1) Weather data of August 6, 1945, were collected by the Hiroshima Regional Headquarters such as temperature, wind velocity, wind direction, rainfall, and cloud cover. 2) Uda and his colleagues recorded 116 testimonies [7], but they required more materials. Masuda was able to find and use a total of 170 materials that Uda et al. had used and kept at Tokyo University of Marine Science and Technology. 3) In 1974, Hiroshima city and Hiroshima prefecture conducted a questionnaire survey of black rain. From the ca. 20,000 subjects, 17,369 responses were collected, but most were lost; 1,045 were available. 4) Just before the establishment of the Black Rain Association, its later Chairman Hanamoto administered a questionnaire to 243 families, of whom 83 responded. 5) In 1978 and 1979, Secretary-general Murakami of the Black Rain Association convened meetings at 17 places and interviewed residents about black rain. He left a map on a scale of 1:50,000 in which black rain information of 25 areas was available. 6) On June 13 and 14, 1987, Masuda, in cooperation with the association, had meetings at five locations where a total of 340 people gathered, 72 of whom provided him with relevant information. On August 5, 1987, interviews were conducted at 10 places, yielding 111 testimonies. 7) In cooperation with the Association, a questionnaire survey was administered; 1,188 answers were collected. 8) Newspaper articles and interviews on TV were collected; a total of 61 data were adopted. 9) Memoirs and recordings describing experiences were collected from 37 books and journals; 358 data were obtained.



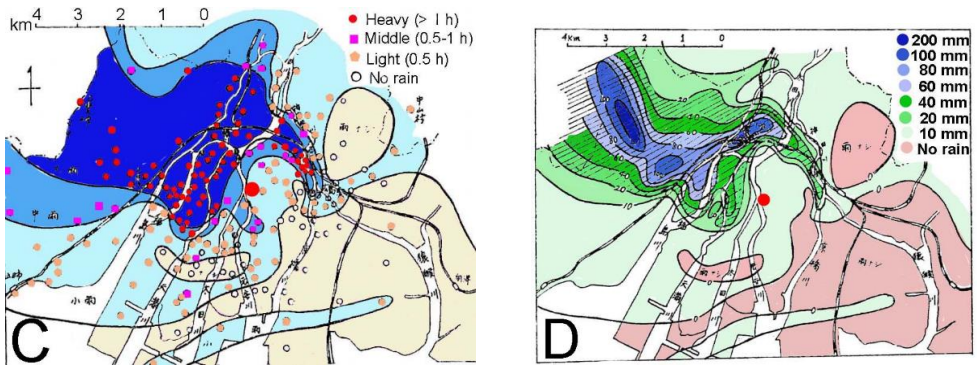


Figure 2. Rainfall maps: A, outlines of Uda, Masuda, and Ohtaki map; B, raining period in a large sale; C, rainfall in the central area of Hiroshima city; and D, estimated volumes of rain in the central area. Degrees of rain were determined by the rain duration as follows: heavy, ≥1 hr; middle, <1 hr – ≥30 min; and light, <30 min (C). The original maps are colorless, but are colored here for ease of understanding.

Masuda collected many data to produce the Masuda map (Fig. 2A) [8]. The period during which data of papers were accepted was 1945–1988. During about 43 years, memories might become dim. In the early days after the A-bombing, people tended to conceal the fact that they were A-bomb survivors because they were sometimes discriminated against socially, e.g., engagements were often canceled. When the heavy rain area of the Uda map (Fig. 2A) made in 1953 was designated as "Special Areas for Physical Examination" in 1976, some exaggerated responses were expected thereafter, given so that a person could obtain a certificate.

When the slightest rain was included, the black rain area was 1,250 km^2 with 45 km north–northwest length and 36 km east–west width, ca. four times larger than the Uda map area (Figs. 2A, B). Rain areas are more complicated than those of the Uda map. A marked difference between the two maps is that the epicenter is in the heavy area in the Uda map (Fig. 1B), but is in the light area in the Masuda map (Fig. 2C). Because the rain started after 1 hr from the detonation (Fig. 1A) and stopped before 10 AM (Fig. 1C), the rain must have lasted for less than 1 hr. Therefore, the Masuda map (Fig. 2B) must be correct. Uda might think that the rain must be heavy in the central area. Figure 2D shows the deduced rain volumes. The northwest parts to the epicenter received heavy rains.

The Masuda map was examined by an expert committee established by Hiroshima city and Hiroshima Prefecture. It consisted of 12 members, but Masuda was excluded. In May, 1991, after 10 meetings over two years, the conference concluded that the Masuda map could not be adopted as the black rain map because the effects of black rain on humans had not been established. His map is not shown in HPMM.

2.3. Ohtaki map

In 2008, Hiroshima city conducted a questionnaire survey of about 37,000 residents who might have experienced black rain. The rain start time, stopping time, and location were asked and 23,780 people responded. Effective responses were limited: those with both start and end times were 1,084; those with only a start time were 481. Analyses indicated that black rain started about 9 AM, reached its heaviest level of precipitation at around 10 AM, spread northwestward from the epicenter, and disappeared around 30 km north–northwest from the hypocenter at 3 PM. The black rain area was estimated as 5–6 times greater than the Uda map and slightly greater than the Masuda map (Fig. 2A) [9].

The Ohtaki map entails some issues. Data were obtained from a survey sponsored by Hiroshima city. The mayor must plan to support citizens sincerely to the greatest extent possible, but a politician must think carefully about voting behavior. The survey was administered 53 years after the A-bombing; responders' memories might be vague. Many or most respondents, the vast majority of whom were 60 years old and older, must have wanted to have a certificate allowing them certain health and other benefits. A tendency to exaggeration of responses can be inferred.

The Ohtaki map was examined by the MLHW, which concluded that specification of black-rain-areas was difficult. This map has been displayed in HPMM since 2010 (see Fig. 2 (right) in an earlier report by the author [10]).

3. Black Rain was Radioactive

3.1. Proceedings of new radiation dosimetry system DS02 of the atomic bombing

Proceedings of the workshop 'new radiation dosimetry system DS02 of the atomic bombing in Hiroshima and Nagasaki' include several reports describing that black rain was radioactive [11]. Shizuma measured three samples: 1) 28 soil samples collected by Nishina of RIKEN within 5 km from the epicenter on August 9, 1945; 2) 117 rock samples stored at the Petrological Laboratory, the Department of Science, Hiroshima University; and 3) black rain streaks on wall panels [12]. He was able to detect the γ-ray spectrum of Cs-137 in all three samples, indicating that fallout carried down by black rain contained an A-bomb product.

Yashima's house was located in the Takasu area, 3.2 km west to the epicenter. The roof of his house was shifted by the blast wind, leaving a gap between the roof and the room. Black rain came into the room, leaving many black streaks on the wall panels. The rain was sticky. The streaks showed slight thickness. Two wall panels were given to HPMM,

where they can be viewed. U-235 was used to make the Hiroshima A-bomb. The ratio of U-235/U-238 was expected to be higher than 0.00736, the natural ratio. Indeed, the rain samples showed slightly higher ratios than 0.00736 [13].

3.2. Obo report indicates hazardous effects by residual radiation

Obo had been running his hospital in Hiroshima city. He wanted to ascertain the relation between the A-bomb radiation and cancer. A-bomb survivors (3,946) and NIC (629) who lived in the area 0–7.0 km from the epicenter were interviewed in January–July 1957 with the help of Hiroshima University students. Examinees were asked about the place at the A-bombing, presence or absence of ARS, and if they entered the central area with a radius of 1 km from the epicenter within 3 months after the blast. The survivors were divided into two groups: those bombed outdoors and indoors. Each group was divided further into two subgroups: those who entered the central area (entrants) and those who did not (non-entrants). NIC were divided into entrants and non-entrants [3, 4].

Radiation from the A-bomb can reach 3 km from the epicenter, but 50–60% outdoor and 20–40% indoor bombed survivors showed ARS, indicating hazardous effects of residual radiation. Non-entrant survivors residing beyond 4.5 km showed a few percent of ARS irrespective of the outdoor or indoor bombing, but about 30% entrant survivors experienced ARS without regard to outdoor or indoor bombing, indicating strong residual radiation in the central area. More direct evidence of residual radiation was found: around 10–50% NIC entrants showed ARS within three weeks, depending on the entrance date. No ARS, however, were visible in NIC non-entrants. Among the areas of residual radiation, the induced radioactivity was limited to a 2 km radius from the epicenter. It disappeared in a few days. Therefore, the hazardous effects outside the 2 km circle must be attributable to fallout included within the black rain.

3.3. Committee for Approval of Survivors estimates residual radiation

The Committee for Approval of Survivors presented the criticism that exposure doses of survivors estimated from the initial radiation only were greatly underestimated beyond 1.5 km [14]. In fact, the ARS of residents in remote areas and NIC cannot be explained without the effects of residual radiation. The Committee examined and analyzed the Obo report [3] and estimated the average exposure doses of NCI: 1.5 Gy (equivalent to the initial radiation at 1,200 m from the epicenter) on the A-bombing day; 0.7 Gy after a week; 0.35 Gy after two weeks; 0.18 Gy after three weeks; and 0.09 Gy after one month.

3.4. Technical report of Oak Ridge National Laboratory: ORNL-TM-4017

The census taken in 1950 revealed that there were about 280,000 A-bomb survivors in Japan and that around 200,000 lived in Hiroshima or Nagasaki. The master sample questionnaire (MSQ) was administered to 200,000 people during 1956–1961. The results became basic data, from which about 93,000 were chosen for LSS. MSQ was applied to 27,000 NIC. Other MAQ data were added to reach totals of 138,000 and 23,000, respectively, in Hiroshima and in Nagasaki.

During 1954–1965, 20,356 Hiroshima and 8,373 Nagasaki survivors were interviewed for their shielding histories. Rain (when, where, what kind, etc.) was included in question items until a format change in September, 1958. Results were recorded on microfilm. The copies were stored in ORNL, which held 11,915 Hiroshima and 2,046 Nagasaki survivors' records. These survivors were more than 1,600 m from the epicenter. Yamada and Jones selected 222 black rain-exposed Hiroshima survivors from the microfilm data. Their radiation symptoms were extracted from MSQ data. Separately, a database was constructed by combining the MSQ data and shielding histories. They were called the ABCC magnetic tape records. This contained 75,100 Hiroshima and 24,900 Nagasaki survivors, from which black-rain-exposed 65 Hiroshima subjects and 16,045 control people who lived in southeast portion of Hiroshima were selected. Consequently, a total of 287 survivors were extracted to ascertain the effects of black rain. A technical report was produced: ORLN-TM-4017 [5]. The original is kept at the Department of Energy.

Major findings extracted from the report are shown in Table 1. Even though the rain-exposed population was small (287), the hazardous effects of black rain are clear. The authors seemed to urge implicitly RFRF as relevant data to reflect the black rain effects.

Table 1. Specific radiation symptoms versus initial exposure

Symptoms with onset within 21 days	Black rain survivors[a]	Control survivors[b]
Fever	32 (13.56%)	212 (1.32%)
Vomiting	18 (7.62%)	88 (0.55%)
Diarrhea (non-bloody)	39 (16.53%)	122 (0.76%)
Diarrhea (bloody)	13 (5.51%)	37 (0.23%)
Oropharyngeal lesions		
Sore throat	13 (5.51%)	212 (0.13%)
Sore mouth	10 (4.24%)	14 (0.09%)
Sore gums	5 (2.12%)	7 (0.04%)
Purpura		
Gingival bleeding	11 (4.66%)	25 (0.16%)
Purpura	7 (2.97%)	14 (0.09%)
Other bleeding	1 (0.43%)	1 (001%)
Non-purpuric bleeding	11 (4.66%)	231 (1.44%)
Epilation		

Slight (less than 1/4)	142 (60.17%)[c]	646 (4.03%)
Moderate (1/4 to 3/4)	13 (5.51%)	47 (0.29%)
Sever (more than 3/4)	2 (0.85%)	20 (0.12%)
Present, but not specified	5 (2.11%)	12 (0.07%)

[a], Initial exposure: < 10 mGy, 74; 10–100 mGy, 121; 100–200 mGy, 41; and > 200 mGy, 51.
[b], Initial exposure: < 200 mGy.
[c], Some cases without epilation were apparently added erroneously to the slight epilation group and the actual number must be less than 142 [15].

3.5. Induced radiation

The A-bomb blast released a huge amount of energy: thermal radiation (35%), blast energy (50%), and nuclear radiation (15%). Of the 15%, 5% was the initial radiation released within 30 s. It was used to estimate the exposure doses. The remaining 10% was residual radiation, which consisted of induced radiation and fallout. Fallout accounted for most of the residual radiation. Hazardous effects of fallout on survivors and NIC might be readily apparent, but quantitative estimation has been quite difficult mainly because of the complicated rainfall status and the lack of reliable radiation data.

Induced radiation is produced by the action of neutrons in making non-radioactive substances into radioactive ones. The extent of radiation from the A-bomb was ca. 3 km from the epicenter, but the extent of neutrons was limited to 2 km. Induced radiation can be determined more precisely than that of fallout. Half-lives of induced nuclides were short and fell off rapidly with distance from the epicenter and with time. The maximum cumulative dose was estimated as 800 mGy [16]. The dose would be about one-third as large after a day and only a few percent after a week. For example, a person entering the Hiroshima epicenter area after 1 day and working 10–20 hr a day for a week would have been exposed to about 100 mGy. If the person had been working at a distance of 500 m, then exposure would have been 10 mGy. On August 6, 1945, 84 NIC entered the central area and 40 people (47.6%) showed ARS [3, 4]. When people stayed in this area for 1 hr, 4 hr, 1 day, 2 days, and 4 days, the respective percentages with ARS were 11.7, 28.6, 42.5, 50.0, and 70.0. These people were definitely irradiated by both induced and fallout radiation.

4. A-bomb Survivors get Cancer Less Frequently and Live Longer

4.1. Reasons the BEIR VII report is flawed

NAS put forward the BEIR VII report based on a LSS study in 2006 as evidence supporting LNT. This report seems to have been intended from the start to support the old LNT, ignoring a half century of scientific development. Much evidence indicates that black rain carried down fallout onto wide areas and that it caused hazardous health effects on inhabitants outside the reach of the initial radiation. Therefore, exposure doses are underestimated. Main flaws in the BEIR VII report include the following:

- The dose-response of leukemia is clearly linear-quadratic. That of solid cancers fits better to a linear-quadratic than linearity, but no statistical significance was found between the two; the BEIR VII report adopted linearity. This forced logic is unacceptable.
- The highest dose in Fig. 4 of the BEIR VII report is 2 Gy. Excess relative risk (ERR) usually shows a downturn of more than 2 Gy because highly exposed people would die before cancer development. Concealing a downturn by limiting doses up to 2 Gy, the BEIR VII report is successful in giving the impression of linearity.
- The BEIR VII report combined all data <100 mGy into one data point. More than 80% of all survivors belong to this <100 mGy category. Combining data into arbitrary groups is often said to be a statistical trick. Such combination is successful in giving the impression of linearity.
- The BEIR VII report is based on the false assumption that zero dose exposure and zero ERR in NIC, but this is invalid because most NIC were exposed to residual radiation. Setting aside this assumption, Bayesian analysis of LSS shows a threshold and hormetic response [17].
- Living organisms, including humans, have defense mechanisms against ionizing radiation such as reactive oxygen species (ROS) quenching, DNA repair, apoptosis, and anticancer immunity. The BEIR VII report ignores these mechanisms acquired through the evolutional processes of billions of years. The report was based on faulty assumptions [18].

4. 2. A-bomb survivors get cancer less frequently

RERF publishes an LSS report once every five years. The quantities of A-bomb survivors and solid cancer deaths were extracted from the latest three articles and were compared with Japanese national averages (Table 2). Rates of cancer deaths in both A-bomb survivors and NIC are lower than those of Japanese nationwide. The finding is readily acceptable when one acknowledges that low-dose radiation is hormetic under appropriate conditions and that both A-bomb survivors and NIC were exposed to hormetic radiation. Approximately 95% survivors had been exposed to < 0.5 Gy (probably in the hormetic range).

Table 2. Solid cancer mortality in the lifespan study of A-bomb survivors compared to Japanese cancer mortality. Japanese average cancer deaths were calculated by dividing cancer deaths by total deaths each year during 1958–2009 [19].

Reporters	Year	Survey period	No. *hibakusha* or [NIC]	No. cancer deaths (%)	% Japanese average cancer deaths
Preston et al. [20]	2007	1958–1998	105,427 [25,427]	17,448 (**16.6**) [3,994 (**15.7**)]	**21.4** (1958–1998)
Ozasa et al. [21]	2012	1958–2003	86,611 [26,529]	10,929 (**12.6**) [NA[a]]	**22.3** (1958–2003)
Grant et al. [22]	2017	1958–2009	80,205 [25,239]	17,316 (**21.5**) [5,222 (**20.6**)]	**23.3** (1958–2009)

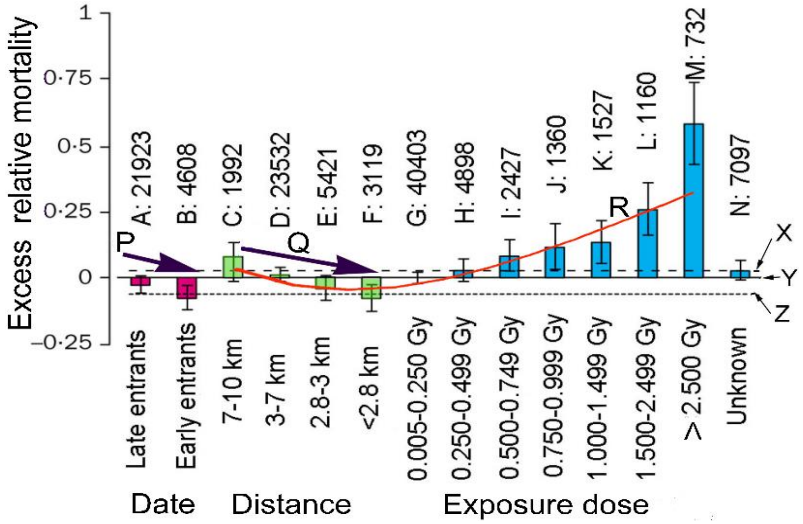
[a], not available

4.3. A-bomb survivors live longer

Stewart and Kneale [23] showed that deaths in 1950–1982 from all non-malignant diseases in LSS population were significantly lower in survivors exposed to low doses than in unexposed persons. Cologne and Preston [24], however, concluded that the lifespan of A-bomb survivors was shortened. They assumed zero exposure and zero hazardous effects in NIC, the negative control cohort. Analyses were made based on LNT. Their data are reproduced in Fig. 3.

We can draw the conclusion that A-bomb survivors live longer, on average, from Fig. 3.

- Excess relative mortality of early entrants (Fig. 3A) is greater than that of late entrants (Fig. 3B), indicating that people with higher exposure lived longer than those with lower exposure (arrow P). The key to resolving this contradiction is the inference that radiation hormesis stimulates human bodily defense mechanisms.
- Excess relative mortality is inversely proportional to distance from the epicenter (arrow Q), again indicating that people with higher exposure lived longer than those with lower exposure.
- Excess relative mortality shows a typical J-shaped curve (arrow R), a hallmark of radiation hormesis. The crossing of the J and the x-axis implies a threshold at around 0.250–0.499 Gy (Fig. 3, H). When residual radiation is examined, the threshold is expected to be around 1 Gy. Survivors in Hiroshima were irradiated acutely. People in Fukushima were irradiated chronically: the threshold in Fukushima would be 10–100 times higher than that in Hiroshima.



Figuer 3. Excess relative mortality by entrance date, distance from the hypocenter, or radiation dose. Figure 1 and Table 1 of an earlier report [24] are combined. A, late entrants (NIC, entered after 1 month); B, early entrants (NIC, entered within 1 month); C–F, <0.005 Gy dose groups with different distance from the epicenter; G–M, different dose groups; and N, people (0.11–3 km) with unknown doses. Numerals shown above A–N denote the number of people studied. Solid lines X, Y, and Z respectively represent the averages of C and D (n = 25,524), of C–F (n = 34,064), and of E and F (n = 8,540).

5. Discussion

Reportedly, about 1 g of U-235 was converted to energy during the Hiroshima A-bomb explosion. According to the equation $E = mc^2$, 1 g of mass produces an energy of 9×10^{13} J/g. A radius of 2 km area (1.25×10^7 m^2) was burned down in Hiroshima city (Fig. 1D). Maruyama and Yoshikawa deduced that houses made of wood had been built with a 30% coverage ratio (3.76×10^6 m^2) and that the unit of mass was 100 kg/m^2, giving a mass of 3.76×10^{11} g [25]. We assume that the wood consisted of cellulose made from glucose. Because the heat of combustion for glucose is 1.55×10^4 J/g, the heat produced by the burned houses is estimated as 5.82×10^{15} J, which is 65 times greater than that produced by the A-bomb. Therefore, the major destructive power of the Hiroshima disaster was not represented by the A-bomb

itself, but by anthropogenic organic materials such as houses, buildings, and human bodies. The Hiroshima inferno was ignited by the A-bomb.

A lot of water was produced by the inferno. It contributed to the formation of black rain. The molecular weight of glucose is 180, so 3.76×10^{11} g means 2.08×10^{9} mol. Because 1 mol of glucose produces 6 mol of water, 1.25×10^{10} mol water was produced. The molecular weight of water is 18, 2.25×10^{11} g or 2.25×10^{5} tons of water was produced. About 70% of a human body consists of water, so a person with 70 kg has 50 kg water. When the remaining parts of a body are burned, H_2O, CO_2, and other inorganic compounds are produced. There were many people, animals, trees, and other objects and organisms burned and charred, thereby producing water. The large amount of water thus produced must have contributed to make the black rain that carried most fallout down onto the ground.

Rainfall around the epicenter was apparently limited (Figs. 2C, D). This does not mean, however, that radioactivity levels around it were low because the initial rain might be fallout-rich. One can infer that NICs who experienced ARS (Fig. 3 in an earlier report by the author [4]) must have been irradiated heavily with residual radiation, whereas those who lived long lives (Fig. 3) or who were unaffected by cancer (Table 2) must have been irradiated with a hormetic range of radiation. Exposure doses of LSS cohort were estimated only on the initial radiation. The contribution of residual radiation might be readily apparent as discussed here. Although they have relevant data, NAS [2] and RERF [6] are reluctant to admit the facts. Once they acknowledge the facts, LNT might collapse like a castle in the air. Because the analysis of LSS at RERF itself shows hormesis and a threshold [17], it is apparently high time to acknowledge the effects of residual radiation and to establish a new paradigm, e.g., setting parsimoniously a threshold of 100 mGy for acute radiation and of 1 Gy for chronic radiation

Abbreviations

ARS: acute radiation symptoms
ERR: excess relative risk
HPMM: Hiroshima Peace Memorial Museum
LNT: linear no-threshold model
LSS: Life Span Study of A-bomb survivors in Hiroshima and Nagasaki
MHLW: Ministry of Health, Labour and Welfare
MSQ: master sample questionnaire
NAS: National Academy of Sciences of the United States of America
NIC: not-in-the-city control subjects
ORNL: Oak Ridge National Laboratory
RERF: Radiation Effects Research Foundation
ROS: reactive oxygen species

References

[1] Anonymous (1956). Genetic effects of atomic radiation. Science, 123, 1157-1164.
[2] National Research Council of the National Academies. Health risks from exposure to low levels of ionizing radiation: BEIR VII – Phase 2. 2006. http://www.philrutherford.com/Radiation_Risk/BEIR/BEIR_VII.pdf.
[3] Obo, G. (1957). Statistical observation of disorders induced by residual radiation of atomic bomb. Nihon Iji Shinpo, No. 1746, 21-25. (in Japanese)
[4] Sutou, S. (2017). Rediscovery of an old article that the area around the epicenter in Hiroshima was heavily contaminated with residual radiation, indicating that exposure doses of A-bomb survivors were largely underestimated. J. Radiat. Res., 58, 745-754. https://doi.org/10.1093/jrr/rrx029.
[5] Yamada, H., & Jones, T.D. (1972). An examination of A-bomb survivors exposed to fallout rain and a comparison to a similar control population. ORNL-TM-4017, Oak Ridge National Laboratory.
https://inis.iaea.org/collection/NCLCollectionStore/_Public/04/058/4058759.pdf.
[6] Sakata, R., Eric, J., Grant, E.J., Furukawa, K., Misumi, M., Cullings, H., Ozasa, K., & Shore, R.E. (2014). Long-Term Effects of the Rain Exposure Shortly after the Atomic Bombings in Hiroshima and Nagasaki. Radiat. Res., 182, 599-606.
[7] Uda, M., Sugawara, Y., & Kita, T. (1953). Meteorological research report on A-bomb disaster in Hiroshima, *in* Reports on research into A-bomb disasters, Part I: Science and Engineering (Japan Society for the Promotion of Science), pp. 98-136. (in Japanese)
[8] Masuda, Y. (1989). Re-investigation of "black rain" after Hiroshima A-bomb. *Tenki* (Weather), 35, 69-79. (in Japanese)
[9] Ohtaki, M. (2011). Re-construction of spatial-time distribution of 'black rain' in Hiroshima based on statistical analysis of witness of survivors from atomic bomb. *In* Michio, A. & Yutaka, O. (eds.). Revisit the Hiroshima A-bomb with Database: 131- 144. Hiroshima City. http://www.hisof.jp/03database/0206.pdf.
[10] Sutou, S. (2018). Low-dose radiation from A-bombs elongated lifespan and reduced cancer mortality relative to un-irradiated individuals. Sutou Genes and Environment (2018) 40:26. https://doi.org/10.1186/s41021-018-0114-3.
[11] Hasai, H., Hoshi, H., Shibata, S., & Imanaka, T. (eds.) (2005). Proceedings of the workshop 'new radiation dosimetry system DS02 of the atomic bombing in Hiroshima and Nagasaki'. Kyoto: Kyoto University.
http://www.rri.kyoto-u.ac.jp/PUB/report/04_kr/img/ekr011.pdf.
[12] Shizuma, K. (2005). Estimation of cumulative exposure from radioactive fallout. *In* Hasai, H., Hoshi, H., Shibata, S., & Imanaka, T. (eds.). Proceedings of the workshop 'new radiation dosimetry system DS02 of the atomic bombing in Hiroshima and Nagasaki'. Kyoto: Kyoto University, pp. 155-163. http://www.rri.kyoto-u.ac.jp/PUB/report/04_kr/img/ekr011.pdf. (in Japanese)
[13] Fujikawa, Y., Shizuma, K., Endo, S., Fukui, M. (2005). U-235/U-238 ratios detected in the black rain from the Hiroshima A- bomb. *In* Hasai, H., Hoshi, H., Shibata, S., & Imanaka, T. (eds.). Proceedings of the workshop 'new radiation dosimetry system

DS02 of the atomic bombing in Hiroshima and Nagasaki'. Kyoto: Kyoto University, pp. 164-18. http://www.rri.kyoto-u.ac.jp/PUB/report/04_kr/img/ekr011.pdf. (in Japanese)
[14] Sawada, S. (2007). Committee for approval of survivors. Residual radiation and internal exposure. The Ministry of Health, Labour and Welfare, 2007. http://www.mhlw.go.jp/shingi/2007/10/dl/s1004-7b.pdf. (in Japanese)
[15] Honda, K. (2012). Human body influence of the residual radiation which ORNL-TM-4017 asks. J. Japan Statist. Soc., 42, 103-117. http://www.mhlw.go.jp/shingi/2007/10/dl/s1004-7b.pdf. (in Japanese)
[16] Okajima, S., Fujita, S., & Harley, H. (1987). Radiation doses from residual radioactivity. *In* US-Japan joint reassessment of atomic bomb radiation dosimetry in Hiroshima and Nagasaki. DS86. Dosimetry System 1986. Vol. 1. Chapter 6, DS86 final report, pp. 205-226. https://www.rerf.or.jp/library/scidata/scids/ds86/images/v1/data/Chapter6/Chapter6.pdf.
[17] Furukawa, K.M., Cologne, J.B., & Cullings, H.M.A. (2016). Bayesian semiparametric model for radiation dose-response estimation. Risk Anal., 36, 1-13. https://onlinelibrary.wiley.com/doi/full/10.1111/risa.12513.
[18] Siegel, J.A., Greenspan, B.S., Maurer, A.H., Taylor, A.T., Phillips, W.T., Nostand, D.V., Sacks, B., & Silberstein, E.B. (2018). The BEIR VII estimates of low-dose radiation health risks are based on faulty assumptions and data analyses: a call for reassessment. J. Nucl. Med., 59, 1017-1019. https://www.ncbi.nlm.nih.gov/pubmed/29475999.
[19] Vital Statistics Japan Ministry of Health, Labour, and Welfare (cancer mortality (1958-2017). https://ganjoho.jp/reg_stat/statistics/dl/index.html.
[20] Preston, D.L., Ron, E., Tokuoka. S., Funamoto, S., Nishi, N., Soda, M., Mabuchi, K., & Kodama, K. (2007). Solid cancer incidence in atomic bomb survivors: 1958-1998. Radiat. Res., 168, 1–64.
[21] Ozasa, K., Shimizu, Y., Suyama, A., Kasagi, F., Soda, M., Grant, E.J., Sakata, R., Sugiyama, H., & Kodama, K. (2012). Studies of the mortality of atomic bomb survivors, report 14, 1950-2003: an overview of cancer and non cancer diseases. Radiat. Res.,177, 229-243. https://bioone.org/journals/radiation-research/volume-177/issue-3/RR2629.1/Studies-of-the-Mort ality-of-Atomic-Bomb-Survivors-Report-14/10.1667/RR2629.1.full.
[22] Grant, E.J., Brenner, A., Sugiyama, H., Sakata, R., Sadakane, A., Utada, M., Cahoon, E.K., Milder, C.M., Soda, M., Cullings, H.M., Preston, D.L., Mabuchi, K., & Ozasa, K. (2017). Solid Cancer incidence among the life span study of atomic bomb survivors: 1958-2009. Radiat. Res., 187, 187, 513–537. https://www.rrjournal.org/doi/pdf/10.1667/RR14492.1. Health Phys., 54, 567-569.
[24] Cologne, J.B., & Preston, D.L. (2000). Longevity of atomic-bomb survivors. Lancet, 356, 303-307.
[25] Maruyama, T., & Yoshikawa, T. (2005). Residual radioactivity and radiation dose due to black rain by the atomic bomb in Hiroshima. *In* Hasai, H., Hoshi, H., Shibata, S., & Imanaka, T. (eds.). Proceedings of the workshop 'new radiation dosimetry system DS02 of the atomic bombing in Hiroshima and Nagasaki'. Kyoto: Kyoto University, pp. 184-195. http://www.rri.kyoto-u.ac.jp/PUB/report/04_kr/img/ekr011.pdf. (in Japanese)

International Conference on Cancer Research 2019

Website: www.CancerConf.org

June 10-11, London, UK



Study of the Prevalence of Chronic Diseases (Cancer, Diabetes, Heart Disease) and Its Relationship with the Elderly's Quality Of Life

Samira Sangi [1]*, Majid Zargham Hajabi [2], Leila Zolghadr [3], Faegheh Miryousefiata [4], Sareh Sangi [5]

1. PhD Candidate of Educational Psychology, Qom Branch, Islamic Azad University, Qom, Iran.
2. PhD, Faculty Member, Department of Psychology, Qom Branch, Islamic Azad University, Qom, Iran.
3. Masters of Statistics, Qom Branch, Islamic Azad University, Qom, Iran.
4. Medical Student, Osmangazi University, Eskisehir, Turkey
5. Young Researchers and Elite Club, Qom Branch, Islamic Azad University, Qom, Iran.

** Corresponding author: sareh.sangy@gmail.com*

Abstract

Introduction: Elderly is one of the most sensitive stages of life, and in the near future, a high percentage of the population is made up of the elderly. This period of life is often associated with an increased risk of chronic illness. The aim of this study was to determine the incidence of chronic diseases and its impact on the quality of life of the elderly.

Methods: In this cross-sectional study in 2018, 203 elderly subjects were selected through a multi-stage sampling method in elderly of Kahrizak sanatorium in Tehran. The history of chronic diseases was collected through checklist and face-to-face interviews. Quality of life assessment was performed using standard quality of life questionnaire (SF36). Data were analyzed using independent t-test and chi-square in SPSS software version 18.

Results: The results showed that 167 subjects aged 82.22% had at least one chronic disease and the quality of life of people with chronic diseases was significantly lower in all areas than in healthy subjects (P > 0/05).

Conclusion: The findings of this study indicate the high prevalence of chronic diseases in the elderly and its impact on the quality of life of the elderly. Therefore, it is necessary to focus on the elderly and take appropriate measures to improve the quality of life of this group of people.

Keywords:

Aging,

Chronic Diseases,

Quality of Life.

1. Introduction

Long life is one of the achievements of the twenty-first century. The aging phenomenon of the world population is due to the reduction in the mortality rate due to advances in medical sciences, health and education, as a result of an increase in the rate of life expectancy (1). Elderly is one of the most critical stages of life and is a growing process that in the near future will account for a high percentage of the global population. The United Nations estimates that the world's elderly population will double by 20 billion in 2025 (1.2 billion) (2). According to the organization, Iran, after the UAE and Bahrain, ranked third in terms of population aging. Based on the statistics of the country's civil registration organization, the population growth rate over 60 years old in Iran from 2011-2050 is more than 26%, and it is expected that by the year 2050 about 33% of the population will be over 60 years old (3). As the age increases, the risk of one or more chronic illnesses increases, so that most of the elderly over the age of 60 have at least one chronic illness (4). Chronic illness is a long-term disease that causes physical changes in the body and limits the function of the patient. Chronic illness is usually difficult, and its treatment is long and difficult to recover, and in some cases there is no clear definitive treatment (5). At the moment, the number of deaths from chronic diseases and diseases of the aging period is

increasing rapidly. The cost and duration of the treatment are 20 to 30 times more severe than the disease, and the impact of these care on the elderly's lifespan and function is very low. (6). People with chronic illness often experience a disorderly illness that has a negative impact on the quality of life associated with health. On the other hand, the aging of the elderly with these diseases has a double effect on the decline in quality of life (7). Quality of life has a broad and multidimensional concept and has at least four aspects: daily activity of life, social function (work, home management), mental performance, and the ability to engage in enjoyable activities (recreation, entertainment, etc.) (8). What contemporary science takes into consideration is not just prolonging life, but it should be noted that the extra years of human life ultimately lead to calm and physical and mental health, and if such conditions are not met, scientific advances to supply Longer life will be fruitless. Evaluating the quality of life of the elderly will examine their health status, the effectiveness of medical and health interventions, disease assessment, cost estimation, and the effectiveness of health care policies in the elderly and help plan. (9) Forjaz Joao et al. Spain, the disability caused by chronic diseases is associated with poor quality of life. In this study, the prevalence of chronic diseases (59.5%) and high blood pressure (55.3%) are the most prevalent among the elderly (10). The results of Bazrafshan et al. Research show the effect of some factors such as diseases, level of education on marital status, age, income and occupation on the quality of life of the elderly (11). Considering the increasing number of elderly people and the serious risks of chronic illnesses and the fact that chronic illness can increase the burden of responsibility of the elderly family and financially cost, so doing studies to assess the health status of the physical and their psychology to raise the level of quality of life in this period is mandatory. Studies in Iran indicate that the studies conducted in this regard are mainly related to the effects of demographic characteristics such as age, sex, literacy and economic status on the quality of life of the elderly and the role of these variables in the study of chronic diseases not taken. Also, their impact on the dimensions and sub-dimensions of quality of life is not expressed separately. The aim of this study was to investigate the effects of chronic diseases and some demographic information on the quality of life of the elderly in Kahrizak sanatorium in Tehran. It is expected that the results of this study can provide appropriate and practical solutions to identifying effective factors in the quality of life of the elderly.

2. Method

This cross-sectional study was conducted. The minimum sample size of the study, taking into account the magnitude of the error of the type I at the level of 0.05, and the reported prevalence of chronic diseases in the elderly was 92.2% (9) and the estimated error was 0.1, the prevalence, using the formula for estimating the size of a ratio, 136 people were estimated. Finally, in order to increase the power of study, 203 elderly people over 60 years of age at Kahrizak sanatorium were enrolled using multi-stage sampling. In order to create the most variation in the sample, at first different sections of the sanatorium were identified and then from each section, with the inquiry of each section, the elderly over the age of 60 were selected. Before completing the questionnaire, the goals of the study were clearly explained to the participants in the study, and interviews were conducted only by those with oral consent to participate in the study. Data were collected through a two-part questionnaire and interviewed. The first part of the questionnaire included questions about the demographic characteristics of the subjects as well as questions about the history of chronic diseases. The purpose of this study is to identify any of the diseases of articular pains, hypertension, high blood lipids, low back pain, osteoporosis, cardiovascular disease, type 2 diabetes, depression, diseases and digestive disorders, chronic respiratory diseases, Myocardial infarction is cancer. The second part of the questionnaire was about the quality of life assessment of the elderly. For this purpose, the standard of quality of life questionnaire (SF36) was used. The questionnaire includes eight areas of physical function, limitation of the role played by physical problems, general health, physical pain, happiness and vitality, social function, role playing from emotional problems, mental health. The first four areas are related to physical and mental health. The following areas are related to the mental health dimension. Valuation of questions in each field by converting the total score of that area to the minimum score of zero and the maximum score of 100. In all areas, the score of zero points represents the lowest level of quality of life and the score of 100 represents the highest level of quality of life in the relevant area. In previous studies, the Persian version of the SF36 questionnaire has been standardized and its validity and reliability have been reported to be desirable (12). Data were collected by SPSS software version 18 and descriptive statistics were presented using mean and standard deviations for quantitative and frequency variables and percentages for qualitative variables. Statistical analysis of the data was also performed according to the nature of the independent variables using independent t-test and chi-square test.

3. Results

In the study, 203 elderly people living in the Kahrizak sanatorium participated in the study. The mean (SD) age of the elderly was 66.99 ± 8.28. Nearly a third of the elderly are illiterate, and only 10 percent of them have high school diplomas. The descriptive information of the variables studied in the study is presented in Table 1.

Table 1. Distribution of the variables studied in the elderly of Kahrizak sanatorium

Variable	Variable levels	Abundance	Percentage
Sex	Man	92	54.67
	Female	11	45.33
Age	60 to 74	128	63.05
	75 and above	75	36.94
education level	illiterate	76	37.43
	Literacy reading and writing	106	52.21
	Diploma and higher	21	10.34
Financial affiliation	Yes	115	56.65
	No	88	43.35

The results showed that 167 (82.26%) of the elderly were suffering from at least one chronic disease, and 36 (17.74%) had no chronic disease. The variables of sex, age, and level of education were significantly correlated with the incidence of chronic diseases (P> 0.05). The outbreak of chronic diseases has been reported in terms of the variables studied in Table 2.

Table 2. Frequency distribution of chronic disease in the elderly of Kahrizak sanatorium in terms of the variables studied

Variable	Variable levels	Chronic disease				Significance level (P> 0/05)
		Yes		No		
		Frequency	percentage	Frequency	percentage	
Sex	Man	70	76.08	22	23.92	0.036
	Female	97	87.38	14	12.62	
Age	60 to 74	98	76.56	30	23.44	0.005
	75 and above	69	92	6	8	
education level	illiterate	67	88.16	9	11.84	0.001
	Literacy reading and writing	106	16.04	17	83.96	
	Diploma and higher	11	52.38	10	47.62	
Financial affiliation	Yes	97	84.34	18	15.66	0.375
	No	88	79.54	18	20.56	

In terms of quality of life in the elderly studied, the highest and lowest mean of quality of life scores in the sub-scales of physical health were related to physical and physical health, respectively. Also under the mental health scale, the highest and lowest mean scores were related to the fields of vitality and vitality and social functioning. Based on the results of this study, the mean scores in all eight areas of quality of life in healthy elderly were higher than the elderly with chronic diseases, which was significant in all areas (P> 0.05).

In examining the relationship between gender and quality of life, it was determined that mean score of quality of life in physical activity and limitation of role played by physical problems were significantly higher in males (P> 0.05), and in other areas, there was a significant difference between There were no women and men. In the study of relationship between age and quality of life, it was found that the elderly belonging to the age group of 60 to 74 years in the field of physical activity had a higher mean score than the elderly of 75 years and this difference was statistically significant (P> 0.05), and In other areas, the difference between the two groups was not significant.

4. Discussion

According to the findings of the present study, a significant percentage of elderly people were referred to at least one of the chronic diseases. This is while higher than the incidence of chronic diseases in the United States (13). In a study by Habibi et al. On the prevalence of chronic diseases in the elderly in Tehran's west, 8.86% of the samples suffered from at least one chronic illness (14). Concerning the relationship between the incidence of chronic disease and gender, the findings show that there is a meaningful relationship between them. These results indicate that the incidence of chronic diseases in women is more than that of men, and this can be due to some of the complications of aging in women. One of the consequences of aging in women is menopause, which can lead to complications such as cardiovascular disease, osteoporosis, incontinence or lack of urine control. Until recently, researchers believed that physical changes that occurred during menopause in women was the main cause of the development of aging psycosis (15).Therefore, in this study, the high prevalence of chronic diseases in women than men may be due to menopause. In this study, the prevalence of chronic diseases in the elderly belonging to the age group of 75 years and above was more than that of

Haomiao group (60-74 years). He believes that age increases the incidence of chronic diseases (16). Also, the percentage of chronic disease in elderly people with higher level of education was significantly lower than those with low education. The British Institute of Cardiology and the British Journal of Brainwashing Safety in a statistical survey concluded that low-educated people suffered from premature aging, due to improper use of brain cells and DNA-related communications, faster than their peers. While those with university education are at an advanced age (17,18). Also, people who are in a better position are knowledgeable because of smoking, not exercising and not observing diets according to their elderly status, destroying their lives. In this study, there was no significant relationship between economic status and chronic diseases, which may be due to the financial support of the family and relatives of the elderly. There was a significant correlation between the incidence of chronic diseases and quality of life in such a way that people with chronic diseases had lower quality of life than healthy elderly and this finding was consistent with the findings of other studies (6, 7 and 9).

As stated above, quality of life has two dimensions: physical and mental, and each dimension has four domains. Here, we intend to discuss the role of demographic factors of the elderly with chronic diseases in the areas of quality of life.

Concerning the relationship between quality of life and the gender variable, the results indicate that there is a significant relationship between the physical function and the limitation of the role played by the physical problems between the sexes and the quality of life, and men have a better quality of life than women. With the advent of aging, malnutrition occurs due to the inability to ingest certain foods, such as protein foods, as well as to reduce the absorption capacity of the gastrointestinal tract. Lack of nutrition in the elderly reduces muscle mass and decreases bodily strength. (19,20). But this problem is more prevalent in women than men because the male body is more muscular than the female body, so that the muscles of an adult are 40% higher than that of a woman and the average physical strength of a man is 2 times the force of a woman His wife is his. This difference makes men more capable of physical and physical abilities than women (21). In the study of relationship between age and quality of life, it was found that the elderly belonging to the age group of 60 to 74 years had a higher mean score in physical activity than those aged 75 years and older. This difference was statistically significant. Malnutrition, Alzheimer's, muscle problems, osteoporosis, hypertension, fat and high blood sugar, fatigue, weakness, and reduced mobility, and hundreds of other diseases are the consequences of aging and aging (22), which can justify the findings. . This finding is consistent with the results of the study by Bowling et al. (23,24). The quality of life scores of elderly people who were financially dependent were significantly lower in all aspects of the eight dimensions of quality of life than those who had financial autonomy. Other studies have shown that quality of life and health are affected by incomes, and in poorer elderly people are more likely to develop illnesses, which reduces their quality of life (6).

5. Conclusion

Regarding the high prevalence of chronic diseases and the low quality of life of the elderly living in the Kahrizak sanatorium, the development and implementation of health and nursing programs is more useful. Conducting workshops to learn about the effects of aging and providing solutions to overcome these problems, providing advice and building counseling sessions and recreational facilities for the elderly can help to improve the physical and mental dimension of the quality of life of the elderly.

6. Reference

1. Assessment of the correlation between lifestyle an quality of sleep in elderly who referred to retirement center in RASHT, Holistic Nursing and Midwifery. 2007؛17(2):15-22[in Persian].
2. Exploration of family reinforcing factors in elderly care through thematic analysis. Nursing of the vulnerable journal. 2015؛1(1): 50-64 [in Persian].
3. Khalvati M, Nafei A, Ostadhashemi L. Social exclusion domains of the elderly: A systematic review. . 2015؛18(12): 10. [in Persian].
4. Hosseini, SR, Zabihi, A, Savadkohi S, Bijani A. PREVALENCE POPULATION IN AMIRKOLA (2006-2007). Journal of Babol University Of Medical Sciences. 2008;10(2):68-75.[in Persian]
5. Bani Asadi T, Jamalpour A. Improvement of Senile Chronic Disease Management with Health Information Technologies. Journal of Iran Health Information Management. 2012;7(1):38-43 .[in Persian]
6. Habibi A, Nemadi-Vosoughi M, Habibi S, Mohammadi M. Quality of Life and Prevalence of Chronic Illnessesamong Elderly People: A Cross-Sectional Survey. journal of health. 2012;3(1):58-66 .[in Persian]

7. Schlenk EA, Erlen JA, Dunbar-Jacob J, McDowell J, Engberg S, Sereika SM, et al. Health-related quality of life in chronic disorders: a comparison across studies using the MOS SF-36. Quality of Life Research. 1997;7(1):57-65.
8. Yohannes AM, Roomi J, Waters K, Connolly MJ. Quality of life in elderly patients with COPD: measurement and predictive factors. Respiratory medicine. 1998;92(10):1231-6.
9. Esmaeili Shahmirzadi S, Shojaeizadeh D, Azam K, Salehi L, Tol A, Moradian Sorkhkolaei M. The Impact Of Chronic Diseases On The Quality Of Life Among The Elderly People In The East Of Tehran Payavard Salamat. 2012;6(3):225-35 .[in Persian]
10. Forjaz MJ, Rodriguez-Blazquez C, Ayala A, Rodriguez-Rodriguez V, de Pedro-Cuesta J, Garcia-Gutierrez S, et al. Chronic conditions, disability, and quality of life in older adults with multimorbidity in Spain. European journal of internal medicine. 2015;26(3):176-81.
11. Quality of elderly's life in shiraz ,jahandidegan club. Iranian Journal of Ageing. 2008;3(1):33-41. [in persian]
12. Montazeri A ,Goshtasebi A, Vahdaninia A, Gandek B. The Short Form Health Survey (SF-36): translation and validation study of the Iranian version. Quality of Life Research. 2005;14(3):875 82. [in persian]
13. Bauer UE, Briss PA, Goodman RA, Bowman BA. Prevention of chronic disease in the 21st century: elimination of the leading preventable causes of premature death and disability in the USA. The Lancet. 2014;384(9937):45-52.
14. Quality Of Life in elderly people of west of Tehran. Iranian Journal of Nursing Research. 2008;2(7):29-35. [in persian]
15. Soltani O. Menopausal prevalence and related factors Among women referred to Mostafa khomeini hospital of Ilam, in 2001. Journal of Ilam University of Medical Sciences. 2002;10(37-38):44-9.[in Persian]
16. Jia H, Lubetkin EI. The impact of obesity on health-related quality-of-life in the general adult US population. Journal of public health. 2005;27(2):156-64.
17. Steptoe A, Hamer M, Butcher L, Lin J, Brydon L, Kivimäki M, et al. Educational attainment but not measures of current socioeconomic circumstances are associated with leukocyte telomere length in healthy older men and women. Brain, behavior, and immunity. 2011;25(7):1292-8.
18. Hekmatpou D, Jahani F, Behzadi F. Study the Quality of Life among Elderly Women in Arak in 2013. Arak University of Medical Sciences Journal. 2014;17(2):1-8. [in persian]
19. Mokhtari F, Ghasemi N. Comparison of Elderlys "Quality of life and mental health living in nursing homes and members of retiered club of Shiraz city". Iranian Journal of Ageing. 2011;5(4):0. [in persian]
20. mahan lk, stump ss. Nutrition principles krause. Tehran: jamee negar 2012. 299 p. [in persian]
21. hosseini sgh. Biological differences between men and women Book Showcases. 2000;17:220-59. [in persian]
22. Sadeghipoor Rodsari H, Maaref H, Holakooie Naeeni K. Evaluation of social, economic and health requirements of elderly residing in the area under the supervision of Tehran University of Medical Sciences. Tehran University Medical Journal. 1998;56(6):88-92. [in persian]
23. Bowling A, Hankins M, Windle G, Bilotta C, Grant R. A short measure of quality of life in older age: The performance of the brief Older People's Quality of Life questionnaire (OPQOL-brief). Archives of Gerontology and Geriatrics. 2013;56(1):181-7.
24. Turvey CL, Wallace RB, Herzog R. A revised CES-D measure of depressive symptoms and a DSM-based measure of major depressive episodes in the elderly. International Psychogeriatrics. 1999;11(02):139-48.

International Conference on Cancer Research 2019

Website: www.CancerConf.org

June 10-11, London, UK



The Cytotoxic Properties and Anticancer Impacts of Zinc oxide Nanoparticles On Human Breast, MCF7 Cell Lines

Ghasem Rahimi Kalateh Shah Mohammad [1]*, Vahid Pouresmaeil [1]

[1] *Biochemistry Department, Islamic Azad University, Mashhad Branch, Iran*

* *Corresponding author: jasemrahimi.jr@gmail.com*

Abstract

Nanotechnology enable us to manipulate the substances at nanoscale level. Metallic nanomaterials such as Zn O nanoparticles synthesized with chemical methods, which has the disadvantage of using deleterious chemicals. Green chemistry allows the design and synthesis of nanoparticles, with reducing or elimination of hazardous materials. One of the important applications of zinc oxide nanoparticles is to use as an antibacterial and anticancer agent. In this study, we synthesized Zn O nanoparticle using Hyssopus officinalis plant extract and evaluate its their cytotoxicity on MCF7 breast cancer cell line.

Materials and Methods: The MTT (3-(4,5-dimethylthiazol-2-yl)-2,5-diphenyltetrazolium bromide) cell viability assay was done on MCF7 cell line. Cells were seeded on 96-well plates and incubated for 24 hours. After 24 hours, cells were treated with different concentrations of Zn O nanoparticles (8, 16, 32, 64 and 128 µg / ml) and incubated for next 24, 48 and 72 hours. Then, treatments removed and MTT was added to each well. DMSO was used in order to dissolve insoluble blue crystals and absorbance was read at 570 nm.

Results: Results showed that Zn O nanoparticles synthesized in Hyssopus officinalis plant extract are able to inhibit MCF7 cells. However, this inhibition was at low concentrations of Zn O nanoparticles and the values of IC50 (in 24, 48 and 72-hour treatment) respectively was calculated at 16, 10 and 5 µg/ml NPs.

Conclusion: Results of this study indicated the inhibitory effects of Zn O nanoparticles synthesized in Hyssopus officinalis plant extract on cancer cells. However, in vitro studies should perform in order to confirm these effects. Finally, these results demonstrate the anticancer potential of Zn O nanoparticles, which could be used as therapeutic agent in cancer therapy.

Keywords:

Green Chemistry,

Zn O Nanoparticles,

Hyssopus Officinalis,

MCF7 Cell Line,

Breast Cancer..

1. Introduction

In recent years, many attempts have been made to produce nanoparticles due to their specific optical, chemical, electrical and photoelectric properties, which confirmed the various uses of these materials in the fields of catalysts, optics, biomedical knowledge, mechanics, magnetism and Energy is[1] . Zinc is a rare element in the body and is also used as a food supplement in foods, so some researchers consider zinc oxide nanoparticles as low toxicity substances. Various studies have been conducted on the toxicity of zinc oxide nanoparticles, the main cause of which is the toxicity of zinc oxide nanoparticles, related to microorganisms and factors related to the release of metal cations [2]. Concerning the formation of zinc oxide nanoparticles that are synthesized both in chemical and green form, it has to be said that in the process of various plant extracts, which are very common today, it is completely safe and safe compared to chemical synthesis[3]. The different structures of nanoparticles make them possible to be used in many fields, including biosensors, Nano medicine, and bio nanotechnology [4]. Moreover, the applications of nanoparticles (NPs) in the health, food, chemistry and cosmetics industries are developing rapidly. It should be noted that the synthesis of nanoparticles is feasible by different methods, which are known as green, chemical or physical synthesis [5-7]. Expensive equipment and the difficult conditions of synthesis in the physical methods [8] as well as dangerous and toxic chemicals for patients and researchers in the chemical methods, have increased the applications of green synthesis approaches [9]. The

synthesis of nanoparticles through plants, bacteria, fungi and algae is called green synthesis. The advantage of this approach is the pure amounts of ZnO NPs production on a large scale [10].

It is known that ZnO has the individual potential for applying in the biomedical and cancer fields, due to its specific chemical properties [11]. However, numerous studies have shown that the acute and chronic proximity to ZnO ultimately leads to cytotoxicity and genotoxicity in plants and animals [12-14]. It has been shown that the ZnO-NPs toxicity is due to its involvement in the ROS generation and the oxidative stress induction [15-17].

Methods and materials

Green synthesis of Zinc oxide nanoparticles and approval tests

The fresh green leaves and stem of *Hyssops officinalis* were harvested from 10 g of the collected parts were washed thoroughly thrice with water followed by sterile distilled water (DW). After cutting and soaking the plant in 200 mL distilled water, they were shade-dried for

10-15 days and then powdered by a domestic blender. Heating the 0.3 g of produced powder was performed at 50°C for 2 h in 100 mL DW. 1 mm Zinc acetate [Zn $(O_2CCH_3)_2(H_2O)_2$] was added in 50 ml DW and mixed by magnetic stirrer at 25 ° C for 1 h. A mixture containing of 20 mL NaOH, 50 mL Zinc acetate, and 25 mL of plant extract was made subsequently and mixed for 3 h. The yellow color was indicated the ZnO NPs synthesis. Centrifuging at 8000 rpm at 60°C for 15 min was performed to collect the pellet. The pellet was dried at 80°C for 2 h and stored for future studies [18, 19].

The X-ray diffractometer (PAN analytical X-Pert PRO) was used to measure the pattern of density, purity, and size of the ZnO NPs. X-ray diffraction (XRD) analysis using CuKα radiation (1.54060 Å) X-ray crystallography was applied. FTIR spectroscopy was applied to define the FTIR spectra in a resolution of 4 cm^{-1} [20]. Finally, to analyze the shape and size of NPs, SEM and TEM were used respectively. The average size of produced nanoparticles was 20 nm.

MTT assy

To study the impact of ZnO NPs on cell viability, 3-(4,5-dimethylthiazole-2-yl)-2,5-diphenyl tetrazolium bromide (MTT) was applied. 75×10^3 cells of Huh7 cell line were seeded into each plate of 17 culture plates. Moreover, HupG2 and Huvec cells were seeded in two groups of five plates by the same way. After an overnight incubation, the mediums were replaced with a fresh modified medium containing ZnO NPs. Incubation plane was designed into two classes of treatments, dose-dependent and time-dependent viability assays. For dose-dependent MTT assays, different ZnO NPs concentrations were added into the medium of all of 27 cultured cells and incubated for 24 hours. For time-dependent MTT assays, certain doses of ZnO NPs, were used to measure the viability of Huh7 cell line for 48 hour incubation. The doses, which were used are indicated in Figures 9 and 10.

Upon the incubations were completed, the ZnO NPs-modified medium was removed, and 100 µL of medium containing MTT 0.5 mg/mL was added into all culture plates. Then, 3 hours incubation at 37°C was performed. 100 µL of dimethylsulfoxide (Sigma) was replaced with MTT-medium and shaked for 10 minutes to stabilize the formed formazan. Versamax microplate reader (Molecular Devices, Sunnyvale, CA) was used at a wavelength of 570 nm to measure the absorbance (background effect was removed at 690 nm).

Statistical analysis

Statistical significance was determined by one-way analysis of variance (ANOVA) followed by Dunnett's multiple comparison test. Significance was ascribed at $p < 0.05$.

Results

The viability of the treated hepatocyte cell lines by ZnO NPs using *Hyssopus officinalis* plant extract

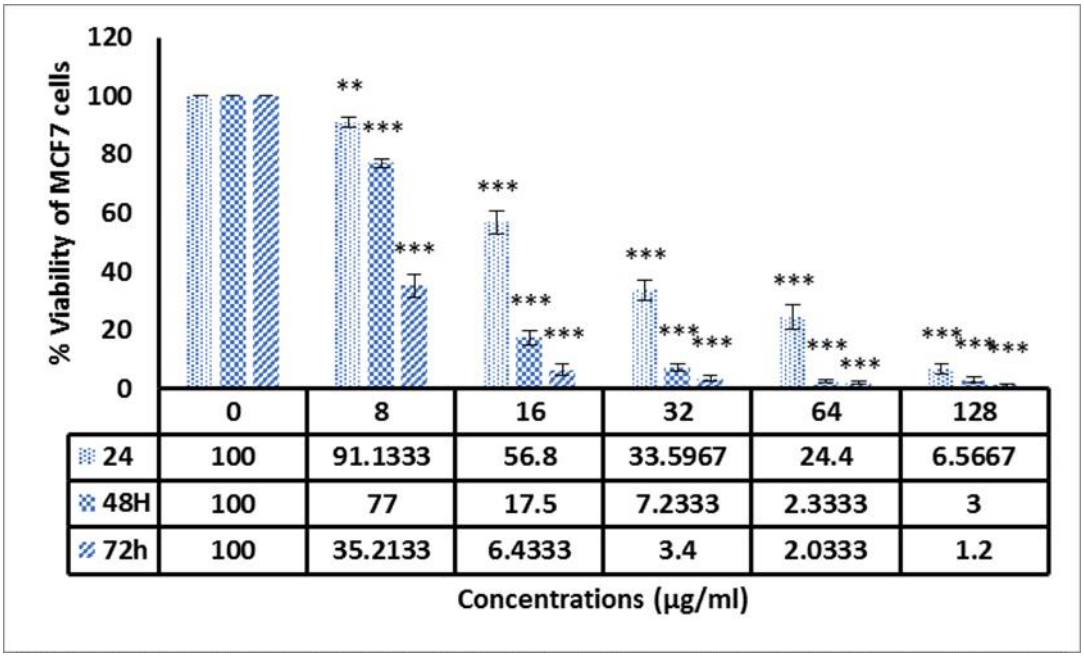
The results of MTT assay analysis for MCF7 cell lines were designed in Figures 1. The IC50 value for MCF7 cell lines (in 24, 48 and 72-hour treatment) respectively was calculated at 16, 10 and 5 µg/ml NPs.

According to the results obtained from breast cancer cells that were treated with ZnO nanoparticles in a green way from the *Hyssopus officinalis* plant extract, it was considered that with increasing concentration and increasing time, the effects of ZnO nanoparticles on the growth of cancer cells increased, so that these nanoparticles At a concentration of 128 µg / ml, it has the highest cytotoxic effect on MCF7 cells at different times.

Morphological Images of MCF7 Cells

According to the results, in the form of the effect of zinc oxide nanoparticle toxicity at concentrations of 12 and 24 µg / ml, compared to the control group. As it is seen, the size and number of cells treated with the nanoparticle is reduced and the cell deformation can be attributed to changes in their appearance, such as cytoplasmic decline, germination of cells, and changes in nucleus pigmentation. By increasing the concentration of the nanoparticle, the number of cells decreases and decomposes, which indicates the cytotoxic effects associated with the concentration of zinc oxide nanoparticles synthesized by the green method from the *Hyssopus officinalis* plant extract.

The viability of the treated hepatocyte cell lines by ZnO NPs



	0	8	16	32	64	128
24	100	91.1333	56.8	33.5967	24.4	6.5667
48H	100	77	17.5	7.2333	2.3333	3
72h	100	35.2133	6.4333	3.4	2.0333	1.2

Figure 1: MCF7 cells treated with zinc oxide nanoparticles produced from the *Hyssopus officinalis* plant extract (The significance levels was defined by (**P < 0.01) and (***P < 0.001)).

Morphological Images of MCF7 Cells

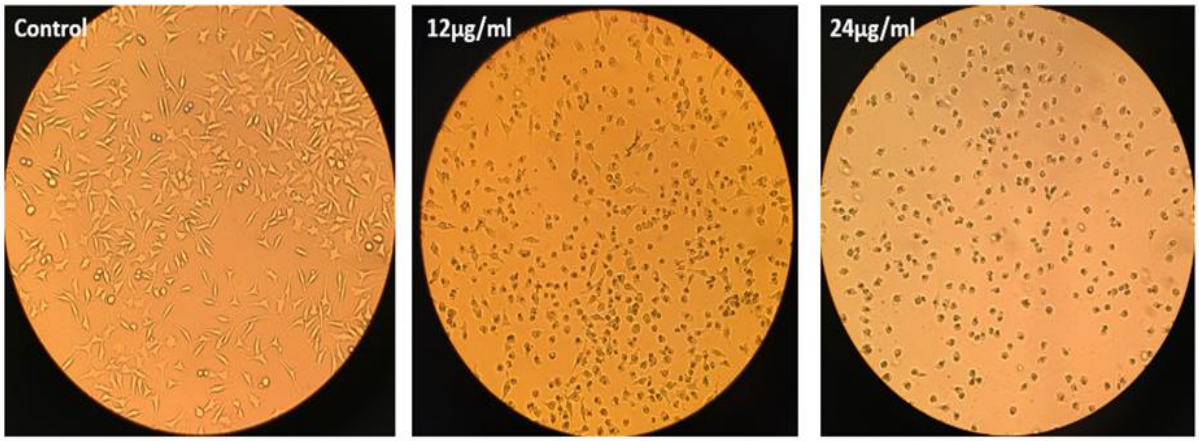


Figure 2: Morphology of cells treated with zinc oxide nanoparticles synthesized from *Hyssopus officinalis* plant extract compared to control.

Discussion

Cytotoxicity parameters such as MTT, NRU and LDH assays represent the damage in mitochondrial, lysosomal and cell membranes, respectively that eventually triggers cell death37. These assays serve as sensitive and integrated measures of cell integrity and of the inhibition of cell proliferation. cytotoxicity results were consistent with the observed higher MMP loss in cells treated with Al-doped ZnO nanoparticles than those of pure ZnO nanoparticles. Damage to

lysosomal membranes is known to release lysosome protease into intracellular spaces, which affects the neighboring cells and triggers cell death due to apoptosis. LDH leakage from cells is further evidence for the penetration of nanoparticles into cells and cell membrane damage16,38. Liver and breast cancer are the most traumatic diseases because they affect the major organs of the body. Nanomedicine recently emerged as a better option for the treatment of these deadly diseases. As a result, many nanoparticles have been used to treat cancer cell lines. Of the various nanoparticles, zinc oxide exhibits biocompatibility[21].

The toxicity effects of ZnO NPs are shown in several types of human cell lines including hepatocytes, kidney and alveolar adenocarcinoma, depending on the nanoparticle's size and dosage used [31-33]. It is known that the ZnO NPs toxicity is related to the Zn ionization to Zn2+ and production of free radicals from the NPs surface, which results in metabolic and ionic imbalance of the cell [34-36]. ZnO NPs lead to induce the oxidative stress by the generation of ROS, therefore, the lack of sufficient antioxidant system causes the cell death and genotoxicity [36]. Some studies argued that ZnO nanoparticles induce toxicity due to the dissolution of the particles into Zn^{2+} ions and metal ions doping can reduce the ZnO cytotoxicity by reducing ZnO dissolution[22]. However, some investigators demonstrated that ZnO nanoparticles liberate Zn^{2+} ions in aqueous state, but the levels of Zn^{2+}ions released were insufficient to promote cytotoxicity in human cells unless the particulate matter is in contact with the cells[23].

We found that zno NPs improves the inherent selective cytotoxicity of ZnO nanoparticles toward human breast cancer cells while posing no toxicity to normal cells. ZnO nanoparticles were found to induce apoptosis in MCF-7 cells. Overall, our data suggested a novel approach through which the inherent selective cytotoxicity of ZnO nanoparticles against human breast cancer cells can be improved. Further research on anticancer activity of ZnO nanoparticles from *Hyssopus officinalis* plant extract in different types of cancer cells is warranted.

Conclusion

Our results indicated a novel approach through which the inherent selective cytotoxicity of ZnO nanoparticles from *Hyssopus officinalis* plant extract against cancer cells can be further improved.

Acknowledgments

Hence, we thank and appreciate the guidance of the professors of the Faculty of Basic Sciences of the Islamic Azad University of Mashhad which collaborated in different stages of this research. The work done in this research was done at a personal expense.

Contributing Contributors

All authors had standards of writing on the basis of the International Committee's recommendations to medical journal publishers.

Conflict of interest

The authors state that there are no conflicts of interest in the current research.

References

1. Mandal, D., et al., *The use of microorganisms for the formation of metal nanoparticles and their application.* Applied microbiology and biotechnology, 2006. **69**(5): p. 485-492.
2. Ben-Slama, I., et al., *Sub-acute oral toxicity of zinc oxide nanoparticles in male rats.* Journal of Nanomedicine & Nanotechnology, 2015. **6**(3): p. 1.
3. Sabir, S., M. Arshad, and S.K. Chaudhari, *Zinc oxide nanoparticles for revolutionizing agriculture: synthesis and applications.* The Scientific World Journal, 2014. **2014**.
4. Ashe, B., *A Detail investigation to observe the effect of zinc oxide and Silver nanoparticles in biological system*. 2011.
5. Rao, M.D. and P. Gautam, *Synthesis and characterization of ZnO nanoflowers using C hlamydomonas reinhardtii: A green approach.* Environmental Progress & Sustainable Energy, 2016. **35**(4): p. 1020-1026.
6. Afifi, M., O.A. Almaghrabi, and N.M. Kadasa, *Ameliorative effect of zinc oxide nanoparticles on antioxidants and sperm characteristics in streptozotocin-induced diabetic rat testes.* BioMed research international, 2015. **2015**.

7. Chen, J., et al., *Nitric oxide ameliorates zinc oxide nanoparticles-induced phytotoxicity in rice seedlings.* Journal of hazardous materials, 2015. **297**: p. 173-182.
8. Chandrasekaran, R., et al., *Formulation of Carica papaya latex-functionalized silver nanoparticles for its improved antibacterial and anticancer applications.* Journal of Molecular Liquids, 2016. **219**: p. 232-238.
9. Dhandapani, P., et al., *Bio-approach: ureolytic bacteria mediated synthesis of ZnO nanocrystals on cotton fabric and evaluation of their antibacterial properties.* Carbohydrate polymers, 2014. **103**: p. 448-455.
10. Yuvakkumar, R., et al., *Novel green synthetic strategy to prepare ZnO nanocrystals using rambutan (Nephelium lappaceum L.) peel extract and its antibacterial applications.* Materials Science and Engineering: C, 2014. **41**: p. 17-27.
11. Rasmussen, J.W., et al., *Zinc oxide nanoparticles for selective destruction of tumor cells and potential for drug delivery applications.* Expert opinion on drug delivery, 2010. **7**(9): p. 1063-1077.
12. Adamcakova-Dodd, A., et al., *Toxicity assessment of zinc oxide nanoparticles using sub-acute and sub-chronic murine inhalation models.* Particle and fibre toxicology, 2014. **11**(1): p. 15.
13. Lin, D. and B. Xing, *Phytotoxicity of nanoparticles: inhibition of seed germination and root growth.* Environmental Pollution, 2007. **150**(2): p. 243-250.
14. Wang, B., et al., *Acute toxicological impact of nano-and submicro-scaled zinc oxide powder on healthy adult mice.* Journal of Nanoparticle Research, 2008. **10**(2): p. 263-276.
15. Li, N., T. Xia, and A.E. Nel, *The role of oxidative stress in ambient particulate matter-induced lung diseases and its implications in the toxicity of engineered nanoparticles.* Free Radical Biology and Medicine, 2008. **44**(9): p. 1689-1699.
16. Nel, A., et al., *Toxic potential of materials at the nanolevel.* science, 2006. **311**(5761): p. 622-627.
17. Xia, T., et al., *Comparison of the mechanism of toxicity of zinc oxide and cerium oxide nanoparticles based on dissolution and oxidative stress properties.* ACS nano, 2008. **2**(10): p. 2121-2134.
18. Ahmed, S., et al., *Green synthesis of silver nanoparticles using Azadirachta indica aqueous leaf extract.* Journal of Radiation Research and Applied Sciences, 2016. **9**(1): p. 1-7.
19. Santhoshkumar, J., S.V. Kumar, and S. Rajeshkumar, *Synthesis of zinc oxide nanoparticles using plant leaf extract against urinary tract infection pathogen.* Resource-Efficient Technologies, 2017. **3**(4): p. 459-465.
20. Mishra, V. and R. Sharma, *Green synthesis of zinc oxide nanoparticles using fresh peels extract of Punica granatum and its antimicrobial activities.* International Journal of Pharma Research and Health Sciences, 2015. **3**(3): p. 694-699.
21. Wahab, R., et al., *ZnO nanoparticles induced oxidative stress and apoptosis in HepG2 and MCF-7 cancer cells and their antibacterial activity.* Colloids and surfaces B: Biointerfaces, 2014. **117**: p. 267-276.
22. Xia, T., et al., *Decreased dissolution of ZnO by iron doping yields nanoparticles with reduced toxicity in the rodent lung and zebrafish embryos.* ACS nano, 2011. **5**(2): p. 1223-1235.
23. Moos, P.J., et al., *ZnO particulate matter requires cell contact for toxicity in human colon cancer cells.* Chemical research in toxicology, 2010. **23**(4): p. 733-739.

International Conference on Cancer Research 2019

Website: www.CancerConf.org

June 10-11, London, UK



A Comprehensive Study of Possible Crosstalk between Angiogenic and Metabolic Signaling Pathways in Cancer

Hamid Latifi-Navid [1]*, Sepideh Taghizadeh [1], Zahra-Soheila Soheili [1], Shahram Samiei [1], Ehsan Ranaie Pirmardan [1]

[1] *Molecular Medicine Department, National Institute of Genetic Engineering and Biotechnology, Tehran, Iran*

** Corresponding author: hlatifin@gmail.com*

Abstract

Purpose:

Tumor angiogenesis is a fundamental, complex and dynamic process necessary for the growth of solid tumors. Vascular system is a highly branched network lined by endothelial cells (ECs), it supplies tissues with oxygen (O2) and nutrients. During angiogenesis, ECs must increase associated metabolic activities to facilitate incorporation of nutrients into biomass. Understanding EC metabolism reveals new perspectives on disease mechanisms in the vascular system and provides new therapeutic approaches for disorders complicated with aberrant vessel growth. Metabolic pathways, such as glycolysis, play distinct, essential roles during vessel formation. In adults, most ECs are quiescent for extended periods, however, they rapidly switch to growth upon proangiogenic stimulation. Signaling pathways that control angiogenic switch control EC metabolism, eliciting a metabolic state permissive for growth and proliferation. Interfering with these metabolic adaptions renders ECs less sensitive to angiogenic signals. Another compensatory mechanism to hypoxia is metabolic symbiosis, a process in which cells in the oxygenated milieu use lactate to produce ATP, which is associated with the activation of glycolytic genes. The aim of this study is network analysis of known angiogenic pathways and related metabolic signaling pathways, looking for their intrinsic communication and determine plausible bottlenecks as novel targets in cancer disease.

Methods:

We investigated the association between angiogenesis, metabolic symbiosis and endothelial cell metabolic pathways using protein-protein interaction, gene-gene interaction and text mining approach by bioinformatics tools. By recruiting the markers of angiogenesis, metabolic symbiosis and endothelial cell metabolism in AMD, we designed an intersection network that includes information on how these three biological phenomena are linked.

Results:

We selected 92 important genes from multiple signaling pathways. The network of those genes was visualized using the Cytoscape software, highly interconnected regions (clusters), hub nodes with the highest degree-and nodes which control most of the information flow- in the network were identified by using Molecular Complex Detection (MCODE) and centrality analysis respectively.

Conclusion:

The results are leading us to the promising new directions in revealing cancer mechanisms and development of possible new treatment.

Keywords:

Crosstalk,

Angiogenic,

Metabolic,

Cancer.

International Conference on Cancer Research 2019

Website: www.CancerConf.org

June 10-11, London, UK



A Comprehensive Study of Possible Crosstalk between Angiogenic and Metabolic Signaling Pathways in Cancer

Seyed MohammadReza Soltani Moghadas [1]*

[1] *Naturopathic Researcher, Islamic Azad University, Iran*

** Corresponding author: Raysoltani123@gmail.com*

Abstract

Sea buckthorn or Elaeagnus rhamnoides is thorny tree with the height of 1 to 3m growing in Europe, western and central Asia to the west of china and northwest of Himalaya and in Iran it is found in Alborz mountain to Azerbayijan and Taleghan and Karaj valley. It has long and narrow leaves, sharped with the length of 5-6and one cm width. Its fruit is sphere, yellow and orange with sour taste. Different parts of plant particularly its fruits have phenolic compounds, vitamins (especially vitamin C), unsaturated fatty acids, and phytosterols such as beta-sitosterol beign investigated by some researchers. These fruits have useful antioxidant, anti-inflammatory and anticancer effects. It has also anti-proliferation properties and can induce apoptosis and stimulate the immune system; sea buckthorn oil counteracts many side effects of chemotherapy by restoring kidney and liver function, increasing appetite, and keeping general good health. Although the anticancer activity of sea buckthorn has been confirmed by many in vitro and in vivo animal studies, measurements should be taken for the development of well-controlled clinical experiments to determine the therapy and preventive does in this area. The present study discusses briefly about whether sea buckthorn is used as an anti-inflammatory and anticancer drug or not.

Keywords:

Sea buckthorn,

Antioxidant,

Anticancer,

Herbal treatment.

Introduction

Sea buckthorn (Elaeagnus rhamnoides (L.) A. or Hippophae rhamnoides) is a member of the Elaeagnaceae family. It is a forest species extending to Europe, western and central Asia to the west of china and North West of Himalaya and in Iran, it is extended from Alborz Mountain to Azerbaijan, Taleghan and Karaj valley. The results of a study showed that the collected samples from Alborz, Mazandaran, Eastern Azerbayijan and Ghazvin provinces belong to E.rhamnoides subsp. Caucasica but the samples collected from western Azerbaijan province are introduced with two noucleotide differences as a new sub-species as E. rhamnoides subsp. Azerbaijanica (Ahani, Jalilvand and Vaezi, 2016). Sometimes, this species is mistaken for Melia azederach L due to the Persian name similarity (Sadeghipour Rudsari et al., 1956).

Its local names are Kam, Keham (Karaj valley), Kah (in Taleghan), Chali (in Gharetape and Ishlegh in Mianeh)(Kokord (western Azerbayijan) around Tehran, it is called willow thorn and in Arabic, it is called "Shokolghesar " as its root is used as a latherwort to wash clothes. Some Arabs call it also Roman Ghasul (Ghasul means latherwort) and in old medicine books, it is called as "Aboghanes". All the organs of this plant such as its leaves, roots, seeds, and berries (known as seaberry) have a wide range of anti-inflammatory, anticancer, antioxidant, and anti-atherosclerotic activities (Zeb, 2006; Basu et al., 2007; Kumar et al., 2011; Suryakumar and Gupta, 2011; Xu et al., 2011; Christaki, 2012; Teleszko et al., 2015; Olas, 2016; Ulanowska et al., in press).

Vitamins (especially A, C, and E), lipids, carotenoids, amino acids, unsaturated fatty acids, and phenolic compounds that are found in the berries (Olas, 2016; Gradt et al., 2017; Ulanowska et al., in press) are presented in Table. The amount of minerals and vitamins in the fruits depends on the climate conditions, size, growth of the plant, and the method used to process and stores the plant material (Fatima et al., 2012; Malinowska and Olas, 2016). Gao et al. (2000) report changes

in antioxidant properties, besides other types of biological activity, in sea buckthorn berries during maturation stage, which were strongly correlated with the content of total phenolic compounds and ascorbic acid. Moreover, the antioxidant activity increased significantly and is related to the increase in total carotenoid content.



Figure 1- Sea buckthorn shrub

Table 1- The chemical composition of isolated parts of the sea buckthorn (44; modified).

Part of sea buckthorn	**Chemical composition**
Fruits (berries)	Vitamins (C, E, B, K1, D, A, folic acid)
	Micro and rare elements (potassium, magnesium,
	calcium, iron, sodium, manganese, zinc, copper, nickel)
	Carotenoids
	Phenolic compounds
	Lipids
	Amino acids
	Organic acids
	Proteins
	Sugars
	Pectins
Leaves	Vitamins (E, folic acid)
	Calcium, magnesium, potassium
	Carotenoids
	Phenolic compounds
	Amino acids
	Chlorophyll
	Proteins
	Pectins
Seeds	Carotenoids
	Phenolic compounds
	Lipids
	Proteins
Roots	Carotenoids
	Phenolic compounds
	Lipids- Proteins
Bark	Phenolic compounds

The main sources of ingredients are found not only in the raw fruits, but also in preparation of its products such as jams, juices, marmalades, or tinctures. Sea buckthorn fruits can be also used to make cookies (Li and Hu, 2015). Hu (2005) reports that sea buckthorn seed can be used to make oil and the leaves can used to make tea. While teas made from the seeds have laxative properties and help weight loss, infusions of the leaves have antidiarrheal properties; in addition, fruit teas strengthen the immune system, and fights against skin diseases (Sarwa, 2001; Frohne, 2010). The positive and unique properties of sea buckthorn have been known since at least the 12th century BC.

Nowadays, its products are used in many industries, especially the pharmaceutical, cosmetic and food industries. According to historical records, sea buckthorn was first used as a drug in China, and in modern era, the plant was formally listed in the Chinese pharmacopoeia in 1977 (The Comitte of Medicine and Treatment of China, 1977). Modern studies have shown that the different parts of sea buckthorn can be applied as natural remedies for cardiovascular diseases, as well as diseases of the skin, liver, and stomach. The therapeutic potential of its bioactive compounds is shown in Table . This study reviews the current knowledge about the different organs of sea buckthorn, and discusses whether they may represent an option for the treatment of cancer or not. It is worth to mention that the source information for this paper is derived not only from in vitro models, but also in vivo models.

Anticancer activity of sea buckthorn

A number of medicinal herbs compounds, particularly phenolic compounds such as proanthocyanidins, curcumin, and resveratrol, have offered significant benefits in cancer chemotherapy (Barrett, 1993; Bagchi and Preuss, 2004; Bagchi et al., 2014; Shanmugam et al., 2015; Ko et al., 2017) and radiotherapy (Cetin et al., 2008).

It is well proved that higher dietary use of phenolic compounds, especially procyanidins and flavonoids are associated with a lower risk of cancer (Barrett, 1993; Bagchi and Preuss, 2004; Duthie et al., 2006; Zafra-Stone et al., 2007; Cetin et al., 2008; Seeram, 2008; Bagchi et al., 2014; Chen et al., 2014; Wang et al., 2014; Giampieri et al., 2016; Kristo et al., 2016).

Sea buckthorn has a wide range of biological and pharmacological activities, including anticancer properties. Although their molecular mechanisms remain unknown, these compounds are present in different organs and their products, especially in the extract and oil (Xu et al., 2011).

The antitumor activity of sea buckthorn can be attributed to antioxidant compounds, particularly phenolic compounds such as flavonoids, including kaempferol, quercetin, and isorhamnetin as these compounds protect cells from oxidative damage that can lead to genetic mutation and to cancer (Christaki, 2012).

In vitro studies

Various in vitro studies have shown that sea buckthorn has anticancer activity. For example, Zhang et al. (2005) investigated changes in the expression of apoptosis-related genes in the human breast carcinoma cell Bcap-37 induced by flavonoids from sea buckthorn seed. Their bioinformatics analysis showed that the expression of 32 analyzed genes, including CTNNB1, IGFBP4, GADD34, and caspase 3 with the apoptosis of Bcap-37 cells, was affected by flavonoid treatment.

Teng et al. (2006) revealed that isorhamnetin (3′-methoxy-3,4′5,7-tetra hydroxyl flavone; a flavonoid isolated from sea buckthorn) has cellular toxicity effects against hepatocellular carcinoma cells (BEL-7402), with an IC50 of about 75 cc/μg after 72h treatment. Li et al. (2015) also found isorhamnetin has anti-proliferation effects on lung cancer cells in vitro as its concentrations ranging from 10 to 320 cc/μg were administrated orally in C57BL/6 mice (50 mg/kg/day) for 7 days. The authors suggest that the mechanism of isorhamnetin action may involve the apoptosis of cells induced by the down-regulation of oncogenes and up-regulation of apoptotic genes. Other observations showed that isorhamnetin inhibits the proliferation of cells from the human colorectal cancer cell (HT-29, HCT 116, and SW480), and stops cell cycle at the G2/M phase, and suppresses cell proliferation by inhibiting the PI3K-Akt-mTOR path. In addition, isorhamnetin reduces the phosphorylation levels of Akt (Ser473), phosphat-p70S6 kinase, and phosph-4E-BP1 (t37/46) protein, and enhances the expression of cyclin B1 protein at concentrations of 20 and 40 μM (Li et al., 2014).

In a study on human breast cancer cells MDA-MB-231, Wang et al. (2014) found that sea buckthorn procyanidins isolated from the seeds to have inhibitory effects on fatty acid synthase (FAS): as a key enzyme for long-chain fatty acid biosynthesis and its high levels are found in cancer cells. This inhibition is dose-dependent at concentrations ranging from 0 to 0.14 μg/ml. A concentration of 0.087 μg/ml inhibited 50% of FAS activity. Moreover, cell growth was suppressed by treatment with sea buckthorn procyanidins at concentrations ranging 10 and 60 μg/ml. In addition, the tested procyanidins were found to induce cell apoptosis in a dose-dependent method. The authors suggest that these procyanidins can induce MDA-MB-231 cell apoptosis by inhibiting intracellular FAS activity.

Olsson et al. (2004) compared the effect of 10 different extracts of fruits and berries, including sea buckthorn fruit, on the proliferation of HT29 semi-colon cancer cells and MCF-7 breast cancer cells. They observed that sea buckthorn

had the highest inhibition effect for the proliferation of HT29 and MCF-7 cells at its two highest concentrations (0.25 and 0.5%). The authors suggest that the inhibition of cancer cell proliferation was associated with concentrations of carotenoids and vitamin C. Moreover, they proposed the presence of a synergistic action between carotenoids, vitamin C, and anthocyanins. In addition, McDougall et al. (2008) found that sea buckthorn fruit extract had antiproliferative effects against cervical and a semi-colon cancer cells growing in vitro.

Boivin et al. (2007) determined the antiproliferative activity of the extract of 13 types of berries, including sea buckthorn, at concentrations of 10–50 μg/ml against five cancer cells in vitro: AGS stomach adenocarcinoma, ACF-7—mammary gland adenocarcinoma, PC-3—prostatic adenocarcinoma, Caco-2—colorectal adenocarcinoma, and MDA-MB-231—mammary gland adenocarcinoma. It was shown that sea buckthorn fruit extract, like blackberry and black chokeberry had anti-proliferative properties. However, no significant association was found between the anti-proliferative properties of the berry extracts and their antioxidant capacity, and the inhibition of cancer cell proliferation by the extract did not involve caspase-dependent apoptosis. Despite this fact, suppression of tumor necrosis factor (TNF)-induced activation of nuclear factor kappa-light-chain-enhancer of activated B cells (NFκB) was observed.

Recently, Guo et al. (2017) studied the phytochemical compounds of the berries of four different subspecies of sea buckthornH. rhamnoides L. subsp. sinensis (Sinensis), H. rhamnoides L. subsp. yunnanensis (Yunnanensis), H. rhamnoides L. subsp. mongolica (Mongolica), and H. rhamnoides L. subsp. turkestanica (Turkestanica) , as well as their antioxidant and antiproliferative properties against HepG2 human liver cancer cells in vitro. Of these species, H. rhamnoides L. subsp. sinensis demonstrated the highest phenolic content (about 39 mg gallic acid (GA) equiv./g dry weight) and corresponding total antioxidant activity, while the greatest cellular antioxidant and antiproliferative properties were observed in H. rhamnoides L. subsp. yunnanensis. These properties were attributed to the action of phenolic acids and flavonoid aglycones.

Zhamanbaeva et al. (2014) studied the effects of ethanol extract from sea buckthorn leaves on the growth and differentiation of human acute myeloid leukemia cells (KG-1a, HL60, and U937). Although a plant extract was found to inhibit cell growth according to cell strain and extract dose, the study does not identify the chemical content of the tested extract. They used three concentrations of the extract: 25, 50, and 100 μg/ml. The findings of the study suggest that the antiproliferative effect of sea buckthorn extract on acute myeloid leukemia cells was determined by activation of the S phase checkpoint, which probably led to the decrease of the cell cycle and stimulation of apoptosis.

Table 2- Sea buckthorn bioactive compounds and their therapeutic effects (44; modified).

Therapeutic effect	Bioactive compound
Antioxidant Analgesic Protection against destructive changes, thrombosis, and muscle cramps	Tocopherol
Antioxidant Involved in the synthesis of collagen Protection and restoration of the mucous membranes and epithelia Enhancing the immune system	Carotenoids
Anti-atherosclerotic action, anti-inflammatory and antibacterial properties The prophylaxis and treatment of hypercholesterolemia-induced cardiovascular disorders by lowering serum cholesterol concentrations Reducing the risk of stomach ulcers	Phytosterols
Protecting against cerebrovascular and cardiovascular disorders Stimulating the immune system Promoting cognitive function and bone health.	Unsaturated fatty acids

Positive effect on such neurological disorders as depression, schizophrenia, and Alzheimer's disease	
Fast wound healing Protecting against cerebrovascular and cardiovascular disorders	Organic acids
Antioxidant Involved in collagen synthesis Maintaining correct cell membrane integrity	Vitamin C
Prevention of bleeding Reducing the risk of stomach ulcers Helping the reconstruction of skin damage	Vitamin K
Antioxidant Reducing the risk of cardiovascular disease Involved in regulating heart rhythm Prevention of tumors Relieving the symptoms of aging	Phenolic compounds

The tested extracts considerably inhibit microsomal lipid peroxidation and protect normal erythrocytes against hypo-osmotic shock. A recent study by Kim et al. (2017) proposes that sea buckthorn extract containing about 70 mg/g phenolic compounds and about 460 μg/g catechin, may inhibit the rapid proliferation of rat C6 glioma cells when administered at 0.62, 6.2, and 62 μg/ml, probably by inducing the early events of apoptosis. The authors also suggest that the reduction of C6 glioma cell proliferation and viability following administration of the plant extract was associated with a drop in the production of reactive oxygen species as critical for the proliferation of tumor cells. Moreover, sea buckthorn not only strengthens the expression of the pro-apoptotic protein Bcl-2- X (Bax), but also promotes its localization in the nucleus. Various studies show that sea buckthorn oil also has anti-tumor properties. This oil can be placed in capsules, gelatin, and oral liquids (Yang and Kallio, 2002). Moreover, toxicity studies revealed no adverse effects in individuals administered with sea buckthorn oil (Upadhyay et al., 2009). Kumar et al. (2011) showed that sea buckthorn oil plays an important role in cancer therapy, including chemotherapy and radiotherapy complications, and using sea buckthorn oil may help fight against many side effects or treatment, restore kidney and liver function, increase appetite, and generally keep good health. Wang et al. (1989) observed that seed oil reduced tumor growth by 3–50%. Zhang et al. (Zhang, 1989) indicated that seed oil (1.59 g/kg body weight) significantly inhibited the growth rate of transplanted melanoma (B16) and sarcoma (S180) tumors in mice. Wu et al. (1989) attribute the protective effect of sea buckthorn seed oil against cervical cancer to the presence of vitamins A and E. Finally, Sun et al. (2003) found that flavonoids extracted from sea buckthorn seeds inhibit liver cancer cell BEL-7402 inducing apoptosis. The seeds and berry pulp of sea buckthorn contains various other bioactive compounds, including unsaturated fatty acids and phytosterols. Unsaturated fatty acids have a multidirectional influence on human health, for example, by stimulating the immune system. In addition, phytosterols have anticancer properties (Sajfratova et al., 2010; Dulf, 2012). More details about the composition and useful health aspects of sea buckthorn are presented by Olas (2018). The effect of sea buckthorn on cancer cells in different in vitro models is described in Table 3.

Table 3- The effect of sea buckthorn on cancer cells in in vitro models.

Reference	Effect	Concentration	Cancer cells	Extract/chemical compound or other form obtained from sea buckthorn
			Extract or other forms obtained from sea buckthorn	
Fruits extract	Cell of breast cancer,	10–50 µl/ml of medium	Inhibition of tumor cell	Boivin et al., 2007
Extracting from fruits in different solvents	prostate, stomach, and a semi-colon	<0.1–2% (v/v) of medium	proliferation of all tested line	Grey et al., 2010
Ethanol-water extract from berries	Cancer cells of a semi-colon and liver	0.025–0.5% the dry weight in medium	Inhibition of tumor cell proliferation of all tested	Olsson et al., 2004
Ethanol-water extract from berries	Cancer cells of the breast and a semi-colon	10–100 µg/ml	lines; extract with ethyl acetate also caused	Zhamanbayeva et al., 2016
Ethanol extract from berries	Acute myeloid leukemia cells	25, 50, and 100 µg/ml	apoptosis of these cells	Zhamanbaeva et al., 2014
Leaf extract	Acute myeloid leukemia cells	0.62, 6.2, and 62 µg/ml	Inhibition of tumor cell proliferation of all tested	Kim et al., 2017
Isorhamnetin isolated from berries of sea buckthorn	C6 glioma cells	25–300 µg/ml of medium (IC50 = 75 µg/ml)	lines	Teng et al., 2006
Isorhamnetin isolated from berries of sea buckthorn	Cancer cells of the liver	10–320 µg/ml	Anti-proliferative action	Li et al., 2015
Isorhamnetin isolated from berries of sea buckthorn	Lung cancer cells	20 and 40 µM	Anti-proliferative action	Li et al., 2014
Procyanidins isolated from seeds	Colorectal cancer cells	10–60 µg/ml	Anti-proliferative action	Wang et al., 2014
	Breast cancer cells		Cytotoxicity against cancer cells-a fall in their vitality, fragmentation and chromatin condensation	
			Anti-proliferative action	
			Anti-proliferative action Inducing apoptosis	

IN VIVO studies

Sea buckthorn had anticancer properties in both in vitro and in vivo studies on animal models. A study of the chemotherapy effect of sea buckthorn fruits by Padmavathi et al. (2005) showed that dimethylobenzenoantracen-induced skin papillomagenesis in mice is inhibited. The authors suggest that inhibition of carcinogenesis may be attributed to the concomitant induction of phase II enzymes, i.e., glutathione S-transferase, glutathione peroxidase, catalase, superoxide dismutase, and glutathione reductase in mouse liver. Moreover, the authors also suggest that the anticancer activity of sea buckthorn fruits may be based on its increase of the DNA-binding activity of interferon regulatory factor-1 (IRF-1), a known antioncogenic transcription factor causing growth suppression and apoptosis. Nersesyan and Muradyan (2004) report that sea buckthorn extract protects mice against the genotoxic action of cisplatin: a famous anticancer drug which also is very toxic to normal cells. Sea buckthorn extract (300 ml) was given to mice by gavage for 5 or 10 days. 3 hours after the last gavage, mice received cisplatin at concentrations of 1.2 or 2.4 mg/kg. Yasukawa et al. (2009) found that 70% ethanol extract of sea buckthorn branches (1 mg of plant extract/mouse) had antitumor properties in an in vivo two-stage carcinogenesis test with two groups of 15 mice; 7,12-dimethylbenzanthracene as an indicator, and 12-O-tetracecanoyl-phorbol-13-acetate as a promotor. Of the three phenolic compounds (catechin, gallocatechin, and epigallocatechin) and the triterpenoid ursolic acid isolated from the extract, epigallocatechin, and ursolic acid showed the most active ones. Wang et al. (2015) found that not only the phenolic compounds or phenolic extracts/some species sea buckthorn have anticancer properties: HRWP-A, a water-soluble homogenous polysaccharide with repeating units of (1 → 4)-β-D-galactopyranosyluronic residues, of which 85.2% are esterified with methyl groups,

also shows anticancer and immunostimulating activities in vivo. An antitumor activity test demonstrated that HRWP-A could significantly inhibit lung carcinoma growth in mice with tumur. In addition, this compound enhanced lymphocyte proliferation, strengthened macrophage activities, and promoted natural killer cell activity in mice with tumor. The authors used three different doses of polysaccharide (50, 100, and 200 mg/kg), which were administrated intragastrically each day for 14 days.

Conclusion

Although most of the studies have emphasized the anticancer activities of sea buckthorn, its suitable use in pharmaceutical and prevention applications is not clearly indicated and clinical tests except in vivo and in vitro are not performed. The studies have shown that sea buckthorn may play an important role in prevention and treatment of cancer and it is also important in healing the health of patients receiving chemotherapy by improving the immune system performance and reduction of blood cells damage. The effective substances in different parts of sea buckthorn have a wide range of useful properties including antioxidant, anti-inflammatory and anti-proliferation activities. They also strengthen the immune system of the body. However, before considering sea buckthorn a good option in cancer treatment, we need further studies regarding its effects and side-effects with the collaboration of cancer

References

1. Saddati, Seyed Ehsan, Vaezi, Jamil, Jalilvand, Hamid, Ahani, Hamid. 2016. New sub-species of (Elaeagnus rhamnoides (L.) A.Nelson) in Iran based on molecular data, genetic studies and improvement of pasture and forest plants of Iran. No. 2. Period 24, p.208-220.
2. Sadeghipourrudsari, H. R. Haeri Ruhani, S. A. Parandin, R. A. Vosughi, M. Sepehri, H. Haji Akhundi, A., Khanavi, M. 1956. The investigation of anti-fertility effects of Melia azedarach L fruit oil in Iran on male rats. Spring medicinal herbs. No. 13. Period 5. P. 23-26.
3. Agrawala, P. K., and Goel, H. (2002). Protective effect of RH-3 with special reference to radiation induced micronuclei in mouse bone marrow. Indian J.Exp. Biol. 40, 525–530.
4. Bagchi, D., and Preuss, H. G. (2004). Phytopharmaceuuticals in Cancer Chemoprevention, 1st Edn. Bocca Raton, FL: CRC Press.
5. Bagchi, D., Swaroop, A., Preuss, H., and Bagchi, M. (2014). Free radical scavenging, antioxidant and cancer chemoprevention by grape seed proanthocyanidin: an overview. Mutat. Res. 768, 69–73. doi: 10.1016/j.mrfmmm.2014.04.004.
6. Barrett, J. C. (1993). Mechanisms of multistep carcinogenesis and carcinogen risk assessment. Environ. Health Perspect. 100, 9–20. doi: 10.1289/ehp.931009.
7. Basu, M., Prasad, R., Jayamurthy, P., Pal, K., Arumughan, C., and Sawhney, R. C. (2007). Anti-atherogenic effects of seabuckthorn (Hippophaea rhamnoides) seed oil, Phytomedicine 14, 770–777. doi: 10.1016/j.phymed.2007.03.018.
8. Boivin, D., Blanchette, M., Barrette, S., Moghrabi, A., and Beliveau, R. (2007). Inhibition of cancer cell proliferation and suppression of TNF-induced activation of NFκB by edible berry juice. Anticancer Res. 27, 937–948.
9. Cetin, A., Kaynar, L., Kocyigit, I., Hacioglu, S., Saraymen, R., Ozturk, A., et al. (2008). The effect of grape seed extract on radiation-induced oxidative stress in the rat liver. Turk. J. Gastroenterol. 19, 92–98.
10. Chen, L., Xin, X., Yuan, Q., Su, D., and Liu, W. (2014). Phytochemical properties and antioxidant capacities of various colored berries. J. Sci. Food Agric. 94, 180–188. doi: 10.1002/jsfa.6216.
11. Christaki, E. (2012). Hippophae rhamnoides L. (Sea Buckthorn): a potential source of nutraceuticals. Food Pub. Health 2, 69–72. doi: 10.5923/j.fph.20120203.02.
12. Dulf, F. V. (2012). Fatty acids in berry lipids of six sea buckthorn (Hippophae rhamnoides L. subspecies carpatica) cultivars grown in Romania. Chem. Cent.J. 6, 1–12. doi: 10.1186/1752-153X-6-106.
13. Duthie, S., Jenkinson, A., Crozier, A., Mullen, W., Pirie, L., Kyle, J., et al. (2006). The effects of cranberry juice consumptions on antioxidant status and biomarkers relating to heart disease and cancer in healthy human volunteers. Eur. J. Nutr. 45, 113–122. doi: 10.1007/s00394-005-0572-9.Evidence, eds Y. Liu, Z. Wang, and J. Zhang (Vienna: Springer Science and Business Media), 411.
14. Fatima, T., Snyder, C., Schroeder, W., Cram, D., Datla, R., Wishart, D., et al. (2012). Fatty acid composition of developing sea buckthorn (Hippophae rhamnoides L.) berry and the ranscriptome of the mature seed. PLoS

ONE 7:e34099. doi: 10.1371/journal.pone.0034099.

15. Frohne, D. (2010). Leksykon Ro´slin Leczniczych MedPharm. Wroclaw, 276. Gao, X., Ohlander, M., Jeppsson, N., Bjork, L., and Trajkovski, V. (2000). Changes in antioxidant effects and their relationship to phytonutrients in fruits of sea buckthorn (Hippophae rhamnoides L.) during maturation, J. Agric. Food Chem. 48, 1485–1490. doi: 10.1021/jf991072g.
16. Giampieri, F., Alvarez-Suarez, J., Gasparrini, M., Forbes-Hernandez, T., Afrin, S., Bompadre, S., et al. (2016). Strawberry consumption alleviates doxorubicininduced toxicity by suppressing oxidative stress. Food Chem. Toxicol. 94, 128–127. doi: 10.1016/j.fct.2016.06.003.
17. Goel, H. C., Gupta, D., Gupta, S., Garg, A. P., and Bala, M. (2005). Protection of mitochondrial system by Hippophae rhamnoides L. against radiationinduced oxidative damage in mice. J. Pharm. Pharmacol. 57, 135–143. doi: 10.1211/0022357055218.
18. Goel, H. C., Indraghanti, P., Samanta, N., and Ranaz, S. V. (2004). Induction of apoptosis in thymocytes by Hippophae rhamnoides: implications in radioprotection. J. Environ. Pathol. Toxicol. Oncol. 23, 123–137. doi: 10.1615/JEnvPathToxOncol.v23.i2.50.
19. Goel, H. C., Kumar, I. P., Samanta, N., and Rana, S. V. (2003a). Induction of DNAprotein cross-links by Hippophae rhamnoides: implications in radioprotection and cytotoxicity. Mol. Cell Biochem. 245, 57–67. doi: 10.1023/A:1022809625826.
20. Goel, H. C., Prasad, J., Singh, S., Sagar, R. K., Kumar, I. P., and Sinha, A. K. (2002). Radioprotection by a herbal preparation of Hippophae rhamnoides,RH-3, against whole body lethal irradiation in mice. Phytomedicine 9, 15–25. doi: 10.1078/0944-7113-00077.
21. Goel, H. C., Salin, C., and Prakash, H. (2003b). Protection of jejunal crypts by RH- 3 (a preparation of Hippophae rhamnoides) against lethal whole body gamma irradiation. Phytother Res. 17, 222–226. doi: 10.1002/ptr.1109.
22. Gradt, I., Kuhn, S., Morsel, J., and Zvaigzne, G. (2017). Chemical composition of sea buckthorn leaves, branches and bark. Proc. Natl. Acad. Sci. U.S.A. 3, 211–216. doi: 10.1515/prolas-2017-0035.
23. Grey, C., Widen, C., Adlercreutz, P., Rumpunen, K., and Duan, R. (2010). Antiproliferative effects of sea buckthorn (Hippophae rhamnoides L.) extracts on human colon and liver cancer cell lines. Food Chem. 120, 1004–1010. doi: 10.1016/j.foodchem.2009.11.039.
24. Guo, R., Guo, X., Li, T., Fu, X., and Liu, R. (2017). Comparative assessment of phytochemical profiles, antioxidant and antiproliferative activities of Sea buckthorn (Hippophae rhamnoides L.). Food Chem. 221, 997–1003. doi: 10.1016/j.foodchem.2016.11.063.
25. Hu, S. (2005). "Hippophae rhamnoides L. – Sea buckthorn, shaji," in Food Plants of China (The Chinese University Press), 572.
26. Kim, S., Hwang, E., Yi, S., Song, K., Lee, H., Heo, T., et al. (2017). Seabuckthorn leaf extracts inhibits glioma cell growth by reducing reactive oxygen species and promoting apoptosis. Appl. Biochem. Biotechnol. 1 82, 1663–1674.doi: 10.1007/s12010-017-2425-4.
27. Ko, J. H., Sethi, G., Um, J. Y., Shanmugam, M. K., Arfuso, F., Kumar, A., et al. (2017). The role of resveratrol in cancer therapy. J. Mol. Sci. 18:2589. doi: 10.3390/ijms18122589.
28. Kristo, A., Klimis-Zacas, D., and Sikaliidis, A. (2016). Protective role of dietary berries in cancer, Antioxidants 5:37. doi: 10.3390/antiox5040037.
29. Kumar, I. P., Namita, S., and Goel, H. C. (2002). Modulation of chromatin organization by RH-3, a preparation of Hippophae rhamnoides, a possible role in radioprotection. Mol. Cell. Biochem. 238, 1–9. doi: 10.1023/A:1019905 211392.
30. Kumar, R., Kumar, G. P., Chaurasia, O. P., and Singh, S. (2011). Phytochemical and pharmacological profile of seabuckthorn oil: a review. Res. J. Med. Plant 5, 491–499. doi: 10.3923/rjmp.2011.491.499.
31. Li, C. H., Yang, X., Chen, C. H., Cai, S., and Hu, J. (2014). Isorhamnetin suppresses colon cancer cell growth through the PI3K-Akt-mTOR pathway. ol. Med.Rep. 9, 935–940. doi: 10.3892/mmr.2014.1886.
32. Li, Q., Ren, F., Yang, C., Zhou, L., Liu, Y., Xiao, J., et al. (2015). Anti-proliferation effects of isorhamnetin on lung cancer cells in vitro and in vivo. Asian Pac. J. Cancer Prev. 16, 3035–3042. doi: 10.7314/APJCP.2015.16.7.3035.

33. Li, Y., and Hu, C. (2015). "Hippophae rhamnoides L. (Shaji, Common Seabuckthorn)," in Dietary Chinese Herbs: Chemistry, Pharmacology and Clinical.

34. Malinowska, P., and Olas, B. (2016). Sea buckthorn – valuable plant for health. Kosmos 2, 285–292. doi: 10.1186/s12944-017-0469-7.

35. McDougall, G., Ross, H., Ikeji, M., and Stewart, D. (2008). Berry extracts exert different antiproliferative effects against cervical and colon cancer cells grown in vitro. J. Agric. Food Chem. 56, 3016–3023. doi: 10.1021/jf073469n.

36. Nersesyan, A., and Muradyan, R. (2004). Sea-buckthorn juice protects mice against genotoxic action of cisplastin. Exp. Oncol. 26, 153–155.

37. Olas, B. (2016). Sea buckthorn as a source of important bioactive compounds in cardiovascular diseases. Food Chem. Toxicol. 97, 199–204. doi: 10.1016/j.fct.2016.09.008.

38. Olas, B. (2018). The composition and beneficial health aspects of sea buckthorn (Hippophae rhamnoides L.) oil. J. Ethnopharm. 213, 183–190. doi: 10.1016/j.jep.2017.11.022.

39. Olsson, M., Gustavsson, K., Andersson, S., Nilsson, A., and Duan, R. (2004). Inhibition of cancer cell proliferation in vitro by fruit and berry extracts and correlations with antioxidant levels. J. Agric. Food Chem. 52, 7264–7271.doi: 10.1021/jf030479p.

40. Padmavathi, B., Upreti, M., Singh, V., Rao, A. R., Singh, R. P., and Rath, P. C. (2005). Chemoprevention by Hippophae rhamnoides: effects on tumorigenesis, phase II and antioxidant enzymes, and IRF-1 transcription factor. Nutr. Cancer51, 59–67. doi: 10.1207/s15327914nc5101_9.

41. Prakash, H., Bala, M., Ali, A., and Goel, H. C. (2005). Modification of gamma radiation induced response of peritoneal macrophages and splenocytes by Hippophae rhamnoides (RH-3) in mice. J. Pharm. Pharmacol. 57, 1065–1072. doi: 10.1211/0022357056668.

42. Sajfratova, M., Lickova, I., Wimmerova, M., Sovova, H., and Wimmer, Z. (2010). β-Sitosterol: supercritical carbon dioxide extraction from sea buckthorn (Hippophae rhamnoides L.) seeds. Int. J. Mol. Sci. 11, 1842–1850.doi: 10.3390/ijms11041842.

43. Sarwa, A. (2001). Wielki Leksykon Ro´slin Leczniczych. Warszawa: Ksia¸zka i Wiedza.

44. Seeram, N. (2008). Berry fruits: compositional elements, biochemical activities, and the impact of their intake on human health, performance, and disease. J. Agric. Food Chem. 56, 627–629. doi: 10.1021/jf071988k.

45. Shanmugam, M., Rane, G., Mathi, K. M., Arfuso, F., Chinnathambi, A., Zayed, M. E., et al. (2015). The multifaceted role of curcumin in cancer prevention and treatment. Molecules 20, 2728–2769. doi: 10.3390/molecules20022728.

46. Sun, B., Zhang, P., Qu, W., Zhang, X., Zhuang, X., and Yang, H. (2003). Study on effect of flavonoids from oil-removed seeds of Hippophae rhamnoides on inducing apoptosis of human hepatoma cell. Zhong Yao Cai 26, 875–877.

47. Suryakumar, G., and Gupta, A. (2011). Medicinal and therapeutic potential of Sea buckthorn (Hippophae rhamnoides L.). J. Ethnopharmacol. 138, 268–278. doi: 10.1016/j.jep.2011.09.024.

48. Teleszko, M., Wojdylo, A., Rudzinska, M., Oszmianski, J., and Golis, T. (2015). Analysis of lipophilic and hydrophilic bioactive compounds content in sea buckthorn (Hippophae rhamnoids L.) berries. J. Agric. Food Chem. 63, 4120–4129. doi: 10.1021/acs.jafc.5b00564.

49. Teng, B., Lu, Y., Wang, Z., Tao, X., and Wei, D. (2006). In vitro anti-tumor activity of isorhamnetin isolated from Hippophaer rhamnoides L. against BEL-7402 cells. Pharm. Res. 54, 186–194. doi: 10.1016/j.phrs.2006.04.007.

50. The State of Pharmacopoeia Commission of PR China (1977). Pharmacopeia of the People's Republic of China 1997, Beijing.

51. Ulanowska, K., Skalski, B., and Olas, B. (in press). Sea-buckthorn (Hippophae rhamnoides L.) as a source of compounds with antitumor and radioprotective activity. Postepy Hig. Med. Dosw.

52. Upadhyay, N. K., Kumar, R., Mandotra, S. K., Meena, R. M., Siddiqu, M. S.Sawhney, R. C., et al. (2009). Safety and wound healing efficacy of sea buckthorn (Hippophae rhamnoides L.) seed oil in experimental rats. Food Chem. Toxicol. 47, 1146–1153. doi: 10.1016/j.fct.2009.02.002

53. Wang, H., Gao, T., Du, Y., Yang, H., Wei, L., Bi, H., et al. (2015). nticancer and immunostimulating activities of a novel homogalacturonan from Hippophae rhamnoides L. berry. Carbohydr. Polym. 131, 288–296.doi: 10.1016/j.carbpol.2015.06.021

54. Wang, H., Ge, H., and Zhi, J. (1989). "The components of unsaponifiable matters in sea buckthorn fruit and seed oil," in Proceedings first International Symposium on Sea Buckthorn (Xi'an), 81–90.

55. Wang, Y., Nie, F., Ouyang, J., and Wang, X. (2014). Inhibitory effects of sea buckthorn procyanidins on fatty acid synthase and MDA-MB-231 cells. Tumor Biol. 35, 9563–9569. doi: 10.1007/s13277-014-2233-1.

56. Wu, A., Su, Y., Li, J., Liu, Q., Lu, J., Wei, X., et al. (1989). "The treatment of chronic cervicitis with Hippophae oil and its suppository (129 cases analysis)," in Proceedings first International Symposium on Sea Buckthorn, 404–406.

57. Xu, Y. J., Kaur, M., Dhillon, R. S., Tappia, P. S., and Dhalla, N. S. (2011). Health benefits of sea buckthorn for the prevention of cardiovascular diseases. J. Funct. Foods 3, 2–12. doi: 10.1016/j.jff.2011.01.001

58. Yang, B., and Kallio, H. (2002). Composition and physiological effects of sea buckthorn (Hippophae) lipids. Trends Food Sci. Technol. 13, 160–167. doi: 10.1016/S0924-2244(02)00136-X

59. Yasukawa, K., Kitanaka, S., Kawata, K., and Goto, K. (2009). Anti-tumor promoters phenolics and triterpenoid from Hippophae rhamnoides. Fitoterapia 80, 164–167. doi: 10.1016/j.fitote.2009.01.006

60. Zafra-Stone, S., Yasmin, T., Bagchi, M., Chatterjee, A., Vinson, J., and Bagchi, D. (2007). Berry anthocyanins as novel antioxidants in human health and disease prevention. Mol. Nutr. Food. Res. 51, 675–683. doi: 10.1002/mnfr.200700002.

61. Zeb, A. (2006). Anticarcinogenic potential of lipids from hippophae – evidence from the recent literature. Asian Pac. J. Cancer Prev. 7,32–34.

62. Zhamanbaeva, G., Murzakhmetova, M., Tuleukhanov, S., and Danilenko, M. (2014). Antitumor activity of ethanol extract from Hippophae rhamnoides L. leaves towards human acute myeloid leukemia cells in vitro. Bull. Exp. Biol. Med. 158, 221–224. doi: 10.1007/s10517-014-2734-3.

63. Zhamanbayeva, G., Aralbayeva, A., Murzakhmetova, M., Tuleukhanov, S., and Danilenko, M. (2016). Cooperative antiproliferative and differentiationenhancing activity of medicinal plant extracts in acute myeloid leukemia cells. Biomed. Pharmacother. 82, 80–89. doi: 10.1016/j.biopha.2016. 04.062.

64. Zhang, P. (1989). Anti-cancer activities of sea buckthorn seed oil and its effects on the weight of immune organs Seabuckthorn 2, 31–34.

65. Zhang, P., Mao, Y. C., Sun, B., Qian, M., and Qu, W. J. (2005). Changes in apoptosis-related genes expression profile in human breast carcinoma cell line Bcap-37 induced by flavonoids from seed residues of Hippophae rhamnoides. L. Ai Zheng 24, 454–460.